Valorization of commercial food waste via anaerobic processes

Gabriel Capson-Tojo

Gabriel CAPSON TOJO

PhD thesis 2017

VALORISATION DES BIODÉCHETS ALIMENTAIRES COMMERCIAUX PAR DES PROCÉDÉS ANAÉROBIES

VALORIZATION OF COMMERCIAL FOOD WASTE VIA ANAEROBIC PROCESSES

INRA
SCIENCE & IMPACT

Membre fondateur de
agreenium

THÈSE POUR OBTENIR LE GRADE DE DOCTEUR DE MONTPELLIER SUPAGRO

En génie des procédés

École doctorale GAIA – Biodiversité, Agriculture, Alimentation, Environnement, Terre, Eau
Portée par l'Université de Montpellier

Unité de recherche Laboratoire de Biotechnologie de l'Environnement (LBE, INRA UR050)

Valorisation des biodéchets alimentaires commerciaux par des procédés anaérobies

Présentée par Gabriel CAPSON TOJO
Le 12 décembre 2017

Sous la direction de Renaud ESCUDIE
et Jean-Philippe DELGENES

Devant le jury composé de

Patrick DABERT, Directeur de recherche, IRSTEA Rennes, France	Rapporteur
Fernando FERNANDEZ POLANCO, Professeur, Université de Valladolid, Espagne	Rapporteur
Renaud ESCUDIE, Directeur de recherche, INRA LBE, France	Co-directeur
Hassen BENBELKACEM, Maître de conférences HDR, INSA Lyon, France	Examinateur
Catherine FAUR, Professeur, Université de Montpellier, France	Examinatrice
Maxime ROUEZ, Ingénieur de recherche, CIRSEE SUEZ, France	Encadrant
Christophe HEVIN, Ingénieur, ADEME, France	Invité
Anne TREMIER, Directrice de recherche, IRSTEA Rennes, France	Invitée

UNIVERSITÉ DE MONTPELLIER

Montpellier SupAgro

Valorization of commercial food waste via anaerobic processes

The increasing production of food waste worldwide and new international regulations call for the development of novel processes for the treatment of this waste. Among all the existing possibilities, anaerobic processes represent a sustainable-modern approach that allows waste treatment and valorization. This PhD thesis aims at understanding the biochemical processes governing anaerobic digestion of food waste, eventually providing a stable process applicable at industrial scale.

As a first step, a screening was performed to elucidate the main parameter affecting anaerobic digestion of food waste, evaluating different substrate loads, solid contents, co-digestion proportions and microbial inocula from different origins. After concluding the critical importance of the inoculum used and the substrate load, different strategies for process stabilization for methane production were tested using consecutive batch reactors. This served for confirming the positive effect of supplementation of trace elements and to identify the main issue that was found: accumulation of propionic acid. Aiming at finding a solution, the final experiments were focused on assessing the capability of carbon-based conductive materials to solve this problem. The dosing of these materials favored the digestion kinetics, improving greatly the methane volumetric productivities.

This thesis provides novel insights, both on the main mechanisms governing food waste anaerobic digestion and on the implications that they present for the valorization of this waste. In addition, potential solutions for the complications found are given, aiding to the development of a feasible industrial digestion process.

Keywords: Biomethane; hydrogen; ammonia; hydrogenotrophic methanogenesis

Valorisation des biodéchets alimentaires commerciaux par des procédés anaérobies

La production croissante de déchets alimentaires dans le monde et des nouvelles réglementations internationales exigent le développement de nouveaux procédés pour le traitement de ce type de déchets. Parmi toutes les possibilités existantes, les procédés anaérobies représentent une approche durable qui permet le traitement et la valorisation de ces déchets. Ce doctorat vise à comprendre les processus biochimiques régissant la digestion anaérobie des déchets alimentaires, en fournissant des éléments pour le développement de procédés applicables à l'échelle industrielle.

Dans un premier temps, un screening a été effectué pour élucider les paramètres principaux affectant la digestion anaérobie des déchets alimentaires, en évaluant différentes charges de substrat, teneurs en matière sèche, proportions de co-digestion et des inocula microbiens de différentes origines. Après avoir conclu à l'importance cruciale de l'inoculum utilisé et de la charge du substrat, différentes stratégies de stabilisation des procédés de méthanisation ont été testées à l'aide de réacteurs discontinus consécutifs. Ce travail a permis de confirmer l'effet positif de la supplémentation du milieu réactionnel en oligoéléments sur les performances de production de biogaz et à identifier le principal verrou: l'accumulation d'acide propionique. Dans le but de trouver une solution, deux expériences ont été axées sur l'évaluation de la capacité des matériaux conducteurs à base de carbone à résoudre ce problème. Le dosage de ces matériaux favorise la cinétique de la digestion, améliorant significativement les productions volumétriques du méthane.

Cette thèse fournit des connaissances nouvelles, à la fois sur les principaux mécanismes régissant la digestion anaérobie des déchets alimentaires et sur les implications qu'elles présentent pour la valorisation de ces déchets. En outre, des solutions possibles pour lever les verrous opérationnels ont été développés, permettant de fournir des recommandations pour l’implantation d’un procédé de digestion à l’échelle industrielle.

Mots-clés: Biométhane; hydrogène; ammoniac; méthanogenèse hydrogénotrophe

Certification

I hereby declare that this thesis is my own work. Where other sources of information have been used, they have been acknowledged and referenced in the list of used literature and other sources. All the partners agree with the confidentiality of this manuscript, valid within 24 months after the thesis defense.

The director(s) and supervisor(s):

Dr. Renaud Escudié

Dr. Philippe Delgenès

Dr. Marion Crest

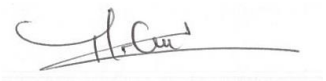

Dr. Maxime Rouez

The author:

Gabriel Capson Tojo

Acknowledgments

And here we go, after 10751 e-mails, a “few” meetings, around 500 meals in the “Routier”, 49 tons of waste weighed and XXX beers in L’Antre de L’échoppe, this thesis has come to an end. The list of people that have helped me out through this journey is so large that I am sure I will miss someone. Here is the best I can do.

The first people to include here are the ones who gave this opportunity and trusted me to carry out this project, my thesis directors and supervisors: **Renaud ESCUDIE**, **Jean-Phillipe DELGENES**, **Maxime ROUEZ** and **Marion CREST**. You are all directly responsible for making this thesis possible and, even if it is far from being enough, I want to give you my deepest “thank you” for the confidence that you have laid on me during these three years and for your amazing qualities, both professional and personal. I have been really lucky to have you as supervisors, not only for your advices and guidance, but also for your constant sense of humor and open-minded point of view. I have to give a special thanks to Renaud for his patience and support (I know by my own experience that I can be a bit “insisting” sometimes ;)). I also want to thank Marion and Maxime for their friendship when I went to the CIRSEE or when you came down to the LBE, it is a pity that I will miss the SUEZ lab in Narbonne!

I have to continue with my “un-official” supervisors, **Jean-Phillipe STEYER** and **Eric TRABLY**. Even if you are not my directors on paper, this thesis would have never been possible without your constant support and advices. And I also want to thank **Nicolas BERNET** for his supervision as lab director in the last year of my thesis. Most importantly, I want to thank you all for your constant sense of humor and your super-friendly attitude. It is because of you all (together with the other permanents) that the atmosphere in the lab is that awesome!

I also want to express my gratitude to the members of the jury for having evaluated the work carried out during this thesis. Particularly, I want to thank **Fernando FERNANDEZ POLANCO** and **Patrick DABERT** for their exhaustive work as thesis reporters and **Catherine FAUR**, **Hassen BENBELKACEM**, **Christophe HEVIN** and **Anne TREMIER** for accepting being part of the jury as examiners and invited members. I also want to acknowledge **Pierre FONTANILLE** for his useful advices during my thesis committees.

Going back to the LBE, I have to thank **Diane RUIZ** and **Chloé GIRARD**, the two people that did all the hard lab-work during the last year of my thesis. Your work was of outstanding quality and a big part of what is presented in this document has been achieved because of you. I hope that I have been able to help you as much as you have helped me and hopefully the

experience was not very traumatic (you know, nice smells, 30 GC injections per day, digestate everywhere, exploding reactors…). I have been really lucky to have you both as interns! Thanks!

In the same line I want to express my gratitude to **Clémence PAGES** for helping me to start so many batch experiments (we managed to understand each other even when I did not speak French), to **Denis LOISEL** and **Pascal GRAS** (we had really nice moments weighing and grinding waste and unclogging pressurized reactors), to **Philippe SOUSBIE** for all his advices when I was working with the pilots (and for the nice travelling chatter) and to **Gaëlle SANTA-CATALINA** for her support and her patience for carrying out microbial analyses (and also for her constant good humor). Here I also want to acknowledge **Eric LATRILLE**, for helping me out with modelling, data acquisition, statistics, etc., (basically everything) throughout these three years. Finally, my biggest "Thank you!" to **Sylvie FARINE**, **Nadine LE THINH**, **Alexandra MESEGUER**, **Ingrid ODON** and **Annie VIDAL**. It's because of you and your great job that we are able to do "some" research ☺.

And there we go with colleagues and friends... There are so many people that have supported me both inside and outside the lab that I do not really know how to start here, so I will do it with the first person I met: **Afifi**. Man, luckily you were there when I arrived to help me out, thanks a lot for everything! A very special line has to be dedicated here to my two "churris", **Angel** and **Julie**. I cannot thank you enough for all the great moments that we have had. And anyway, far from being a farewell, with you two this is a beginning. We have many years ahead to have even better times (although is going to be tough if we want to beat the previous)! **Alice**, **Quentin** and **Elias**, I have to thank you also for your friendship along these three years. We have always (and always will) understood each other, even if when I arrived we were not able to speak (no words needed, they are overrated). I will be waiting for you in my home! **Felipe** and **Yolanda**, thanks also for having become part of my family abroad, you know that sometimes being far away from home is not easy and it is meeting people like you that makes is worthy! Moreover, now I can say I have met genuine "Pelotudos". And **Chabi** and **Irene** (and **Jimmy**), I know it is quite weird that you are here, but your post-it in my computer saying "Hoy va a ser un día estupendástico" and "recuerda darle amor a las microalgas", has helped me a lot (really, it has, mainly when one gets "morriña" attacks). And of course here comes my family from Cuxac d'Aude: **Florian** "le Roux", **Roman** "Gross Porc hyper-brutal-de-guerre", **Cyrille** "Princess Sisi" and **Adrien** le "Pulpe". Thanks you all for teaching me the wonders of the French culture, such as "crème fraiche" and "beurre (bien sûr, salé)". I think that after these three years we can agree with a couple of things: "le canard

c'est la vie" and "our neighbor is awesome". Of course, here I also have to mention **Wendy** (et **Ben**), **Virginie**, **Marie-Lou**, **Clément**, **Lucile**, **Antonella**, **Elie**, **Elsa**, **Violette**, **Julien**, **Anish**, **Mariana**, **Silvio**, **Iza**… Thanks you all! These three years have been an unforgettable experience because of you!

I also want to acknowledge **Ignacio HERNANDEZ** (*a.k.a.* **Piro**) for accepting to make this awesome illustration of "The Green City" for my thesis. It is because of small details like this one that one can feel a bit at home wherever one roams. And I must say that it ended up better than my original idea of the food-waste-monster destroying stuff.

Here my Family has a very special place. It is because of you that I have been able to accomplish everything that I have done. Especially I have to thank my mother **Emilia**, **Santi** and my grandmother **Emilia** for their continuous support and the patience that they have had during the last years (it has been a while since I am not home for more than a couple of weeks…). Muchas gracias a todos!!!

And I leave the most important one for the end. A simple "thank you" is not enough to express my gratitude to my girlfriend **Laura** who, even from far away (sometimes a bit too far), has always supported me in all the projects that have allowed me to accomplish this part of my life. I promise I am not going anywhere else without you. No matter where (Australia, Miami (Ohio) or Cuntis), our adventure "starts" now! Mil gracias pequena!!!

"The good thing about **science** is that it's true whether or not you believe in it"

Neil de Grasse Tyson

"The **environment** is everything that isn't me"

Albert Einstein

"The saddest aspect of life right now is that science gathers **knowledge** faster than society gathers wisdom".

Isaac Asimov

"Bah! Genius is not inspired. Inspiration is **perspiration**."

Thomas Edison

"**Global warming** isn't a prediction. It is happening"

James Hansen

"We are in danger of destroying ourselves by our greed and stupidity. We cannot remain looking inwards at ourselves on a small and increasingly **polluted** and **overcrowded** planet"

Stephen Hawking

Contents

Contents

Contents

List of figures

List of figures

List of tables

List of tables

List of abbreviations and symbols

3D-EEM	3 Dimension excitation emission matrix fluorescence spectroscopy
A	Empiric parameter dependent on the dielectric constant of water
A_i	Parameter dependent on the ion size
a_0, a_i, a_{ii}, a_{ij}	Quadratic parameters
ABPs	Animal by-products
AcoD	Anaerobic co-digestion
AD	Anaerobic digestion
AF	Acidogenic fermentation
AGVs	Acides gras volatiles
AM	Acetoclastic methanogenesis
AMPTSII	Automatic methane potential test system
ANOVA	Analysis of variance
AnMBR	Anaerobic membrane bioreactor
B	Empiric parameter dependent on the dielectric constant of water
BAs	Biodéchets alimentaires commerciaux
BMP	Biochemical methane potential
CA	Charbon actif
CAGN	Communauté d'Agglomération du Grand Narbonne
CB	Cardboard
C_i	Molar concentration of ion i
COD	Chemical oxygen demand
COD_{bio}	Biodegradable chemical oxygen demand
CSTR	Continuous stirred tank reactor
DA	Digestion anaérobie
DC	déchets de type carton
DCO	Demande chimique d'oxygène
DIET	Direct interspecies electron transfer
DF	Dark fermentation
DNA	Deoxyribonucleic acid
DOE	Design of experiments
EPS	Extra polymeric substances
Eq	Equation
ETMs	Eléments traces métalliques
f_i	Activity coefficient of ion i
FAN	Free ammonia nitrogen

List of abbreviations and symbols

FAO	Food and Agriculture Organization
FS	Fermentation sombre
FW	Food waste
GAC	Granular activated carbon
GC	Gas chromatography
GW	Green waste
GWP	Global warming potential
HAc	Acetic acid
HBu	Butyric acid
HCA	Hierarchical clustering analysis
HCap	Caproic acid
HLa	Lactic acid
HM	Hydrogenotrophic methanogenesis
HPLC	High-performance liquid chromatography
HPr	Propionic acid
HRT	Hydraulic retention time
HVal	Valeric acid
HY	Hydrogen yield
INRA	Institut National de la Recherche Agronomique
I	Ionic strength
IC	Inorganic carbon
ICh	Ion chromatography
K_a	Acid-base equilibrium constant
L	Lag phase
LAB	Lactic acid bacteria
LBE	Laboratoire de Biotechnologie de l'Environnement
LCA	Life cycle analysis
M	Cumulative methane yield
M_{max}	Final methane yield
m_0	Initial useful mass of the reactor
m_{t-1}	Mass of the reactor at time t-1
MIET	Mediated interspecies electron transfer
MS	Matière sèche
MV	Matière volatile
MY	Methane yield
N_g	Number of times the population was doubled
OFMSW	Organic fraction municipal solid waste

OLR	Organic loading rate
OTU	Operational taxonomic unit
PCA	Principal component analysis
PCR	Polymerase chain reaction
PW	Paper waste
qPCR	Real-time polymerase chain reaction
R	Ideal gas constant
R^2	Coefficient of determination
R_m	Maximum methane production rate
rRNA	Ribosomal ribonucleic acid
S_0	Initial amount of substrate added
S/X	Substrate to inoculum ratio/rapport substrat inoculum
SAO	Syntrophic acetate oxidation
sCOD	Soluble chemical oxygen demand
SMPs	Soluble metabolic products
SPO	Syntrophic propionate oxidation
SRT	Solids retention time
SSFW	Source segregated food waste
t	Time
T	Temperature
TAN	Total ammonia nitrogen
TC	Total carbon
TEs	Trace elements
TKN	Total Kjeldahl nitrogen
TOC	Total organic carbon
TPASBR	Temperature phased anaerobic sequencing batch reactor
TS	Total solids
UASB	Up-flow anaerobic sludge blanket
VFAs	Volatile fatty acids
VHPR	Volumetric hydrogen production rate
VMPR	Volumetric methane production rate
VS	Volatile solids
VSS	Volatile suspended solids
WAS	Waste activated sludge
WRRFs	Water resource recovery facilities
X_i	Initial concentration of 16S copies
x_i	Factors studied

List of abbreviations and symbols

$\mathbf{X_f}$	Final concentration of 16S copies
y	Model response
$\mathbf{Y_{prod}}$	Product yield
$\mathbf{z_i}$	Charge of ion i
$\mathbf{\Delta G^0}$	Standard Gibbs free energy of the reaction
$\mathbf{\Delta G'}$	Variation of Gibbs free energy
$\mathbf{\Delta prod_{t,t-1}}$	Amount of product generated between time t and time t-1
$\mathbf{\sigma}$	Standard error associated with the measurement

Publications and communications

Scientific publications

Capson-Tojo, G., Rouez, M., Crest, M., Steyer, J.-P., Delgenès, J.-P., Escudié, R., 2016. Food waste valorization via anaerobic processes: a review. Rev. Environ. Sci. Biotechnol. 15, 499–547. *(Section 1.2)*

Capson-Tojo, G., Trably, E., Rouez, M., Crest, M., Steyer, J.-P., Delgenès, J.-P., Escudié, R., 2017. Dry anaerobic digestion of food waste and cardboard at different substrate loads, solid contents and co-digestion proportions. Bioresour. Technol. 233, 166–175. *(Section 3.2)*

Capson-Tojo, G., Trably, E., Rouez, M., Crest, M., Bernet, N., Steyer, J.-P., Delgenès, J.-P., Escudié, R., 2017. Cardboard proportions and total solids contents as driving factors in dry co-fermentation of food waste. Bioresour. Technol. 248, Part A, 229-237. *(Section 3.3)*

Capson-Tojo, G., Rouez, M., Crest, M., Trably, E., Steyer, J.-P., Bernet, N., Delgenès, J.-P., Escudié, R., 2017. Kinetic study of dry anaerobic co-digestion of food waste and cardboard for methane production. Waste Manag. 69, 470-479. *(Section 3.4)*

Capson-Tojo, G., Ruiz, D., Rouez, M., Crest, M., Steyer, J.-P., Bernet, N., Delgenès, J.-P., Escudié, R., 2017. Accumulation of propionic acid during consecutive batch anaerobic digestion of commercial food waste. Bioresour. Technol. 245, Part A, 724-733. *(Section 4.2)*

Capson-Tojo, G., Trably, E., Rouez, M., Crest, M., Bernet, N., Steyer, J.-P., Delgenès, J.-P., Escudié, R., 2017. Methanosarcina sp. as essential methanogen for efficient anaerobic digestion of high-solids food waste. Waste Manag. *Submitted on December 4th 2017. (Section* 3.5*)*

Capson-Tojo, G., Moscoviz R., Ruiz D., Santa-Catalina G., Trably E., Rouez, M., Crest, M., Steyer, J.-P., Bernet, N., Delgenès, J.-P., Escudié, R. Addition of granular activated carbon and trace elements to favor VFA consumption during anaerobic digestion of food waste. *To be submitted after patent acceptance. (Section 5.2)*

Capson-Tojo, G., Girard C., Rouez, M., Crest, M., Steyer, J.-P., Bernet, N., Delgenès, J.-P., Escudié, R. Biochar and industrial $FeCl_3$ as additives to favor the consumption of VFAs during anaerobic digestion of food waste for methane production. *To be submitted after patent acceptance. (Section 5.4.2)*

International communications

Capson-Tojo, G., Rouez, M., Crest, M., Trably. E., Steyer, J.-P., Delgenès, J.-P., Escudié, R., 2016. Stabilization of anaerobic digestion of food waste for methane production. ORBIT 2016: Organic Resources and Biological Treatment. 10th International Conference on "Circular Economy and Organic Waste". Hersonissos, Greece. *(Oral presentation)*

Capson-Tojo, G., Rouez, M., Crest, M., Steyer, J.-P., Delgenès, J.-P., Escudié, R., 2017. Stabilization of anaerobic digestion of food waste for methane production. 1st International ABWET Conference: Waste-to-bioenergy: Applications in Urban areas. Paris, France. *(Oral presentation)*

Capson-Tojo, G., Rouez, M., Crest, M., Trably, E., Bernet, N., Steyer, J.-P., Delgenès, J.-P., Escudié, R., 2017. Déchets de papier/carton comme co-substrat pour stabiliser la digestion anaérobie des biodéchets alimentaires commerciaux. Journée Recherche Innovation Biogaz Méthanisation. Beauvais, France. *(Oral presentation)*

Publications and communications

Capson-Tojo, G., Rouez, M., Crest, M., Trably. E., Steyer, J.-P., Delgenès, J.-P., Escudié, R., 2017. Optimization of urban food waste valorization: cardboard as suitable co-substrate for dry anaerobic co-digestion. The 15th IWA Conference on Anaerobic digestion. Beijing, China. *(Oral presentation)*

Capson-Tojo, G., Rouez, M., Crest, M., Trably. E., Steyer, J.-P., Delgenès, J.-P., Escudié, R., 2017. *Methanosarcina* sp. as key archaea to avoid acidification in dry anaerobic digestion of food waste. The 15th IWA Conference on Anaerobic digestion. Beijing, China. *(Poster)*

Résumé

Introduction et objectifs

En raison de l'augmentation de la demande mondiale en matières et en énergies liée à l'accroissement de la population mondiale et du niveau de développement des pays, de l'épuisement des ressources naturelles et de l'empreinte environnementale des technologies de production conventionnelle, il ne fait aucun doute que nous devons axer le développement de notre société sur des approches durables de production et de consommation. Les concepts tels que la bioraffinerie environnementale et l'économie circulaire sont à la base de cette option, en considérant les déchets comme des ressources qui représentent un fort potentiel de valorisation. Plus spécifiquement, de nouvelles réglementations internationales exigent le développement de nouvelles techniques de valorisation des biodéchets alimentaires commerciaux (notés BA).

Les procédés anaérobies représentent une alternative particulièrement prometteuse, en offrant un double objectif: (i) le traitement des déchets et (ii) la production de différents produits à valeur ajoutée. Parmi toutes les options qui existent, la digestion anaérobie (DA) ou méthanisation apparaît comme une alternative intéressante pour la valorisation des BA via la production de méthane et d'un digestat pouvant être utilisé, par exemple, en agriculture. Cependant, des complications sont associées à la méthanisation des BA, principalement en raison de l'accumulation d'azote ammoniacal et des acides gras volatils (AGVs). Bien que des alternatives différentes aient été appliquées pour stabiliser la DA des BAs, telles que l'addition d'éléments traces métalliques (ETMs), la recirculation de la fraction solide du digestat ou la co-digestion avec d'autres substrats, une grande hétérogénéité des résultats obtenus est rapportée, principalement en raison des caractéristiques différentes des BA digérés, de l'inoculum microbien utilisé et de la diversité des conditions opératoires appliquées. De plus, peu de recherches se sont également focalisées sur l'optimisation de ces différentes stratégies de stabilisation. Par conséquent, il existe un manque de connaissances concernant les meilleures options pour stabiliser le procédé et les conditions opérationnelles optimales, en particulier pour la DA des BAs non dilués (contenant une teneur en matière sèche élevée).

Pour répondre à ces enjeux, un projet de collaboration entre SUEZ et l'INRA-LBE a été lancé. Ce projet de recherche a été créé pour répondre au besoin social de développer des nouvelles technologies de traitement (autres que la mise en décharge et l'incinération) pour la valorisation des BAs. En tenant compte des nouvelles directives européennes pour la

valorisation des déchets organiques, le gouvernement français a approuvé des nouveaux règlements (article 204 de la loi du 12 juillet 2010) qui imposent la collecte séparée des BAs des grands producteurs et sa valorisation par le retour au sol. Par rapport à cette règlementation, les entreprises/institutions concernées ont deux options: (i) la valorisation interne des déchets par compostage ou (ii) l'utilisation de fournisseurs de services externes qui effectuent la collecte des déchets et leur valorisation par compostage ou DA. La collaboration entre SUEZ et l'INRA-LBE permet de créer une synergie en couplant les connaissances de la recherche et les intérêts industriels, en vue de fournir une solution industriellement réalisable pour le service demandé. C'est dans ce contexte que cette thèse a eu lieu, ayant pour objectif scientifique d'accroître les connaissances sur le traitement/valorisation des BAs par des procédés anaérobies en posant des questions de recherche spécifiques. Les objectifs scientifiques du doctorat ont principalement porté sur la compréhension des processus biochimiques mis en jeu au cours de la DA des BAs, et sur la recherche d'options fiables de stabilisation pour la réalisation d'un procédé efficace.

La première partie de la thèse a eu comme objectif principal l'évaluation et la sélection des principaux facteurs affectant la valorisation des BAs par des procédés anaérobies. L'influence de la teneur en matière sèche (MS), du rapport substrat-inoculum (S/X) et du rapport de co-digestion (avec du carton) sur les performances de DA et fermentation sombre (FS) a notamment été étudiée. De plus, différents inocula microbiens ont été utilisés et leurs communautés microbiennes ont été identifiées afin d'élucider le type de microorganismes impliqués dans chaque processus et leur importance. La deuxième étape de la thèse a porté sur l'évaluation de trois stratégies de stabilisation de la méthanisation des BAs en utilisant des réacteurs discontinus successifs: (i) utilisation d'une température basse, (ii) co-digestion des BAs avec des déchets de type carton (DC) et (iii) addition des ETMs. Différentes options pour favoriser la consommation des AGVs accumulés (*i.e.* ajout d'ETMs, de charbon actif (CA) et dilution du digestat) ont également été étudiées. Enfin, la dernière approche expérimentale a été consacrée à élucider l'effet de l'ajout des matériaux conducteurs à base de carbone avec ETMs sur l'accumulation d'AGVs pendant DA des BAs. L'ajout de CA a d'abord été appliqué pour étudier les mécanismes impliqués dans le processus, et l'ajout de biochar obtenu par pyrolyse de bois a été ensuite utilisé comme une alternative moins chère, visant à développer un processus industriellement applicable pour la valorisation des BAs par DA.

Valorisation des BAs via DA sèche: sélection des principaux facteurs et importance de l'inoculum

L'objectif d'une première étude a été d'évaluer la faisabilité de la valorisation des BAs par co-digestion anaérobie sèche avec des déchets de type carton (DC) en utilisant des réacteurs 'batch' discontinus: ce type de réacteur a permis de tester différentes conditions simultanément. Plus précisément, l'influence de la charge initiale du substrat sur la performance des réacteurs a été étudiée pour la première fois avec ce type de substrats. La charge a été modifiée en faisant varier le rapport S/X (ratio substrat sur inoculum), la teneur en MS et les proportions de co-substrats. En faisant varier ces paramètres opérationnels, différentes voies métaboliques ont été sélectionnées (Figure F.1). Le ratio S/X constitue un paramètre critique qui affecte le pH, ainsi que la nature des produits finaux obtenus. Une production efficace de méthane a seulement été obtenue à un rapport S/X faible (0,25 g MV·g MV^{-1}), avec *Methanosarcina* comme archaea majoritaire. Des processus de fermentation sombre (FS) ont prédominé à de plus forts ratios S/X (1 et 4 g MV·g MV^{-1}), en produisant de l'hydrogène et d'autres métabolites. Dans ce cas, des teneurs en MS élevées, des substrats de co-digestion contenant une plus forte proportion de BAs, ou des rapports S/X élevés ont entraîné des dégradations de substrat plus faibles et des proportions de lactate plus élevées dans les métabolites produit, diminuant ainsi les rendements d'hydrogène. Des conversions de substrats (≤ 48 %) et des rendements en hydrogène (≤ 62 ml·g MV^{-1}) plus élevés ont été obtenus à des faibles charges. Cette étude a montré que différents composés à haut valeur ajoutée (*i.e.* comme méthane, hydrogène ou AGVs) peuvent être produits dans des conditions "sèches" (fortes teneurs en MS) par co-digestion des BAs et DC: la charge de substrat initiale est dans ce cas le paramètre opératoire critique, qui est par ailleurs facile à contrôler.

Une deuxième étude de cette section a permis d'évaluer la faisabilité de la fermentation sombre (FS) pour la production d'hydrogène et des AGVs à partir de BAs à des fortes teneurs en MS, en utilisant des DC comme co-substrat. L'influence du rapport de co-digestion (0-60% de DC en base sèche) et de la teneur en MS initiale (20-40%) sur la performance de la FS discontinue a été étudiée. Une attention particulière a été portée sur l'effet de ces paramètres sur les rendements finaux des différents métabolites obtenus et sur la structure des communautés microbiennes après la fermentation. Les rendements maximaux en hydrogène ont été obtenus lors de la mono-fermentation des BAs à forte teneur en MS (89 ml H_2·g MV^{-1}). Les rendements en hydrogène étaient plus faibles à des proportions de DC plus élevées. Ces rendements d'hydrogène inférieurs à des proportions plus élevées de DC ont été traduits en des rendements plus élevés d'acide caproïque (jusqu'à 70,1 g DCO·kg DCO^{-1}), produit par

la consommation d'acide acétique et d'hydrogène. Les conversions de substrat les plus élevées ont été obtenues à des faibles proportions de DC, ce qui indique un effet de stabilisation lié à des capacités de tampon des DC plus élevées en co-fermentation. La diversité des communautés microbiennes impliquées (avec *Clostridiales* en tant qu'espèces principales) dépendait principalement des teneurs en MS. Cette étude ouvre de nouvelles possibilités pour l'utilisation des proportions de DC pour contrôler la production de produits à forte valeur ajoutée dans la fermentation sèche des BAs. En effet, les résultats obtenus dans ces deux premières expériences prouvent qu'une large gamme de produits à haute valeur ajoutée peut être obtenue lors de la valorisation anaérobie des BAs.

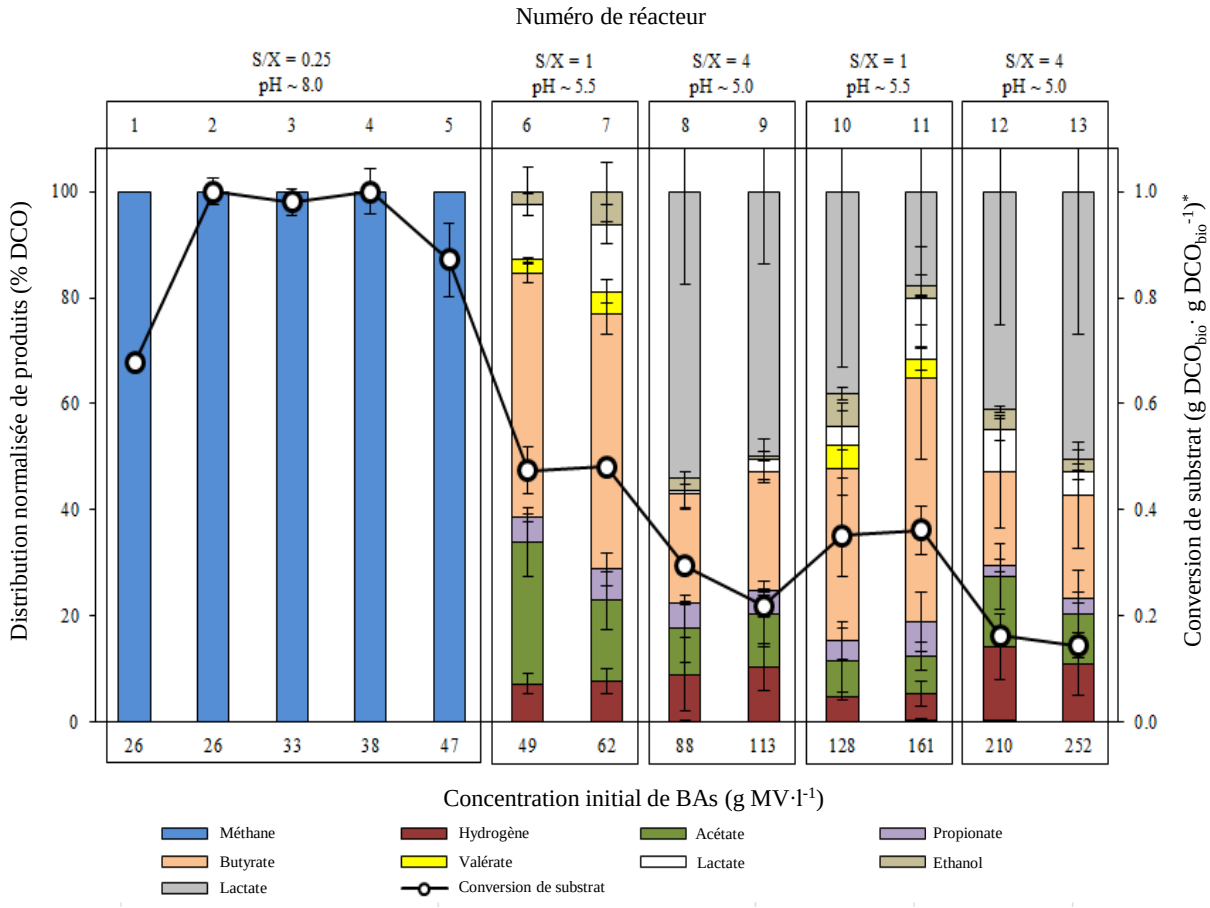

* La conversion du substrat a été calculée en fonction de la quantité initiale de DCO biodégradable ajoutée comme substrat (estimée à partir des potentiels méthanogènes)

Figure F.1. Répartition des produits finals métaboliques et conversion du substrat selon la concentration initiale de BAs. Le rapport S/X initial et les valeurs finales du pH sont également présentés

Une troisième expérience s'est focalisée sur la production de méthane à partir de BAs, qui permet leur stabilisation complète. L'objectif était d'évaluer l'effet du rapport S/X (0,25 à 1 g MV·g MV^{-1}) et de la teneur initiale en MS (20-30%) sur la cinétique et la performance de la

DA des BAs. La mono-digestion et la co-digestion avec des DC ont été étudiées en utilisant des réacteurs batch discontinus, afin d'évaluer l'effet de l'ajout de CB sur le procédé. Pour la première fois, dans des conditions sèches en mode batch, une attention particulière a été portée sur la dynamique de production/consommation des AGVs et de production de méthane. L'influence des paramètres décrits précédemment sur les rendements de méthane a aussi été évaluée. Toutes les conditions ont produit du méthane efficacement (71 à 93% de la valeur du BMP atteints). Cependant, en raison du manque d'activité méthanogène, des AGVs se sont accumulés au début de digestion et des phases de latence dans la production de méthane ont été observées. En augmentant les rapports S/X, l'accumulation d'acide observée initialement était plus prononcée, avec des rendements cumulés de méthane plus faibles. Des quantités plus élevées de composés organiques simples liés au métabolisme microbien (comme les enzymes, les acides aminés et les produits microbiennes solubles) ont été observées à des S/X plus élevées. Bien que provoquant des phases de latence légèrement plus longues, une teneur initiale en MS élevée n'a pas compromis les rendements en méthane. Concernant l'effet de la co-digestion, il a également été observé que l'addition des DC réduit l'accumulation d'acides et entraine une baisse des rendements à des charges de substrat croissantes. Cependant, l'addition en DC a également provoqué des concentrations plus élevées d'acide propionique, qui constitue un intermédiaire métabolique difficile à dégrader. Néanmoins, si un consortium microbien adapté est utilisé, la co-digestion sèche des BAs et du DC dans les zones urbaines est une intéressante option de valorisation.

Enfin, comme des performances de méthanisation très différentes ont été observées lors des trois expériences précédentes, une quatrième étude a été menée avec le but de comprendre cette variabilité. L'objectif de cette étude était de comparer les performances de production de méthane des trois inocula microbiens utilisés précédemment, qui possédaient des origines différentes et donc une composition microbienne initiale spécifique. Une attention particulière a été portée sur les communautés d'archaea dans les inocula et les digestats après méthanisation. Alors que les tests menés avec des inocula riches en *Methanosarcina* sp. ont conduit à une production efficace de méthane, des AGVs se sont accumulés et aucune production de méthane a été observée dans les réacteurs inoculés faiblement avec cette archaea. De plus, des charges de substrat plus élevées ont été tolérées lorsque de grandes proportions de *Methanosarcina* sp. étaient initialement présentes dans l'inoculum. Indépendamment de l'inoculum utilisé, *Methanosarcina* sp. était l'archaea méthanogène dominante dans toutes les expériences où du méthane a été produit, ce qui suggère que cette archaea est essentielle pour atteindre une DA efficace à des concentrations élevées d'azote

ammoniacal et d'AGVs. La composition initiale des communautés d'archaea dans l'inoculum est donc cruciale, principalement dans les systèmes discontinus et pendant le démarrage du méthaniseur, ce qui peut avoir de fortes implications dans les installations industrielles traitant des BA et des DC.

Pour conclure, au cours de ce chapitre, différents produits à valeur ajoutée ont été générés lors de la valorisation des BAs par des procédés anaérobies en voie sèche. Les résultats obtenus ouvrent plusieurs questions de recherche, ainsi que des alternatives industrielles, qui doivent être étudiées afin de répondre à l'objectif principal de cette thèse: développer un procédé efficace de méthanisation des BAs. Ainsi, à partir des résultats précédents, il a été décidé de passer à des études en réacteurs pilotes en régime batch successif, en utilisant l'inoculum qui avait montré la meilleure performance. Différentes stratégies de stabilisation, telles que l'ajout d'ETMs, le fonctionnement à basse température et la co-digestion avec des DC, ont été testées.

Accumulation de l'acide propionique comme principal problème lors de la digestion anaérobie des biodéchets alimentaires pour la production de méthane

L'objectif principal de cette expérience était d'élucider si la DA des BAs en batch successifs était un procédé efficace de valorisation. De plus, ce mode d'opération permet également de reproduire le mode de fonctionnement des réacteurs pistons avec recirculation du digestat, qui sont des procédés de méthanisation en voie sèche utilisés au niveau industriel. Différentes stratégies permettant de favoriser la consommation ou de limiter l'accumulation des AGVs ont été évaluées: (i) utilisation d'une température basse (30 °C *vs.* 37 °C, afin de réduire les proportions d'ammoniac libre), (ii) la co-digestion des BAs avec DC (visant à diluer la teneur en azote et à augmenter la capacité tampon) et la complémentation avec des ETMs (visant à améliorer la consommation d'AGVs en favorisant la synthèse des enzymes). En outre, le digestat d'un réacteur a été utilisé pour tester différentes options pour permettre la consommation des AGVs accumulées.

Dans l'ensemble des stratégies mises en place, bien que le méthane ait été produit efficacement (~500 ml $CH_4 \cdot g\ MV^{-1}$, 16 l $CH_4 \cdot l_{réacteur}^{-1}$), les concentrations d'acide propionique ont augmenté progressivement au cours des alimentations successives des réacteurs (jusqu'à 21,6 $g \cdot l^{-1}$). L'accumulation de ce composé a provoqué des phases de retard dans la production de méthane et a finalement conduit à une acidification du réacteur à des charges de substrat élevées. La stratégie consistant à co-digérer des DA avec DC n'a pas permis de stabiliser le

procédé, et a même conduit à la concentration de propionate la plus élevée. L'ajout d'ETMs a permis d'améliorer la cinétique de production de méthane et d'atteindre des charges de substrat plus élevées, mais cependant n'a pas pu éviter l'accumulation de propionate. Des expériences réalisées en utilisant des digestats contenant de fortes concentrations en propionate ont démontré que l'ajout de CA, la supplémentation en ETMs et la dilution du digestate peuvent constituer des moyens pour favoriser la consommation d'acide propionique. D'autres recherches doivent être menées pour élucider l'effet de ces options très prometteuses pour prévenir l'accumulation d'acides et/ou favoriser leur consommation.

Pour conclure, ce travail expérimental a permis de mettre en évidence que l'accumulation d'acide propionique était le facteur clef limitant la production de méthane dans des réacteurs discontinus successifs. D'un point de vue industriel, il s'agit d'un problème important. En effet, avant de relancer un digesteur, il est indispensable d'attendre que l'acide propionique soit consommé, ce qui limite les charges de substrat appliquées dans les réacteurs et donc leurs productivités. Une autre conséquence des résultats obtenus est que la stratégie de co-digestion des BAs avec DC ne peut être retenue, puisqu'elle a conduit à des concentrations de propionate les plus élevées.

Par conséquent, des pistes additionnelles ont été explorées pour trouver une solution à la problématique de l'accumulation d'acide propionique, soit en évitant son accumulation en premier lieu ou en favorisant sa consommation. Dans ce cadre, différents additifs ont été testés dans le chapitre expérimental suivant: l'ajout de matériaux conducteurs à base de carbone (*e.g.* CA ou biochar) et la supplémentation en ETMs.

Matériaux conducteurs à base de carbone et oligoéléments pour favoriser la consommation d'AGVs et stabiliser la DA des BAs pour la production de méthane

Dans la première section expérimentale de ce chapitre, l'impact de l'ajout d'un CA granulaire et d'ETMs a été évalué sur la performance de réacteurs batch consécutifs de DA traitant des BAs. Une attention particulière a été portée sur la cinétique de production-consommation d'AGVs et sur les communautés microbiennes établies. Comme il a été précédemment démontré que les ETMs permettait d'améliorer le processus de digestion (et la dégradation de propionate), ils ont été également ajoutés simultanément avec les matériaux conducteurs de carbone sélectionnés.

Dans un premier temps, les résultats obtenus (Figure F.2) ont suggéré que l'addition de CA seul améliorait la cinétique de la consommation d'acide acétique ainsi que la production de

méthane. L'ajout d'ETMs a permis une consommation plus rapide de l'acide propionique accumulé. Donc, dans une deuxième alimentation en mode batch, l'ajout simultané de CA et d'ETMs a été étudié. Il a été démontré que cette option améliore la cinétique de dégradation de tous les AGVs initialement accumulés, ce qui permet de réduire considérablement la durée du batch et augmente ainsi les productions moyennes de méthane. L'analyse des communautés microbiennes a montré que les méthanogènes hydrogénotrophes étaient les archaeas prédominants. De plus, l'addition de CA a favorisé la croissance des bactéries syntrophiques et des archaea, en améliorant ainsi les interactions entre ces microorganismes. L'ajout de CA granulaire et d'ETMs peut constituer une solution réaliste pour stabiliser la méthanisation des BAs.

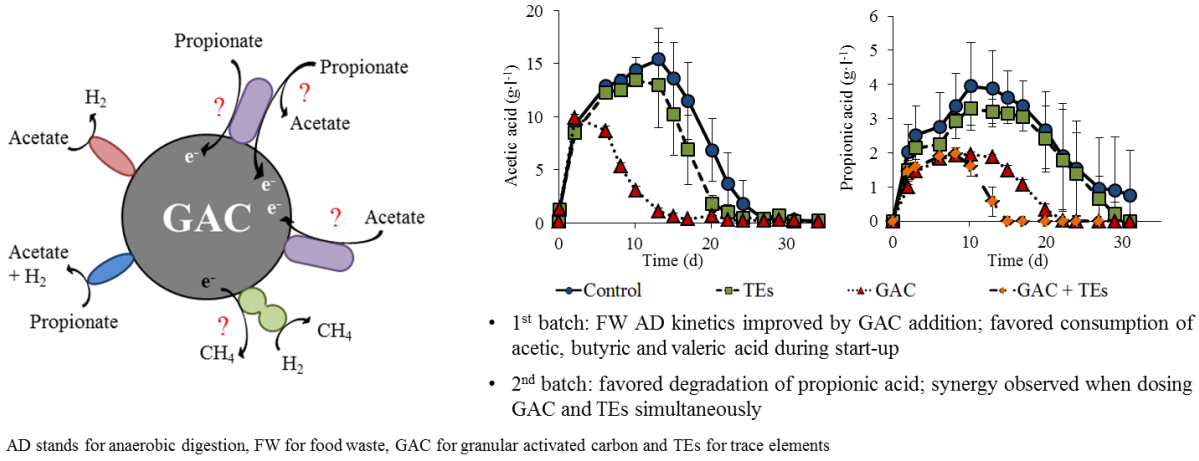

Figure F.2. Principaux résultats correspondant à l'ajout de CA et OE dans les réacteurs batch traitant des BA

Dans l'optique d'une application industrielle, le CA et les ETMs étant des composés trop coûteux, une dernière expérimentation de cette thèse a visé à tester l'utilisation d'un biochar et du $FeCl_3$ industriel comme substituts de CA et d'ETMs, respectivement. Tout d'abord, grâce à un plan d'expérience (biochar 10-100 $g \cdot l^{-1}$ et ETMs 0.1-0.2 g $Fe \cdot l^{-1}$), des réacteurs batch ont été utilisés pour optimiser les concentrations de ces deux matériaux et pour évaluer l'influence de l'augmentation des charges de substrat. L'ajout de biochar et de $FeCl_3$ industriel favorise la cinétique de la digestion dans les réacteurs discontinus, avec des résultats optimaux à la plus forte concentration de biochar appliquée (100 $g \cdot l^{-1}$). L'addition de biochar a amélioré les taux de de production de méthane (liés à la consommation d'acétate) et les productivités moyennes de méthane (liées à la consommation de propionate). L'utilisation de charges en substrat plus élevées augmente la durée du batch afin d'atteindre la production finale de méthane sans accumulation de propionate, mais elle améliore également les taux volumiques de production

de méthane, avec des valeurs allant jusqu'à 1,30 $l \cdot l^{-1} \cdot d^{-1}$ avec un ratio S/X de 2 g $VS \cdot g\ VS^{-1}$ lors de l'alimentation. De plus, des essais en réacteurs pilotes continus ont également été réalisés, afin de tester l'ajout de biochar et de $FeCl_3$ et d'envisager une extrapolation à une installation à l'échelle industrielle. Les réacteurs continus ont confirmé les résultats obtenus en conditions batch, avec des taux de production de méthane plus élevés et des concentrations plus faibles d'acétate et de propionate lorsque le biochar et le $FeCl_3$ ont été ajoutés. Ces matériaux apparaissent comme une option possible pour stabiliser la DA des BAs à grande échelle, en favorisant la consommation d'AGVs et en permettant des charges en substrat plus élevées.

Conclusions and perspectives

Les résultats obtenus ont montré que les BAs peuvent être efficacement transformés par des procédés anaérobies (*i.e.* DA et FS) en différents produits à haute valeur ajoutée tels que le méthane, les AGVs, l'hydrogène et/ou le digestat. Cependant, en raison de la faible teneur en eau des BAs, des concentrations élevées de matières organiques et d'espèces ioniques ont été mesurées dans les réacteurs. Par conséquent, la méthanisation des BAs est confrontée à deux problèmes principaux: (i) un inoculum microbien adapté (riche en archaea hydrogénotrophe) doit être utilisé et (ii) les AGVs (principalement acide propionique) s'accumulent facilement. La supplémentation en ETMs et en matériaux conducteurs à base de carbone (*i.e.* CA et biochar) apparaît comme une solution efficace pour stabiliser le procédé, en favorisant la consommation d'AGVs et en améliorant la cinétique de la production de méthane. Les travaux menés au cours de la thèse ont permis de réaliser des progrès, à la fois sur les principaux mécanismes régissant la DA des BAs et sur leurs implications au niveau de la mise en œuvre des bioprocédés. D'un point de vue industriel, l'addition de biochar et de $FeCl_3$ apparaît comme une option réaliste pour stabiliser la DA des BAs, à la fois pour des systèmes continus ou discontinus.

D'un point de vue scientifique, les résultats présentés dans cette thèse ont ouvert plusieurs perspectives de recherche. Face à la nécessité d'utiliser un inoculum microbien adapté pour obtenir une méthanisation efficace des BAs, des recherches supplémentaires doivent être effectuées, en analysant les performances de DA avec des substrats simples à différentes concentrations d'espèces inhibitrices, des valeurs de pH et des capacités de tampon. La modélisation des changements dans les populations d'archaeas et de bactéries peut être un outil puissant qui devrait être appliqué afin d'améliorer la compréhension globale des

mécanismes régissant DA des substrats complexes, tels que les BAs. Suite aux travaux menés dans ce doctorat, il n'est pas clairement identifié en quoi et comment les matériaux conducteurs à base de carbone améliorent ce procédé. Des travaux de recherche centrés sur les interactions microbiennes pourraient être effectués, ce qui pourrait permettre notamment d'identifier de nouvelles bactéries électro-actives. La récupération du biofilm attaché sur la surface des matériaux conducteurs est une approche prometteuse qui pourrait également permettre d'identifier ces interactions. Le couplage de cette méthodologie avec une modélisation thermodynamique et des analyses métagénomiques pourrait fournir des informations essentielles pour comprendre les mécanismes et pour évaluer leur potentiel pour améliorer les performances de DA.

En ce qui concerne les perspectives industrielles, l'approche la plus prometteuse tirée de cette thèse est l'application du biochar et du $FeCl_3$ pour la stabilisation de la DA. Cependant, les résultats obtenus sont clairement de nature préliminaire, ce qui implique que les modalités d'ajout de ces composés doivent encore être optimisées. En particulier, des études complémentaires doivent être effectuées pour déterminer l'importance des caractéristiques du biochar (*i.e.* surface spécifique, volume des pores, taille des pores, distribution des pores, hydrophobicité ou conductivité) sur les processus biochimiques mis en œuvre. Une fois ces caractéristiques identifiées, les paramètres opératoires utilisés lors de la production du biochar par pyrolyse doivent également être évalués: matière première utilisée, température et pression appliquées, prétraitements appliqués au biochar. Finalement, les concentrations de biochar (et en $FeCl_3$), en lien avec les charges de BAs appliquées, doivent également être optimisées, dans des expériences de méthanisation en mode discontinu et continu.

Introduction

Our world is rapidly moving towards a turning point in which we will have to decide if we keep relying on traditional old-fashioned production technologies or if we base our society upon sustainable approaches. Concepts such as environmental biorefineries and circular economy are the basis of the latter, considering wastes as resources that must be further valorized. In this context, the valorization of commercial food waste (accounting for 1.3 billion tons of waste every year (FAO, 2012)) is of critical importance. Anaerobic processes represent a particularly promising alternative for this purpose, offering the dual role of waste treatment and generation of biogas and digestate as value-added products. However, anaerobic treatment of highly concentrated and biodegradable organic wastes (such as food waste) is a challenging process, usually associated with different issues, such as accumulation of ammonia nitrogen and volatile fatty acids.

To gain understanding on this process and to facilitate the construction of an industrial anaerobic digestion plant, a project was started with SUEZ and the INRA-LBE (Institut National de la Recherche Agronomique - Laboratoire de Biotechnologie de l'Environnement) as partners. This project had the following main objectives:

- To perform an extensive characterization of commercial food wastes from potential producers in the region of the Grand Narbonne.
- To evaluate the main alternatives for food waste valorization via anaerobic processes, determining at the same time the most influential operational parameters and their impact on the process performance.
- To develop a feasible process for food waste treatment and valorization at industrial scale.

It was within this collaboration that this thesis was developed, aiming to fulfill the presented goals. Furthermore, this thesis also had as objective to increase the existing scientific knowledge on the basics of food waste treatment via anaerobic processes, assessing the main parameters affecting the process and identifying the main biochemical mechanisms involved. A schematic representation of the dual general goals of the thesis is presented in Figure 1. In addition, the precise objectives of the thesis are given at the end of Chapter 1 (Section 1.3).

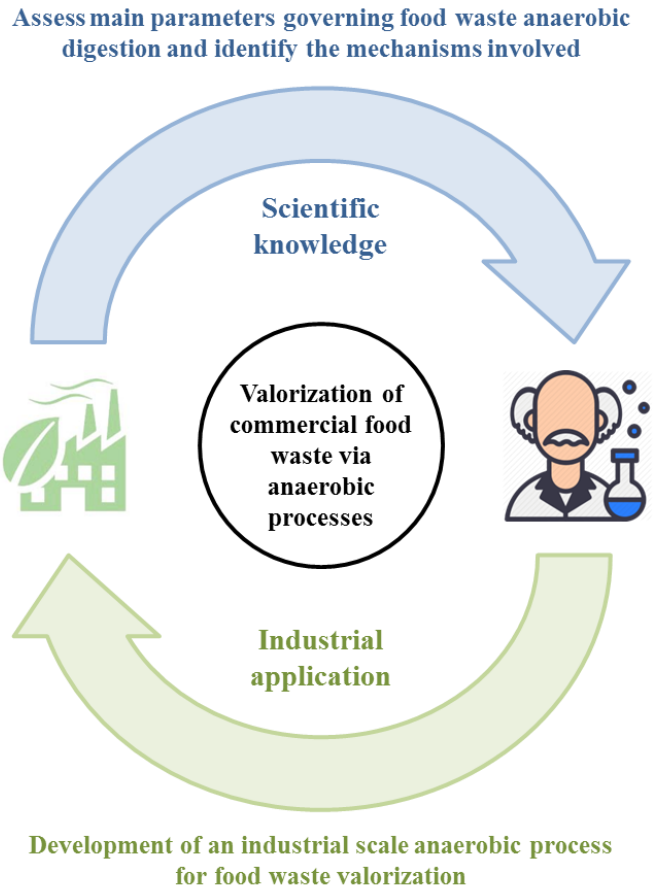

Figure 1. Schematic representation of the dual goal of the thesis, including both research and industrial interests

To favor its comprehension, this manuscript is divided in six main sections. First, an introductory literature review is presented (Chapter 1), followed by a general description of the materials and methods applied (Chapter 2). Afterwards, the main results (corresponding most of them to published or submitted scientific articles) are shown and discussed (Chapter 3 to Chapter 5). The document is finished with a summary of the main conclusions and perspectives (Chapter 6).

The first chapter of the thesis introduces the state-of-the-art technologies dealing with treatment of food waste by anaerobic processes. The main alternatives addressed are anaerobic digestion for methane production, anaerobic fermentation for hydrogen and/or volatile fatty acids production and 2-stage systems. These processes are described and compared, evaluating at the same time their primary complications and the latest developments achieved to overcome these difficulties. The most relevant economic and environmental research is also presented, including several life cycle analyses and case studies. Recommendations for future research for the anaerobic processes reviewed and options for process integration are also given.

Chapter 2 gives an overview of the materials and methods used to carry out this work. All the general equipment and procedures are described, including the substrates and the microbial inocula, the additives applied as enhancers of the digestion process, the reactors, the analytical and molecular biology methods and the mathematical calculations (both for modelling and statistical analysis).

The third chapter is dedicated to the screening of the main factors affecting dry anaerobic digestion (and fermentation) of food waste. Three different batch experiments started with different inocula evaluated the anaerobic treatment of food waste with cardboard as co-substrate. The parameters assessed were the initial total solids contents, the co-digestion proportions and the substrate to inoculum ratio (equivalent to the substrate load). The different value-added products that can be produced by anaerobic digestion and dark fermentation of food waste, depending on the working conditions and the microbial inoculum used, are discussed. Finally, the critical influence of the substrate to inoculum ratio and the selection of an adequate inoculum on the products obtained are deeply analyzed.

Chapter 4 introduces the main issue that was faced during consecutive batch anaerobic digestion of food waste: accumulation of propionic acid. In this section, a pilot scale experiment comparing different options to avoid this issue (*i.e.* working at low temperatures, food waste co-digestion with cardboard and supplementation of trace elements) is described. Possible reasons behind this problem and potential solutions are also discussed. Additional batch experiments were also performed, evaluating the effect of addition of granular activated carbon, further supplementation of trace elements and dilution on the consumption of propionic acid once it is accumulated in a digester.

Chapter 5 evaluates the addition of carbon conductive materials and trace elements into the reactor to stabilize the anaerobic digestion process. To understand the effect of these materials on the digestion performance, the addition of granular activated carbon and trace elements is firstly discussed. To study a potential industrial scale application, the addition of biochar and industrial $FeCl_3$ is also assessed in Chapter 5.

To conclude, the most relevant outcomes of this thesis as well the roads to follow with the greatest potential are summarized in Chapter 6.

Three appendixes at the end of the document include: complementary experiments focused on the application of green waste as co-substrate for stabilizing methane production from food waste (Appendix A), the results of the commercial food waste characterization (Appendix B) and the supplementary material presented to facilitate the comprehension of the manuscript (Appendix C).

Chapter 1. Literature review and objectives

1.1 General context

This thesis is the outcome of a collaboration project with SUEZ and the INRA-LBE as main partners. The research project was originated to respond to the social need of developing novel treatment technologies (*i.e.* other than landfilling and incineration) for commercial food waste (FW) valorization. Taking into consideration new European directives for organic waste valorization (Directive 2088/98/CE), the French government has approved new regulations (article 204 from law of July 12th 2010, law Grenelle 2) that impose the separate collection of commercial FW from large producers and its valorization through land return. This new regulation has a progressive implementation. While in 2013 it affected the actors producing over 80 tons of waste per year, in 2016 it affected already those producing over 10 tons per year. In this context, the concerned companies/institutions have two options: (i) internal waste valorization through composting or (ii) hiring external service providers that carry out the waste collection and its valorization by composting or anaerobic digestion. Within this second possibility, SUEZ wants to play a major role in the coming years, offering modern services for valorization of commercial food waste through anaerobic treatment.

However, a lack of knowledge exists both on the characteristics of this novel source-segregated waste and on the anaerobic processes that allow its treatment and valorization. The collaboration between SUEZ and INRA-LBE created a synergy that merged industrial and research knowledges and interests, aiming at providing an industrially-feasible solution for the demanded service. It was within this context that this thesis took place, having as scientific objective increasing the existing knowledge on FW treatment via anaerobic processes and answering to the research questions that arose during the course of the research.

Chapter 1 intends to explain the state-of-the-art technologies dealing with the treatment of FW by anaerobic processes. Thus, Section 1.2 introduces the first part of the thesis work, which consisted on a thorough literature review. The basics of FW production and its characteristics, as well as those of anaerobic processes, are discussed. The main processes applied for FW treatment (namely single-stage mono- and co-digestion for methane production, dark fermentation for hydrogen and volatile fatty acid production and 2- stage systems for production of both hydrogen and methane) are also critically analyzed and recommendations for further research are given. Finally, general conclusions are drawn in Section 1.3, where the precise objectives of the thesis are also given.

1.2 Food waste valorization via anaerobic processes: a review

Capson-Tojo, G., Rouez, M., Crest, M., Steyer, J.-P., Delgenès, J.-P., Escudié, R., 2016. Food waste valorization via anaerobic processes: a review. Reviews in Environmental Science and Bio/Technology 15, 499–547. doi:10.1007/s11157-016-9405-y

Abstract

The increasing production of food waste worldwide and new international regulations call for the development of new technologies to treat this biowaste. Anaerobic processes are able to treat efficiently organic wastes, producing at the same time different value-added compounds. In addition, due to the lower costs and environmental impacts associated with these processes when compared to other options, they are among the most promising technologies for food waste treatment. This article reviews the state-of-the-art dealing with treatment of food waste by anaerobic processes, with emphasis on the most recent research carried out. The different processes that are assessed are anaerobic digestion for methane production, anaerobic fermentation for hydrogen and/or volatile fatty acids production and 2-stage systems. The primary issues associated with each alternative are presented, paying special attention to accumulation of ammonia and volatile fatty acids in the reactor. In addition, the latest developments to overcome the complications of each system are also described, focusing on how they improve its stability and performance. Moreover, the relevant economic and environmental research has also been reviewed, including several life cycle analyses that compare anaerobic processes with other technologies used for food waste treatment. Different case studies are also presented. Finally, recommendations for future research for the anaerobic processes studied and options for process integration are discussed. Moving towards the idea of a circular economy, a potential biorefinery for food waste valorization is also proposed.

1.2.1 *Introduction*

1.2.1.1 Food waste production and valorization potential

The production of food waste (FW), which can be defined as the "mass of food lost or wasted in the part of food supply chains leading to edible products for human consumption" (Gustavsson et al., 2011), is an issue of global importance. This waste is generated mainly by food processing and distribution and represents a significant proportion of the total food produced worldwide. According to the Food and Agriculture Organization (FAO), about 1.3 billion tons of food, fully one third of the production for human consumption, is lost along the

food supply chain every year (FAO, 2012). In countries such as the United States of America, the United Kingdom or Japan, between 30 % and 40 % of the total food generated is discarded (Gunders, 2012; Kosseva, 2009). On a global scale, the production of urban FW has been predicted to increase by 44 % from 2005 to 2025 due to economic and population growth, particularly in developing countries (Melikoglu et al., 2013). In Europe, the amount of FW is expected to increase from 89 million tons in 2006 to 126 million tons in 2020 (Monier et al., 2010). Figure 1.1 (adapted from (Melikoglu et al., 2013; Spanish Ministry of Agriculture Food and the Environment, 2013; Thauvin and Vernier, 2013; United Nations, 2011; C. Zhang et al., 2014)) shows the FW production from different countries in 2010.

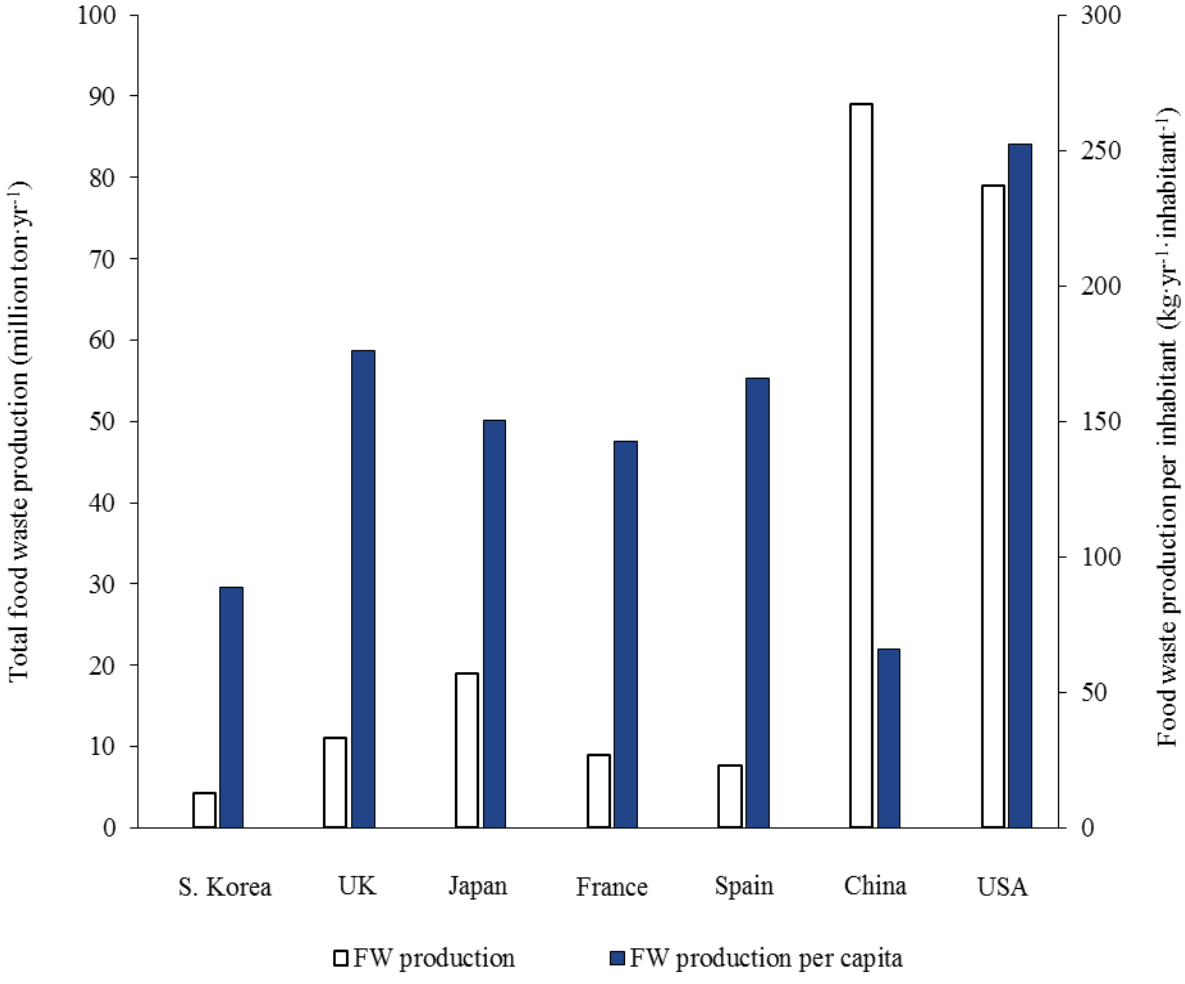

Figure 1.1. Amount of food waste produced in different countries in 2010. Adapted from (Melikoglu et al., 2013; Spanish Ministry of Agriculture Food and the Environment, 2013; Thauvin and Vernier, 2013; United Nations, 2011; C. Zhang et al., 2014)

According to the Directive 75/442/EEC of the Economic European Community (European Community, 1975), re-use and recycling are the most favored options of waste management after waste prevention. In this context, traditional direct disposal and treatment techniques, such as landfilling or incineration, which are currently widely applied for FW, are the least sustainable choices. Landfilling leads to several environmental issues, including leaching, greenhouse gas emission (*i.e.* methane) and odor production. Moreover, this practice has increasing costs imposed by EU landfill directives, which will eventually limit its application (European Community, 1999). Due to the high water content of FW, incineration is an energy-demanding and inefficient process that also causes air pollution. Two other common practices for FW treatment are aerobic composting and the production of animal feed (Kumar et al., 2010; San Martin et al., 2016). These options involve FW valorization, but generating low value-added products in the case of compost and increasing the risks of disease propagation in the case of animal feed application. Thus, there is an urgent need to develop and optimize technologies for FW valorization and recycling. In their bibliometric study, H. Chen et al. (2016) found a considerable increase in the number of publications dealing with FW in the last years, evidencing the growing need to find alternative treatments for FW.

In 2011, a study aiming to deal with the future world demands ranked FW 3rd out of 15 identified potential resource opportunities (Dobbs et al., 2011), mainly because of its chemical complexity, which makes it a source of several valuable compounds. To date, products such as chemicals (enzymes, organic acids, glycerol, animal feed, among others), materials (bioplastics, biopolymers, nanoparticles, fibers, among others) or fuels (such as methane, hydrogen, biodiesel, ethanol) have been obtained from FW (Kim et al., 2014; Lin et al., 2013; San Martin et al., 2016; Uçkun Kiran et al., 2014; Wang et al., 2015; R. Zhang et al., 2007). Chemicals generate the greatest revenues (around $1000/ton biomass), but the market demand for these products is still small due to the advantages of the traditional production processes and a post-treatment step is often required (Tuck et al., 2012). Transportation fuels are in the second place ($200-400/ton biomass). However, in this case their market applicability is huge and, depending on the process used for their production, it is possible to achieve a complete waste stabilization.

Between the different options for valorization and treatment of organic matter, anaerobic digestion (AD) is a well-known low-cost technology that can efficiently treat wastes, producing different value-added compounds (methane, hydrogen or volatile fatty acids among others) (Chynoweth et al., 2001). Some recent studies based on Life Cycle Analysis (LCA)

have already suggested that AD is preferred over the traditional methods for treatment of FW (Khoo et al., 2010; Xu et al., 2015).

Therefore, this review focuses on the valorization of FW by anaerobic processes. In addition, as mixed anaerobic consortia are usually preferred over pure cultures (lower cost, non-sterile conditions, greater stability and higher diversity of biochemical functions…) (Venkata et al., 2016), only this type of processes have been addressed.

The different options that have been reviewed are: single-stage AD for methane production (including co-digestion and dry AD), fermentation for hydrogen generation, (*i.e.*, dark fermentation - DF), fermentation for synthesis of volatile fatty acids (VFAs), (*i.e.*, acidogenic fermentation - AF) and 2-stage reactors for production of both hydrogen and methane. Figure 1.2 represents the number of peer-reviewed articles extracted from the literature, classified by valorization process and desired product. All these alternatives have been assessed in this study.

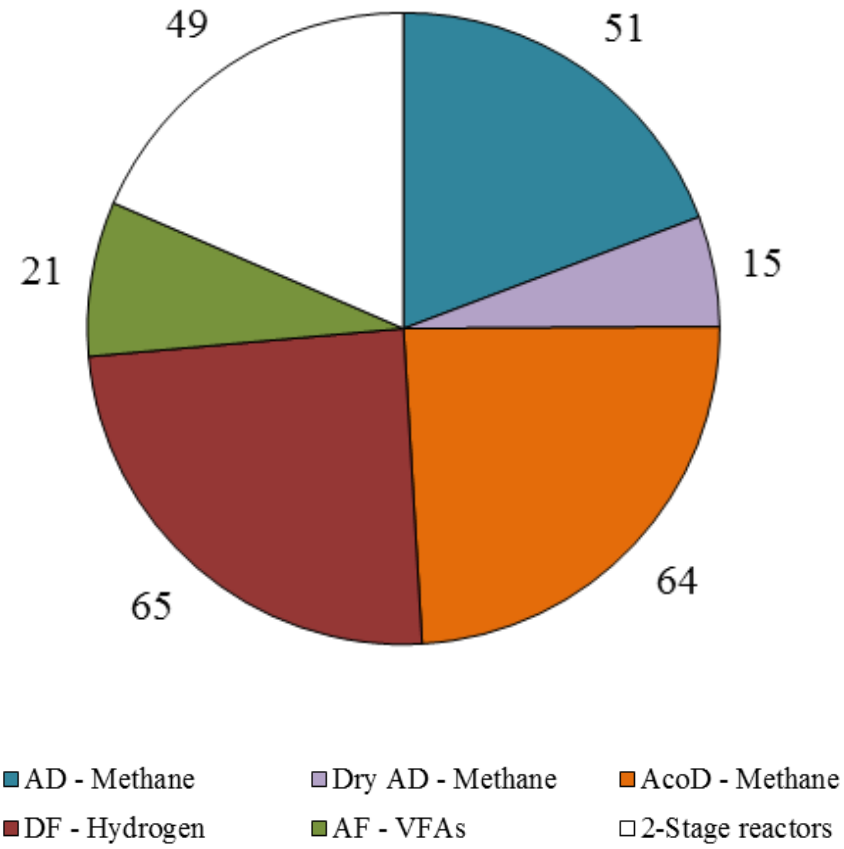

Figure 1.2. Number of peer-reviewed articles found in the literature involving FW treatment by anaerobic processes: anaerobic digestion (AD), dry anaerobic digestion (Dry AD), anaerobic co-digestion (AcoD), dark fermentation (DF), acidogenic fermentation (AF) and 2-stage reactors

1.2.1.2 Food waste characteristics around the world

As shown in Table 1.1, the composition of FW varies worldwide, depending mainly on the dietary and cultural habits, the economical level of the region and the climate. As a consequence, the physicochemical characteristics of FW differ depending on sources and regions in the world (Table 1.2). However, FW has general features that can be extrapolated worldwide. FW has relatively high total solids (TS) contents (~20 %), with around 90 % corresponding to volatile solids (VS). It is mainly composed of easily degradable carbohydrates (Uçkun Kiran et al., 2014), as suggested by the high carbohydrate percentage and the low cellulose-like and lignin-like proportions. The other two main components are proteins (15-25 %) and lipids (13-30 %). Proteins have a high nitrogen content and as a result, FW has a relatively low C/N ratio when compared to other substrates. Other important features of FW are the high concentrations of macroelements (*i.e.*, Phosphorus, Sodium, Potassium, Calcium or Magnesium) present in it and its relatively low content of trace elements (*i.e.*, Iron, Selenium, Nickel or Molybdenum) (Banks et al., 2012; Pham et al., 2014). All of these characteristics make FW a suitable substrate for anaerobic processes. However, issues like its low C/N ratio and its lack of trace elements (TEs) have to be addressed to optimize the process.

Table 1.1. Composition of FW from different countries. Adapted from VALORGAS (2010), Gustavsson et al. (2011), Melikoglu et al. (2013) and Uçkun Kiran et al. (2014)

% Wet weight	UK	Finland	Portugal	Italy	Europe	China	Thailand	Asia
Fruit and vegetables	61	45	59	69	58	30	13	32
Pasta/rice/cereals	1.5	0.4	0.2	12	3.6	58	47	27
Meat and fish	6.7	4.3	7.3	6.2	6.1	-	0.3	0.1
Dairy products	1.7	2.0	0.7	1.4	1.4	1.7	0.6	3.9
Mixed meals	12	6.3	29	1.4	12	-	-	-
Other foods	17	43	3.6	9.6	18	11	40	37

Table 1.2. Characteristics of food wastes (from different sources and regions) reported in the literature

Reference	(Banks et al., 2012; Y. Zhang et al., 2012a)	(Yirong et al., 2015)	(VALORGAS, 2010; Yirong et al., 2015)	(VALORGAS, 2010; Yirong et al., 2015)	(VALORGAS, 2010; Yirong et al., 2015)	(VALORGAS, 2010)	(De Vrieze et al., 2013)	(Zhang et al., 2011)	(Wanqin Zhang et al., 2015)	(Wanli Zhang et al., 2015a)	(C. Zhang et al., 2013a)	(C. Zhang et al., 2013b)	(Li et al., 2009; C. Zhang et al., 2014)	(Zhou et al., 2014)	(R. Zhang et al., 2007)
Country	UK	UK	UK	Finland	Italy	Portugal	Belgium	Korea	China	China	China	China	China	China	USA
FW Origin	Domestic FW	Domestic FW	Household	Waste company	Household	Household	University restaurant	University restaurant	University restaurant	Restaurant	University restaurant	University restaurant	-	University restaurant	Waste company
TS (%)[1]	23.74 ± 0.08	23.65 ± 0.38	23.70 ± 0.06	27.02 ± 0.12	27.47 ± 0.03	33.80	25.50 ± 0.40	18.10 ± 0.60	21.75 ± 0.34	23.20 ± 0.18	23.10 ± 0.30	18.50 ± 0.10	24.66 ± 0.08	22.71	30.90 ± 0.07
VS (%)[1]	21.71 ± 0.09	21.99 ± 0.49	21.84 ± 0.10	24.91 ± 0.05	23.60 ± 0.09	27.60	24.00 ± 0.60	17.10 ± 0.60	20.06 ± 0.19	21.70 ± 0.15	21.00 ± 0.30	17.00 ± 0.10	23.20 ± 0.02	20.72	26.35 ± 0.14
VS/TS (%)	91.44 ± 0.39	92.96 ± 1.00	91.28 ± 0.20	92.26 ± 0.26	86.60 ± 0.40	81.70	93.46	94.00 ± 1.00	92.21 ± 0.54	93.50	90.90 ± 0.20	92.0	94.08	91.24	85.30 ± 0.65
pH	4.71 ± 0.01	-	5.12 ± 0.01	5.34	6.16	-	-	6.50 ± 0.20	4.80 ± 0.12	4.40	4.20 ± 0.20	5.20 ± 0.30	5.10 ± 0.20	5.02	-
Carbohydrates (%)[2]	41.42 ± 1.55	-	-	-	-	-	-	61.70	-	59.35	-	-	55.20 ± 2.10	-	-
Proteins (%)[2]	15.10 ± 0.10	-	19.44 ± 0.09	14.95 ± 0.04	16.11 ± 0.26	-	-	18.20	-	12.67	-	-	15.00 ± 1.30	-	-
Lipids (%)[2]	23.50 ± 0.30	-	13.51 ± 0.36	14.39 ± 0.05	17.49 ± 0.04	-	-	12.87	28.30 ± 1.30	27.97	-	22.80	23.90 ± 0.80	30.40	-
C (%)[2]	47.60 ± 0.50	52.30 ± 1.10	51.20 ± 1.20	49.40 ± 0.04	47.20 ± 0.01	-	-	46.67	48.24 ± 0.17	-	56.30 ± 1.10	46.50 ± 1.50	54.00	48.30	46.78 ± 1.15
N (%)[2]	3.44 ± 0.04	3.00 ± 0.01	3.12 ± 0.01	2.46 ± 0.03	2.58 ± 0.05	-	-	3.54	2.50 ± 0.11	-	2.30 ± 0.30	2.20 ± 0.30	2.40	2.56	3.16 ± 0.22
C/N	13.90 ± 0.20	17.43	16.41	20.08	18.29	-	-	13.20 ± 0.20	19.30	-	24.50 ± 1.10	21.10	22.50	18.90	14.80
Cellulose (% TS)[2,3]	4.61 ± 0.15	-	-	-	-	-	-	-	4.30 ± 0.30	-	-	-	-	4.12	-
Hemi-cellulose (% TS)[2,3]	3.48 ± 0.34	-	-	-	-	-	-	-	10.05 ± 0.90	-	-	-	-	9.68	-
Lignin-like (%TS)[2,3]	1.51 ± 0.02	-	-	-	-	-	-	-	2.19 ± 0.2	-	-	-	-	1.80	-
P (%)[2]	0.54 ± 0.03	-	0.49 ± 0.01	0.27 ± 0.01	0.35 ± 0.01	0.50	0.28	0.82	-	-	-	-	0.88	-	0.52 ± 0.08
Na (%)[2]	-	-	-	-	-	-	-	0.84 ± 0.05	-	0.81	3.45 ± 0.20	3.45 ± 0.20	2.24	-	-
K (%)[2]	1.43 ± 0.08	-	1.23 ± 0.01	1.00 ± 0.02	1.00 ± 0.01	-	-	0.30	-	0.29	2.30 ± 0.04	2.30 ± 0.04	-	-	0.90 ± 0.11
Ca (%)[2]	-	-	-	-	-	-	0.12	0.07	-	-	0.40 ± 0.01	0.03 ± 0.01	2.44	-	2.16 ± 0.29
Mg (%)[2]	-	-	-	-	-	-	0.08	0.03	-	0.08	0.16 ± 0.01	0.16 ± 0.01	-	-	0.14 ± 0.01
S (ppm)[1]	356.10 ± 23.74	-	497.70 ± 0.00	-	-	-	-	597.30	975.00 ± 43.50	-	-	-	8.60	-	2508.00 ± 87.00

Reference	(Banks et al., 2012; Y. Zhang et al., 2012a)	(Yirong et al., 2015)	(VALORGAS, 2010; Yirong et al., 2015)	(VALORGAS, 2010; Yirong et al., 2015)	(VALORGAS, 2010; Yirong et al., 2015)	(VALORGAS, 2010)	(De Vrieze et al., 2013)	(Zhang et al., 2011)	(Wanqin Zhang et al., 2015)	(Wanli Zhang et al., 2015a)	(C. Zhang et al., 2013a)	(C. Zhang et al., 2013b)	(Li et al., 2009; C. Zhang et al., 2014)	(Zhou et al., 2014)	(R. Zhang et al., 2007)
Fe (ppm)[1]	-	21.05	35.08 ± 0.24	139.29 ± 8.67	427.98 ± 19.78	-	9.52	3.17	50.18 ± 3.20	38.91	100.00 ± 23.00	100.00 ± 23.00	-	-	766.00 ± 402.00
Cu (ppm)[1]	1.71 ± 0.19	-	-	-	-	-	2.06	3.06	-	1.86	-	-	-	-	31.00 ± 1.00
Zn (ppm)[1]	7.83 ± 2.61	-	-	-	-	-	4.83	8.27	-	13.03	160.00 ± 30.00	160.00 ± 30.00	-	-	76.00 ± 22.00
Al (ppm)[1]	-	-	-	-	-	-	-	4.31	-	-	-	-	-	-	1202.00 ± 396.00
Mn (ppm)[1]	20.30	21.76	23.15 ± 0.38	11.11 ± 0.05	23.24 ± 0.36	-	4.69	0.96	-	3.17	110.00 ± 95.00	110.00 ± 95.00	-	-	60.00 ± 30.00
Cr (ppm)[1]	6.88 ± 0.28	-	-	-	-	-	-	0.17	-	-	-	-	-	-	3.00 ± 1.00
Ni (ppm)[1]	1.66 ± 0.69	-	-	-	-	-	0.25	0.19	1.46 ± 0.18	3.55	-	-	-	-	2.00 ± 1.00
Co (ppm)[1]	< 0.06	0.02	0.02 ± 0.00	0.50 ± 0.05	1.30 ± 0.05	-	0.01	-	0.08 ± 0.01	0.04	-	-	-	-	-
Se (ppm)[1]	< 0.07	0.04	0.28 ± 0.14	-	-	-	-	-	0.13 ± 0.04	-	-	-	-	-	-
Mo (ppm)[1]	0.11 ± 0.01	0.09	0.26 ± 0.05	1.16 ± 0.11	2.39 ± 0.08	-	0.10	-	-	0.36	-	-	-	-	-
Cd (ppm)[1]	< 0.02	-	-	-	-	-	-	-	-	-	-	-	-	-	< 1.00
Pb (ppm)[1]	< 2.4	-	-	-	-	-	-	-	-	-	-	-	-	-	4.00 ± 3.00
Hg (ppm)[1]	< 0.0003	-	-	-	-	-	-	-	-	-	-	-	-	-	-
W (ppm)[1]	< 0.25	-	-	-	-	-	-	-	-	-	-	-	-	-	-

1. Wet basis
2. Dry basis
3. Calculated by Van Soest fractionation

1.2.1.3 Fundamentals of anaerobic processes

Anaerobic digestion is a multistage biological process that degrades organic matter to produce biogas and digestate in absence of oxygen for aerobic metabolism (Chynoweth et al., 2001; Kangle et al., 2010). Generally, this process is divided in four main steps: hydrolysis, acidogenesis, acetogenesis and methanogenesis (Appels et al., 2008). Figure 1.3 represents the different steps occurring in anaerobic degradation. During disintegration and hydrolysis, the complex organic material is converted into soluble monomers (*i.e.*, amino acids, monosaccharides and long chain fatty acids) by non-biological and enzymatic processes. Fermentation (namely acidogenesis) then takes place. In this step, these monomers are converted into simpler products, mainly VFAs, hydrogen and carbon dioxide. In complete AD, the compounds generated during acidogenesis are oxidized to produce acetate and hydrogen (acetogenesis step), outputs that are eventually consumed by anaerobic archaea to produce methane (methanogenesis).

However, depending on the operating conditions, methanogenesis (carried out by sensitive archaea) can be the limiting biological step, leading to the accumulation of intermediate compounds such as acetate, butyrate, propionate or hydrogen, which can further inhibit the process. When AD is stopped after fermentation, in a process named dark fermentation (DF), it can be efficiently used for biomass valorization by its conversion into hydrogen and VFAs. Moreover, the metabolic pathways can be driven to produce compounds other than methane or hydrogen, such as ethanol, caproate or lactate.

This review aims to summarize the state-of-the-art dealing with the treatment of food waste by anaerobic processes, *i.e.* single-stage anaerobic digestion, dark and acidogenic fermentations and 2-stage anaerobic digestion. Each process has been assessed in a separate section, describing the main complications associated with each option and the solutions that are being developed to overcome them. Recommendations for future research are also given in each section. Finally, the main energy and environmental factors as well as the current options for digestate management and the approach of biorefinery for FW valorization have been assessed.

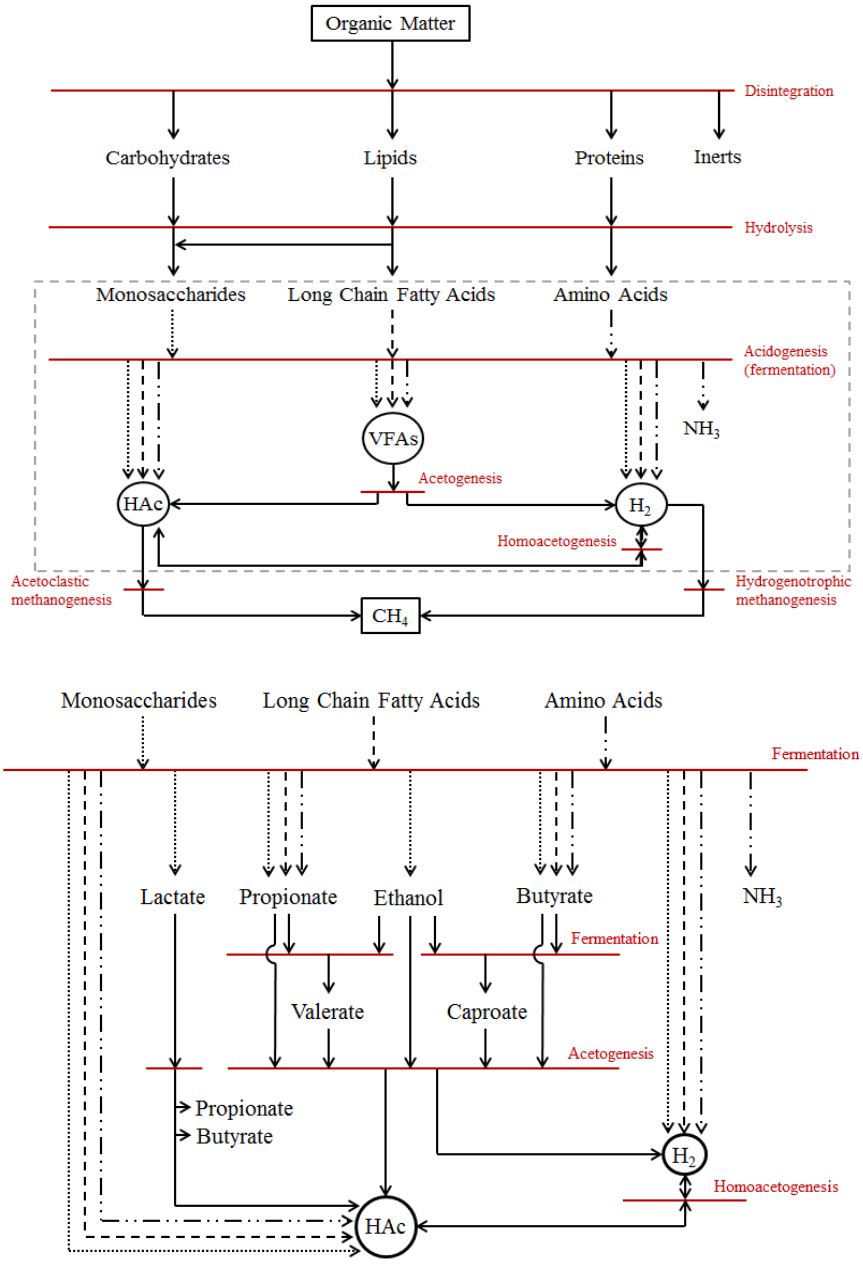

Figure 1.3. Different steps involved in anaerobic degradation of organic biomass. The figures represent the complete anaerobic digestion process (above) and a close-up of the metabolic pathways related to anaerobic fermentation (grey shaded region in A; below). HAc stands for acetic acid. Adapted from Batstone et al. (2002b), Dahiya et al. (2015), Ghimire et al. (2015a), Motte et al. (2013), Salminen and Rintala, (2002) and Yin et al. (2014)

1.2.2 *Single-stage anaerobic digestion of FW for methane production*

The first approach to be considered is the AD of FW for methane production. Single-stage mono-digestion of FW has been heavily studied, mainly due to its simplicity and economic viability when compared to other processes. Many authors have studied the feasibility of this process by determining the biochemical methane potentials (BMPs) of FW (Table 1.3). These values are higher than those reported for other common substrates, such as waste activated

sludge (WAS) (157 ml $CH_4 \cdot g\ VS^{-1}$) (X. Liu et al., 2012), dairy manure (243 ml $CH_4 \cdot g\ VS^{-1}$) (Labatut et al., 2011), or wheat straw (233 ml $CH_4 \cdot g\ VS^{-1}$) (Ferreira et al., 2014). This suggests that FW can be an excellent substrate for AD. In addition, a recent study evaluated the variability of FW characteristics and its influence on its BMP (Fisgativa et al., 2016). They concluded that, even if FW features can depend on the geographical origin, the type of collection and the season, the biochemical methane potentials did not vary significantly (~460 ml $CH_4 \cdot g\ VS^{-1}$).

Table 1.3. Various biochemical methane potentials (BMPs) of FW reported in the literature

Country	FW Origin	BMP (ml $CH_4 \cdot g\ VS^{-1}$)	Reference
Italy	Synthetic FW	648 ± 11 - 402	(Ariunbaatar et al., 2014)
Italy	SS-FW[1]	338 - 566	(Facchin et al., 2013)
UK	SS-FW[1]	445 ± 4 - 456 ± 7	(Y. Zhang et al., 2012b)
Ireland	University restaurant	467 - 529	(Browne and Murphy, 2013)
Korea	Bibimbab (Korean FW)	472	(Cho et al., 1995)
Korea	FW leachate	≤ 478	(Lee et al., 2009)
Korea	University restaurant	480 ± 21	(Zhang et al., 2011)
Singapore	University restaurant	410 ± 14	(Rajagopal et al., 2013a)
China	University restaurant	260	(Yong et al., 2015)
China	Restaurant	480	(Wanqin Zhang et al., 2015)
Canada	Synthetic FW	210 ± 6 - 340 ± 1	(Marin et al., 2010)

1. Source segregated food waste

However, this process is not without operational challenges. Two main problems have been identified when considering FW as mono-substrate: its high biodegradation rate and its low C/N ratio (Jabeen et al., 2015; Shen et al., 2013). The rapid biodegradation of FW leads to an imbalance in the production-consumption of VFAs, overwhelming the methanogenic archaea and eventually leading to the failure of the process due to VFA accumulation and decrease in the pH. Alternatively, the high protein content of FW causes a reduction of the C/N ratio of this substrate (Table 1.2), with values far from the ratio of 25, generally considered as optimal (Mao et al., 2015). As shown in Figure 1.3, the organic N present in the organic biomass is reduced to ammonia nitrogen during the degradation of organic compounds, a well-known inhibitor of AD in its free form (FAN) NH_3 (Rajagopal et al., 2013b). If this compound is accumulated in the system, it may eventually cause VFA accumulation due to inhibition of methanogens, especially the acetoclastic, which are more

sensitive to FAN than bacteria. Because of these problems, many authors have reported unsuccessful AD of FW due to VFA accumulation (Bouallagui, 2003; Climenhaga and Banks, 2008; Ghanem et al., 2001; Izumi et al., 2010; Ma et al., 2011; Nand et al., 1991; Qiang et al., 2013, 2012; Ranade et al., 1987; Tampio et al., 2014; Wei et al., 2014; Yirong et al., 2015; Zhang and Jahng, 2012; Y. Zhang et al., 2012b; Zhou et al., 2011).

This potential process failure can however be avoided by several means. Some studies have conducted continuous methane production even if high concentrations of VFAs and total ammonia nitrogen (TAN) were present in the reactors (Banks et al., 2012, 2008; Banks et al., 2011a; Climenhaga and Banks, 2008). In fact, this continuous operation was possible due to the accumulation of TAN in the system, which acted as buffer for the VFAs, avoiding a sudden decrease in the pH. Although this "inhibited-steady state" allowed a continuous operation, decreases in the methane yields and unstable performances have been reported. Another solution is the reduction of the organic loading rate (OLR) (or the substrate to inoculum ratio, S/X ratio, under batch conditions) to limit the acidification effect (Banks et al., 2012; Bouallagui, 2003; Climenhaga and Banks, 2008; Ghanem et al., 2001; Kawai et al., 2014; Ma et al., 2011; Nagao et al., 2012; Nand et al., 1991; Neves et al., 2004; Ranade et al., 1987; Tampio et al., 2014; Zhou et al., 2011). However, the volumetric methane production rate is jeopardized (*e.g.*, from 0.4 to 2.7 $l \cdot l^{-1} \cdot d^{-1}$ at OLRs of 1.0 and 5.5 g $VS \cdot l^{-1} \cdot d^{-1}$, respectively (Wanqin Zhang et al., 2015)) and for a given amount of treated FW, the reactor size can increase enormously. Other alternatives used to achieve stable FW mono-digestion have been reported in the literature: co-digestion with suitable co-substrates, side ammonia stripping (Serna-Maza et al., 2015, 2014), buffer addition (Latif et al., 2012), pH adjustment (Ma et al., 2011), TEs supply (Banks et al., 2012; Climenhaga and Banks, 2008; Facchin et al., 2013; Feng et al., 2010; Qiang et al., 2013, 2012; Tampio et al., 2014; Wei et al., 2014; Yirong et al., 2015; L. Zhang et al., 2012; Zhang and Jahng, 2012; Wanqin Zhang et al., 2015), utilization of granular sludge (Neves et al., 2008, 2004), digestate recirculation (Nagao et al., 2012) or uncoupling solid retention time (SRT) from hydraulic retention time (HRT). All these alternatives are further discussed below. Because of its wide application, anaerobic co-digestion (AcoD) of FW is discussed in a separate section.

1.2.2.1 Main options for efficient FW mono-digestion

Table 1.4 summarizes some of the main results found in the bibliography dealing with stabilization of FW mono-digestion for methane production.

Table 1.4. Some of the main results of FW mono-digestion for methane production presented in the literature

FW origin	Reactor Type	Scale (l)	S/X (VS/VS)	HRT (d)	T (ºC)	OLR (g $VS \cdot l^{-1} \cdot d^{-1}$)	MY (ml $CH_4 \cdot g\ VS^{-1}$)	VMPR ($l \cdot l^{-1} \cdot d^{-1}$)	VS reduction (%)	TAN[14] ($mg \cdot l^{-1}$)	VFAs[15] (mg $COD \cdot l^{-1}$)	Stabilization	Reference
Synthetic	Batch	1.0	0.5	-	32-34	-	647-402	-	nr	-	-	BMP conditions[11]	(Ariunbaatar et al., 2014)
Synthetic	Batch	0.12	9.2-6.1	-	33	-	340-210	-	nr	-	-	BMP conditions[11]	(Marin et al., 2010)
Synthetic	Batch	1.2	nr	-	37	-	375-470[3]	-	nr	-	-	FW pretreatment	(Izumi et al., 2010)
Synthetic	Batch	0.15, 1.5	2.0	-	35	-	340-495	-	-	-	≤ 21000	Zero-valent iron addition	(Kong et al., 2016a)
Synthetic, restaurant	Batch	0.16	1.3	-	37	-	360-430	-	94.0-99.6	-	-	Granular sludge, buffer addition	(Neves et al., 2008)
University restaurant	Batch	0.5-5.0	0.3	-	35	-	467-529	-	nr	-	-	BMP conditions[11]	(Browne and Murphy, 2013)
Restaurant, Household	Batch	0.5	0.3	-	35	-	378, 316	-	nr	-	-	Low S/X	(Lü et al., 2015)
Cafeteria	Batch	1.0	0.7	-	35	-	≤ 314.7	-	nr	620-4670	-	Nitrification for N removal	(Sheng et al., 2013)
Supermarket	Batch	1.0	47.6-0.9	-	35	-	0-445	-	nr	-	-	Spatial separation inoculum-waste	(Lü et al., 2012)
Management company	Batch	0.5	1.8, 2.7	-	50	-	425, 445	-	81	-	-	-	(R. Zhang et al., 2007)
Management company	Batch	1.2	0.3-4.0	-	37	-	435-318	-	nr	-	-	Low S/X	(Kawai et al., 2014)
SS-FW	Batch	nr	0.3-0.4	-	37	-	338-566	-	nr	-	-	TEs addition	(Facchin et al., 2013)
FW leachate	Batch	0.5	0.1	-	25-55	-	516-275	-	nr	-	-	BMP conditions[11]	(Lee et al., 2009)
Hydrolyzed FW	Batch	nr	0.6	-	35	-	198-468	-	≤ 80.4	-	-	FW pretreatment (pH control)	(Kiran et al., 2015)
Canteen	Batch, semicontinuous	0.8	nr	31.2-3.5	35	3.0-16.0	659-518, 390-450	nr	nr	135-735	2700-15400	Separation solid and liquid fractions, OLR	(C. Zhang et al., 2013a)
Source Sorted	Semicontinuous	35	-	30[1]	36	2.0	425	nr	83.9	≤ 2500	≤ 16000	Sludge recirculation. Unstable digestion	(Y. Zhang et al., 2012b)
Source Sorted	Semicontinuous	4.0	-	nr	35, 55	2.0	470-450	nr	nr	1500-4200	0, >1000	TEs addition	(Yirong et al., 2013)
Source Sorted	Semicontinuous	11.0	-	78-47	37	3.0-4.0	552-392	nr	nr	nr	nr	TEs addition	(Blasco et al., 2014)
Source Sorted	Semicontinuous + stripping	35.0	-	107	36	2.0[5]	487-476	nr	82.3-83.8	1000-5100[6]	260-290	TEs addition, side stripping	(Serna-Maza et al., 2014)
Source Sorted	Semicontinuous + stripping	75.0	-	115.5	36	2.0[5]	434-492	nr	84	4907-4808[6]	152-143	TEs addition, side stripping	(Serna-Maza et al., 2015)

FW origin	Reactor Type	Scale (l)	S/X (VS/VS)	HRT (d)	T (ºC)	OLR (g $VS \cdot l^{-1} \cdot d^{-1}$)	MY (ml $CH_4 \cdot g\ VS^{-1}$)	VMPR ($l \cdot l^{-1} \cdot d^{-1}$)	VS reduction (%)	TAN[14] ($mg \cdot l^{-1}$)	VFAs[15] (mg $COD \cdot l^{-1}$)	Stabilization	Reference
University restaurant	Semicontinuous	4.5	-	40	37	1.0-5.0	≤ 550	≤ 2.7	nr	≤ 2250	≤ 30000	TEs addition, OLR	(Wei et al., 2014)
University restaurant	Semicontinuous	0.15	-	20-30	37	2.2-6.6	352-450	nr	nr	1265-2758	471-10481	TEs addition	(Zhang and Jahng, 2012)
University restaurant	Batch, Semicontinuous	0.3	2.3	30-15	37	2.0-6.0	504-372	nr	69.5-78.4	nr	< 2000	TEs addition	(Wanli Zhang et al., 2015b)
University restaurant	Continuous	5.0	-	25-180	nr	1.5	300-650	nr	nr	>5700	>15000	TEs addition, HRT	(Climenhaga and Banks, 2008)
Restaurant	Semicontinuous	4.5	-	40	37	1.0-5.5	106-491	0.4-2.7	nr	nr	1200-35000	TEs addition, OLR	(Wanqin Zhang et al., 2015)
Supermarket, catering facilities	Semicontinuous	106	-	29	38	2.8	560[13]	nr	nr	1800-1900	10707	Substrate pH control, TEs addition	(Bajón Fernández et al., 2015)
Management company	Semicontinuous	3.0	-	8, 16, 60[1]	37	3.7-12.9	417-455	2.7-6.6	84.4-92.5	nr	≤ 19210	HRT, OLR, sludge recirculation	(Nagao et al., 2012)
Domestic	Semicontinuous	4.0	-	nr	55	2.0-4.0	430	nr	nr	5000-6000	10000-35000	TEs addition	(Yirong et al., 2015)
Domestic	Semicontinuous	11	-	117-31	37	2.0-6.0	483-373	nr	80.6-63.0	1200-4200[4]	90-267	TEs addition, OLR	(Tampio et al., 2014)
Domestic	Semicontinuous	4.0	-	95-38	36	2.0-5.0	700-750[2]	1.5-3.8[2]	nr	5000-6000	500-30000	TEs addition	(Banks et al., 2012)
Pasteurized FW	Semicontinuous	6	-	20-60	37, 55	1.0-3.0	401-480	nr	-	1109-2258	300-7000	Sludge recirculation	(Zamanzadeh et al., 2016)
Synthetic	Batch, CSTR	0.08, 10	nr	100-30	35	1.9-6.3[7]	~400	nr	78.0	1100	0-5000	TEs addition	(Qiang et al., 2012)
Synthetic	CSTR	12	-	100-30	55	1.9-6.3[7]	430-475	nr	72.0-80.0	≤ 1127	≤ 3800	TEs addition, HRT, Alternate feeding	(Qiang et al., 2013)
Domestic	Industrial plant	900000	-	80	42	2.5	402	1.0	nr	≤ 5000	≤ 15000	Inhibited steady state	(Banks et al., 2011a)
Domestic	Pilot plant	1500	-	31.5-20	36, 56	4.1-5.7	390, 410	nr	67.0, 70.0	≤ 5200	7000-45000	Inhibited steady state	(Banks et al., 2008)
University restaurant	Anaerobic baffled reactor	53.5	-	30	35	0.5-1.0	215.57[12]	nr	86.4	nr	nr	Phase separation	(Ahamed et al., 2015)
Liquidized FW	UASB	2.0	-	10-4	30-55	2.0-12.5[7]	0.29-0.91[9]	nr	≤ 93.7[8]	nr	3600-9000	Buffer addition	(Latif et al., 2012)

1. Solids retention time
2. Biogas
3. ml biogas·g $CODtotal^{-1}$
4. $mg \cdot kg^{-1}$
5. g $VS \cdot kg^{-1} \cdot d^{-1}$
6. Concentrations per kg
7. g $COD \cdot l^{-1} \cdot d^{-1}$
8. % COD
9. l·g COD $removed^{-1} \cdot d^{-1}$
10. Nominal retention time (based on FW volume)
11. Standard conditions for BMP determination: buffer addition and TEs supplementation
12. ml biogas·g VS $removed^{-1} \cdot d^{-1}$
13. ml $CH_4 \cdot g\ VS^{-1} \cdot d^{-1}$
14. When values of TAN were not reported, the values refer to NH_4^+-N
15. When the units were not specified, the concentrations were assumed to be expressed in COD

nr stands for "non-reported"

1.2.2.1.1 Batch experiments

Starting with the experiments carried out in batch conditions, the first point to mention is the high variability between the methane yields obtained. The first explanation is the inherent variability of the FW according to its origin. As presented in Table 1.2, the characteristics of this waste vary widely worldwide and depending on the source. Secondly, the previous adaptation of the inoculum plays a major role when digesting FW, even for BMP determination (Browne and Murphy, 2013; Kong et al., 2016b). Due to the risk of VFA and TAN accumulation when treating this waste, the tolerance of the initial bacterial community to these compounds has a critical importance. Particularly, the ratio of archaea hydrogenotrophs/acetotrophs in the inoculum may play a major role, as the first group is known to be more resistant to inhibition (De Vrieze et al., 2012). This could explain why some authors have achieved efficient methane production at relatively high S/X ratios (>1.77 VS/VS) (R. Zhang et al., 2007) and others needed low values (<0.5) to avoid inhibition (Kawai et al., 2014; Lü et al., 2015). Lü et al. (2012) did not achieve an efficient digestion even at low S/X ratios due to initial VFA accumulation. To avoid this problem, they proposed a new inoculation strategy, separating the inoculum and the waste in different reactors and adding the substrate gradually. They obtained methane yields up to 445 ml $CH_4 \cdot g\ VS^{-1}$. Other strategies have been applied to stabilize the process, such as addition of TEs (Facchin et al., 2013), nitrification for N removal (Sheng et al., 2013), addition of zero-valent iron (Kong et al., 2016a) or use of granular sludge (Neves et al., 2008). Besides all these alternatives, a low S/X ratio (≤0.5) is recommended when digesting FW without buffer addition to avoid inhibition by initial VFA peaks. However, as the initial FW concentration also plays a major role in acidification of AD under batch conditions, this parameter must be carefully selected to avoid inhibition.

1.2.2.1.2 Continuous and semi-continuous experiments

Concerning continuous and semi-continuous operations, equivalent strategies have been evaluated, such as avoiding reactor overloading by OLR and HRT control or stabilization of the digestion by TEs supplementation. The instability of continuous mono-AD of FW has been reported by several authors (Ma et al., 2011; Mata-Alvarez et al., 1992; Nand et al., 1991). Banks et al. (2008, 2011a) showed efficient digestion performances at OLRs of 5.72 and 2.50 g $VS \cdot l^{-1} \cdot d^{-1}$, but with high VFAs and TAN concentrations, suggesting a process prone to failure and with lower methane yields than other options. This corresponds to the

aforementioned “inhibited-steady state”, in which the high VFA concentrations are buffered with the also high TAN concentrations, avoiding a pH drop.

Lately, several studies have been directed towards the addition of TEs to stabilize the digestion. Failure of FW digestion without supplementation of these microelements is indeed prone to occur, whereas the process are stable when adding them, even at high OLRs (Climenhaga and Banks, 2008; Wei et al., 2014; L. Zhang et al., 2012; Zhang and Jahng, 2012; Wanqin Zhang et al., 2015). Banks et al. (2012) avoided VFAs accumulation with OLRs up to 8 g $VS \cdot l^{-1} \cdot d^{-1}$ by adding TEs, in the form of a solution containing Iron, Cobalt, Molybdenum, Nickel, Selenium, Tungsten, Aluminium, Bore, Zinc, Copper and Manganese. Alternatively, without metals, the VFA concentrations continually increased at loads of 2 g $VS \cdot l^{-1} \cdot d^{-1}$ and the process failed at 3 g $VS \cdot l^{-1} \cdot d^{-1}$. Their results suggest that, at the high TAN concentrations associated with FW AD, syntrophic acetate oxidation and hydrogenotrophic methanogenesis are predominant pathways for methane production (Banks et al., 2012). This is in agreement with the greater resistance of hydrogenotrophic methanogens to high TAN and VFAs concentrations. Therefore, due to the synthesis of the enzymes required for syntrophic hydrogenotrophic methanogenesis (particularly for formate oxidation), there is a lack of TEs that leads to an initial accumulation of propionate, followed by a pH drop and then by failure of the process. They concluded also that Selenium and Cobalt were essential elements to avoid acidification of the system. Other authors suggested the importance of Iron, Cobalt and Nickel as TEs used for bacterial growth. As an example, Qiang et al. (2012, 2013) achieved stable digestion and even recovered an acidified reactor by adding these elements. They also optimized the TEs requirements for thermophilic (276, 4.96 and 4.43 $mg \cdot kg^{-1}$ COD-removed for Iron, Cobalt and Nickel) and mesophilic conditions (200, 6.0 and 5.7 $mg \cdot kg^{-1}$ COD-removed for Iron, Cobalt and Nickel). Zhang and Jahng (2012) also avoided acidification (with OLRs up to 6.64 g $VS \cdot l^{-1} \cdot d^{-1}$) by TEs supplementation, adding Molybdenum as an essential TE and remarking the critical role of Iron. New research has tried to optimize the TEs dosage by integrating this option with other alternatives, such as FW pretreatment (autoclaving) (Tampio et al., 2014), ammonia stripping to reduce TAN concentrations below toxic levels (Serna-Maza et al., 2015, 2014) or addition of ethylenediamine-N,N'-disuccinic acid (EDDS) to improve the availability of metals, decreasing the TEs dosage required (*i.e.*, Iron, Cobalt, Molybdenum and Nickel by 50 %) (Wanli Zhang et al., 2015b).

A different promising approach to stabilize the process is uncoupling the HRT and the SRT, *e.g.* by solid digestate recirculation or applying membranes for biomass retention. This

allows to increase the biomass concentration in the reactor, retaining also the TEs linked mainly to the solid phase (C. Zhang et al., 2013a; Zhang et al., 2011), while increasing the C/N ratio by removing the soluble TAN from the liquid phase. Nagao et al. (2012) achieved a stable digestion at 9.2 g $VS \cdot l^{-1} \cdot d^{-1}$ by applying recirculation of the solid fraction of the digestate (after centrifugation). Also, (C. Zhang et al., 2013a) designed a Dual System, digesting separately the liquid and the solid fractions of FW in two different reactors. They achieved stable operations at OLRs of 6 and 8 g $VS \cdot l^{-1} \cdot d^{-1}$ in each reactor, respectively.

Considering the option of operating at thermophilic conditions (~ 55 °C °C), research has shown that when increasing the temperature, the proportion of FAN also increases and, as FAN is the most toxic form of ammonia, this can compromise the process (Chen et al., 2008). Several authors have reported a more unstable process (and even process failure at low OLRs) at thermophilic conditions when compared to mesophilic when digesting FW, even with TEs supplementation (Banks et al., 2008; Latif et al., 2012; Yirong et al., 2015, 2013; Zamanzadeh et al., 2016).

1.2.2.2 Anaerobic co-digestion (AcoD) of FW

AcoD can be defined as the simultaneous digestion of two or more organic substrates (Kangle et al., 2010). This process is a feasible option to overcome the aforementioned issues, improving the economic viability of AD plants by treating two or more wastes simultaneously and increasing at the same time the methane production. By mixing substrates, AcoD leads to positive interactions, such as macro- and micro-nutrients balance, adjustment of the moisture content or dilution of inhibitory compounds (Mata-Alvarez et al., 2014). These benefits can induce synergetic effects, *e.g.* by avoiding microbial inhibition and process instabilities, which may increase the global methane production, *e.g.* by allowing the application of greater OLRs in the reactors. Because higher OLRs lead to greater volumetric methane production rates (VMPRs), currently the operational OLR together with waste transportation costs are the main factors to be considered in industrial AD (Mata-Alvarez et al., 2014).

As shown in Table 1.5, several co-substrates have been applied to stabilize FW AD, *e.g.* by nutrient balance, TEs supplementation, dilution of inhibitors or by increasing the buffer capacity of the system. These positive effects have been proved by many experiments, in which, where the mono-digestion systems failed, co-digestion showed stable and efficient performances even at higher loads of substrate (Carucci et al., 2005; Dai et al., 2013; Drennan and DiStefano, 2014; El-Mashad et al., 2008; Liao et al., 2014; Lin et al., 2011; Owamah and Izinyon, 2015; Ye et al., 2013; Wanli Zhang et al., 2015a; Y. Zhang et al., 2012a).

Separating the experiments by co-substrate digested, sludge (sewage, waste activated or dewatered sludge) has been used for nutrient balance (C/N ratio adjustment), for supplying TEs and for increasing the buffering capacity of the system. (H.-W. Kim et al., 2011) achieved stable digestion at high OLRs using a Temperature Phased Anaerobic Sequencing Batch Reactor system (TPASBR), digesting a mixture of 40:60 FW:Sludge (g VS:g VS). Heo et al. (2003) obtained similar optimal co-digestion proportions (50:50), without observing signs of VFA accumulation at OLRs up to 3.2 g $VS \cdot l^{-1} \cdot d^{-1}$. De Vrieze et al. (2013) used sludge as source of Iron for the digestion, obtaining VMPRs up to 1.15 $l \cdot l^{-1} \cdot d^{-1}$ in mesophilic conditions. Even if higher residual VFAs concentrations have been found in thermophilic conditions, this process was stable. Gou et al. (2014) found even greater methane yields at 55 °C than at 35 °C using WAS as co-substrate in proportions 1:2. They obtained efficient digestions until OLRs of 5 and 7 g $VS \cdot l^{-1} \cdot d^{-1}$ for mesophilic and thermophilic conditions, respectively.

The application of manure as co-substrate has been mainly used to increase the buffering capacity of the digester. In all the cases shown in Table 1.5, AcoD showed better performances than mono-digestion. Only (M. Wang et al., 2014) faced TAN build-up in all their reactors, concluding that the N content of chicken manure was too high to be used as co-substrate for FW. In contrast, C. Zhang et al. (2013b) found an optimal co-digestion ratio of 2:1 FW:Cattle Manure (g VS:g VS) and achieved a stable process at a load of 10 g $VS_{FW} \cdot l^{-1} \cdot d^{-1}$. Agyeman and Tao (2014) obtained high methane yields at an optimal OLR of 2 g $VS \cdot l^{-1} \cdot d^{-1}$ and El-Mashad et al. (2008) achieved also stable methane productions at 4 g $VS \cdot l^{-1} \cdot d^{-1}$. It must be pointed out that manure as co-substrate creates a system similar to the “inhibited steady state” explained in the previous section. Thus, in this case special attention must be paid to the TAN concentrations in the reactors to prevent inhibition.

Table 1.5. Some of the main results of FW co-digestion for methane production presented in the literature

FW origin	Co-substrate	Aim	Co-digestion ratio (g VS:g VS)	Reactor Type	Scale (l)	S/X (VS/VS)	HRT (d)	T (ºC)	OLR (g $VS \cdot l^{-1} \cdot d^{-1}$)	MY (ml $CH_4 \cdot g\ VS^{-1}$)	VMPR ($l \cdot l^{-1} \cdot d^{-1}$)	VS reduction (%)	TAN[16] ($mg \cdot l^{-1}$)	VFAs[17] (mg $COD \cdot l^{-1}$)	Reference
Restaurant	Sewage sludge	Nutrient balance	2:1-1:2[3]	BMP	0.4, 1.8	5.0	-	37	-	71-290	nr	25-61	750-2010	-	(J. Zhang et al., 2015)
University restaurant	Sewage sludge	Nutrient balance	1:1, 6:1, 10:1[2]	Semicontinuous	1975.0	-	27, 22, 19	35	7.9, 10.8, 14.0[6]	237-457[9]	nr	44-69	nr	2734-3545	(Ratanatamskul et al., 2014)
Restaurant	Sewage sludge	Nutrient balance, dilution inhibitors	40:60	TPASBR[14]	8.0	-	8, 7	35, 55	3.5, 6.1	180, 200	0.69, 1.24	42, 45	nr	nr	(H.-W. Kim et al., 2011)
Sanitized, no-lipids	Sludge	Add recalcitrant TS, nutrient balance	95:5-70:30[2]	Batch	0.4	0.5	-	38	-	350-330	-	nr	nr	nr	(Koch et al., 2016)
University restaurant	Sludge	Dilution inhibitors	77.8:22.2-59:41	Batch, sequencing	0.2, 1.2	nr	56-26, 31	35	2.0-4.1, 3.5	< 90	nr	nr	nr	nr	(Carucci et al., 2005)
University restaurant	Waste Activated Sludge	Adjust C/N ratio	1:2	Semicontinuous	2.0	-	33.3-4.2	35, 45, 55	1.0-8.0	400-0	2.10-0	75-0	nr	0-4000	(Gou et al., 2014)
Bibimbab	Waste Activated Sludge	Adjust C/N ratio, buffer capacity	10:90, 30:70, 50:50	Semicontinuous	3.5	-	10, 13, 16, 20	35	1.3-3.2	192-375	nr	34-56	680-1160	0	(Heo et al., 2003)
University restaurant	Waste Activated sludge	Fe supply	1:0-0:1	Semicontinuous	0.8	-	20	34, 54	1.2-3.1	nr	0.15-1.15	82-50	nr	< 2070	(De Vrieze et al., 2013)
Chinese cafeterias	Dewatered Sludge	Dilution inhibitors	1:0-0:1	Semicontinuous	6.0	-	8-30[5]	35	4.0-21.8	509-620	0.95-8.22	27-86	≤ 4100	≤ 1309	(Dai et al., 2013)
University restaurant	Sludge, grass clippings, garden waste	Adjust C/N ratio	67-45:10:16-32:7-13	BMP, semicontinuous	0.3, 7.5	0.5	30-10	Mesophilic, 55	0.6-7.8	433-315	0.89-2.77	nr	1724-1517	60-590	(Fitamo et al., 2016)
University restaurant	Cattle manure	Buffering capacity, nutrient balance	1:1	Batch	1.0	1.0, 2.0	-	35	-	299-458	nr	53-78	nr	nr	(Li et al., 2009)
University restaurant	Cattle manure	Buffering capacity, nutrient balance	2, 3, 4	Batch, semicontinuous	0.8	nr		35	8.0-18.0	388-410, 347-388[10]	nr	nr	487-677	nr	(C. Zhang et al., 2013b)
University restaurant	Cattle manure, Sewage sludge	Improve MY	2:7:1, 1:7:2[2]	Semicontinuous	5.0	-	22, 20, 18	36, 55	1.2-1.5	616-329	0.75-0.49	60-53	940-570[8]	140-790	(Marañón et al., 2012)
Restaurant	Cattle manure	Nutrient balance	1	Semicontinuous	1.8	-	160-54	36	0.7-3.0	630-470	1.53-1.40	83-67	3090-3420	nr	(Agyeman and Tao, 2014)

FW origin	Co-substrate	Aim	Co-digestion ratio (g VS:g VS)	Reactor Type	Scale (l)	S/X (VS/VS)	HRT (d)	T (ºC)	OLR (g $VS \cdot l^{-1} \cdot d^{-1}$)	MY (ml $CH_4 \cdot g\ VS^{-1}$)	VMPR ($l \cdot l^{-1} \cdot d^{-1}$)	VS reduction (%)	TAN[16] ($mg \cdot l^{-1}$)	VFAs[17] (mg $COD \cdot l^{-1}$)	Reference
Restaurant FW	Dairy manure	Buffering capacity	1:0, 32:68, 48:52, 0:1	Semicontinuous	18.5	-	20	35	2.0, 4.0	120-320	1.12-0.23	46-62	nr	914-6778	(El-Mashad et al., 2008)
University restaurant	Cow manure, fat (intermittent)	Improve MY	1:1[3]	Semicontinuous	5.0	-	15	37	4.6[6]	210-260	nr	64-66	nr	< 1400[1]	(Neves et al., 2009)
University restaurant	Pig Manure, Rice straw	Adjust C/N ratio	0.4:1.6:1-2:0:1	Batch	2.0	3.0		37	-	3-384	nr	52-56	nr	0-30000	(Ye et al., 2013)
Restaurant	Chicken Manure	Buffering capacity, nutrient balance	1:1, 2:1	Semicontinuous	3.5	-	100-25	35	2.6-0.9	653-493	1.28-0.48	nr	3200-1900	nr	(M. Wang et al., 2014)
Domestic	Cattle slurry, Card packaging	Adjust C/N ratio, supply TEs	1:4-3:4, 5:5	Semicontinuous	4, 75	-	30[5]	36	2.0-4.0	50-400	0.43-1.23	nr	800-5000	0-3000	(Y. Zhang et al., 2012a)
University restaurant	Paper waste, Livestock waste	Adjust C/N ratio	7:3[2]	Semicontinuous	40.0	-	30-100	35	2.0-10.0[7]	250, 260[11]	2.70, 0.92	80, 72	nr, < 8000	< 1800, nr	(Kim and Oh, 2011)
Restaurant	Paper water, Plastic	Simulate OFMSW	1:2:1, 2:1:1[3]	Batch	1.5, 500.0	2.0		38	-	592, 370	0.55-2.60	69	890-1207	0	(Wan et al., 2013)
University restaurant	Paper waste lime mud	Buffering capacity, nutrient balance	50:1-50:7	Batch	0.5	4.4		37		167-273	nr	< 45	200-375	4500-0	(J. Zhang et al., 2014)
Grocery stores	Yard waste	System stability, increase TS %	0:1, 1:9, 2:8	Batch	1.0	1.0, 2.0, 3.0	-	36	-	0-120	nr	20-43	nr	nr	(Brown and Li, 2013)
Restaurant	Green waste	System stability, increase TS %	1:0-0:1	Batch	0.5	1.0	-	37	-	410-271	1.00-4.00	40-50	< 4243	nr	(X. Chen et al., 2014)
University restaurant	Tall fescue	Adjust C/N ratio	8.9-0.7	Batch, semicontinuous	1.0, 2.0	nr	nr	37	5.7-28.5	≤ 296	≤ 3.50	3-80	nr	nr	(G. Chen et al., 2016)
Restaurant	Landscape waste	Adjust C/N ratio, increase TS %	until 20% TS in reactors	Semicontinuous	260.0-280.0	-	25-175[5]	35	2.0-15.0[6]	229-272	0.46	nr	≤ 7010	512-25700[1]	(Drennan and DiStefano, 2014)
University restaurant	Rice husks	Adjust C/N ratio	10.5:1, 1.3:1, 0.5:1, 0.2:1	Batch	1.0	0.25, 0.5, 1, 1.5, 2	-	37	-	584-71	nr	78-24	nr	594	(Haider et al., 2015)
University restaurant	Rice husks	Adjust C/N ratio	1:2	Continuous plug flow	80.0	-	26, 25, 14	37	5.0, 6.0, 9.0	446, 399, 215	2.23, 2.36, 1.89	82, 73, 35	nr	1935, 2413, 8344	(Jabeen et al., 2015)
Restaurant	Olive husks	Adjust C/N ratio	1:0, 1:1	BMPs	0.3	0.6	-	37	-	339-505	nr	33-53	< 2000	nr	(Pagliaccia et al., 2016)

FW origin	Co-substrate	Aim	Co-digestion ratio (g VS:g VS)	Reactor Type	Scale (l)	S/X (VS/VS)	HRT (d)	T (ºC)	OLR (g $VS \cdot l^{-1} \cdot d^{-1}$)	MY (ml $CH_4 \cdot g\ VS^{-1}$)	VMPR ($l \cdot l^{-1} \cdot d^{-1}$)	VS reduction (%)	TAN[16] ($mg \cdot l^{-1}$)	VFAs[17] (mg $COD \cdot l^{-1}$)	Reference
University restaurant	Maize husks	Adjust C/N ratio	6.41:1	Continuous	nr	-	68-15	37	1.0-4.5	400-482	nr	81-74	300-1300	500-400	(Owamah and Izinyon, 2015)
University restaurant	Straw	Adjust C/N ratio	1:4-8:1[2]	Batch	1.0	0.8	-	35	-	157-392	nr	nr	nr	75-126	(Yong et al., 2015)
University restaurant	Distiller's grains	Buffering capacity	1:10, 1:8, 1:6, 1:4[3]	Batch	0.5	2.2	-	Mesophilic	-	108-160[12]	nr	nr	1300-1800	< 5000	(Wang et al., 2012)
University restaurant	Brown water	Buffering capacity	75g:1L	Batch	0.2	2.0	-	35	-	318-233	nr	nr	nr	nr	(Lim and Wang, 2013)
University restaurant	Brown water	Buffering capacity	75g:1 L	BMP, sequential	0.4, 5.3	nr	16-20	33	1.0-3.0	540-590, 210-460	nr	64-76	nr	< 2500[1]	(Rajagopal et al., 2013a)
University restaurant	Pretreated wastewater	Increase biogas productivity	0~0.5[4]	Continuous AnMBR[15]	2100	-	40-70[5]	25-29	0.5-1.0[6]	45-202[13]	0.02-0.19	nr	nr	nr	(Pretel et al., 2016)
University restaurant	FVW	Buffering capacity	1:1, 2:1, 1:2	BMP, semicontinuous	4.0	nr	nr	35	3.0	560, 0.06-490	0.19-1.50	≤ 75	647-2359	70-8887	(Lin et al., 2011)
University restaurant	Floatable FW oil	Stabilize digestion	1:0 - 1:5	Batch	0.25	0.5-3	-	35	-	697-926	nr	88-91	1405-1320	0-6492	(Meng et al., 2015)
University restaurant	Landfill leachate	Buffering capacity	40gTS:0mL - 40gTS:852mL	Batch	1.5	nr	-	35	-	1-466	nr	nr	600-2813	2000-11000	(Liao et al., 2014)
University restaurant	Piggery wastewater	Supply TEs	1:0-8.3:1.7[4]	Semicontinuous	0.2	-	20-40	37	2.6-4.9	0-600	0-1.75	nr	1000-3500	0-18000	(Zhang et al., 2011)
University restaurant	MSW incineration plant leachate	Supply TEs	1:0-7.7:2.3	BMP, semicontinuous	0.3	nr	20-15-10	37	4.0-6.0-8.3	480, 376-506	1.70-4.19	67-82	nr	0-9000	(Wanli Zhang et al., 2015a)
Synthetic	Seaweed Waste	Supply TEs	1:0-0:1[3]	Batch	0.1	1.0	-	36	-	184-252	nr	25-45	nr	nr	(Cogan and Antizar-Ladislao, 2016)

1. g $COD \cdot l^{-1}$
2. Wet weight ratio
3.TS ratio
4. COD ratio
5. Solid Retention Time
6. g $COD \cdot l^{-1} \cdot d^{-1}$
7. g $TS \cdot l^{-1} \cdot d^{-1}$
8. $mg \cdot kg^{-1}$
9. ml $CH_4 \cdot g\ VSremoved^{-1}$
10. ml $CH_4 \cdot g\ VS^{-1} \cdot d^{-1}$
11. ml $CH_4 \cdot g\ COD^{-1} \cdot d^{-1}$
12. ml $CH_4 \cdot g^{-1} \cdot d^{-1}$
13. ml $CH_4 \cdot g\ COD^{-1}$
14. Temperature Phased Anaerobic Sequential Batch Reactor (the commas separate the results at each temperature)
15. Anaerobic membrane bioreactor
16. When values of TAN were not reported, these concentrations refer to NH_4^+-N
17. When the units were not specified, the concentrations were assumed to be expressed in COD

nr stands for "non-reported"

Co-digesting substrates rich in lignocellulosic compounds with FW under continuous operation, Kim and Oh (2011) obtained promising results using paper waste as co-substrate. With a ratio 7:1 FW:paper (g TS:g TS), they achieved stable methane productions without significant VFA accumulations at OLRs up to 10 g $TS \cdot l^{-1} \cdot d^{-1}$. Similarly, Drennan and DiStefano (2014) achieved a stable process using landscape waste (green waste mainly composed of deciduous leaves) as co-substrate at an OLR of 2 g $COD \cdot l^{-1} \cdot d^{-1}$. However, the process was inhibited at 15 g $COD \cdot l^{-1} \cdot d^{-1}$. Long term operation at intermediate loads should be tested to optimize the process. Using rice husks, Jabeen et al. (2015) obtained high methane yields at OLRs of 5 and 6 g $VS \cdot l^{-1} \cdot d^{-1}$. Even if the concentrations of VFAs were over 2 $g \cdot l^{-1}$ in those conditions, the methane production was not inhibited until the load was raised to 9 g $VS \cdot l^{-1} \cdot d^{-1}$. Owamah and Izinyon (2015) also achieved a stable process, feeding 4.5 g $VS \cdot l^{-1} \cdot d^{-1}$ with maize husks as co-substrate (ratio 6.41:1 g VS:g VS). Recently, (G. Chen et al., 2016) applied OLRs up to 15.8 g $VS \cdot l^{-1} \cdot d^{-1}$ co-digesting FW and tall fescue (ratio of 1.52 g VS:g VS) without observing acidification and with a VMPR of 3.5 $l \cdot l^{-1} \cdot d^{-1}$. Also, Fitamo et al. (2016) achieved stable and efficient operation at HRTs as low as 15 d mixing FW with sludge, garden waste and grass clippings. All the substrates aforementioned, from paper waste to garden waste, are rich in lignocellulosic compounds and therefore allowed an increase of the applicable OLRs and improved the digestion stability by balancing the C/N ratio of the substrate (Brown and Li, 2013) and by increasing the buffering capacity. The contribution of these materials to the buffering capacity is linked to a reduction of the easily degradable fraction in the substrate (Motte et al., 2014a; Wang et al., 2012), slowing down the hydrolysis and avoiding accumulation of VFAs, and to a higher alkalinity of the substrate itself (Wang et al., 2012). Other organic wastes such as brown water or vegetable and fruit waste have efficiently stabilized the AD process at OLRs of 3 g $VS \cdot l^{-1} \cdot d^{-1}$ (Lin et al., 2011; Rajagopal et al., 2013a). Moreover, FW has also been applied to improve the biogas productivity when digesting pretreated urban wastewater. Using an Anaerobic Membrane Bioreactor (AnMBR), Pretel et al. (2016) increased the methane yields up to 167% by addition of FW when compared with monodigestion of wastewater.

Finally, as TEs are known to improve AD of FW (previous section), co-substrates rich in those elements have also been tested, avoiding the potential cost of adding a pure TEs solution. Zhang et al. (2011) used piggery wastewater, containing significant amounts of Zinc, Copper, Iron, Manganese, Magnesium and Aluminium, for this purpose. They obtained stable methane yields at OLRs up to 4.86 g $VS \cdot l^{-1} \cdot d^{-1}$. Also, they proved that the TEs remained mainly in the solid fraction of the wastewater and they were able to achieve high methane

yields at high OLRs using only the solid fraction as co-substrate. Using a similar approach, (Wanli Zhang et al., 2015a) applied the fresh leachate from the storage tank of a municipal solid waste incineration plant (containing Zinc, Copper, Iron, Manganese, Magnesium, Aluminium, Nickel, Molybdenum and Cobalt) as co-substrate. By its addition, they achieved stable methane productions at OLRs as high as 8.1 g $VS \cdot l^{-1} \cdot d^{-1}$ and even 8.3 g $VS \cdot l^{-1} \cdot d^{-1}$ (although the concentrations of VFAs were high; up to 9000 mg $COD \cdot g^{-1}$). They also managed to recover an acidified reactor by adding this co-substrate. (Y. Zhang et al., 2012a) co-digested FW with cattle slurry (for TEs addition) and card packaging (to increase the C/N ratio). This allowed an increase of the OLR up to 4 g $VS \cdot l^{-1} \cdot d^{-1}$. Lately, Cogan and Antizar-Ladislao (2016) have also proved the feasibility of FW co-digestion with seaweed as substrate for TEs supplementation.

1.2.2.3 Towards the optimization of FW anaerobic digestion for methane production

To synthetize the information presented above and to extract concise conclusions about the allowable OLRs, a graphical summary of the data is shown in Figure 1.4. This figure presents the methane yields and the corresponding VFAs concentrations at different OLRs. To verify the positive effect of the aforementioned stabilization techniques (*i.e.* TEs supplementation, AcoD or solid digestate recirculation) on the digestion performance, the processes in which these techniques have been applied (namely Enhanced Processes in Figure 1.4) are presented separately from those in which no stabilization method was used (namely Food Waste sole in Figure 1.4). Whatever the conditions, the concentrations of VFAs increased when increasing the OLRs. However, a clear difference can be appreciated when applying the stabilization techniques. In AD of FW sole, considerable VFAs concentrations appear even at low OLRs (2 g $VS \cdot l^{-1} \cdot d^{-1}$). At higher loadings, these reactors showed signs of acidification and in most of the cases, very low methane yields at loads of 4 g $VS \cdot l^{-1} \cdot d^{-1}$ or higher. On the other hand, the systems where stabilization techniques were applied were able to maintain high methane yields without appreciable accumulation of VFAs up to OLRs of 8 g $VS \cdot l^{-1} \cdot d^{-1}$, increasing greatly the VMPRs. At higher OLRs, the concentrations of VFAs in the reactors started to increase, suggesting reactor overloading. Therefore, it can be stated that the aforementioned stabilization methods were successfully applied to keep high methane yields at greater OLRs, improving the VMPRs.

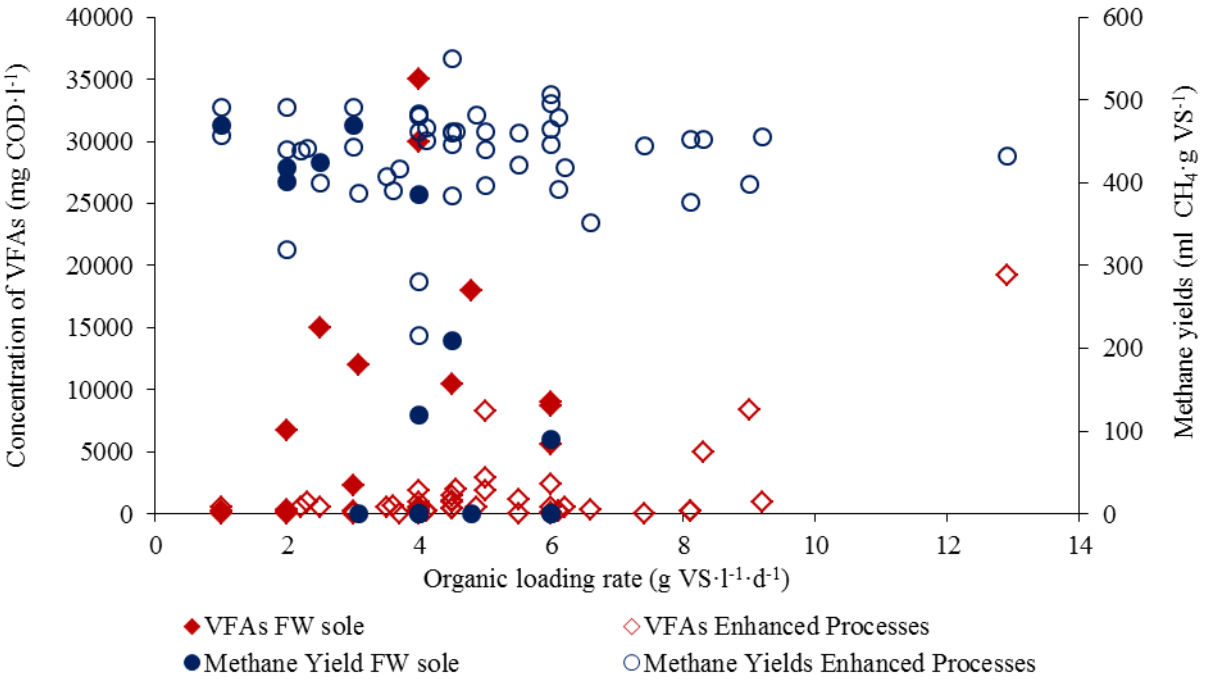

Figure 1.4. Influence of the applied OLR on the methane yields and the VFAs concentrations in steady state. The processes using a stabilization technique (*i.e.*, TEs supplementation or co-digestion; namely Enhanced Process) are presented separately from the reactors digesting directly FW (namely FW sole). Data taken from Banks et al., 2011a, El-Mashad et al. 2008, Jabeen et al. 2015, Nagao et al. 2012, Owamah and Izinyon 2015, Tampio et al. 2014, Wei et al. 2014, Zhang et al. 2011, Zhang and Jahng 2012, Wanli Zhang et al. 2015a, 2015b and Wanqin Zhang et al. 2015

More research should be carried out to further develop the most promising options, such as TEs supplementation via waste co-digestion (Cogan and Antizar-Ladislao, 2016; Zhang et al., 2011; Wanli Zhang et al., 2015a; Y. Zhang et al., 2012a), reduction of the TEs requirements (Wanli Zhang et al., 2015b) or process stabilization via solid digestate recirculation (Nagao et al., 2012). The TEs dosage, co-digestion proportions, recirculation rates and HRTs are particularly important factors that have to be optimized. As solid digestate recirculation does not require any additional reagent, this option could be particularly interesting from an economic point of view. Also, coupling the TEs addition with solid recirculation could reduce the TEs requirements, which remain in the solid fraction.

In addition, dry anaerobic digestion (>20 % TS) can also represent a promising option to investigate for the treatment of FW, due to the advantages of this process when compared to traditional wet digestion (*e.g.*, lower water requirement, lower digestate production and smaller reactor volume) (Karthikeyan and Visvanathan, 2013). Forster-Carneiro et al. (2008) obtained high methane yields at high TS contents (20-30 %) using dried FW as substrate and controlling the pH to avoid inhibition. Cho et al. (2013) used also dried FW as feed, achieving

a stable operation by digestate recirculation, with yields of 500 ml $CH_4 \cdot g\ VS^{-1}$, a TS content of 20 % and OLRs up to 5 g $VS \cdot l^{-1} \cdot d^{-1}$. Yang et al. (2015) digested raw FW and adjusted the pH in the reactor to obtain a stable digestion, with a TS content of 15 %. However, as drying the FW is an energy consuming process (usually carried out by heating), FW co-digestion with a substrate with lower water content appears as a more feasible option. Co-substrates rich in lignocellulosic materials fulfill this requirement and, as explained before, they can be used at the same time to increase the C/N ratio and to provide buffer capacity. Jabeen et al. (2015), Drennan and DiStefano (2014), X. Chen et al. (2014), Brown and Li (2013), Zhan-jiang et al. (2014), Wang et al. (2012) and Kim and Oh (2011) used different materials for this purpose (*i.e.,* rice straw, distiller's grains, paper, landscape, green or yard wastes), achieving efficient methane productions (Table 1.5) at high TS contents (20-40 %).

In a radically different approach, Pretel et al. (2016) co-digested FW efficiently in an AnMBR pilot plant treating urban wastewater, increasing the net energy production when compared with wastewater monodigestion and decreasing the operational costs of the plant. This is an interesting technology for moving towards water resource recovery facilities (WRRFs), a concept involving a holistic approach for the treatment of different waste streams in a single plant.

Finally, as FW can be considered as a solid substrate, a point must be made on the effect of pretreatment processes on the performance of FW AD. Different methods such as mechanical (ultrasound, high pressure…), thermal, chemical (acid, alkali, ozonation…) or biological pretreatments are often applied to reduce the required HRTs or to improve the biogas production when digesting solid wastes, generally by enhancing the hydrolysis of the substrate (Kondusamy and Kalamdhad, 2014). However, as FW is a highly biodegradable substrate, the rate limiting step is the methanogenesis and an excessive substrate pretreatment may even enhance the accumulation of VFAs. Thus, FW pretreatment has not been widely applied. In fact, microwave pretreatment (Shahriari et al., 2013) and autoclaving (160 °C, 6.2 bar) (Tampio et al., 2014) have been found to jeopardize the production of biomethane from FW. On the other hand, increases in the BMPs of FW have been reported after ozonation and thermal pretreatment at temperatures lower than 120 °C (Ariunbaatar et al., 2014). Nevertheless, only the thermal pretreatment produced net energy gains compared to AD of untreated FW. Optimal pretreatment conditions were found at 80 °C for 1.5 h, obtaining 647.5±10.6 ml $CH_4 \cdot g\ VS^{-1}$ (52 % higher than untreated FW). Recently, Ariunbaatar et al. (2015a) extended these results using BMP tests at different conditions, obtaining again an

optimum BMP value at 80 °C for 1.5 h and concluding that the energy produced by the increased biomethane production was sufficient to pretreat the substrate. Pretreatment of FW at low temperatures is an interesting option that may increase the biogas yield, providing at the same time the hygienization of the substrate. This process still remains to be tested in continuous operation.

1.2.3 *Single-stage fermentation for hydrogen and VFAs production*

In addition to methane, anaerobic processes can also be applied to produce hydrogen and VFAs by dark fermentation (DF) and acidogenic fermentation (AF), respectively. In the case of hydrogen, this molecule is a carbon-free clean fuel with a high energy content that can be used for several purposes, such as electricity production, direct combustion, or the synthesis of chemicals (Ghimire et al., 2015a). For the concomitant VFAs produced during AD, these fatty acids (from C2 to C5) are potentially renewable carbon sources that can be used as platform molecules for fuels, chemicals or for other purposes (Chang et al., 2010; K. Wang et al., 2014). VFAs from FW have been used for biological nutrient removal (Lim et al., 2000), production of electricity by microbial fuel cells (Y. Chen et al., 2013), production of biogas (Wang et al., 2015), production of biodiesel (Fontanille et al., 2012), or for the synthesis of value-added chemicals, such as ethanol (Ma et al., 2014; Uçkun Kiran and Liu, 2015), yeast flavor (Mantzouridou et al., 2015), fatty acids (Pleissner et al., 2015) or polyhydroxyalkanoates (H. Chen et al., 2013).

Among the alternatives for hydrogen and mixed VFAs production, DF and AF have lower energy requirements and are more environmentally friendly than other methods (Chang et al., 2010; Dahiya et al., 2015; Kim et al., 2014; K. Wang et al., 2014). In addition, anaerobic fermentation can accommodate a great variety of substrates and, in the case of hydrogen, DF has high hydrogen production rates when compared to other processes (Levin et al., 2004).

1.2.3.1 Main factors affecting dark fermentation for hydrogen production

The composition of FW makes it a very suitable substrate for DF, mainly because monosaccharides are the preferred substrates for hydrogen production by DF (Guo et al., 2014). In fact, the hydrogen yields obtained by DF are correlated with the carbohydrate content of the substrates (Guo et al., 2014; Kobayashi et al., 2012). As carbohydrates are the main component of FW (Table 1.2), this biomass has a tremendous valorization potential by DF. Thus, extensive research has been carried out using FW as substrate for DF (Figure 1.2). Some of the latest results found in the bibliography are presented in Table 1.6.

Table 1.6. Some of the main results of FW dark fermentation for hydrogen production presented in the literature

FW origin	Co-substrate	Reactor Type	Scale (l)	S/X (VS/VS)	HRT (d)	T (ºC)	OLR (g $VS \cdot l^{-1} \cdot d^{-1}$)	HY (ml $H_2 \cdot g\ VS^{-1}$)	VHPR ($l \cdot l^{-1} \cdot d^{-1}$)	VS reduction (%)	TAN[26] ($mg \cdot l^{-1}$)	VFAs (mg $COD \cdot l^{-1}$)[27, 28]	Inoculum pretreatment	pH	Reference
Synthetic	-	Batch	0.3	opt 7.8[6]	-	36	-	37-101	-	nr	nr	nr	no	4.0-6.0[24]	(Chen et al., 2006)
Synthetic	-	Batch	0.02	1.6[7]	-	37, 60, 70	-	0-98[13]	-	nr	nr	700-5800	Autoclave, BES	6.5	(Danko et al., 2008)
Synthetic	-	Batch	0.5	1.0-8.0	-	37	-	0.4-2.7[17]	nr	nr	nr	103-26[22]	Heat	6.0[24]	(Laothanachareon et al., 2014)
Cafeteria	-	Batch	0.3	4.0[8]	-	35	-	0-120	nr	nr	nr	0-70[22]	Enrichment	6.0-8.0[24]	(Zhu et al., 2009)
Cafeteria	-	Batch	0.2	∞	-	35	-	1.3-1.9[17]	-	nr	nr	~ 40000	FW heated	5.0	(D.-H. Kim et al., 2011a)
Cafeteria	-	Batch	0.6, 3	∞	-	35	-	0-153	0-9.98	≤ 50	nr	≤ 33991	FW heated	5.0	(Kim et al., 2009)
Cafeteria	-	Batch	0.2	∞	-	35-60	-	16-137	0.65-8.67	50	nr	30000	-	6.0	(D.-H. Kim et al., 2011c)
University restaurant	-	Batch	0.1	2.7-4.2	-	35	-	38-154	-	nr	nr	1500-6500	no	4.3-5.6	(Cao and Zhao, 2009)
University restaurant	-	Batch	0.2	22.6	-	55	-	62-86[13]	-	43-22[20]	nr	≤ 12400	Heat	4.8	(Elsamadony et al., 2015)
University restaurant	-	Batch	0.1	0.2-0.4[8]	-	45-65	-	0-120[16]	-	nr	nr	> 24330	Heat	5.0-9.0[24]	(Ismail et al., 2009)
University restaurant	-	Batch	nr	∞	-	35	-	161-27	28.9-1.6	41-33	nr	0-16000	FW pretreated	8.0[24]	(Kim et al., 2014)
University restaurant	-	Batch	0.1	0.3-4.4[9]	-	30	-	15-105	nr	nr	nr	nr	Heat	5.5[24]	(Sreela-or et al., 2011a)
University restaurant	-	Batch	1.0	0.3-32.2	-	35	-	121-51	nr	nr	500-10000[25]	nr	No	nr	(Pan et al., 2013)
Restaurants	-	Batch	0.1	1.5-9.0	-	35-60	-	0.4-583.0[16]	nr	nr	nr	16130-4210	Heat	4.5-5.5	(Nazlina et al., 2009)
Waste Facility	-	Batch	0.2	∞	-	37	-	42-118	-	nr	nr	9700-16900	-	5.5	(Elbeshbishy et al., 2011a)
Garbage company	-	Batch	1.2	∞	-	15-65	-	65-63	nr	46-73	nr	nr	-	7.0	(Komemoto et al., 2009)
FW hydrolysate	-	Batch	0.5	nr	-	37	-	220	-	nr	nr	nr	Heat	4.0-4.6	(Han et al., 2015b)
FW leachate	-	Batch	0.1	0.4-1.0[8]	-	35	-	0.1-2.1[17]	nr	nr	nr	9500-17500	Alkali treatment	5.5-6.5	(Kim et al., 2013)
University restaurant	-	Sequential batch	4.5	-	1.0-6.7[11]	35	nr	13-81	0.3-2.7	55-76[19]	nr	19700-25800	Heat	> 5.3	(Kim et al., 2008)
University restaurant	-	Sequential batch	4.5	-	1.0-1.3	35	nr	≤ 63	nr	nr	nr	≤ 26400	Heat	5.3	(Kim and Shin, 2008)
University restaurant	-	Sequential batch	150.0	-	1.5	35	nr	0.3-0.5[17]	nr	nr	nr	23400-32700	Heat	5.3	(Kim et al., 2010)
University restaurant	-	Batch, semicontinuous	0.3, 3, 0.7	∞	0.7-1.0	37	nr	63-162	7.2-20.3	33-53	nr	16000-25000	-	6.0	(Jang et al., 2015)

FW origin	Co-substrate	Reactor Type	Scale (l)	S/X (VS/VS)	HRT (d)	T (ºC)	OLR (g VS·l^{-1}·d^{-1})	HY (ml H_2·g VS^{-1})	VHPR (l·l^{-1}·d^{-1})	VS reduction (%)	TAN[26] (mg·l^{-1})	VFAs (mg COD·l^{-1})[27, 28]	Inoculum pretreatment	pH	Reference
Waste Facility	-	Semicontinuous	2.0	-	2.0	37	46-46[12]	180-332[14]	2.6-4.8	15-24[19]	nr	15300-18100	Sonicated	5.0-6.0	(Elbeshbishy et al., 2011b)
Synthetic	-	Semicontinuous	3.0	-	0.5-2.0	34	11-45	21-13	0.2-0.6	53-47	78-15	8500-6100	No	5.5	(Redondas et al., 2012)
FW hydrolysate	-	CMISR[3]	3.2	-	0.3	55	8-40	≤ 86[15]	≤ 8.5	nr	nr	≤ 532	Aeration	> 4.0	(Han et al., 2015a)
Cafeteria	-	HF-MBR[4]	5.0	-	0.8-0.4	55	70-125[12]	63-111	≤ 10.7	nr	nr	15399-20933	Heat	5.5	(Lee et al., 2014)
Kitchen wastes	-	I-CSTR[5]	3.0	-	4.0-1.3	35	27-100[12]	70-96[14]	0.7-3.0	56-23[19]	320-670	10900-8900	-	5.5	(Li et al., 2011)
University restaurant	-	CSTR	0.7	-	3.5-2.0	35	nr	88-261	0.1-0.4	nr	nr	493-1084	Heat	5.0	(Reungsang et al., 2013)
University restaurant	Aged landfill refuse	Batch	0.3	~ 1.5	-	36	-	≤ 188	nr	nr	nr	18000-35000	Heat	4.7-5.5	(Li et al., 2008)
University restaurant	Sewage sludge	Batch	0.6	∞	-	35	-	129-162	5.3	40	300-500	38300	FW heated	6.0	(D.-H. Kim et al., 2011b)
University restaurant	Olive husks	Batch	0.3	0.6	-	37	-	5-87	nr	35-53	≤ 2000	nr	No	8.0-7.0[24]	(Pagliaccia et al., 2016)
University restaurant	Sludge	Batch	0.1	nr	-	30	-	12-103	nr	nr	nr	nr	Heat	nr	(Sreela-or et al., 2011b)
University restaurant	White mud	Batch	0.5	2.0[10]	-	55	-	92-145	nr	nr	175-350	nr	Heat	3.8-6.2	(Zhang and Wang, 2013)
University restaurant	Lime mud	Batch	0.5	2.0[10]	-	55	-	80-138	nr	nr	nr	nr	Heat	4.4-5.1	(J. Zhang et al., 2013)
Refectory	Slaughterhouse waste	Batch	0.8	nr	-	36	-	40-145	-	36-76	nr	< 6000[21]	Heat	5.1-5.5	(Boni et al., 2013)
Processing facility	Primary sludge, WAS[2]	Batch	0.3	2.0[6]	-	55	-	12-165[14]	nr	15-26[19]	nr	nr	Heat	5.5[24]	(Zhou et al., 2013)
nr	Paper waste	Sequential batch	1.0	-	21.0[11]	55	-	1.2-51.2[18]	nr	15-53	nr	13450-8119[23]	No	7.0-6.0[24]	(Valdez-Vazquez and Poggi-Varaldo, 2009)
University restaurant	OFMSW[1]	Semicontinuous	nr	-	6.6-1.9[11]	55	19-66	34-38	2.5-0.6	nr	nr	16580-20727	no	5.5	(Angeriz-Campoy et al., 2015)

1. Organic fraction municipal solid waste
2. Waste activated sludge
3. Continuous mixed immobilized sludge reactor
4. Hydrogen fermentation membrane bioreactor
5. Intermittent-continuous stirred tank reactor
6. g COD·g VSS^{-1}
7. g COD·g VS^{-1}
8. Volume·Volume^{-1}
9. g VS·g VSS^{-1}
10. g·g^{-1}
11. Solids retention time
12. g COD l^{-1}·d^{-1}
13. ml H_2·g COD^{-1}
14. ml H_2·g VSS^{-1}
15. ml H_2·g FW^{-1}
16. ml H_2·g Carbohydrate^{-1}
17. mol H_2·mol hexose^{-1}
18. ml H_2·g VS removed^{-1}
19. VSS %
20. COD %
21. mg·kg^{-1}
22. mM
23. mg COD organic acids·kg^{-1}
24. Initial pH
25. TAN added initially
26. When values of TAN were not reported, these concentrations refer to NH_4^+-N
27. If present, ethanol and lactic acid are added-up as COD
28. When the units were not specified, the concentrations were assumed to be expressed in COD

nr stands for "non-reported"

It is important to notice that, contrary to what occurs in FW AD, TAN build-up is not a primary complication in single-stage DF. This is because methanogens, which are the species most vulnerable to TAN, are not required. In fact, as they consume hydrogen via hydrogenotrophic methanogenesis (Figure 1.3), they are undesirable. To inactivate these archaea, pretreatment of the inoculum is the most widely applied technique. This process must suppress as much as possible the activity of hydrogen-consuming microorganisms, maintaining at the same time the activity of hydrogen producers, such as *Clostridium* or *Enterobacter* (Elbeshbishy et al., 2011a). Thus, inoculum pretreatment methods usually aim to enrich the sludge in hydrogen producers such as *Clostridium* species, which, due to their ability to form spores, have a better chance to survive than non-spore formers (Ghimire et al., 2015a). Using FW as substrate, this has been achieved by several means, *e.g.* by thermal pretreatment (Elsamadony et al., 2015), sonication (Elbeshbishy et al., 2011b), aeration (Han and Shin, 2004) or BES (sodium 2-bromoethasulfonic acid) addition (Danko et al., 2008). Due to its simplicity, relatively low price and effectivity, heat treatment has been the most widely applied alternative for FW DF. However, other options like integrated sonication (ultrasonic prove within the reactor itself) should be considered due to the high yields they have achieved (180-332 ml $H_2 \cdot g\ VSS^{-1}$) (Elbeshbishy et al., 2011b).

In addition, much lower HRTs are often applied in DF compared to AD (≥ 4 d). With a constant concentration of the substrate, this allows much higher OLRs (≥ 8 g $VS \cdot l^{-1} \cdot d^{-1}$). Moreover, lower HRTs also lead to smaller reactors and to the wash-out of undesired slow-growing microorganisms (*i.e.* methanogens). Concerning to batch systems, working under higher S/X ratios (optimum of 3.9-8 for DF (Pan et al., 2008)) also leads to lower volumes of the reactors.

Another main difference of DF compared to AD is that the hydrolysis of the substrate is in this case the rate limiting step (Han et al., 2015a; Yasin et al., 2013). Thus, substrate pretreatment becomes a more interesting option to improve the efficiency of FW DF. Elbeshbishy et al. (2011a) tested several pretreatment methods (*i.e.* ultrasonication, heat, acid and base methods) in batch conditions and concluded that sonication was an effective treatment method for FW. They obtained optimal results when combining acid and ultrasonic treatment, with a hydrogen yield of 118 ml $H_2 \cdot g\ VS^{-1}$. In a continuous system with different sonication configurations, Elbeshbishy et al. (2011b) obtained optimal results using integrated sonicated systems, with a yield of 332 ml $H_2 \cdot g\ VSS^{-1}$. Jang et al. (2015) concluded that a basic pretreatment of FW (pH from 9.0-13.0) was the best option for start-up of DF without inoculum addition, preventing the growth of hydrogen consuming microorganisms and

improving the hydrolysis step at the same time. After akali-preteatment at pH 11.0, they reached average hydrogen yields and productivities of 121 ± 1 ml $H_2 \cdot g\ VS^{-1}$ and 4.39 ± 0.32 l $H_2 \cdot l^{-1} \cdot d^{-1}$ in batch operation. Applying a similar approach, some authors have assessed the effect of FW pretreatment on hydrogen production without the addition of any external inoculum (Elbeshbishy et al., 2011a; Jang et al., 2015; D.-H. Kim et al., 2011a, 2011b, 2011c, Kim et al., 2014, 2010, 2009). In this case, the objective of the treatment is the suppression of lactic acid bacteria (LAB), which consume the substrate to produce lactic acid through a pathway with no associated hydrogen production (Figure 1.3). Using FW, Kim et al. (2014) evaluated the effect of FW acid treatment, verifying the viability of this option and a greater suppression of LAB at lower pH values. Kim et al. (2009) compared three different pretreatment options, namely acid, alkali or temperature shock, concluding that heat treatment was the most effective one (153.5 ml $H_2 \cdot g\ VS^{-1}$).

In addition, another option to increase substrate solubilization is to work at higher temperatures, resulting in an enhanced hydrolysis. However, no consensus exists on this point. Although some authors have reported greater yields at thermophilic temperatures (Ismail et al., 2009; D.-H. Kim et al., 2011c; Nazlina et al., 2009), others have found the contrary, with higher yields at mesophilic temperatures (Danko et al., 2008) and even with greater solubilization of the substrate under those conditions (Komemoto et al., 2009). These differences may be caused by several reasons, such as acclimation of the inoculum, the inherent bacterial population in the FW, different working pH of the system or varying buffering capacities.

The initial and the working pH of the system and the buffering capacity play a critical role on the predominant metabolic pathways followed. Moreover, as methanogens do not consume the generated VFAs, there is a concomitant VFA accumulation as hydrogen is produced. This may eventually lead to a decrease in the pH of the system, modifying the fermentation products and decreasing the hydrogen yields. This occurs because while at optimal pH values (6.5-7.5 (Ismail et al., 2009; Nazlina et al., 2009; Zhu et al., 2009)) the metabolic pathways favored are those associated with hydrogen production (mainly generation of acetic and butyric acids), as acids accumulate in the reactor and the pH starts to decrease, other products with lower associated hydrogen yields (*i.e.*, ethanol or propionic acid) start to be produced. Eventually, if the pH drops low enough, lactic acid will start to accumulate due to metabolic shifts occurring in acidic environments (Motte et al., 2014b). This acid does not generate any hydrogen during its production and, moreover, it affects greatly the pH, causing a further decrease in the pH. Because of this, the pH of the system is usually regulated by the addition

of buffers, avoiding acidification of the reactors (Han et al., 2015b; Jang et al., 2015; D.-H. Kim et al., 2011a; Sreela-or et al., 2011a, 2011b; Zhu et al., 2009).

To improve the economic feasibility of the process at an industrial scale, some studies have tried alternatives to the use of buffers. Co-digestion appears to be a promising option. Boni et al. (2013) effectively co-digested FW with slaughterhouse waste (from a butcher shop) to provide buffering capacity, obtaining hydrogen yields up to 145 ml $H_2 \cdot g\ VS^{-1}$ even at pH values lower than the optimal range. Waste sludge has also been used as an effective co-substrate for FW DF (D.-H. Kim et al., 2011b; Sreela-or et al., 2011b; Zhou et al., 2013), stabilizing the hydrogen production by adjusting the C/N ratio of the substrate, by providing buffer capacity and by supplying TEs. Synergistic effects have also been observed when co-digesting FW with lime mud and white mud (from paper-making and ammonia-soda processes, respectively) without addition of external buffer (J. Zhang et al., 2013; Zhang and Wang, 2013). This co-substrate improved the performance of DF by increasing the buffering capacity, supplying TEs and balancing the macronutrients in the substrate.

1.2.3.2 Main factors affecting acidogenic fermentation for production of VFAs

The main difference between DF and AF is the lower working pH required in AF. As shown in Table 1.7, many authors have tried to find the optimal pH value for the products they were trying to obtain. In the case of mixed VFAs production, most of the research points towards an optimal range of 5.5-6.5 (Dahiya et al., 2015; Jiang et al., 2013; Lim et al., 2008; K. Wang et al., 2014), the range which has been the most widely applied (Kim et al., 2006; Lim et al., 2000; Yin et al., 2014). However, when trying to obtain other products such as lactic acid, optimal conditions are around pH 4, values at which no further conversion of lactate into acetic or butyric acids can occur (K. Wang et al., 2014; Y. Wu et al., 2015). Therefore, in AF the pH is also usually controlled by alkali addition to avoid the acidification of the reactors.

Table 1.7. Some of the main results of FW acidogenic fermentation for production of VFAs presented in the literature

FW origin	Co-substrate	Product aimed	Reactor Type	Scale (l)	S/X (VS/VS)	HRT (d)	T (ºC)	OLR (g $VS \cdot L^{-1} \cdot d^{-1}$)	Yield (g·g VS^{-1})	Initial pH	VS reduction (%)	NH_4-N (mg·l^{-1})	Main VFAs obtained	VFAs[12] (g $COD \cdot l^{-1}$)	Reference
Synthetic	-	VFAs	Batch	4.6	∞-14.4	-	35	-	0.05-0.18[8]	3.8-4.5	52.4-71.7	< 100	HBu, HAc, HPr	6.8-11.8	(Xu et al., 2012)
Synthetic	-	VFAs	Batch	4.5	5.5-20.9	-	35	-	0.47-0.80[8]	6.0	42.5-50.0	< 1800	HAc, HPr, HBu, HVa	26.1-62.6	(Wang et al., 2015)
Cafeteria	-	VFAs	Batch	2.0	11.2	-	35	-	nr	6.5	10.6-37.7	nr	HAc, HBu	0.8-5.6	(Kim et al., 2006)
Cafeteria	-	VFAs	Batch	2.0	nr	-	35	-	0.38-0.40	5.5	nr	180-356	HAc, HBu, HPr	3.8-7.2	(Lim et al., 2000)
University restaurant	-	VFAs	Batch	2.0	3.0	-	35, 55, 75	-	nr	7.0	nr	nr	HAc, HBu	10-16.8	(He et al., 2012)
University restaurant	-	VFAs	Batch	0.5	4.0[3]	-	30	-	0.44-0.91[9]	6.0	nr	300-750	HBu, HAc, HPr	1.8-34.0	(Yin et al., 2014)
University restaurant	-	VFAs	Batch	0.5	4.0[3]	-	30	-	0.12-0.92[10]	4.0, 5.0, 6.0	nr	100-800	HBu, HAc, HPr	3-52	(K. Wang et al., 2014)
University restaurant	-	VFAs	Batch	0.5	4.0[3]	-	30	-	0.67-0.76[9]	6.0	nr	nr	HAc, HBu, HPr	22-23.9	(D. Shen et al., 2016)
University restaurant	-	VFAs, H_2	Sequencing batch	0.4	-	nr	28	15[5]	nr	5.0-11.0	30.0-66.0[11]	nr	HAc, HBu, HPr	3.5-6.3	(Dahiya et al., 2015)
Synthetic	-	VFAs	Batch, semicontinuous	4.5	19.9	5	35-55	5-16[6]	0.03-0.50	5.0-7.0	59.4-32.5	2208-423	HAc, HBu, HPr	3.9-47.9	(Jiang et al., 2013)
Cafeteria	-	VFAs	Semicontinuous	2.0	-	4, 8, 12	25, 35, 45	5, 9, 13[6]	0.22-1.50[8]	5.0, 5.5, 6.0	nr	0-51	HAc, HBu, HPr	5-30	(Lim et al., 2008)
FVW	-	Lactic acid	Semicontinuous	4.5	-	3	35	11	nr	4.0, 5.0	nr	68	HLa, HAc	10-29.5	(Y. Wu et al., 2015)
Synthetic	-	VFAs	SLS-CSTR[2]	3.7	-	15	37	2	nr	6.0, 9.0	60.0-80.0[11]	nr	HAc, HBu, HPr	11-25	(Karthikeyan et al., 2016)
University restaurant	WAS[1]	VFAs	Batch	5.0	nr	-	5-65	-	0.05-0.67[8]	4.0-12.0	nr	nr	HAc, HPr, HBu, HVal	nr	(Y. Chen et al., 2013)
Synthetic	Dewatered sludge	VFAs	Sequencing batch	0.5	-	9	35	nr	nr	5.0, 7.0, 9.0, 11.0	nr	nr	nr	≤ 25.9	(H. Chen et al., 2013)
Soybean meal	Wheat-rice stone	VFAs	Batch, Rotational drum	3.6	1:1, 1:2[4]	10	35	nr	0.09-0.97[9]	7.4-7.5	11.1-68.2	nr	HAc, HBu, HPr	7.4-11.7	(Lu et al., 2013)
Synthetic	Dewatered sludge	VFAs	Semicontinuous	0.5	-	4-12	35	4-12[7]	nr	4.4-7.5	nr	nr	nr	3.7-29.1	(Hong and Haiyun, 2010)
nr	Brown water	VFAs	Semicontinuous	3.0	-	4	35	5	nr	4-4.12	nr	96-110	HAc, HBu	7.8-11.1	(Lim et al., 2014)

1. Waste Activated Sludge
2. Solid-Liquid-Separating Continuous Stirred Tank Reactor
3. TS ratio
4. Wet weight ratio
5. g $COD \cdot l^{-1} \cdot d^{-1}$
6. g $TS \cdot l^{-1} \cdot d^{-1}$
7. g $VSS \cdot l^{-1} \cdot d^{-1}$
8. VFAs expressed in COD units
9. g·g VS $removed^{-1}$
10. g·g VSS $removed^{-1}$
11. COD %
12. When the units were not specified, the concentrations were assumed to be expressed in COD

nr stands for "non-reported"

HAc, HBu, HPr, HVal and HLa stand for acetic acid, butyric acid, propionic acid, valeric acid and lactic acid, respectively

The most important parameters for FW single-stage AF are similar to those reported for hydrogen production. The rate limiting step of the process is also the hydrolysis and therefore, different FW pretreatments have been tested to enhance this step. Kim et al. (2006) applied an enzymatic pretreatment, improving the VFAs production (up to 5,600 g $COD \cdot l^{-1}$, 3.3 times higher than in the control) and concluding that an enzyme mixture was the optimal option. Yin et al. (2014) applied a hydrothermal treatment, reporting a two-fold increase of the FW solubilization (COD units), which improved the VFA yields up to 0.908 g·g $VS_{removed}^{-1}$. D. Shen et al. (2016) also obtained higher VFA yields, up to 0.763 g·g $VS_{removed}^{-1}$, after hydrothermal treatment of FW, using phosphoric acid as catalyst.

Also the temperature has an important role in AF. Generally, optimal performances have been reported to occur under mesophilic temperatures. Lim et al. (2008) and Y. Chen et al. (2013) determined optimal conditions at 35 and 37 °C, respectively. However, Jiang et al. (2013) obtained slightly better yields at 45 °C. Surprisingly, He et al. (2012) reported greater VFA concentrations, up to 16.8 $g \cdot l^{-1}$ at 70 °C, due to improved hydrolysis of the substrate. This different optimal temperature may be caused by the fact that the pH was not controlled in the later study, and the acidification effect was more pronounced at lower temperatures (pH of 3.7 at 35 °C), jeopardizing the fermentation process. A possible explanation for the higher pH values at greater temperatures may be higher TAN concentrations due to a greater hydrolysis of the FW, which buffered the pH of the system. Moreover, the hydrolysis is also compromised at acidic pH values, limiting the conversion of protein to TAN. Interestingly, due to the low final pH (3.70-4.45), He et al. (2012) obtained high ethanol concentrations (up to 15 $g \cdot l^{-1}$) at 35 °C.

In semi-continuous operation, the effect of the OLR on the process was assessed by Lim et al. (2008) and Jiang et al. (2013) at pH values of 5-6 and 5-7, respectively. They concluded that, within the range studied, increasing the OLR led to a decrease in the VFA yields but, at the same time, to an increase in the VFA concentrations in the reactors, improving the productivity. Interestingly, both authors also reported higher proportions of acetic acid, and lower values for butyric and propionic acids, when increasing the OLR. Moreover, at the highest loadings, greater concentrations of lactic and caproic acids were reported (Lim et al., 2008). This means that VFAs speciation could be regulated to some extent by the reactor load.

In addition, Karthikeyan et al. (2016) have recently developed a novel reactor, able to uncouple the SRT from the HRT in a simple way and reaching VFAs concentrations up to 25 $g \cdot l^{-1}$.

Finally, some authors have researched the co-fermentation of FW with other biowastes, such as WAS, dewatered sludge or brown water. Like for DF, the objective was to balance nutrients (*i.e.* increase the C/N ratio) and to provide buffer capacity. Y. Chen et al. (2013) obtained VFAs yields up to 0.67 g COD·g VS^{-1} co-digesting FW and WAS and, with dewatered sludge as co-substrate, H. Chen et al. (2013) and Hong and Haiyun (2010) reached VFAs concentrations of 26 and 29 g COD·l^{-1}, respectively. It must be mentioned that in these three studies with sludge as co-substrate, the optimal pH values, 8.0, 9.0 and 7.0 respectively, were found to be higher than for any other mono-digestion experiment. The explanation for that may be, not only the different characteristics of the substrates (*i.e.* C/N ratio), but also the indigenous bacterial population present in the sludge, which might have favored the VFA production. Brown water has also been used as co-substrate, obtaining concentrations of VFAs of 7.8-11.1 g COD·l^{-1} even at pH values around 4. An interesting approach was investigated by Lu et al. (2013), in which wheat-rice stone, a porous natural clay, was used as adsorption material to alleviate inhibition and to provide nutrients at the same time. By addition of this material and by leachate recirculation, which lowered VFA concentrations and buffered inhibition, they achieved stable VFAs production without pH regulation, with final pH values of 4.9-5.2 and yields up to 0.97 g·g $VS_{removed}^{-1}$.

1.2.3.3 Towards the optimization of FW fermentation

Table 1.8 presents a summary of the different key decision points that can be extracted from the data discussed above. Two main options exist to provide buffering capacity and to avoid reactor acidification: co-fermentation and external buffer addition. The application of a chemical buffer may lead to a very stable pH, but the high costs associated to this process make co-fermentation a much more attractive alternative. However, another degree of freedom, co-substrates proportions, is added to the system. A suitable co-substrate for FW fermentation should increase the buffer capacity, be readily available for collection together with FW and be highly biodegradable.

Table 1.8. Comparison of different alternatives that represent key decision points for optimization of FW fermentation (✓ stands for positive impact and × for negative impact)

	Source of buffering capacity		**Source of inoculum for DF**		**Substrate pretreatment**	
	Co-substrate	**External buffer**	**Enriched sludge**	**Treated FW**	**Yes**	**No**
Stability	✓	✓	✓	✓	✓	✓
Operational costs	✓	×	✓	×	×	✓
Hydrogen / VFAs production	✓	✓	×	✓	✓	×
VS reduction	✓	✓	✓	✓	✓	×

For DF, there is also a need to optimize the source of the microbial inoculum. The use of an enriched external sludge is a reliable option, but the volumetric hydrogen production may be jeopardized at high proportions of inoculum due to the volume of the reactor that is used by the sludge. In fact, some of the highest VHPRs reported in the literature, *e.g.* 28.9 $l \cdot l^{-1} \cdot d^{-1}$ (Kim et al., 2014) and 20.3 $l \cdot l^{-1} \cdot d^{-1}$ (Jang et al., 2015), have been obtained without addition of external inoculum. Moreover, the need of preparing new inoculum in batch processes every time the fermentation starts disappears, making this option more feasible and with completion times (including lag periods) equivalent to those of continuous processes (Kim et al., 2009). On the other hand, if treated FW is used directly as source of bacteria, the volumetric hydrogen production may be promoted, but the related operational costs increase due to the necessity of pretreating the incoming waste. A complete techno-economic evaluation has to be carried out before selecting an option. However, as FW treatment may be used simultaneously to produce the inoculum and to increase the hydrogen yields and the VS degradation, this strategy has a great potential to increase the feasibility of FW DF in the future.

In the literature dealing with fermentation of FW, most of the studies have been performed in batch mode and therefore more research in continuous regime is required. This would allow to test the stability and the robustness of the process and to investigate different approaches, such as fermentation in dry conditions (TS >20%) or the uncoupling of the SRT and the HRT, which could potentially increase the buffering capacity of the system and allow greater OLRs (Karthikeyan et al., 2016; Lee et al., 2014). In addition, promising options such as co-fermentation with substrates that eliminate the need for pH control (Lim et al., 2014; Lu et al., 2013) or microaeration (Lim et al., 2014) and non-strict anaerobic conditions (Yin et al., 2014) to improve the fermentation efficiency, warrant further exploration. Combinations of different alternatives such as SRT uncoupling and co-fermentation also have a great potential to overcome the main issues associated with FW fermentation. The results presented above suggest that anaerobic fermentation, particularly AF, remains as a non-mature process that requires optimization. Nevertheless, due to the high added-value of the products that can be potentially produced by anaerobic fermentation, coupling this process with a second stage of AD for stabilizing the residues from fermentation could be an attractive approach.

1.2.4 *Hydrogen and methane production in 2-stage systems*

A different alternative for biowaste treatment via anaerobic digestion is the application of multistage systems, mainly consisting of two reactors in series. While in single-stage

processes all the reactions of AD occur in one reactor, in 2-stage systems, hydrolysis, acidogenesis and acetogenesis take place in a first stage, producing mainly hydrogen, carbon dioxide and VFAs. Afterwards, in a conventional 2-stage system, these products are transformed into methane through methanogenesis in a second digester, physically separated from the first stage (Kondusamy and Kalamdhad, 2014). The purpose of this design is to provide optimal conditions for the various microorganisms that carry out the different biological processes (Grimberg et al., 2015). 2-stage systems can be used for two main purposes. If methane is the desired product, this configuration can serve to achieve stable AD in the 2nd stage. On the other hand, this process can also be directed towards hydrogen production in the 1st stage. In this last case, AD takes places in a 2nd stage to treat the effluents from the 1st reactor, producing methane.

In the first option, all the products from the 1st stage, including hydrogen and carbon dioxide, are used as substrates for the 2nd stage. Other than the physical separation of the microbial communities, this strategy offers the benefit of favoring the shift towards hydrogenotrophic methanogenesis due to the biogas recirculation from the 1st stage. Hydrogenotrophic methanogens are more resistant to ammonia and VFA inhibition than acetothrops and therefore, a more stable digestion is achieved and the methane content in the biogas can be increased (Luo and Angelidaki, 2013). This alternative has been widely applied using FW as substrate (Grimberg et al., 2015; Lim et al., 2013; Rajagopal et al., 2013a; Ratanatamskul et al., 2015; Shahriari et al., 2013; Shen et al., 2013; Ventura et al., 2014; Xu et al., 2011; Yabu et al., 2011; Yan et al., 2016), proving its feasibility under different conditions and with methane yields up to 535 ml $CH_4 \cdot g\ VS^{-1}$.

Regarding the 2nd option (hydrogen production in the first stage), the 2nd stage digester is used to transform the remaining organic matter from the first reactor into methane, obtaining a stable digestate. The hydrogen and methane produced can be used separately or can be mixed together to produce hythane (average composition of 10 % H_2, 60 % CH_4 and 30 % CO_2 (Dung Thi et al., 2016)). The production of hydrogen and methane has also been widely investigated with FW as feedstock (Cavinato et al., 2012; Chu et al., 2012, 2010; Kobayashi et al., 2012; Micolucci et al., 2014; Wang and Zhao, 2009), obtaining high yields for both gases (*e.g.* 122.5 ml $H_2 \cdot g\ VS^{-1}$ and 412.0 ml $CH_4 \cdot g\ VS^{-1}$ (Kobayashi et al., 2012)). These two main integrated systems, as well as other combinations of processes, are discussed below.

1.2.4.1 Main factors affecting 2-stage systems

The parameters with greater influence on 2-stage systems are similar to those mentioned before for AD and DF processes, pH being one of the most critical ones. As previously, the main issues encountered are FAN build-up and VFA accumulation in the reactors. Similar optimal operational conditions have been reported for both 2-stage strategies (AD stabilization and H_2/CH_4 production). This is because a high hydrogen yield will increase the performance of both systems. In the case of AD, more hydrogen means not only more substrate for hydrogenothrops but also higher proportions of acetic and butyric acids, which are easily converted into methane. Because of the same reasons, in systems that aim to produce both gases, the hydrogen yields in the 1st phase will be directly related to the methane yields in the 2nd stage (Zhu et al., 2011). Therefore, in 2-stage systems it is of outmost importance to optimize hydrogen production in the 1st stage.

As shown in Table 1.9, while the 2nd stage is kept at pH values of 6.0-8.5 and is operated at HRTs of 5-80 d (optimal conditions for the growth of methanogenic archaea), the 1st stage is usually maintained at lower pH values of 4.0-6.0 and at lower HRTs of 0.5-10 d, consequently with greater OLRs. The low HRTs avoid the presence of slow-growing acid and hydrogen consuming organisms in the 1st reactor. However, due to acid accumulation the pH tends to decrease as DF takes places in this stage, which may lead to lactate or ethanol production, lowering the hydrogen yields (Chen et al., 2015; Chu et al., 2012; B. Zhang et al., 2007). pH values over 5 in the 1st stage have been recommended to avoid this issue (Chen et al., 2015; Chu et al., 2012), and therefore, the pH is usually increased by addition of external chemicals (*e.g.*, NaOH) (Chen et al., 2015; Chu et al., 2012, 2010; Lee and Chung, 2010; Liu et al., 2013; Ventura et al., 2014; Xu et al., 2011; Yabu et al., 2011; Zhu et al., 2011). Since this approach has high associated costs, recirculation of the digestate from the methanogenic reactor has been proposed as an alternative for pH control in the 1st stage (Chinellato et al., 2013; Chu et al., 2010; Kim et al., 2012; Kobayashi et al., 2012; Lee et al., 2010; Micolucci et al., 2014; L.-J. Wu et al., 2015). As in mono-digestion, due to the reduction of the organic nitrogen present in the FW, this digestate is characterized by high concentrations of TAN. Therefore, it can be used as base to increase the pH, as source of alkalinity and as nutrient supplier. In fact, when external chemical addition is not applied, failures of the 1st stage have been reported without digestate recirculation (Ariunbaatar et al., 2015b; L.-J. Wu et al., 2015). Thanks to this recirculation, Kim et al. (2012) achieved a reduction of 75 % of the external alkali required, removing the need of water for dilution and increasing the hydrogen production by 48 %. Chu et al. (2010) recirculated only the solid fraction of the digestate and

Ariunbaatar et al. (2015b) only the liquid fraction, achieving stable operations in both cases. Moreover, Lee et al. (2010) demonstrated the economic feasibility of a 2-stage thermophilic process with digestate recirculation producing hydrogen and methane from FW without external buffer addition.

However, when applying digestate recirculation for pH control special attention must be paid to the FAN concentrations in the reactors as TAN is recycled. Micolucci et al. (2014) developed an effective control strategy for hythane production from FW by controlling the digestate recirculation rate, considering both the pH in the 1st stage and the ammonia concentrations to avoid inhibitory issues. To decrease TAN concentrations, different alternatives such us denitrification of the digestate prior to its recirculation (Lee et al., 2010) or ammonia stripping in the 1st stage (Yabu et al., 2011) have been proved to be effective. Besides, VFA and TAN accumulation can be avoided by controlling the OLR. Optimal OLRs for the 1st stage of around 20 g $VS \cdot l^{-1} \cdot d^{-1}$ have been found for systems with digestate recirculation (Chinellato et al., 2013) and with external buffer addition (Wang and Zhao, 2009), with greater loads leading to lactate and propionate production in the 1st stage, decreasing the hydrogen or methane yields and eventually causing VFA and FAN build-up.

Another option to increase the buffering capacity of the system and to dilute TAN concentrations is AcoD. Using co-substrates such as WAS (Liu et al., 2013), sewage sludge (Ratanatamskul et al., 2015; Zhu et al., 2011), dairy manure (Li et al., 2010) or brown water (Rajagopal et al., 2013a), synergies have been observed, obtaining better performance than the mono-digestion systems and even avoiding the need of pH control in the 1st stage (Li et al., 2010; Lim et al., 2013).

Finally, a key variable affecting the process is the temperature. Due to the advantages of working at thermophilic conditions, many authors have researched this option besides being more prone to ammonia inhibition because of the displacement of the chemical equilibrium NH_3-NH_4^+ towards FAN. Thermophilic temperatures have been effectively applied in 2-stage systems digesting FW, obtaining high biogas yields and avoiding inhibition by optimization of the OLRs and HRTs (Cavinato et al., 2012; Chu et al., 2012; Lee and Chung, 2010). Moreover, some studies have compared different combinations of mesophilic and thermophilic conditions in each of the stages. Chu et al. (2010) obtained greater biogas productions under thermophilic temperatures in both stages. Also, Ventura et al. (2014) reported the highest gas yields with a mesophilic 1st stage and a thermophilic 2nd stage, but the process was found to be less stable at higher temperatures in the 2nd reactor.

Table 1.9. Most recent results of FW 2-stage AD presented in the literature (the values from both stages are separated by commas; if a parameter is the same for both stages, one value is presented)

FW origin	Co-substrate	Reactor Type	Scale (l)	S/X (VS/VS)	HRT (d)	T (ºC)	OLR (g $VS \cdot l^{-1} \cdot d^{-1}$)	HY (ml $H_2 \cdot g\ VS^{-1}$)	VHPR ($l \cdot l^{-1} \cdot d^{-1}$)	MY (ml $CH_4 \cdot g\ VS^{-1}$)	VMPR ($l \cdot l^{-1} \cdot d^{-1}$)	Stable pH[13]	VS reduction (%)	TAN[21] ($mg \cdot l^{-1}$)	VFAs[22] (mg $COD \cdot l^{-1}$)	Reference
Synthetic	-	Batch	0.5	2.5-10.0, 2.5-10.0	-	37	-	55.1[7]	0.9	94.8[7]	-	6.0, 7.0	90.0	nr	≤ 47, ≤ 10[18]	(Nathao et al., 2013)
University restaurant	-	Sequential batch	3.6	-	2.0-4.0, 24.0-15.0	35	7.5-22.5[4], 2.0-3.8[5]	0.4-0.9[8]	0.6-1.8	0.2-0.25[11]	0.4-0.9	5.3, nr	80.0-97.0[14], 58.0-71.0[15]	nr	nr, 1273-2200	(Kim et al., 2012)
Synthetic	-	Sequential batch, Semicontinuous	nr, 19.0	-	2.0-6.0, 80.0-30.0	55	nr	nr	nr	414-487	nr	7.0-8.0, 8.0	nr	1000-3000 , ≤ 3000[16]	500-900 ≤ 50 [19]	(Yabu et al., 2011)
Synthetic	-	Semicontinuous	0.2, 2.0	-	2.0-4.0, 18.0-36.0	30-37	1.2-0.3	~0	~0	759	nr	4.0-5.5, ~7.0	100 (% BMP)	≤ 1026	3450, 96	(Ariunbaatar et al., 2015b)
Synthetic	-	Semicontinuous	1.0, 5.0	-	2.0, 10.0	55	nr	66.0	1.7	364	1.5	5.5, 7.1-7.6	nr	313, 540	nr, 0	(Chu et al., 2012)
Synthetic	-	Semicontinuous	0.3, 0.6	-	9.0-20.0	35	nr, 1.2-3.4	0	0	1.11-1.31[12]	nr	nr, 8.4-8.3	87.3-61.7	nr	497-8900	(Shahriari et al., 2013)
University restaurant	-	Semicontinuous	5000.0	-	nr	37	0.8	0	0	446	nr	5.2, 8.4	93.0	nr	38900, 6300[17]	(Grimberg et al., 2015)
University restaurant	-	Semicontinuous	1.5, 6.0	-	6.0, 24.0	55, 35	14.2, 2.6	41.2	0.6	521	1.3	4.0-5.4, 7.3-7.6	28.4, 53.6	981, 1111	4334, 0[17]	(L.-J. Wu et al., 2015)
Restaurant	-	Semicontinuous	10.0, 40.0	-	1.3, 5.0	55, 35-55	64.4, 16.3[5]	205.0	5.6	464	3.5	5.5, 7.5-7.8	nr	nr, 1500-1700	12800, 3900-440	(Chu et al., 2010)
Restaurants	-	Semicontinuous	200.0, 800.0	-	10.0-4.0, 40.0-16.0	40	15.1-37.8, 2.9-8.2	71.0-49.0	nr	551-480	nr	5.2-5.8, 6.7-7.3	25.5-16.9, nr	258-427, 881-2625	13851-15126, 457-631	(Wang and Zhao, 2009)
Recycling company	-	Semicontinuous	10.0, 30.0	-	5.0, 20.0	35-55	3.2-4.4	nr	nr	370-440	0.9-1.2	5.0-5.5, 7.2-8.0	23.1-27.3, 51.9-58.6	nr	~6000, ~500-13000	(Ventura et al., 2014)
Heat-treated liquid FW	-	Semicontinuous	500.0, 2300.0	-	2.8-0.9, 6.4-3.9	33, 36	7.1-71.3, 1.6-6.4[5]	1.8[9]	0.6-3.9	nr	≤ 5.4	5.3, 7.4	95.0[14], nr	nr	6576, 5803	(Lee and Chung, 2010)
SS-FW	-	Semicontinuous	2.0, 5.0	-	3.0, 12.0	52	15.0-30.0, 3.0-6.0[6]	117.0-0	nr	484-77	nr	5.8-4.6, 7.9-5.7	nr	2910-1708, 2471-3295	6664-13756, 3850-17494	(Chinellato et al., 2013)
University restaurant	-	Semicontinuous Baffled reactor	8.0, 40.0	-	2.9, 14.4	55	nr	5.9-147.3	5.2-0.2	393-470	nr	5.5-5.6, nr	74.1-78.7[15]	116-1766, nr	10642-18581, nr[17]	(Kobayashi et al., 2012)
University restaurant	-	Semicontinuous Packed reactor	10.0, 40.0	-	3.8-1.3, 15.4-5.1	55	19.5-58.5, 4.2-11.8[5]	≤ 114.0	nr	≤ 451	≤ 2.1	5.4-5.7, 7.4-7.9	≤ 81.7, ≤ 88.1	1230, nr	≤ 44800, ≤ 11700	(Lee et al., 2010)
University restaurant	Waste Activated Sludge	Batch	0.15	2.3, 3.0[2]	-	37	-	2.5-121.1	0.2-3.5	108-354	0.1-0.4	5.5, 7.0	34.4-55.7	22-53, 239-311	159-3494, 0-987	(Liu et al., 2013)
University restaurant	Rice straw	Sequential batch	5.0	-	10.0-5.0	35	4.0-12.0	nr	nr	≤ 535	nr	3.5-6.0, 7.1-7.2	nr	nr, 551-588	44000, 111-48 [20]	(Chen et al., 2015)

FW origin	Co-substrate	Reactor Type	Scale (l)	S/X (VS/VS)	HRT (d)	T (ºC)	OLR (g $VS \cdot l^{-1} \cdot d^{-1}$)	HY (ml $H_2 \cdot g\ VS^{-1}$)	VHPR ($l \cdot l^{-1} \cdot d^{-1}$)	MY (ml $CH_4 \cdot g\ VS^{-1}$)	VMPR ($l \cdot l^{-1} \cdot d^{-1}$)	Stable pH[13]	VS reduction (%)	TAN[21] ($mg \cdot l^{-1}$)	VFAs[22] (mg $COD \cdot l^{-1}$)	Reference
Synthetic	Bulking agents	Batch, Semicontinuous	4.6, 10.0	42.8	nr	35	≤ 2.0[5]	nr	nr	180-250	nr	3.0-6.0, nr	49.7-71.7	≤ 40, 368-825	3000-5000, nr	(Xu et al., 2011)
Restaurant	Sewage sludge	Semicontinuous	1.0, 5.0	-	1.3, 12.5	35	nr	0.04-48.0	nr	≤ 522	nr	5.5-6.0, 6.8-7.2	25.0-33.0, nr	nr	≤ 5000, 0	(Zhu et al., 2011)
University restaurant	Sewage sludge	Semicontinuous	750.0, 1875.0	-	24.0-16.0	Mes[3]	8.7-16.0[5]	0	0	nr	0.3	4.2, 6.8	74.0	nr	475-555	(Ratanatamskul et al., 2015)
University restaurant	Dairy Manure	Semicontinuous	var, 3.5	-	1.0-3.0, 12.0-10.0	35	1.2-6.1	0	0	nr	≤ 5.5	5.0-3.2, 7.2-7.4	40.0-64.0	400-2100	1560-8380, 0-4140	(Li et al., 2010)
University restaurant	Brown water	Semicontinuous	5.3	-	10.0-6.0, 30.0-29.0	35	0.5-0.8	0	0	0.92[10]	nr	3.72, 6.98	79.1-81.4	≤ 689	3532-19367, 62-1146	(Lim et al., 2013)
Municipal biowaste	Paper, inerts	Semicontinuous	200.0, 380.0	-	3.3, 12.6	55	18.4, 4.8	60	0.8	476	1.5	5.2, 8.1	52	705, 1190	12241, 640	(Micolucci et al., 2014)
University restaurant	Brown water	Semicontinuous	1.2, 4.1	-	4.0-2.0, 20.0-16.0	33	1.0-3.3[5]	0	0	400-210	nr	4.0, 5.5-6.9	69.4-63.4	nr	2000-3000	(Rajagopal et al., 2013a)
University restaurant	Fruit Vegetable Waste	Semicontinuous	5.0, 8.0	-	10.0, 10.0	35	2.0-10.0, 1.0-5.0	0.028-0.005[10]	nr	0.546-0.198[10]	nr	nr, 7.1-6.7	nr	nr	3643-15415, 94-8906	(Shen et al., 2013)
Municipal biowaste	Paper, inerts	CSTR[1]	200.0, 760.0	-	3.3, 12.6	55	16.8, 4.8	66.7	1.1-0.7	720	2.0-1.6	5.7, 8.4	nr	970-1976, 1005-2240	11701, 1107	(Cavinato et al., 2012)

1. Continuous stirred tank reactor
2. S/X in 2nd stage calculated considering initial charge in 1st stage
3. Mesophilic temperatures
4. g $Carbohydrates \cdot l^{-1} \cdot d^{-1}$
5. g $COD \cdot l^{-1} \cdot d^{-1}$
6. Load to whole system
7. Yield per gram VS removed
8. mol H_2·mol $carbohydrates^{-1}$
9. mol H_2·mol $glucose^{-1}$
10. $l \cdot g\ VS^{-1} \cdot d^{-1}$
11. ml CH_4·g COD^{-1}
12. $l \cdot l^{-1} \cdot g$ VS $removed^{-1} \cdot d^{-1}$
13. Stable pH stands for the pH at the end of the experiment (batch) or at the stationary state (semicontinuous)
14. % Carbohydrates
15. % COD
16. mg $N \cdot kg^{-1}$
17. VFAs expressed in g HAc equivalent
18. mM VFA + ethanol
19. mmol HAc $equivalent \cdot kg^{-1}$
20. VFAs + ethanol
21. When values of TAN were not reported, these concentrations refer to NH_4^+-N
22. When the units were not specified, the concentrations were assumed to be expressed in COD

nr stands for "non-reported" and "var" for variable

1.2.4.2 Comparison of single-stage and 2-stage systems for FW AD

Recently, Schievano et al. (2014) demonstrated that 2-stage AD systems can increase the energy recovery from biomass when compared to single-stage AD. However, this conclusion is always dependent on the characteristics of the substrate and specific requirements of each process, such as aimed products and economic or space limitations, among others. Dealing with FW, several studies have obtained higher biogas yields and more stable processes, *i.e.*, more resistant to organic shocks, using 2-stage configurations (Ariunbaatar et al., 2015b; Grimberg et al., 2015; Nathao et al., 2013; Pisutpaisal et al., 2014; Shahriari et al., 2013; Shen et al., 2013). However, in these studies none of the stabilization techniques for FW single-stage mono-digestion described previously was applied. Recently, L.-J. Wu et al. (2015) compared single-stage and temperature-phased 2-stage AD of FW, adding TEs in both cases, and obtained similar biogas yields (447.7 ml $CH_4 \cdot g\ VS^{-1}$ for single-stage AD and 41.2 ml $H_2 \cdot g\ VS^{-1}$ and 521 ml $CH_4 \cdot g\ VS^{-1}$ for 2-stage AD). Further research should be carried out comparing 2-stage systems with novel single-stage strategies, such as co-digestion, HRT and SRT uncoupling or TEs supplementation. Moreover, recent studies pointed out that TAN can accumulate more easily in 2-stage processes, this alternative being more sensitive to FAN toxicity (Ariunbaatar et al., 2015b; Lim et al., 2013). Rajagopal et al. (2013a) obtained even higher methane yields and a more stable process using a sequencing-batch reactor compared to a 2-stage system. The issue of excessive TAN and VFAs concentrations entering the 2nd stage and jeopardizing the methanogenesis can be a major problem when considering 2-stage AD of FW, particularly if digestate recirculation to the 1st stage is applied (Kondusamy and Kalamdhad, 2014).

To conclude, 2-stage processes are a promising option to optimize FW AD, but the larger investment and operational costs when compared to single-stage reactors, require that there is a clear benefit in terms of process stability or biogas yields. In addition, currently most of the industrial processes rely on the simplicity and the robustness of single-stage AD (Rapport et al., 2008). However, if hydrogen generation is the primary objective, AD in the 2nd stage remains as a promising option for treatment of the digestate from the 1st stage. The integration of this system within the biorefinery concept for production of several value-added compounds (such as hydrogen, VFAs and methane) is particularly interesting.

1.2.5 *Other considerations and process integration*

1.2.5.1 Energy, environmental and economic factors

Many studies have proven the feasibility of FW AD/DF and compared this treatment option with other ways of dealing with FW. In this context, most of the research has been based on the approach of Life Cycle Analysis (LCA) and Life Cycle Cost (LCC) to identify the environmental and the economic burdens associated with each process.

Other than FW prevention, which will be always preferred over any treatment process (Bernstad and Andersson, 2014), alternatives such as incineration, composting or animal feeding production have been compared with AD from an environmental and economic point of view. Bernstad and la Cour Jansen (2011) compared the environmental impacts of incineration, composting and AD in a full scale study in Sweden. They concluded that the lowest global warming potential (GWP) and the minimal formation of photochemical ozone were associated with AD, coupled with the use of biogas as vehicle fuel and with the digestate applied as chemical fertilizer. However, the use of biogas for electricity generation led to a better energy balance. The main benefits of AD were related to energy (biogas) and fertilizer (digestate) substitution, indicating the importance of the utilization of both products. It is interesting to note that due to the importance of nutrient enrichment and acidification when applying AD, the type of soil for digestate application (namely sandy or clay) was found to be a relevant factor for the environmental impact of the process. A similar study from Singapore (Khoo et al., 2010) also found that centralized FW AD was preferable over incineration and composting from an environmental point of view. As indicated above, the main contributions to the reduction of the global warming impacts were related to energy generation and compost production from AD digestate. Xu et al. (2015) compared FW AD, FW AcoD with sludge and FW landfilling in China. Their results indicated that FW AD was the option with the lowest environmental impacts, concluding also that landfilling was unsuitable for FW treatment. In a recent Swedish study, Eriksson et al. (2016) evaluated different options for FW collection and treatment of digestate and reject water. Source separation and centralized FW sorting had similar environmental impacts, but the latter option presented lower net costs. They also found that direct spread of digestate on arable land was the best alternative for digestate management, both economically and environmentally. In addition, they concluded that digestate drying and pelleting had negative climate impacts, greater when compared with application of digestate on land, due to the loss of ammonia from the sludge during the drying process. An important outcome from this work is that carbon dioxide should not be used as

single environmental indicator for comparison of FW AD systems. This occurs because the carbon in FW is of biological origin and thus, does not have emission of greenhouse gases associated. Moreover, due to the importance of nutrient release in this case, categories such as eutrophication and acidification must be assessed when studying the environmental performance of FW AD. Another LCA from China (Jin et al., 2015) concluded that the FW pretreatment and AD system, and therefore the biogas yield, were the key processes affecting the global energy consumption and the environmental impacts.

In addition, Bernstad and la Cour Jansen (2012) and Bernstad et al. (2016) presented reviews of the existing LCAs dealing with different FW management options. They concluded that the main differences in the GWPs obtained in those studies were caused by methodological discrepancies and variations in the boundaries of the systems. Thus, they proposed the establishment of more detailed guidelines for LCA to increase the quality of these studies and to promote potential cross-study comparisons.

Moving forward, other studies have been carried out to prove the feasibility of FW AD/DF, evaluating the techno-economics of the process as well as the main bottlenecks to overcome. Han et al. (2016) recently analyzed the viability of the construction of an industrial process for hydrogen production by DF of FW in China. The process consisted of an enzymatic pretreatment step for FW hydrolysis, followed by DF using pre-heated sludge as inoculum to avoid methanogenesis and with buffer addition for pH control. Treating 1,095 tons of FW per day and producing 42,858 $m^3 \cdot yr^{-1}$of hydrogen (128,574 $kWh \cdot yr^{-1}$; 117 $kWh \cdot ton^{-1}$), they concluded that the process was economically feasible, with a payback period of 5 years and an overall revenue of US$146,473 per year. However, the price of hydrogen affected greatly the revenue of the plant and thus, the economic viability of the process relies on the evolution of the price of this product in the future. Also in China, a framework for FW collection and recycling for biogas production by AD has been recently proposed for the city of Hong Kong (Woon and Lo, 2015). In another case study from Canada, the authors evaluated the integration of small-scale AD of FW in urban buildings (Curry and Pillay, 2012). They suggested that this technology could be efficiently used for FW recycling locally, leading to energy savings and avoiding at the same time the transportation and the landfilling of this waste, currently applied. Treating 165 tons of FW, they produced 18,350 m^3 of biogas, leading to an annually energy recovery of 144,688 kWh and an energy surplus of 134,600 $kWh \cdot yr^{-1}$ (816 $kWh \cdot ton^{-1}$). Just by avoiding the FW transportation, they calculated savings of US$131 per ton. In addition, Banks et al. (2011a) obtained a net energy yield of 405 $kWh \cdot ton^{-1}$ digesting FW collected mainly from domestic kitchens. They concluded that the main

bottleneck of the process was the long-term accumulation of propionic acid and ammonia. The high ammonia concentration buffered the VFA accumulation, avoiding a drop in the pH, but they obtained lower methane yields, which jeopardized the performance of the overall process. De Clercq et al. (2016) also presented a Chinese case study for methane production from restaurant FW in megacities, and reported that FW AD in Beijing had the potential of producing approximately 300 million m^3 of methane per year, or $2.99 \cdot 10^9$ kWh assuming a calorific value of methane of 9.968 $kWh \cdot m^{-3}$ (Lorenz et al., 2013). At 100% utilization, this value represents 3.35% of the natural gas consumption of the city in 2012. Moreover, they identified low biogas production, inefficient waste collection, suboptimal monitoring and process control and inefficient biogas utilization as the main bottlenecks to be overcome in the future.

1.2.5.2 Digestate management and hygienization

In addition to biogas, AD produces digestate, which is suitable for application in agricultural land as a valuable fertilizer and soil conditioner (Arthurson, 2009). Residues from FW AD are rich in mineralized nitrogen, potassium and phosphorus and have low concentrations of heavy metals (Banks et al. 2011a, Banks et al. 2011b). Thus, they can be used as a substitute for mineral fertilizers, benefiting farmers and avoiding other traditional digestate management options such as landfilling and incineration, both of which are associated with significant environmental, social and financial issues (Arthurson, 2009). Since pollutants and pathogens may be present in the digestate (Owamah et al., 2014), regulations exist to ensure that the concentrations of these potentially dangerous compounds are far from posing any risk to human health or to the environment. In addition, another essential point to be considered is the public acceptance of digestate recycling and its acceptance by farmers, who may be reluctant to this approach if it does not provide obvious benefits.

Regarding the European regulations dealing with FW, which are among the most restrictive ones, FW contaminated or containing meat or any other product of animal origin are considered animal by-products (ABPs) and are therefore subject to ABPs regulations. FW, including biowaste from restaurants, markets and households, fall within the least dangerous group of ABPs (3) (European Community, 2009). For these residues, hygienization is required before their application on land. According to the current regulation, “any biogas production process must be equipped with a pasteurization/hygienization unit (particle size lower than 12 mm; minimum 70 ºC; minimum 60 min)” (European Community, 2011). To

fulfil this requirement FW must be pretreated for removal of impurities and for pasteurization, usually before entering the digester.

Nevertheless, regulations also offer other alternatives which are often applied. Instead of pasteurization upstream, it is possible to compost the digestate produced before land usage, which also ensures its stabilization and an adequate pathogen removal. However, the low biodegradability of digestate leads to a low rise in temperature during composting and thus, co-composting with other organic substrates is usually necessary to ensure disinfection (Zeng et al., 2015). The law also states that "the competent authority can authorize the utilization of other processes provided that an adequate decrease of the biological risks is guaranteed". Moreover, especially for waste coming from kitchen or restaurants, the competent authority is also allowed to define specific hygienization demands other than those suggested in the regulation, provided that an adequate decrease of the biological risks is guaranteed.

The possibility of approval by local authorities of different options for dealing with digestate has led to the development of other hygienization alternatives. The main limitation of pasteurization is its extensive energy requirements. Banks et al. (2011a) performed an energy balance of an AD plant treating FW, concluding that digestate pasteurization represented 34 % of the total heat requirement of the treatment plant. Therefore, most of the other options aim to skip this step. A particularly interesting approach is integrated thermophilic sanitation (Grim et al., 2015). This alternative for hygienization, which is already approved by the Swedish Environmental Protection Agency, consists on direct sanitation by AD at thermophilic temperatures (52-60 ºC), with a minimum exposure time in the digesters. Kjerstadius et al. (2013) proved that AD of sewage sludge during 55 ºC and 2 h reached the EU and Swedish limits for pathogen reduction. Following this approach, Grim et al. (2015) concluded that the substitution of pasteurization for integrated thermophilic sanitation in a full-scale plant in Sweden could reduce the plant heat demand by 46 %.

In order to make recycling of digestate by on land application a feasible proposition, the safety of the different hygienization approaches, including novel alternatives, and the value of this residue as fertilizer must be confirmed (Arthurson, 2009). Moreover, regulations should be reviewed to allow less energy demanding hygienization processes (Iacovidou et al., 2012) and to stimulate the agricultural sector to develop this huge market opportunity for digestate from AD.

1.2.5.3 Process integration: biorefinery for food waste valorization

The concept of biorefinery is based upon the idea of bioprocess integration to convert biomass into a variety of marketable products and energy (Mohan, 2016). The objective is to design a waste treatment facility that is self-sufficient, environmentally sustainable and economically beneficial. From the infinite number of biorefinery models that can be proposed, a promising option is the so-called "acidogenic model", described by Venkata et al. (2016). This process may combine a 1st DF step for hydrogen, alcohol and VFA production and purification, with a 2nd step for generation of methane by AD. Recently, Sawatdeenarunat et al. (2016) reviewed the concept of anaerobic biorefinery, indicating several options for biogas, digestate and liquid effluent valorization. They pointed out the enhancement that this process integration could pose for the economic viability of AD processes, mentioning also FW as a biomass with huge potential as feedstock.

Following this biorefinery approach, different studies have been performed to evaluate the integration of several processes for FW treatment. Lü et al. (2016) demonstrated the influence of the storage time on the BMP of FW. This step acted as a pretreatment, increasing the acidification efficiency at larger storage times. This proves the importance of process integration at the earliest stages of FW management. Using FW as substrate, different authors have demonstrated the feasibility of bioprocess integration to obtain several products, such as ethanol and methane (Koike et al., 2009), hydrogen by dark-photofermentation and methane (Ghimire et al., 2015b), hydrogen by yeast fermentation and photosynthetic bacteria (Mekjinda and Ritchie, 2015), hydrogen by DF and photofermentation (Zong et al., 2009), lactic acid, hydrogen by photofermentation and methane in a 3-phase system (Kim and Kim, 2013), lactic acid and methane (Kim et al., 2016) or hydrogen by extractive electrofermentation and photofermentation (Redwood et al., 2012). In a recent study, Wen et al. (2016) assessed the economics and environmental performance of a FW treatment pilot plant integrating AD with protein feed and biodiesel production. They concluded that the facility showed strong environmental and economic performances, mainly due to the diversification of outputs.

In an attempt to integrate the anaerobic processes described in this review, a model biorefinery is proposed in Figure 1.5. In this biorefinery, after FW conditioning and pretreatment, DF would take place in the 1st reactor, producing hydrogen and other fermentation products. The liquid fraction (mainly composed of VFAs) would be separated for purification and valorization (*e.g.*, as carbon source for nitrogen removal or for algae growth for nutrient recovery). The concentrated fraction would be feed into a dry AD reactor,

producing methane and digestate. A co-substrate could be added if required, *e.g.* to provide buffer capacity, to increase the TS content or for TEs supplementation. A solution containing TEs could also be added if needed. The liquid fraction of the resulting digestate would be used for pH control in the DF reactor and the solid fraction would be partially recirculated to the AD stage to inoculate and to achieve a more stable process. The remaining solid digestate (already hygienized by thermophilic AD) could be used directly for soil amendment as fertilizer. Due to the high TS content of FW, both DF and AD processes could be carried out under dry (TS ≥ 20 %) or semi-dry (10% ≥ TS > 20 %) conditions. Commercial designs suitable for the working conditions of each stage could be applied. Systems commonly applied worldwide such as DRANCO or Valorga processes (vertical continuous reactors; common OLRs of 10-15 kg $VS \cdot m^{-3} \cdot d^{-1}$) for the DF reactor and Kompogas (horizontal continuous reactor; common OLRs of ~4 kg $VS \cdot m^{-3} \cdot d^{-1}$) for the AD reactor could be used (Karthikeyan and Visvanathan, 2013).

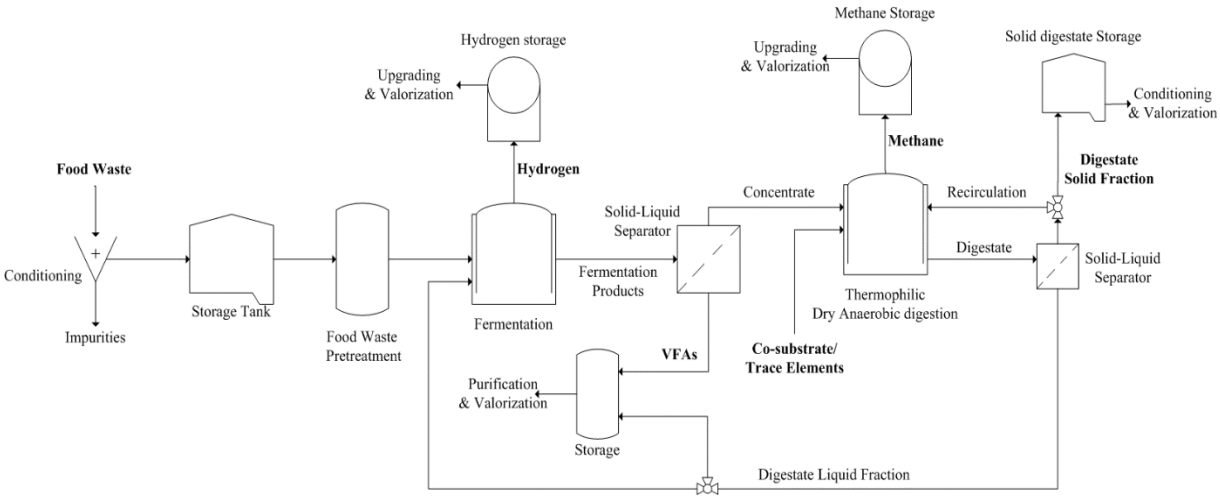

Figure 1.5. Scheme of a proposed biorefinery for FW valorization, integrating DF, recuperation of VFAs and AD

A biorefinery such as the one presented above should show high energy efficiencies, applying mostly zero-waste production processes and allowing industries to generate environmental friendly products (Venkata et al., 2016). To evaluate the feasibility of such facilities, more research is required for process optimization. Also, studies applying a holistic approach are needed to assess the economics and environmental performance of these systems, considering the entire process as an integrated waste treatment strategy.

Finally, the application of pure cultures must be mentioned in this section even if these processes are out of the main scope of this document. These options have the main advantage of producing high value-added compounds (*i.e.* ethanol, lactate or caproate) and therefore,

they have the potential for improving greatly the economic viability of a FW biorefinery if coupled with any of the processes mentioned above. Some promising alternatives have already been tested with FW as substrate, such as ethanol production by *Saccharomyces cerevisiae* (Uçkun Kiran and Liu, 2015), lactic acid production by *Bacillus coagulans* after production of lipid-rich *Chlorella pyrenoidosa* biomass for nutrient recovery from FW hydrolysate (Pleissner et al., 2015) or fatty acids production by *A. niger* for biodiesel generation (Papanikolaou et al., 2011). Further information about the application of pure cultures using FW as substrate can be found elsewhere (Girotto et al., 2015; Pham et al., 2014; Uçkun Kiran et al., 2014).

1.2.6 *Conclusions*

The increasing FW production worldwide and new regulations create the need for the development of new technologies for FW treatment. Anaerobic processes are a promising alternative. Single-stage AD appears as a reliable alternative for methane production. Besides the complications associated with this process, caused primarily by TAN and VFA accumulation, several options have been proven to be effective to stabilize the AD, such as TEs addition, solid digestate recirculation or co-digestion with other biomasses. Regarding DF, FW has a great potential for biohydrogen production, even without addition of external inoculum or without pretreatment. The production of VFAs remains as a non-mature promising alternative that deserves further research due to its great economic potential. For both fermentations, co-digestion to supply buffering capacity has been effectively used, avoiding the need of an external buffer. 2-stage systems appear also as a promising option to produce hydrogen and methane from FW. Recent advances such as digestate recirculation to control the pH in the 1st stage or co-digestion have a tremendous potential to improve the performance of 2-stage AD. Eventually, an integrated biorefinery approach should be taken, moving towards a circular economy and obtaining the most out of the FW. Scientific, social and political advances must be pursued and achieved before this idea can become a reality, moving our society to a cleaner and more sustainable future.

1.3 General conclusions and objectives of the PhD thesis

Several options exist for the anaerobic treatment of FW. Among them, single-stage AD appears as a reliable alternative for FW valorization via methane production. However, different complications are associated with this option, mainly due to TAN and VFA accumulation. Although different alternatives have been applied for stabilizing AD FW, such

as TEs addition, solid digestate recirculation or co-digestion with other substrates, a wide heterogeneity exists on the obtained results, mainly due to the different characteristics of the FW digested and the microbial inoculum used and because of the different operational conditions applied. In addition, barely any optimization focused on these alternatives has been carried out. Dealing with AD of undiluted FW (with high TS contents), a lack of knowledge exists regarding the best options to stabilize the process and the optimal operational conditions.

In this context, the scientific objectives of the thesis were mainly focused on understanding the biochemical processes governing the bioreactors and on finding a reliable stabilization option for achieving an efficient FW AD. Figure 1.6 shows a schematic representation of the objectives pursued in each chapter of the thesis.

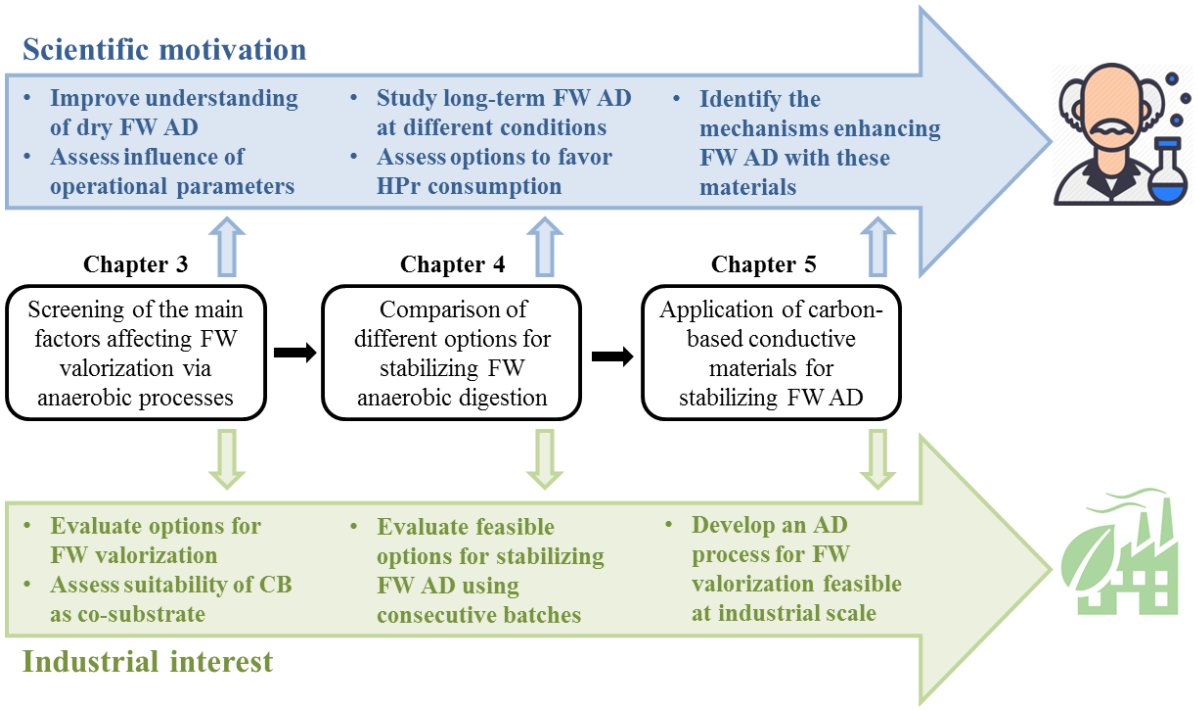

Figure 1.6. Schematic representation of the objectives pursued in each chapter of the thesis, both from a scientific and an industrial point of view. FW stands for food waste, AD for anaerobic digestion, HPr for propionic acid and CB for cardboard

As it can be observed, the global goal of the experiments presented in Chapter 3 was to evaluate and screen the main factors affecting FW valorization via anaerobic digestion processes. The influence of the TS content, the S/X ratio and the co-digestion ratio (co-digestion with CB) on the AD and DF performances was studied. In addition, different microbial inocula were used and analyzed, aiming to elucidate the type of the microorganisms involved in each process and their relevance.

The second stage of the thesis (Chapter 4) was focused on the evaluation of three different alternatives for stabilizing FW AD using consecutive batch reactors: (i) working at low temperatures, (ii) co-digestion of FW with CB and (iii) addition of TEs. Different options to favor the consumption of the accumulated VFAs (*i.e.* addition of TEs, GAC and digestate dilution) were also investigated.

Finally, Chapter 5 was dedicated to elucidate the effect of adding carbon-based conductive materials (together with TEs) on the VFA accumulation during FW AD. GAC was firstly applied to study the mechanisms involved on the process and woody biochar was used afterwards as a cheaper alternative, aiming to develop an industrially-feasible process for FW valorization via AD.

Deeper discussions on the particular objectives can be found in the respective sections. Moreover, a summary of the experiments carried out, their objectives and the materials applied is given in Table 2.3.

Chapter 2. Materials and methods

2.1 Overview of materials and methods

This chapter aims to introduce the materials used during the thesis, as well as the experimental methodologies followed. The substrates used and the general equipment are precisely described. In addition, the applied analytical methods, the molecular biology techniques and the mathematical and statistical approaches used to treat the experimental data are also explained. At the end of this chapter a summary is given (Section 2.8), including the different materials and methods applied in each experiments. The specific experimental designs used in the experiments are presented in the corresponding sections.

2.2 Substrates and inocula

2.2.1 *Synthetic food waste*

A model FW was prepared according to the VALORGAS report (VALORGAS, 2010) and used as substrate for the experiments presented in Chapter 3. Its composition is shown in Table 2.1. The FW mixture was finely milled and blended to ensure its homogeneity.

Table 2.1. Components of the model food waste

Component	Ingredient	Proportion (% in wet basis)
Fruits and vegetables	Apples	25.9
	Lettuce	25.9
	Potato	25.9
Pasta/rice/flour/cereals	Couscous	4.80
Bread and bakery	Bread	6.20
Meat and fish	Chicken	4.10
	Beef	4.10
Dairy products	Cheese	1.90
Confectionery/snacks	Biscuits	1.50

2.2.2 *Commercial food waste*

Within the project of the thesis a FW test collection was started. The FW flux was measured weekly and the different sampling campaigns carried out throughout the three years allowed to assess the FW characteristics and its seasonal variations (results presented in Appendix B). In this manuscript, only the results corresponding to the FW used as substrate for the AD experiments presented in Chapter 4 and Chapter 5 are shown. The waste collection was carried out in the region of the Grand Narbonne, in the south of France. Five different mayor FW producers were used as representative examples of potential FW suppliers: (1) fast

food restaurant, (2) restaurant, (3) supermarket, (4) fruit and vegetable supermarket and (5) fruit and vegetable distribution. Pictures of these wastes are shown in Figure 2.1. A proportional mixture (wet weight basis) of the different FWs was used as substrate for the experiments.

Figure 2.1. Pictures of the commercial food wastes used as substrates: fast food restaurant (upper left), restaurant (upper center), supermarket (upper right), fruit and vegetable supermarket (down left) and fruit and vegetable distribution (down right)

2.2.3 *Paper and cardboard waste*

As it will be further explained, compact cardboard (CB) and paper waste (PW) were used as co-substrate for FW AD. The CB used (branded ‘‘Cartonnages Michel’’) had a density of 1.42 $kg \cdot m^{-3}$ and was shredded to less than 1 mm. The PW consisted of regular white office paper shredded to less than 1 cm.

2.2.4 *Microbial inocula*

As it will be further discussed in Section 3.5, inocula issued from different industrial facilities were used for this thesis.

For the experiments carried out at high TS contents (Sections 3.2 and 3.3), the microbial inoculum consisted on a mixture of (i) a centrifuged granular sludge issued from a mesophilic

industrial UASB (Up-flow Anaerobic Sludge Blanket) reactor treating sugar factory effluents and (ii) a dried digestate originated from a thermophilic industrial plant treating the organic fraction of municipal solid waste used only to increase the TS content. This latter digestate was dried at 105 °C for at least 24 hours and the resulting material was finely milled and sieved at 1 cm. Both fractions were mixed in a proportion 1:2 (wet weight basis), obtaining an inoculum with TS of 74.19 % (59.06 % VS/TS) and 70.78 % (70.85 % VS/TS) for Sections 3.2 and 3.3, respectively. The high TS proportion of the inoculum allowed starting the reactors at TS contents up to 40 %. Although this process resulted in a very particular inoculum, this was the only possible way to achieve the desired TS contents in the reactors. This allowed elucidating clearly the influence of this parameter on the AD process. In addition, the dried digestate added was the source of solids closest to those that can be found in a regular high-solid digestate.

The inoculum used for the rest of the experiments (Section 3.4, Chapter 4 and Chapter 5) was initially collected from an industrial plant digesting different organic streams at high TAN/FAN concentrations (5.04 g $TAN \cdot l^{-1}$; 0.615 g $FAN \cdot l^{-1}$). Thus, it was assumed that the microbial population was already adapted to high FAN concentrations, such as those existing during FW AD. The sludge had a TS content of 5.81±0.02 %, with 59.13±0.08 % corresponding to volatile solids (VS).

2.3 Additives tested to stabilize the AD process

2.3.1 *Trace elements*

Trace elements (TEs) were added into some reactors during the experiments presented in Chapter 4 and Chapter 5. The concentrations of TEs supplied were: 100 $mg \cdot l^{-1}$ Fe, 1 $mg \cdot l^{-1}$ Co, 5 $mg \cdot l^{-1}$ Mo, 5 $mg \cdot l^{-1}$ Ni, 0.2 $mg \cdot l^{-1}$ Se, 0.2 $mg \cdot l^{-1}$ Zn, 0.1 $mg \cdot l^{-1}$ Cu, 1 $mg \cdot l^{-1}$ Mn. These values were calculated from optimal results reported in the literature (Banks et al., 2012; Zhang and Jahng, 2012; Wanli Zhang et al., 2015b). The required volume of a concentrated solution (x100) containing $FeCl_2 \cdot 4H_2O$, $CoCl_2 \cdot 6H_2O$, $Na_2MoO_4 \cdot 2H_2O$, $NiCl_2 \cdot 6H_2O$, Na_2SeO_3, $ZnCl_2 \cdot 2H_2O$, $CuCl_2 \cdot 2H_2O$, $MnCl_2 \cdot 4H_2O$ was used for doping the reactors.

2.3.2 *Industrial $FeCl_3$*

As a cheaper alternative to the addition of pure TEs, industrial $FeCl_3$ (commonly applied for pH regulation in wastewater treatment plants and AD plants) was dosed into the reactors (Chapter 5). The composition of the industrial $FeCl_3$ solution (supplied by SUEZ) is shown in Table 5.9.

2.3.3 *Granular activated carbon*

Granular activated carbon (GAC) was used as AD enhancer in different experiments of Chapter 5. The GAC corresponded to activated charcoal powder bought from Sigma-Aldrich (Missouri, United States of America; CAS 7440-44-0).

2.3.4 *Biochar*

Two different types of biochar were also supplemented into some reactors: pine-wood biochar (Section 5.3) and natural slow-pyrolyzed wood charcoal (Section 5.4.2). Before application the biochar was grinded and sieved (600 µm).

2.4 Reactors

2.4.1 *Discontinuous laboratory-scale reactors*

These reactors, with a total volume of 600 ml, were used to carry out the batch assays of Section 3.2. They consisted simply in glass vessels closed with a rubber cover that allowed sampling the gas from the headspace. A picture of these reactors is shown in Figure 2.2A1.

Figure 2.2. Pictures and schemes of the different reactors used during the thesis: (A1) discontinuous laboratory-scale reactors, (A2) AMPTSII system, (A3) discontinuous dry AD reactors and (B1 and B2) pilot-scale reactors

2.4.2 *Automatic methane potential test system (AMPTSII)*

The batch experiments described in Chapter 5 were incubated in an Automated Methane Potential Testing System (AMPTSII) (Bioprocess Control, Sweden). The AMPTSII system (Figure 2.2A2) consisted of 15 parallel reactors with a total volume of 500 ml and placed in a

thermostatic bath that automatically regulated the temperature. They were connected to CO_2 traps (NaOH solutions) and to gas flow meters to determine continuously the methane flow rate. The AMPTSII allowed agitating the reactors during one minute every 10 minutes at 40 rpm. Other than allowing an automatic measurement of the biogas produced, this system has the advantage of allowing sampling the digestate easily, through a hole present in each reactor than can be used as sampling port. Thus, the follow-up of the VFA kinetics was facilitated. It must be mentioned that, due to the small diameter of the sampling port, this sampling system cannot be used at high TS contents in the reactor. Because of this problem, the reactors presented in Section 2.4.3 were used.

2.4.3 *Discontinuous dry AD reactors*

During the experiments discussed in Sections 3.3 and 3.4 (and the batches in 4.2), it was required to sample the reacting medium to evaluate the dynamics of metabolites production-consumption during the digestion process. However, opening the reactors for sampling in high-solid systems leads to the introduction of air, which disturbs the anaerobic conditions in the reactor and modifies the physico-chemical equilibria (*e.g.* favoring CO_2 desorption). Therefore, a sampling system developed in the LBE was used (Motte et al., 2013). The corresponding reactor is depicted in Figure 2.2A3.

These vessel reactors were equipped with a "ball" valve on their tops, which allowed introducing a metallic sampler. During regular operation, a rubber septum on the top of the valve (opened) allowed monitoring the biogas production. When a sample was to be taken, the valve was closed and the septum was removed. Afterwards, the metallic sampler was fixed over the valve and the sampling volume was flushed with nitrogen. With no air in the sampling device, the blue valves shown in Figure 2.2A3 were closed and the ball valve was opened, allowing the sampling device to get into the reactor. Once the sample was taken, the valve was closed, the device removed and, after flushing the empty space with nitrogen, the septum was again placed over the valve. Finally, the valve was opened again. Using this sampling system, the disturbances of the headspace (only caused by nitrogen) were lower than one % in volume.

2.4.4 *Pilot-scale reactors*

The reactors consisted of cylindrical vessels made of stainless steel that were continuously mixed by inner stirring blades. The reactors had a double-wall system filled with water that regulated automatically the temperature. Two different reactor sizes were used, with total

volumes of 15 and 49 l. As it will be further explained in Section 2.5.2.2, the reactors had holes in the upper covers that allowed the biogas to be continuously measured. A schematic representation is shown in Figure 2.2B1 (15 l) and B2 (49 l). These reactors were fed in consecutive batch regime (Chapter 4 and Appendix A) and semi-continuously (fed five times per week) (Chapter 5).

2.5 Analytical methods

2.5.1 *Physicochemical characterization of the substrates*

The substrates were extensively characterized before starting the experiments. The TS and VS contents were measured according to the standard methods of the American Public Health Association (APHA, 2005).

After acid hydrolysis of the substrate with sulfuric acid (solution 10 % v/v H_2SO_4 98 % with one g $TS \cdot l^{-1}$ of substrate; agitation for 24 hours), the protein concentration was determined by the modified Lowry method (Frølund et al., 1996) and the carbohydrate concentration by the Dubois method (Dubois et al., 1956). The lipid content was measured using a gravimetric method (APHA, 2005) based on accelerated solvent extraction with heptane as solvent using an ASE®200, DIONEX (100 bar, 105 °C, 5 cycles of 10 min static and 100s purge) coupled to an evaporator MULTIVAPOR P-12, BUCHI. The proportions of cellulose, hemicellulose and lignin-like compounds in the substrates were determined according to the Van Soest procedure (Van Soest, 1963).

Total Kjeldahl nitrogen (TKN) and ammonia nitrogen contents were measured with an AutoKjehdahl Unit K-370, BUCHI. Total organic carbon (TOC) and inorganic carbon (IC) were determined using a Shimadzu TOC-V_{CSN} total organic carbon analyzer coupled to a Shimadzu ASI-V tube rack. The total carbon (TC) content corresponded to the sum of TOC and IC. The pH was measured using a WTW pHmeter series inoLab pH720. The chemical oxygen demand (COD) was analyzed using an Aqualytic 420721 COD Vario Tube Test MR (0-1500 $mg \cdot l^{-1}$). Two ml of sample were pipetted into each tube and then they were placed inside a HACH COD reactor at 150 °C for two hours. COD concentrations were determined using an Aqualytic MultiDirect spectrophotometer.

The biochemical methane potentials (BMPs) of the substrates were determined by measuring the amount of methane produced after the addition of a known quantity of substrate under non-limiting conditions (high inoculation ratio) (Angelidaki et al., 2009). The inoculum used was issued from an UASB reactor treating the effluent from a sugar factory

located in Marseille. A precise mass of substrate (around one g VS) was added into glass reactors with a total volume of 500 ml and mixed with the corresponding amount of sludge to keep a substrate to inoculum (S/X) ratio of 0.5 g VS·g VS^{-1}. To ensure optimal conditions for the digestions, different solutions were added: a bicarbonate buffer at 2.6 $g \cdot l^{-1}$ in the BMP reactor, a solution containing macroelements for microbial growth (concentrations in reactor of 229 $mg \cdot l^{-1}$ NH_4Cl, 86 $mg \cdot l^{-1}$ of KH_2PO_4, 52 $mg \cdot l^{-1}$ of $MgCl_2$, 26 $mg \cdot l^{-1}$ of $CaCl_2 \cdot 2H_2O$, 100 $mg \cdot l^{-1}$ of $Na_2S \cdot 9H_2O$) and a solution containing microelements (concentrations in reactor of 20 $mg \cdot l^{-1}$ $FeCl_2 \cdot 4H_2O$, 5 $mg \cdot l^{-1}$ $CoCl_2 \cdot 6H_2O$, 1 $mg \cdot l^{-1}$ $MnCl_2 \cdot 4H_2O$, 1 $mg \cdot l^{-1}$ $NiCl_2 \cdot 6H_2O$, 0.5 $mg \cdot l^{-1}$ of $ZnCl_2$, 0.5 $mg \cdot l^{-1}$ of H_3BO_3, 0.5 $mg \cdot l^{-1}$ of Na_2SeO_3, 0.4 $mg \cdot l^{-1}$ $CuCl_2 \cdot 2H_2O$, 0.1 $mg \cdot l^{-1}$ of $Na_2MoO_4 \cdot 2H_2O$). After addition of all the components, the volume was adjusted to 400 ml, the headspace was flushed with nitrogen and the vessels were closed. Blanks experiments (without substrate) were performed to take into account the endogenous respiration. Prior to its utilization, the activity of the inoculum was verified using ethanol as substrate (0.5 g COD·g VS^{-1}). The reactors were incubated at 35 °C under constant agitation. Each experiment was carried out in triplicate.

The concentrations of micro/macro-elements were measured by Aurea Agroscience© (Ardon, France) as follows: metallic trace elements were analyzed by water extraction, according to the norm NF EN 13346. The determination of the Cd, Cr, Cu, Ni, Pb, Al, Mo, Co, Zn and As concentrations was performed by plasma emission spectrometry, in accordance with the NF EN ISO 11885. Hg was measured by elementary analysis (internal method), according to the norm NF EN ISO 12338. The concentrations of total P, K, Mg, Ca, S and Na were measured according to NF EN ISO 11885.

2.5.2 *Gas quantification and analysis*

Different methods were applied according to the reactors used and specific requirements.

2.5.2.1 Pressure difference

The amount of biogas produced in the BMPs and in the discontinuous reactors presented in Sections 2.4.1 and 2.4.3 was determined by measuring the pressure in the headspace (using a Manometer LEO 2 Keller with a resolution of one mbar), according to Equation 2.1.

$$\Delta V_i = \left[\frac{(y_i \cdot P_i - y_{i-1} \cdot P_{i-1}) \cdot V_{Headspace}}{T}\right] \cdot \frac{T_0}{P_0} \qquad \text{Equation 2.1}$$

Where ΔV_i is the volume of gas produced between time i and i-1, y_i is the percentage of the gas to determine (one for the total biogas production) at time i, P_i is the pressure at time i,

y_{i-1} is the percentage of the gas to determine at time i-1, P_{i-1} is the pressure at time i-1, $V_{Headspace}$ is the volume of the headspace of the reactors, T is the temperature and T_0 and P_0 are the standard temperature and pressure conditions to normalize the volumes of gas produced (0 °C and 1013 hPa). Blanks reactors (containing only sludge) were always carried out to take into account the endogenous respiration to be subtracted from the cumulative biogas productions.

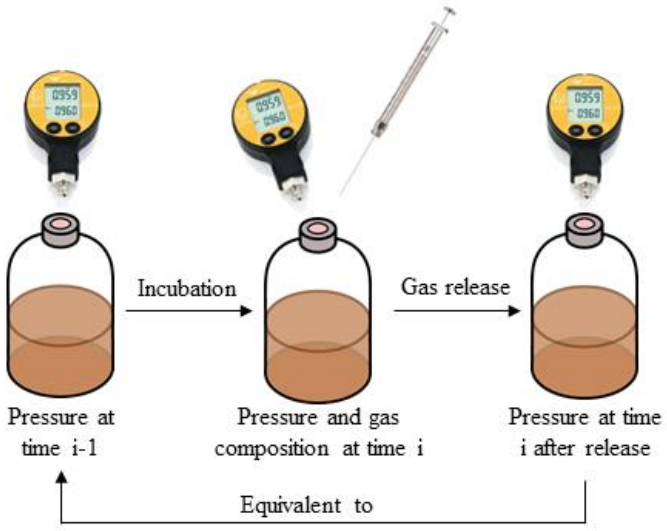

Figure 2.3. Follow-up of the gas production by pressure difference

2.5.2.2 Volumetric flow meters

The biogas production in the pilot reactors used in Chapter 4 and Chapter 5 was measured using volumetric flow meters (Ritter, Bochum, Germany). According to the expected biogas volume to be produced, Drum-type or MilliGascounters were connected to the reactors. In both cases, the flow meters allowed to register the biogas produced continuously. This, together with regular measurement of the biogas composition, enabled to determine the kinetics of biogas production, as well as that of methane. To calculate the methane produced in the interval of time between two measurements of the gas composition, the total amount of biogas generated was multiplied by the arithmetic average of both methane contents.

2.5.2.3 Automatic methane potential test system (AMPTSII)

As aforementioned, the reactors in the AMPTSII were connected to CO_2 traps (100 ml flasks containing 80 ml of 3M NaOH solutions with thymolphthalein as indicator) and to gas automatic gas flow meters to determine continuously the methane flow rate.

2.5.2.4 Gas chromatography (GC)

The composition of the biogas produced was determined by gas chromatography (GC; Clarus 580, Perkin Elmer) equipped with a thermal conductivity detector. The columns used

were an RtQbond column (for H_2, O_2, N_2 and CH_4) and an RtMolsieve column (for CO_2) and the gas vector was argon at a pressure of 3.5 bars.

2.5.3 *Analysis of metabolites and ionic species*

The digestate samples were heavily analyzed according to the objective of the experiments. Figure 2.4 shows a schematic representation of all the possible treatments applied.

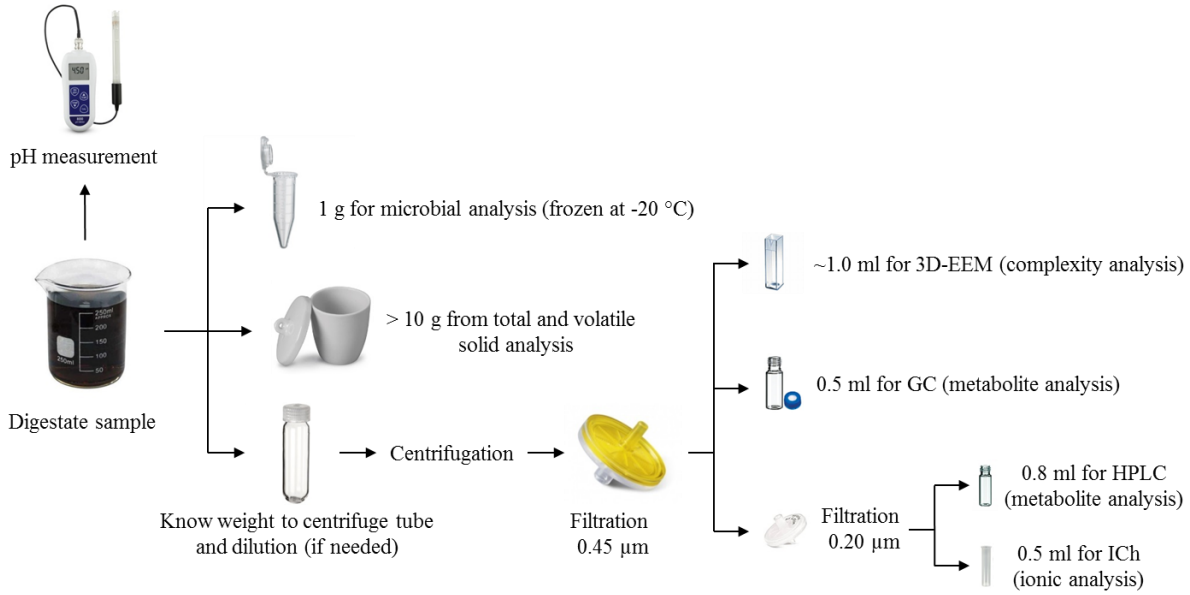

Figure 2.4. Schematic representation of the procedure followed to analyze the digestates

Immediately after digestate sampling, the pH was measured to minimize the effect of gas desorption. Afterwards, around one g of sample was placed into an Eppendorf tube (previously sterilized) and kept frozen at –20 °C until the microbial analysis was carried out. To be able to interpret the real-time polymerase chain reaction (qPCR) results, the amount of sample was precisely determined using a high-precision balance. Another fraction of the digestate sample was using for measuring the TS and VS contents (if required). To reduce the errors caused due to the heterogeneity of the digestates, a minimum of 10 g of digestate was used and the measurement was carried out in triplicate. A last fraction of the digestate was used for analysis of the soluble compounds. For this purpose, a known amount of sample was placed into centrifuge tubes and diluted with water (if needed for extraction of the soluble compounds). After centrifugation of the samples (15 min at 18600 rpm), the supernatant was filtered at 0.45 µm, and 0.5 ml was used for metabolite analysis by gas chromatography (GC). The rest of the supernatant was further filtered at 0.20 µm, and 0.8 ml and 0.5 ml were used for metabolite analysis by high-performance liquid chromatography (HPLC) and for analysis of the ionic species by ion chromatography (ICh), respectively.

2.5.3.1 Gas chromatography (GC)

The concentration of VFAs was determined by GC (Perkin Clarus 580). The GC consisted of an injector (at 250 °C), a capillary column (Elite-FFAP crossbond carbowax; 15 m; at 200 °C) and a flame ionization detector (at 280 °C). The mobile phase was nitrogen gas at a flow rate of six $ml \cdot min^{-1}$. Before analysis, the samples were mixed with a solution of one $g \cdot l^{-1}$ of éthyle-2-butyrique acid at proportions 1:1 volume (acting as internal standard).

2.5.3.2 High-performance liquid chromatography (HPLC)

The concentrations of soluble metabolites other than VFAs (*i.e.* lactic acid or ethanol) were measured by HPLC. The HPLC was equipped with a refractive index detector (Waters R410), an autosampler (Water 717 plus), a pre-column (Micro-Guard cation H refill cartbridges, Bio-rad) for filtering potential remaining residues and a column Aminex HPX-87H, 300 x 7.8 mm (Bio-Rad). The temperature of the column was 35 °C and H_2SO_4 4 mM was used as mobile phase at a flow rate of 0.4 $ml \cdot min^{-1}$.

2.5.3.3 Ion chromatography (ICh)

The concentrations of ions (namely NH_4^+, Na^+, K^+, Ca^{2+}, Cl^-, SO_4^{2-}) was measured by ICh, using a DIONEX ICS-3000. Two different systems (one for cations and another for anions) were run in parallel. Each of them consisted of an isocratic pump, a pre-column to avoid ionic contamination and polar compounds, a chemical suppressor to minimize the conductivity of the eluent (CSRS-300-2 mm for anions and ASRS-300-2 mm for cations), the respective separation system and a conductimeter to determine the total conductivity (and thus the concentration) for each ion. The separation system for cations detection consisted of a guard column (CG16 3 mm) and a separation column (CS16 3 mm). HMSA was used as eluent. For anions, the separation system consisted of a second pre-column (CG11 2 mm), a guard column (AG15 2 mm), a separation column (AS15 2 mm) and a carbonate trap (CR-ATC). KOH was used as eluent in this case. And automatic sampler (AS 40) was coupled to the system. The temperature of the columns was of 35 °C, the concentrations of the eluents was 10 mM and the flow rate for anions and cations was 0.30 and 0.35 $ml \cdot min^{-1}$, respectively.

2.5.4 *Fluorescence spectroscopy analysis*

The composition and the complexity of the soluble matter in the digestates obtained after AD in Section 3.4 were assessed by 3 Dimension Excitation Emission Matrix Fluorescence Spectroscopy (3D-EEM). The sample was centrifuged, filtered to 0.45 µm and diluted to a COD concentration of 3-10 $mg \cdot l^{-1}$ (Jimenez et al., 2015). As described in Jimenez et al. (2015), the spectra obtained by 3D-EEM can be decomposed on seven zones according to the

fluorescence of each biochemical molecules, which varies according to their complexity. Thus, fluorescent regions I, II and III represent simple compounds (Tyrosine-like simple aromatic proteins, Tryptophan-like simple aromatic proteins and soluble microbial products, respectively) and regions IV, V, VI and VII stand for complex matter (fulvic acid-like, glycolated proteins-like, lignocellulosic-like and humic acid-like, respectively). A technical description of the methodology applied can be found elsewhere (Jimenez et al., 2015).

2.5.5 *Granulometry*

The particle size distribution of the GAC and the biochar used in Chapter 5 was determined using a Z2 Coulter Counter granulometer. Before analysis, the samples had to be filtered in case particles with a diameter higher than 60 µm were present in the solution. The maximum concentration of particles in the samples was 10^5 events par ml.

2.6 Molecular biology techniques and microscopic observations

The structure of the bacterial and archaeal communities in the inocula and the digestates were studied following the procedure described in Figure 2.5.

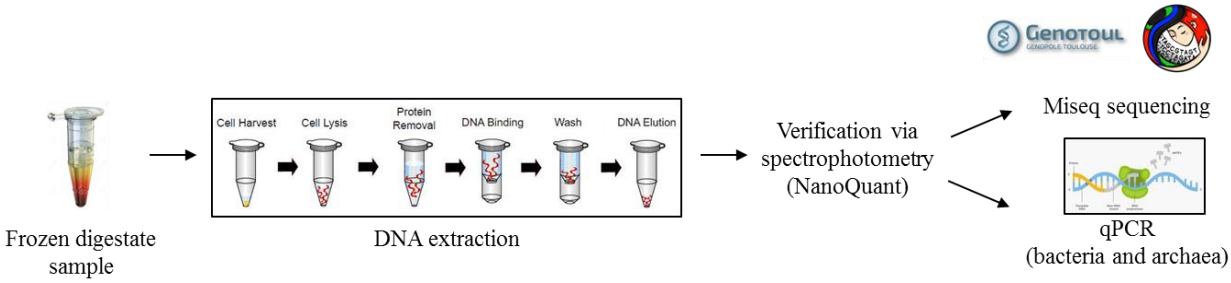

Figure 2.5. Schematic representation of the procedure followed to study the microbial communities

The frozen samples were directly taken for DNA extraction. Afterwards, the quality and quantity of the extracted DNA was verified using spectrophotometry and, if the extraction had been successful, the samples were used for 16S rRNA quantification by real-time polymerase chain reaction (qPCR) and for 16S metagenomic sequencing.

2.6.1 *DNA Extraction*

The DNA was extracted using a Fast DNA SPIN kit for soil in accordance with the instructions of the manufacturer (MP Biomedicals). The quality and quantity of the extracted DNA were verified by spectrophotometry using an Infinite 200 PRO NanoQuant (Tecan Group Ltd., Männedorf, Switzerland).

2.6.2 *Real-time polymerase chain reaction (qPCR)*

The real-time PCR plates were prepared using 96-well PCRs (Eppendorf, Hamburg, Germany) in a Mastercycler ep gradient S (Eppendorf, Hamburg, Germany). The components added to the plates were: 6.5 µl of Express qPCR Supermix with premixed ROX (Invitrogen, France), 8 nM TaqMan probe, 2 µl of DNA extract with three appropriate dilutions, 10 nM of primers (see Table 2.2) and water (to obtain a final volume of 12.5 µl).

Table 2.2. Primers used for the qPCR analyses

Specificity	Name	Sequence 5'-3'
Bacteria	BAC338F	ACTCC TACGG GAGGC AG
	BAC805R	GACTA CCAGG GTATC TAATC C
	BAC16F	TGCCA GCAGC CGCGG TAATA C
Archaea	ARC787F	ATTAG ATACC CSBGT AGTCC
	ARC1059R	GCCAT GCACC WCCTC T
	ARC915F	AGGAA TTGGC GGGGG AGCAC

According to the procedure described in Braun et al. (2011), the PCR consisted on an initial incubation of 20 s at 95 °C, followed by 40 cycles of denaturation (95 °C, 15 s; 60 °C, 1 min). For the quantification, one standard curve was created by using 10-fold dilutions in sterilized water (Aguettant Laboratory, Lyon, France) of the PCR products from known environmental clones. The clones used for calibration of bacteria and archaea were DF10 and LC103, respectively. The quantification of the initial DNA concentrations was performed by spectrophotometry using an Infinite 200 PRO NanoQuant (Tecan Group Ltd., Männedorf, Switzerland). According to Klappenbach et al. (2001), the average numbers of archaeal and bacterial cells were estimated by dividing the average number of 16S rRNA gene copies per cell by factors of 1.76 and 4.1, respectively.

To evaluate the growth or decay of a microbial population, the number of times the population was doubled (N_g; growth rate) was calculated by:

$$N_g = \frac{\ln(\frac{X_f}{X_i})}{\ln(2)} = \log_2(\frac{X_f}{X_i}) \qquad \text{Equation 2.2}$$

Where X_i and X_f are the initial and final concentrations of 16S copies respectively.

The qPCR measurements were performed in triplicate to assess the technical standard error associated with the measurement (σ). The raw qPCR results were log2 transformed and the

variance between replicates was used to calculate σ. It was considered that no growth (or decay) existed when values of N_g lower than twice σ were observed.

2.6.3 *MiSeq sequencing*

The primer pairs 515-532U and 909-928U and their respective linkers were used to amplify the V4-V5 regions of the 16S rRNA genes (over 30 amplification cycles were applied at an annealing temperature of 65 °C). These primer pairs target both bacterial and archaeal 16S rRNA genes, capturing most of their diversity (Wang and Qian, 2009). The PCR mixtures had a total volume of 50 µl, containing: 0.5 units of Pfu Turbo DNA polymerase (Stratagene), the corresponding buffer, each deoxynucleotide at 200 mM, each primer at 0.5 mM and 10 ng of genomic DNA. The following PCR sequence was carried out (using a Mastercycler thermal cycler; Eppendorf): after 94 °C for 2 min, 35 cycles of 94 °C for 1 min, 65 °C for 1 min, and 72 °C for 1 min were applied, with a final extension at 72 °C for 10 min. The obtained products were purified and analyzed using the Illumina MiSeq cartridge (v3 chemistry) for sequencing of paired 300 bp reads at the GenoToul platform (http://www.genotoul.fr). Mothur (version 1.35.0) was used for sequence assembling, cleaning and alignment and for assignation of the taxonomic affiliation, as described in Venkiteshwaran et al. (2016). It must be mentioned that the Operational Taxonomic Units (OTUs) are generally defined from 16S rRNA copies.

2.6.4 *Microscopic observations*

The presence of bacterial and archaeal biofilms was qualitatively assessed using coloration and fluorescence microscopy in Section 5.2. DNA was colored using DAPI (4',6-diamino-2-fenilindol). A diluted digestate sample was mixed with the DAPI solution (25 $\mu g \cdot ml^{-1}$) at a volumetric ratio of 19:1 and the mixture was incubated at ambient temperature for 20 min. The natural fluorescence of methanogenic archaea at 420 nm (due to the coenzyme F_{420}) was used for their observation. To avoid crushing the GAC particles (and thus the biofilm), the samples were fixed in agar (1.5% in Tris pH 7.5 0.1M) and covered with a layer of Milli-Q water (around 1 mm deep). A submergible lens (Olympus UM Plan FLN 60x/1.00) coupled to a microscope Olympus BX53, a motorized reflected fluorescence system (Olympus BX3-RFAA) and a control box (Olympus U-CBM) was used.

2.7 Data treatment and analysis

2.7.1 *Process modelling*

2.7.1.1 Modified Gompertz equation

The cumulative methane yields (M) presented in Sections 3.2 and 4.2 were fit to the modified Gompertz equation (Zwietering et al., 1990), adjusting the three parameters of the equation: final methane yield, (M_{max}, ml $CH_4 \cdot g\ VS^{-1}$), maximum methane production rate, (R_m, ml $CH_4 \cdot g\ VS^{-1} \cdot d^{-1}$), and lag phase (L, d). The corresponding expression is shown in Equation 2.3.

$$M(t) = M_{max} \cdot exp\left\{-exp\left[\frac{R_m}{M_{max}} \cdot (L - t) + 1\right]\right\} \qquad \text{Equation 2.3}$$

The cumulative methane productions obtained in Section 3.4 were also fitted to this model. In this case, the units of M_{max} and R_m were ml CH_4 and ml $CH_4 \cdot d^{-1}$, respectively.

2.7.2 *Statistical analysis*

2.7.2.1 Regression analysis

Linear and non-linear regression analyses were performed to adjust some of the obtained data to theoretical models and linear correlations between variables were investigated. The least squares method was used in both cases. To evaluate the goodness of fit of non-linear models, the predicted values were plotted against the real data. The resulting coefficient of determination (R^2) and the p-value obtained from an F-test (determining the percentage of variance explained by the model) were used as fitting indicators. The statistical analyses were computed using the statistical software R 3.2.5 (The R Foundation for Statistical Computing, Vienna, Austria). The functions “nls” and “cor” (from the package “corrplot”) were used.

2.7.2.2 Analysis of variance (ANOVA)

To evaluate if significant differences existed amongst the results obtained, analyses of variance (one-way ANOVAs) were applied in different sections. Tukey’s Post Hoc tests were performed to compare means when the differences were found to be significant. The ANOVAs were carried out using the software R (version 3.2.5, R Development Core Team 2010). The level of significance was set at 5 % (p-value < 0.05).

2.7.2.3 Principal component analysis (PCA)

To investigate relationships between the initial working parameters (*i.e.* TS content, S/X ratio and co-digestion ratio) and the fermentation products, principal component analyses

(PCAs) were carried out in Chapter 3. PCA is a mathematical procedure based on orthogonal linear transformation of the data. The input variables (whose correlation is to be studied) are transformed into uncorrelated principle components. These components are ordered according to the percentage of explained variability of the data that they represent. Therefore, the most relevant components have been chosen. The MixOmics R software package was used to perform the PCAs.

2.7.2.4 Hierarchical clustering analysis (HCA)

A dual hierarchal clustering analysis (HCA) was used to study the results from metagenomics in Section 3.3. To carry out the HCA, an Euclidean distance matrix was calculated with center-scaled variables. The clustering method applied was the "complete" linking method (Defays, 1977), contained in the "stats" R package. The definition of the number of groups present in the dendrogram was carried out following a heuristic approach, according to the initial conditions in the reactors. This will be further discussed in the corresponding section.

2.7.2.5 Design of experiments (DOE)

The design of experiments (DOE) methodology was applied in Section 5.4.2. This process allowed retrieving the maximum information from a reduced number of experimental conditions. This is achieved through modelling of the response of the system using quadratic expressions (Equation 2.4).

$$y = a_0 + \sum_{i-1}^{k} a_i \cdot x_i + \sum_{i-1}^{k} a_{ii} \cdot x_i^2 + \sum_{i<j}^{k} a_{ij} \cdot x_i \cdot x_j \qquad \text{Equation 2.4}$$

Where, y is the selected response to be predicted (and optimized), x_i are the factors studied and a_i, a_{ii} and a_{ij} are the parameters corresponding to each factor. They represent the linear, quadratic and interactional effects, respectively. The coefficient a_0 is required to adjust mathematically the model. Both the experimental design and the process modelling were carried out using the software Statgraphics Centurion XVI (version 16.1.03 StatPoint Technologies Inc.). To evaluate the goodness of fit of the obtained models, the R^2 and the p-values from the F-test applied to the global model and to each individual constant of the model were calculated. To keep the general structure of the document, the applied experimental design is presented in the corresponding section (Table 5.10).

2.7.3 *Thermodynamic calculations*

To support the experimental findings presented in Chapter 4, the lines of zero variation of Gibbs free energy were calculated for four reactions at different concentrations of acetic acid and hydrogen partial pressures. For this purpose, Equation 2.5 was used:

$$\Delta G' = \Delta G^0 + R \cdot T \cdot ln\left(\frac{[C]^c \cdot [D]^d}{[A]^a \cdot [B]^b}\right) \qquad \text{Equation 2.5}$$

Where, ΔG' is the variation of Gibbs free energy ($J \cdot mol^{-1}$), ΔG^0 the standard Gibbs free energy of the reaction ($J \cdot mol^{-1}$), R the ideal gas constant (8.314 $J \cdot mol^{-1} \cdot K^{-1}$), T the temperature (K) and $[I]^i$ are the concentrations and the stoichiometric coefficients in the reaction aA + bB ↔ cC + dD. The following conditions were assumed: 298 K, pH 7, 1 mM organic acids and 0.1 M HCO_3^- (Batstone et al., 2002). The ΔG^0 were taken from Zeeman (2005).

2.7.4 *General data treatment*

The methane yields were generally calculated by dividing the total volume of methane produced by the initial mass of VS of substrates. In the case of co-digestion experiments, the yields (of methane or other fermentation products) have been expressed in different units to allow un-biased comparisons. If so, this is specified in each section.

In addition, when sampling of the digestates was performed during the fermentation process to evaluate the kinetics of production-consumption of soluble metabolites, the withdrawn amount of digestate was considered. The yields of the different products were progressively corrected according to the quantity of digestate sampled, according to Equation 2.6.

$$Y_{prod} = \frac{\sum_{t=0}^{n} \Delta prod_{t,t-1}}{S_0} = \frac{\sum_{t=0}^{n} (prod_t - prod_{t-1}) \cdot \frac{m_0}{m_{t-1}}}{S_0} \qquad \text{Equation 2.6}$$

Where, Y_{prod} is the yield of the product, $\Delta prod_{t,t-1}$ is the amount of product generated between time t and time t-1, S_0 is the initial amount of substrate added, $prod_t$ and $prod_{t-1}$ are the amounts of products at t or t-1, respectively, m_0 is the initial useful mass of the reactor, and m_{t-1} is the mass of the reactor at time t-1.

Moreover, the headspace volume in the reactors also varied due to digestate sampling and thus, its value was also corrected to avoid errors when calculating the produced biogas by applying Equation 2.1.

Equation 2.7, derived from J. L. Chen et al., (2014), was used to calculate the concentration of free ammonia nitrogen (FAN) as a function of the pH, the temperature (T) and the total ammonia concentration (TAN) in the media.

$$NH_3 = NH_4^+ \cdot \frac{K_a}{\left(10^{-pH} \cdot \left[\frac{K_a}{10^{-pH}} + 1\right] - K_a\right)} \quad \text{Equation 2.7}$$

Where, K_a has a value of $1.097 \cdot 10^{-9}$ (35 °C) and the concentrations are expressed in $mg \cdot l^{-1}$.

To take into account the ionic strength of the media and avoid overestimating the FAN concentrations in Section 3.4 and Chapter 5 (with high concentrations of ionic species), an activity coefficient was calculated according to Equations 2.8-2.10 (Rajagopal et al., 2013b).

$$I = \frac{1}{2} \cdot \sum_i^n c_i \cdot z_i^2 \quad \text{Equation 2.8}$$

$$\log f_i = -A \cdot z_i^2 \cdot \frac{\sqrt{I}}{1 + B \cdot A_i \cdot \sqrt{I}} \quad \text{Equation 2.9}$$

$$NH_3 = TAN \cdot \frac{K_a \cdot f_{NH3}}{(10^{-pH} + K_a \cdot f_{NH3})} \quad \text{Equation 2.10}$$

Where, I is the ionic strength, c_i is the concentration of each ion (M), z_i is the charge of each ion, f is the activity coefficient, A and B are parameter depending on the dielectric constant of water, A_i is related to the size of each ion (value of 3 for NH_4^+) and TAN is the concentration of total ammonia nitrogen. The concentrations of the main ions present in the reactors were taken into account in this calculation (Cl^-, PO_4^{2-}, Na^+, NH_4^+, K^+, Mg^{2+}, H^+ and Ca^{2+}) (Rajagopal et al., 2013b).

Finally, it must be mentioned that the errors presented in the tables and figures of the document represent the standard deviations of the measurements.

2.8 Summary

To facilitate the follow-up of the experiments and the understanding of the reader, a summary of the experiments carried out, including their specific objectives and the parameters studied is presented in Table 2.3. In addition, the inocula, the substrate, the reactor type and the additives applied in each particular section are also described.

Finally, Table 2.4 summarizes the experimental techniques and methods applied in each experiment.

Table 2.3. Summary of the experiments carried out, their objectives and the materials applied

Chapter	Section	Objective	Parameters varied	Inoculum	Substrate	Reactor	Additives
Chapter 3	3.2	Evaluate feasibility of FW valorization via dry anaerobic co-digestion with CB	TS content; S/X ratio; co-digestion ratio	Mixture of centrifuged granular sludge dried digestate	Model FW; compact CB	Discontinuous laboratory-scale reactors	n.a.
	3.3	Assess feasibility of FW dry fermentation with CB as co-substrate	TS content; co-digestion ratio	Mixture of centrifuged granular sludge dried digestate	Model FW; compact CB	Discontinuous dry AD reactors	n.a.
	3.4	Study kinetics of methane production in mono-digestion of FW and its co-digestion with CB	TS content; S/X ratio; co-digestion ratio	Mixture of industrial digestate rich in TAN and compost	Model FW; compact CB	Discontinuous dry AD reactors	n.a.
	3.5	Study AD performance of three different microbial inocula	TS content; S/X ratio; co-digestion ratio	Three inocula shown above	Model FW; compact CB	Three reactors shown above	n.a.
Chapter 4	4.2	Compare the performances of co-digestion with PW, low reactor temperature and addition TEs for digestion stabilization	S/X ratio	Industrial digestate rich in TAN	Commercial FW; PW	Pilot scale reactors; discontinuous dry AD reactors	TEs
Chapter 5	5.2	Improve digestion kinetics by adding GAC and TEs	S/X ratio	Industrial digestate rich in TAN	Commercial FW	AMPTSII	TEs; GAC
	5.3	Asses maximum methane production rate in reactors containing GAC and TEs and test biochar and $FeCl_3$ as substitutes	S/X ratio	Industrial digestate rich in TAN	Commercial FW	AMPTSII	TEs; GAC; biochar; industrial $FeCl_3$
	5.4.2	Optimize dosage of biochar and $FeCl_3$ and substrate load in batch reactors; evaluate performance of continuous reactors doped with biochar and $FeCl_3$	Organic loading rate; concentration of biochar and $FeCl_3$; S/X ratio	Industrial digestate rich in TAN; digestate from pilot reactors	Commercial FW	AMPTSII; Pilot scale reactors	Biochar; industrial $FeCl_3$

FW stands for food waste, CB for cardboard, TS for total solids, S/X for substrate to inoculum, AD for anaerobic digestion, TAN for total ammonia nitrogen, TEs for trace elements, PW for paper waste, GAC for granular activated carbon and n.a. for not applied

Table 2.4. Experimental techniques and methods used in each experiment

Stage	Section	Technique	Objective/parameter measured
Characterization of substrates[1]	General[2]	Gravimetric method	Total and volatile solid content
		Lowry method	Protein content
		Dubois method	Carbohydrate content
		Gravimetric method	Lipid content
		Van Soest procedure	Cellulose, hemicellulose and lignin-like fractions
		Automatic titration	TKN and TAN
		Combustion catalytic oxidation-nondispersive infrared method	Total and inorganic carbon
		Dichromate oxidation-spectrophotometry	Chemical oxygen demand
		Inductively coupled plasma atomic emission spectroscopy	Metallic trace elements[3], macroelements[4]
Chapter 3: screening of main factors affecting FW AD	3.2, 3.3, 3.4	Pressure difference	Gas quantification
	3.2, 3.3, 3.4	GC[5]	Gas composition
	3.2, 3.3	HPLC[5]	Concentration metabolites
	3.4	GC[5]	Concentration metabolites
	3.2, 3.3, 3.4	ICh[5]	Concentration ionic species
	3.4	Fluorescence spectroscopy	Complexity soluble matter
	3.2, 3.3, 3.4	qPCR[5]	Quantification microorganisms
	3.2, 3.3, 3.4	Sequencing	Composition microbial communities
	3.2, 3.3	PCA[5]	Relationship variables and metabolites
	3.3	Dual HCA[5]	Structure of bacterial population
	3.4	Modified Gompertz	Kinetics methane production
	3.2, 3.3, 3.4	Regression analysis	Evaluate correlations
	3.2, 3.3, 3.4	ANOVA	Find statistical differences
Chapter 4: issue comparison of different stabilization options	4.2	Flow meters	Gas quantification
	4.2	GC[5]	Gas composition
	4.2	GC[5]	Concentration metabolites
	4.2	ICh[5]	Concentration ionic species
	4.2	Thermodynamic calculations	Support experimental results
	4.2	Modified Gompertz	Kinetics methane production
Chapter 5: application of carbon-based conductive materials	5.2, 5.3, 5.4.2	AMPTSII	Methane quantification
	5.4.2	Flow meters	Gas quantification
	5.4.2	GC[5]	Gas composition
	5.2, 5.3, 5.4.2	ICh[5]	Concentration ionic species
	5.4.2	Granulometry	Granulometry biochar
	5.2	qPCR[5]	Quantification microorganisms
	3.2, 3.3, 3.4	Sequencing	Composition microbial communities
	5.2	Fluorescence microscopy	Microscopic observations
	5.2, 5.3, 5.4.2	ANOVA[5]	Find statistical differences
	5.4.2	DOE[5]	Optimize a selected output

1. The assembly of results of the commercial FW characterization is presented and discussed in Appendix B
2. General stands for methods applied throughout the whole duration of the thesis
3. Cd, Cr, Cu, Ni, Pb, Al, Mo, Co, Zn and As
4. P, K, Mg, Ca, S and Na
5. TKN stands for total Kjeldahl nitrogen, TAN for total ammonia nitrogen, CG for gas chromatography, qPCR for real-time polymerase chain reaction, HPLC for high-performance liquid chromatography, ICh for ion chromatography, PCA for principal component analysis, HCA for hierarchical clustering analysis, ANOVA for analysis of variance and DOE for design of experiments

Chapter 3. FW valorization via dry AD: screening of main factors and importance of inoculum

3.1 General introduction

The main objective of this chapter was to evaluate and screen the main factors affecting the performance of AD processes for FW valorization at high solids contents, to produce fermentative metabolites and methane. Other than their shared goal, the experiments discussed in this chapter have been lumped together because they had a particularity when compared to the studies presented in the rest of the manuscript: the initial TS contents of the reactors were artificially increased in all the experiments. This procedure allowed to investigate the digestion performances at high TS contents, which otherwise would have been impossible due to the initial high water contents of the inocula. The interest of this approach lied on the initial intention of digesting continuously FW under dry conditions (*i.e.* in a dry plug flow reactor, such as a Kompogas system), which was thought to be feasible due to the high TS contents of the substrate itself. With the objective of further increasing the initial TS contents of the substrate and its C/N ratio, all the experiments presented in this chapter evaluated the co-digestion of FW with compact CB (see Section 2.2).

With this purpose, four different studies are presented. The first experiment (Section 3.2) evaluated the feasibility of FW valorization via batch dry anaerobic co-digestion with CB, screening the influence of the TS content, the S/X ratio and the co-digestion ratio on the digestion performance. In the second study (Section 3.3), the S/X ratio was fixed, varying only the co-digestion ratio and the initial TS contents (according to the TS contents of the substrate). As inefficient methane production in the two previous experiments prevailed, a different microbial inoculum was used in the third experiment (Section 3.4). In this case, the kinetics of methane production in mono-digestion of FW and during its co-digestion with CB were investigated: again, different TS contents, S/X ratios and co-digestion proportions were applied. Finally, in Section 3.5 the performances of the inocula used in the previous experiments were compared, paying special attention to the structure of the microbial communities before and after the digestion process. The four sections presented below correspond to published and submitted articles in international journals. Deeper explanations, as well as links between the different sections, are given in the respective subchapters. A summary of the objectives of these experiments and the parameters studied is presented in Table 3.1.

Table 3.1. Summary of the objectives and the parameters varied in the experiments presented in Chapter 3

Section	Objective	Parameters varied
3.2	Evaluate feasibility of FW valorization via dry anaerobic co-digestion with CB	TS content; S/X ratio; co-digestion ratio
3.3	Assess feasibility of FW dry fermentation with CB as co-substrate	TS content; co-digestion ratio
3.4	Study kinetics of methane production in mono-digestion of FW and its co-digestion with CB	TS content; S/X ratio; co-digestion ratio
3.5	Study AD performance of three different microbial inocula	TS content; S/X ratio; co-digestion ratio

FW stands for food waste, CB for cardboard, TS for total solids, S/X for substrate to inoculum and AD for anaerobic digestion

3.2 Dry anaerobic digestion of food waste and cardboard at different substrate loads, solid contents and co-digestion proportions

Capson-Tojo, G., Trably, E., Rouez, M., Crest, M., Steyer, J.-P., Delgenès, J.-P., Escudié, R., 2017. Dry anaerobic digestion of food waste and cardboard at different substrate loads, solid contents and co-digestion proportions. Bioresource Technology 233, 166–175. doi:10.1016/j.biortech.2017.02.126

Abstract

The increasing food waste production calls for developing efficient technologies for its treatment. Anaerobic processes provide an effective waste valorization. The influence of the initial substrate load on the performance of batch dry anaerobic co-digestion reactors treating food waste and cardboard was investigated. The load was varied by modifying the substrate to inoculum ratio (S/X), the total solids content and the co-digestion proportions. The results showed that the S/X was a crucial parameter. Within the tested values (0.25, 1 and 4 g VS·g VS^{-1}), only the reactors working at 0.25 produced methane. *Methanosarcina* was the main archaea, indicating its importance for efficient methanogenesis. Acidogenic fermentation was predominant at higher S/X, producing hydrogen and other metabolites. Higher substrate conversions (≤48 %) and hydrogen yields (≤62 ml·g VS^{-1}) were achieved at low loads. This study suggests that different value-added compounds can be produced in dry conditions, with the initial substrate load as easy-to-control operational parameter.

Graphical abstract

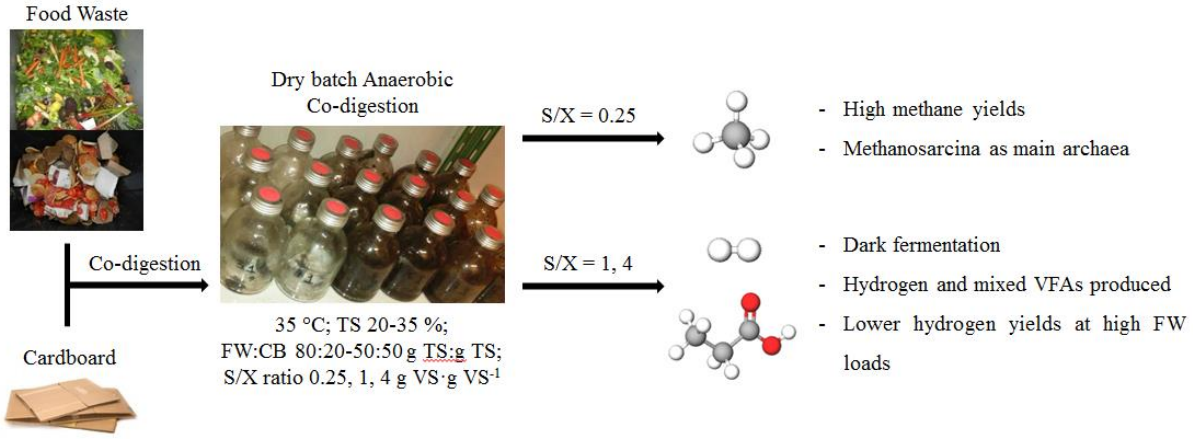

3.2.1 *Introduction*

The production of food waste (FW), which can be defined as the mass of food lost or wasted during the part of the food supply chains leading to edible products for human consumption, is a global problem (Gustavsson et al., 2011). Currently, about 1.3 billion tons of food (one third of the production for human consumption) is wasted every year (FAO, 2012). Moreover, this number is expected to increase in the coming years due to economic and population growth, particularly in developing countries. On a global scale, the production of urban FW is expected to increase by 44 % from 2005 to 2025 (Melikoglu et al., 2013). In Europe, this raise is expected to be from 89 million tons in 2006 to 126 million tons in 2020 (Monier et al., 2010).

Nowadays, most of the FW is disposed in landfills or incinerated, practices associated with different issues, such as rising costs of waste disposal, lack of space, leaching, public environmental concern and emission of toxic and greenhouse effect gases (Curry and Pillay, 2012; Uçkun Kiran and Liu, 2015). Therefore, it is necessary to develop and optimize technologies that allow a proper treatment of this biowaste. Anaerobic processes stand as a well-established technology that permits an effective and environmental-friendly treatment of waste and its valorization in the form of several products, such as biomethane, biohydrogen, alcohols or volatile fatty acids (VFAs) (Banks et al., 2012; Kim et al., 2014; Wang et al., 2015). Particularly, anaerobic digestion (AD) in dry conditions (> 20 % total solids; TS) is a promising alternative, due to several advantages when compared to wet digestion, *e.g.* lower water requirement and/or smaller reactor volume (Karthikeyan and Visvanathan, 2013).

However, AD of FW is a complex process, associated in many cases with the accumulation of ammonia and VFAs, leading to inefficient performances and even to process failure (Agyeman and Tao, 2014; Dai et al., 2013; El-Mashad and Zhang, 2010; Owamah and

Izinyon, 2015; Wan et al., 2013; M. Wang et al., 2014; L. Zhang et al., 2012). Co-digestion, *i.e.* simultaneous treatment of two or more substrates, has been proved to be an economically feasible option to overcome these complications (Dai et al., 2016; Lin et al., 2011). Co-digestion may favor the methanogenic/acidogenic processes by balancing the nutrient and carbon contents, diluting inhibitory compounds, adjusting the moisture content or increasing the buffering capacity of the system (Mata-Alvarez et al., 2011). Particularly for FW dry AD, a suitable co-substrate should have a high C/N ratio, a high TS content and provide enough buffering capacity to avoid sudden pH drops. Paper/cardboard waste (CB) fulfills all these requirements, with negligible N contents, having high buffering capacities and TS contents and being slowly biodegradable. In addition, CB is a particularly convenient co-substrate for centralized co-digestion with commercial FW in urban areas, where FW and CB are usually the main organic solid waste streams (Kim and Oh, 2011; Y. Zhang et al., 2012a). To give an idea of the importance of CB waste streams, in a study dealing with the composition of municipal solid waste in different countries in the 90s, paper and cardboard waste represented up to 36.8 % of the total municipal waste (Hogg et al., 2002).

Besides the great potential of this option, few studies have been carried out to assess the feasibility of FW and CB dry co-digestion. Y. Zhang et al. (2012a) co-digested FW and CB in wet AD at a ratio 53:47 g VS·g VS^{-1}, achieving effective methane production at a load of 3 g $VS \cdot l^{-1} \cdot d^{-1}$ and proving that CB addition led to less accumulation of ammonia and VFAs. In a recent study, Asato et al. (2016) co-digested FW and CB (wet AD) at different COD loads and co-digestion proportions. They concluded that concentrations of FW ≥ 18.75 g $COD \cdot l^{-1}$ caused inhibition, while mixtures with ≥ 75 % of CB avoided failure of methanogenesis. In dry conditions, Kim and Oh (2011) achieved a stable methane production (up to 260 ml $CH_4 \cdot g\ COD^{-1} \cdot d^{-1}$) without significant VFA accumulation at OLRs up to 10 g $TS \cdot l^{-1} \cdot d^{-1}$ and with a co-digestion ratio FW:paper of 7:1 g TS·g TS^{-1}. To our knowledge, no other study has been performed dealing with FW and CB co-digestion at high TS contents. In addition, no study has been performed to optimize critical variables for dry co-digestion of FW and CB, such as the substrate load, the co-digestion ratio or the TS contents. Moreover, taking into account the huge variability of the FW characteristics worldwide, producing comparable experiments (always supplying extensive characterizations of the substrates and the inoculum) is much more important than when using more simple/homogeneous substrates.

Accordingly, the aim of this study was to evaluate the feasibility of FW valorization by dry anaerobic co-digestion with CB using batch systems, which allowed testing different conditions simultaneously. More precisely, the influence of the initial FW load (varied by

modifying the substrate to inoculum ratio (S/X), the TS content and the FW:CB proportions) on the performance of a dry batch anaerobic co-digestion system using CB as sole stabilization agent, was investigated for the first time. In addition, the physicochemical characteristics of the substrates and the microbial communities in the reactors were studied extensively.

3.2.2 *Materials and methods*

3.2.2.1 Substrate and microbial inoculum

A model FW was prepared according to the VALORGAS report (VALORGAS, 2010) and used as substrate (Table 3.2). The FW mixture was finely milled and blended to ensure its homogeneity. Compact cardboard (branded ‘‘Cartonnages Michel’’) with a density of 1.42 $kg \cdot m^{-3}$ was shredded to less than 1 mm and used as co-substrate.

Table 3.2. Components of the model food waste

Component	Ingredient	Proportion (% in wet basis)
Fruits and vegetables	Apples	25.9
	Lettuce	25.9
	Potato	25.9
Pasta/rice/flour/cereals	Couscous	4.80
Bread and bakery	Bread	6.20
Meat and fish	Chicken	4.10
	Beef	4.10
Dairy products	Cheese	1.90
Confectionery/snacks	Biscuits	1.50

The microbial inoculum consisted on a mixture of (i) a centrifuged granular sludge issued from a mesophilic industrial UASB reactor treating sugar factory effluents and (ii) a dried digestate originated from a thermophilic industrial plant treating the organic fraction of municipal solid waste used only to increase the TS content. This latter digestate was dried at 105 °C for at least 24 hours and the resulting material was finely milled and sieved at 1 cm. Both fractions were mixed in a proportion 1:2 (wet weight basis), to obtain a final TS content of 74.19 % (59.06 % VS/TS; VS standing for volatile solids). This high TS proportion of the inoculum allowed starting the reactors with TS contents up to 35 %. Although this process resulted in a very particular inoculum, this was the only possible way to achieve the desired TS contents in the reactors. This allowed elucidating clearly the influence of this parameter on the AD process. In addition, the dried digestate added was the source of solids closest to those that can be found in a regular high-solid digestate.

3.2.2.2 Dry batch anaerobic co-digestion

The batch assays were carried out in flasks with a total volume of 600 ml. The initial FW concentrations in the reactors were adjusted by modifying the initial TS content (20, 27.5 and 35 %), the S/X (0.25, 1 and 4 g VS·g VS^{-1}) and the FW:CB co-digestion ratio (80:20, 65:35 and 50:50 g TS·g TS^{-1}). Thirteen different combinations of these independent variables were defined following an optimal statistical design and varying the initial FW load from 26.4 to 252 g VS·l^{-1} (Table 3.3). After addition of all the components needed (*i.e.*, FW, CB, inoculum and tap water), the flasks were sealed and the volume of the headspace was accurately determined by measuring the pressure in the vessel before and after adding a known volume of gas. The reactors were then flushed with nitrogen to ensure anaerobic conditions and incubated at 35 °C for a maximum of 98 days. Such a long incubation period was necessary to account for the long lag phases in the methane production observed in some reactors. To correct the endogenous contribution to the biogas from the inoculum, three blanks (one per TS content) were carried out. Each condition was performed in triplicate.

Table 3.3. Experimental design used

Reactor number	TS content (%)	Co-digestion ratio (g TS·g TS^{-1})	S/X (g VS·g VS^{-1})	Initial FW concentration (g VS·l^{-1})
1	20	80:20	0.25	26.4
2	27.5	50:50	0.25	26.5
3	27.5	65:35	0.25	33.4
4	35	50:50	0.25	37.7
5	35	65:35	0.25	47.0
6	20	50:50	1	48.6
7	20	65:35	1	62.0
8	20	50:50	4	87.6
9	20	65:35	4	113
10	27.5	80:20	1	128
11	35	80:20	1	161
12	27.5	80:20	4	210
13	35	80:20	4	252

3.2.2.3 Analytical methods

3.2.2.3.1 Physicochemical characterization of the substrates

Both substrates were characterized before starting the experiments. The TS and VS contents were measured according to the standard methods of the American Public Health

Association (APHA, 2005). After acid hydrolysis of the substrate with sulfuric acid (solution 10 % v/v H_2SO_4 98 % with 1 g $TS \cdot l^{-1}$ of substrate; agitation for 24 hours), the protein concentration was determined by the modified Lowry method (Frølund et al., 1996) and the carbohydrate concentration by the Dubois method (Dubois et al., 1956). The lipid content was measured using a gravimetric method (APHA, 2005) based on accelerated solvent extraction with heptane as solvent using an ASE®200, DIONEX (100 bar, 105 °C, 5 cycles of 10 min static and 100s purge) coupled to an evaporator MULTIVAPOR P-12, BUCHI . The proportions of cellulose, hemicellulose and lignin-like compounds in the substrates were determined according to the Van Soest procedure (Van Soest, 1963). Total Kjeldahl nitrogen (TKN) and ammonia nitrogen contents were measured with an AutoKjehdahl Unit K-370, BUCHI. Total Organic Carbon (TOC) and Inorganic Carbon (IC) were determined using a Shimadzu TOC-V_{CSN} Total Organic Carbon Analyzer coupled to a Shimadzu ASI-V tube rack. The Total Carbon (TC) content corresponded to the sum of TOC and IC. The pH was measured using a WTW pHmeter series inoLab pH720. The chemical oxygen demand (COD) was analyzed using an Aqualytic 420721 COD Vario Tube Test MR (0-1500 $mg \cdot l^{-1}$). Two mL of sample were pipetted into each tube and then they were placed inside a HACH COD reactor at 150 °C for 2 hours. COD concentrations were determined using an Aqualytic MultiDirect spectrophotometer. The biochemical methane potentials (BMPs) of the substrates were determined according to Motte et al. (2014a).

The concentrations of micro/macro-elements were measured by SAS Laboratoire© (Ardon, France) as follows: metallic trace elements were analyzed by water extraction, according to the norm NF EN 13346. The determination of the Cd, Cr, Cu, Ni, Pb, Al, Mo, Co, Zn, Se and As concentrations was performed by plasma emission spectrometry, in accordance with the NF EN ISO 11885. Hg was measured by elementary analysis (internal method), according to the norm NF EN ISO 12338. The concentrations of total P, K, Mg, Ca, S and Na were measured according to NF EN ISO 11885.

3.2.2.3.2 Gas quantification and analysis

The amount and composition of the biogas produced were determined as previously described by Cazier et al. (2015). The volumes were normalized (at 0 °C and 1013 hPa) and the endogenous respiration was considered by subtracting the gas generated in the blanks.

3.2.2.3.3 Analysis of metabolites and final products of the digestion

The concentrations of VFAs, ionic species and other metabolic products (*i.e.* lactic acid or ethanol) were measured according to Cazier et al. (2015) and Motte et al. (2013).

3.2.2.4 Microbial community analysis

Samples of the initial inoculum and from the batch reactors at the end of the experiments were analyzed to determine the structure of the microbial communities. Polymerase Chain Reaction (PCR), quantitative PCR (qPCR) and DNA sequencing techniques were used. A precise description of the methodology employed can be found elsewhere (Moscoviz et al., 2016).

3.2.2.5 Data analysis

To evaluate the existence of significant statistical differences between comparable experiments, one-way ANOVA tests were computed. When the differences were found to be significant ($\alpha = 0.05$), Tukey's Post Hoc tests were performed to compare means.

Non-linear regression analyses were performed to adjust some of the obtained data to theoretical models and linear correlations between variables were investigated. The least squares method was used in both cases.

The experimental data corresponding to the methane production were fit to the Gompertz equation (Zwietering et al., 1990) to estimate the kinetic parameters of the process.

Equation 3.1, derived from J. L. Chen et al. (2014), was used to calculate the concentration of free ammonia nitrogen (FAN) as a function of the pH, the temperature (T) and the total ammonia concentration (TAN) in the media.

$$NH_3 = NH_4^+ \cdot \frac{K_a}{\left(10^{-pH} \cdot \left[\frac{K_a}{10^{-pH}} + 1\right] - K_a\right)} \qquad \text{Equation 3.1}$$

Where K_a has a value of $1.097 \cdot 10^{-9}$ (35 °C) and the concentrations are expressed in $mg \cdot l^{-1}$.

In order to investigate the relationships between the initial working parameters (TS content, S/X and FW:CB ratio) and the fermentation products, a Principal Component Analysis (PCA) was carried out. The MixOmics R software package was used to perform the PCA.

All the analyses were computed using the statistical software R 3.2.2 (The R Foundation for Statistical Computing, Vienna, Austria). A significance level value of 5 % ($\alpha = 0.05$) and N = 3 were used when needed.

3.2.3 *Results and discussion*

3.2.3.1 Characterization of substrates

Table 3.4 shows the characteristics and the composition of both substrates. The synthetic FW was mainly composed of carbohydrates (697 g·kg TS^{-1}), with a TS content of 21.6 % (96.2 % VS) and a relatively high BMP (498 ml CH_4·g VS^{-1}; obtained after 35 days). These values are within the range of BMPs (210-648 ml CH_4·g VS^{-1}) reported in the literature (Capson-Tojo et al., 2016). The results also suggested that CB is a suitable co-substrate to stabilize FW dry digestion, *i.e.* by increasing the C:N ratio and the TS content, supplying trace elements such as Cu, Fe, Mn or Ni or diluting potentially toxic compounds such as Na^+ or K^+, as well as providing alkalinity to the medium.

The results of the Van Soest fractionation (Table 3.4) pointed out another beneficial characteristic of the CB as co-substrate. The soluble fractions were indeed much lower for CB (8.53 %) than for FW (66.6 %) and its hydrolysis kinetics should therefore be slower. This may lead to a moderation of the issue of initial VFA accumulation, common in batch AD of FW (Capson-Tojo et al., 2016).

Table 3.4. Characteristics and composition of the substrates

Parameter/Element	Unit	Model Food Waste	Cardboard
TS	% (w. b.)	21.6±0.7	92.7±3.7
VS	% TS	96.2±0.1	77.5±0.2
pH	Unit pH	5.60	7.10
COD	g COD·g TS^{-1}	1.37±0.05	1.19±0.05
BMP	ml CH_4·g VS^{-1}	498±42	250±3
NH_4	g·kg TS^{-1}	0.051	0.002
TKN	g·kg TS^{-1}	27.08±1.64	2.00±0.02
TC	g·kg TS^{-1}	442±7	366±6
C:N	$g \cdot g^{-1}$	16.3	183
Carbohydrates	g·kg TS^{-1}	687±15	958±5
Proteins	g·kg TS^{-1}	169±10	0
Lipids	g·kg TS^{-1}	72.3±1.5	0
Water soluble fraction[1]	%	66.6±0.3	8.5±0.9
Soluble fraction[1]	%	11.5±0.9	11.8±1.3
Hemicellulose fraction[1]	%	18.2±0.5	9.5±0.6
Cellulose fraction[1]	%	2.0±0.2	52.1±0.3

Parameter/Element	Unit	Model Food Waste	Cardboard
Lignin fraction[1]	%	0.7±0.1	10.7±0.1
Ash fraction[1]	%	1.0±0.0	7.4±0.3
Total P_2O_5	g·kg TS^{-1}	7.02	0.45
Total CaO	g·kg TS^{-1}	3.80	68.2
Total MgO	g·kg TS^{-1}	1.21	1.88
Total K_2O	g·kg TS^{-1}	14.6	< 0.53
Total Na	g·kg TS^{-1}	3.27	0.56
B	mg·kg TS^{-1}	7.49	14.4
Co	mg·kg TS^{-1}	< 9.07	< 8.55
Cu	mg·kg TS^{-1}	23.5	43.5
Fe	mg·kg TS^{-1}	421	866
Mn	mg·kg TS^{-1}	16.4	34.4
Mo	mg·kg TS^{-1}	0.408	0.976
Zn	mg·kg TS^{-1}	38.7	35.0
Cd	mg·kg TS^{-1}	< 0.186	< 0.175
Cr	mg·kg TS^{-1}	8.19	7.87
Hg	mg·kg TS^{-1}	0.012	0.013
Ni	mg·kg TS^{-1}	2.32	4.18
Pb	mg·kg TS^{-1}	< 4.59	14.8

1. Calculated by Van Soest fractionation

3.2.3.2 Performance of the dry anaerobic digestion reactors

The performances of the reactors varied widely according to their initial conditions (*i.e.* S/X, TS content and FW:CB ratio). Figure 3.1 presents a summary of the main results obtained, including the final distribution of metabolic end-products, the final pH values and the final substrate conversion according to the initial load of FW. In this graphic, the vertical axis on the left represents the distribution of products (*i.e.*, gas and soluble metabolites) at the end of the experiments (in COD %) and the vertical axis on the right stands for the substrate conversion. This conversion variable is the result of the sum of the metabolites obtained at the end of the experiment (in COD units) divided by the biodegradable COD of the added substrates (COD_{bio}), estimated from the BMP tests of both substrates. In Figure 3.1, these two variables are plotted together with the initial food waste concentration in the reactors (g $VS \cdot l^{-1}$). In addition, to underline the importance of the S/X, the reactors were grouped according to this operating parameter (grey rectangular lines).

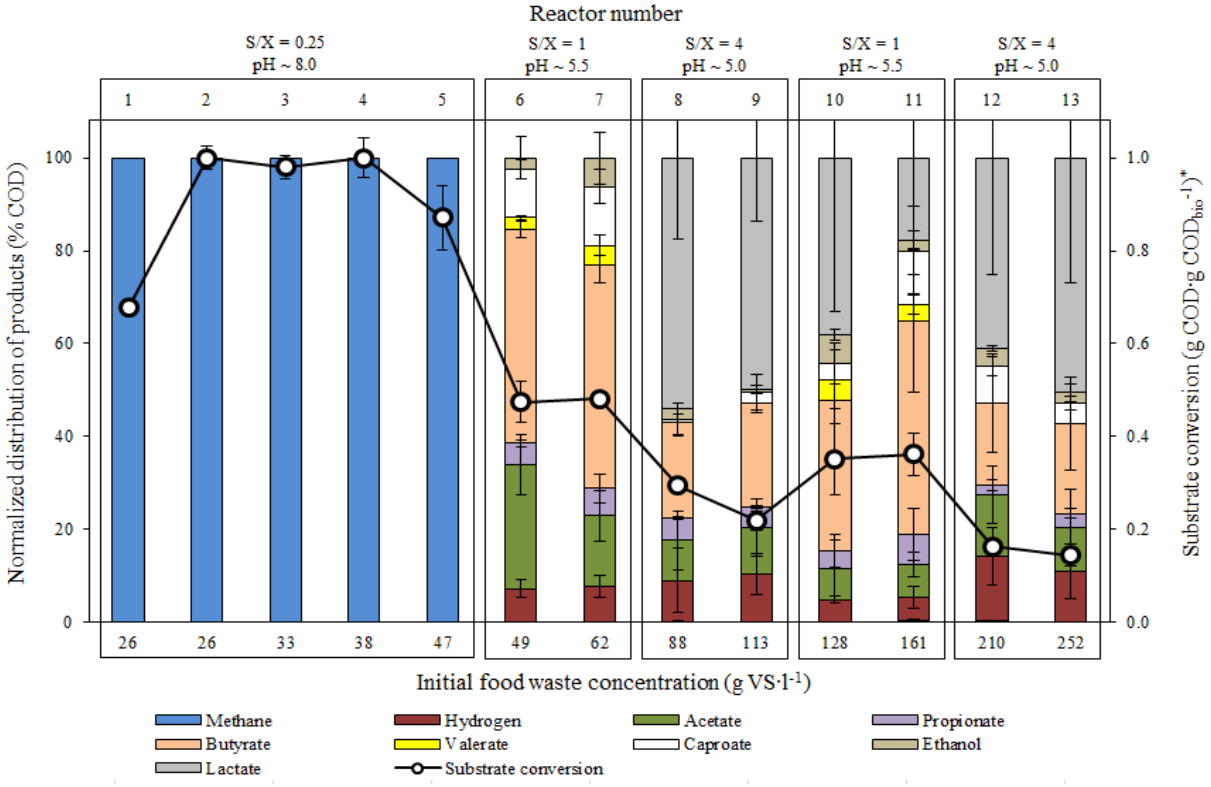

* The substrate conversion was calculated according to the inicial amount of biodegradable COD added as substrate (estimated from the BMPs)

Figure 3.1. Distribution of metabolic end-products and substrate conversion according to the initial concentration of FW. The initial S/X and the final pH values are also presented

As it can be appreciated, the substrate conversion was greatly affected by the initial load of FW, observing generally a decreasing trend in the conversion when increasing the FW concentration. These lower conversions at higher FW concentrations occurred likely due to acidification of the reactors, which decreased the final pH of the system (top of Figure 3.1) and led to modifications in the metabolic pathways. These differences are evident when paying attention to the composition of the final products (Figure 3.1). In the reactors with an S/X of 0.25 g VS·g VS^{-1}, the final pH was always above 8.0 and methane and carbon dioxide were the only products obtained. These conditions showed the highest substrate degradations, always over 60 % and in three cases close to 100 % (reactors 2, 3 and 4). At higher values of the S/X (*i.e.* 1 and 4 g VS·g VS^{-1}), the final pH was always below 5.5 and no methane was produced. In those conditions, dark fermentation (AD stopped after generation of acids; DF) took place, accumulating hydrogen and different metabolites instead of methane. Basically, at S/X higher than 0.25 g VS·g VS^{-1} the alkalinity of the medium was not sufficient to avoid a pH drop when VFAs started to accumulate at the beginning of the AD process, which led to inhibition of the archaea. Thus, the main operating parameter affecting the pH in the reactors, and therefore the metabolic pathways, was found to be the S/X.

3.2.3.3 Methane production at low S/X (0.25 g VS·g VS^{-1})

The obtained results showed that in the reactors with S/X of 0.25 g VS·g VS^{-1}, efficient methanogenesis occurred. In those systems, the methane yields were always over 67 % of the BMP (estimated by addition of the BMPs for FW and CB). For reactors 2, 3 and 4, these values were around 100 %, indicating a maximal conversion of the substrate. However, as shown in Figure 3.1, the substrate conversions and the methane yields were not equal for all the methanogenic reactors. The evolution of the methane yields during the experiments, shown in Figure 3.2, may help to understand this behavior. The reactors with loads of 26 g VS·l^{-1} (26A) and 47 g VS·l^{-1} (rectors 1 and 5) showed significantly lower final yields after 98 days of operation (varying from 409.3 mL CH_4·g VS^{-1} in reactor 3 to 306.9 ml CH_4·g VS^{-1} in reactor 1) and much larger lag phases (almost 50 days by adjustment to the Gompertz equation) than the other conditions. These long lag periods might be consequence of a more intense accumulation of VFAs at the beginning of the digestion (Kawai et al., 2014; Liu et al., 2009), causing the need of a stronger adaptation of the microbial consortia.

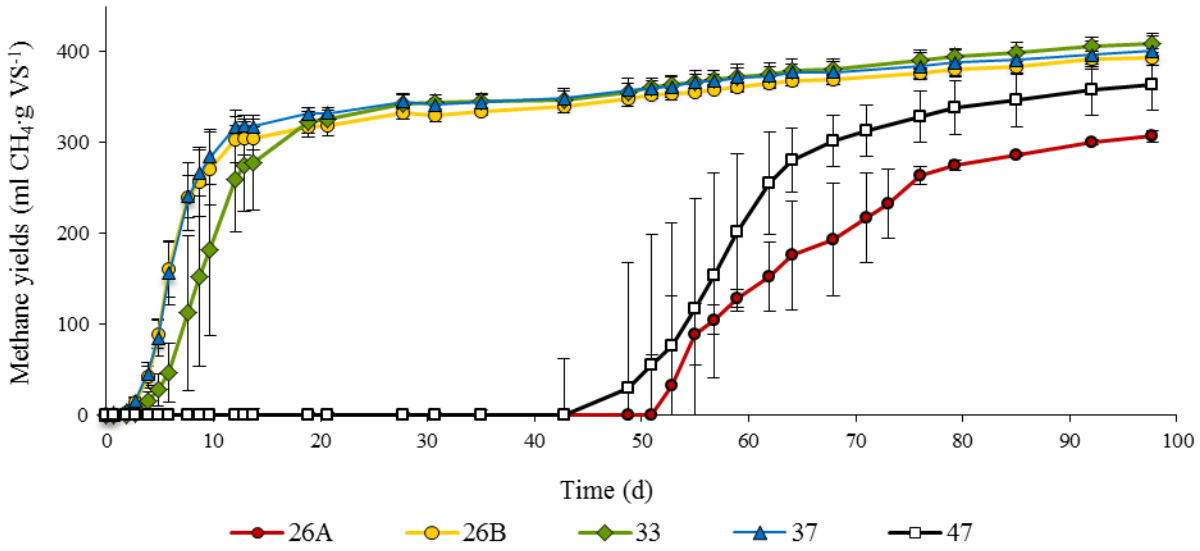

Figure 3.2. Methane yields in the reactors with an S/X ratio of 0.25 g VS·g VS^{-1} (1 to 5). The legend represents the initial food waste concentrations (g VS·l^{-1}) applied

A change in the structure of the microbial community could also explain the lower methane yields, as a greater amount of substrate would be used for microbial growth and adaptation. Figure 3.3 presents the results of the microbial analysis for the reactors producing methane (with an S/X of 0.25 g VS·g VS^{-1}). As shown in Figure 3.3A, representing the relative abundance of archaeal Operational Taxonomic Units (OTUs), the archaeal population clearly varied when compared with the initial inoculum (Inoculum; NA). Starting with the initial inoculum, *Methanosarcina* represented around 5 % of the OTUs and *Methanosaeta*

around 20 %. Amongst the reactors producing methane, the only ones in which the archaeal growth led to significant concentrations of archaeal OTUs at the end of the experiments, *Methanosarcina* accounted for more than 50 % of the archaeal OTUs and the proportions of *Methanosaeta* were negligible after the digestion. This suggests that a microbial selection occurred towards *Methanosarcina*. This could be explained by the greater resilience of *Methanosarcina* to high FAN and VFA concentrations when compared to *Methanosaeta* (Batstone et al., 2002b).

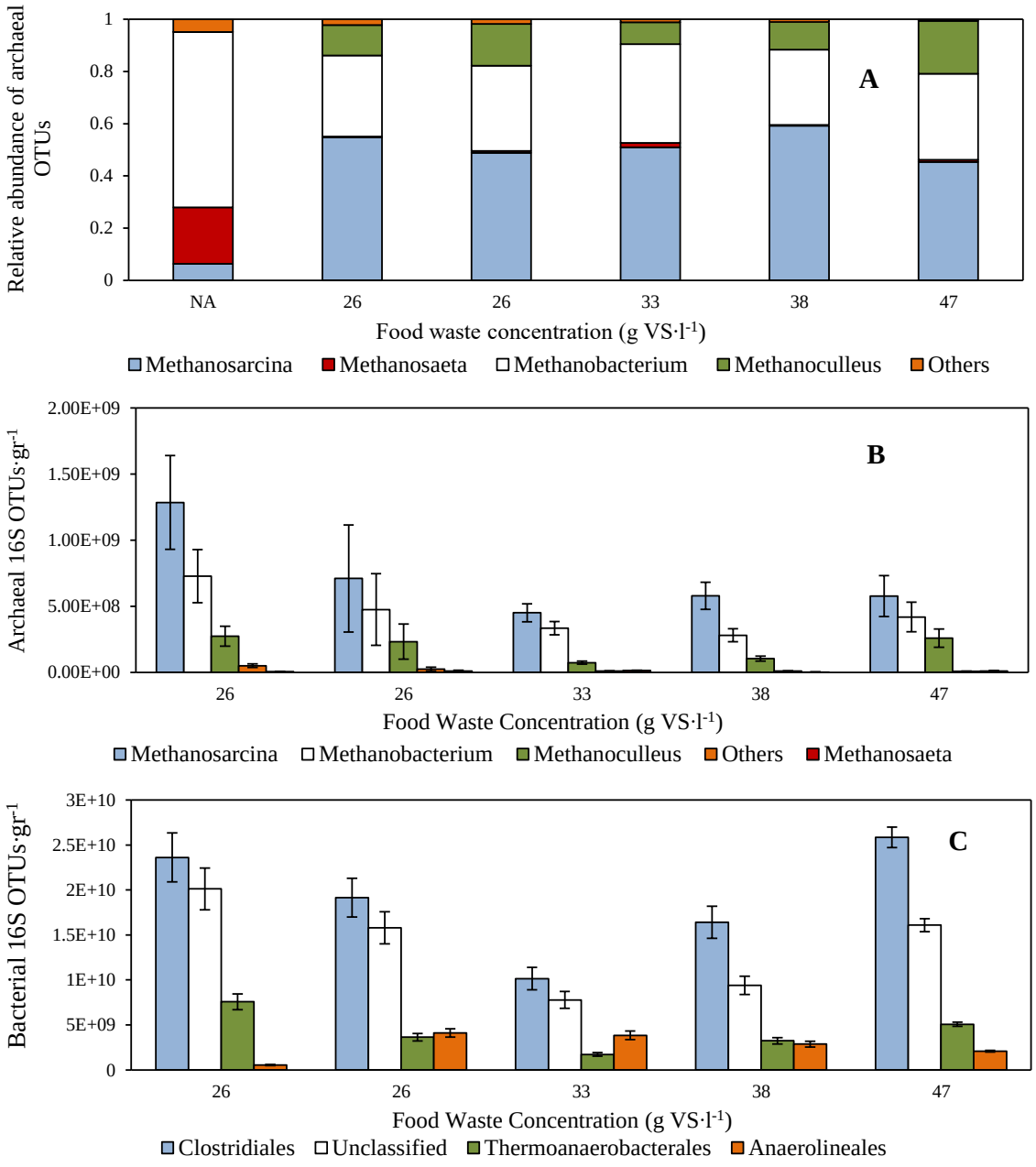

Figure 3.3. Relative abundance of Archaeal OTUs (A), concentrations of archaeal 16S OTUs (B) and concentrations of bacterial 16S OTUs (C) in the inoculum and in reactors 1 to 5 (S/X of 0.25 g VS·g VS^{-1}) at the end of the batch experiments. NA stands for "not applicable"

In fact, the concentration of FAN (only significant in the systems producing methane) increased linearly (R^2 of 0.987) with the initial TS content in the reactors, ranging from 360 to 795 mg FAN·l^{-1} (2.61-3.70 g TAN·l^{-1}). This elevated concentration of FAN/TAN may be responsible for the microbial selection towards *Methanosarcina* mentioned above. As explained by De Vrieze et al. (2012), *Methanosarcina* sp. are more tolerant to ammonia stress than other methanogens, particularly *Methanosaeta* sp., which cannot thrive at TAN concentrations greater than 3 g·l^{-1}. Therefore, a population selection according to their resistance to TAN/FAN would favor the digestion. Moreover, while *Methanosaeta* are strict acetotrophs, *Methanosarcina* are able to perform both hydrogenotrophic and acetotrophic methanogenesis. Thus, it can be stated that, due to the high concentrations of FAN observed, the main metabolic pathway for methane production that occurred in the reactors was hydrogen production by acetogenesis and syntrophic acetate oxidation coupled to hydrogenotrophic methanogenesis (Qu et al., 2009). The microbial selection observed suggests a great importance of the initial archaeal structure of the inoculum when batch-digesting FW. Besides non observing inhibition, it is clear that FAN accumulation can become an issue when digesting FW.

However, a quantitative analysis of the microbial population was required to explain the different performances and the lower methane yields obtained in reactors 1 and 5. Figures 3.3B and 3.3C show the concentrations of the most significant OTUs in the reactors at the end of the experiments for archaea and bacteria, respectively. The reactor with the lowest FW load (reactor 1) had a significantly higher concentration of *Methanosarcina* than the others and, in both reactors showing significant lag phases and lower methane yields (reactors 1 and 5), the concentration of *clostridiales* OTUs (main responsible for hydrogen and VFA production during fermentation) was significantly higher than in the rest. This can be explained by a more extended initial acidification period, in which acidogenesis took place, leading to a greater growth of *clostridiales* and decreasing the pH, inhibiting methane production until a proper archaeal population (mainly composed of *Methanosarcina*) was developed. This extended fermentation stage and the concomitant bacterial/biofilm growth and COD consumption may aid to explain the lower methane yields observed in reactors 1 and 5. However, although they may contribute, the obtained differences in the microbial growths only cannot explain the significantly lower methane yields obtained (considering the COD consumed). In addition, also the synthesis of other compounds such as soluble microbial products or extrapolymeric substances may have reduced the methane yields. Interestingly, other authors have also reported lower methane yields after initial acidification (with the

consequent lag phases) using FW as substrate for wet AD. Liu et al. (2009) obtained lower biogas yields (from 716 to 358 ml $CH_4 \cdot g\ VS^{-1}$) at higher S/X (from 1.6 to 3.1 g $VS \cdot g\ VSS^{-1}$) for co-digestion of FW and green waste due to more pronounce acidifications at high loads. As they did not find signs of residual VFAs present at the end of the digestion, they hypothesized that either the acidogenesis or the hydrolysis steps were jeopardized at high S/X. In addition, Kawai et al. (2014) studied the mono-digestion of FW at different loads, concluding also that the S/X was inversely proportional to the methane yield due to reversible initial VFA accumulation. Furthermore, they achieved yields over 400 ml $CH_4 \cdot g\ VS^{-1}$ only at S/X lower than 1.0 g $VS \cdot g\ VS^{-1}$. They attributed the lower yields to the initial pH drop caused by the initial accumulation of VFAs. In this study, no residual VFAs were detected after AD. The fate of the COD not becoming VFAs nor methane in FW AD after long lag phases (and initial VFA accumulations) must be elucidated and further research should be performed on this topic. Hypotheses that can be drawn to explain the lower methane yields after VFA accumulation are lower degrees of hydrolysis or more intense synthesis of soluble microbial under stressful AD conditions, such us high VFA concentrations or relatively low pH values.

The long lag phases in the methane production occurring in reactors 1 and 5 might have been caused by a more intense initial acid accumulation, due to: (i) the high proportion of FW in the substrate in reactor 1 (only reactor producing methane with 80 % of FW in the experimental design) and (ii) the high FW load and TS content in reactor 5 (47 g VS $FW \cdot L^{-1}$ and 35 % TS). These characteristics may have caused a rapid increase in the VFAs concentrations during the first days in both reactors. In reactor 1, the FW concentration was low due to dilution with water, which did not supply any extra alkalinity to the medium. In addition, this reactor had the lowest proportion of CB, which might have also led to a lower alkalinity when compared to the other reactors and might have also favored a faster VFA accumulation at the beginning of the AD process. In addition, as demonstrated by Abbassi-Guendouz et al. (2012), increasing the TS contents may cause the first-order hydrolysis rates to decrease in batch experiments. Thus, in the case of reactor 1, its low TS content (20 %) may also have prolonged the acidification effect due to faster hydrolysis kinetics. However, as the high TS content (and associated FW concentration) in reactor 5 might have been responsible for the lag phase, it can be hypothesized that both the TS content and the substrate composition might have led to excessive VFAs concentrations, decreasing the methane yields and slowing down the kinetics of the methanogenesis. An optimum combination of the TS content of the system and the FW:CB proportions of the substrate remains to be found.

At this point, it must be mentioned that the physicochemical characteristics of the inoculum are also of critical importance. The results presented in this study were obtained using an inoculum with relatively high TS and VS contents, meaning that the initial substrate concentrations for a defined S/X were also relatively high. This led to a system easier to acidify when compared to other processes using an inoculum with lower contents of solids and higher alkalinities. A previously adapted inoculum with a higher proportion of *Methanosarcina* and lower initial TS content should be tested at different S/X. This would allow the optimization of the AD process as well as the comparison of experiments using different inoculums. In addition, optimal combinations of the FW:CB ratio and the TS content at different S/X should be found to assess the impact of these operating parameters at different loads.

3.2.3.4 Production of hydrogen and metabolites at high S/X (1 and 4 g VS·g VS^{-1})

In the reactors with an S/X higher than 0.25 g VS·g VS^{-1} (*i.e.* 1 and 4 g VS·g VS^{-1}), no methane was produced and a much lower substrate conversion was achieved (Figure 3.1). Moreover, the substrate conversion was found to be negatively correlated to the initial FW concentration. As shown in Figure 3.4A, the final substrate conversion showed a decreasing trend when increasing the FW charge.

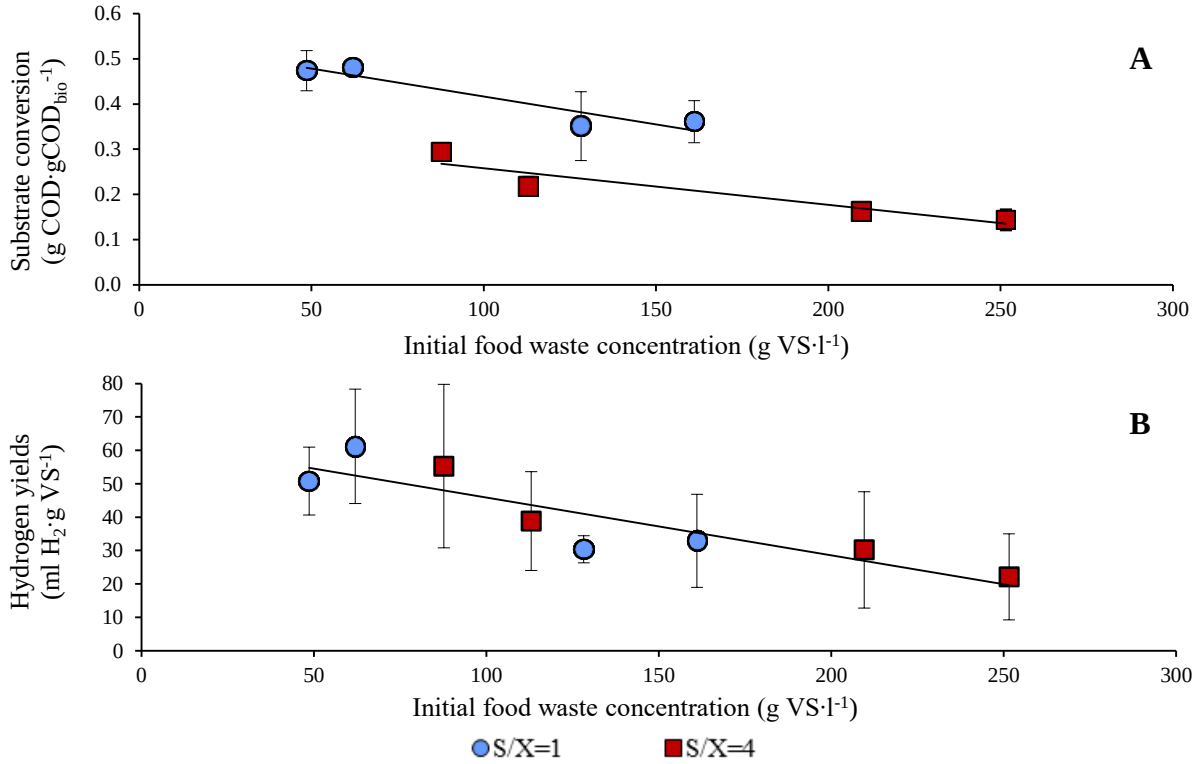

Figure 3.4. Influence of the initial FW concentration on the substrate conversion (A) and the hydrogen yields (B) in the reactors 6 to 13 (S/X of 1 and 4 g VS·g VS^{-1})

In these reactors, the hydrogen yields ranged from 22.1 to 61.2 ml·g VS^{-1}. The highest values obtained were in agreement with results presented in the literature (Ghimire et al., 2015a), confirming an efficient FW conversion by DF. As for the substrate conversion, a generally decreasing trend was found when plotting the obtained hydrogen yields against the FW concentration. This occurred due to a greater accumulation of organic acids and alcohols in the reactors at higher charges of substrate, which led to changes in the pH of the system, modifying the microbial pathways followed. At low pH values (~5.0), non-hydrogen producing pathways, such as those related to ethanol and lactate production (Eqs. 3.2 and 3.3; Batstone et al., 2002) were favored.

$$C_6H_{12}O_6 \rightarrow 2CH_3CH_2OH + 2CO_2 \qquad \text{Equation 3.2}$$

$$C_6H_{12}O_6 \rightarrow 2CH_3CHOHCOOH \qquad \text{Equation 3.3}$$

In fact, lactate accumulation was found to be the reason for the decreasing hydrogen yields in the reactors with an S/X of 4 g VS·g VS^{-1} (Motte et al., 2013). A directly proportional correlation was found between the lactate concentrations and the initial FW concentration (R^2 of 0.944). This means that less substrate was available for hydrogen production and, moreover, as lactic acid has a relatively low pKa (3.08), the accumulation of this compound affected greatly the pH, favoring the acidification of the medium. In the reactors with an S/X of 1 g VS·g VS^{-1}, the production of lactic acid was observed only in the two most heavily charged reactors (number 10 and 11), showing also the lowest hydrogen yields. Moreover, it was also observed that the ratio butyric/acetic acid increased linearly with the FW charge in those conditions (R^2 of 0.914). As butyric acid production yields less hydrogen than that of acetic acid (Eqs. 3.4 and 3.5) (Ghimire et al., 2015a), an increase of this ratio represents a detriment on the hydrogen yields when homoacetogenesis (Eq. 3.6; Batstone et al., 2002) does not take place. Thus, the metabolic shift towards butyric acid production instead of acetic acid was responsible for the decreasing hydrogen yields in the reactors with an S/X of 1 g VS·g VS^{-1}.

$$C_6H_{12}O_6 + 2H_2O \rightarrow 2CH_3COOH + 2CO_2 + 4H_2 \qquad \text{Equation 3.4}$$

$$C_6H_{12}O_6 \rightarrow CH_3CH_2CH_2COOH + 2CO_2 + 2H_2 \qquad \text{Equation 3.5}$$

$$2CO_2 + 4H_2 \rightarrow CH_3COOH + H_2O \qquad \text{Equation 3.6}$$

However, special attention must be paid when considering the butyric/acetic acid ratio. Although this ratio has been reported to be a good indicator of the biohydrogen yields

associated with the metabolic pathways followed (Khanal et al., 2004), controversy exists when applying this approach (Ghimire et al., 2015a). The reason for that is that, if homoacetogenesis takes place, hydrogen is also consumed for production of acetic acid. Therefore, some authors have found direct correlations between the hydrogen yields and the yields of butyric acid, and not those of acetic (Guo et al., 2014). Thus, our results suggest that, in these experiments, homoacetogenesis did not occur in a great extent.

Finally, another possible explanation for the lower substrate conversion at higher FW loads is inhibition of hydrolysis due to local accumulation of hydrogen (Abbassi-Guendouz et al., 2012; Cazier et al., 2015), an issue that has been previously reported at high TS contents.

To evaluate the general influence of each initial working parameter (TS content, S/X and FW:CB ratio) on the synthesis of the different products, a PCA analysis was carried out: the products were expressed as g $COD \cdot g\ COD_{bio}^{-1}$, the TS content in %, the S/X in g $VS \cdot g\ VS^{-1}$, the FW:CB ratio in g $TS \cdot g\ TS^{-1}$ and the initial FW concentration in g $VS \cdot l^{-1}$. Figure 3.5 shows the corresponding correlation circles.

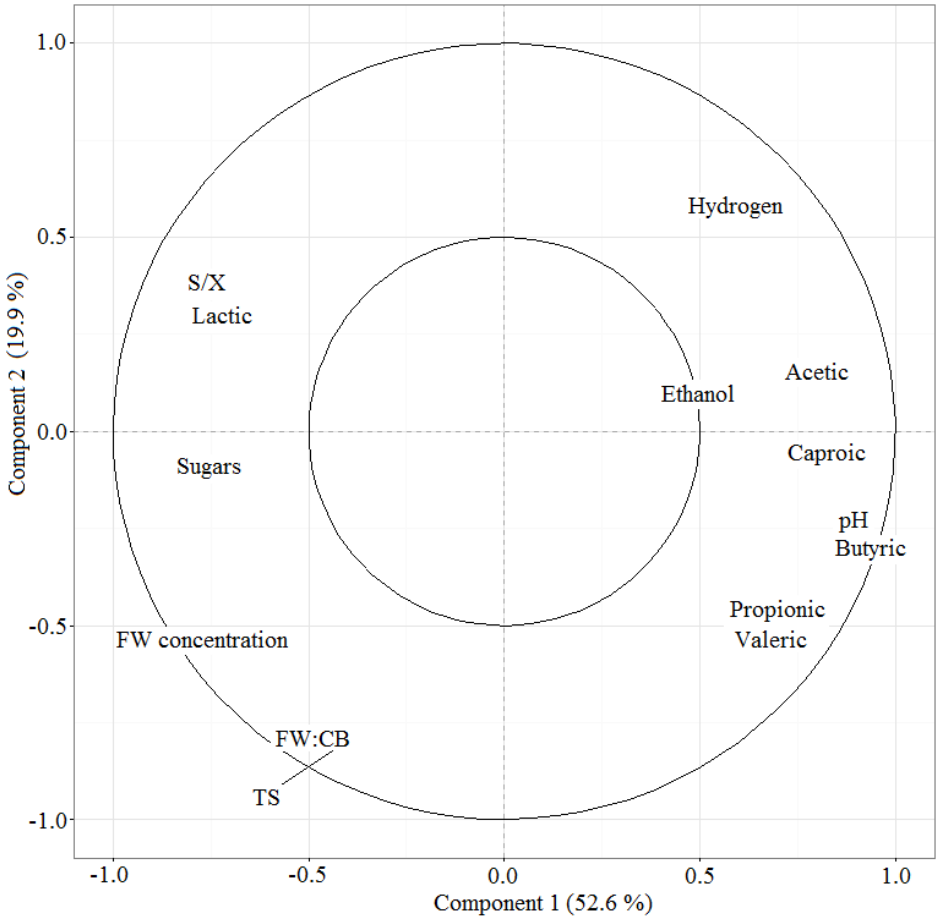

Figure 3.5. Correlation circle of the initial working parameters and the final yields of metabolites. It is based on the projection in plans formed by the two first principal components, accounting for 72.5 % of the variance

As it can be observed, both the TS content and the FW:CB ratio of the substrate (as well as the initial FW concentration) were negatively correlated to the hydrogen yield and positively correlated to the yields of lactate and non-degraded sugars (glucose, fructose, xylose and lactose) left in the media. In agreement with Equations 3.4 and 3.5, the hydrogen yield was correlated to the production of acetic acid. Surprisingly, it was also positively related to the ethanol and the caproic acid yields, meaning that probably Equation 3.7 (Ghimire et al., 2015a) was a mayor pathway for the production of ethanol.

$$C_6H_{12}O_6 + 2H_2O \rightarrow CH_3COOH + CH_3CH_2OH + 2CO_2 + 2H_2 \qquad \text{Equation 3.7}$$

However, the yields of these two products in the reactors (and therefore their final concentrations) were of minor importance when compared to others, such as acetic or butyric acids.

In accordance to Equations 3.8 and 3.9 (Motte et al., 2013), the yields of valeric and caproic acids were strongly correlated to the yields of ethanol (for both) and those of propionic and butyric acids, respectively.

$$CH_3CH_2OH + CH_3CH_2COOH \rightarrow CH_3CH_2CH_2CH_2COOH + H_2O \qquad \text{Equation 3.8}$$

$$CH_3CH_2OH + CH_3CH_2CH_2COOH \rightarrow CH_3CH_2CH_2CH_2CH_2COOH + H_2O \qquad \text{Equation 3.9}$$

These results were in agreement with the previous statements, showing that the increasing FW concentrations led to greater degrees of acidification, decreasing the pH, raising the lactate yields and jeopardizing the hydrogen production. The yields for the different metabolites were also in accordance with the literature (Wang et al., 2015). Maximum yields of 0.127, 0.231, 0.121, 0.0612 and 0.0295 g COD·g COD_{bio}^{-1} for acetic acid, butyric acid, lactic acid, caproic acid and ethanol respectively, suggest that FW could be used for production of these value-added products at a large scale. Due to the aforementioned acidification effect, greater yields of all the organic acids other than lactate were observed at S/X of 1 g VS·g VS^{-1} when compared to the S/X of 4 g VS·g VS^{-1}. In the reactors with an S/X of 1 g VS·g VS^{-1}, increasing the FW load decreased the acetic acid yields, increasing at the same time those of butyric, valeric and caproic acids and ethanol.

The results shown above suggest that a two-stage system coupling DF and AD, with an intermediate extraction process for recovery of value-added metabolites (therefore not entering the AD system) is an interesting option that should be tested using FW and CB as substrates. In the first stage, as hydrogen and organic acids are to be produced, high S/X

should be applied, aiming at the optimal conditions (*i.e.* FW:CB ratios and TS %) to obtain the highest yields of the desired products. After recovery of the useful products, the remaining COD leaving the DF process (between 50 to 85 % of the input COD_{bio}) could enter the AD stage (at much lower loads) for final waste treatment and stabilization, producing methane at the same time. This is a very interesting option in urban areas, where FW and CB are the main components of solid waste. In addition, these wastes are generally taken to the same treatment facilities, which facilitates their centralized co-digestion.

Finally, the microbial communities in the reactors where DF took place (S/X of 1 and 4 g VS·g VS^{-1}) were also analyzed. The concentrations of microbial OTUs at the end of the experiments were lower than those found in the reactors where AD occurred. While in the methanogenic reactors the average concentration of bacterial 16S OTUs was $4.25 \cdot 10^{10}$ OTUs·gr^{-1}, this value was $5.80 \cdot 10^{9}$ OTUs·gr^{-1} for the DF reactors. This might be explained by the much lower substrate conversion obtained by DF when compared to AD, which was translated into a lower microbial growth. Moreover, as methanogenesis did not occur in those systems, negligible amounts of archaeal OTUs were detected. Regarding the composition of the bacterial communities in these reactors, the relative abundance of OTUs is shown in Figure 3.6.

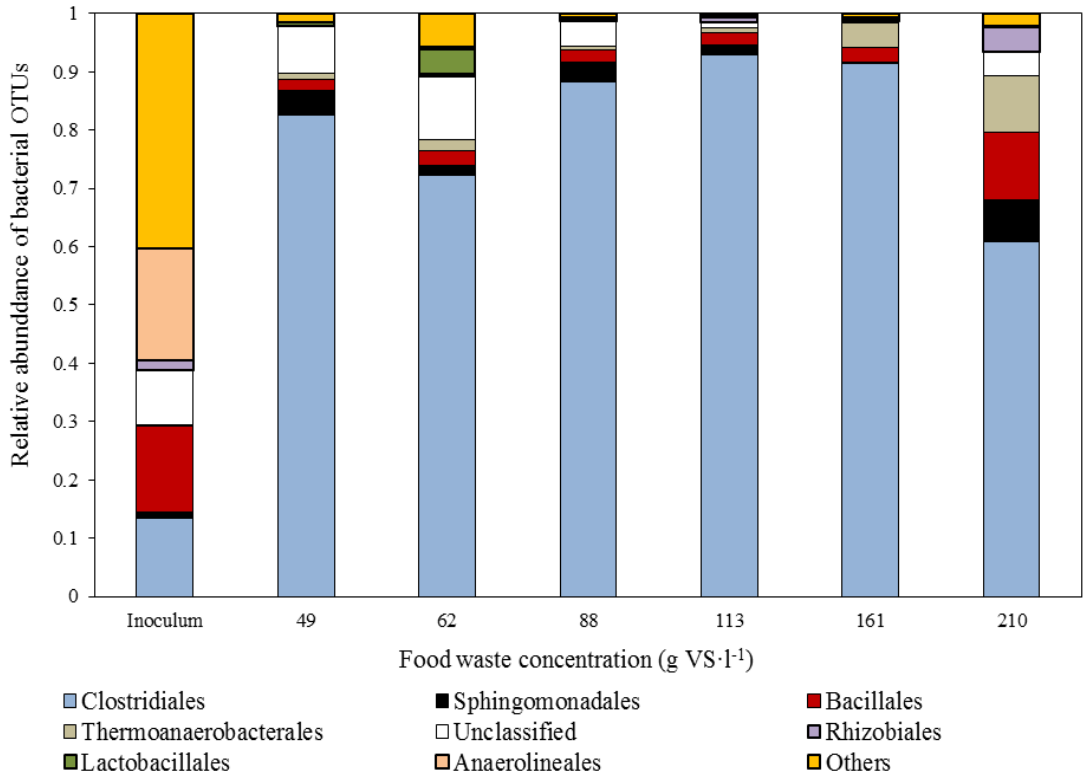

Figure 3.6. Relative abundance of bacterial OTUs in the inoculum and in reactors with S/X of 1 and 4 g VS·g VS^{-1} at the end of the batch experiments

The predominant order in all the reactors at the end of the DF was *Clostridiales*, with proportions ranging from 61 % to 93 %. The abundance of *Clostridiales* was much lower in the inoculum (13 %), indicating a clear microbial selection towards the growth of these microorganisms. Moreover, the microbial diversity was also much lower after the fermentation (see "Others" in Figure 3.6) and barely no *Anaerolineales* (important in the inoculum and after AD, see Figure 3.3) were detected. The relevance of *Clostridiales* for DF has been previously presented in the literature (Ghimire et al., 2015a), which confirms that these bacteria were the main responsible for the production of hydrogen and other metabolites.

3.2.4 *Conclusions*

By varying the selected operational parameters, different metabolic pathways occurred. The S/X was a critical parameter, affecting the pH due to lack of alkalinity and thus affecting the final products. Efficient methane production was achieved at low S/X (0.25 g VS·g VS^{-1}), with *Methanosarcina* as essential archaea for AD. At higher S/X, hydrogen and metabolites were produced, obtaining lower substrate degradations. For DF, higher TS contents, FW:CB or S/X resulted into lower degradations and greater lactate proportions, decreasing the hydrogen yields. This study shows that different value-added compounds can be produced in dry conditions by anaerobic co-digestion of FW and CB.

3.2.5 *Main outcomes and coming experiments*

Two main conclusions can be drawn from this experiment: (i) different value-added products could be obtained by simply varying the substrate load and (ii) efficient methane production could only be achieved at low S/X ratios (0.25 g VS·g VS^{-1}) at the working conditions tested.

According to the information presented above and with the aim of optimizing the production biomethane from FW, it seemed logical to carry out experiments at low S/X ratios (*e.g.* 0.25 g VS·g VS^{-1}) and different TS contents and FW:CB proportions in the substrate. This would allow investigating the influence of these variables on the methane production, which would not be inhibited at low working S/X ratios. With this initial purpose, the experiment presented in Section 3.3 was designed (Table 3.5). A similar inocula to the one previously used was prepared and the S/X ratio was fixed to 0.25 g VS·g VS^{-1}. In addition, the reactors presented in Section 2.4.2 (allowing digestate sampling) were used, thus enabling to follow-up the dry AD kinetics. However, contrary to our expectations, all the reactors

resulted in acidification, performing DF and producing negligible amounts of methane (but obtaining instead high hydrogen and VFA yields). Therefore, even if the results presented in Section 3.3 show interesting conclusions, it must be clarified that the initial objective was not fulfilled. Nevertheless, the coming experiment serve to evaluate dry DF as treatment method, opening new possibilities for FW valorization and, as it will be further explained, producing significant amounts of very high value-added products, such as caproic acid.

It must be mentioned that another main outcome from the previous work was the significant growth of *Methanosarcina* sp. over that of other archaea. This result suggested the critical influence of microbial acclimation on the AD performance.

3.3 Cardboard proportions and total solids contents as driving factors in dry co-fermentation of food waste

Capson-Tojo, G., Trably, E., Rouez, M., Crest, M., Bernet, N., Steyer, J.-P., Delgenès, J.-P., Escudié, R., 2017. Cardboard proportions and total solids contents as driving factors in dry co-fermentation of food waste. Bioresource Technology 248 Part A, 229-237. doi:10.1016/j.biortech.2017.06.040

Abstract

This study evaluated the influence of the co-substrate proportions (0-60 % of cardboard in dry basis) and the initial total solid contents (20-40 %) on the batch fermentation performance. Maximum hydrogen yields were obtained when mono-fermenting food waste at high solids contents (89 ml $H_2 \cdot g\ VS^{-1}$). The hydrogen yields were lower when increasing the proportions of cardboard. The lower hydrogen yields at higher proportions of cardboard were translated into higher yields of caproic acid (up to 70.1 g $COD \cdot kg\ COD_{bio}^{-1}$), produced by consumption of acetic acid and hydrogen. The highest substrate conversions were achieved at low proportions of cardboard, indicating a stabilization effect due to higher buffering capacities in co-fermentation. *Clostridiales* were predominant in all operational conditions. This study opens up new possibilities for using the cardboard proportions for controlling the production of high added-value products in dry co-fermentation of food waste.

Graphical abstract

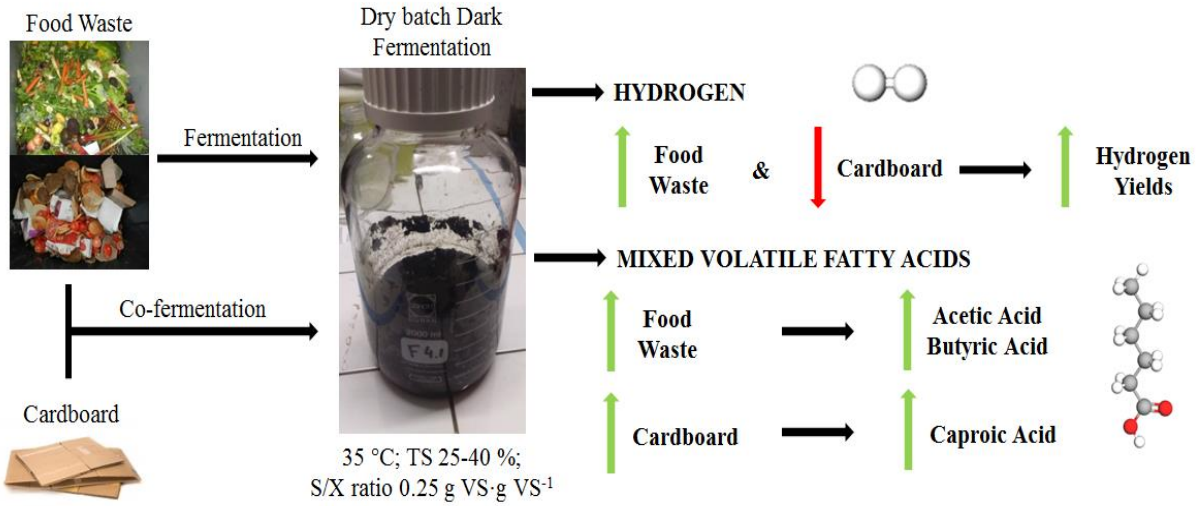

3.3.1 *Introduction*

The production of food waste (FW) is currently an issue of global importance. This biowaste represents one third of the total food generated for human consumption, accounting for 1.3 billion tons of waste every year (FAO, 2012). In addition, the economic and population growth will cause an increase in the production of urban FW, which is expected to raise by 44 % from 2005 to 2025 (Melikoglu et al., 2013). The traditional treatment techniques for FW, mainly landfilling and incineration, lead to several environmental issues, such as leaching, emission of greenhouse gases and odor production. Moreover, the costs associated with these practices are expected to increase in the coming years.

Therefore, it is necessary to develop and optimize technologies that allow an efficient FW treatment, integrating its disposal with its valorization and recycling. In the context of a rising global energy demand, the development of clean and renewable energy sources is a mayor goal to be achieved in the future. The production of hydrogen and volatile fatty acids (VFAs) by dark fermentation (DF) of FW is a promising alternative that can serve for both purposes: (i) FW treatment and (ii) generation of renewable energy (hydrogen) and carbon sources (VFAs).

Hydrogen is a carbon-free clean fuel with a high energy content (122 $kJ \cdot g^{-1}$). It can be used for electricity production, in direct combustion or for the synthesis of chemicals (Ghimire et al., 2015a). The concomitant VFAs produced during DF are a renewable carbon source that can be used for several purposes and that have high added-value in some cases (*i.e.* caproic acid). Mixed VFAs from FW have been applied for production of electricity (Y. Chen et al., 2013), production of biogas or biodiesel (Fontanille et al., 2012), biological nutrient removal

(Lim et al., 2000) and for the synthesis of value-added chemicals, such as ethanol (Kiran et al., 2015), yeast flavor (Mantzouridou et al., 2015), long-chain fatty acids (Pleissner et al., 2015) or polyhydroxyalkanoates (H. Chen et al., 2013). Among the options for hydrogen and VFA production, DF has low energy requirements, it is environmentally friendly, it has high hydrogen production rates and it can accommodate a great variety of substrates (Dahiya et al., 2015; Kim et al., 2014; K. Wang et al., 2014).

FW has a relatively high total solids (TS) content (~20 %), with around 90 % corresponding to volatile solids (VS). These VS correspond mainly to easily degradable carbohydrates (50-70 %) (Uçkun Kiran et al., 2014). These characteristics make FW a very suitable substrate for DF, mainly because the hydrogen yields obtained by DF have been found to be correlated with the contents of carbohydrate in the substrates (Guo et al., 2014). Moreover, the high TS content of FW allows the operation under dry conditions (20-40 % TS), which requires smaller reactor volumes and produces less digestate than wet DF. However, FW also contains proteins (15-25 %) and lipids (13-30 %), components which may jeopardize the process. The high protein proportions may cause nutrient imbalance due to a low C/N ratio. Another issue that may appear during DF is a drop in the pH of the reactors due to accumulation of VFAs, leading to production of lactate or ethanol and thus decreasing the hydrogen yields. To avoid these problems, the addition of another substrate for co-fermentation with FW has been applied to balance nutrients (*i.e.*, increase C/N ratio) and to provide buffering capacity (*e.g.* by slowing down acid accumulation or by directly increasing the alkalinity). Boni et al. (2013) effectively co-fermented FW with slaughterhouse waste to provide buffering capacity, obtaining hydrogen yields up to 145 ml $H_2 \cdot g\ VS^{-1}$ (compared to 74 ml $H_2 \cdot g\ VS^{-1}$ of FW alone). Waste sludge has also been used as an effective co-substrate for FW DF, stabilizing the hydrogen production by adjusting the C/N ratio of the substrate and by providing buffer capacity (D.-H. Kim et al., 2011b; Sreela-or et al., 2011b; Zhou et al., 2013). Lime mud and white mud, from paper-making and ammonia-soda processes, respectively, have also led to synergistic effects when co-fermented with FW (J. Zhang et al., 2013; Zhang and Wang, 2013) due to an increased buffering capacity and an enhanced macronutrients balance. Recently, Zheng et al. (2017) co-fermented *Sophora flavescens* residues (a medicinal plant) and FW for production of lactic acid, achieving high conversions by balancing the C/N ratio and the pH. In addition, Pagliaccia et al. (2016) co-digested FW with olive husks for hydrogen production, observing synergetic effects and obtaining hydrogen yields up to 87 ml $H_2 \cdot g\ VS^{-1}$.

Due to its high C/N ratio, its relatively slow biodegradability and its high TS content, an interesting option for dry co-fermentation with FW is cardboard waste (CB). In addition, FW and CB (which may account for up to 37 % of the total municipal waste) are usually the main organic solid waste streams in urban areas, which makes CB an appropriate option for centralized DF with FW in those regions (Hogg et al., 2002; Kim and Oh, 2011; Y. Zhang et al., 2012a).

Therefore, the aim of this study was to evaluate the feasibility of FW dry DF with CB as co-substrate for production of hydrogen and VFAs. The influence of the proportions of CB in the substrate and the initial TS contents on the performance of batch DF was investigated. Special attention was paid to the influence of these parameters on the final yields of the different metabolites obtained and to the structures of the microbial communities after fermentation.

3.3.2 *Materials and methods*

3.3.2.1 Substrate and microbial inoculum

A synthetic FW was prepared according to the VALORGAS report (VALORGAS, 2010). In agreement with this document, the main components of the FW were: fruits and vegetables (78 %), meat (8.2 %), bread (6.2 %), cereals (4.8 %), dairy products (1.8 %) and snacks (1.5 %). A more precise composition of the substrate can be found elsewhere (Capson-Tojo et al., 2017d). To ensure its homogeneity, the mixture was milled and blended. Compact cardboard (branded ‘‘Cartonnages Michel’’) with a density of 1.42 $kg \cdot m^{-3}$ was used as co-substrate. It was shredded to less than 1 mm before its usage.

The inoculum was a mixture of two different sludges: (i) centrifuged granular sludge from a mesophilic industrial UASB reactor treating effluents from a sugar factory and (ii) a dried digestate (at 105 °C for 24 h; sieved at 1 cm) from a thermophilic industrial plant treating the organic fraction of municipal solid waste. This latter digestate was added to increase the initial TS content of the inoculum. This allowed working at high initial TS contents in the reactors (up to 40 %). Both sludges were mixed in a proportion 1:2 (wet weight basis), obtaining a final TS content of 70.78 % (70.85 % VS/TS).

3.3.2.2 Batch dry dark co-fermentation

The specific conditions of the experiments, as well as the particular objectives of the experimental set-up, are presented in Table 3.5.

Table 3.5. Experimental design used in the study. All the conditions were started with 60 g of FW as substrate, at 35 °C and with a S/X of 0.25 g VS·g VS^{-1}

Reactor number	Objective	Substrate TS content (%)	CB in substrate (% dry basis)	Initial substrate concentration (g COD_{bio}·kg^{-1})	Initial FW concentration (g VS·l^{-1})
$FW^{20\%}$	FW fermentation at increasing TS contents	20	-	42.5	29.9
$FW^{25\%}$		25	-	53.2	37.4
$FW^{30\%}$		30	-	64.0	45.0
$(FW+CB)^{25\%}$	Adjustment of the TS content of the substrate by CB addition	25	18	48.5	31.7
$(FW+CB)^{30\%}$		30	36	52.0	30.3
$(FW+CB)^{35\%}$		35	50	55.3	28.6
$(FW+CB)^{40\%}$		40	60	58.3	26.7
$(FW+CB+H_2O)^{25\%}$	Complementary reactors (same substrate composition that previous at lower initial TS content)	25	36	43.4	25.3
$(FW+CB+H_2O)^{30\%}$		30	50	47.4	24.5
$(FW+CB+H_2O)^{35\%}$		35	60	50.9	23.3

The first three conditions ($FW^{20\text{-}30\%}$) were fed with FW as sole substrate at three different TS contents (control reactors). The next four conditions ($(FW+CB)^{25\text{-}40\%}$) were defined to study the application of CB to increase the initial TS content of the substrate from 25 to 40 %. Depending on the TS content, the proportion of CB in the co-fermentation reactors ranged between 18 and 60% in dry basis. Finally, the complementary reactors ($(FW+CB+H_2O^{25\text{-}35\%})$) were designed to differentiate the influence of the TS content on the DF performance from that of the CB % in the substrate. These reactors had the same CB proportions than reactors $(FW+CB)^{30\text{-}40\%}$ but lower TS contents (the same of $(FW+CB)^{25\text{-}35\%}$). All the reactors were run with a substrate to inoculum (S/X) ratio of 0.25 g VS·g VS^{-1}. After adding 60 g of FW into the vessels, the respective amounts of CB, sludge and distilled water (according to Table 3.5) were supplemented and the mixture was thoroughly homogenized. The volume of the headspace was determined by measuring the difference in pressure after addition of a known volume of gas. The reactors were sealed and flushed with nitrogen to ensure anaerobic conditions. The incubation was carried out at 35 °C and lasted for a period of 83 days. The glass reactors used had a total volume of 2.5 l, with working volumes ranging from 280 to 540 ml (according to the added amounts of sludge and CB). As described in Motte et al. (2015), the reactors used allowed sampling of the sludge during the fermentation process, avoiding disturbances of the headspace. The reactors had a specifically designed ball valve in their heads that allowed the introduction of a sampling device. After digestate collection, the system also permitted flushing out with nitrogen the small amounts of air that could have contacted the closed valve through the sampling device. This way, we ensured that minimal

amounts of oxygen could enter the reactors. All the conditions were run in duplicate. In order to allow unbiased comparisons between the different conditions, the substrate concentrations shown in Table 3.5 were calculated according to the biodegradable COD (COD_{bio}) added initially. This value was estimated from the experimental biochemical methane potentials (BMPs) of the substrates. The COD transformed into methane in the BMPs was assumed to be the fraction of biodegradable COD in the substrates.

3.3.2.3 Analytical methods

3.3.2.3.1 Physicochemical characterization of the substrates

The TS and VS contents were determined according to the standard methods of the American Public Health Association (APHA, 2005). The substrates were hydrolyzed with sulfuric acid for measurement of the protein and carbohydrates concentrations by the modified Lowry method (Lowry, 1951) and the Dubois method (Dubois et al., 1956), respectively. A gravimetric method (APHA, 2005) based on accelerated solvent extraction using an ASE®200, DIONEX coupled to a MULTIVAPOR P-12, BUCHI with heptane as solvent (100 bar, 105 °C, 5 cycles of 10 min static and 100s purge) was used to determine the lipid contents. The concentrations of Total Kjeldahl nitrogen (TKN) and ammonia nitrogen were measured with an AutoKjehdahl Unit K-370, BUCHI. Total organic carbon (TOC) and inorganic carbon (IC) were determined using a Shimadzu TOC-V_{CSN} Total Organic Carbon Analyzer coupled to a Shimadzu ASI-V tube rack. The total carbon (TC) was calculated as the sum of TOC and IC. The pH was measured by a WTW pHmeter series inoLab pH720. The chemical oxygen demand (COD) was analyzed using an Aqualytic 420721 COD Vario Tube Test MR (0-1500 $mg \cdot l^{-1}$). 2 ml of sample were pipetted into each tube and then they were placed inside a HACH COD reactor at 150 °C for 2 h. The COD concentrations were determined using an Aqualytic MultiDirect spectrophotometer.

3.3.2.3.2 Biogas quantification and analysis

The volume and composition of the biogas generated were determined as described in Cazier et al. (2015). The volumes of gas are expressed in normal conditions (at 0 °C and 1013 hPa) and the yields are expressed per gram of COD_{bio} added initially. A blank reactor was used to determine the amount of gas produced by endogenous respiration.

3.3.2.3.3 Analysis of fermentation products

The concentrations of the different metabolic products, *i.e.* VFAs, ionic species, lactic acid or ethanol, among others, were measured according to Motte et al. (2013). The concentration of free ammonia nitrogen (FAN) was calculated as a function of temperature, pH, and

concentration of total ammonia nitrogen (TAN), according to Rajagopal et al. (2013b). As for the gas yields, in order to make the yields of final metabolites comparable between the different substrates, they were expressed per gram of COD_{bio} of substrate fed.

3.3.2.4 Microbial analysis

Samples of the initial inoculum and from the batch reactors at the end of the fermentation experiments were analyzed. Polymerase Chain Reaction (PCR), quantitative PCR (qPCR) and DNA sequencing techniques were used. A precise description of the methodology employed can be found elsewhere (Moscoviz et al., 2016).

3.3.2.5 Data analysis

The least squares method was applied to study linear correlations between variables. Principal component analyses (PCA) were performed to analyze the relationships between fermentation products of the DF. The PCAs were carried out using the software package MixOmics in R. In addition, a dual hierarchal clustering analysis was used to study the results from metagenomics. The statistical analyses were computed using the statistical software R 3.2.5 (The R Foundation for Statistical Computing, Vienna, Austria). In addition, it must be mentioned that the errors bars shown in Figure 3.7, as well as the errors presented in Table 3.6 and Table 3.7 correspond to the standard deviations of the experimental results.

3.3.3 *Results and discussion*

3.3.3.1 Characterization of substrates

The main characteristics of the substrates are presented in Table 3.6. The results for the synthetic FW were similar to those reported in the literature (Capson-Tojo et al., 2016). It was mainly composed of carbohydrates (697 g·kg TS^{-1}) and it had relatively high contents of TS (21.6 %), of which 96.2 % corresponded to VS. The results for the CB suggest that it is a suitable co-substrate for FW dry DF. In this context, CB can be used to increase the C/N ratio and the TS content of the substrate. In addition, it can also supply alkalinity to the system. A more extensive characterization of the substrates can be found in Capson-Tojo et al. (2017b).

Table 3.6. Characteristics and composition of the substrates

Parameter/Element	Unit	Model Food Waste	Cardboard
TS	% (w. b.)	21.6 ± 0.7	92.7 ± 3.7
VS	% TS	96.1 ± 0.1	77.6 ± 0.2
pH	Unit pH	5.60	7.10
COD	g COD·g TS^{-1}	1.37 ± 0.05	1.19 ± 0.05
Carbohydrates	g·kg TS^{-1}	687 ± 15	958 ± 5

Parameter/Element	Unit	Model Food Waste	Cardboard
Proteins	g·kg TS^{-1}	169 ± 10	0
Lipids	g·kg TS^{-1}	72.3 ± 1.5	0
TKN	g·kg TS^{-1}	27.1 ± 1.6	2.00 ± 0.02
TC	g·kg TS^{-1}	441 ± 6	366 ± 6
C/N	-	16.3	183.0

3.3.3.2 Performance of the dry anaerobic co-fermentation reactors

As it can be observed in Table 3.7, different products, as well as different total substrate conversions, were obtained. The substrate conversions and the product yields were calculated by dividing the sum of the products obtained at the end of the experiment (in COD units) by the COD_{bio} added initially. In order to avoid accounting twice for the COD corresponding to hydrogen production-consumption, the hydrogen yields presented correspond only to the volumes of hydrogen removed from the reactors.

Table 3.7. Total substrate conversions and final yields of products (g COD·kg COD_{bio}^{-1})

Reactor	Substrate Conversion	Acetic acid	Butyric acid	Propionic acid	Valeric acid	Caproic acid	Hydrogen
$FW^{20\%}$	627 ± 3.0	248 ± 16	224 ± 11	25.4 ± 0.5	33.5 ± 4.4	60.4 ± 5.2	35.3 ± 0.2
$FW^{25\%}$	631 ± 1.8	237 ± 4	235 ± 0	25.8 ± 3.0	32.3 ± 5.6	57.8 ± 8.7	42.7 ± 1.6
$FW^{30\%}$	620 ± 0.0	238 ± 0	238 ± 0	25.4 ± 0.1	28.7 ± 0.2	42.8 ± 0.0	46.9 ± 0.2
$(FW+CB)^{25\%}$	622 ± 0.9	264 ± 1.0	239 ± 10	27.3 ± 0.5	19.6 ± 0.1	40.4 ± 2.3	31.0 ± 2.7
$(FW+CB)^{30\%}$	647 ± 0.1	280 ± 3.0	245 ± 4	26.6 ± 0.7	20.5 ± 1.7	51.0 ± 0.1	23.8 ± 0.0
$(FW+CB)^{35\%}$	616 ± 0.4	245 ± 5	237 ± 2	26.1 ± 2.7	24.0 ± 0.0	63.5 ± 9.2	20.2 ± 1.3
$(FW+CB)^{40\%}$	565 ± 1.0	181 ± 8	242 ± 13	25.8 ± 1.0	38.5 ± 5.3	70.1 ± 5.7	8.3 ± 0.7
$(FW+CB+H_2O)^{25\%}$	698 ± 0.6	329 ± 3	234 ± 3	27.4 ± 1.2	25.6 ± 7.1	49.1 ± 1.1	22.7 ± 1.4
$(FW+CB+H_2O)^{30\%}$	675 ± 1.0	278 ± 5	275 ± 11	28.2 ± 0.1	20.2 ± 1.0	53.9 ± 4.1	18.9 ± 1.2
$(FW+CB+H_2O)^{35\%}$	603 ± 1.5	212 ± 7	255 ± 9	27.7 ± 0.5	25.2 ± 0.2	69.6 ± 2.2	12.8 ± 1.9

The achieved substrate conversions were high for a DF process, ranging from 565 to 698 g COD·kg COD_{bio}^{-1}. The substrate conversions varied slightly, mainly due to the substrate composition. The reactors fed with the same substrate showed very close conversions (*e.g.* $FW^{20\text{-}30\%}$, with values of 620-631 g COD·kg COD_{bio}^{-1}). Interestingly, the highest substrate conversions were obtained in the reactors fed with a mixture of 36 % of CB (*i.e.* $(FW+CB)^{30\%}$ and $(FW+CB+H_2O)^{25\%}$), observing a synergy when this co-substrate was added. A possible explanation for the higher conversions may be that when adding small amounts of CB to the substrate, the initial substrate concentration is diluted (see Table 3.5). In addition, CB may have acted as buffer. Therefore, small quantities of CB added to the substrate may avoid or

slow down the pH drop during the acidification process, allowing longer and more extended fermentations. This hypothesis was supported by the final pH values in reactors (Figure 3.7C), which were higher at low co-digestion ratios. Moreover, while in reactors with higher initial FW concentrations (such as ($FW+CB^{25\%}$)) significant lactic acid peaks were observed initially (data not shown), the maximum concentration of this acid (which may act as sign for acidification due to overloading) was much lower, and even negligible, in reactors fed with higher CB proportion.

In addition, the conversions were higher in the water supplemented reactors ($FW+CB+H_2O^{25-35\%}$), suggesting that the addition of water to the reactors (*i.e.* working at lower TS contents) may have favored the DF process due to lower VFA concentrations at lower TS contents.

3.3.3.2.1 Effect of the operational parameters on the hydrogen production

Figure 3.7A and Figure 3.7B show the obtained hydrogen yields. As it can be observed, high hydrogen yields were achieved, with a maximum of 62.8 ml $H_2 \cdot g\ COD_{bio}^{-1}$ (corresponding to 46.9 g $COD \cdot g\ COD_{bio}^{-1}$ and 89 ml $H_2 \cdot g\ VS^{-1}$) in mono-digestion of FW at 30 % TS ($FW^{30\%}$). This value agrees with those found in the literature, suggesting an efficient DF performance (Ghimire et al., 2015a). Different maximum hydrogen yields within the range of the results presented in this study have been reported under different conditions, such as 87 ml $H_2 \cdot g\ VS^{-1}$ (Pagliaccia et al., 2016) when co-fermenting FW and olive-husks, 105 ml $H_2 \cdot g\ VS^{-1}$ after optimization of mono-digestion with buffer addition (Sreela-or et al., 2011a), 101 ml $H_2 \cdot g\ VS^{-1}$ for FW co-fermentation with sludge (Sreela-or et al., 2011b) or 145 ml $H_2 \cdot g\ VS^{-1}$ when co-fermenting FW with slaughterhouse waste (Boni et al., 2013).

As shown in Figure 3.7A, the hydrogen yields were affected linearly by the TS contents. However, while these values increased with the TS content in the mono-digestion systems (49.5-62.8 ml $H_2 \cdot g\ COD_{bio}^{-1}$), it was negatively correlated to the initial TS concentration in the co-digestion reactors (11.6-43.4 ml $H_2 \cdot g\ COD_{bio}^{-1}$). High TS contents have been found to reduce the hydrolysis rates with lignocellulosic biomass as substrate for DF, jeopardizing also the hydrogen yields (Motte et al., 2013). Nevertheless, the decrease in the hydrogen yields observed in the co-digestion systems cannot be attributed to the TS content only. As it can be observed in Figure 3.7B, the hydrogen yields were similar in the reactors fed with the same substrate (same CB proportion in the substrate) regardless the initial TS content. Therefore, it can be stated that the addition of CB affected negatively the obtained hydrogen yields. The main reason for that is the recalcitrant lignocellulosic biomass present in the CB. The

carbohydrates in CB are mainly cellulose, hemicellulose and lignin, which are less biodegradable than those found in FW. When compared to FW, the hydrolysis of the organic matter in CB occurred at a much lower extent and was much slower. Therefore, the organic matter present in the CB did not contribute significantly to the hydrogen yields during the first days of DF, when hydrogen production took place.

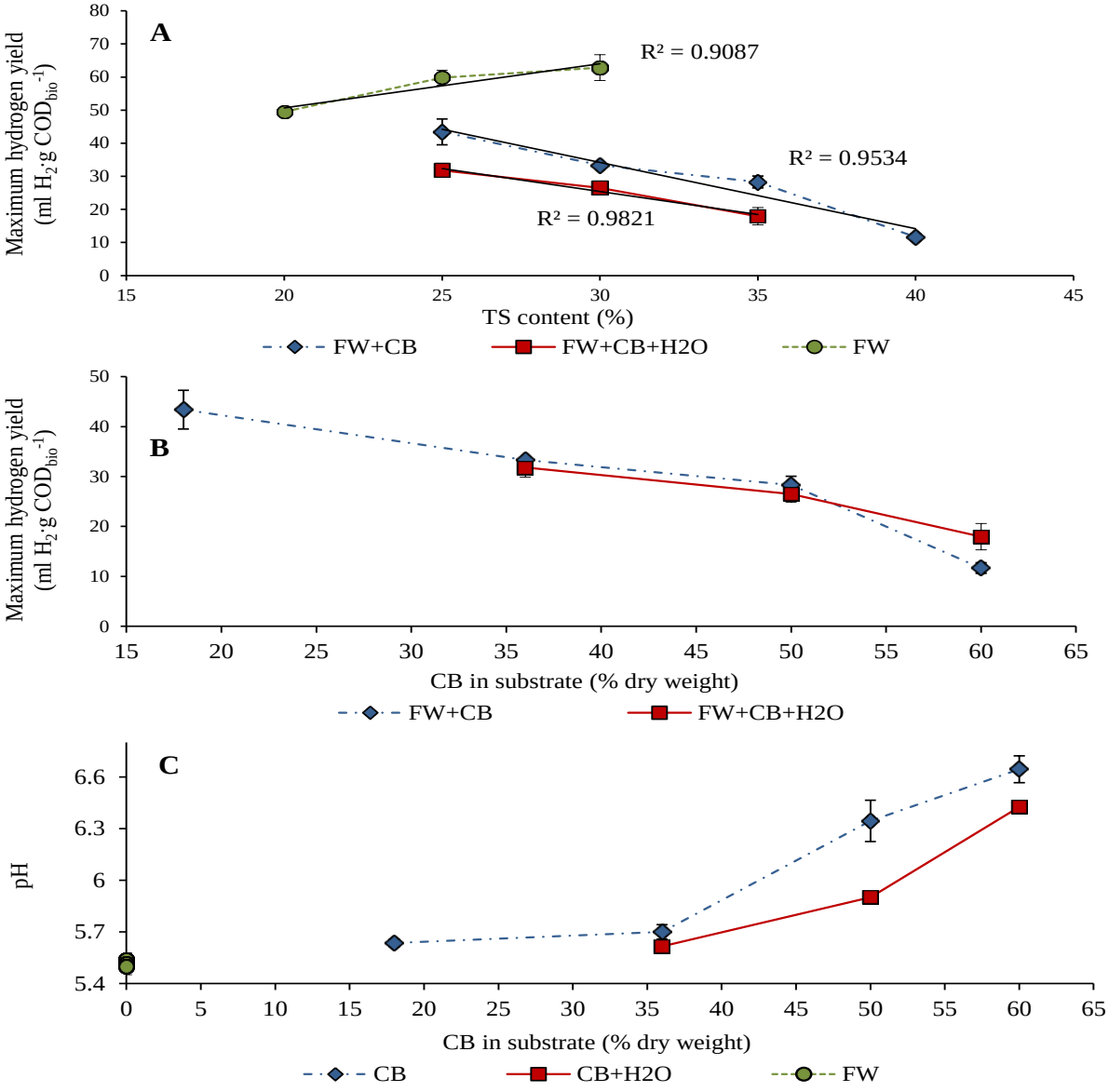

Figure 3.7. Maximum hydrogen yields in the reactors according to the initial TS content (A) and the initial co-digestion ratios (B) and final pH values in the reactors (C)

A possible explanation for the increasing hydrogen yields at higher TS contents in the mono-digestion reactors might be that the high initial TS contents limited to some extent the hydrolysis kinetics. This might have slowed down the production of acids and avoided a more pronounced pH drop besides the lower water content at the beginning of DF (when hydrogen

is produced). In fact, the minimum pH values in the mono-digestion reactors (after 10 days) did not differ significantly (5.38-5.45). Therefore, even if the VFA concentrations were higher at greater TS contents (up to 36.5 g COD·l^{-1} in $FW^{30\%}$), the higher TS contents (and consequent lack of water) acted as buffer, which avoided a decrease in the pH. This hypothesis is supported also by the pH values in the co-fermentation reactors. In those systems, even if the hydrogen yields were similar at the same co-digestion ratios, lower pH values were reported at lower TS contents (see ($FW+CB^{20-40\%}$) *vs.* ($FW+CB+H_2O^{25-25\%}$) in Figure 3.7C). Wang et al. (2015) also observed increasing hydrogen yields at increasing TS contents under semi-dry conditions (maximum at 13 % TS), obtaining maximum yields of 148.9 ml H_2·g VS^{-1} during FW mono-digestion with an adjusted pH of 6.0. The maximum yield reported by Wang et al. (2015) was higher than ours (89 ml H_2·g VS^{-1}). However, it must be considered that in their experiment they aimed to optimize the DF conditions for hydrogen production (the pH was controlled and the working TS contents were much lower), which was not the objective of this study.

3.3.3.2.2 Effect of the operational parameters on the production of volatile fatty acids

As shown in Table 3.7, high VFA yields were obtained, with values for the total VFAs ranging from 557 to 675 g COD·kg COD_{bio}^{-1}. As for the substrate conversions, the yields of total VFAs depended mainly on the composition of the substrate, with similar values for the mono-digestion reactors and the highest yields obtained when adding small amounts of CB. Again, lower values were observed at higher proportions of CB and higher TS contents. This parallelism exists because the main products were VFAs (mainly acetic and butyric acids) and therefore the substrate conversion and the yields of these acids were directly related.

The predominant VFAs were similar in all the reactors, with acetic and butyric acids being the mayor species, followed by caproic acid and finally by propionic and valeric acids. These values are in agreement with the literature. After phosphoric acid pretreatment of FW, maximum VFA yields of 0.763 g·g $COD_{removed}^{-1}$ (with acetate and butyrate as main species, followed by propionate and traces of valerate) were achieved by D. Shen et al. (2016). In addition, at an initial pH of 10, a maximum yield of 0.253 g COD·g $COD_{initial}^{-1}$ (with acetate and butyrate as main species, followed by propionate and traces of valerate) has been reported (Dahiya et al., 2015). Also, an optimum of 0.918 g·g $VSS_{removed}^{-1}$ was obtained (with butyrate followed by acetate and propionate) by K. Wang et al. (2014) at an initial pH 6.0. When testing semi-dry conditions (around 13 % TS content as maximum), an optimum of 0.799 g COD·g VS^{-1} was achieved at low TS contents during FW mono-digestion when controlling

the pH at 6.0 (propionate as main VFA, followed by butyrate, acetate and valerate) (Wang et al., 2015). In addition, hydrothermal pretreatment of FW led to improvements of the VFA yields, up to of 0.908 g·g $VSS_{removed}^{-1}$ (with butyrate followed by acetate, propionate and valerate) (Yin et al., 2014). Finally, when co-fermenting FW with waste activated sludge at optimal conditions, yields up to 0.670 g COD·g VS^{-1} have been achieved (acetic as main species, followed by propionic, butyric and valeric) by Y. Chen et al. (2013).

Interestingly, this study shows a main difference with the others reported: the relatively high yields of caproic acid achieved (up to 70.1 ± 5.7 g COD·g COD_{bio}^{-1}). Other than the inoculum used and the operational conditions, this difference is likely to be a consequence of the fermentation time. While most of the studies dealing with FW DF last for short periods of time (*i.e.* 5-6 days maximum) or have short retention times, this experiment lasted for 83 days, which allowed an extensive fermentation to occur. As the production of caproate showed a lag phase (not observed for any other acid) of 5 days minimum (data not shown), much longer fermentation periods than those required for other acids must be applied to observe significant caproate biosynthesis using DF. This can be an interesting approach due to the high added-value of caproic acid when compared to other VFAs produced by DF.

In an attempt to evaluate the relationships between the studied parameters (*i.e.* co-digestion ratio and TS content) and the final yields of the VFAs obtained, PCA analyses were carried out. The yields of final metabolites were expressed as g COD·kg COD_{bio}^{-1} for the PCAs. As the behaviors were different in the mono-digestion and the co-digestion systems, two different analyses were performed. The obtained results are presented in Figure 3.8.

As it can be observed, two totally different behaviors were observed according to the substrate used (*i.e.* mono-digestion and co-digestion).This is because, while higher TS contents led to higher substrate (FW) concentrations in the mono-digestion reactors, in the co-digestion systems it caused the opposite effect: the increasing TS contents were associated with more CB added, which caused lower initial FW concentrations (Table 3.5) and higher buffer capacities in the system.

Therefore, in the mono-digestion reactors (Figure 3.8A), the TS content was found to be negatively correlated to the valeric, caproic and acetic acids yields and positively correlated to the yields of butyric acid (with no correlation to the yield of propionic acid). Different conclusions can be extracted from these results. First of all, it must be mentioned that, as higher butyric acid yields and lower acetic acid yields were observed at higher TS, this means that the ratio butyric/acetic acid increased at high TS. This indicator can be used as an indicator of the stability of the DF process (Ghimire et al., 2015a), with increasing values at

lower pH and higher VFA concentrations. As it has already been mentioned, the final concentrations of VFAs increased with the TS, which probably caused a metabolic shift towards butyrate production due to product-induced inhibition at the relatively low working pH values (5.50-5.54). In addition, as the increase of the butyric/acetic acid ratio did not cause lower hydrogen yields (actually the opposite occurred), it can also be concluded that the reaction of homoacetogenesis played a major role for hydrogen consumption-acetic acid production (Ghimire et al., 2015a). Higher initial TS contents (thus final VFA concentrations) also led to lower yields of caproic and valeric acids. This can also be explained by the negative effect of higher final concentrations of VFAs on the fermentation process.

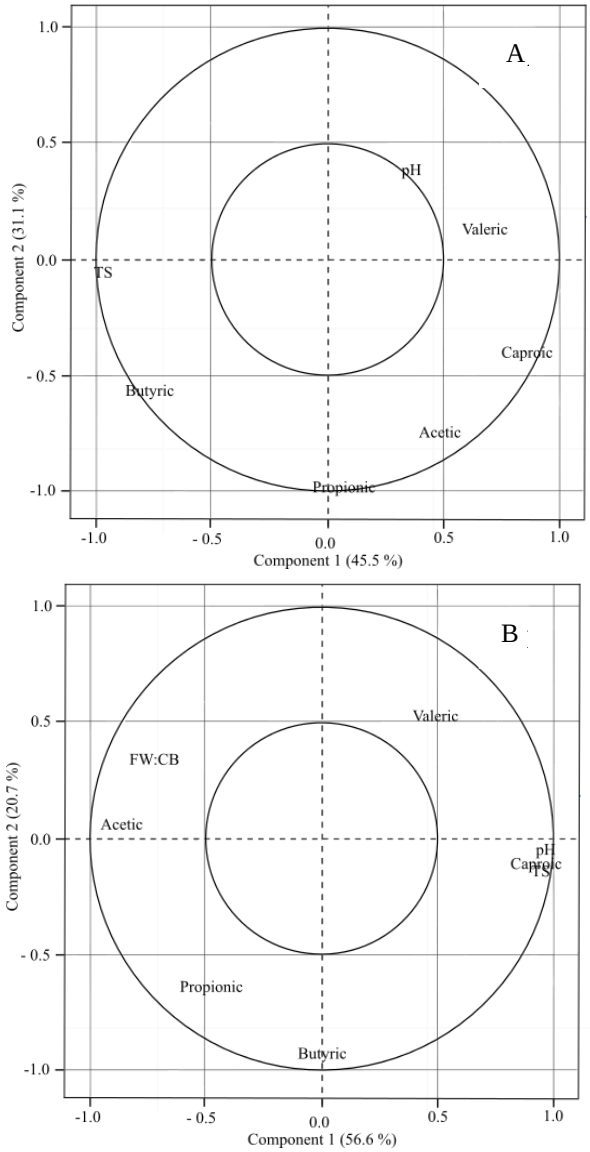

Figure 3.8. Correlation circles of the final yields of VFAs (expressed as g COD·kg COD_{bio}^{-1}), the final pH, the initial TS contents and the co-digestion ratios for the mono-digestion reactors (A) and the co-digestion reactors (B). They were formed by the projection in plans formed by the two first principal components, accounting for 76.6 % (A) and the 77.3 % (B) of the variance

On the other hand, in the co-fermentation systems (Figure 3.8B), the final yields of propionic, butyric and valeric acids were relatively not affected by the initial working conditions. However, the initial working conditions clearly affected the yields of acetic and caproic acids. As mentioned before, in this case, the TS contents were adjusted by the amount of CB, so obviously the TS was negatively correlated to the FW:CB ratio. In addition, in Figure 3.8B a proportionality can be observed between the TS and final pH (in opposition with the FW:CB ratio), which also suggests the great buffering capacity of the CB. Concerning to the yields of acetic acid, they were higher at lower proportions of CB in the substrates and lower TS contents (also in the mono-digestion reactors; see Figure 3.8A). Inversely, the yields of caproic acid were higher at higher proportions of CB in the substrates and higher TS contents, suggesting that both variables may have stimulated the synthesis of this added-value VFA. As high TS contents during FW mono-digestion did not lead to higher caproate yields, it can be hypothesized that the pathways of caproate formation were favored in the conditions were the pH was kept at high values (6.3-6.6) due to the increased buffer capacity related to addition of CB. In fact, the highest yields of caproic acid were obtained in the reactors with the highest proportions of CB (60 % CB dry basis), with values of 70.1 ± 5.6 g COD·kg COD_{bio}^{-1} $(FW+CB)^{40\%}$ and 69.6 ± 2.2 g COD·kg COD_{bio}^{-1} $(FW+CB+H_2O)^{35\%}$.

Interestingly, other than been negatively correlated to the yields of acetic acid, the yields of caproic acid were also negatively related to the maximum hydrogen yields obtained (R^2 of 0.894 for the reactors $(FW+CB)^{25-40\%}$ and of 0.972 for the reactors $(FW+CB+H_2O)^{25-35\%}$). This suggests that caproic acid was synthetized by elongation of acetate, using hydrogen as electron donor (Equation 3.10), as described in Steinbusch et al. (2011). Other than hydrogen, a common electron donor for caproate synthesis in mixed culture is ethanol (Equation 3.11) (Weimer et al., 2015). The following simplified reactions represent both pathways (Steinbusch et al., 2011; Weimer et al., 2015).

$$3C_2H_3O_2^- + 2H^+ + 4H_2 \rightarrow C_6H_{11}O_2^- + 4H_2O \qquad \Delta G^0 = -177\ kJ{\cdot}mol^{-1} \qquad \text{Equation 3.10}$$

$$C_2H_3O_2^- + 2C_2H_6O \rightarrow C_6H_{11}O_2^- + 2H_2O \qquad \Delta G^0 = -79\ kJ{\cdot}mol^{-1} \qquad \text{Equation 3.11}$$

Thus, in order to verify that hydrogen (and not ethanol) was the main electron donor for caproate production, ethanol was added into the reactors with the highest yields of caproic acid after the fermentation. Following the approach presented in Grootscholten et al. (2013), this allowed to test if this alcohol was the limiting reactant. No further caproate production

was observed after ethanol addition (data not shown), suggesting also that Equation 3.10 was the main pathway for producing caproic acid in the reactors.

Optimum conditions for caproate production have been found at controlled pH of 7 with *Clostridium Kluyveri* as main fermenter (Steinbusch et al., 2011). Thus, the higher pH values when adding CB could be an explanation for the higher yields of caproic acid at higher percentage of CB. More research must be carried out to verify if there was also a substrate-induced effect increasing the yields of caproic acid when CB was added. However, as cellulosic materials have been found to be suitable substrates for caproic acid production (and not for hydrogen production) (Kenealy et al., 1995; Weimer et al., 2015), this could also explain the higher yields at higher CB contents.

3.3.3.3 Microbial analysis after the co-fermentation

To identify relationships and to facilitate the interpretation of the results from metagenomics, a dual hierarchal clustering analysis (Figure 3.9) was carried out, using the relative abundances of the main bacteria (≥ 5 %) as input data (Venkiteshwaran et al., 2016).

Clostridiales were the main bacteria in all the reactors (with abundances ranging from 78 to 90 %), with only one main OTU corresponding to *Enterobacteriales*, probably due to traces of oxygen present in the reactors (Chatellard et al., 2016). *Clostridium butyricum* (OTU 1) was found to a predominant species in the reactors, with abundances ranging from 9 to 41 %. *C. butyricum* is a very common fermenter during DF, known to play a major role in the production of hydrogen, butyrate and acetate. Moreover, this microorganism did not form any cluster with others, suggesting that its growth was independent from other bacteria. Although the microbial populations were similar within the reactors, some differences were observed, which lead to the identification of three main clusters. The first cluster (upper part of the graph) included the conditions working at low TS contents (20-25 %) and with low proportions of CB or only fed with FW. In this cluster, *C. butyricum* was predominant, but also high relative abundances of OTUs 2 (*Neglecta timonensis*; 23-4 %) and 6 (*Clostridium sporosphaeroides*; 0-17 %) were identified. Both are also *clostridia* and belong within the same OTU cluster. The second cluster was formed by the reactors with initial TS contents of 30 %. In these conditions, *C. butyricum* was clearly predominant (much more than in the previous cluster), representing between 35 to 41 % of the bacterial OTUs. Finally, the last cluster was formed by the reactors working at the highest TS contents (35-40 %). In those cases, even if *C. butyricum* was also a main species (9-17 %), similar proportions of *C. paraputrificum* (8-16 %), *E. cloacae* (8-17 %) and *L. massiliensis* (9-10 %) (OTUs 4, 9 and 3

respectively; all in the same cluster) were also present. It is important to mention that these differences were not caused by a lack of bacterial growth in some conditions. The results of the qPCRs showed that significant amounts of bacterial 16S copies were found in all the digestates, varying from $2.30 \cdot 10^8 \pm 2.40 \cdot 10^7$ up to $4.88 \cdot 10^{10} \pm 3.32 \cdot 10^9$ copies 16S·g^{-1}.

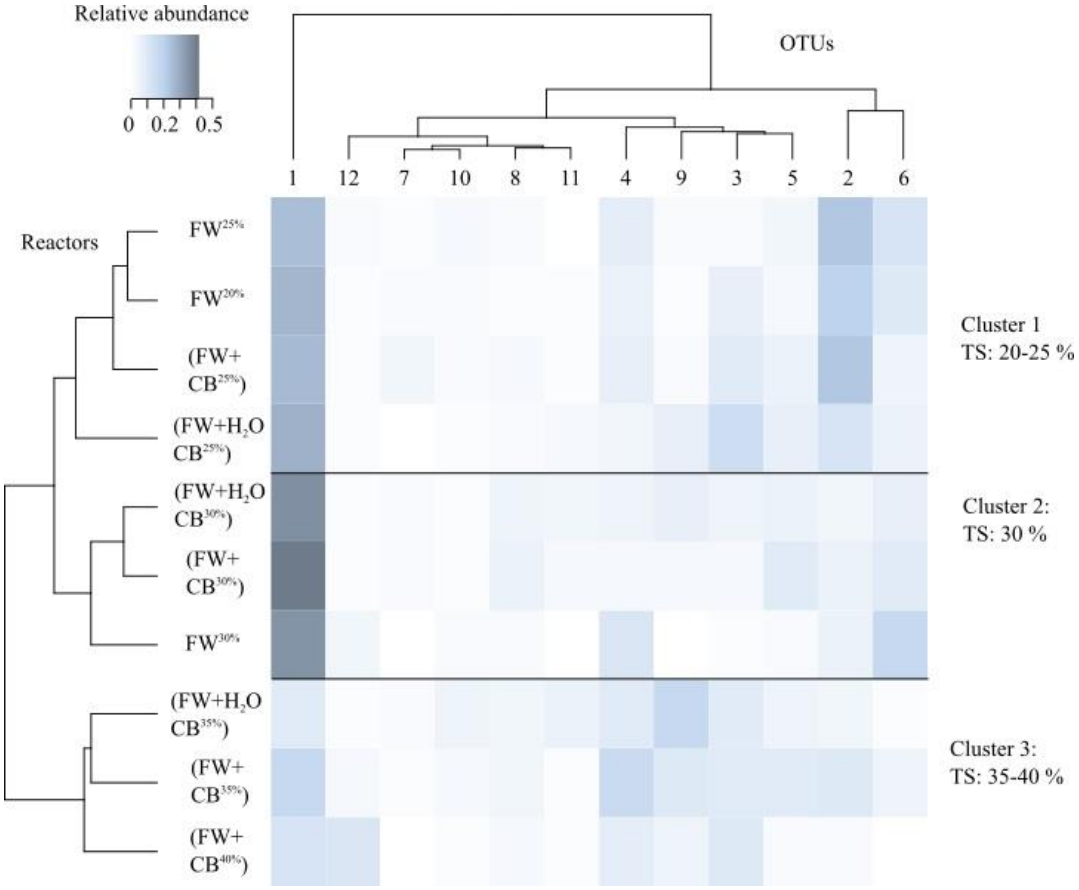

OTU	Class	Order	Family	Closest relative affiliation	Similarity (%)
1	Clostridia	Clostridiales	Clostridiaceae_1	*Clostridium butyricum*	98
2	Clostridia	Clostridiales	Ruminococcaceae	*Neglecta timonensis*	95
3	Clostridia	Clostridiales	Unclassified	*Clostridium paraputrificum*	100
4	Gammaproteobacteria	Enterobacteriales	Enterobacteriaceae	*Enterobacter cloacae*	100
5	Clostridia	Clostridiales	Ruminococcaceae	*Ruminiclostridium thermocellum*	89
6	Clostridia	Clostridiales	Clostridiaceae_1	*Clostridium sporosphaeroides*	94
7	Clostridia	Clostridiales	Clostridiaceae_1	*Oxobacter pfennigii*	92
8	Clostridia	Clostridiales	Unclassified	*Acutalibacter muris*	94
9	Clostridia	Clostridiales	Ruminococcaceae	*Lascolabacillus massiliensis*	91
10	Clostridia	Clostridiales	Ruminococcaceae	*Clostridium cellulosi*	93
11	Clostridia	Clostridiales	Ruminococcaceae	*Clostridium carnis*	99
12	Clostridia	Clostridiales	Ruminococcaceae	*Dethiobacter alkaliphilus*	89

Figure 3.9. Dual hierarchal clustering analysis of the relative abundances of the dominant bacterial OTUs (based on 97 % similarity) present in the reactors after fermentation. Only the OTUs with relative abundances higher than 5 % are presented

All these results suggest that, other than the composition of the substrates, the TS content affected to some extent the structure of the microbial communities. In addition, the Shannon diversity index increased linearly with the TS contents (R^2 values of 0.729, 0.828 and 0.925 for reactors FW+CB$^{25\text{-}40\%}$, FW+CB+$H_2O^{25\text{-}35\%}$ and FW$^{20\text{-}30\%}$, respectively), with values ranging from 0.57 to 1.00 (data not shown). Therefore, more diverse ecosystems were observed at increasing TS contents. The influence of the TS content on the microbial communities and on population selection during DF has been previously reported. However, while previous authors presented 19 % TS as a limit of operation for hydrogen production using wheat straw as substrate (Motte et al., 2014a), in this study high hydrogen yields have been achieved at much more elevated TS contents (*i.e.* 30 % TS) with FW as substrate. In addition, due to the low loads applied (0.25 g VS·g VS^{-1}), excessive acidification of the reactors was avoided, favoring the growth of hydrogen-producing *Clostridia* over that of lactic acid bacteria even if high TS contents were used. Moreover, while the main bacterial species in the inoculum was found to be *Bacilalles* (data not shown), *Clostridiales* were the main species after fermentation in all the conditions. Thus, it can be stated that, while the substrate conversions and the hydrogen and VFA yields were mainly affected by the substrate composition, this was not the case for the final structure of the microbial communities, which were mainly influenced by the TS contents in the reactors. This suggests that the production of different metabolites was not determined by the growth of predominant bacteria, but rather by metabolic changes occurring within the same microbial species. This hypothesis deserves to be confirmed by carrying out further research.

Finally, it must be mentioned that from all the different microorganisms known to produce caproic acid (*i.e. C. Kluyveri*, *Eubacterium pyruvativorans* or *Rhodospirillum rubrum*) (Angenent et al., 2016; Spirito et al., 2014), only *C. Kluyveri* was found in the reactors. However, while *C. Kluyveri* was predominant in other studies focused on caproate production from acetate (Steinbusch et al., 2011), this microorganism was a minority in our experiment, with relative abundances ranging from 0.25 to 0.71 %. Therefore, it was not possible to conclude that this microorganism was responsible for the production of caproic acid. In addition, in an attempt to find possible relationships between the main microbial OTUs and the obtained metabolic products, a correlation matrix was calculated with the relative abundances of the main OTUs, the substrate conversion and the metabolite yields as entries (data not shown). No significant relationships were found between the yields of caproic acid and any OTU. The follow-up of the fermentation process, including the DF dynamics (including both metabolites and populations), is an interesting approach that should be

evaluated in the future to elucidate the microbial species (and the metabolic pathways) responsible for the obtained results. This would eventually allow driving the DF towards the production of the most interesting compounds.

3.3.4 *Conclusions*

Maximum hydrogen yields were obtained with FW at high TS contents (62.8 ml $H_2 \cdot gCOD_{bio}^{-1}$). CB addition caused lower hydrogen yields, but stabilized DF by increasing the buffering capacity, obtaining the highest substrate conversions at low proportions of CB. The lower hydrogen yields when adding CB were translated into higher yields of caproic acid (up to 70.1 g COD·kg COD_{bio}^{-1}), which was produced mainly by consumption of acetic acid and hydrogen. The microbial communities (with *Clostridiales* as main species) depended mainly on the TS contents. This study suggests that the FW/CB proportion can be used as an easy-to-control parameter for producing high added-value products.

3.3.5 *Main outcomes and coming experiments*

As aforementioned, the initial goal of this experiment (assess the effect of the studied parameters on the methane production kinetics) was not satisfied. However, the results obtained were clearly useful from a scientific point of view and when considering a global process for biowaste valorization. Other than concluding than hydrogen could be efficiently produced at high TS contents with FW as substrate for DF, very high concentrations of high value-added products were achieved (up to 36.5 g $COD \cdot l^{-1}$ of total VFAs). The efficient production of both hydrogen and a highly-concentrated VFAs effluent indicates that dry DF of FW (with or without CB) is an option with a huge potential for integration with AD in a future biorefinery for FW valorization (*e.g.* Figure 1.5). This is without any doubt an option that deserves further research, mainly because it could improve greatly the economics of FW treatment and valorization, playing a critical role in future societies based on the concept of circular economy.

Nevertheless, as the main objective of this PhD was to achieve an efficient methane production via FW AD, several direct questions still remained unanswered: why even at an S/X ratio of 0.25 g $VS \cdot g\ VS^{-1}$ the reactors were acidified? What was the difference between the previous experiment (producing methane) and this one (not at all)? What can be done to overcome this problem?

In an attempt to clarify these doubts, it was decided to carry out the experiment presented in Section 3.4 (Table 3.9), in which a new inoculum was used. Even if at this point the results

from the analysis of the microbial communities of the inocula and the digestates were not available, it was already suspected that the problem could be related to the initial composition of the archaeal communities in the inocula (coming from a reactor treating easily degradable sugars and not adapted to high TAN/FAN and VFA concentrations) (De Vrieze et al., 2012). Therefore, it was decided to change the inocula for another that would be already adapted to these harsh stressing conditions. Thus, digestate from an industrial plant managed by SUEZ that fulfilled the requirements (high TAN concentrations) was used as inoculum. This digestate contained initially 5.04 g $TAN \cdot l^{-1}$ and 0.615 g $FAN \cdot l^{-1}$.

This new experiment would allow to verify if the acidification was actually related to the initial inoculum used and, at the same time, to evaluate the kinetics of methane production at different S/X ratios, FW:CB ratios and TS contents. With these objectives, the experimental plan described in Table 3.9 was carried out.

3.4 Kinetic study of dry anaerobic co-digestion of food waste and cardboard for methane production

Capson-Tojo, G., Rouez, M., Crest, M., Trably, E., Steyer, J.-P., Bernet, N., Delgenès, J.-P., Escudié, R., 2017. Kinetic study of dry anaerobic co-digestion of food waste and cardboard for methane production. Waste Management 69, 470-479. doi:10.1016/j.wasman.2017.09.002

Abstract

Dry anaerobic digestion is a promising option for food waste treatment and valorization. However, accumulation of ammonia and volatile fatty acids often occurs, leading to inefficient processes and digestion failure. Co-digestion with cardboard may be a solution to overcome this problem. The effect of the initial substrate to inoculum ratio (0.25 to 1 g $VS \cdot g\ VS^{-1}$) and the initial total solids contents (20-30 %) on the kinetics and performance of dry food waste mono-digestion and co-digestion with cardboard was investigated in batch tests. All the conditions produced methane efficiently (71-93 % of the biochemical methane potential). However, due to lack of methanogenic activity, volatile fatty acids accumulated at the beginning of the digestion and lag phases in the methane production were observed. At increasing substrate to inoculum ratios, the initial acid accumulation was more pronounced and lower cumulative methane yields were obtained. Higher amounts of soluble organic matter remained undegraded at higher substrate loads. Although causing slightly longer lag phases, high initial total solids contents did not jeopardize the methane yields. Cardboard

addition reduced acid accumulation and the decline in the yields at increasing substrate loads. However, cardboard addition also caused higher concentrations of propionic acid, which appeared as the most last acid to be degraded. Nevertheless, dry co-digestion of food waste and cardboard in urban areas is demonstrated as an interesting feasible valorization option.

Graphical abstract

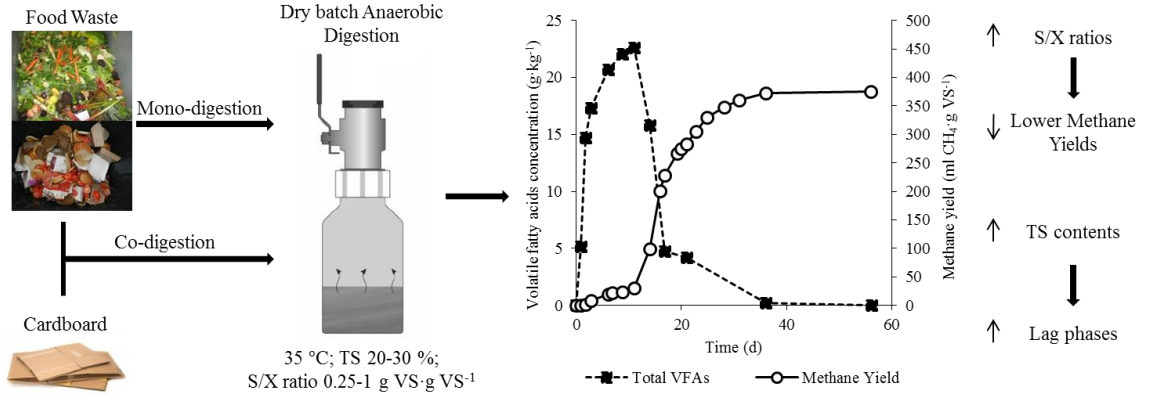

3.4.1 *Introduction*

The treatment and valorization of food waste (FW) is currently a global issue that needs to be addressed urgently. While traditional methods for FW treatment (*i.e.* landfilling and incineration) are associated with several environmental issues and increasing costs, anaerobic digestion (AD) appears as an effective environmental-friendly industrial process that allows at the same time valorization of the waste into biogas and digestate. From an industrial point of view, AD at high total solid (TS) contents and high loadings is particularly interesting due to the higher associated volumetric biogas production rates (Karthikeyan and Visvanathan, 2013). However, when digesting highly biodegradable substrates rich in nitrogen such as FW, accumulation of volatile fatty acids (VFAs) and free ammonia nitrogen (FAN) usually occurs (Banks et al., 2012, 2008; Capson-Tojo et al., 2016; L. Zhang et al., 2012), limiting the loading capacity of the system. This excessive acidification of the digesters may eventually cause a drop of the pH, leading to failure of the digestion process with low methane yields and high chemical oxygen demand (COD) concentrations in the digestates (Capson-Tojo et al., 2016).

Different alternatives have been developed recently to avoid VFA accumulation when digesting FW (Capson-Tojo et al., 2016), such as supplementation of trace elements (L. Zhang et al., 2012), addition of zero-valent iron (Kong et al., 2016a) or co-digestion (Mata-Alvarez et al., 2011). Between those, co-digestion (*i.e.* simultaneous digestion of two or more substrates) appears as an efficient low-cost option that can be used to avoid accumulation of

VFAs. Co-digestion may improve the process by diluting inhibitory compounds, by balancing the C/N ratio and the concentrations of nutrients, by adjusting the moisture content or by increasing the buffering capacity (Mata-Alvarez et al., 2011). Several co-substrates, such as landfill leachate (Liao et al., 2014), paper waste (Kim and Oh, 2011), sewage sludge (Dai et al., 2013), piggery wastewater (Zhang et al., 2011), rice husks (Haider et al., 2015) or green waste (Kumar et al., 2010), have been effectively applied for stabilization of FW AD. Among these options, paper/cardboard waste (CB) can be a suitable co-substrate for FW dry AD, since it has a high C/N ratio, a high TS content and because of its low biodegradability. Furthermore, FW and CB are the two main organic solid waste streams in urban areas (*i.e.*, CB representing up to 35 % of the municipal waste), which facilitates their centralized co-digestion (Hogg et al., 2002; Kim and Oh, 2011; Y. Zhang et al., 2012a).

Besides the potential of this alternative, few studies have been carried out to optimize FW and CB dry co-digestion. At high TS contents (30-50 %) Kim and Oh (2011) used paper waste to adjust the C/N ratio of FW, with a co-digestion ratio of 7:1 g TS FW:g TS CB. They achieved stable methane production (with yields up to 250 ml $CH_4 \cdot g\ COD^{-1}$) without significant VFA accumulation at OLRs up to 10 g $TS \cdot l^{-1} \cdot d^{-1}$. Moreover, Asato et al. (2016) co-digested FW and CB under wet conditions (TS in the inoculum lower than 10 %) at different co-digestion proportions and substrate loadings. Their results showed that mixtures with ≥ 75 % of CB avoided failure of methanogenesis (occurring at concentrations of FW ≥ 18.75 g $COD \cdot l^{-1}$), suggesting that CB addition helped the process operation. In a recent paper at TS contents between 20 and 35 %, Capson-Tojo et al. (2017b) concluded that the substrate to inoculum ratio (S/X) and the structure of the microbial community in the inoculum were crucial for an efficient AD process. With an S/X of 0.25 g $VS \cdot g\ VS^{-1}$ methane yields ranging from 307 to 409 ml $CH_4 \cdot g\ VS^{-1}$ were obtained, depending on the FW concentration and the co-digestion ratio. However, to our knowledge there is no study aiming at understanding the influence of the substrate loading and/or the TS content on the dynamics of VFA production/consumption and the methane yields during dry anaerobic batch co-digestion of FW and CB. As both parameters are critical to assess the feasibility of the AD process and to optimize its performance, their study is essential. Moreover, studying the AD kinetics at dry conditions may potentially lead to a deeper understanding of the process.

Accordingly, the objective of this study was to evaluate the influence of the initial organic load (*i.e.* S/X ratio in batch systems) and the initial TS content on the performance of dry FW mono-digestion and FW co-digestion with CB in batch systems. At the same time, the effect of CB addition itself was also assessed. For the first time under dry conditions using batch

reactors, particular attention was paid to the dynamics of VFA production/consumption and methane generation. In addition, the influence of the aforementioned parameters on the final methane yields was assessed. Aiming to elucidate the fate of the organic matter not being transformed into methane, the characteristics of the residual soluble organic matter remaining in the digestates were also studied, as well as the structure of the final microbial communities.

3.4.2 *Materials and methods*

3.4.2.1 Substrate and inoculum

A model FW was synthetized according to the VALORGAS report (VALORGAS, 2010) as in Capson-Tojo et al. (2017b). Compact cardboard (branded ‘‘Cartonnages Michel’’; shredded to 1 mm) with a density of 1.42 $kg \cdot m^{-3}$ was used as co-substrate. The characteristics of these substrates are shown in Table 3.8.

Table 3.8. Main characteristics of the substrates (Capson-Tojo et al., 2017d)

Parameter/Element	Unit	Food Waste	Cardboard
TS	% (w. b.)	21.6±0.7	92.7±3.7
VS	% TS	96.2±0.1	77.5±0.2
pH	Unit pH	5.60	7.10
COD	g $COD \cdot g\ TS^{-1}$	1.37±0.05	1.19±0.05
BMP	ml $CH_4 \cdot g\ VS^{-1}$	498±42	250±3
NH_4	$g \cdot kg\ TS^{-1}$	0.051	0.002
TKN	$g \cdot kg\ TS^{-1}$	27.08±1.64	2.00±0.02
TOC	$g \cdot kg\ TS^{-1}$	442±7	366±6
C/N	$g \cdot g^{-1}$	16.3	183
Carbohydrates	$g \cdot kg\ TS^{-1}$	687±15	958±5
Proteins	$g \cdot kg\ TS^{-1}$	169±10	0
Lipids	$g \cdot kg\ TS^{-1}$	72.3±1.5	0

* TS stands for total solids; VS for volatile solids; COD for chemical oxygen demand; BMP for biochemical methane potential; TKN for total Kjeldahl nitrogen; TC for total carbon

The inoculum was collected from an industrial plant treating a mixture of different organic streams. As the concentrations of TAN in the sludge were elevated (5.04 g $TAN \cdot l^{-1}$; pH 8.1; 336 mg $FAN \cdot l^{-1}$), it was assumed that the microbial population were already adapted to high TAN/FAN concentrations (like those found during FW AD). The sludge had a TS content of 5.81±0.02 %, with 59.13±0.08 % corresponding to volatile solids (VS).

3.4.2.2 Dry batch anaerobic co-digestion

When compared to continuous systems, batch reactors facilitate testing different conditions simultaneously much more easily and therefore they are particularly convenient for AD assays at different TS contents and inoculation ratios. To evaluate the influence of the S/X (*i.e.*, substrate loading), the initial TS content and the substrate composition, eight different conditions were defined (Table 3.9).

Table 3.9. Experimental design of the batch reactors

Purpose	# Reactor	TS_0 (%)	S/X (g VS·g VS^{-1})	FW added (g)	CB added (g)	Initial FW concentration (g VS·l^{-1})
FW at 3 S/X	FW-20-0.25	20	0.25	20	0.0	7.07
	FW-20-0.50	20	0.50	40	0.0	13.7
	FW-20-1.00	20	1.00	80	0.0	25.7
FW and CB at 3 S/X	(FW+CB)-20-0.25	20	0.25	15	2.0	4.90
	(FW+CB)-20-0.50	20	0.50	30	4.0	9.57
	(FW+CB)-20-1.00	20	1.00	60	8.0	18.3
Influence TS content	FW-30-0.25	30	0.25	20	0.0	6.19
	(FW+CB)-30-0.25	30	0.25	15	2.0	4.29
Endogenous respiration at different compost proportions	Blank1	20	-	0	0	0
	Blank2	20	-	0	0	0
	Blank3	20	-	0	0	0
	Blank4	30	-	0	0	0

* TS_0 stands for initial total solid content; S/X for substrate to inoculum ratio; VS for volatile solids; FW for food waste; CB for cardboard

The first three reactors (FW-20-0.25, FW-20-0.50, FW-20-100) consisted in mono-digestion batch reactors fed with FW at a given TS content (20 %) and different S/X (0.25, 0.50, 1.0 g VS·g VS^{-1}, respectively). To evaluate the effect of co-digestion, the same conditions were applied in reactors (FW+CB)-20-0.25 to (FW+CB)-20-1.00, but feeding a mixture of FW and CB. The co-digestion ratio was fixed at 7.48 g FW·g CB^{-1} (raw weights), obtaining a substrate with an initial TS content of 30 %. Finally, two other conditions, FW-20-0.25 and (FW+CB)-30-0.25, were applied to test the influence of the initial TS content: an S/X of 0.25 g VS·g VS^{-1} was applied, with an initial TS content of 30 %. To adjust the initial TS content in the reactors, dried stabilized compost was added into all the vessels. To correct the endogenous contribution to the biogas from the inoculum and the compost, four different blanks (one per S/X and TS content to consider the influence of the added compost) were carried out.

All reactors had a total volume of 2.5 l and were incubated at 35 °C. In order to have similar operating volumes in the reactors (0.6-0.7 l), different initial amounts of FW were added into the vessels. Afterwards, the respective amounts of CB, inoculum and compost (according to Table 3.9) were supplemented and the mixture was thoroughly homogenized. The headspace volume was determined by measuring the difference in pressure after addition

of a known volume of gas and applying the ideal gas law. The reactors were sealed and flushed with nitrogen to ensure anaerobic conditions. The reactors used were specifically designed to allow sampling of the dry digesting medium during the AD process without disturbing the gas in the head space (Motte et al., 2015). These reactors were equipped with a "ball" valve on their tops, which allowed introducing a metallic sampler. During regular operation, a rubber septum on the top of the valve (opened) allowed monitoring the biogas production. When a sample was to be taken, the valve was closed and the septum was removed. Afterwards, the metallic sampler was fixed over the valve and the sampling volume was flushed with nitrogen. Then, the ball valve was opened, allowing the sampling device to get into the reactor. Once the sample was taken, the valve was closed and the device removed, and, after flushing the empty space with nitrogen, the septum was again placed over the valve. Finally, the valve was opened again. All the conditions were run in duplicate.

3.4.2.3 Analytical methods

3.4.2.3.1 Physicochemical characterization of the substrates

The TS and VS contents were measured according to the standard methods of the American Public Health Association (APHA, 2005). The protein and carbohydrate concentrations were measured by the modified Lowry method (Frølund et al., 1996) and the Dubois method (Dubois et al., 1956), respectively. A gravimetric method (APHA, 2005) based on accelerated solvent extraction using an ASE®200, DIONEX coupled to a MULTIVAPOR P-12, BUCHI with heptane as solvent (100 bar, 105 °C, 5 cycles of 10 min static and 100s purge) was used to determine the concentrations of lipids. Total Kjeldahl nitrogen (TKN) and NH_4^+ concentrations were measured with an AutoKjehdahl Unit K-370, BUCHI. Total organic carbon (TOC) and inorganic carbon (IC) were determined using a Shimadzu TOC-V_{CSN} Total Organic Carbon Analyzer coupled to a Shimadzu ASI-V tube rack. The total carbon (TC) was calculated as the sum of TOC and IC. The pH was measured by a WTW pHmeter series inoLab pH720. The COD was analyzed using an Aqualytic 420721 COD Vario Tube Test MR (0-1500 $mg \cdot l^{-1}$). 2 ml of sample were pipetted into each tube and then they were placed inside a HACH COD reactor at 150 °C for 2 h. The COD concentrations were determined using an Aqualytic MultiDirect spectrophotometer. The biochemical methane potentials (BMPs) of the substrates were determined according to Motte et al. (2014b).

3.4.2.3.2 Gas quantification and analysis

The amount and composition of the biogas produced were determined as described in Cazier et al. (2015). The volumes were normalized (at 0 °C and 1013 hPa) and the endogenous respiration was considered by subtracting the gas generated in the blanks (Cazier et al., 2015).

3.4.2.3.3 Analysis of metabolites and final products of the digestion

The concentrations of VFAs, ionic species and other metabolic products (*i.e.*, lactic acid or ethanol) were measured by gas and ion chromatography, according to Cazier et al. (2015) and Motte et al. (2013).

3.4.2.4 Microbial community analysis

Samples of the initial inoculum and from the batch reactors at the end of the experiments were analyzed to estimate microbial growth and the structure of the microbial communities. Polymerase Chain Reaction (PCR), quantitative PCR (qPCR) and DNA sequencing techniques were applied. A precise description of the methodology used can be found elsewhere (Moscoviz et al., 2016). According to Moscoviz et al. (2016), the COD equivalent to the microbial growth was calculated assuming average values for the 16S rRNA copies per cell (1.7 for archaea and 4.7 for bacteria) and a chemical composition of the biomass of $C_4H_7O_2N$. Average cell weights were assumed to range between $2.8 \cdot 10^{-13}$ g and $8.0 \cdot 10^{-13}$ g for bacteria (*E. coli*) and between $2.0 \cdot 10^{-13}$ g and $5.8 \cdot 10^{-13}$ g for archaea (*Methanosaeta concilii*) (Milo et al., 2010).

3.4.2.5 Fluorescence spectroscopy analysis

The composition and the complexity of the soluble organic matter in the digestates obtained after AD were assessed by 3 Dimension Excitation Emission Matrix Fluorescence Spectroscopy (3D-EEM). The sample was centrifuged, filtered to 0.45 µm and diluted to a COD concentration of 3-10 $mg \cdot l^{-1}$ (Jimenez et al., 2015). As described in Jimenez et al. (2015), the spectra obtained by 3D-EEM can be decomposed on seven zones according to the fluorescence of each biochemical molecules, which varies according to their complexity. Thus, fluorescent regions I, II and III represent simple compounds and regions IV, V, VI and VII stand for complex matter. The first two regions (Tyrosine-like and Tryptophan-like) represent essential aminoacids and the third region represents soluble microbial products (SMPs), which stand for the pool of organic compounds (*e.g.* polysaccharides, proteins, nucleic acids, organic acids, amino acids, antibiotics, steroids, exocellular enzymes, structural components of cells or products of energy metabolism) that are released during substrate

metabolism and biomass decay, excluding VFAs (Barker and Stuckey, 1999). Regions IV, V, VI and VII include complex organic matter usually related with organic matter decay (*i.e.* fulvic and humic acids, regions IV and VII, respectively), large proteins (*i.e.* glycolated proteins, region V) and complex carbohydrate polymers (*i.e.* lignocellulosic matter, region VI). To simplify the results, the distributions of fluorescence from the regions corresponding to simple compounds were added-up. The same was done for the complex organic matter. A technical description of the methodology applied can be found elsewhere (Jimenez et al., 2015).

3.4.2.6 Data analysis

The concentration of FAN was calculated as explained in Rajagopal et al., (2013b), as a function of temperature, pH, and concentration of TAN. To consider the ionic strength of the media, an activity coefficient was calculated, taking into account the concentrations of the main ions present in the reactors (Cl^-, PO_4^{2-}, Na^+, NH_4^+, K^+, Mg^{2+}, H^+ and Ca^{2+}) (Rajagopal et al., 2013b). This approach allowed avoiding an overestimation of the FAN concentrations of up to 32 % when compared with the ideal solution approach. The yields of methane and metabolites produced during the digestion were progressively corrected according to the amount of digestate sampled for the dynamic analysis. The methane yields were calculated by dividing the volume of methane by the initial mass of VS of substrates (corrected).

Non-linear regression analyses were used to adjust some of the obtained results to theoretical models (*i.e.* modified Gompertz equation) and potential linear correlations between variables were assessed. The least squares method was used in both cases. To evaluate the goodness of fit of non-linear models, the predicted values were plotted against the real data. The resulting R^2 and the p-value obtained from an F-test (determining the percentage of variance explained by the model) were used as indicators.

The cumulative methane productions were fit to the modified Gompertz equation (Zwietering et al., 1990), adjusting the three parameters of the equation: final methane production, (M_{max}, ml CH_4), maximum methane production rate, (R_m, ml $CH_4 \cdot d^{-1}$), and the lag phase, (L, d). The corresponding expression is shown in Equation 3.12.

$$M(t) = M_{max} \cdot exp\left\{-exp\left[\frac{R_m}{M_{max}} \cdot (L - t) + 1\right]\right\} \qquad \text{Equation 3.12}$$

A significance level value of 5 % (α = 0.05) was used. The statistical analyses were computed using the statistical software R 3.2.5 (The R Foundation for Statistical Computing, Vienna, Austria). The functions "nls" and "cor" (from the package "corrplot") were used.

3.4.3 *Results and discussion*

3.4.3.1 Characterization of substrates

The main characteristics of FW and CB are shown in Table 3.8. These characteristics are typical for both substrates. For the model FW, the values are similar to those presented in the literature (Capson-Tojo et al., 2016), with a TS content of 21.6 % and VS/TS of 96.2 %. As it has been also previously reported, this substrate consists mainly of easily degradable carbohydrates, has a high BMP value (498 ml $CH_4 \cdot g\ VS^{-1}$) and a relatively low C/N ratio. On the other hand, CB shows a much higher TS content (92.7 %), consists of hardly degradable carbohydrates (cellulosic compounds) and has a much lower BMP. A more extensive characterization of both substrates can be found in Capson-Tojo et al. (2017b).

3.4.3.2 Kinetics of the digestion process

Figure 3.10 presents the dynamic evolution of the cumulated methane productions for the 8 operating conditions. Table 3.10 reports the corresponding kinetic parameters calculated using the Gompertz equation. The high R^2 ($\geq$ 0.994) and the low p-values ($\leq 1.72 \cdot 10^{-21}$) presented in Table 3.10 suggest a good fit of the experimental results to the Gompertz model applied.

Table 3.10. Best-fitting parameters corresponding to the representation of the cumulative methane productions by the Gompertz equation

# Reactor	TS_0 (%)	S/X (g VS·g VS^{-1})	Cumulative methane (ml CH_4)	Maximum methane production rate (ml $CH_4 \cdot d^{-1}$)	Lag phase (d)	R^2	p-value F-test
FW-20-0.25	20	0.25	1916	156	5.37	0.997	< 0.0001
FW-20-0.50	20	0.50	3470	279	7.73	0.995	< 0.0001
FW-20-1.00	20	1.00	6241	515	9.95	0.994	< 0.0001
(FW+CB)-20-0.25	20	0.25	1597	124	4.88	0.996	< 0.0001
(FW+CB)-20-0.50	20	0.50	3485	199	6.26	0.994	< 0.0001
(FW+CB)-20-1.00	20	1.00	5800	533	10.5	0.995	< 0.0001
FW-30-0.25	30	0.25	1992	182	8.43	0.998	< 0.0001
(FW+CB)-30-0.25	30	0.25	1563	147	8.22	0.996	< 0.0001

* TS_0 stands for initial total solid content; S/X for substrate to inoculum ratio; FW for food waste; CB for cardboard

At this point, it must be mentioned that all the blanks at 20 % TS were not significantly different (independently of the S/X ratio applied) and had identical kinetics (results not

shown), indicating that the added compost did not influence the obtained results. In addition, the gas produced in the blanks represented always less than 10 % of the total gas productions. On the other hand, as the blank at 30 % TS had different kinetics of methane production than the others, this condition was used to estimate the endogenous respiration from reactors FW-30-0.25 and (FW+CB)-30-0.25.

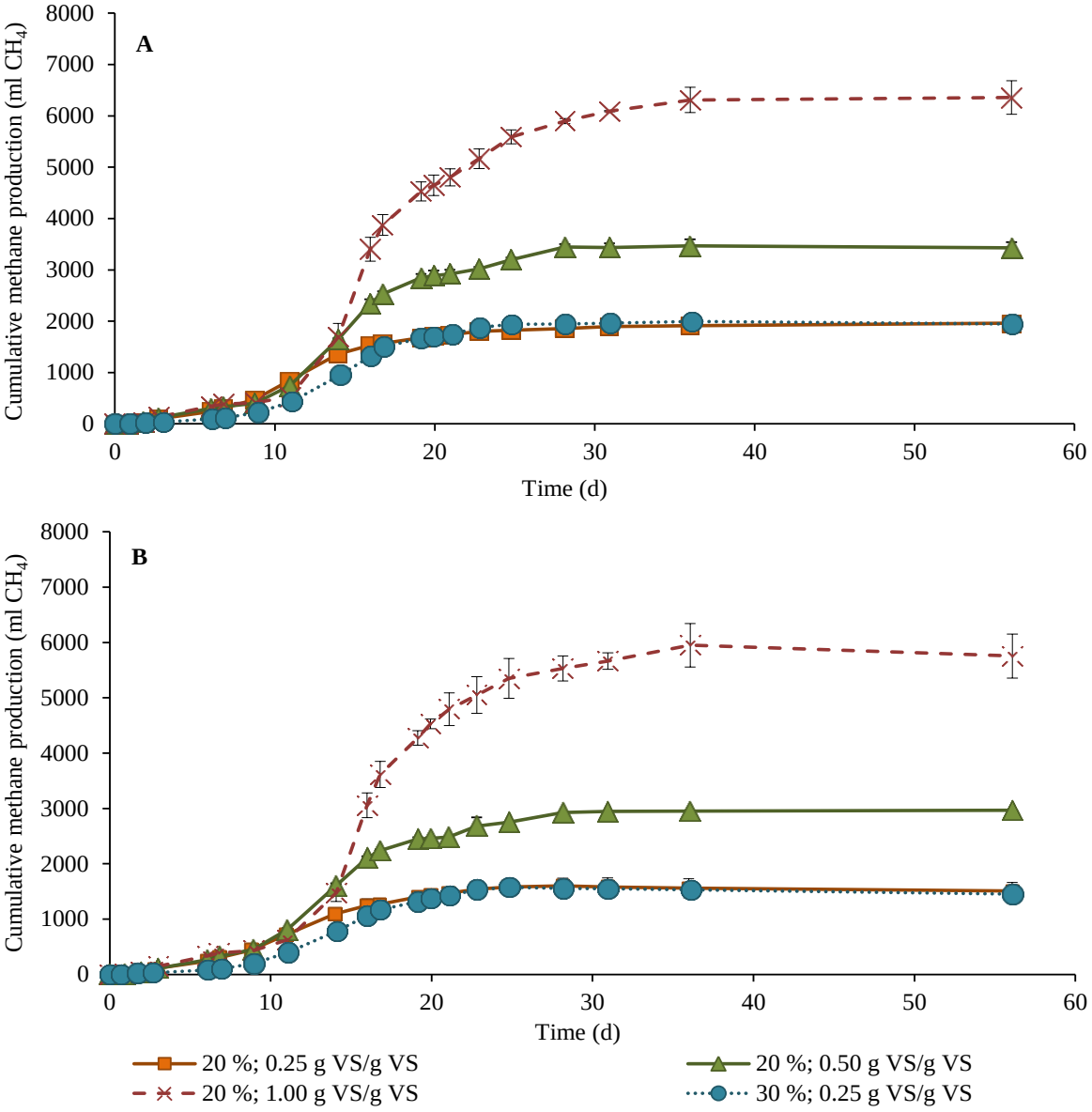

Figure 3.10. Evolution of the cumulative methane productions during anaerobic mono-digestion of FW (A) and co-digestion of FW and CB (B). The legend represents the operating conditions: TS contents (%) and S/X (g VS·g VS^{-1})

The kinetics of methane production clearly depended on the operating conditions. In both mono- and co-digestion reactors, lag phases in the methane production were observed. These lag phases were associated with initial accumulation of VFAs at the beginning of the digestion process (Figure 3.11).

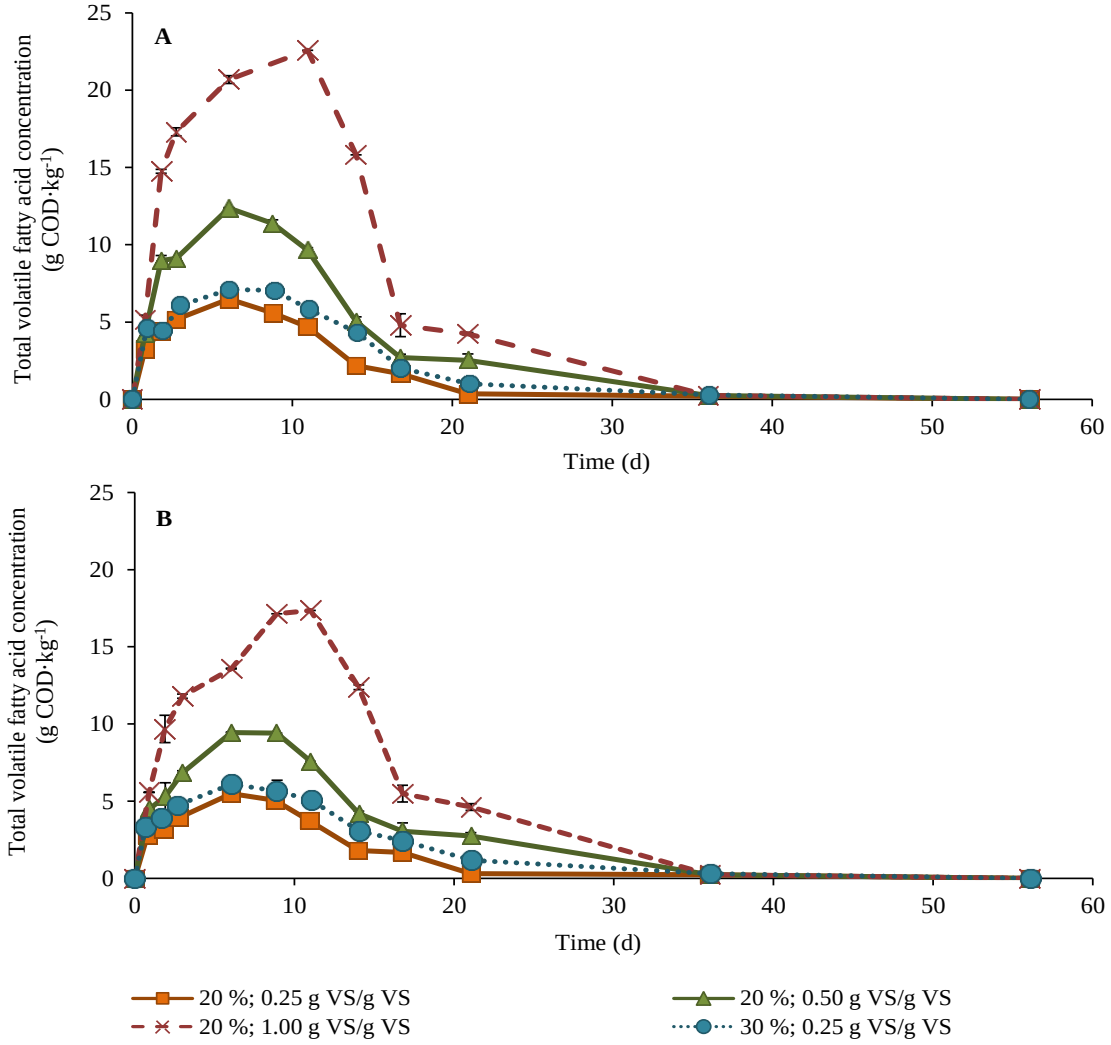

Figure 3.11. Concentration of total volatile fatty acids during anaerobic mono-digestion of FW (A) and co-digestion of FW and CB (B). The legend represents the operating conditions: TS contents (%) and S/X (g VS·g VS^{-1})

This build-up of acids can be attributed to the high biodegradability of FW. It can be hypothesized that this feature caused a fast FW hydrolysis, with its subsequent conversion into VFAs. In these conditions, the methanogenesis becomes the rate limiting step of the digestion process and VFAs start to accumulate. At greater initial concentrations of FW (higher S/X), more substrate was acidified and the obtained peaks of VFAs were more pronounced, causing greater pH drops (Figure 3.12). However, the minimum pH value was 7.78, associated with concentrations of VFAs of 22.6 g COD·kg^{-1} (FW-20-1.00). This indicates high buffering capacities in the reactors, higher at greater proportions of CB (lower pH drops). Thus, the pH values were far from being inhibitory for methanogens and cannot explain the lag phases. In fact, even if the lag phases estimated with the Gompertz equation (Table 3.10) increased with the S/X (from 5.37 to 9.95 with FW as substrate and from 4.88 to 10.5 d in the co-digestion reactors), it can be observed that all the curves working at the same

TS content are overlapped during the first 10-15 d when looking at the initial phase of methane production (Figure 3.10). This indicates that the kinetics of methane production were similar during this period. Therefore, it can be stated that the methane production was limited in all the reactors by a lack of methanogenic activity, which led to a rise in the VFA concentrations in the reactors, higher at greater S/X values. After this period, an active community of methanogenic archaea was developed and the VFAs were degraded, producing efficiently methane. In the reactors with TS contents of 30 % (*i.e.* FW-30-0.25 and (FW+CB)-30-0.25), the lower water contents led to slightly higher concentrations of VFAs when compared to reactors at 20 % and the same S/X (*i.e.* FW-20-0.25 and (FW+CB)-20-0.25), causing also slightly lower minimum pH values. In addition, longer lag phases (shown in Figure 3.10 and Table 3.10) were observed at 30 % when compared to operation at 20 %. This suggests that the growth of methanogenic archaea was jeopardized at higher TS contents, causing the higher VFA peaks.

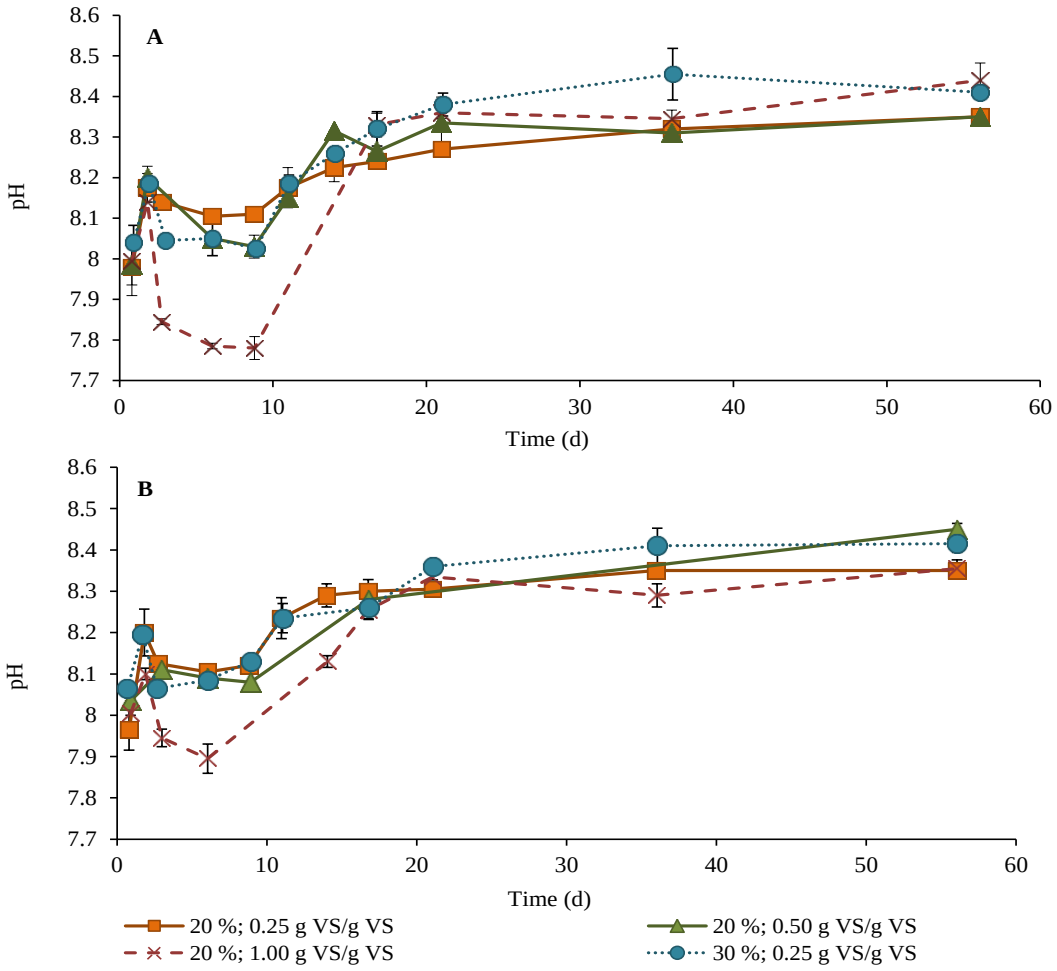

Figure 3.12. Evolution of the pH in the reactors during anaerobic mono-digestion of FW (A) and co-digestion of FW and CB (B). The legend represents the operating conditions: TS contents (%) and S/X (g VS·g VS^{-1})

The initial accumulation of VFAs and the lag phases of methane production observed may have occurred for several reasons. As no irreversible inhibition was observed, the most probable reason might have been the adaptation of the archaea to the initial overloading of substrate. Previous authors have reported long adaptation periods of methanogens (from 0 to 40 d) during AD at high concentrations of TAN/FAN, such those in this study (Van Velsen, 1979). The concentrations of these species in the inoculum were already of 5.04 g TAN·l^{-1} and 336 mg FAN·l^{-1}, reaching values up to 5.39±0.24 g TAN·kg^{-1} and 808±44 mg FAN·kg^{-1} in the digestates after AD (Table 3.11). In addition, these high TAN/FAN concentrations are responsible for the predominance of the hydrogenotrophic pathway for methane production (Banks et al., 2008). Acclimation periods for hydrogenotrophic methanogens similar to those found in this study have also been reported. According to the dilution rate, Ako et al. (2008) reported lag phases of around 5-13 d on the specific methanogenic activities of these microorganisms with inorganic substrates (hydrogen and carbon dioxide) as feed. The values shown in Table 3.10, ranging from 4.88 to 10.5 d are totally in agreement with those reported in the literature. Therefore, the results suggest that at the beginning of the AD the methanogens were overwhelmed, which led to initial VFA peaks that were greater at higher loadings of substrate. Another fact supporting that the growth of archaea caused the lag phases is that, even if the minimum pH values were higher and the VFA peaks were lower in the reactors co-digesting FW and CB (suggesting less intense VFA accumulation), this was not translated into significantly shorter lag phases, which were similar for both mono- and co-digestion. Another conclusion that can be drawn is the longer adaptation period (longer lag phases) of the methanogens according to the TS content.

Table 3.11. Concentrations of sCOD, TAN and FAN in the digestates and 3D-EEM results corresponding to the soluble fraction of the digestates

# Reactor	TS_0 (%)	S/X (g VS·g VS^{-1})	sCOD (g COD·kg^{-1})	TAN (g·kg^{-1})	FAN (mg·kg^{-1})	Fluorescence simple compounds (%)(1)	Fluorescence complex matter (%)(2)
FW-20-0.25	20	0.25	7.75±0.42	4.80±0.47	643±80	41.2±0.1	57.1±3.8
FW-20-0.50	20	0.50	7.84±0.23	5.39±0.24	713±4.0	41.7±0.4	58.3±0.2
FW-20-1.00	20	1.00	8.38±0.43	5.05±0.16	808±44	44.6±0.8	55.4±1.0
(FW+CB)-20-0.25	20	0.25	7.74±0.52	4.96±0.14	663±2	39.3±0.3	60.2±0.3
(FW+CB)-20-0.50	20	0.50	8.72±1.57	4.93±0.08	803±32	42.1±2.1	57.9±2.1
(FW+CB)-20-1.00	20	1.00	10.1±0.89	4.97±0.15	670± 49	48.2±2.0	51.8±2
FW-30-0.25	30	0.25	8.34±0.22	2.62±0.10	419±28	37.3±0.7	62.7±1.3
(FW+CB)-30-0.25	30	0.25	8.26±0.41	3.20±0.22	509±52	40.5±0.5	59.4±0.5

(1) Addition of fluorescence from regions representing simple compounds: I (tyrosine-like simple aromatic proteins), II (tryptophan-like simple aromatic proteins) and III (soluble microbial products)
(2) Addition of fluorescence from regions representing complex matter: IV (fulvic acid-like matter), V (glycolated proteins-like), VI (lignocellulosic-like) and VII (humic acid-like)

Despite being clearly within the range reported for inhibition of methanogenesis by TAN/FAN (J. L. Chen et al., 2014), efficient methane production was achieved in all the conditions. As most of the TAN was already present in the initial inoculum, no trends were found relating the initial loadings of substrates with the amounts of TAN detected. In fact, irreversible inhibition did not occur besides the high VFA concentrations due to the high TAN/FAN concentrations in the reactors and the high buffering capacity provided by the substrates (mainly CB). If the pH in the reactors had dropped, the VFAs equilibria would have been displaced towards their non-dissociated form (pKa 4.76-4.88), which would have caused severe methanogenic inhibition (Anderson et al., 1982). However, during continuous operation special attention must be paid if high concentrations of acetic acids are maintained at high FAN/TAN concentrations, mainly due to acetogenic inhibition (Banks et al., 2008; Wang et al., 1999).

To exemplify more easily the kinetics observed, Figure 3.13 presents the evolution of the methane yields and the concentrations of individual VFAs in the reactors showing more pronounced initial VFA accumulations (*i.e*. FW-20-1.00 and (FW+CB)-20-1.00; S/X of 1 g VS·g VS^{-1}).

In all the reactors, the main VFA produced was acetic acid, reaching concentrations up to 13.6 $g \cdot kg^{-1}$ and 11.7 $g \cdot kg^{-1}$ in reactors FW-20-1.00 and (FW+CB)-20-1.00, respectively. However, this acid, as well as butyric acid, was rapidly consumed when the exponential phase of methanogenesis started. On the other hand, the concentrations of propionic acid continued to increase and it was not consumed until the concentrations of any other VFAs were almost zero. Difficulties for degrading propionate during AD of FW have been previously reported (Banks et al., 2012). During syntrophic acid oxidation and hydrogenotrophic methanogenesis, which is the mechanism supposed to be predominant during high solids AD of FW (Banks et al., 2012; Capson-Tojo et al., 2017d), hydrogen and formate act as electron shuttles (Zhao et al., 2016b). For propionate oxidation towards acetate to be thermodynamically favorable, the concentrations of hydrogen and formate must be very low (Batstone et al., 2002a) and, furthermore, high acetic acid concentrations may also cause a product-induced feedback inhibition of propionate oxidation (Zhao et al., 2016b). Therefore, the concentrations of these three compounds must be kept low for propionate to be degraded. This might be the reason of the increasing propionate concentrations reported during continuous AD of FW (Banks et al., 2011a). In this study, very low concentrations of hydrogen in the biogas were detected only during the first 2 days of the AD process (up to 6 % in the gas on the 2nd day and below 0.5 % afterwards), accounting for negligible proportions of the input COD. Controversially,

although the addition of CB reduced the intensity of VFAs accumulation, it did not have any beneficial effect on the consumption of propionate. As examples, the concentrations of propionic acid on day 21 in reactors FW-20-1.00 and (FW+CB)-20-1.00 were 2.1 g·kg^{-1} and 2.5 g·kg^{-1}, respectively. The reason for that may be the slower degradability of CB, which may have led to slower production/consumption of the other VFAs, making the oxidation of propionate thermodynamically unfeasible. This may be an issue during long-term co-digestion of FW and CB.

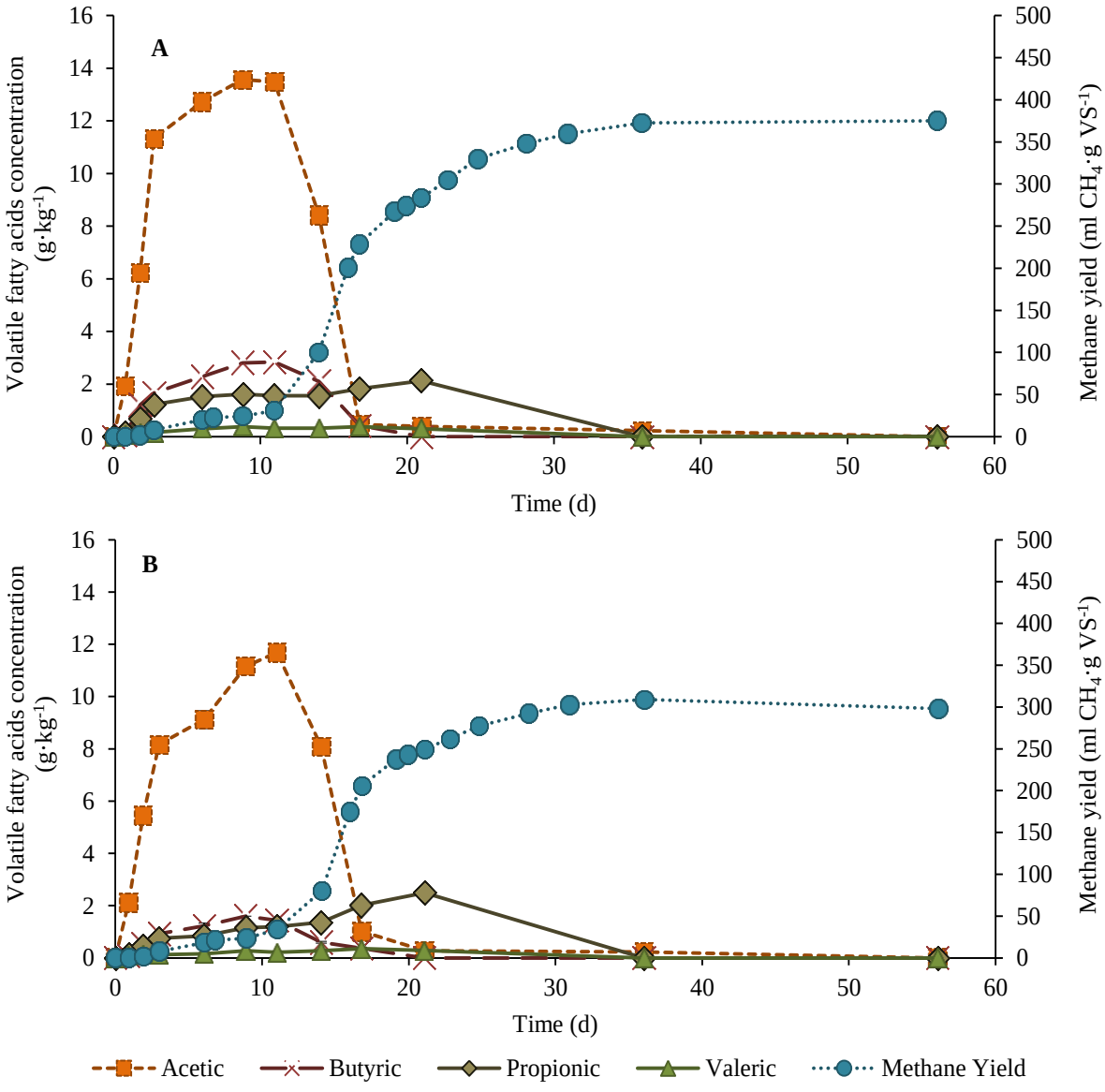

Figure 3.13. Concentrations of volatile fatty acids and methane yields during anaerobic digestion in reactor FW-20-1.00 (A; food waste mono-digestion; substrate to inoculum ratio of 1 g VS·g VS^{-1}; 20 % total solids) and reactor (FW+CB)-20-1.00 (B; food waste and cardboard co-digestion; substrate to inoculum ratio of 1 g VS·g VS^{-1}; 20 % total solids)

The obtained results suggest that CB can be potentially used in full-scale systems to stabilize FW AD at high TS contents, reducing the TAN/FAN concentrations in the reactors, the VFA peaks and increasing the buffering capacities.

3.4.3.3 Overall performance of the digestion

3.4.3.3.1 Influence of the operational parameters on the cumulative methane yields

Table 3.12 shows the experimental methane yields obtained. As it can be observed, while the TS contents did not have any effect on the experimental methane yields (FW-20-0.25 vs. FW-30-0.25 and (FW+CB)-20-0.25 vs. (FW+CB)-30-0.25), the yields decreased when increasing the initial S/X. Lower methane yields at higher substrate loadings have been previously reported using FW as substrate for wet AD. In a co-digestion experiment degrading FW and green waste, Liu et al. (2009) also obtained lower biogas yields at higher S/X. They concluded that, as the final pH values in the reactors were over 7.2, there were no remaining VFAs in the digestate. Therefore, they postulated that either the hydrolysis or the acidogenesis steps were negatively affected at high S/X. However, the fate of the COD not degraded into methane was not discussed and the final concentrations of VFAs in the reactors were not measured. In another study, Kawai et al. (2014) mono-digested FW at different S/X, concluding also that the methane yield was inversely proportional to this parameter. Moreover, they achieved methane yields over 400 ml $CH_4 \cdot g\ VS^{-1}$ only at S/X lower than 1.0 g $VS \cdot g\ VS^{-1}$. They attributed these lower yields to the so-called "reversible acidification". This term referred to the initial pH drop (lower than 6 in some reactors) caused by initial accumulation of VFAs, which were consumed afterwards. They stated that, when reversible acidification takes place, the final methane yields are often lower than those achieved when this process does not occur. Like in the present study, they did not find any residual VFAs present in the digestate. No explanation was given dealing with the fate of the COD which had not been reduced to methane. Finally, lower methane yields at S/X of 0.25 g $VS \cdot g\ VS^{-1}$ after initial VFA accumulation with FW and CB as substrates were also reported by Capson-Tojo et al. (2017b).

Concerning the influence of the substrate composition on the methane yields, as the BMP of the CB is lower than that of FW, the methane yields of the co-digestion reactors were lower than those of the mono-digestion systems. In addition, the percentages of the BMP were also lower after CB addition. While for FW the maximum yield corresponded to 93.4±2.9 % of the BMP (S/X of 0.25 g $VS \cdot g\ VS^{-1}$), for co-digestion the maximum was 79.53±7.6 % (also S/X of 0.25 g $VS \cdot g\ VS^{-1}$). This suggests that the supplementation of CB led to a lower conversion of

the substrate into methane. However, the addition of CB also diminished the negative impact of higher S/X. While the BMP percentage of FW-20-1.00 was 18 % lower than that of FW-20-0.25, the difference between (FW+CB)-20-1.00 and (FW+CB)-20-0.25 was indeed only 8.5 %.

Table 3.12. Experimental results of the final methane yields

# Reactor	TS_0 (%)	S/X (g VS·g VS^{-1})	Methane yield (ml CH_4·g VS^{-1})	% of BMP
FW-20-0.25	20	0.25	464±14	93.4± 2.9
FW-20-0.50	20	0.50	405±12	81.3± 2.5
FW-20-1.00	20	1.00	375±17	75.4± 6.4
(FW+CB)-20-0.25	20	0.25	334±32	79.5± 7.6
(FW+CB)-20-0.50	20	0.50	321	76.5
(FW+CB)-20-1.00	20	1.00	298	71.0
FW-30-0.25	30	0.25	464±24	93.2± 4.9
(FW+CB)-30-0.25	30	0.25	333±14	79.3± 3.4

* TS_0 stands for initial total solid content; S/X for substrate to inoculum ratio; VS for volatile solids; BMP for biochemical methane potential; FW for food waste; CB for cardboard

Other than the lower extent of hydrolysis or acidogenesis, a possible explanation for the lower methane yields at higher substrate loadings may be the same microbial growth and adaptation that caused the lag phases, due to more stressful AD conditions (with higher VFA and TAN concentrations). These processes would uptake COD (otherwise used for methane production) for microbial growth and for the synthesis of extra polymeric substances (EPS) and SMPs (Le and Stuckey, 2017; Lü et al., 2015). To elucidate this hypothesis, the digestates from the reactors were heavily analyzed.

3.4.3.3.2 Analysis carried out to elucidate the fate of the residual organic matter

First of all, in order to test the hypothesis of a more intense microbial growth at higher loadings, qPCRs of the inoculum and the digestates from reactors FW-20-0.25 and FW-20-1.00 were performed. A significant increase in the number of both bacterial and archaeal 16S rRNA operational taxonomic units (OTUs) was found in both reactors when compared to the inoculum. While in the inoculum the number of archaeal and bacterial OTUs were $2.82 \cdot 10^7$ $g \cdot g^{-1}$ (wet weight) and $5.87 \cdot 10^8$ $g \cdot g^{-1}$, respectively, these numbers were $6.19 \cdot 10^7$ $g \cdot g^{-1}$ (archaea) and $3.00 \cdot 10^9$ $g \cdot g^{-1}$ (bacteria) and $1.20 \cdot 10^8$ $g \cdot g^{-1}$ (archaea) and $4.00 \cdot 10^9$ $g \cdot g^{-1}$ (bacteria) in reactors FW-20-0.25 and FW-20-1.00. The number of OTUs was found to be positively correlated to the initial FW concentrations, with R^2 of 0.990 and 0.779 for archaea and bacteria, respectively, indicating a proportional growth of the microorganisms (more

intense growth when more substrate was added). It is important to mention that *Methanosarcina* was the main methanogenic species in all the samples, with relative abundances from 53 to 62 % (in accordance with difference studies (Capson-Tojo et al., 2017d; Poirier et al., 2016)). These results clearly point out the importance of the initial inoculum for efficient AD batch operation, not only of its composition, but also of the concentrations of microorganisms, which must be in accordance with the FW loading to be applied. Nevertheless, when considering the amount of COD that this biomass growth could account for, the obtained values for the microbial growth (1.9-5.6 % and 0.8-2.2 % of the total COD supplied as substrate in FW-20-0.25 and FW-20-1.00, respectively) cannot justify the lower methane yields obtained at increasing S/X.

Thus, in an attempt to elucidate the fate of the COD that had neither been transformed into methane nor into biomass, the concentrations of soluble COD (sCOD) remaining in the digestates were measured (Table 3.11).

The sCOD increased linearly with the substrate loadings (R^2 of 0.961 for FW and 0.992 for CB), with values from 7.74±0.52 g COD·kg^{-1} to 10.1±0.89 g COD·kg^{-1} in reactors (FW+CB)-20-0.25 and (FW+CB)-20-1.00, respectively (Table 3.11). In addition, to take into account the recalcitrant sCOD coming from the inoculum and the compost, the differences between the sCOD in each reactor and the optimum conditions for methane production (*i.e.* FW-20-0.25 and (FW+CB)-20-0.25 for each substrate) were calculated. This resulted in increases of the residual sCOD up to 0.627 g·kg^{-1} (FW-20-1.00) for reactors fed with FW and up to 2.37 g·kg^{-1} ((FW+CB)-20-1.00) for the co-digestion reactors. These values (and the concentrations of sCOD presented in Table 3.11) clearly show that the concentrations of recalcitrant sCOD in the co-digestion systems were much more influenced by the initial loading of substrates than those in the mono-digestion reactors. In fact, when calculating the methane that this sCOD could account for, it represented increments of 5.8 % and 7.4 % of the BMP for (FW+CB)-20-0.50 and (FW+CB)-20-1.00, respectively. Adding this extra methane production (calculated from the measured sCOD) to the experimental methane yields obtained, the differences between the methane yields in the reactors using FW and CB as substrates were negligible at the different S/X tested. This means that the remaining sCOD could explain the difference observed in the methane yields for the co-digestion reactors. However, when repeating these calculations with FW as sole substrate, the increases in the methane yields for FW-20-0.50 and FW-20-1.00 due to the sCOD accounted only for 0.55 % and 1.67 % of the BMP, values far from the differences of 12.1 % and 18 % when compared to FW-20-0.25.

Therefore, the amount of sCOD could not explain the decreasing methane yields at higher loadings in the mono-digestion reactors.

In an attempt to understand these results, the composition/structure of the sCOD was studied by 3D-EEM, a method that allows estimating the nature of the organic matter. The results (Table 3.11) show that although the distributions were similar in all the digestates due to the influence of the initial inoculum (initially much greater mass of sludge and compost was added in comparison to that of substrate), clear tendencies were present. For both substrates, increasing the S/X resulted in higher proportions of simple compounds (related to amino acid/enzyme production and SMPs (Jimenez et al., 2015)) and lower proportions of complex organic matter generally present in stable digestates and composts (coming from the initial inoculum). These differences were more pronounced in the co-digestion reactors, with the fluorescence from simple compounds increasing from 39.3±0.3 % to 48.2±2.0 % and the fluorescence from complex matter decreasing from 60.2±0.3 % to 51.8±2.0 % at increasing S/X ratios. The higher increases in the proportions of simple compounds with CB as co-substrate are in agreement with the results of the sCOD and suggest that this COD might have been used for producing enzymes, amino acids and SMPs required for the digestion process. In comparison, for the mono-digestion experiments, smaller raises in those proportions (as well as in sCOD) were observed at increasing S/X. Putting together the results of the sCOD and the fluorescence analysis, it can be concluded that, even if a more intense production of simple compounds (such as enzymes, amino acids and SMPs) occurred during mono-digestion, it could not explain the lower methane yields in this case. New results have found that, under stressful conditions (particularly at high TAN concentrations), the production of SMPs is much more important than under non-stressed conditions (Le and Stuckey, 2017). In addition to the high TAN/FAN concentrations in all the reactors in this study, higher S/X ratios led to higher transient VFA peaks, which might have led to a more intense synthesis of different simple compounds to favor microbial growth. In addition to these simple compounds, the synthesis of EPS (*i.e.* for biofilm formation) could also explain the decrease in the methane yields at greater loadings (Lü et al., 2015). These COD sinks can remain linked to the solid phase, avoiding their measurement as sCOD. To find out if these hypotheses are right and the reason of their occurrence, further research must be carried out. In addition, the hypothesis of a less performant hydrolysis step suggested by previous research remains as a feasible possibility (Kawai et al., 2014; Liu et al., 2009). The presented results suggest that the initial structure of the microbial inocula (including the soluble

products related to their metabolism) is of critical importance to achieve an efficient AD at high substrate loads, particularly in batch processes and during start-up of full-scale reactors.

3.4.4 *Conclusions*

Efficient methane production was achieved in all the conditions (71-93 % of BMP). However, biomass adaptation led to VFA accumulation and lag phases in the methane production at the beginning of AD. Increasing loadings of substrate caused more pronounced acid accumulations and lower methane yields. Although causing slightly larger lag phases, higher initial TS contents did not jeopardize the methane yields. The addition of cardboard caused less intense acid accumulations and smaller differences in the methane yields at increasing loadings. Propionate was found to be the most recalcitrant acid to be degraded and higher peaks of this acid were observed when CB was added. Higher amounts of simple organic compounds related to microbial metabolism (such as enzymes, amino acids and SMPs) were observed at higher S/X. More research needs to be carried out to elucidate the fate of the organic matter not being transformed into methane neither to sCOD. Nevertheless, if an adapted microbial consortium is used, dry co-digestion of these substrates in urban areas is an interesting feasible valorization option.

3.4.5 *Main outcomes and coming experiments*

Compared to the previous experiments presented in this chapter, efficient methane production was achieved at relatively high substrate loads and TS contents. A major conclusion of this experiment was that higher TS contents did not jeopardize the methane yields using FW as substrate, which suggests that FW dry AD could be efficiently used for industrial-scale valorization. Moreover, although the addition of CB stabilized the AD process, higher peaks of propionic acid were observed in the co-digestion reactors, which may eventually jeopardize the AD process. As it will be further discussed in Chapter 4, this was the main problem found during FW mono-digestion, which was worsen when co-digested with CB. Finally, the results also suggested the importance of using an adapted microbial consortium as inoculum.

However, the question of why the behavior of the three batch experiments presented above was so different remained unanswered. To find an explanation for this observation, the results from the analysis of the microbial communities from these experiments were further studied, trying to link the predominant species found in the successful AD reactors to their performance. This was the objective of the coming study: find general trends that would allow

determining the reasons behind the different AD performances observed. With this purpose, comparable conditions from the previous experiments (Sections 3.2, 3.3 and 3.4) were selected, according to the substrates used (*i.e.* co-digestion proportions), the initial TS contents and the S/X ratios used (see Table 3.13). The performances of the three different inocula were compared, paying particular attention to the composition of the archaeal communities in the inocula and after digestion.

3.5 *Methanosarcina* sp. plays a main role during methanogenesis from high-solids food waste and cardboard

Capson-Tojo, G., Trably E., Rouez, M., Crest, M., Bernet, N., Steyer, J.-P., Delgenès, J.-P., Escudié, R., 2017. Methanosarcina sp. as essential methanogen for efficient anaerobic digestion of high-solids food waste. Waste Management. *Submitted on December 4th 2017*.

Abstract

Anaerobic digestion of food waste is a complex process often hindered by high concentrations of volatile fatty acids and ammonia. Methanogenic archaea are more sensitive to these inhibitors than bacteria and thus the structure of their community is critical to avoid reactor acidification. In this study, the performances of three different inocula were compared using batch digestion tests of food waste and cardboard mixtures. Particular attention was paid to the archaeal communities in the inocula and after digestion. While the tests started with inocula rich in *Methanosarcina* sp. led to efficient methane production, VFAs accumulated in the reactors where inocula initially were poor in this archaea and no methane was produced. In addition, higher substrate loads were tolerated when greater proportions of *Methanosarcina* sp. were initially present in the inoculum. Independently of the inoculum origin, *Methanosarcina* sp. was the dominant methanogen in the digestates from the experiments that efficiently produced methane. These results suggest that the initial archaeal composition of the inoculum is crucial during reactor start-up to achieve stable anaerobic digestion at high concentrations of ammonia and organic acids.

Graphical abstract

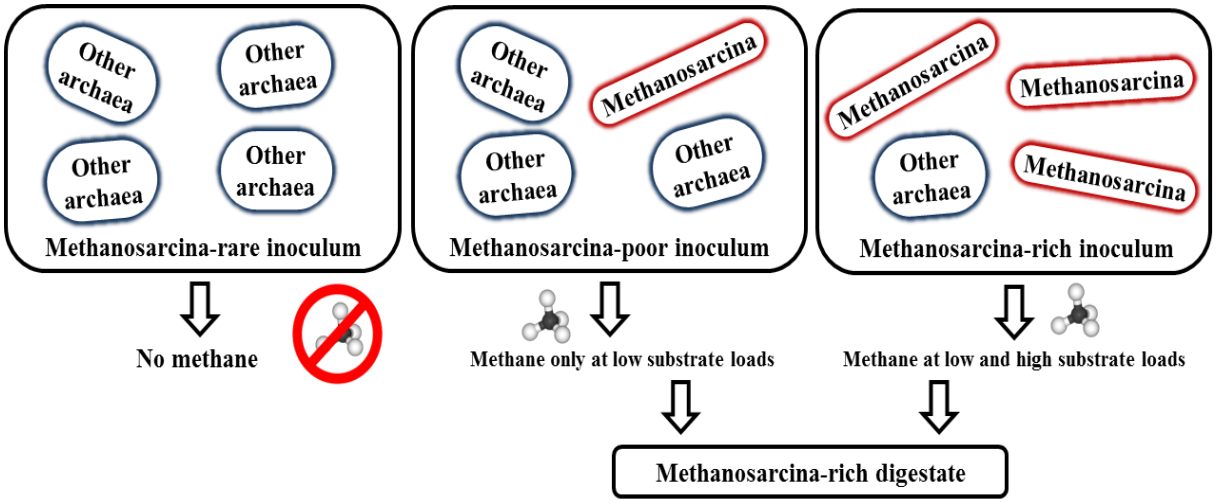

3.5.1 *Introduction*

Novel technologies for treatment and valorization of the organic fraction of municipal solid waste (OFMSW) must be developed to deal with an increasing production and new international regulations. Anaerobic digestion (AD) is a well-known process used for efficient treatment of organic waste with high total solids (TS) contents (≥ 20 %), converting them into biogas and digestate, both added-value end-products. However, AD of highly biodegradable substrates such as food waste (FW), which is a major component of OFMSW, is often associated with accumulation of volatile fatty acids (VFAs), which are detrimental to the AD process. In addition, FW is rich in organic nitrogen, which is reduced to ammonia during AD, leading to high concentrations of total ammonia nitrogen (sum of NH_3 and NH_4^+; TAN) in the digesters (L. Zhang et al., 2012). Accumulation of both VFA and/or TAN might lower the methane yields and can even lead to failure of the AD process (Banks et al., 2008). The reactors are particularly vulnerable to these inhibitions during the start-up period (Fernández et al., 2001). This occurs because the microbial communities are not adapted to the stressful conditions imposed by the substrates and the operational parameters (*i.e.* high organic loading rates). Therefore, to achieve efficient methane yields and productivities with FW as substrate, it is crucial to have well-adapted microbial communities in the digesters, which are resistant to high VFA and free ammonia nitrogen (NH_3; FAN) concentrations.

Methanogenic archaea are generally more sensitive to inhibitors than bacteria and thus methanogenesis is usually the first process affected by common inhibitors, such as FAN or VFAs (De Vrieze et al., 2012). Nonetheless, not all methanogenic archaea have the same resistance to these inhibitors and thus the composition of the archaeal microbial community varies according to the operating conditions (Abbassi-Guendouz et al., 2013). Due to their

high substrate affinity, acetotrophs such as *Methanosaeta* sp. are generally predominant under unstressed conditions and thus acetotrophic methanogenesis is the predominant pathway for methane production. On the other hand, under stressful AD conditions, these methanogens are preferentially inhibited and mixotrophic microorganisms (*i.e.* able to consume acetate and hydrogen to produce methane), such as *Methanosarcina* sp. which are more resistant to inhibitors (*i.e.* FAN or VFAs), become predominant (De Vrieze et al., 2012; Venkiteshwaran et al., 2016). In fact, while *Methanosaeta* sp. cannot grow at TAN concentrations greater than 3 $g \cdot l^{-1}$, *Methanosarcina* sp. have been found at much higher TAN concentrations (De Vrieze et al., 2012; Poirier et al., 2016). As an illustration, Capson-Tojo et al. (2017b) found *Methanosarcina* sp. to be the dominant methanogens at TAN concentrations up to 3.7 $g \cdot l^{-1}$ (795 mg $FAN \cdot l^{-1}$) using FW as substrate in AD batch tests.

Over the past years, the importance of the microbial communities for efficient AD processes has gained attention and many studies have been carried out to further understand the structures of the communities of both bacteria and archaea in AD reactors. In a recent study carried out by Zhang et al. (2016) with sewage sludge and FW as substrates (with final NH_4^+ concentrations up to 2.01 $g \cdot l^{-1}$), it was observed that *Methanosaeta* sp. was the main archaea at the beginning of the batch experiment (70.53 % of the operational taxonomical units; OTUs). Afterwards, *Methanosarcina* sp. grew during acid production (with transient VFA concentrations up to 24 $g \cdot l^{-1}$) and overpassed in abundance *Methanosaeta* sp. because of its greater resistance to VFA and TAN inhibition. Finally, other hydrogenotrophic methanogens (*i.e. Methanoculleus* sp.) grew once acetate was totally consumed. Using a high solid-state AD box-type container fed with FW at high TS contents (from 34.4 to 44.5 %) and TAN concentrations (2.5 $g \cdot l^{-1}$), Walter et al. (2016) observed that *Methanosarcina* sp. was the dominant species accompanied by different hydrogenotrophs (*i.e. Methanobacterium* sp., *Methanoculleus* sp., and *Methanocorpusculum* sp.). Consistently, Zamanzadeh et al. (2016) found *Methanosaeta* sp. as the main archaea in mesophilic continuous AD of FW at low concentrations of FAN ($\leq$ 200 $mg \cdot L^{-1}$). This further supports that the concentration of TAN-FAN is a key factor that can result in shifts of the archaeal populations. In a recent batch study, Poirier et al. (2016) identified the key microbial phylotypes resisting to extreme ammonia concentrations (up to 50 g $TAN \cdot l^{-1}$). They achieved high methane yields at TAN concentrations as high as 25 g $TAN \cdot l^{-1}$, with *Methanosarcina* sp. and *Methanoculleus* sp. as main methanogens and with relative abundances of *Methanosaeta* sp. lower than 5 % in all AD reactors.

The objective of this study was to evaluate, for the first time, the AD performance of three microbial inocula from different origins and with different initial archaeal compositions using FW and cardboard (CB) as substrates. These wastes are the main components of OFMSW (Kim and Oh, 2011; Y. Zhang et al., 2012a) and are generally collected at the same facilities, and thus their co-digestion is facilitated. Also, they constitute a good waste model substrate, since the initial proportions of carbon and nitrogen could be easily adjusted. Batch tests were performed at different substrate loads, TS contents (≥ 20 %) and co-digestion proportions. Special attention was paid to the archaeal communities and to the FAN and VFA levels.

3.5.2 *Materials and methods*

3.5.2.1 Substrate and microbial inoculum

A synthetic FW was prepared according to the VALORGAS report (VALORGAS, 2010). It was composed of fruits and vegetables (80.7 %), meat (8.2 %), pasta (4.8 %), bread (6.2 %), dairy products (1.9 %) and biscuits (1.9 %). Its precise composition has been detailed elsewhere (Capson-Tojo et al., 2017b). Being FW and CB the most common components of OFMSW, CB (branded ‘‘Cartonnages Michel’’ and shredded to less than 1 mm) was added as co-substrate to simulate this waste (Hogg et al., 2002), increasing at the same time the C/N ratio of the substrate and thus diluting the TAN concentrations in the reactors and favoring the AD process (Capson-Tojo et al., 2017b). Three different inocula from industrial plants were used: mixture of a centrifuged granular sludge issued from a mesophilic industrial UASB reactor treating sugar factory effluents with a dried digestate. This digestate was used to increase the TS content of the inoculum and was sampled in a thermophilic industrial plant treating OFMSW (Inoc-UASB1); a mixture of sludge and dried digestate issued from the same sources than Inoc-UASB1 but sampled at a different moment (Inoc-UASB2); a sludge issued from an AD industrial plant treating a mixture of different organic waste streams mixed with dried compost (99 % TS; 81 % VS) to increase the TS content of the inoculum (Inoc-OW). The amount of compost added was 0.17 g per g of inoculum (w/w).

3.5.2.2 Dry batch anaerobic co-digestion tests

Different co-digestion ratios (4-1 g TS FW·g TS CB^{-1}), initial TS contents (20-35 %) and substrate to inoculum (S/X) ratios (0.25-1.00 g VS·g VS^{-1}) were tested. To allow un-biased comparisons of the performances of each inoculum, comparable pairs of experiments (*i.e.* working at similar operational conditions) were defined. Table 3.13 summarizes the 10 different experimental conditions that were considered in this study (in triplicate). The five

selected comparable pairs (with similar initial S/X ratios, co-digestion ratios and TS contents but started with different inocula) are represented by the letters A to E (Table 3.13). This experimental set-up enabled to produce results which primarily depended on the inoculum source, while evaluating at the same time different initial operational conditions. Therefore, the obtained results were not dependent on the particular operational conditions applied, but only on the type of inoculum used. With this set-up the performances of each pair were also totally independent between them.

After adding the required volumes of sludge into the flasks, the corresponding amounts of substrates (according to Table 3.13) were supplemented. Finally, the TS contents were adjusted adding water and the flasks were flushed with nitrogen and sealed. As aforementioned, to allow working at the high TS contents desired, the inocula used were mixed with dried digestates (Inoc-UASB1 and Inoc-UASB2) and compost (Inoc-OW). Different blank reactors were carried out to account for the biogas production that could have been produced by degradation of these materials (Capson-Tojo et al., 2017b, 2017c, 2017d). The working volumes were different according to the operational conditions and the reactor size, varying from 0.4 l to 0.7 l. The duration of the batch experiments was variable (56-98 days). In the systems producing methane, the batch experiments were stopped when a plateau in the biomethane production was observed. On the other hand, longer batch periods were applied when acidification occurred (to ensure that the acid accumulation was irreversible). All the reactors were incubated at 37 °C.

Table 3.13. Operational conditions of the batch experiments and obtained methane yields. "UASB1", "UASB2" and "OW" stand for the inoculum used and the letters A-E indicate comparable pairs

Pair	Inoculum	Substrate	S/X (g VS·g VS^{-1})	Co-digestion ratio (g TS FW·g TS CB^{-1})	Initial TS (%)	Methane yield (ml CH_4·g VS^{-1})
A	UASB2	FW+CB	0.25	1.00	27.5	393±9.0
	UASB1	FW+CB	0.25	1.00	30.0	7.9±1.9*
B	UASB2	FW+CB	0.25	1.86	27.5	409±11
	UASB1	FW+CB	0.25	1.75	30.0	11±2.7*
C	UASB2	FW+CB	0.25	1.00	35.0	401±16
	UASB1	FW+CB	0.25	1.00	35.0	17±2.3*
D	OW	FW	0.25	-	20.0	464±14
	UASB1	FW	0.25	-	20.0	0.7±0.9*
E	OW	FW	1.00	-	20.0	375±17
	UASB2	FW+CB	1.00	4.00	27.5	0±0*

* These values were considered as indicators of an inefficient AD process

3.5.2.3 Analytical methods

3.5.2.3.1 Physicochemical characterization of the substrates

The TS and Volatile Solids (VS) contents were determined according to the Standard Methods (APHA, 2005). The protein and carbohydrate concentrations were measured by the modified Lowry method (Frølund et al., 1996) and the Dubois method (Dubois et al., 1956), respectively. The lipid content was determined using a gravimetric method (APHA, 2005), the pH was measured with a WTW pHmeter series inoLab pH720, total Kjeldahl nitrogen (TKN) and TAN contents were determined with an AutoKjehdahl Unit K-370, BUCHI and the total organic carbon (TOC) with a Shimadzu TOC-V_{CSN} Total Organic Carbon Analyzer. A more precise description of the analytical methods can be found in Capson-Tojo et al., (2017b). The biochemical methane potentials (BMPs) of the substrates were determined according to Motte et al. (2014). The C/N ratio was calculated as TOC divided by TKN. The FAN concentrations were calculated according to J. L. Chen et al. (2014) as a function of temperature, pH, and concentration of TAN.

3.5.2.3.2 Gas quantification and analysis

The total biogas volume was periodically determined by measuring the pressure in the reactor headspace and the gas composition was analyzed by gas chromatography coupled to a catharometer detector, as detailed in Cazier et al. (2015). The methane yields were calculated by dividing the total volume of methane by the amount of VS initially added as substrate.

3.5.2.3.3 Analysis of metabolites and final products of the digestion

The concentrations of VFAs and ionic species after digestion were measured by gas chromatography and high-performance liquid chromatography, according to Motte et al. (2013). The reactors used in the experiments carried out using the Inoc-OW and Inoc-UASB1 allowed sampling of the digestate during the digestion and therefore, the kinetics of production-consumption of metabolites were also analyzed. The sampling device is described in Capson-Tojo et al. (2017c).

3.5.2.4 Microbial community analysis

The microbial communities of the inocula and the digestates were characterized by 16S rDNA sequencing. One ml of each sample was first taken and stored at -20 °C until analysis. The DNA was extracted using a Fast DNA SPIN kit for soil in accordance with the instructions of the manufacturer (MP Biomedicals). The quality and quantity of the extracted DNA were verified by spectrophotometry using an Infinite 200 PRO NanoQuant (Tecan

Group Ltd., Männedorf, Switzerland). The primer pairs 515-532U and 909-928U and their respective linkers were used to amplify the V4-V5 regions of the 16S rRNA genes (over 30 amplification cycles were applied at an annealing temperature of 65 °C). These primer pairs target both bacterial and archaeal 16S rRNA genes, capturing most of their diversity (Wang and Qian, 2009). The PCR mixtures had a total volume of 50 µl, containing: 0.5 units of Pfu Turbo DNA polymerase (Stratagene), the corresponding buffer, each deoxynucleotide at 200 mM, each primer at 0.5 mM and 10 ng of genomic DNA. The following PCR sequence was carried out (using a Mastercycler thermal cycler; Eppendorf): after 94 °C for two min, 35 cycles of 94 °C for one min, 65 °C for one min, and 72 °C for one min were applied, with a final extension at 72 °C for 10 min. The obtained products were purified and analyzed using the Illumina MiSeq cartridge (v3 chemistry) for sequencing of paired 300 bp reads at the GenoToul platform (http://www.genotoul.fr). Mothur (version 1.35.0) was used for sequence assembling, cleaning and alignment and for assignation of the taxonomic affiliation, as described in Venkiteshwaran et al. (2016).

3.5.3 *Results and discussion*

3.5.3.1 Physicochemical characterization of substrates and inocula

The physico-chemical characteristics of the substrates and the inocula are presented in Table 3.14. The observed composition of the FW was similar to those found in the literature (Capson-Tojo et al., 2016), with TS contents of 21.6 % and VS/TS of 96.2 %. In agreement with previously reported results, the FW was mainly composed of carbohydrates and had a relatively low C/N ratio, far away from the optimum values of 25 reported in the literature (Mao et al., 2015). The high BMP value of the FW (498 mL $CH_4 \cdot g\ VS^{-1}$) highlights its great potential for valorization by AD. In contrast, CB had a high C/N ratio, suggesting that CB can be effectively used as co-substrate for diluting the TAN from FW organic nitrogen. A more extensive characterization of both substrates can be found in Capson-Tojo et al., (2017b).

Inoc-UASB1 and Inoc-UASB2 had very similar physico-chemical characteristics, with high TS (70.8 and 74.2 %) and low TAN concentrations (1.49-1.50 $g \cdot l^{-1}$). In contrast, Inoc-OW had much lower TS (5.8 %) and much higher TAN contents (5.04 $g \cdot l^{-1}$). Due to this high TAN concentrations (higher than in the two other inocula), it was expected that the microbial community in Inoc-OW was more adapted to typical FW AD conditions, *i.e.* high TAN and high transient VFA concentrations.

Table 3.14. Physico-chemical characteristics of the substrates and the inocula

Parameter/Element	Model food waste	Cardboard	Inoc-UASB1	Inoc-UASB2	Inoc-OW
TS % (wet basis)	21.6±0.7	92.7±3.7	70.8±2.2	74.2±3.1	5.81±0.02
VS (% TS)	96.2±0.1	77.5±0.2	70.9±1.4	59.1±0.4	59.1±0.1
pH	5.60	7.10	-	-	8.01
Carbohydrates ($g \cdot kg\ TS^{-1}$)	687±15	958±5	-	-	-
Proteins ($g \cdot kg\ TS^{-1}$)	169±10	0	-	-	-
Lipids ($g \cdot kg\ TS^{-1}$)	72.3±1.5	0	-	-	-
BMP ($ml\ CH_4 \cdot g\ VS^{-1}$)	498±42	250±3	-	-	-
TAN ($g \cdot l^{-1}$)	0	0	1.50	1.49	5.04
TKN ($g \cdot kg\ TS^{-1}$)	27.08±1.64	2.00±0.02	-	-	-
TOC ($g \cdot kg\ TS^{-1}$)	442±7	366±6	-	-	-
C/N	16.3	183	-	-	-

3.5.3.2 Anaerobic digestion performances

As shown in Table 3.13, while one batch test of each comparable pair produced methane efficiently, the other (working under equivalent operational conditions but started with a different inoculum) did not produce methane significantly (methane yields marked with *). This occurred because VFA rapidly accumulated at the beginning of the batch AD process. To illustrate this fact, Figure 3.14 presents the evolution of the total VFA concentrations in the experiments carried out using Inoc-OW as inoculum (efficient methane production; Figure 3.14A) and Inoc-UASB1 as inoculum (no methane production; Figure 3.14B). As it can be observed, if the initial archaea did not consume the produced VFA, the pH dropped and the methanogenesis process was inhibited. The acidified systems corresponded to all the tests inoculated with Inoc-UASB1 and the experiment started at an S/X ratio of 1.00 g $VS \cdot g\ VS^{-1}$ with Inoc-UASB2. In the tests started with Inoc-UASB1, VFA concentrations up to 33.7 g $COD \cdot l^{-1}$ (45 % COD acetic acid, 39 % butyric acid, 8 % caproic acid, 4 % propionic acid and 3 % valeric acid) were detected, causing a pH drop to values down to 5.6 (Table 3.15).

In contrast, all the batch tests inoculated with Inoc-OW produced methane efficiently, as well as the experiments carried out at low loads (S/X ratio of 0.25 g $VS \cdot g\ VS^{-1}$) with Inoc-UASB2. Although high transient VFA concentrations, up to 22.6 g $COD \cdot l^{-1}$, were observed in these reactors (Figure 3.14A), the methanogens efficiently consumed the accumulated VFAs, producing methane and avoiding a pH drop. A possible explanation for the different results obtained using the Inoc-OW is that the high initial TAN concentrations in this inoculum buffered the initial peak of VFAs (up to 22.6 g $COD \cdot kg^{-1}$; 64 % COD acetic acid, 23 % butyric acid, 10 % propionic acid and 3 % valeric acid), alleviating the pH drop. However,

such TAN-buffering effect cannot explain the different performances observed in pairs A, B and C, which compared Inoc-UASB1 and Inoc-UASB2, with similar initial TAN concentrations. In order to elucidate the reasons behind these observations, analyses of the microbial communities were performed. At this point, it must be mentioned that the methanogenic activity of all the used inocula was previously verified using ethanol as substrate. In fact, all the blank tests defined to determine the endogenous respiration produced significant amounts of methane.

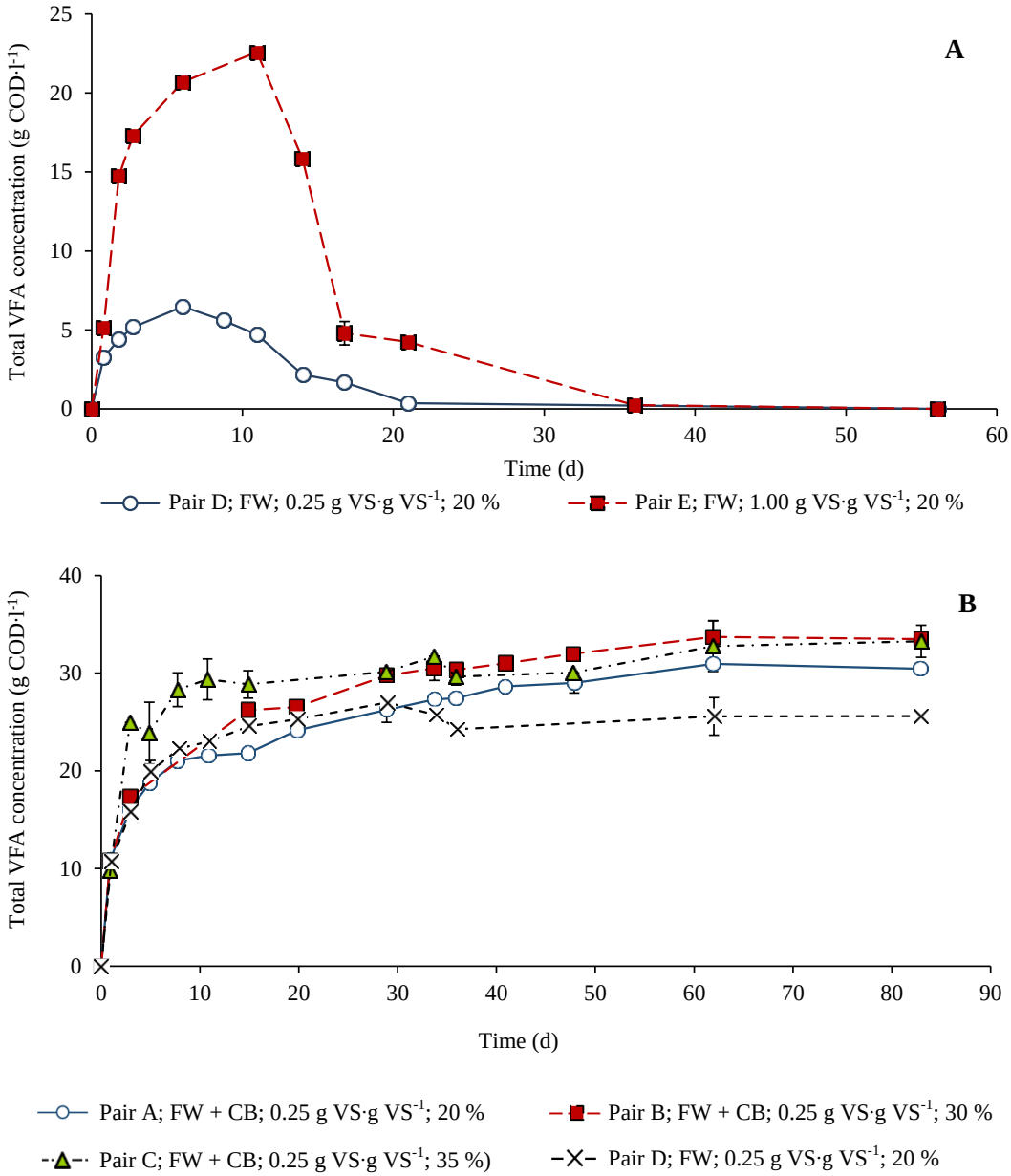

Figure 3.14. Evolution of the total VFA concentrations in the experiments carried out using Inoc-OW (A) and Inoc-UASB1 (B) as inocula. The legends indicate the pairs defined in Table 3.13, the substrate used, the S/X ratio and the initial TS content

Table 3.15. Concentrations of VFAs, TAN and FAN at the beginning and the end of the batch tests presented in Table 3.13. The values of the pH and the incubation times are also presented

Pair	Inoculum	Incubation time (d)	pH		Total VFAs (g COD·l^{-1})		TAN (mg·l^{-1})		FAN (mg·l^{-1})	
			Initial	Final	Initial	Final	Initial	Final	Initial	Final
A	UASB2	98	na[1]	8.4±0.0	nd[2]	nd[2]	470	2600±160	na[1]	567±20
	UASB1	83	na[1]	5.9±0.2	nd[2]	33.7±0.3	450	1060±30	na[1]	0.94±0.4
B	UASB2	98	na[1]	8.3±0.0	nd[2]	nd[2]	470	2900±210	na[1]	576±32
	UASB1	83	na[1]	5.9±0.1	nd[2]	33.3±0.5	530	1250±30	na[1]	1.27±0.25
C	UASB2	98	na[1]	8.5±0.0	nd[2]	nd[2]	600	3200±180	na[1]	795±55
	UASB1	83	na[1]	6.3±0.0	nd[2]	24.7±1.6	350	1340±10	na[1]	2.61±0
D	OW	56	8.1	8.3±0.0	nd[2]	nd[2]	4140	4800±480	570	948±119
	UASB1	83	na[1]	5.7±0.2	nd[2]	25.6±0.6	310	1090±140	na[1]	0.41±0
E	OW	56	8.1	8.4±0.0	nd[2]	nd[2]	3770	5050±160	519	1171±50.1
	UASB2	98	na[1]	5.4±0.5	nd[2]	64.4±14.5	370	1800±90	na[1]	1.12±1.00

1. Not available due to the high TS contents of the inoculum
2. Not detectable due to too low concentrations

3.5.3.3 Microbial composition of the inocula and the digestates

In an attempt to explain the different behaviors observed, the structures of the microbial communities of the initial inocula and the digestates sampled at the end of each batch tests were analyzed. Due to their relevance for methane production, the composition of the archaeal communities was specifically investigated. Figure 3.15 and Figure 3.16 show the relative abundances of archaea found in the three inocula (Figure 3.15) and in the batch tests producing methane (Figure 3.16). As the numbers of archaeal OTUs were negligible in the acidified experiments, they are not presented.

As shown in Figure 3.15, the initial archaeal communities varied widely according to the inoculum origin. Inoc-UASB1 and Inoc-UASB2 (non-acclimated to high TAN or VFA concentrations) were rich in the hydrogenotroph *Methanobacterium* sp. and the acetotroph *Methanosaeta* sp., both relatively vulnerable to TAN inhibition, *i.e.* not surviving over 3 g TAN·l^{-1} (De Vrieze et al., 2012). In contrast, *Methanosarcina* sp. was already the dominant species in the Inoc-OW, with the highest initial TAN concentrations, followed by the hydrogenothrops *Methanothermobacter* sp. and *Methanobrevibacter* sp. Therefore, for practical reasons these inocula were classified according to their initial relative abundance of *Methanosarcina* sp.: negligible proportions in Inoc-UASB1 (0.47 %; MS-Rare), 6.36 % of the total archaeal OTUs in Inoc-UASB2 (MS-Poor) and up to 52.6 % in Inoc-OW (MS-Rich). As the experiments performed with Inoc-UASB1 (MS-Rare) did not produce any methane and those inoculated with Inoc-OW (MS-Rich) generated methane at higher substrate loads that those inoculated with Inoc-UASB2 (MS-Poor), these results suggest that *Methanosarcina*-

scarce inocula were sensitive to inhibition when compared to inocula with higher initial proportions of *Methanosarcina* sp.

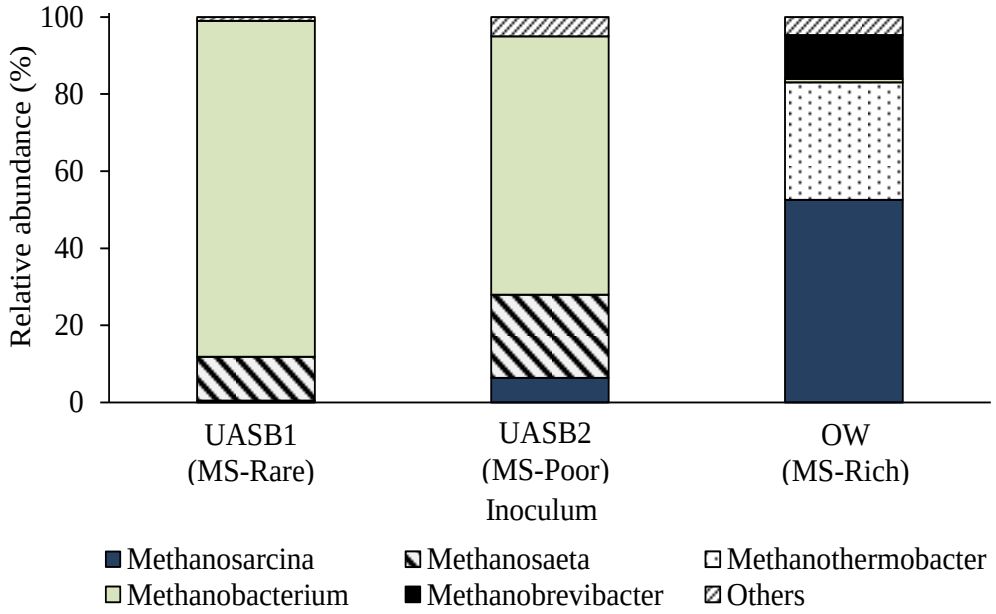

Figure 3.15. Relative abundances of archaeal OTUs in the inocula. The inocula were named "MS-Rare", "MS-Poor" and "MS-Rich" according to their low to high initial relative abundances of *Methanosarcina* sp.

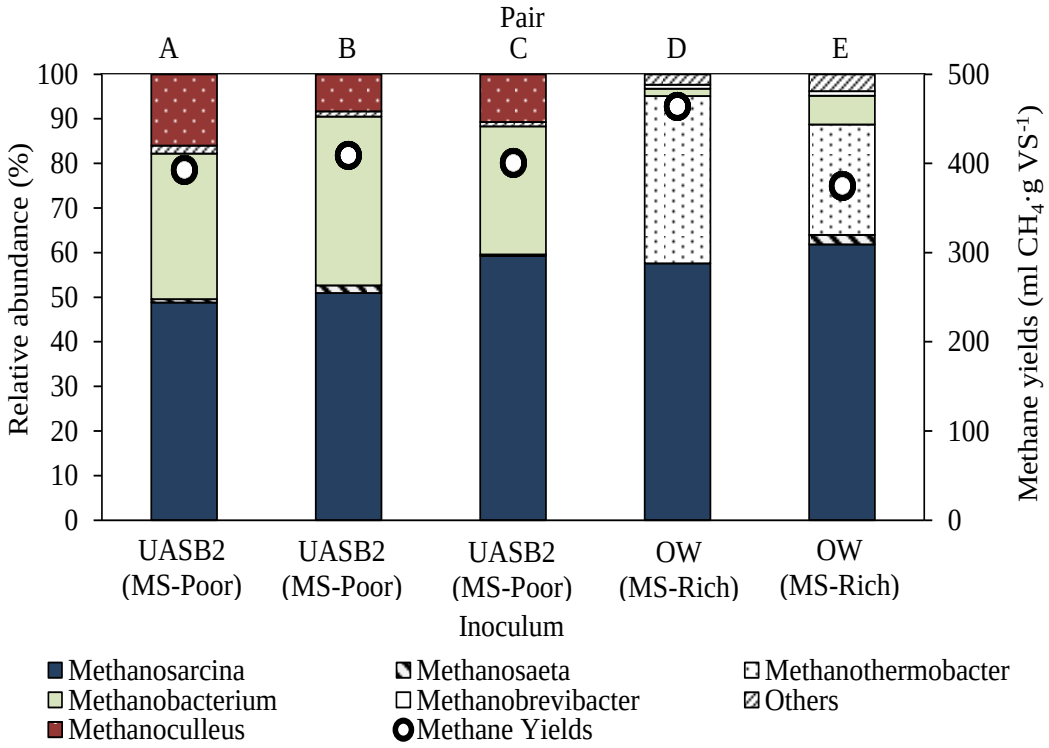

Figure 3.16. Relative abundances of archaeal OTUs in the digestates issued from the batch tests that produced methane. The methane yields are also presented. The inocula were named "MS-Poor" and "MS-Rich" according to their initial relative abundances of *Methanosarcina* sp.

The archaeal populations in the digestates after methane production (shown in Figure 3.16) support this assumption. Regardless of the initial inoculum, the predominant species in all the batch tests that produced methane was *Methanosarcina* sp., with relative abundances ranging from 48.8 % to 61.8 %. This suggests that, at the high TAN levels (up to 5.05 $g \cdot l^{-1}$) and transient VFA concentrations (up to 22.6 $g \cdot l^{-1}$) that are associated with batch high-solids AD environments (Table 3.15) the growth of members of this genus was favored, which is in agreement with different results presented in the literature (Hao et al., 2015).

This can be explained by the high resistance of *Methanosarcina* sp. to inhibition by these compounds (De Vrieze et al., 2012). As aforementioned, acetotrophs such as *Methanosaeta* sp. are generally predominant under unstressed conditions due to their higher substrate affinity and favored thermodynamics when compared to hydrogenotrophs. However, under stressful AD conditions (*i.e.* high FAN or VFAs concentrations) these methanogens are inhibited and the growth of mixotrophic and hydrogenotrophic microorganisms, which are more resistant to inhibitors, is favored (De Vrieze et al., 2012; Venkiteshwaran et al., 2016). Therefore, hydrogenotrophic methanogenesis, which otherwise would have been a secondary methane-producing pathway, becomes predominant. This finding is in agreement with a recent study using ^{14}C radiolabelling, which showed that at TAN concentrations over 2 $g \cdot l^{-1}$, hydrogenotrophic methanogenesis was predominant (68-75 % of the methane produced) over the acetoclastic pathway (Jiang et al., 2017). Therefore, the growth of hydrogenotrophic/mixotrophic microorganisms (such as *Methanosarcina* sp.) was favored under these conditions.

In addition, when comparing the tests that produced methane with the others, the importance of *Methanosarcina* sp. to achieve efficient methanogenesis is also highlighted. Using Inoc-UASB1 (MS-Rare), where the proportion of this group of archaea was initially negligible, no efficient methane production was achieved under any condition, even at relatively low organic loads (0.25 g $VS \cdot g\ VS^{-1}$). On the other hand, the experiments operated under equivalent conditions but inoculated with Inoc-UASB2 (MS-Poor; with 6.36 % of *Methanosarcina* initially) showed efficient methane production, likely due to the presence and the emergence of this group of methanogens. This is supported by the fact that a minimum of 48.8 % of *Methanosarcina* was observed in these tests after AD, indicating that the growth of this group of archaea prevailed. Moreover, when looking at the results obtained using Inoc-OW (MS-Rich; 52.5 % *Methanosarcina* initially), high methane yields were achieved at substrate loads up to 1 g $VS \cdot g\ VS^{-1}$, values where Inoc-UASB1 (MS-Poor; with lower initial proportions of *Methanosarcina*; 6.36 %) led to acidification and no methane was produced.

These results are in accordance with a recent review article focused on the microbial communities of FW AD. In their bibliographic study, P. Wang et al. (2017) pointed out that *Methanosarcina* sp. was a predominant methanogen during dry FW AD and that the presence of this archaea could potentially act as an indicator of a stable and efficient dry AD process. It must also be mentioned that, together with this particular archaea, the development of other microorganisms growing in syntrophy with *Methanosarcina* sp. might have also been of critical importance. The growth of other hydrogenotrophic methanogens (such as *Methanothermobacter* or *Methanoculleus*) might have contributed greatly to the metabolic shift towards hydrogenotrophic methanogenesis as main methane-producing pathway. Moreover, if it is assumed that this was the main route for methane production using FW and CB as substrates (Capson-Tojo et al., 2017a), the growth of syntrophic acetate oxidizers has also been essential to degrade acetate to hydrogen, facilitating the production of methane by the hydrogenotrophs. Finally, the fact that all the reactors producing methane (regardless of the inoculum used) had *Methanosarcina* sp. as predominant methanogen suggest that the relevance of its growth was independent of the particular characteristics of each inoculum (*i.e.* initial VS concentration or sludge mixture).

These results highlight the critical relevance of the initial composition of the archaeal populations in the inoculum to achieve efficient AD, especially during reactor start-up. In particular, the results suggest the great importance of *Methanosarcina* sp. and other hydrogenotrophs within the archaeal populations to achieve efficient dry AD of FW. The structure of the archaeal community used to start up batch FW AD may also explain the high variability of the substrate loading limits reported in the literature, ranging from below 0.5 g VS·g VS^{-1} to over 2 g VS·g VS^{-1} (Capson-Tojo et al., 2016). These results could have great implications in industrial scale AD installations, in particular for the start-up of continuous AD systems and for the initial conditions applicable for batch AD systems.

3.5.4 *Conclusions*

AD performances of three different inocula were compared using FW and CB as substrates. Particular attention was paid to the compositions of the archaeal communities in the inocula and in the digestates. Regardless of the inoculum used, *Methanosarcina* sp. was the dominant methanogen in all the experiments where methane was produced, suggesting that these archaea played a critical role in methane production at high TAN and VFA concentrations. Higher proportions of *Methanosarcina* sp. in the inocula also allowed greater substrate loads. The initial composition of the archaeal communities in the inoculum was

found to be crucial, mainly in batch systems and during reactor start-up. This may have huge implications for industrial-scale installations treating FW and CB.

3.6 General conclusions and perspectives

This chapter allowed obtaining different value-added products from FW via its valorization through dry anaerobic processes. In addition, the main factors affecting the AD and DF processes were also elucidated. Also a deeper understanding on the basics and the microbial interactions existing during each process was gained.

With the first experiment (Section 3.2), the feasibility of FW and CB valorization via dry AD was proved, concluding also that the S/X ratio was a critical parameter determining the metabolic pathways: at low values (0.25 g VS·g VS^{-1}) AD could be achieved and at higher values DF took place due to VFA accumulation. The results presented in Section 3.3 served to verify that hydrogen production (with the concomitant VFAs) by dry DF is a feasible alternative for FW valorization. In addition, different products could be obtained by varying the operational parameters and the co-digestion ratios, which opened new possibilities for driving biological processes to obtain the desired products. Even if this strategy was not further researched in this thesis, this alternative has a huge potential for improving the economic viability of future environmental biorefinery, allowing the synthesis of products (at high concentrations) with much higher prices than energy carriers such as methane. Section 3.4 served to assess the kinetics of FW AD for methane production, concluding at the same time that high substrate loadings may lead to lower methane yields (even though the methane volumetric productivities were higher) and that CB may serve as co-substrate to stabilize the AD process. Finally, Section 3.5 permitted to verify the tremendous importance of the archaeal composition of the microbial consortium for achieving an efficient dry AD process, with *Methanosarcina* sp. as predominant methanogen in FW AD. To facilitate the understanding of the conclusions obtained in this chapter, they are summarized in Table 3.16.

To conclude, the obtained results open up several research questions, as well as industrial alternatives, that had to be answered/tested if the main objective of this thesis (to develop an efficient FW treatment process via AD) was to be achieved. Thus, with the aforementioned information, it was decided to move forwards towards the operation of consecutive batch AD pilot reactors, using the inoculum that had shown the best performance (that of Section 3.4). Simultaneously, different strategies for stabilization of FW AD, such as TEs addition, working at low temperatures and FW co-digestion, were tested. It must be mentioned that, as

at this point we knew that the TS content in the reactors would not be as high as those tested previously (due to to the high biodegradability of FW), the initial TS contents were not artificially increased in the experiments presented in Chapter 4 and Chapter 5.

Table 3.16. Summary of the conclusions of Chapter 3 and research perspectives

Section	**3.2**	**3.3**	**3.4**	**3.5**
Objective	Evaluate feasibility of FW valorization via dry anaerobic co-digestion with CB	Assess feasibility of FW dry fermentation with CB as co-substrate	Study kinetics of methane production in mono-digestion of FW and its co-digestion with CB	Compare AD performances of three different inocula
Main conclusion	Several products obtained; S/X ratio as critical parameter determining the metabolic pathways	Maximum H_2 yields with FW and high TS; with CB: lower H_2 yields and higher HCap yields	Higher substrate loads reduced the methane yields; CB acted as stabilizing agent	*Methanosarcina* sp. as essential archaea for an efficient methane production from FW via dry AD
Novelty	Feasibility of FW and CB valorization via dry AD and DF	Production of highly concentrated VFAs from FW and CB	Study kinetics of AD at high TS contents	Importance of archaeal community on AD performance
Agreement with literature	AD valorization (Asato et al., 2016); DF at high S/X ratios (Cao and Zhao, 2009)	Similar H_2 yields (Pagliaccia et al., 2016); highest yields at high TS contents (Wang et al., 2015)	Lower methane yields at high FW loads (Kawai et al., 2014; Liu et al., 2009)	*Methanosarcina* sp. as predominant methanogen in dry FW AD (P. Wang et al., 2017)
Hypotheses and perspectives	• An adapted inoculum should allow an efficient FW AD (semi)continuously • CB is a potential option for stabilizing FW AD • Different reactor configurations using FW as substrate must be studied • Different co-substrates to stabilize FW AD should be evaluated • An optimization of the substrate load must be carried out, aiming to determine maximum values avoiding acidification			

FW stands for food waste, CB for cardboard, AD for anaerobic digestion, S/X for substrate to inoculum, TS for total solids, HCap for caproic acid, VFAs for volatile fatty acids and HPr for propionic acid

Chapter 4. Accumulation of propionic acid as main issue during food waste anaerobic digestion for methane production

4.1 General introduction

The next stage of the PhD project consisted on the pilot scale AD of FW using consecutive batch reactors. After solving the main issue faced at the beginning of the experiment (the need of using an adapted microbial inoculum), the AD tests were scaled-up and potential strategies for AD stabilization were tested. Successive batch reactors were used in this study, mainly because of two reasons: (i) it is a process that can be applied at industrial scale and (ii) the obtained results can be used to simulate a plug-flow reactor with digestate recirculation (another industrially feasible alternative).

Thus, the main goal of this experiment was to elucidate if consecutive batch AD of FW was a process that could provide an efficient FW valorization, evaluating at the same different possibilities to favor the consumption of the VFAs accumulated at the beginning of the batch AD process. In this context, and according to the literature, three different approaches were tested to avoid this VFA build-up: (i) working at low temperatures (aiming to reduce the FAN proportions), (ii) co-digestion of FW with PW (aiming to dilute the nitrogen input and provide buffering capacity) and (iii) supplementation of TEs (aiming to favor VFA consumption by promoting the synthesis of enzymes). A summary of the objectives of these experiments and the materials used is presented in Table 4.1

This chapter presents the obtained results, introducing also the second main issue that was found along the project: the accumulation of propionic acid. At the end of the chapter, potential solutions to overcome this problem are also presented. Section 4.2 corresponds to a scientific publication.

Table 4.1. Summary of the objectives and the parameters varied in the experiments presented in Chapter 4

Section	Objective	Parameters varied
4.2	Compare the performances of co-digestion with CB, low reactor temperature and addition TEs for digestion stabilization	S/X ratio

CB stands for cardboard, TEs for trace elements and S/X for substrate to inoculum

4.2 Accumulation of propionic acid during consecutive batch anaerobic digestion of commercial food waste

Capson-Tojo, G., Ruiz, D., Rouez, M., Crest, M., Steyer, J.-P., Bernet, N., Delgenès, J.-P., Escudié, R., 2017. Accumulation of propionic acid during consecutive batch anaerobic digestion of commercial food waste. Bioresource Technology 245, Part A, 724-733. doi:10.1016/j.biortech.2017.08.149

Abstract

The objective of this study was to test three different alternatives to mitigate the destabilizing effect of accumulation of ammonia and volatile fatty acids during food waste anaerobic digestion. The three options tested (low temperature, co-digestion with paper waste and trace elements addition) were compared using consecutive batch reactors. Although methane was produced efficiently (~500 ml $CH_4 \cdot g\ VS^{-1}$; 16 l $CH_4 \cdot l\ reactor^{-1}$), the concentrations of propionic acid increased gradually (up to 21.6 $g \cdot l^{-1}$). This caused lag phases in the methane production and eventually led to acidification at high substrate loads. The addition of trace elements improved the kinetics and allowed higher substrate loads, but could not avoid propionate accumulation. Here, it is shown for the first time that addition of activated carbon, trace elements and dilution can favor propionic acid consumption after its accumulation. These promising options should be optimized to prevent propionate accumulation.

Graphical abstract

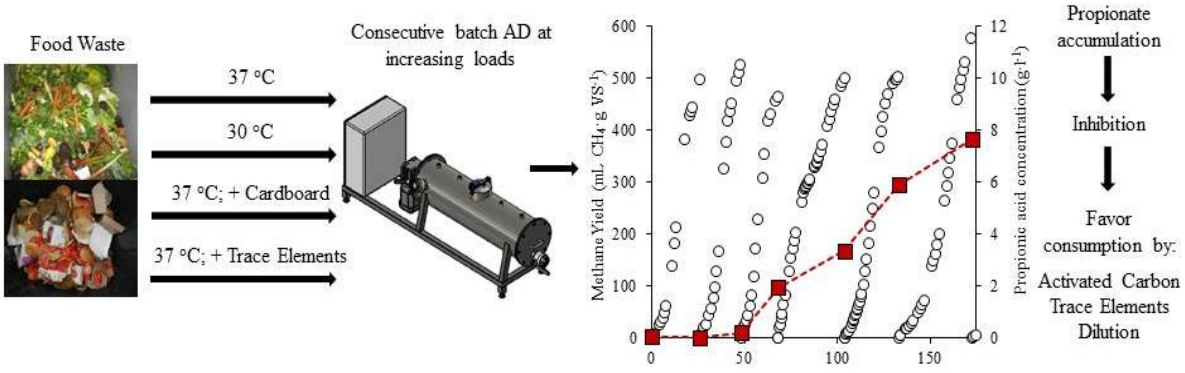

4.2.1 *Introduction*

Moving our society towards a circular economy and a sustainable future, food waste (FW) must be considered as a resource. In addition, the European Directive 2008/98/CE imposes the valorization of commercial FW from large producers through soil return. Among all the options for FW valorization, anaerobic digestion (AD) allows the conversion of organic

matter into biogas and digestate. Considering FW as a substrate for AD, it has been stated that these two end-products may have huge implications for production of renewable energy (Thi et al., 2016) and for recovery of nutrients (Stoknes et al., 2016), respectively. Moreover, the benefits of AD when compared to other treatment methods, such as landfilling, incineration or composting have been previously proved (Bernstad et al., 2016).

However, AD of FW is a complex process associated with several issues. In short term, as FW is mainly composed of easily degradable carbohydrates, reactor overloading and initial accumulation of volatile fatty acids (VFAs) have been frequently reported due to unbalance of the acidogenesis/acetogenesis and methanogenesis steps (Capson-Tojo et al., 2016). In addition, during long term operation several authors have reported high concentrations of total ammonia nitrogen (TAN) and thus free ammonia nitrogen (FAN), which is toxic to microorganisms (Banks et al., 2008; Rajagopal et al., 2013b). This occurs due to the high protein content of FW. Proteins are rich in organic N, which is reduced to TAN during AD. The high TAN concentrations achieved during AD of FW have been found to be responsible for inhibiting acetoclastic methanogens, which are known to be more sensitive to high TAN/FAN concentrations (inhibited over 2.8-3.0 g $TAN \cdot l^{-1}$) than hydrogenotrophic or mixotrophic archaea (De Vrieze et al., 2012). Thus, these latter archaea are the predominant species at the high TAN concentrations associated with FW AD (Jiang et al., 2017). As a conclusion, different studies have suggested that syntrophic acetate oxidation (SAO) and hydrogenotrophic methanogenesis (HM) are predominant pathways for methane production during AD of FW (Banks et al., 2012; Capson-Tojo et al., 2017d; Yirong et al., 2015). In these systems, syntrophic interactions between different groups of bacteria and archaea are particularly important to avoid accumulation of intermediate metabolites such as VFAs, molecular hydrogen or formate. If any of the aforementioned compounds start to build-up in the reactors, it eventually causes acidification of the AD process, decreasing the pH down to values at which the production of methane no longer occurs. Thus, accumulation of VFAs during FW AD has been reported by several authors, causing inefficient AD and eventually process failure (Banks et al., 2008; Wanqin Zhang et al., 2015).

Different options have been proposed to overcome this issue. Among them, co-digestion (*i.e.* simultaneous digestion of two or more substrates) and supplementation of trace elements (TEs) are among the most promising alternatives for achieving stable FW AD (Capson-Tojo et al., 2016). Several co-substrates have been co-digested with FW, such as green waste (X. Chen et al., 2014), manure (Ebner et al., 2016), sludge (Kim et al., 2017), macroalgae (Cogan and Antizar-Ladislao, 2016) or cardboard/paper waste (Asato et al., 2016; Capson-Tojo et al.,

2017d; Kim and Oh, 2011). Among those co-substrates, lignocellulosic-rich organic matter appears as a convenient option due to their much slower hydrolysis rates when compared with FW (reducing the risk of initial VFA accumulation), their high C/N ratio (diluting N concentrations) and their higher alkalinity. Paper/cardboard waste (PW) is particularly suitable for centralized commercial FW co-digestion, mainly because both wastes are usually the main organic solid waste streams in urban areas (Kim and Oh, 2011; Y. Zhang et al., 2012a). Other than co-digestion, the supplementation of TEs has also been found to stabilize AD of FW (Banks et al., 2012; Zhang and Jahng, 2012; Wanli Zhang et al., 2015b). As the results by Banks et al. (2012) suggest, a lack of TEs exists during AD of FW because of the requirements for synthesis of the enzymes needed for syntrophic HM, particularly for the production of formate dehydrogenase for formate cleavage. In their study, the build-up or formate and/or hydrogen led to accumulation of propionic acid (HPr) in the reactors, whose degradation is thermodynamically favorable only within a small range of concentrations of these species (Batstone et al., 2002a). Different TEs have been found to be required for both mesophilic and thermophilic AD of FW, such as iron, selenium, cobalt, molybdenum, nickel or tungsten (Qiang et al., 2013, 2012; Wanqin Zhang et al., 2015). By adding mixtures of these elements, it has been possible to avoid accumulation of VFAs, even at higher organic loading rates (OLRs) than in the reactors without them (Zhang et al., 2011; Wanli Zhang et al., 2015b; Wanqin Zhang et al., 2015). Some authors have even recovered acidified reactors by TEs supplementation (Qiang et al., 2013, 2012).

Besides their wide industrial applicability, consecutive batch reactors have been barely used for solid FW AD. As these systems allow testing several conditions in parallel, they are particularly convenient for AD studies at laboratory and pilot scale. To the knowledge of the authors, no study has been carried out to compare the aforementioned stabilization options (*i.e.* co-digestion and TEs addition) and their ability to avoid accumulation of VFAs at different substrate loads. Moreover, a simple option to decrease the FAN concentration in the reactors is working at low temperatures, displacing the NH_3-NH_4^+ equilibrium towards NH_4^+ and therefore lowering the impact of NH_3 inhibition.

The objective of this study was to compare the performance of three options for AD stabilization using pilot-scale consecutive batch reactors: working at low temperatures (30 °C *vs.* 37 °C), co-digestion of FW with PW and supplementation of TEs. The total solids (TS) contents and the concentrations of VFAs and TAN after each consecutive batch were measured. In addition, the digestate from a pilot reactor was used to test different options for

favoring the consumption of the VFAs that had progressively accumulated (mainly HPr). An extensive characterization of commercial FWs from different sources was also carried out.

4.2.2 *Materials and methods*

4.2.2.1 Inoculum and substrate

The inoculum used to start the pilot reactors was collected from an industrial plant digesting different organic streams at high TAN/FAN concentrations (5.04 g $TAN \cdot l^{-1}$; 0.615 g $FAN \cdot l^{-1}$). Thus, it was assumed that the microbial population was already adapted to high FAN concentrations, such as those existing during FW AD. The sludge had a TS content of 5.81±0.02 %, with 59.13±0.08 % corresponding to volatile solids (VS). Concerning the commercial FW, the waste collection was carried out in the region of the Grand Narbonne, in the south of France. Five different mayor FW producers from the region were used as representative examples of potential FW suppliers: (1) fast food restaurant, (2) restaurant, (3) supermarket, (4) fruit and vegetable supermarket and (5) fruit and vegetable distribution. A proportional mixture (wet weight) of the different FWs was used as substrate for the experiments.

4.2.2.2 Consecutive batch reactors for stabilization of anaerobic digestion

Four different pilot reactors were run in parallel to test the different strategies for AD stabilization. The particular working conditions are shown in Table 4.2.

Table 4.2. Working conditions in the pilot reactors

Reactor	Substrate	Initial working volume (l)	Working temperature (°C)
Control	FW[1]	20	37
T30	FW[1]	7.5	30
Co-PW	FW[1] + PW[2]	7.5 – 10	37
Sup-TEs	FW[1] + TEs[3]	8.4 – 10	37

1. Food waste
2. Paper waste
3. Trace elements

The Control reactor was fed with FW and incubated at 37 °C. The reactor T30 had equivalent working conditions, but was kept at 30 °C to lower the FAN proportions. The Co-PW reactor was operated similarly, but a supplementary amount of PW was added as co-substrate (75 % FW:25 % PW w/w). This co-digestion ratio was selected because similar values have been previously applied successfully in the literature (Kim and Oh, 2011; Y. Zhang et al., 2012a) and because this is a proportion similar to the one at which FW and PW

are generally found in municipal solid waste (Hogg et al., 2002). The PW used was regular office paper grinded to less than 1 cm (92.7 % TS; 77.6 % VS/TS). During the start-up of this reactor, a small amount of dried compost was added to the inoculum to increase the initial TS contents to values close to those expected after several consecutive batches using this substrate (around 9 % TS). Finally, the Sup-TEs reactor had equivalent working conditions to those of the Control reactor but was supplemented with TEs at the following concentrations: 100 $mg \cdot l^{-1}$ Fe, 1 $mg \cdot l^{-1}$ Co, 5 $mg \cdot l^{-1}$ Mo, 5 $mg \cdot l^{-1}$ Ni, 0.2 $mg \cdot l^{-1}$ Se, 0.2 $mg \cdot l^{-1}$ Zn, 0.1 $mg \cdot l^{-1}$ Cu, 1 $mg \cdot l^{-1}$ Mn. These values were calculated from optimal results reported in the literature (Banks et al., 2012; Zhang and Jahng, 2012; Wanli Zhang et al., 2015b). The required volume of a concentrated solution (x100) containing $FeCl_2 \cdot 4H_2O$, $CoCl_2 \cdot 6H_2O$, $Na_2MoO_4 \cdot 2H_2O$, $NiCl_2 \cdot 6H_2O$, Na_2SeO_3, $ZnCl_2 \cdot 2H_2O$, $CuCl_2 \cdot 2H_2O$, $MnCl_2 \cdot 4H_2O$ was used for doping the reactor.

Concerning the reactor loading, the same procedure was applied in all the systems. The first load was 0.087 kg FW·kg $inoculum^{-1}$ (corresponding to an initial substrate to inoculum ratio (S/X) of 0.25 g VS·g VS^{-1}), continuing with 0.173 FW·kg $inoculum^{-1}$ (two-fold initial load) and 0.260 kg FW·kg $inoculum^{-1}$ (three-fold initial load). The reactors were fed when a biogas plateau was reached or when yields of approximately 500 ml $CH_4 \cdot g\ VS^{-1}$ (common biochemical methane potential (BMP) value for FW (Capson-Tojo et al., 2016)) were obtained. When feeding, the required amount of digestate was removed to keep a constant working volume in the reactors. It is important to consider that, as the kinetics of biogas production in the reactors differed, the reactors were not fed at the same times and a different number of feeding cycles was achieved in each condition throughout the operational period. Table 4.3 aims to summarize the loading regime applied in the four reactors (*i.e.* Control and three stabilization strategies). The Control reactor and the reactors T30 and Co-PW were started at the first selected load (Cycle 1; 0.087 kg FW·kg $inoculum^{-1}$). It must be mentioned that this first cycle was used for adaptation of the inoculum and therefore the three reactors had the same working conditions (37 °C and FW as substrate; grey-shaded methane yields in Figure 4.1). The specific conditions of T30 and Co-PW were started in Cycle 2 (with the same load of Cycle 1). In the 3rd cycle, the load was doubled in all the pilots, and the Sup-TEs reactor was started with inoculum issued from the Control reactor and with the same load that was applied in the other pilots (0.173 kg FW·kg $inoculum^{-1}$). This allowed the comparison between the different conditions. To permit a straight-forward comparison between the Control and the Sup-TEs after the start-up of the latter, the first 2 feeding cycles of the

Control (used for inoculating Sup-TEs) are also presented in the figure showing the performance on Sup-TEs (grey-shaded methane yields in Figure 4.1).

Table 4.3. Loading regime applied to the pilot reactors (kg FW·kg inoculum^{-1})

Reactor\Cycle #	1	2	3	4	5	6	7
Control	0.087	0.087	0.173	0.173	0.173	0.173	na[1]
T30	0.087[2]	0.087	0.173	0.173	na[1]	na[1]	na[1]
Co-PW	0.087[2]	0.087	0.173	0.173	0.173	na[1]	na[1]
Sup-TEs	0.087[3]	0.087[3]	0.173	0.173	0.255	0.255	0.173

1. Not applicable
2. Conditions equivalent to the Control reactor
3. Results of the Control reactor

The experiments lasted a minimum of 173 days (Co-PW) and a maximum of 187 days (Control). The reactors consisted of cylindrical vessels made of stainless steel that were continuously agitated by inner stirring blades. A more precise description of these reactors can be found elsewhere (Ganesh et al., 2013).

4.2.2.3 Batch essay for investigating the VFA consumption

After 159 days of operation, 4 kg of digestate from the Co-PW reactor were sampled and used to test different options for favoring the consumption of the accumulated VFAs. Table 4.4 summarizes the different working conditions defined.

Table 4.4. Experimental design of the batch essay for favoring VFA consumption. The working temperature was 37 °C. The inoculum was taken from the Co-PW reactor

Reactor	Initial working volume (ml)	TEs concentration (mg Fe·l^{-1})[1]	GAC concentration (g·l^{-1})
Control	288	-	-
TEs	291	100	-
5xTEs	303	500	-
GAC	291	-	10
1/2Dilution	577	-	-

1. Concentrations expressed in mg Fe·l^{-1} to facilitate comprehension. All the TEs mentioned in Section 4.2.2.2 were also added

All these reactors were fed with 288 ml of digestate and incubated at 37 °C for 142 days. The influence on the VFA consumption of the addition of TEs was tested at two different concentrations: (i) the TEs concentration defined previously for the pilot reactor Sup-TEs (corresponding to 100 mg Fe·l^{-1}), and (ii) a reactor with a 5-folded concentration (corresponding to 500 mg Fe·l^{-1}). The effect of the supplementation of granular activated carbon (GAC; Sigma-Aldrich, Missouri, United States of America; CAS 7440-44-0) was also

assessed. Addition of GAC has been reported to favor adsorption of inhibitors, allowing at the same time the formation of biofilms onto its surface, which has been shown to favor syntrophic interactions (Fagbohungbe et al., 2017). In addition, GAC allows direct interspecies electron transfer (DIET), avoiding the formation of electron shuttles (such as hydrogen or formate) and favoring acetic acid (HAc) consumption (Dang et al., 2016; Lee et al., 2016). An initial GAC concentration of 10 $g \cdot l^{-1}$ was selected according to Lee et al. (2016). A last reactor was defined (1/2Dilution) to evaluate the effect on VFA consumption of simply diluting the digestate, aiming to reduce thermodynamic inhibitions. A Control reactor was also defined to perform an un-biased evaluation of the effect of these different options.

The reactors used were specifically designed to allow sampling of the digesting medium during the AD process without disturbing the gas in the headspace (Motte et al., 2015). As a consequence, the dynamics of both the biogas production and the VFA consumption-production were followed.

4.2.2.4 Analytical methods

4.2.2.4.1 Physicochemical characterization of the commercial FW

The characterization of commercial FW is a crucial step prior to its valorization. In addition, its characteristics are source dependent. Therefore, an extensive characterization of the commercial FW from the different suppliers was performed. TS and VS contents were measured according to the standard methods of the American Public Health Association (APHA, 2005). The concentration of carbohydrates was measured by the Dubois method (Dubois et al., 1956). The content of lipids was determined by a gravimetric method based on accelerated solvent extraction using an ASE®200, DIONEX coupled to a MULTIVAPOR P-12, BUCHI with heptane as solvent (100 bar, 105 °C, 5 cycles of 10 min static and 100s purge) (APHA, 2005). Total Kjeldahl nitrogen (TKN) and NH_4^+ concentrations were measured with an AutoKjehdahl Unit K-370, BUCHI. The concentration of proteins was estimated from the TKN contents using a conversion factor of 6.25 g protein·g N^{-1} (Jimenez et al., 2013). Total organic carbon (TOC) and inorganic carbon (IC) were determined using a Shimadzu TOC-V_{CSN} Total Organic Carbon Analyzer coupled to a Shimadzu ASI-V tube rack. The total carbon (TC) was calculated as the sum of TOC and IC. The pH was measured by a WTW pHmeter series inoLab pH720. The BMPs of the substrates were determined according to Motte et al. (2014a).

The concentrations of micro/macro-elements were measured by Aurea Agroscience© (Ardon, France) as follows: metallic trace elements were determined by water extraction,

according to the norm NF EN 13346. The measurement of Cu, Ni, Fe, Mo, Mn, Co and Zn concentrations was performed by plasma emission spectrometry, according to the NF EN ISO 11885. The concentrations of total P, K, Mg, Ca and Na were measured according to NF EN ISO 11885.

Table 4.5 shows the main characteristics of the analyzed FWs from the different suppliers and the mixture used for feeding the reactors.

Table 4.5. Characteristics of the food waste samples

Parameter	Fast food restaurant	Restaurant	Supermarket	Fruit and vegetable supermarket	Fruit and vegetable distribution	Mixture
TS (%)	34.3	40.1	10.2	10.0	10.6	21.0
VS/TS (%)	93.1	88.5	94.4	89.8	85.8	90.3
Carbohydrates ($g \cdot kg\ TS^{-1}$)	396	524	762	776	634	618
Proteins ($g \cdot kg\ TS^{-1}$)	230	190	129	125	262	187
Lipids ($g \cdot kg\ TS^{-1}$)	293	127	62.6	24.0	99.0	121
BMPs ($ml\ CH_4 \cdot g\ VS^{-1}$)	515	449	377	388	371	420
pH	5.20	5.40	4.70	4.70	5.10	5.02
TOC ($g \cdot kg\ TS^{-1}$)	454	431	457	452	439	447
TAN ($g \cdot kg\ TS^{-1}$)	0.69	1.08	0.53	0.40	1.80	0.90
TKN ($g \cdot kg\ TS^{-1}$)	36.7	30.4	20.7	19.9	42.0	30.0
C/N (TOC/TKN)	12.4	14.1	21.7	21.8	10.3	16.1
P_2O_5 ($g \cdot kg\ TS^{-1}$)	7.59	27.0	5.76	6.97	14.2	12.3
CaO ($g \cdot kg\ TS^{-1}$)	14.0	42.4	6.70	12.9	10.0	17.2
MgO ($g \cdot kg\ TS^{-1}$)	1.21	1.86	2.56	2.49	5.16	2.66
K_2O ($g \cdot kg\ TS^{-1}$)	9.33	13.7	31.4	32.8	43.9	26.2
Na ($g \cdot kg\ TS^{-1}$)	9.89	7.69	0.95	0.74	1.97	4.25
Co ($mg \cdot kg\ TS^{-1}$)	< 9.75	< 9.75	< 9.75	< 9.75	< 9.75	< 9.75
Cu ($mg \cdot kg\ TS^{-1}$)	4.92	9.43	12.14	11.68	18.03	11.2
Fe ($mg \cdot kg\ TS^{-1}$)	268	294	731	1227	3049	1114
Mn ($mg \cdot kg\ TS^{-1}$)	12.5	10.3	30.7	30.2	54.3	27.6
Mo ($mg \cdot kg\ TS^{-1}$)	< 0.35	0.47	0.48	0.85	4.49	1.26
Zn ($mg \cdot kg\ TS^{-1}$)	52.6	36.3	20.3	27.6	55.3	38.4
Ni ($mg \cdot kg\ TS^{-1}$)	< 1.99	< 1.99	< 1.99	2.06	3.87	1.19
Acetate ($g \cdot kg^{-1}$)	6.14	5.59	1.39	4.21	4.18	4.30
Propionate ($g \cdot kg^{-1}$)	0.01	$< 5 \cdot 10^{-4}$	$< 5 \cdot 10^{-4}$	$< 5 \cdot 10^{-4}$	$< 5 \cdot 10^{-4}$	$< 5 \cdot 10^{-4}$
Total VFAs ($g\ COD \cdot kg^{-1}$)	7.58	6.72	1.61	4.76	4.73	5.08

The results are in agreement with those commonly presented in the literature (Capson-Tojo et al., 2016). The TS content ranged from 10.1 to 40.0 % and the VS from 85.8 to 94.4 % VS/TS. Carbohydrates were the main component in all the samples (396-776 g·kg TS^{-1}), followed by proteins (125-262 g·kg TS^{-1}) and lipids (24.0-293 g·kg TS^{-1}). Interestingly, the sample from fruit and vegetable distribution (mainly composed of vegetables such as leeks) had the highest concentration of proteins (262 g·kg TS^{-1}), suggesting that some vegetables (*e.g.* leeks) might also contribute greatly to the high nitrogen content of FW (and thus to high TAN concentrations in the AD reactors). The high proportions of proteins led to high TKN concentrations and low C/N ratios (16.1 for the mixture), with values also in accordance with the literature (Capson-Tojo et al., 2016). High BMP values, ranging from 371 to 515 ml CH_4·g VS^{-1} were obtained, suggesting the suitability of this substrate for AD and a high potential energy recovery. As the theoretical methane yields are higher for lipids than for proteins or carbohydrates, higher BMPs were obtained in the samples with high lipid contents and low concentrations of carbohydrates (*i.e.* restaurants). Relatively high concentrations of macroelements (*i.e.* P, Ca, Mg, K or Na) were found but, as the levels were much lower than the reported inhibitory limits (Angelidaki and Ahring, 1992; Appels et al., 2008; Batstone et al., 2000), no inhibition was expected. Interestingly, the concentration of TEs varied widely according to the FW source and typology. In FW mainly composed of vegetables and fruits much higher concentrations of TEs required for AD (such as Cu, Fe, Mn, Mo or Ni) were found when compared to the samples from meat-serving restaurant. This suggests that higher contents of FW mainly composed of fruits and vegetables may increase the TEs concentrations, helping to stabilize the AD process. As expected, Fe showed the highest concentrations, with values up to 3 g·l^{-1} in FW from vegetable waste (fruit and vegetable distribution). Finally, the relatively high concentrations of VFAs (up to 7.58 g COD·kg^{-1}) and TAN (up to 1.08 g·kg TS^{-1}) suggest that the biodegradation of the substrates had already started during the storage period (inherent to the collection process and less than one week), proving also the high biodegradability and fast degradation kinetics of FW.

4.2.2.4.2 Gas quantification and analysis

The amount of biogas produced in the pilot reactors was continually measured using Ritter MilliGascounters MGC-1 V3.0. The composition of the biogas (and the volume of gas produced in the batch essay presented in 4.2.3.2) was determined as described in Cazier et al. (2015). For comparing the kinetics of methane production in the reactors, the experimental data corresponding to the methane yields were fit to the Gompertz equation (Zwietering et al.,

1990) to estimate the kinetic parameters of the process. The least squares method was applied and the predicted values were plotted against the real data to evaluate the goodness of fit of the model. The resulting R^2 and the p-value obtained from a Fisher's exact test were used as indicators.

4.2.2.4.3 Analysis of metabolites and final products of the digestion

The concentrations of VFAs (*i.e.* acetic, propionic, butyric or valeric acids) and ionic species in the digestates were measured according to Motte et al. (2013). The concentration of FAN was calculated as a function of temperature, pH and TAN concentration (J. L. Chen et al., 2014).

4.2.2.4.4 Thermodynamic calculations

To support the experimental findings, theoretical thermodynamic calculations were carried out. For this purpose, Equation 4.1 was used:

$$\Delta G' = \Delta G^0 + R \cdot T \cdot ln\left(\frac{[C]^c \cdot [D]^d}{[A]^a \cdot [B]^b}\right) \qquad \text{Equation 4.1}$$

Where ΔG' is the variation of Gibbs free energy ($J \cdot mol^{-1}$), ΔG^0 is the standard Gibbs free energy of the reaction ($J \cdot mol^{-1}$), R is the ideal gas constant (8.314 $J \cdot mol^{-1} \cdot K^{-1}$), T is the temperature (K) and $[I]^i$ are the concentrations and the stoichiometric coefficients in the reaction aA + bB ↔ cC + dD. When the line of zero ΔG' for a reaction was calculated, the following conditions were assumed: 298 K, pH 7, 1 mM organic acids and 0.1 M HCO_3^-. These values were taken from Batstone et al. (2002a) and the ΔG^0 from Zeeman (2005).

4.2.3 *Results and discussion*

4.2.3.1 Performance of the stabilization strategies in consecutive batch pilot reactors

The methane yields as well as the TS contents and the concentrations of HPr and TAN resulting from the different strategies evaluated for AD stabilization (working temperature of 30 °C (T30), co-digestion with PW (Co-PW), and TEs supplementation (Sup-TEs)) are shown in Figure 4.1.

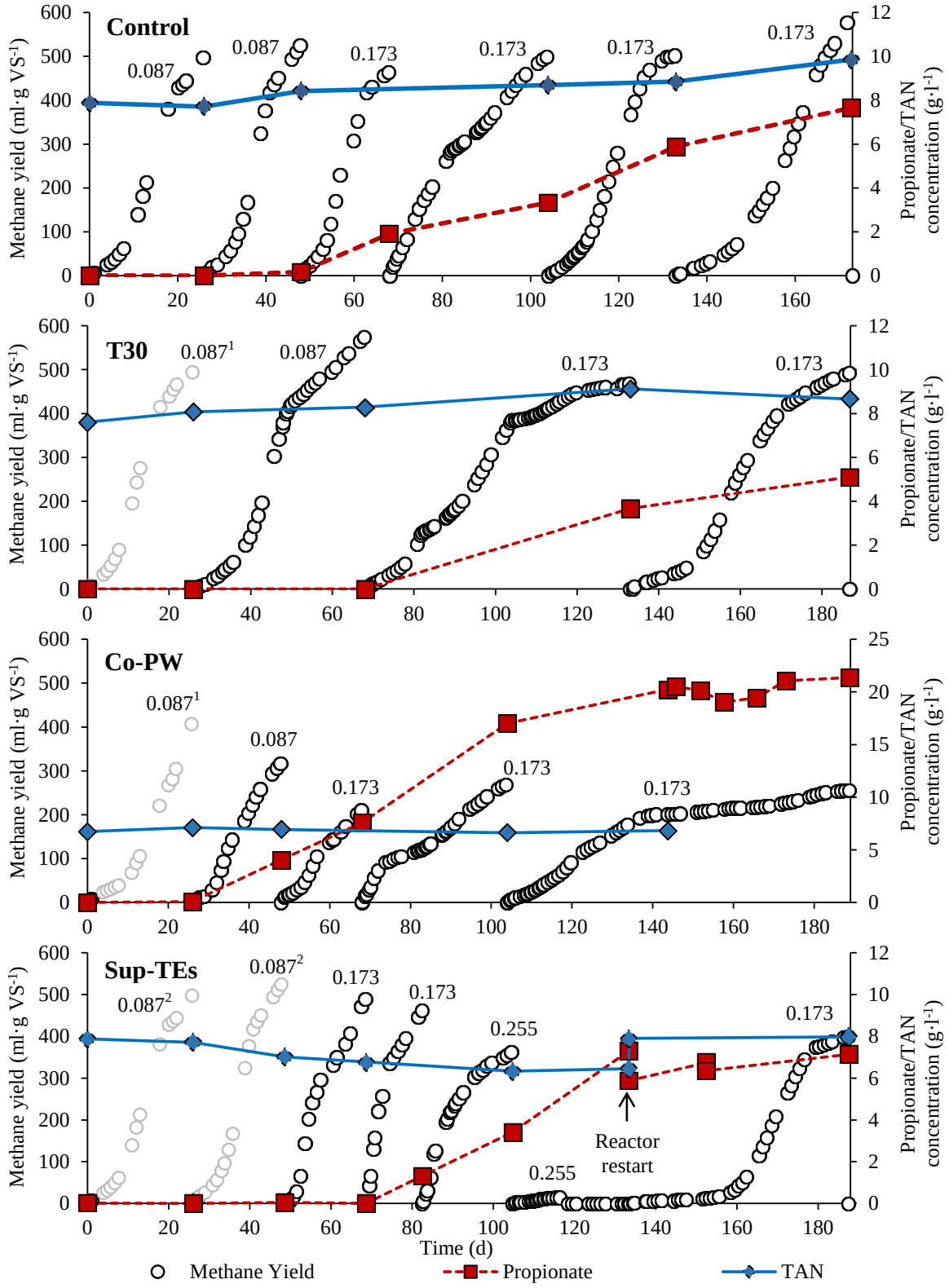

Figure 4.1. Kinetics of methane production in the pilot reactors. The concentrations of propionic acid and TAN after each feeding cycle are also presented. The acetic acid concentrations are shown in Table 4.6. The numbers on the top of the methane curves stand for the loads applied for each batch (kg FW·kg inoculum^{-1}). The grey-shaded methane curves correspond to conditions equivalent to those in the Control reactor (1) and to the results of the Control reactor (2)

4.2.3.1.1 Methane production and gradual propionate accumulation

During the first 2 cycles (with a load of 0.087 kg FW·kg inoculum^{-1}), the reactors were clearly performant, with high methane yields achieved (~500 ml CH_4·g VS^{-1}). However, differences were already observed between the conditions tested. The reactor T30 showed much slower kinetics than that of the Control reactor (*i.e.* 35 days *vs.* 22 days to reach 500 ml CH_4·g VS $^{-1}$, respectively). This occurred simply because the lower reaction temperature slowed down the AD kinetics. This hypothesis was verified by adjusting the experimental results to the Gompertz equation. Taking the second feeding as example, the values of the maximum methane production rate and the lag phase were 48.1 ml CH_4·g VS^{-1}·d^{-1} and 6.09 days for the Control reactor (R^2 0.9964 and p-value of $1.71 \cdot 10^{-23}$) and 29.7 ml CH_4·g VS^{-1}·d^{-1} and 9.41 days for the reactor T30 (R^2 0.994 and p-value of $1.03 \cdot 10^{-41}$). Lower maximum methane production rates and longer lag phases confirmed the slower AD kinetics a 30 °C. In addition, the Co-PW reactor showed lower methane yields at similar digestion times. The maximum methane yields given by the Gompertz equation showed values of 368 ml CH_4·g VS^{-1} in the second cycle for the Co-PW reactor (R^2 0.997 and p-value of $4.04 \cdot 10^{-24}$), while a value of 564 ml CH_4·g VS^{-1} was obtained for the Control reactor. This happened because PW is a more recalcitrant substrate than FW, with a lower BMP (Capson-Tojo et al., 2017d). Therefore, the global methane yields (expressed by total VS of substrate added) decreased. Moreover, it is interesting to mention that in the Co-PW reactor a concentration of HPr of about 4 g·l^{-1} was reached already after the 1st feeding (Cycle 2).

As the performance was satisfactory, the organic load was doubled (0.173 kg FW·kg inoculum^{-1}) in all the reactors in the 3rd and 4th cycles. In addition, the reactor Sup-TEs was started. Again, satisfactory methane yields were achieved (~500 ml CH_4·g VS^{-1}), which led to high volumetric productivities (up to 16 l CH_4·l^{-1}). However, at the end of the 3rd cycle, significant amounts of HPr were detected in all conditions, with concentrations up to 17.0 g·l^{-1} in the Co-PW reactor. This HPr accumulation jeopardized the methane production kinetics and increased the lag phases in the methane production. Taking the results from the Gompertz equation of the Control reactor as example, while in the third feeding (negligible initial HPr concentrations) the maximum methane production rate and the lag phase were 40.4 ml CH_4·g VS^{-1}·d^{-1} and 3.62 days (R^2 0.996 and p-value of $3.82 \cdot 10^{-21}$), these values were 30.5 ml CH_4·g VS^{-1}·d^{-1} and 6.40 days (R^2 0.997 and p-value of $2.42 \cdot 10^{-41}$) for the same reactor in the fifth cycle (with initial HPr concentrations of 3.3 g·l^{-1}), indicating slower AD kinetics. Nevertheless, a clear improvement in the kinetics of methane production and in the reduction of HPr accumulation was observed in Sup-TEs when compared with the other conditions (*i.e.*

methane yields of 462 ml $CH_4 \cdot g\ VS^{-1}$ achieved in 14 days *vs.* 20 days for the Control reactor in the 3rd cycle), suggesting a positive effect of the TEs supplementation. By comparing the kinetic parameters of the Sup-TEs reactor with the Control reactor right after its start-up (3rd cycle), the Gompertz equation served to verify this hypothesis. While the maximum methane production rate and the lag phase in the Sup-TEs reactor were 44.7 ml $CH_4 \cdot g\ VS^{-1} \cdot d^{-1}$ and 2.00 days (R^2 0.978 and p-value of $8.31 \cdot 10^{-15}$), these values were 40.4 ml $CH_4 \cdot g\ VS^{-1} \cdot d^{-1}$ and 3.62 days (R^2 0.996 and p-value of $3.82 \cdot 10^{-21}$) in the Control reactor. Thus, in the 5th feeding cycle, the load was increased in the Sup-TEs reactor to 0.255 kg FW·kg $inoculum^{-1}$. Although methane was produced efficiently, this load increase led to a slightly lower methane yield and to a sharp increase in the HPr concentration, up to 3.4 $g \cdot l^{-1}$. A second feeding with the same load (6th cycle) caused acidification of the reactor, with pH values down to 5.9 and HPr and HAc concentrations of 7.30 $g \cdot l^{-1}$ and 16.1 $g \cdot l^{-1}$, respectively (see Table 4.6, showing the concentrations of both acids after each cycle). This suggested that a load of 0.255 kg FW·kg $inoculum^{-1}$ was too high for the system. To verify if this load would lead to inhibition in all the conditions, an additional experiment (not presented) was carried out. Digestates from the four reactors were used as inoculum for lab-scale batch reactors at a load of 0.255 kg FW·kg $inoculum^{-1}$ (that leading to inhibition in the Sup-TEs pilot). All the batch reactors were acidified (data not shown), confirming the results from the pilot reactors.

Table 4.6. Concentrations of acetic and propionic acids in the pilots after each feeding cycle

Compound	Reactor	Cycle 1	Cycle 2	Cycle 3	Cycle 4	Cycle 5	Cycle 6	Cycle 7
Acetic Acid [2]	**Control**	0.138	0.247	0.214	0.434	1.052	0.270	na[1]
	T30	na[1]	0.117	0.147	0.238	na[1]	na[1]	na[1]
	Co-PW	na[1]	0.285	0.328	0.650	6.41	na[1]	na[1]
	Sup-TEs	na[1]	na[1]	0.106	0.856	1.39	16.1	0.204
Propionic Acid [3]	**Control**	0.004	0.174	1.91	3.33	5.88	7.65	na[1]
	T30	na[1]	0.004	3.64	5.11	na[1]	na[1]	na[1]
	Co-PW	na[1]	4.05	7.57	17.0	21.0	na[1]	na[1]
	Sup-TEs	na[1]	na[1]	0.00	1.32	3.40	7.30	7.135

1. Not applicable
2. Molecular weight of 60.05 $g \cdot mol^{-1}$
3. Molecular weight of 74.08 $g \cdot mol^{-1}$

Therefore, the Sup-TEs reactor was restarted in day 133 with digestate from the Control reactor and the load was reduced to 0.173 kg FW·kg $inoculum^{-1}$ (the maximum applied in the other three reactors). However, even at this load HPr continued to accumulate in the reactors, slowing down the methane kinetics (longer lag phases) and endangering the AD process. With

much lower maximum methane production rates and longer lag phases than previously, the values of the kinetics parameters in the 6th feeding of the Control reactor serve to illustrate this decrease of the AD kinetics: 23.9 ml $CH_4 \cdot g\ VS^{-1} \cdot d^{-1}$ and 13.3 days (R^2 0.998 and p-value of $1.76 \cdot 10^{-36}$), respectively. The co-digestion reactor (Co-PW) showed the most important build-up of HPr, with concentrations up to 21.6 $g \cdot l^{-1}$ detected after the 4th cycle and pH values down to 6.5. Interestingly, the substrate conversion (estimated as the sum of methane and VFAs) remained relatively constant. At this point, the feeding of this reactor was stopped to evaluate if the concentration of HPr would decrease without addition of an external substrate. After two months, no significant decrease was observed.

Concerning the TS contents, average values from 6.5±0.6 to 7.9±0.6 % were observed in the reactors Control, T30 and Sup-TEs. Due to the addition of PW, the Co-PW reactor reached higher TS values, of 11.3±0.3 % after the 3rd Cycle. The high TS contents in Co-PW were caused by the high TS proportion of the PW and its lower degradability when compared with FW.

4.2.3.1.2 Role of the concentrations of FAN and metabolites in propionate accumulation

The FAN concentrations were also affected by the working conditions. Since no specific strategies were applied to reduce the FAN concentrations, the Control and Sup-TEs reactors showed the highest concentrations (1077 and 780 mg $FAN \cdot l^{-1}$, respectively). Applying a temperature of 30 °C in T30 allowed reducing this value to 691 mg $FAN \cdot l^{-1}$ by displacement of the NH_4^+-NH_3 equilibrium towards NH_4^+. In addition, the co-digestion reactor (Co-PW) showed also lower TAN levels (520 mg $FAN \cdot l^{-1}$) because of the high C/N ratio of PW, which diluted the TAN concentrations (up to 7.1 $g \cdot l^{-1}$ in Co-PW *vs.* 9.5 $g \cdot l^{-1}$ in the Control reactor). It must be mentioned that the much lower concentrations of FAN in Co-PW were also related to the lower pH values in this reactor due to the higher HPr concentrations. While in the other reactors the pH ranged between 7.89 and 8.16, the pH in Co-PW ranged between 7.85 and 6.49. This affected greatly the NH_4^+-NH_3 equilibrium, favoring the formation of NH_4^+.

In order to understand why HPr accumulated in the reactors, it was required to pay attention to the high TAN/FAN concentrations and its consequences, as well as to the concentrations of AD metabolites. With this purpose Figure 4.2 and Figure 4.3 are shown. Figure 4.2 represents the different pathways and reactions involved in methane production during AD and Figure 4.3 plots the theoretical lines of zero ΔG' for the same reactions at different acetate concentrations and hydrogen partial pressures. As aforementioned, acetoclastic archaea are inhibited over 2.8-3.0 g $TAN \cdot l^{-1}$ (De Vrieze et al., 2012) and

therefore the acetoclastic pathway (acetoclastic methanogenesis-AM; dashed lines in Figure 4.2) becomes less important than in non-stressed AD conditions. As a consequence, syntrophic acetate oxidation (SAO) and hydrogenotrophic methanogenesis (HM; continuous lines in Figure 4.2) becomes the predominant methane producing pathway (De Vrieze et al., 2012; Jiang et al., 2017). Thus, mediated interspecies electron transfer (MIET), using hydrogen or formate as electron shuttles, becomes a critical step of the global process. These syntrophic interactions are particularly important for syntrophic propionate oxidation (SPO; reaction (i) in Figure 4.2). HPr can only be degraded by coupling SPO and SAO with HM. In addition, as acetic acid (HAc) and hydrogen/formate are products of HPr degradation (reaction (i) in Figure 4.2), SPO becomes thermodynamically unfavorable by product-induced feedback inhibition if these compounds accumulate in the reactor (which is more likely to occur during HM). It must be mentioned that, as the thermodynamics and stoichiometry of hydrogen and formate are virtually identical, only one has been considered in Figure 4.2 and Figure 4.3 (Batstone et al., 2002a).

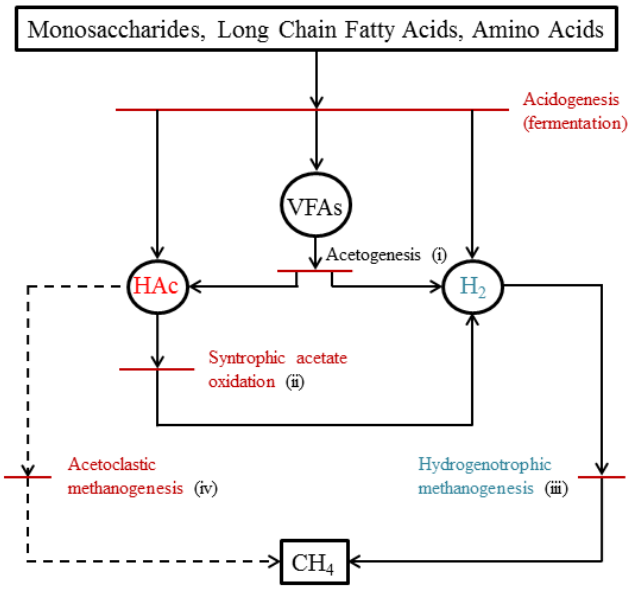

(i) $CH_3CH_2COO^- + 2H_2O \xrightarrow{SPO} CH_3COO^- + HCO_3^- + H^+ + 3H_{2\,(g)}$ $\Delta G'_0 = +76.1\ kJ{\cdot}mol^{-1}$

(ii) $CH_3COO^- + 4H_2O \xrightarrow{SAO} 2HCO_3^- + H^+ + 4H_{2\,(g)}$ $\Delta G'_0 = +104\ kJ{\cdot}mol^{-1}$

(iii) $4H_{2\,(g)} + HCO_3^- + H^+ \xrightarrow{HM} CH_{4\,(g)} + 3H_2O$ $\Delta G'_0 = -135\ kJ{\cdot}mol^{-1}$

(iv) $CH_3COO^- + H_2O \xrightarrow{AM} CH_{4\,(g)} + HCO_3^-$ $\Delta G'_0 = -31.0\ kJ{\cdot}mol^{-1}$

Figure 4.2. Different pathways involved in methane production during AD. The dashed lines represent the pathway inhibited at the high TAN/FAN concentrations associated with FW AD. The main reactions hypothesized to occur during FW AD are shown

As it can be observed in Figure 4.3, while acetoclastic methanogenesis (AM) is thermodynamically favorable in almost the whole range presented (therefore being predominant in non-stressed AD), there is only a small thermodynamic window in which SAO, SPO and HM can occur simultaneously (yellowish region in Figure 4.3). Figure 4.3 offers a possible explanation for the HPr accumulation observed. During batch AD of FW, an initial accumulation of VFAs (mainly HAc) occurs at the beginning of the process (Wanli Zhang et al., 2015b). In the present study, transient HAc concentrations of 17.2 $g \cdot l^{-1}$ (0.29 M) were detected during the first days after reactor loading. In addition, before re-loading the pilots, the minimal concentrations of HAc were higher than $2 \cdot 10^{-3}$ M (Table 4.6). This means that throughout the operational period in all the reactors the concentrations of HAc were mostly within a range where the degradation of HAc was more thermodynamically feasible than that of HPr (region at the right of the vertical red line in Figure 4.3). This jeopardized the growth of syntrophic propionate oxidizers, which are slow-growing microorganisms (de Bok et al., 2004), causing eventually accumulation of HPr. Thus, it can be hypothesized that SPO was not thermodynamically favorable due to the high concentrations of HAc and hydrogen/formate in the reactors.

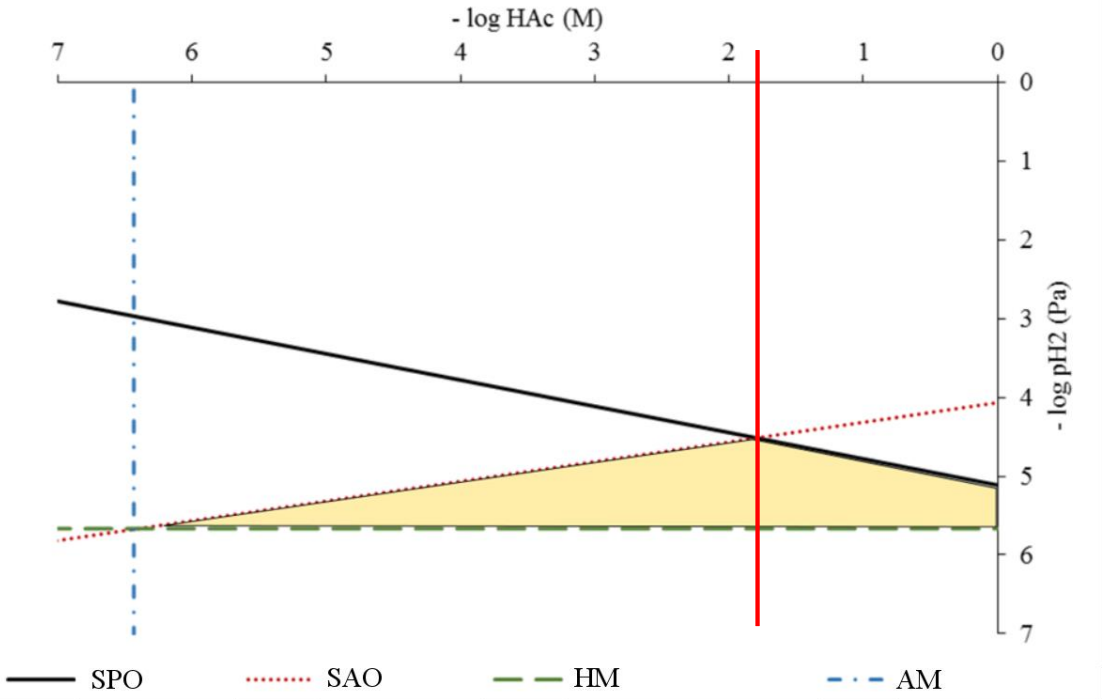

Figure 4.3. Lines of zero ΔG' for the reactions shown in Figure 4.2 at different acetate concentrations and hydrogen partial pressures. They were calculated assuming 298 K, pH 7, 1 mM HPr and 0.1 M HCO_3^-. The ΔG^0 were taken from Zeeman (2005). SPO, SAO, HM and AM stand for syntrophic propionate oxidation, syntrophic acetate oxidation, hydrogenotrophic methanogenesis and acetoclastic methanogenesis, respectively

4.2.3.1.3 Role of the operating mode in propionate accumulation

The first point to mention in this section is that a main drawback of batch operation when compared with continuous mode is the initial substrate overload that occurs after feeding, which can lead to high transient VFA concentrations. In continuous operation, this overloading does not exist and therefore the concentrations of HAc or hydrogen are never as high as in batch operation. As shown in Figure 4.3, if lower concentrations of HAc or hydrogen are present, SPO is favored. In other words, at equivalent loads in continuous reactors, the initial overload of substrate occurring in batch experiments is avoided and therefore the initial accumulation of intermediate compounds is less important, thus reducing the initial accumulation of HPr. Continuous operation in continuous-stirred tank reactors (CSTRs) may be a more appropriate option when compared to batch reactors (even if it is more complex technically).

The observed accumulation of HPr during FW AD has been commonly reported in the literature in continuous or single batch reactors. For example, in an AD plant of 900 m^3 digesting FW, Banks et al. (2011a) observed HPr concentrations up to 14 $g \cdot l^{-1}$ after 426 days of operation at an average OLR of 2.5 g $VS \cdot l^{-1} \cdot d^{-1}$. These results were confirmed by different semi-continuous lab-scale studies, in which HPr build-up during FW AD at low OLRs, directly inhibiting the AD process or jeopardizing its performance (C. Zhang et al., 2013b; Wanli Zhang et al., 2015a, 2015b). However, these studies showed that the addition of TEs or co-substrates rich in those elements (such as piggery wastewater or fresh leachate from the storage of a municipal solid waste incineration plant) avoided the HPr accumulation and stabilized the AD process, even at high OLRs (6-8 g $VS \cdot l^{-1} \cdot d^{-1}$). A possible reason behind the accumulation of HPr in the present study even when TEs were supplied may be the initial substrate overload that exists after feeding during sequential batch operation.

In addition, the strategy used for feeding the successive batch reactors may also have led to a key issue. In the present experiment, the loading strategy consisted on starting a new batch by monitoring only the methane kinetics (*i.e.* the reactors were fed once a biogas plateau or a determined methane yield was achieved) and no attention was paid to the VFA concentrations. Therefore, the reactors were reloaded when the concentrations of HAc were approaching values low enough to allow HPr oxidation (right region of Figure 4.3), increasing again the HAc concentrations and avoiding the development of syntrophic propionic degraders (slow-growing bacteria). Thus, the batch time was never long enough to allow HPr degradation. This also implies that if the process is to be scaled-up, the biogas production should not be the sole parameter to evaluate if the re-loading is feasible. The VFA

concentrations must also be monitored. It must be mentioned that this issue would not have been observed after only one batch operation.

Co-digesting FW with a substrate having a higher C/N ratio (*i.e.* PW) did not avoid HPr accumulation. In fact, at the co-digestion proportions applied (75 % FW:25 % PW w/w), the dilution of TAN (up to 7.0 $g \cdot l^{-1}$ in the reactor) was not enough to avoid inhibition of acetoclastic methanogens. On the contrary, the co-digestion reactor showed the worst methane production performance and the highest HPr concentrations (up to 21.6 $g \cdot l^{-1}$). As PW is degraded more slowly than FW, a hypothesis explaining this observation could be that the release of VFAs during AD was also slower, causing relatively higher HAc concentrations in the reactor for a longer period of time. Consequently, according to Figure 4.3, SPO was not feasible. Another possible explanation is that PW addition simply favored the synthesis of HPr. More significant HPr accumulation during co-digestion of card packaging and FW when compared to FW mono-digestion were also reported by Y. Zhang et al. (2012a) in continuous reactors. More research must be carried out to elucidate the reasons behind this observation.

4.2.3.2 Favoring consumption of propionic acid after its accumulation

In order to screen different possibilities to avoid HPr accumulation or to favor its consumption, the experimental design presented in Table 4.4 was carried out. As described above, the influence of the addition of TEs and GAC on the VFA consumption was tested using digestate from the Co-PW reactor (with concentrations of HAc and HPr of 6.41 and 21.0 $g \cdot l^{-1}$ respectively). Two different TEs concentrations (equivalent to 100 and 500 mg $Fe \cdot l^{-1}$) and one of GAC (10 $g \cdot l^{-1}$) were tested. The effect of diluting the digestate (doubling its volume adding water) was also assessed. The dynamics of methane production and concentrations of HAc and HPr are presented in Figure 4.4.

According to the results presented in Figure 4.4, three successive phases can be identified. During the first phase, corresponding to about the first 28 days (vertical red line in Figure 4.4), methane production occurred because of the degradation of HAc and readily available residual substrates but HPr was not consumed in any condition. At this end of this phase, the HAc concentration was approximately of 0.4 $g \cdot l^{-1}$ ($7 \cdot 10^{-3}$ M) in all conditions, meaning that SPO should have been thermodynamically feasible if the partial pressure of hydrogen (or the equivalent concentration or formate) is low enough (Figure 4.3). However, in the case of undiluted reactors, a "stable phase" occurred during which the concentrations of HPr and HAc did no vary and no significant production of methane was observed (period between both vertical lines in Figure 4.4). After about 52 days, HPr started to be degraded in those

conditions (vertical blue line in Figure 4.4). Simultaneously, a slight increase in the HAc concentrations was observed since HPr was degraded into HAc (resulting in an increase of the HAc concentrations up to 5.3 $g \cdot l^{-1}$; in agreement with Equation (i) in Figure 4.3) and methane was also produced (probably by SAO and HM). Interestingly, in the case of the diluted reactor (1/2Dilution), SPO started earlier, right after the first phase. This can be explained by the lower concentration of electron shuttles (hydrogen and/or formate) due to the addition of water. In this experiment, the total consumption of HPr took between 66 and 114 days, confirming that the degradation of this VFA is clearly a problem after its build-up.

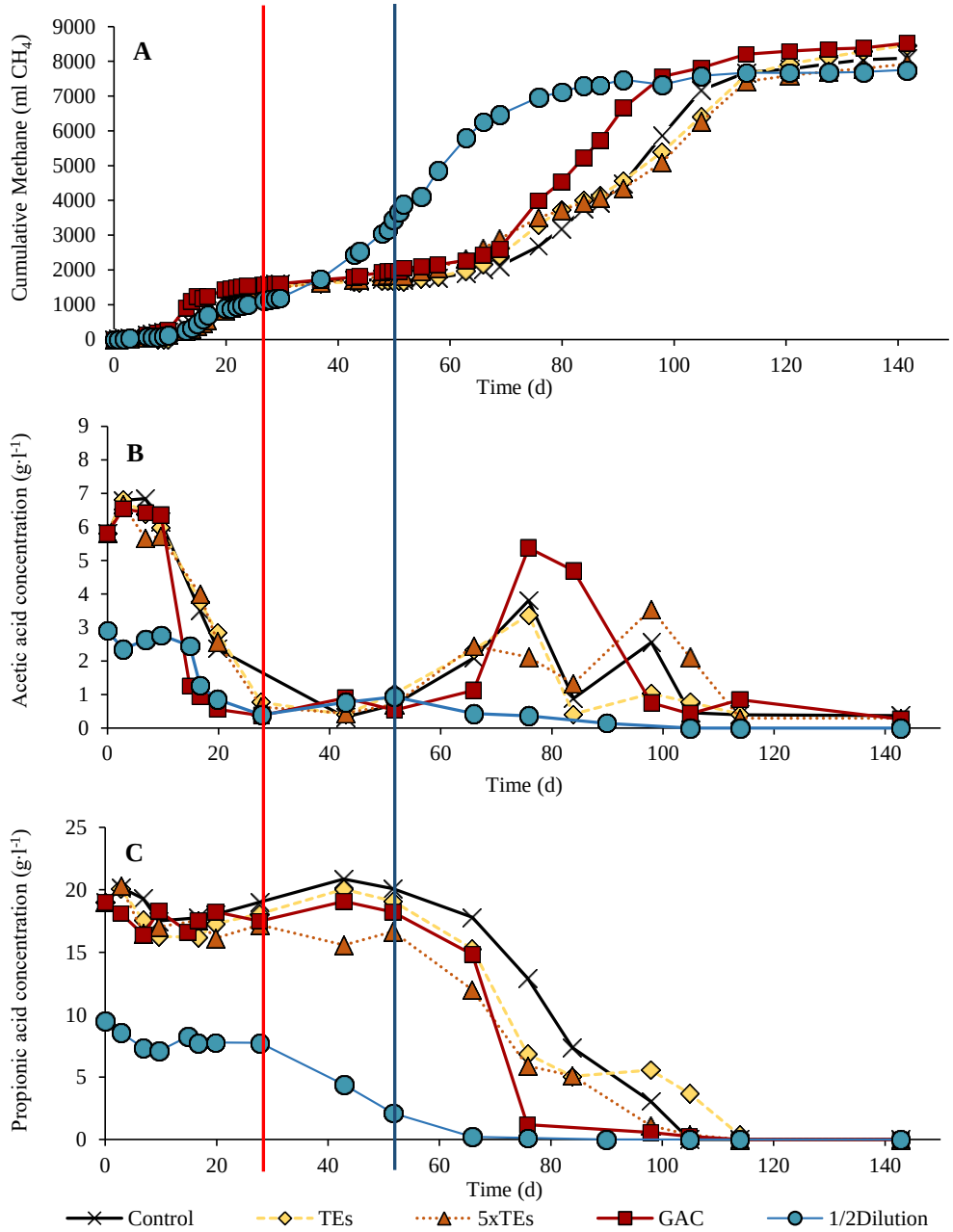

Figure 4.4. Cumulative methane productions (A) and concentrations of acetic acid (B) and propionic acid (C) during the batch experiments. The reactors were incubated at 37 °C for a period of 142 days

Even if the global behavior of the undiluted reactors (Control, addition of TES, addition of GAC) was similar, slight differences can be highlighted. The addition of TEs (5xTEs) improved slightly the kinetics of HPr degradation when compared to the Control reactor, probably by favoring the synthesis of formate dehydrogenase (Banks et al., 2012). Interestingly, SPO was clearly improved when adding GAC. The results indicate that the most plausible explanation is the occurrence of DIET in the reactors. As shown in Figure 4.4B, HAc was degraded faster when GAC was supplemented into the reactors, which favored slightly also the methane production. HAc can be degraded through DIET via direct interaction between an electroactive bacteria and hydrogenotrophic methanogens (Lee et al., 2016), which may explain the better performance in this condition. This led, not only to lower HAc concentrations in the reactors, but also to lower concentrations of electron shuttles, whose formation was avoided (the electrons were directly exchanged). As the concentrations of both HAc and hydrogen/formate were lower, SPO became thermodynamically favorable earlier (Figure 4.3). Moreover, also SPO may have occurred directly through DIET (Zhao et al., 2016b). Other than DIET, the steeper slope of HPr degradation in the GAC reactor also suggests that the growth of HPr oxidizing bacteria during the exponential phase was promoted, probably through biofilm formation onto the GAC surface, allowing syntrophic interactions to occur.

Further research must be carried out to elucidate if the process performance can be improved by allowing the growth of HPr oxidizers, achieving eventually a stable HPr-degrading community (with and without the addition of support materials such as GAC).

In addition, dilution of the substrate can be an option to solve HPr accumulation. Although this alternative is widely applied in industrial AD of solid waste for substrate pretreatment before AD, it leads to greater reactor volumes, lower energy balances and higher amounts of digestate to be dealt with and therefore is a practice to be avoided in the future. Promising options such as GAC addition and TEs optimization (and its combination) have the potential of improving greatly the performance of FW AD (*i.e.* improving the biogas productivities and reducing the retention times) and deserve further research.

4.2.4 *Conclusions*

Methane was efficiently produced in successive batch reactors (~ 500 $mlCH_4 \cdot gVS^{-1}$; 16 $lCH_4 \cdot l^{-1}$) but HPr accumulated in all of them, with concentrations up to 21.6 $g \cdot l^{-1}$. This led to acidification at high substrate loads. Co-digestion with PW led to the highest HPr concentration. Supplementation of trace elements stabilized AD, improving the kinetics and

allowing greater substrate loads. However, it could not avoid HPr accumulation. Batch experiments suggested that GAC addition, TEs supplementation and dilution can favor HPr consumption. Further research must be carried out to elucidate the effect of these promising options to prevent acid accumulation and/or favor its consumption.

4.3 General conclusions and perspectives

This experiment allowed producing methane efficiently in successive batch reactors and identifying what was the main issue faced during the project: HPr accumulation. From an industrial point of view, this is a huge problem that can have dramatic consequences in long-term operation. When using sequential batch reactors, this issue may lead to much longer batch durations before reloading the reactors. Similarly, in plug-flow systems, the OLRs will have to be reduced to ensure that no HPr is present in the digestate before its recirculation. Moreover, the sludge recirculation ratio will probably have to be increased to avoid reactor acidification. In any case, HPr accumulation will limit the substrate loads that can be applied in the reactors, thus jeopardizing greatly the volumetric productivities and the economics of the process. Another industrial consequence of the obtained results was that, as the strategy of FW co-digestion with PW led to the highest HPr concentrations, this possibility was discarded.

This chapter also provided hints that suggested possible solutions to this complication. Although supplementation of TEs could not avoid HPr accumulation, it improved the AD kinetics and allowed higher substrate loads, proving a beneficial effect. Also addition of GAC was found to favor the consumption HPr. Besides dilution was found to have a positive effect, this alternative was discarded due to the negative impact that it would have on the global AD process (*i.e.* water higher requirements and increased digestate production).

Therefore, the further efforts were directed towards finding a solution to the issue of HPr accumulation, either by favoring its consumption or by avoiding its accumulation in the first place. With these purposes on mind, different additives were tested in Chapter 5, according to the results from Chapter 4. Namely, carbon-based conductive materials (*e.g.* GAC and biochar) were evaluated and the influence of TEs supplementation was further studied. Carbon-based conductive materials such as GAC and biochar may aid the AD process by several means, like promoting biofilm formation on their surfaces, mitigating ammonia and acid inhibition through chemical sorption or facilitating the occurrence of DIET, thus improving syntrophic interactions. In addition, as the feeding strategy could have also favored

HPr accumulation, other reactor configurations (*e.g.* CSTR operation) were also tested. The conclusions and the perspectives from this chapter are summarized in Table 4.7.

Another co-digestion possibility for stabilizing FW AD, green waste (GW), was also tested using consecutive batch reactors. The results are presented in Appendix A.

Table 4.7. Summary of the conclusions of Chapter 4 and research perspectives

Section	4.2
Objective	Evaluate sequential FW batch AD as valorization process; compare performances of co-digestion with PW, low reactor temperature and addition TEs for AD stabilization
Main conclusion	Methane was efficiently produced; progressive HPr accumulation occurred in all the reactors; PW co-digestion as worst performant option; TEs and GAC addition as possible options for favoring VFA consumption
Novelty	Identification of HPr accumulation as main issue in sequential batch FW AD; potential solutions to this problem are given
Agreement with literature	HPr as problematic VFA in FW AD (Banks et al., 2008); TEs favor VFA consumption in AD (Yirong et al., 2015); Carbon-based conductive materials favor VFA consumption in AD (Zhao et al., 2016a)
Hypotheses and perspectives	• HPr is accumulated due to high concentrations of HAc and hydrogen • PW addition worsen HPr build-up due to a longer VFA production process • GAC favors VFA consumption through biofilm formation and DIET • Different carbon-based conductive materials should be tested as alternative for stabilizing FW AD • Other reactor configurations (*i.e.* CSTR) must be tested

FW stands for food waste, AD for anaerobic digestion, PW for paper waste, TEs for trace elements, HPr for propionic acid, GAC for granular activated carbon, VFAs for volatile fatty acids, DIET for direct interspecies electron transfer and CSTR for continuous stirred tank reactor

Chapter 5. Carbon-based conductive materials and trace elements to favor VFA consumption and stabilize FW AD for methane production

5.1 General introduction

Before describing the experiments carried out, the theoretical and practical concepts related to the application of carbon-based conductive materials in AD systems must be introduced. Carbon-based conductive materials are stable solids, rich in carbon and are produced from pyrolysis of biomass. Common examples are biochar (pyrolyzed biomass), activated carbon (obtained through post-treatment for activation) or carbon cloth (tissue imbibed with carbon particles). All these carbonaceous materials have particular properties, mainly related to their high specific areas, their hydrophobic surfaces and their relatively high conductivities. Therefore, they are commonly applied for industrial sorption processes (Fagbohungbe et al., 2017).

Dealing with biogas production processes, these materials have been mainly applied for biogas purification, sequestering the CO_2 in the gaseous phase and producing a methane-rich biogas (Linville et al., 2017). Recently, the supplementation of GAC or biochar directly inside the bioreactor has received a lot of attention. Both GAC and biochar have been found to enhance the biogas production in single AD, by promoting biofilm formation on their surfaces and by mitigating ammonia and acid inhibition through chemical sorption (Sunyoto et al., 2016). In the last couple of years, another main advantage of these materials has been discovered: they improve syntrophic interactions, not only by bringing the microbial partners closer via biofilm growth, but also by improving the transfer of electrons between them (Fagbohungbe et al., 2017; Lovley, 2017). Both GAC and biochar can serve as electron acceptors during AD and, once reduced, they are also able to act as electron donors (F. Liu et al., 2012; Prévoteau et al., 2016).

As it has been mentioned before, it has been suggested that SAO (Equation 5.1) and HM (Equation 5.3) are predominant pathways for methane production during AD of FW (Banks et al., 2012; Capson-Tojo et al., 2017d; Westerholm et al., 2012; Yirong et al., 2015).

Syntrophic acetate oxidation (SAO):

$$CH_3COO^- + 4H_2O \rightarrow 2HCO_3^- + H^+ + 4H_{2\,(g)} \qquad \Delta G^0 = +\,104\ kJ{\cdot}mol^{-1} \qquad \text{Eq. 5.1}$$

Syntrophic propionate oxidation (SPO):

$CH_3CH_2COO^- + 2H_2O \rightarrow CH_3COO^- + HCO_3^- + H^+ + 3H_{2\,(g)}$ $\Delta G^0 = +\ 76.1\ kJ{\cdot}mol^{-1}$ Eq. 5.2

Hydrogenotrophic methanogenesis (HM):

$4H_{2\,(g)} + HCO_3^- + H^+ \rightarrow CH_{4\,(g)} + 3H_2O$ $\Delta G^0 = -\ 132\ kJ{\cdot}mol^{-1}$ Eq. 5.3

Acetoclastic methanogenesis (AM):

$CH_3COO^- + H_2O \rightarrow CH_{4\,(g)} + HCO_3^-$ $\Delta G^0 = -\ 31.0\ kJ{\cdot}mol^{-1}$ Eq. 5.4

During this specific methane-producing pathway, syntrophic interactions between hydrogen producing bacteria and methanogens are particularly important if accumulation of intermediate metabolites (such as VFAs, molecular hydrogen or formic acid) is to be avoided. If the concentrations of these compounds start to increase, this leads to acidification of the AD process, mainly because of accumulation of HPr (Banks et al., 2011a). As it has been explained in Chapter 4, this occurs because SPO (Equation 5.2) becomes thermodynamically unfavorable when the concentrations of HAc, molecular hydrogen and/or formic acid start to increase. The immediate consumption of molecular hydrogen by archaea is critical, as its accumulation turns thermodynamically unfavorable the degradation of both HAc and HPr.

During the interactions between acidogenic bacteria and methanogenic archaea, hydrogen and formate act as electron shuttles in HM, allowing mediated interspecies electron transfer (MIET) to occur. Therefore, the processes of consumption-production of these chemical species are critical during HM. SPO is thermodynamically favorable only at low concentrations of hydrogen/formate (Batstone et al., 2002a) and thus the build-up or these species during HM can explain why HPr accumulates frequently during FW AD. This is not the case during AM (Equation 5.4), where HAc is directly transformed into methane.

In this context, the addition of carbon-based conductive materials as AD enhancers is particularly interesting, because of their capabilities of favoring syntrophic interactions and of allowing DIET to occur. As shown in Figure 5.1, DIET consists on the direct transfer of electrons between an electron-donating microorganism (*i.e.* electro-active fermentative bacteria) and an electron-accepting microorganism (*i.e.* hydrogenotrophic archaea). However, DIET is only possible when electrical connections between microorganisms can be forged (*e.g.* through biological structures such as nanowires or via non-biological conductive materials) (Wang et al., 2016). By adding carbon-based conductive materials into the system, the microorganisms attached onto the carbonaceous surface do not need to be in direct contact to interact and the occurrence of DIET is promoted. In addition, this process does not require

electron shuttles. Thus, the problem of accumulation of molecular hydrogen and formate in the reactors is eliminated and SAO or SPO inhibition can be relieved. Potentially, DIET offers two main advantages when compared to MIET in FW AD: (i) faster VFA degradation kinetics are expected due to favored microbial interactions (Cruz Viggi et al., 2014) and (ii) no electron shuttles are formed, favoring the thermodynamics of VFA consumption.

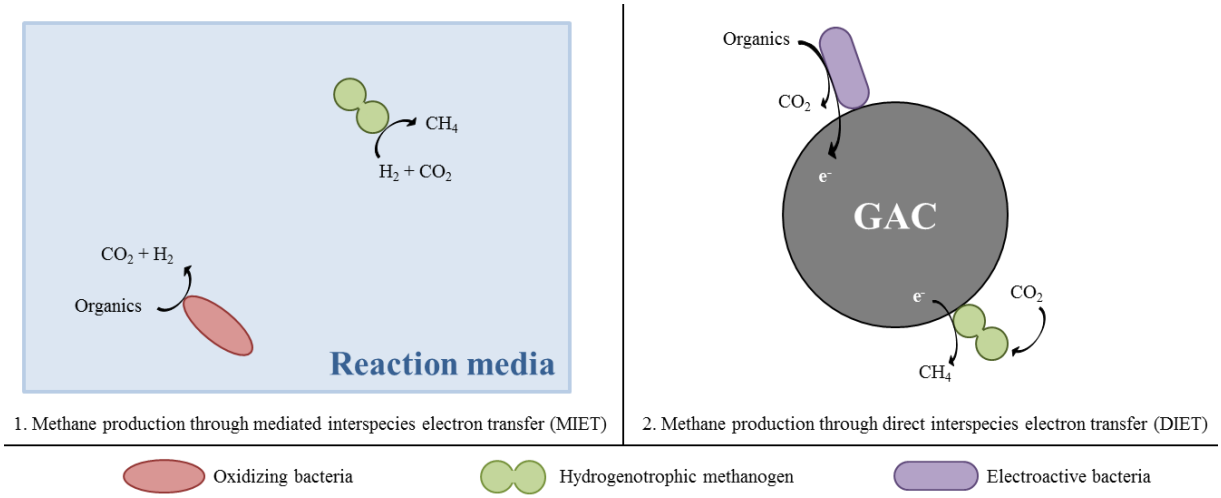

Figure 5.1. Schematic representation of hydrogenotrophic methanogenesis through (1) mediated interspecies electron transfer (MIET) and (2) direct interspecies electron transfer (DIET). GAC stands for granular activated carbon

By adding carbon-based conductive materials into the reactors, recent studies have found improved kinetics of VFA consumption and methane production during AD (Dang et al., 2016; Zhao et al., 2016a). It has been suggested that HAc, butyric acid (HBu) and HPr can be directly metabolized through DIET, improving the degradation kinetics of these particular VFAs for methane production (Cruz Viggi et al., 2014; Dang et al., 2016; Zhao et al., 2016a, 2016b). When considering the degradation of complex organic waste, GAC has been found to stabilize AD of dog food (Dang et al., 2017, 2016), promoting VFA consumption and improving the kinetics of methane production. GAC addition allowed maintaining high methane productivities at OLRs up to 18 kg $COD \cdot m^{-3} \cdot d^{-1}$. Despite the huge room of improvement that these materials offer, no study has been carried out to evaluate the influence of adding carbon-based conductive materials on the performance of FW AD. This is a clearly interesting approach that can help to stabilize the process and to overcome the accumulation of VFAs.

As explained above, HPr accumulation was the main issue to be solved for stabilizing FW AD for methane production. Thus, the addition of carbon-based materials into the reactors appeared as a promising option, not only to promote directly the consumption of HPr, but also

to favor the consumption of HAc and to avoid the formation of molecular hydrogen, both chemical species being responsible for the accumulation of HPr.

Therefore, the main objective of this chapter was to answer the following research question: can addition of carbon-based conductive materials stabilize FW AD? For this purpose, different experiments were carried out.

In the first experimental section of this chapter (5.2), the effect of adding GAC (used as model carbon-based conductive material) on the digestion kinetics was studied, paying particular attention to the VFA production-consumption process and to the established microbial communities. With the objective of maximizing the biogas productivities (and production rates), Section 5.3 was carried out, testing different substrate loads in the most performant reactors from the previous experiment. As TEs had been proved to aid the AD process (and HPr degradation), they were also added, together with the selected carbon conductive materials.

Other than GAC and TEs, the addition of biochar and industrial $FeCl_3$ was also studied, aiming at finding an economically feasible alternative that could be potentially applied at industrial scale. GAC is characterized by an activation post-treatment, which enhances its beneficial properties (such as high specific area) but also increases its price. On the other hand, biochar is a direct product from pyrolysis of biomass and therefore its price is much lower when compared with GAC. Regarding the industrial $FeCl_3$, this solution is itself a mixture of TEs due to its production process (generally acid dilution of several metal scraps). Obviously, this is cheaper and more environmental-friendly than buying the purified salts of the respective TEs and diluting and mixing them in the proper proportions. The composition of the industrial $FeCl_3$ used is shown in Table 5.9. In Section 5.4.2 the dosage of both biochar and industrial $FeCl_3$ was optimized using a batch experimental design (Table 5.10). Afterwards, the procedure used in Section 5.3 was repeated and increasing substrate loads were also applied in the batch reactors from the optimization design showing the best performances. This experimental setup allowed maximizing the biogas production rates and comparing the obtained results with the previous ones using GAC and TEs (Section 5.3). Finally, this section also studied the supplementation of biochar and industrial $FeCl_3$ as AD enhancers in pilot scale continuous reactors, aiming at extrapolating the laboratory scale results. A summary of the objectives of the experiments evaluated in Chapter 5 is given in Table 5.1.

Table 5.1. Summary of the objectives and the parameters varied in the experiments presented in Chapter 5

Section	Objective	Parameters varied	Additives
5.2	Improve digestion kinetics by adding GAC and TEs	S/X ratio	TEs; GAC
5.3	Asses maximum methane production rate in reactors containing GAC and TEs and test biochar and $FeCl_3$ as substitutes	S/X ratio	TEs; GAC; biochar; industrial $FeCl_3$
5.4.2	Optimize dosage of biochar and $FeCl_3$ and substrate load in batch reactors; evaluate performance of continuous reactors doped with biochar and $FeCl_3$	Organic loading rate; concentration of biochar and $FeCl_3$; S/X ratio	Biochar; industrial $FeCl_3$

FW stands for food waste, CB for cardboard, TS for total solids, S/X for substrate to inoculum and AD for anaerobic digestion

5.2 Addition of granular activated carbon and trace elements to favor VFA consumption during anaerobic digestion of food waste

Capson-Tojo, G., Moscoviz R., Ruiz D., Santa-Catalina G., Trably E., Rouez, M., Crest, M., Steyer, J.-P., Bernet, N., Delgenès, J.-P., Escudié, R., 2017. Addition of granular activated carbon and trace elements to favor VFA consumption during anaerobic digestion of food waste. To be submitted after patent acceptance (Section 5.4.2).

Abstract

The effect of supplementing granular activated carbon and trace elements on the anaerobic digestion performance of consecutive batch reactors treating food waste was investigated. Results from the first batch suggest that addition of activated carbon favored biomass acclimation, improving acetic acid consumption and enhancing methane production. Adding trace elements allowed a faster consumption of propionic acid. A second batch proved that a synergy existed when activated carbon and trace elements were supplemented simultaneously. The degradation kinetics of propionate oxidation were particularly improved, reducing significantly the batch duration and improving the average methane productivities. Addition of activated carbon favored the growth of archaea and syntrophic bacteria, suggesting that interactions between these microorganisms were enhanced. Interestingly, microbial community analyses showed that hydrogenotrophic methanogens were predominant. This study shows for the first time that addition of granular activated carbon and trace elements may be a feasible solution to stabilize food waste anaerobic digestion.

Graphical abstract

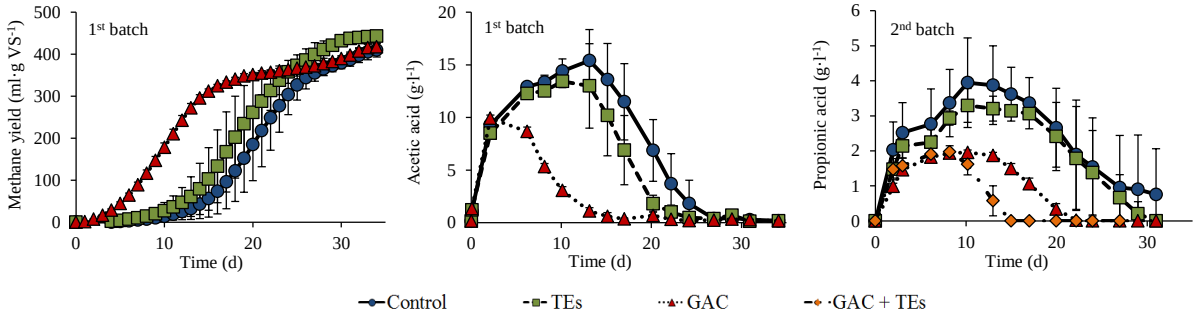

- 1st batch: FW AD kinetics improved by GAC addition due to favored biomass acclimation; TEs favored propionate degradation
- 2nd batch: synergy observed when dosing GAC and TEs simultaneously; enhanced propionate degradation

FW stands for food waste, AD for anaerobic digestion, GAC for granular activated carbon and TEs for trace elements

5.2.1 *Introduction*

The production of food waste (FW) is a global issue and a huge effort is currently being put to reduce the amounts of FW generated and to develop new sustainable technologies for its treatment. Among all the possible processes for FW treatment, anaerobic digestion (AD) stands as an environmental-friendly alternative that offers a triple role: (i) waste stabilization, (ii) production of renewable energy in the form of biogas and (iii) nutrient recovery by digestate application. Thus, within the concepts of circular economy and sustainable industry, AD is clearly an interesting process. Moreover, international regulations (European Directive 2008/98/CE) imposing the valorization of commercial FW from gross producers through soil return are recently being applied, precluding traditional/obsolete methods such as landfilling or incineration.

However, AD of highly concentrated substrates such as FW (18 % volatile solids; VS) is a complex biological process prone to failure if it is not properly managed. As FW is mainly composed of easily degradable carbohydrates, the reactor can be easily overloaded, leading to accumulation of volatile fatty acids (VFAs) due to unbalance of the acidogenesis/acetogenesis and methanogenesis steps (Capson-Tojo et al., 2016). Another issue occurring during FW AD is related to the high protein content of this substrate, which eventually leads to high concentration of total ammonia nitrogen (TAN) in the reactors. Therefore, long term continuous AD experiments have reported high concentrations of free ammonia nitrogen (FAN), which is toxic to microorganisms (Banks et al., 2008; Capson-Tojo et al., 2017b; Fotidis et al., 2014; Rajagopal et al., 2013b). Acetoclastic methanogens are particularly sensitive to high TAN/FAN concentrations (TAN over 2.8-3.0 $g \cdot l^{-1}$). Because of this, hydrogenotrophic and mixotrophic archaea (more resistant to TAN/FAN inhibition and VFA peaks) have been found to be predominant species at high TAN concentrations (De Vrieze et

al., 2012; Jiang et al., 2017). As a consequence, it has been stated that syntrophic acetate oxidation (SAO; Eq. 5.1) and hydrogenotrophic methanogenesis (HM; Eq. 5.3) are predominant pathways for methane production during AD of FW (Banks et al., 2012; Capson-Tojo et al., 2017d; Westerholm et al., 2012). During this processes, syntrophic interactions between bacteria and archaea are crucial to avoid accumulation of intermediate metabolites such as VFAs, molecular hydrogen or formic acid in the reactors. If these compounds accumulate, it leads to acidification of the process, decreasing the pH to values where methane production is stopped.

During HM, hydrogen and formic acid act as sole electron shuttles for methane production, allowing mediated interspecies electron transfer (MIET) to occur (Lovley, 2017). Therefore, the balance between the production-consumption processes of these shuttles is much more relevant in HM when compared with acetoclastic methanogenesis (Eq. 5.4). Propionic acid (HPr) has been reported to be particularly problematic, getting easily accumulated during FW AD and causing inefficient AD and eventually process failure (Banks et al., 2008, 2011a; Capson-Tojo et al., 2016, 2017a, 2017b; Wanqin Zhang et al., 2015). As explained in Capson-Tojo et al. (2017a) and Batstone et al. (2002a), this occurs because syntrophic propionate oxidation (SPO; Eq. 5.2) becomes rapidly thermodynamically unfavorable when main AD intermediates such as acetic acid (HAc), molecular hydrogen or formic acid start to accumulate. Thus, the build-up or these metabolites during HM explains why HPr and HAc accumulate frequently during FW AD.

If VFA accumulation is to be avoided during FW AD, the kinetics of SPO must be improved, by promoting the growth of HPr oxidizers and/or favoring the consumption of hydrogen/formate and HAc (promoting SAO), thus making SPO thermodynamically feasible. The main approach that has been addressed in the literature to avoid HPr accumulation during FW AD is the addition of trace elements (TEs), which are known to enhance degradation rates in AD (Banks et al., 2012; J. L. Chen et al., 2016; Voelklein et al., 2017; Zhang and Jahng, 2012; Wanli Zhang et al., 2015b). As previous research suggests, the synthesis of enzymes is of critical importance during syntrophic HM, particularly for the production of formate dehydrogenase for formate cleavage (Banks et al., 2012). This process requires TEs, such as iron, selenium, cobalt, molybdenum, nickel or tungsten, which have been found to stabilize both mesophilic and thermophilic AD of FW (Banks et al., 2012; Facchin et al., 2013; Qiang et al., 2013, 2012; Zhang and Jahng, 2012; Wanqin Zhang et al., 2015). The concentrations of those in FW is not sufficient and therefore the supplementation of mixtures of TEs has effectively avoided the accumulation of VFAs at high organic loading rates (OLRs) (Zhang et

al., 2011; Wanli Zhang et al., 2015b; Wanqin Zhang et al. 2015) and some studies have even shown that it is possible to recover acidified reactors using TEs (Qiang et al., 2012, 2013).

Another possibility that is currently receiving a lot of attention to favor VFA consumption during AD is the addition of carbon-based conductive materials (Dang et al., 2016), such as granular activated carbon (GAC). Other than favoring the adsorption of inhibitors and allowing the formation of biofilms onto their surface, it has been suggested that these materials can improve syntrophic interactions between microorganisms (Fagbohungbe et al., 2017). Due to their electrical conductivity and their particular surface chemistry, they can serve as electron acceptor during AD and, once reduced, they are also able to act as electron donor (F. Liu et al., 2012). Therefore, GAC has been found to permit direct interspecies electron transfer (DIET) to occur on their surface (Dang et al., 2016). DIET is an alternative to MIET in which the electrons are transferred between the electron-donating and -accepting partners through electrical connections, which can be formed by conductive pili, electron transport proteins or electrically conductive materials (Lovley, 2017). When compared to MIET, DIET is expected to be a faster and more efficient mechanism of electron transfer (Cruz Viggi et al., 2014; Lovley, 2017). In addition, as during DIET electron shuttles (such as hydrogen or formate) are no longer formed, the degradation of VFAs during AD is thermodynamically independent of the concentrations of these species (Dang et al., 2016; Lee et al., 2016). Thus, the application of these materials to favor DIET and avoid VFA accumulation during AD of complex-concentrated substrates (such as FW) appears as an alternative with a huge potential. Finally, a recent preliminary study has proven that the separate addition of GAC and TEs to a digestate containing high concentrations of HPr favored significantly the consumption of this acid (Capson-Tojo et al., 2017a).

The objective of this study was to evaluate for the first time the effect of GAC and TEs addition on the AD performance using consecutive batch reactors fed with FW. Particular attention was paid to the VFA accumulation/consumption kinetics and the evolution of the microbial communities.

5.2.2 *Materials and methods*

5.2.2.1 Inoculum and substrate

The inoculum used to start the reactors was collected from an industrial plant treating different organic streams at high TAN/FAN concentrations (5.04 g TAN·l^{-1}; 615 mg FAN·l^{-1}). This inoculum was selected because it was assumed that the microbial population would already be adapted to high FAN concentrations, like those existing during FW AD. The

inoculum had an initial total solids (TS) content of 5.81±0.02 %, with 59.13±0.08 % corresponding to VS. The FW was collected from different producers from the region of the Grand Narbonne, in the south of France. A proportional mixture (wet weight) of the different FWs was used as substrate. The characterization of the FW mixture used as substrate and the inoculum is provided in Table 5.2.

Table 5.2. Characteristics of the food waste and the inoculum (Capson-Tojo et al., 2017b)

Parameter	Food waste mixture	Inoculum
TS (%)	21.0	5.81
VS/TS (%)	90.3	59.1
Carbohydrates (g·kg TS^{-1})	618	n.m.[1]
Proteins (g·kg TS^{-1})	187	n.m.[1]
Lipids (g·kg TS^{-1})	121	n.m.[1]
BMPs (ml CH_4·g VS^{-1})	420	n.m.[1]
pH	5.02	8.10
TAN (g·kg TS^{-1})	0.90	5.04
TKN (g·kg TS^{-1})	30.0	93.0
C/N	16.1	3.04
Co (mg·kg TS^{-1})	< 9.75	< 9.75
Cu (mg·kg TS^{-1})	11.2	163
Fe (mg·kg TS^{-1})	1114	18003
Mn (mg·kg TS^{-1})	27.6	643
Mo (mg·kg TS^{-1})	1.26	5.45
Zn (mg·kg TS^{-1})	38.4	649
Ni (mg·kg TS^{-1})	1.19	22.3

1. n.m. stands for “not measured”

With TS contents of 21 % (90.3 % VS), being mainly composed of carbohydrates (618 g·kg TS^{-1}) and with relatively low C/N ratios (16.1), the results for the mixed FW are in agreement with typical values presented in the literature (Capson-Tojo et al., 2016). The obtained values also confirm the low concentrations of some TEs (such as Co or Mo) in FW. A deeper discussion of these results as well as a more extensive characterization can be found in Capson-Tojo et al. (2017a).

5.2.2.2 Consecutive batch anaerobic digestion

All the batch reactors were started using 60 g of FW as substrate (raw). The substrate to inoculum (S/X) ratio was set as 1 g VS·g VS^{-1}, which led to FW concentrations of approximately 30 g VS $FW \cdot l^{-1}$. An amount of 368 g of inoculum was then added in each

reactor. The reactors were incubated at 37 °C and had an initial working volume of 430 ± 2 ml. The Control reactor was fed with only FW. The TEs reactor had equivalent working conditions but was supplemented with TEs at the following concentrations: 100 $mg \cdot l^{-1}$ Fe, 1 $mg \cdot l^{-1}$ Co, 5 $mg \cdot l^{-1}$ Mo, 5 $mg \cdot l^{-1}$ Ni, 0.2 $mg \cdot l^{-1}$ Se, 0.2 $mg \cdot l^{-1}$ Zn, 0.1 $mg \cdot l^{-1}$ Cu, 1 $mg \cdot l^{-1}$ Mn. These values were estimated from optimal results reported in the literature (Banks et al., 2012; Zhang and Jahng, 2012; Zhang et al., 2015b). The required volume of a concentrated solution (x100) containing $FeCl_2 \cdot 4H_2O$, $CoCl_2 \cdot 6H_2O$, $Na_2MoO_4 \cdot 2H_2O$, $NiCl_2 \cdot 6H_2O$, Na_2SeO_3, $ZnCl_2 \cdot 2H_2O$, $CuCl_2 \cdot 2H_2O$, $MnCl_2 \cdot 4H_2O$ was used for doping the reactors. Similarly, GAC at a concentration of 10 $g \cdot l^{-1}$ was added into the GAC reactor. The initial concentration of GAC was defined according to Lee et al. (2016). Finally, the reactor GAC + TEs was supplemented simultaneously with the same concentrations of TEs and GAC used above. The GAC was supplied by Sigma-Aldrich (Missouri, United States of America; CAS 7440-44-0). The incubation system was an Automated Methane Potential Testing System (AMPTSII) (Bioprocess Control, Sweden). The AMPTSII system consisted of 12 parallel reactors with a total volume of 500 ml and connected to CO_2 traps (NaOH solutions) and to gas flow meters to determine continuously the methane flow rate. The AMPTSII agitated the reaction media during one minute every 10 minutes at 40 rpm. Other than providing an automatic measurement of the biogas produced, this system has the advantage of allowing an easy sampling of the digestate, through a hole present in each reactor than can be used as sampling port. Thus, the follow-up of the dynamics of VFA accumulation was facilitated. All the conditions were run in triplicate. It is important to mention that recent consecutive batch studies have shown that, even if the accumulated HPr might not account for a high percentage of the final methane yields, this VFA is degraded much slower that the other acids and, if the batch does not last enough time to allow HPr oxidation, this VFA will accumulate after each reactor feeding and will eventually lead to acidification of the reactor. Thus, its degradation defines the batch duration (Capson-Tojo et al., 2017b). Therefore, the reactors were fed a second time after 34 days, when a biogas plateau existed and the HPr from the first feeding had been consumed.

In order to account for inoculum adaptation, a second feeding was performed at the same conditions applied in the first one (S/X ratio of 1 g $VS \cdot g\ VS^{-1}$). The reactors containing TEs or GAC were further supplemented in these reactants/materials according to the amount of digestate removed after the first batch and to the amount of raw FW added as substrate for the second batch.

It is important to mention that recent consecutive batch studies have shown that, even if the accumulation of recalcitrant VFAs (such as HPr) might not account for a high percentage of the final methane yields, if the batch process does not last enough time to allow their total oxidation, these VFAs will accumulate after each reactor feeding and will eventually lead to acidification of the reactor (Capson-Tojo et al., 2017a). Thus, in this study the total degradation of HPr (last VFA to be degraded) defined the batch duration. Therefore, the reactors were fed after 34 days, when a biogas plateau existed and the HPr had been consumed.

Before presenting the results, it must be commented that in the first batch another GAC supplemented reactor was carried out (GAC + Geo). In this case, other than GAC, *Geobacter sulfurreducens* was also added into the reactors. This microorganism is a well-known DIET performer and is also known to grow attached onto GAC particles (F. Liu et al., 2012). The results from these reactors (GAC + Geo) were practically equal to those observed in the GAC reactors (Figure C.1), meaning that the addition of *Geobacter* did not enhance the VFA degradation kinetics. Therefore, this *Geobacter*-inoculated reactor was stopped after the first feeding. In the second batch, these GAC-containing reactors were supplemented with TEs (at the same concentration applied in the TEs reactors) and this new condition was used to elucidate the effect of the simultaneous addition of both AD enhancers (reactor GAC+TEs).

5.2.2.3 Analytical methods

5.2.2.3.1 Physicochemical characterization of the FW

The FW was extensively characterized (Capson-Tojo et al., 2017b). TS and VS contents were determined according to the standard methods of the American Public Health Association (APHA, 2005). The concentration of carbohydrates was measured using the Dubois method (Dubois et al., 1956). The content of lipids was determined by a gravimetric method based on accelerated solvent extraction using an ASE®200, DIONEX (California, United States of America) coupled to a MULTIVAPOR P-12, BUCHI (Aquon, Netherlands) with heptane as solvent (100 bar, 105 °C, 5 cycles of 10 min static and 100s purge) (APHA, 2005). Total Kjeldahl nitrogen (TKN) and NH_4^+ concentrations were measured with an AutoKjehdahl Unit K-370, BUCHI. The concentration of proteins was estimated from the TKN contents (6.25 g protein·g N^{-1} (Jimenez et al., 2013)). Total organic carbon (TOC) and inorganic carbon (IC) were determined using a Shimadzu (Kyoto, Japan) TOC-V_{CSN} Total Organic Carbon Analyzer coupled to a Shimadzu ASI-V tube rack. The C/N ratio was calculated as TOC/TKN. The pH was measured by a WTW (London, United Kingdom)

pHmeter series inoLab pH720. The BMPs of the substrates were determined according to Motte et al. (2014a). The conversion of chemical oxygen demand (COD) was calculated according to the input COD from the substrates and that found as products (methane and VFAs) after AD. The COD of the FW was estimated from the contents in carbohydrates (1.067 g $COD \cdot g^{-1}$), proteins (1.57 g $COD \cdot g^{-1}$) and lipids (2.87 g $COD \cdot g^{-1}$) (Batstone et al., 2002a).

The concentrations of micro-elements were determined by Aurea Agroscience© (Ardon, France). The contents on metallic trace elements were measured by water extraction, according to the norm NF EN 13346. The concentrations of Fe, Cu, Ni, Mn, Mo, Co and Zn were measured by plasma emission spectrometry, according to the NF EN ISO 11885.

5.2.2.3.2 Analysis of metabolites and final products

A plastic tube submerged in the sludge and connected to the cover of the AMPTSII reactors enabled sampling of digestate without modifying the composition of the gas in the headspace. Before sampling, the gas output was blocked and the equivalent volume of digestate to be removed was added as nitrogen gas (with negligible effect in the gas composition), avoiding this way an overestimation of the gas produced. Once sampled, the concentrations of VFAs and ionic species in the digestates were measured by gas and ion chromatography, as described in Motte et al. (2013).

5.2.2.4 qPCR and MiSeq sequencing analysis

To study the evolution of the microbial communities during the AD process, four sampling points were selected from the first batch process. In addition, as the endogenous microbial communities present in the FW are known to have a significant effect on its characteristics (mainly due to pre-degradation during FW storage) (Fisgativa et al., 2017), samples of the FW and the initial inoculum were analyzed separately.

Real-time polymerase chain reaction (qPCR) and DNA sequencing techniques were used to analyze the samples. The DNA extraction was carried out using a Fast DNA SPIN kit for soil (MP Biomedicals). The primer pairs 515-532U and 909-928U and their respective linkers were used to amplify the V4-V5 regions of the 16S rRNA genes (over 30 amplification cycles were applied at an annealing temperature of 65 °C). The products were purified and analyzed using the Illumina MiSeq cartridge (v3 chemistry) for sequencing of paired 300 bp reads at the GenoToul platform (http://www.genotoul.fr). Mothur (version 1.35.0) was used for sequence assembling, cleaning and alignment and for assignation of the taxonomic affiliation,

as described in Venkiteshwaran et al. (2016). A precise description of the methodology employed can be found elsewhere (Moscoviz et al., 2017).

To evaluate the growth or decay of a microbial population, the number of times the population was doubled (N_g; growth rate) was calculated by:

$$N_g = \frac{\ln(\frac{X_f}{X_i})}{\ln(2)} = \log_2(\frac{X_f}{X_i}) \qquad \text{Equation 5.5}$$

Where X_i and X_f are the initial and final concentrations of 16 S copies respectively.

The qPCR measurements of each sample were performed in triplicate to assess the technical standard error associated with the measurement. The raw qPCR results were $\log_2$ transformed and the variance between replicates was used to calculate the standard error of measurement. Values of 0.53 and 0.43 $\log_2$(16 S copies·g^{-1}) were found for bacteria and archaea, respectively. It was considered that no growth (or decay) existed when values of N_g lower than twice σ (1.05 and 0.87 $\log_2$(16 S copies·g^{-1}) for bacteria and archaea) were observed.

5.2.2.5 Data analysis

The methane yields were calculated by dividing the total volume of methane produced by the initial mass of VS of substrates. The yields were corrected to account for the digestate removed. The concentration of FAN was calculated according to Rajagopal et al. (2013b) as a function of temperature, pH, ionic strength and TAN concentration. The concentrations of the main ions present in the reactors (Cl^-, Na^+, NH_4^+, K^+, Mg^{2+}, H^+ and Ca^{2+}) were taken into account in this calculation.

5.2.3 *Results and discussion*

5.2.3.1 Performance of the consecutive batch reactors

5.2.3.1.1 Reactor start-up

As aforementioned, the batch reactors were fed twice consecutively. During the first batch (S/X ratio of 1 g VS·g VS^{-1}; 30 g VS FW·l^{-1}), three different conditions were monitored: a Control reactor, a reactor supplemented with TEs and a reactor supplemented with GAC. The reactors lasted for 34 days and during this period 15 samples were taken to analyze the composition of the reacting medium. Figure 5.2 presents the methane yields, the total

products measured (cumulative g COD) and the concentrations of the main VFAs (acetic acid, propionic acid, butyric acid and valeric acid).

As it can be observed, methane was produced efficiently, but a lag phase on the methane production existed in all the reactors, associated with an initial accumulation of VFAs (mainly HAc and HPr, with traces of HBu and valeric acid). However, while lag phases of around 10 days existed in the Control and TEs reactor, the lag period in GAC lasted for 2 days. This occurred because the addition of GAC promoted the early consumption of HAc (Figure 5.2C), with concentrations up to 9.9 $g \cdot l^{-1}$ in the GAC reactor and up to 15.4 $g \cdot l^{-1}$ in the Control reactor. In addition, while in the GAC reactor the HAc concentrations after 15 days were already low (0.6 $g \cdot l^{-1}$), it was necessary to wait until day 24 to achieve these values in the TEs reactor and until day 27 in the Control. The faster substrate conversion is also suggested by Figure 5.2B (total products as sum of methane plus VFAs in COD units), where it can be observed that the GAC reactors achieved high substrate conversion before the other conditions.

Table 5.3 shows the corresponding methane yields (410-443 ml $CH_4 \cdot g\ VS^{-1}$), as well as the maximum methane production rates (397-419 $ml \cdot d^{-1}$), the maximum rates of HAc and HPr consumption (1.59-1.76 $g \cdot l^{-1} \cdot d^{-1}$ and 0.32-0.58 $g \cdot l^{-1} \cdot d^{-1}$, respectively) and the final COD recoveries (81.9-87.9 %). Interestingly, the values of the maximum HAc consumption rates shown in Table 5.3 were not significantly different (1.59-1.76 $g \cdot l^{-1} \cdot d^{-1}$), suggesting that the favored methane production (and concomitant HAc consumption) in the GAC reactor was mainly related to a favored initial growth of the microorganisms but that, once growing, the AD kinetics (in exponential growth) were similar independently of the initial lag phase observed. In addition, when looking at the maximum methane production rates, it can be observed that they were not significantly different between the reactors (397-419 $ml \cdot d^{-1}$). Concerning the consumption of HBu and valeric acid (HVal), the GAC reactor showed also the best performances, with lower maximum concentrations achieved (Figure 5.2E and Figure 5.2F) and lower times required for their total degradation (Table 5.3). This suggests that GAC addition also favored the consumption of these VFAs. Summarizing, it can be concluded that GAC addition favored biomass acclimation during this first feeding, reducing the observed lag phases.

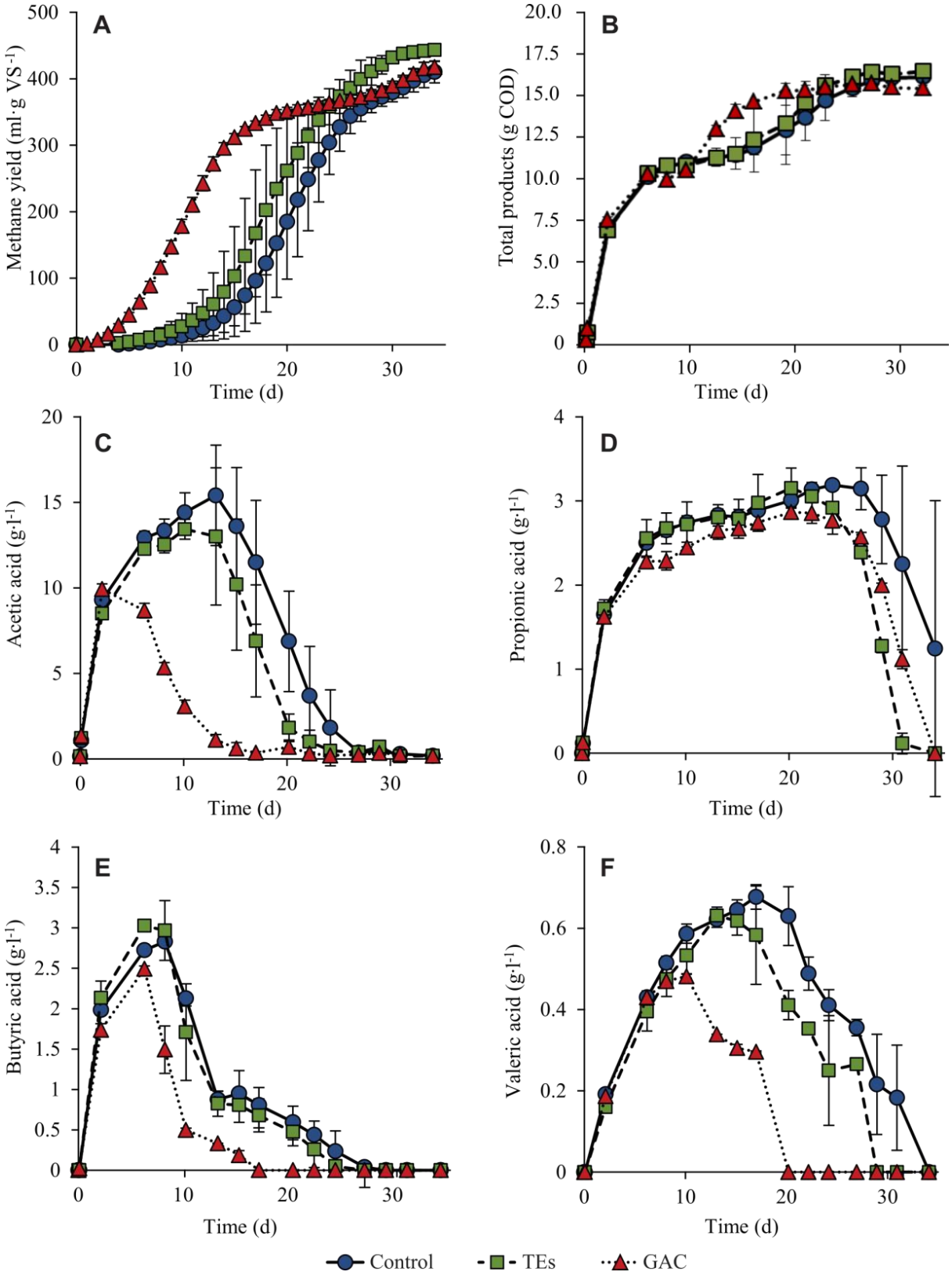

Figure 5.2. Evolution of the (A) methane yields, (B) total products obtained (g COD), and concentrations of (C) acetic, (D) propionic, (E) butyric and (F) valeric acids during the first feeding (~ 30 g VS FW·l^{-1})

Table 5.3. Maximum methane production rates, final methane yields, COD recoveries and final pH values obtained after the first feeding (Batch # 1) and the second feeding (Batch # 2). The maximum consumptions rates of acetic and propionic acids and the times required for total VFA consumption are also shown

Reactor & batch #	Max. CH_4 prod. rate ($ml \cdot d^{-1}$)	CH_4 yield ($ml\ CH_4 \cdot g\ VS^{-1}$)	Final COD recovery (%)[1]	Final pH	Max. HAc cons. rate ($g \cdot l^{-1} \cdot d^{-1}$)	Max. HPr cons. rate ($g \cdot l^{-1} \cdot d^{-1}$)	Time for HAc (d)[2]	Time for HPr (d)	Time for HBu (d)	Time for HVal (d)
Control 1	397 ± 66	410 ± 17	86.0 ± 1.60	8.13 ± 0.02	1.59 ± 0.13	0.32 ± 0.19	27	> 34[3]	29	34
TEs 1	419 ± 27	443 ± 0.3	87.9 ± 0.01	8.12 ± 0.01	1.76 ± 0.32	0.58 ± 0.10	24	31	27	29
GAC 1	406 ± 3	417 ± 9.0	81.9 ± 0.40	8.13 ± 0.01	1.74 ± 0.07	0.44 ± 0.04	15	34	17	20
Control 2	545 ± 58	452 ± 33	92.0 ± 2.37	8.12 ± 0.02	1.68 ± 1.98	0.35 ± 0.23	10	> 31[3]	15	20
TEs 2	584 ± 14	443 ± 7.3	88.7 ± 2.01	8.12 ± 0.03	1.35 ± 0.29	0.28 ± 0.23	10	31	13	15
GAC 2	600 ± 31	456 ± 3.7	90.7 ± 0.74	8.11 ± 0.01	2.01 ± 0.32	0.24 ± 0.00	8	22	13	15
GAC+TEs 2	719 ± 14	456 ± 7.8	90.7 ± 1.58	8.03 ± 0.03	2.22 ± 0.28	0.37 ± 0.05	8	15	10	13

1. Calculated considering the input COD coming from the FW and the COD recovered as final AD products (*i.e.* methane and VFAs)
2. As the acetic acid was also a product of the degradation of other acids, the times shown correspond to the first moment with concentrations lower than 2 $g \cdot l^{-1}$
3. Total consumption not achieved
TEs stands for trace elements, GAC for granular activated carbon, max for maximum, prod for production, HAc for acetic acid, cons for consumption, HPr for propionic acid, HBu for butyric acid and HVal for valeric acid

Surprisingly, even if GAC supplementation improved HAc degradation, this was not translated into a more efficient HPr consumption. As shown in Figure 5.2D, the degradation of HPr did not start until day 22 in all the reactors and was not complete in the Control reaction while it was not finished until days 31 and 34 for reactors supplemented with TEs and GAC, respectively. This suggests that HPr oxidation was not only limited thermodynamically (due to high concentrations of metabolites in the media), but also by the absence of HPr-degrading microorganisms initially. If this second hypothesis was right, the HPr degradation observed during this first batch would have allowed the development of these bacteria which should be afterwards present in the reaction media. Therefore, a second batch should reflect this growth and an improved HPr degradation should be observed. To test the aforementioned hypothesis, a second feeding was performed.

Finally, it must also be mentioned that, besides the high transient VFA concentrations achieved during both feedings, the reactors were not acidified because the high TAN concentrations (10.0-11.1 $g \cdot l^{-1}$; see Table 5.4) acted as pH buffer, keeping the pH at high values, always above 7.20 regardless the VFA concentration and with final values of 8.03-8.13 (Table 5.3).

Table 5.4. Concentrations of TAN and FAN and ionic strengths in the reactors after the second feeding

Reactor	Ionic strength (M)	TAN ($g \cdot l^{-1}$)	FAN ($mg \cdot l^{-1}$)
Control	0.56 ± 0.01	11.1 ± 0.5	1102 ± 133
TEs	0.57 ± 0.07	11.7 ± 0.8	1067 ± 10
GAC	0.47 ± 0.06	10.0 ± 0.7	971 ± 8
GAC + TEs	0.45 ± 0.01	10.2 ± 0.2	878 ± 11

TAN stands for total ammonia nitrogen and FAN for free ammonia nitrogen

5.2.3.1.2 After inoculum adaptation

Once the first batch was finished, the reactors were fed again with an S/X ratio of 1 g VS·g VS^{-1} (30 g VS FW·l^{-1}). In this case, four different conditions were monitored: a Control reactor, a reactor supplemented with TEs, a reactor supplemented with GAC and a reactor supplement with both TEs and GAC (to assess the simultaneous effect of these reactants; see Figure C.1 for more details about the 4^{th} condition started). The batches lasted for 31 days and again 15 samples were taken to analyze the composition of the reacting medium. The corresponding methane yields and production rates and the concentrations of the main VFAs (HAc, HPr, HBu and HVal) are shown in Figure 5.3. As for the first batch, the maximum methane production rates, final methane yields, COD recoveries, final pH values, maximum consumptions rates of acetic and propionic acids and the times required for total VFA consumption are also presented in Table 5.3.

The global behavior was totally different between both feeding cycles, highlighting the importance of microbial adaptation. In this second batch no lag phases in the methane production were observed in any condition and HAc (in this case only up to 9.3 $g \cdot l^{-1}$) started to be degraded after only two days in all the reactors. Moreover, similar kinetics of HAc production-consumption (as well as total COD conversions) were observed in all the reactors. This indicates that the first batch served for biomass growth and acclimation, processes that were favored by adding GAC. When comparing the results presented in Table 5.3 for the two consecutive feedings, it can be appreciated that, while the methane yields did not differ much between the consecutive batchs (410-443 and 443-452 ml $CH_4 \cdot g\ VS^{-1}$, respectively), the maximum methane production rates were much higher in the second one, with values of 545-719 $ml \cdot d^{-1}$ (*vs.* 397-419 $ml \cdot d^{-1}$ in the first feeding). This value was particularly improved in the reactors supplemented with GAC, with the maximum rate obtained in the GAC+TEs reactor (719 $ml \cdot d^{-1}$). Moreover, it can be observed in Table 5.3 that the times required to achieve a total consumption of the accumulated VFAs were also much lower in the second

feeding (*i.e.* 27 days *vs.* 10 days for HAc consumption in the Control reactor). These results indicate that biomass acclimation after the first batch clearly improved the methane production kinetics and the VFA degradation in all conditions. This suggests that biomass acclimation must always be considered when performing batch studies and, particularly, if concentrated substrates known to induce microbial selection in digesters (such as FW) are used (Capson-Tojo et al., 2017d).

The main difference between the GAC supplemented reactors and the other conditions in the second batch can be deducted from Figure 5.3D and Table 5.3: the concentrations of HPr and the times required for its total consumption were much lower in the reactors containing GAC. Again, the GAC+TEs system showed the best performance, with HPr concentrations only up to 1.97 $g \cdot l^{-1}$ (*vs.* 3.94 $g \cdot l^{-1}$ in the Control reactor) and without traces of HPr after day 15 (a value which was 22, 31 and over 31 days for the GAC, TEs and Control reactors, respectively). Therefore, it can be concluded that, even if the kinetics of methane production and the methane yields were similar in all the reactors, the addition of GAC clearly favored the consumption of the accumulated HPr (avoiding at the same time the extent of its build-up). In addition, a further improvement in the HPr degradation was observed when adding TEs into the GAC-supplemented reactors.

As it has already been suggested in Capson-Tojo et al. (2017a), if the batch reactors are reloaded before the HPr degradation is finished, this compound accumulates sequentially, eventually causing acidification of the reactors and inhibition of the methane production process. Thus, if a stable AD process is to be achieved, the time required for total HPr consumption will determine the batch duration, even if the desired methane yields are reached before consuming all the HPr produced. This implies that the reduction of the time required for total HPr degradation when adding GAC + TEs (from over 30 days in the Control to 15 days) leads to an AD process that can potentially treat efficiently the same amount of FW in less than half of the time. This implies that the average daily methane production rates (calculated as total methane volumetric productivity divided by batch duration) are doubled (*i.e.* 0.45 *vs.* 0.95 ml $l \cdot l \cdot d^{-1}$ in the Control and the GAC+TEs reactors, respectively). From an industrial point of view, this is a huge improvement that can potentially render the process economically feasible.

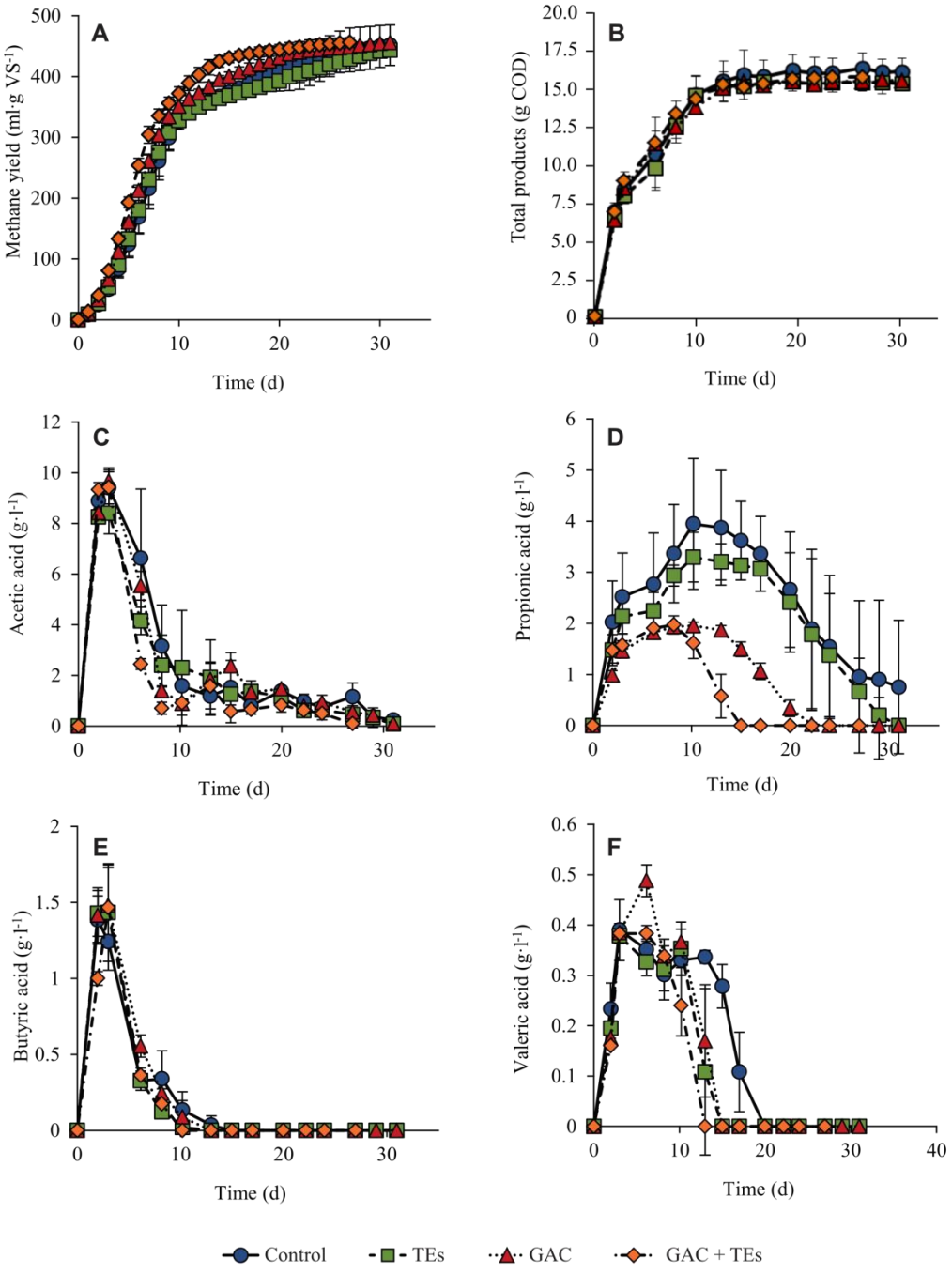

Figure 5.3. Evolution of the (A) methane yields, (B) total products obtained (g COD) and concentrations of (C) acetic, (D) propionic, (E) butyric and (F) valeric acids during the second feeding (~ 30 g VS FW·l^{-1})

The obtained results were further verified by a third feeding cycle at a higher substrate load (two-fold the load applied in the previous batches; ~ 55 g VS FW·l^{-1}), where the same four conditions tested in the second feeding were carried out (Figure C.2). The results confirmed the synergetic effect of GAC and TEs for improving HPr degradation.

In order to understand the obtained results and to elucidate which microorganisms were dominant, an extensive analysis of the microbial communities was carried out, comparing the different conditions and analyzing the evolution of the populations throughout the first batch.

5.2.3.2 Evolution of the microbial communities in the reactors

As aforementioned, four different samples were taken during the first batch (in days 6, 13, 24 and 34). The corresponding sequencing and qPCR results are presented in Figure 5.4.

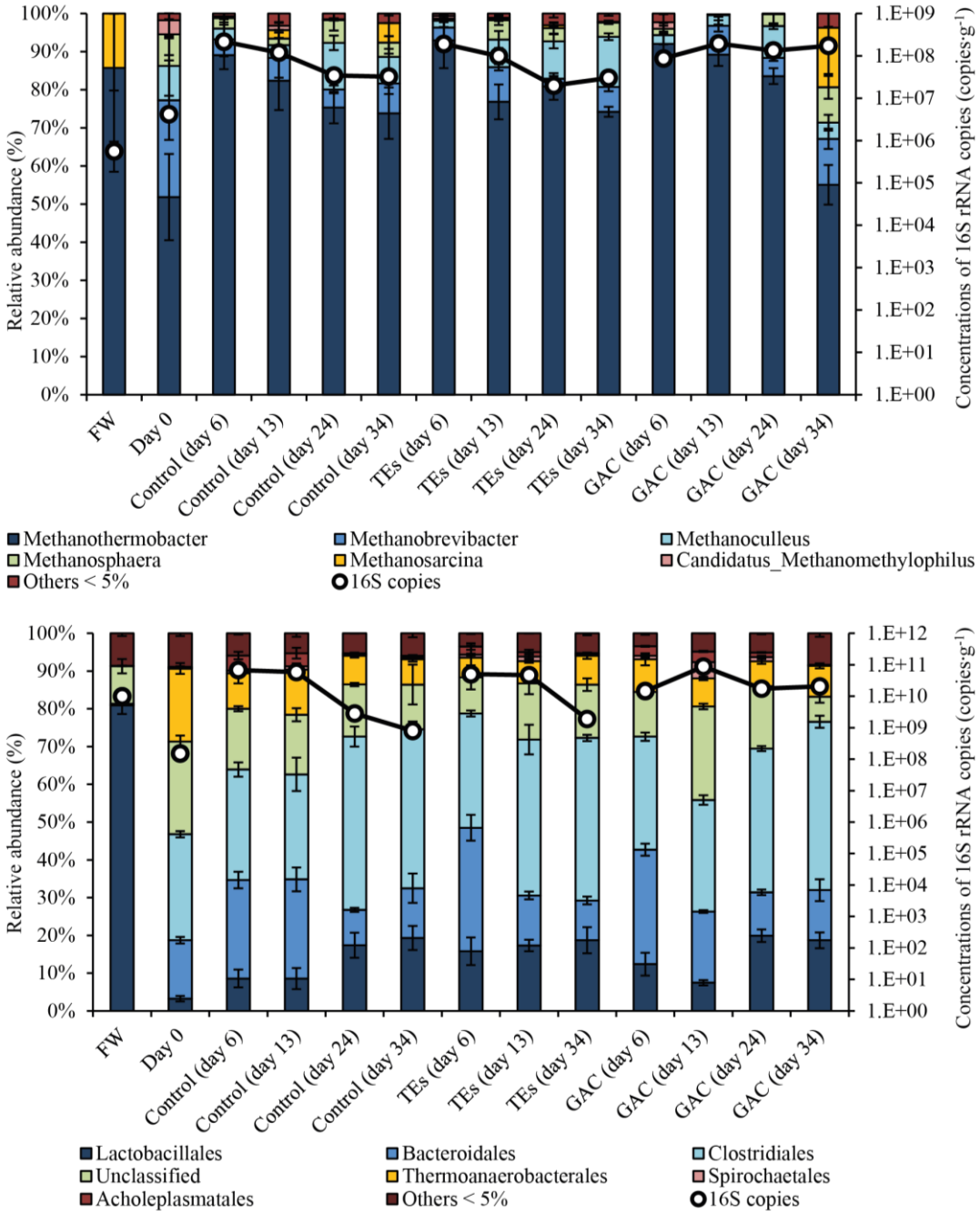

Figure 5.4. Sequencing and qPCR results for the archaea (above) and the bacteria (below) in the food waste and in the reactors. The days indicate the moment of the batch when the samples were taken

Starting with the archaeal populations, the predominant species were similar in all the reactors. In agreement with the literature dealing with AD at high TAN/FAN contents, all the species presented in Figure 5.4 are hydrogenotrophic methanogens, with no traces of *Methanosaeta* sp. being detected (Capson-Tojo et al., 2017c; De Vrieze et al., 2012; Jiang et al., 2017). Considering that the inoculum comes from an AD plant working at high TAN/FAN concentrations (5.04 g $TAN \cdot l^{-1}$) and that these concentrations were even higher after the batches carried out, this is a logical outcome. In addition, other than *Methanosarcina* sp. (which is a mixotrophic microorganism), all the other archaea were strict hydrogen utilizers, indicating that syntrophic VFA oxidation and HM were the main pathways for methane production. The predominant archaea were *Methanothermobacter* sp. (100 % of 16s rRNA gene sequence similarity with *Methanothermobacter tenebrarum*) in all the conditions, followed by *Methanobrevibacter* sp. (97 % of 16s rRNA gene sequence similarity with *Methanobrevibacter acididurans*) and *Methanoculleus* sp. (99 % of 16s rRNA gene sequence similarity with *Methanoculleus bourgensis*). All these species are known to be thermo-tolerant archaea (with some also identified as halotolerant) (Maus et al., 2012; Nakamura et al., 2013; Savant et al., 2002). This indicates that, at the high transient VFA peaks and TAN/FAN concentrations in the reactors (see Table 5.4), common acetotrophic archaea (*i.e. Methanosaeta*) were inhibited, and only the most resistant methanogens were able to thrive. It is also interesting to mention that a general trend can be observed in the archaeal population dynamics when looking at the qPCR results: after a significant growth during the first week, a sudden decay existed, particularly in the Control and TEs reactors, which was followed by a final, less pronounced, archaeal growth. The periods of growth can be attributed to the presence of VFAs and hydrogen at the beginning of the batch process (from FW degradation) and to the HPr degradation at the end, which were used as substrate for methane production after their conversion by bacteria. Interestingly, the GAC reactors sustained the growth of archaea for a longer period than the other two conditions and the concentrations of archaea after AD were higher in those reactors than in the others, reducing the extent of the aforementioned decay. This suggests that the formation of biofilm onto the GAC particles may have favored archaeal survival. In addition, a more diverse archaeal population was observed in the GAC reactor at the end of the batch, with a Shannon index of 1.55 ± 0.10 (*vs.* 1.25 ± 0.09 and 1.30 ± 0.04 for the Control and TEs reactors, respectively). The presence of *Methanosarcina* (known to participate in DIET (Rotaru et al., 2014a)) was particularly higher in this condition when compared to the Control and TEs reactors, suggesting that GAC may have favored its growth.

When looking at the bacterial communities (expressed at order level to favor data analysis) it can be observed that, while *Lactobacillales* (mainly lactic acid-producing bacteria similar to *Lactobacillus plantarum*) were predominant in the FW, *Bacteroidales* and *Clostridiales* were the main microorganisms in all the AD reactors. As these microorganisms are known to participate in the processes of hydrolysis and acidogenesis, respectively, their growth during substrate degradation is a logical outcome. As for archaea, after the day 13 the number of microorganisms decreased rapidly. Several reasons might explain this biomass decay, such as endogenous growth due to lack of substrate or the presence of predators or bacteriophages in the media. Again, this decay was much lower in the GAC-doped reactor, suggesting that GAC allowed keeping higher concentrations of alive bacteria in the media.

In an attempt to elucidate the reasons behind this biomass decay and to further understand the positive effect of GAC addition, the growth rates of the main bacterial OTUs were calculated according to Equation 5.5. The obtained results are presented in Figure 5.5.

The results show that all the reactors followed a similar trend: an initial growth related to FW degradation was observed, followed by a less pronounced growth and a final biomass decay. Interestingly, among the main fermenter bacterial species, numerous syntrophic organisms were detected, such as OTU 7 (belonging to the *Gelria* genus) and OTUs 9 and 10 (*Syntrophomonadaceae* family), with relative abundances over 5 % after AD. This further suggests the importance of these processes during FW AD.

When comparing the reactors, the main conclusion that can be drawn is again related to the influence of GAC addition. While the Control and the TEs reactors showed similar population dynamics, with no significant bacterial growth after day 13, the GAC supplemented reactor showed a continuous growth of *Clostridiales* (OTUs 6 and 10) between days 13 to 35. In the case of OTU 6, it is related to a bacterium known to degrade different sugars and aminoacids to produce HAc and hydrogen (Wu et al., 2010). It belongs to the *Alkaliphilus* genus (96 % of 16S rRNA gene sequence similarity with *Alkaliphilus halophilus*) and its growth was probably favored due to the high pH ($\geq$ 8.03) and ionic strength ($\geq$ 0.45) of the media. Regarding OTU 10, it belongs to the *Syntrophomonas* genus (98 % of 16S rRNA gene sequence similarity with *Syntrophomonas sapovorans*; known syntrophic oxidizing fatty acids of 4-18 carbons when growing with a hydrogen utilizing partner (Roy et al., 1986)). The favored growth of these microorganisms in the presence of GAC further suggests that this material enhanced syntrophic interactions. This can potentially explain the improvement of the HAc and HPr degradation kinetics in the reactors containing GAC particles.

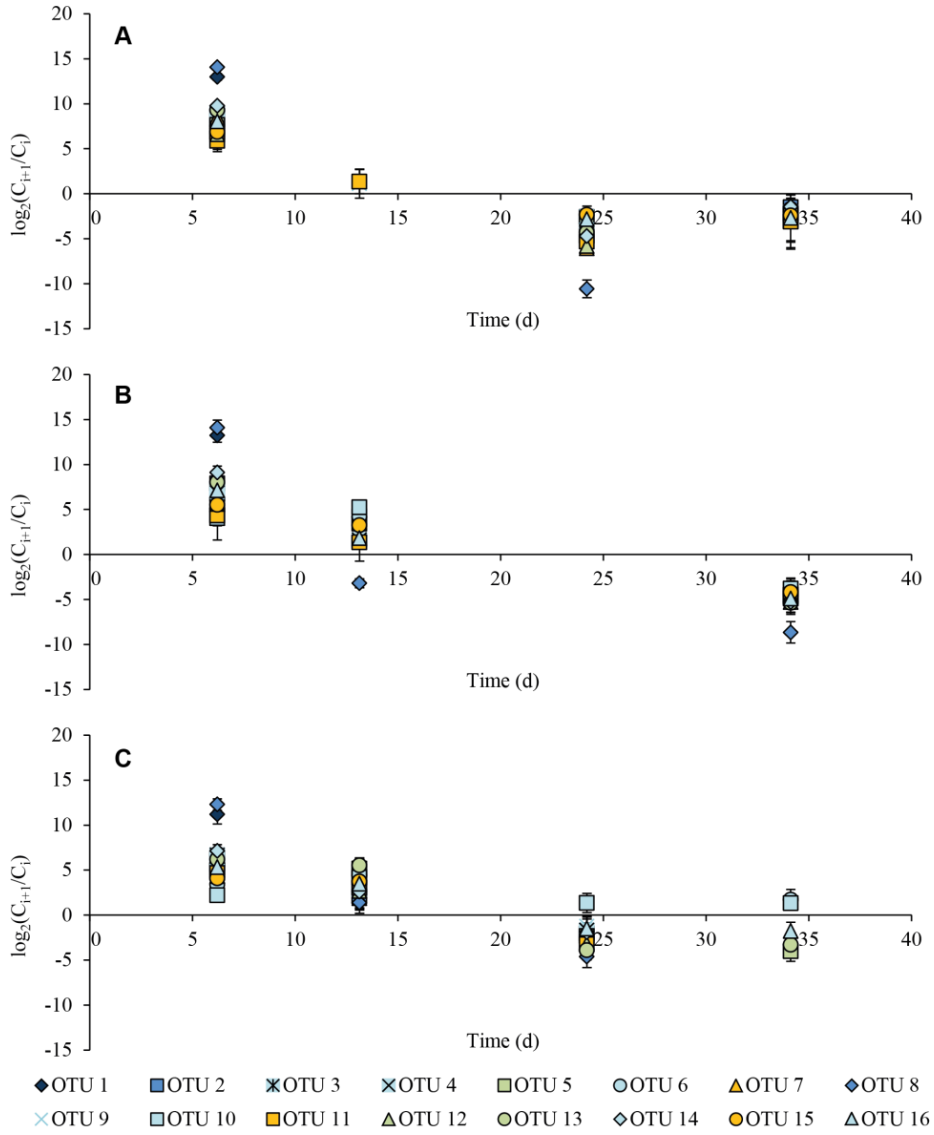

OTU	Class	Order	Family	Genus
1	Bacilli	Lactobacillales	Unclassified	Unclassified
2	Bacteroidia	Bacteroidales	Porphyromonadaceae	Proteiniphilum
3	Clostridia	Clostridiales	Unclassified	Unclassified
4	Clostridia	Clostridiales	Clostridiaceae_1	Clostridium_sensu_stricto_1
5	Spirochaetes	Unclassified	Unclassified	Unclassified
6	Clostridia	Clostridiales	Clostridiaceae_2	Alkaliphilus
7	Clostridia	Thermoanaerobacterales	Thermoanaerobacteraceae	Gelria
8	Bacteroidia	Bacteroidales	Bacteroidaceae	Bacteroides
9	Clostridia	Clostridiales	Syntrophomonadaceae	Unclassified
10	Clostridia	Clostridiales	Syntrophomonadaceae	Syntrophomonas
11	Clostridia	Thermoanaerobacterales	Thermoanaerobacteraceae	Gelria
12	OPB54	Unclassified	Unclassified	Unclassified
13	OPB54	Unclassified	Unclassified	Unclassified
14	Clostridia	Clostridiales	Family_XI	Unclassified
15	Clostridia	Thermoanaerobacterales	Thermoanaerobacteraceae	Syntrophaceticus
16	Clostridia	Clostridiales	Family_XI	Tissierella

Figure 5.5. Growth rates of bacteria in the (A) Control reactors, (B) TEs reactors and (C) GAC reactors during the first batch. The colors represent the orders shown in Figure 5.4. OTU stands for operational taxonomic unit

It is interesting to mention that, contrary to what was expected, no known electro-active bacteria (*i.e. Geobacter* sp.) were detected in the reactors at significant concentrations. This implies that (i) either DIET did not occur significantly in the reactors or (ii) DIET was performed by microorganisms not yet known to be capable of performing it. It must be commented that the harsh conditions during FW AD (*i.e.* high TAN/FAN concentrations, high pH, high ionic strength and high VFA peaks) might have also affected the development of commonly known electro-active microorganisms. Further studies must be carried out to identify potential extremophile electro-active bacteria, able to survive in similar conditions to the ones reported in this study.

Pictures of the GAC particles allowed verifying qualitatively that both bacteria and archaea grew attached to the particles, forming a biofilm onto their surfaces (Figure C.3).

5.2.3.3 Possible mechanisms responsible for the AD improvement when adding GAC

The positive effect of TEs addition on AD has a known explanation: they favor microbial metabolism via synthesis of enzymes required for VFA degradation (Banks et al., 2012). Focusing on the improved HPr degradation, this is likely to be related to the improved synthesis of formate dehydrogenase, which is responsible for formate cleavage (Banks et al., 2012). As this enzyme improves formate degradation, it leads to a thermodynamically favorable oxidation of HAc and HPr (Capson-Tojo et al., 2017b).

However, when trying to find an explanation for the positive effects of the addition of GAC on the VFA degradation, several options are feasible. The first possibility is that GAC allowed the formation of biofilms onto its surface, favoring the syntrophic interactions required for HAc and HPr degradation (Fagbohungbe et al., 2017). By decreasing the distance between the microorganisms performing MIET (using hydrogen and formate as shuttles), the reaction kinetics are accelerated and the concentrations of electron shuttles and other intermediate fermentation products (such as HAc in the case of SPO) in the media are lowered. The lower concentrations of these chemicals species would also improve the thermodynamics of SAO and SPO, making these reactions favorable. As aforementioned, another possible positive effect of GAC is the fact that it allows DIET to occur. As explained in Cruz Viggi et al. (2014), DIET improves the electron transport rates when compared to MIET. In addition, as hydrogen and formate are no longer used as electron shuttles, their concentrations is much lower than during MIET, thus favoring the thermodynamics of SAO and SPO. Some studies using defined co-cultures have given direct evidence of DIET occurring in methanogenic communities with ethanol as substrate (Rotaru et al., 2014a,

2014b) and recent research has provided also direct evidence of DIET occurring in natural methanogenic environments (Holmes et al., 2017). However, as it is deeply discussed in Barua and Dhar (2017), due to the complex nature of the process, most of the evidence of DIET occurring in AD digesters is indirect. Using GAC to stablish electrical connections between microorganisms, different authors have reported an enhanced methanogenesis, *a priori* due to the occurrence of DIET. With ethanol as substrate, F. Liu et al. (2012) were able to reduce the lag phase in methane production. Lee et al. (2016) doubled the methane production rates from acetic acid by GAC addition, enriching the reactors with *Geobacter* sp. (known to perform DIET). Dealing with degradation of HPr, a recent study has also show that GAC addition in ethanol-stimulated batch reactors improved the syntrophic degradation of HPr and HBu, detecting and enrichment of *Geobacter* sp. in the ethanol-doped reactors (Zhao et al., 2016b). Regarding complex substrates, GAC has also provided benefits in poultry blood AD, improving significantly the methane production kinetics in batch reactors (Cuetos et al., 2016). Enhanced AD kinetics have also been observed by adding GAC in a digester treating waste activated sludge, which again led to enrichments in hydrogen-utilizing microorganisms and *Geobacter* sp. (although in low abundances only up to 0.86 %). When considering the degradation of complex organic waste, Dang et al. (2017, 2016) also observed a positive effect in batch AD of dog food waste when adding GAC, with increased methane production rates and less significant VFA accumulation at higher OLRs (up to 18 kg $COD \cdot m^{-3} \cdot d^{-1}$).

Considering the aforementioned information, Figure 5.6 shows all the different possible mechanisms by which GAC addition may have favored VFA degradation. Obviously, the processes described are not exclusive and all of them (or different combinations) may have occurred simultaneously.

Starting with the first possibility (syntrophic acetate and propionate oxidations as major pathways), this alternative presents a process in which DIET did not occur significantly but the syntrophic interactions were improved by biofilm formation. In the second option (acetate oxidation through DIET and syntrophic propionate oxidation), the HAc is mainly degraded by electroactive bacteria and the produced electrons are uptaked by methanogenic archaea (Lee et al., 2016). As in the first option, the HPr is mainly degraded by SPO, a pathway which is favored thermodynamically due to the DIET-mediated HAc degradation, which lowers the concentrations of hydrogen, formate or HAc in the medium. In the third possibility (syntrophic acetate oxidation and propionate degradation through DIET), HAc is degraded by SAO and HPr is degraded by DIET, performed by an electroactive microorganism able to

completely oxidize this acid or to ferment it to HAc (further oxidized by SAO) (Yamada et al., 2015). Finally, the last option (4) represents the case of DIET-mediated oxidation of both HAc and HPr.

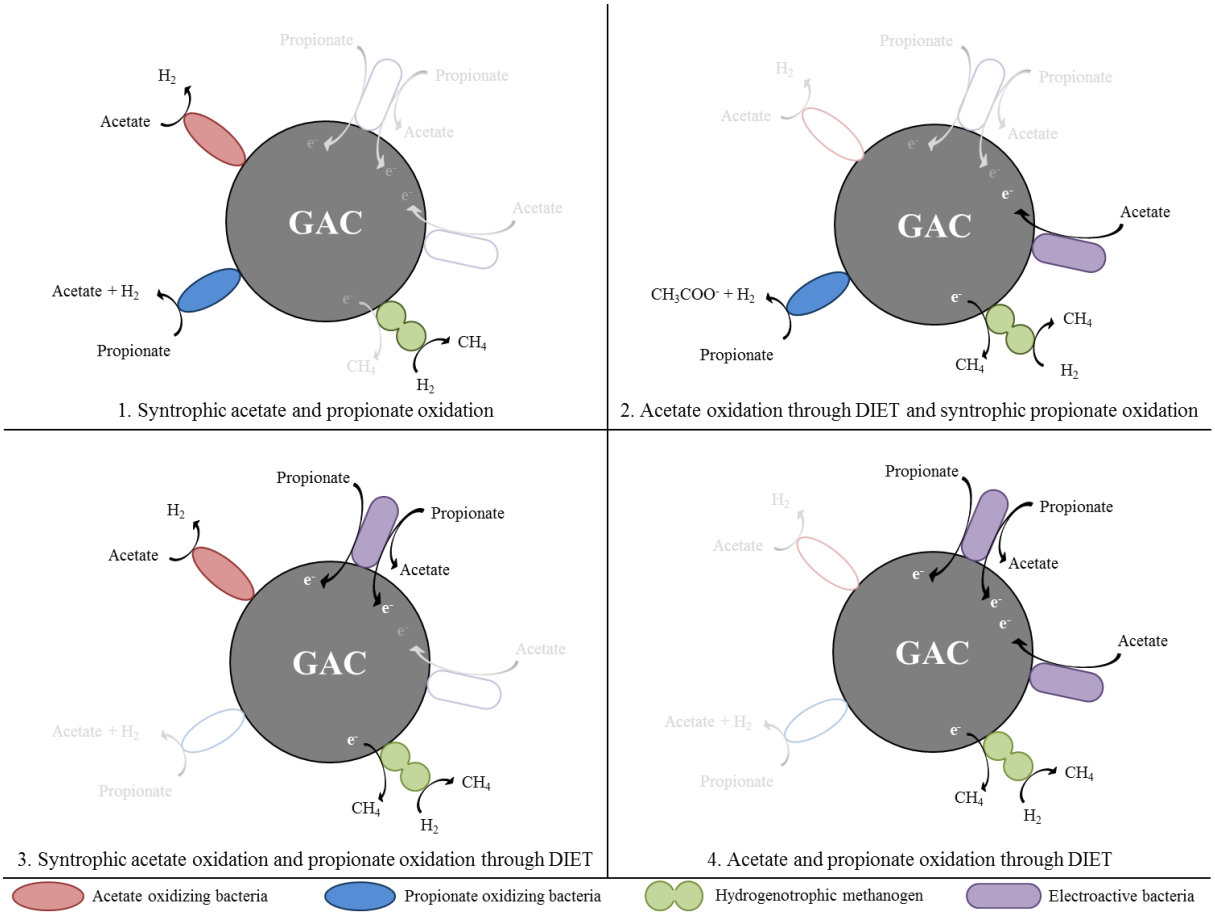

Figure 5.6. Possible mechanisms of VFA degradation favored by the addition of GAC: (1) syntrophic acetate and propionate oxidations, (2) acetate oxidation through DIET and syntrophic propionate oxidation, (3) syntrophic acetate oxidation and propionate degradation through DIET and (4) acetate and propionate oxidations through DIET

Although the analyses of the microbial communities suggest that the first option (syntrophic acetate and propionate oxidations as major pathways) was the main process taking place when GAC was added, the possibility of DIET being carried out by unidentified microorganisms cannot be discarded. In addition, DIET might have been performed even if known microorganisms were a minority (Yang et al., 2017). Further research must be performed to identify the microorganisms being an integral part of the biofilm (*i.e.* using bigger conductive particles that allow recovery of the attached biofilm), aiming at identifying potential electro-active partners thriving at the harsh conditions existing during FW AD (*i.e.* high TAN/FAN concentrations, pH and ionic strengths).

5.2.4 *Conclusions*

During the first batch, GAC addition favored biomass adaptation and reduced the methane production lag phase. After biomass acclimation, the second batch proved that simultaneous supplementation of both GAC and TEs had a synergy effect, improving the degradation kinetics of HPr and the methane productivities. Syntrophic VFA oxidation and hydrogenotrophic methanogenesis were found to be the main methane-producing pathways. GAC addition favored the growth of archaea and bacteria, enhancing syntrophic interactions and allowing higher biomass concentrations. GAC and TEs addition may be a feasible solution to stabilize FW AD by favoring VFA consumption.

5.2.5 *Main outcomes and coming experiments*

The most relevant outcome from the previous experiment is the observed synergy when supplementing both GAC and TEs. For the first time during the PhD, efficient consecutive batch FW AD had been achieved with short batch durations (optimum value of 15 days in the reactors supplemented with GAC and TEs), obtaining high methane yields (443-456 ml $CH_4 \cdot g\ VS^{-1}$) at relatively high initial substrate concentrations (~ 30 g VS $FW \cdot l^{-1}$). The results presented above had huge implications for the project and could also have a strong importance for optimizing and stabilizing FW AD.

However, although the results were promising, the equivalent highest substrate loads reached (~ 2 g $VS \cdot l^{-1} \cdot d^{-1}$) and thus the volumetric production rates achieved (0.9 $l \cdot l^{-1} \cdot d^{-1}$) were far from being close to the values desired in an industrial scale installation (over 4 g $VS \cdot l^{-1} \cdot d^{-1}$, see for instance Figure 1.4). Therefore, an experiment was designed to optimize these variables, aiming at developing a process feasible at large scale. Also aiming at developing a feasible industrial process, biochar and $FeCl_3$ were used as AD enhancer in the coming section.

5.3 Feasibility of supplementation of AD enhancers in an industrial scale application

5.3.1 *Objectives and experimental design*

Two main issues must be addressed when considering the addition of material/substances to enhance the AD performance of an industrial installation: (i) they must allow a high substrate load and (ii) their prices must be low. To address the first point, the objective of this section was to evaluate the effect of increasing substrate loads on the AD performance of batch reactors, aiming at determining the maximum feasible load to avoid acidification and to

maximize the biogas productivities, a critical value to evaluate a potential industrial application. The AD performance of consecutive batch reactors doped with GAC and TEs at increasing substrate loads (30-86 g VS $FW \cdot l^{-1}$) was evaluated. With this purpose, the initial substrate load was doubled every two feeding cycles. This approach was tested on the most performant reactor from the previous experiment: AD supplemented with GAC and TEs (GAC + TEs). Particular attention was paid to the kinetics of methane production and VFA accumulation-consumption. In addition, this experiment also allowed having an idea of the maximum feasible load to avoid acidification.

To address the second point described above (low prices of the AD enhancers), Section 5.3 also introduces a preliminary experiment to evaluate the possibility of using cheaper AD enhancers, obtaining an alternative AD process that would be industrially-feasible from an economic point of view: biochar and $FeCl_3$ as substitutes for GAC and pure TEs. To give an idea of the prices, industrial GAC costs around 12 €·kg^{-1} and the industrial biochar less than 1 €·kg^{-1}. The composition of the industrial $FeCl_3$ solution, with a price of 0.2-0.3 €·kg^{-1}, is shown in Table 5.9. To perform this experiment, a control reactor carried out in the first load of the previous experiment (*i.e.* simply fed with FW) was supplemented in biochar and industrial $FeCl_3$. Table 5.5 shows a summary of the research objectives and the feeding regime applied.

Table 5.5. Experimental design of the consecutive batch experiment

Reactor	Objective	Load 1 (g VS·l^{-1})	Load 2 (g VS·l^{-1})	Load 3 (g VS·l^{-1})	Load 4 (g VS·l^{-1})	Load 5 (g VS·l^{-1})
GAC + TEs	Determine maximum substrate loads and biogas productivities	30	30	54	54	86
Biochar + $FeCl_3$	Evaluate possible substitution of GAC and TEs by Biochar and industrial $FeCl_3$	30[1]	30	54	54	n.p.[2]

1. First feeding without biochar and $FeCl_3$
2. n.p. stands for "not performed"

The first two loads in GAC + TEs correspond to the results presented in the previous section (S/X ratio of 1 g VS·g VS^{-1}; 30 g VS $FW \cdot l^{-1}$). The third, fourth and fifth loads correspond to increasing substrates loads, calculated by doubling the initial mass of FW added (loads 3 and 4) and by tripling it (load 5). The first load, which served for inoculum acclimation, was not carried out in the Biochar + $FeCl_3$, which was directly inoculated with a previously adapted sludge. The reactors were incubated at 37 °C and triplicates of all the conditions were carried out. The concentrations of GAC and TEs were equal to the ones used

previously (10 g·l^{-1} and 100 mg·l^{-1} Fe). Equivalent concentrations of biochar (10 g·l^{-1}) and industrial $FeCl_3$ (100 mg·l^{-1} Fe) were applied in the complementary reactors. The AMPTSII system was used to carry out the experiments.

5.3.2 *Kinetics of anaerobic digestion at increasing FW loads*

5.3.2.1 Reactors supplemented with GAC and TEs

Starting with the reactors in which GAC and TEs were added, the methane yields and production rates, the concentrations of the main acids and the pH are presented in Figure 5.7.

As it can be observed, the first load at 30 g VS·l^{-1} of FW served for inoculum acclimation and, as shown in the previous section, the performance was greatly improved in the second load at the same FW concentration, with much higher methane production rates (from up to 407 ml·d^{-1} in the first feeding to up to 704 ml·d^{-1} in the second one) and faster consumption of VFAs. When increasing the load to 54 g VS·l^{-1} of FW, the performance was satisfactory, obtaining high methane yields (440-450 ml·g VS^{-1}) and greatly improving the methane production rates (up to 1146 ml·d^{-1}). This increase was related directly to the higher substrate loads. However, this higher load also led to higher transitory concentrations of VFAs at the beginning of the digestion process, with concentrations of HAc up to 13.6 g·l^{-1}. The most important consequence of this more intense VFA accumulation was the significant increase of the time required to consume the HPr produced, which increased form 15 days in the second feed at 30 g VS·l^{-1} to 25-30 days when feeding at 54 g VS·l^{-1}. In addition, this higher substrate load affected significantly the initial accumulation of valeric acid (HVal; up to 0.49 g·l^{-1} at 30 g VS FW·l^{-1} and up to 1.36 g·l^{-1} at 54 g VS FW·l^{-1}), which was degraded slower than HAc and HBu. This can be appreciated in Figure 5.7B and Figure 5.7E, which show that a second peak in the methane production rate was observed due to the consumption of HVal. This suggests that HVal may also be a problematic VFA at high substrate loads. It is interesting to mention that no significant differences were observed between the two consecutive loads at 54 g VS ·l^{-1}, suggesting that the inoculum was already adapted and that further cycles at the same load would not improve the AD performance.

As shown in Figure 5.7, further increasing the FW load to 86 g VS FW·l^{-1} resulted in an initial accumulation of VFAs (up to 24.7 g·l^{-1} of acetic acid) which overwhelmed the methanogens and also overpowered the buffering capacity in the reactors. At the high TAN concentrations present in the reaction media (of around 10 g·l^{-1}), very high concentrations of total VFAs (up to 60 g COD·l^{-1}) were needed to acidify the reactors. After two weeks of operation and without any sign of reactor recovery (negligible methane production and pH of

5.9), the system was stopped and the applied load was considered to be an upper limit for the GAC + TEs reactors.

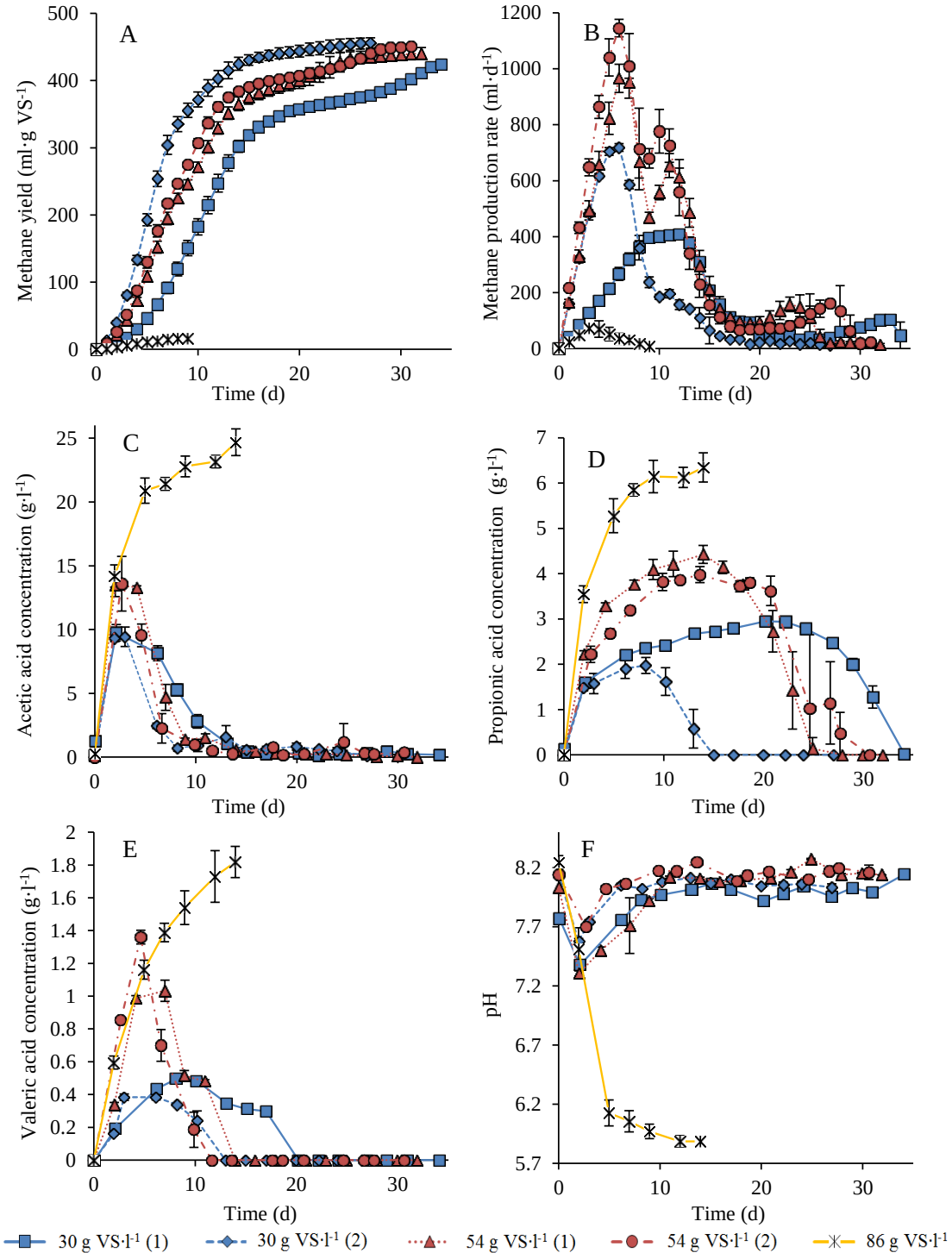

Figure 5.7. Evolution of (A) the methane yields, (B) methane production rates, concentrations of (C) acetic acid, (D) propionic acid and (E) valeric acid and (F) pH in the reactors supplemented with GAC and TEs

To allow a simpler comparison of the obtained results, the obtained methane yields and volumetric productivities in the successful experiments are presented in Table 5.6.

Table 5.6. Final methane yields, required times for total consumption of propionic acid, volumetric productions and volumetric production rates in the reactors supplemented with GAC and TEs

Parameter\Load	**30 g VS·l^{-1} (1)**	**30 g VS·l^{-1} (2)**	**54 g VS·l^{-1} (1)**	**54 g VS·l^{-1} (2)**
Methane yield (ml·g VS^{-1})	424 ± 6	456 ± 8	440 ± 9	451 ± 2
Time for consumption of propionic acid (d)	34	15	25	30
Volumetric methane production (l·l^{-1})	12.7 ± 0.20	14.0 ± 0.25	23.3 ± 0.47	23.9 ± 0.12
Volumetric production rate (l·l^{-1}·d^{-1}) [1]	0.37 ± 0.01	0.94 ± 0.02	0.93 ± 0.02	0.80 ± 0.00

1. This value corresponds to the volumetric productivity divided by the batch duration (*i.e.* time required for consumption of propionic acid)

The first point to underline is that, as the methane yields did not vary significantly between the experiments, the volumetric productions were greatly improved when increasing the substrate load (from 12.7-14.0 to 23.3-23.9 l·l^{-1}). However, as it has been mentioned in previous chapters, if accumulation of HPr is to be avoided during sequential FW AD, the digestion time (*i.e.* batch duration) must be long enough to allow the total consumption of HPr. Thus, even if the volumetric productions were much higher at higher loads, as the batch durations were also larger (from 15 to 25-30 days), the daily volumetric methane productivities (volumetric production rates) were not improved at higher loads (0.94 to 0.93-0.90 l·l^{-1}·d^{-1}). This implies that when considering the upscaling of the process, if a stable AD is to be achieved, not the maximum treatable substrate load but the maximum load allowing a short batch time must be pursued. This adds another variable to an already complex process but, on the other hand, it opens a new approach for optimizing consecutive batch AD as technology for solid waste treatment.

5.3.2.2 Reactors supplemented with biochar and $FeCl_3$

To evaluate if supplementation of biochar and $FeCl_3$ would also stabilize the AD process at similar FW concentrations, the experiments at 30 and 54 g VS FW·l^{-1} were repeated but using biochar and industrial $FeCl_3$ as AD enhancers. The corresponding results are presented in Figure 5.8 and Table 5.7.

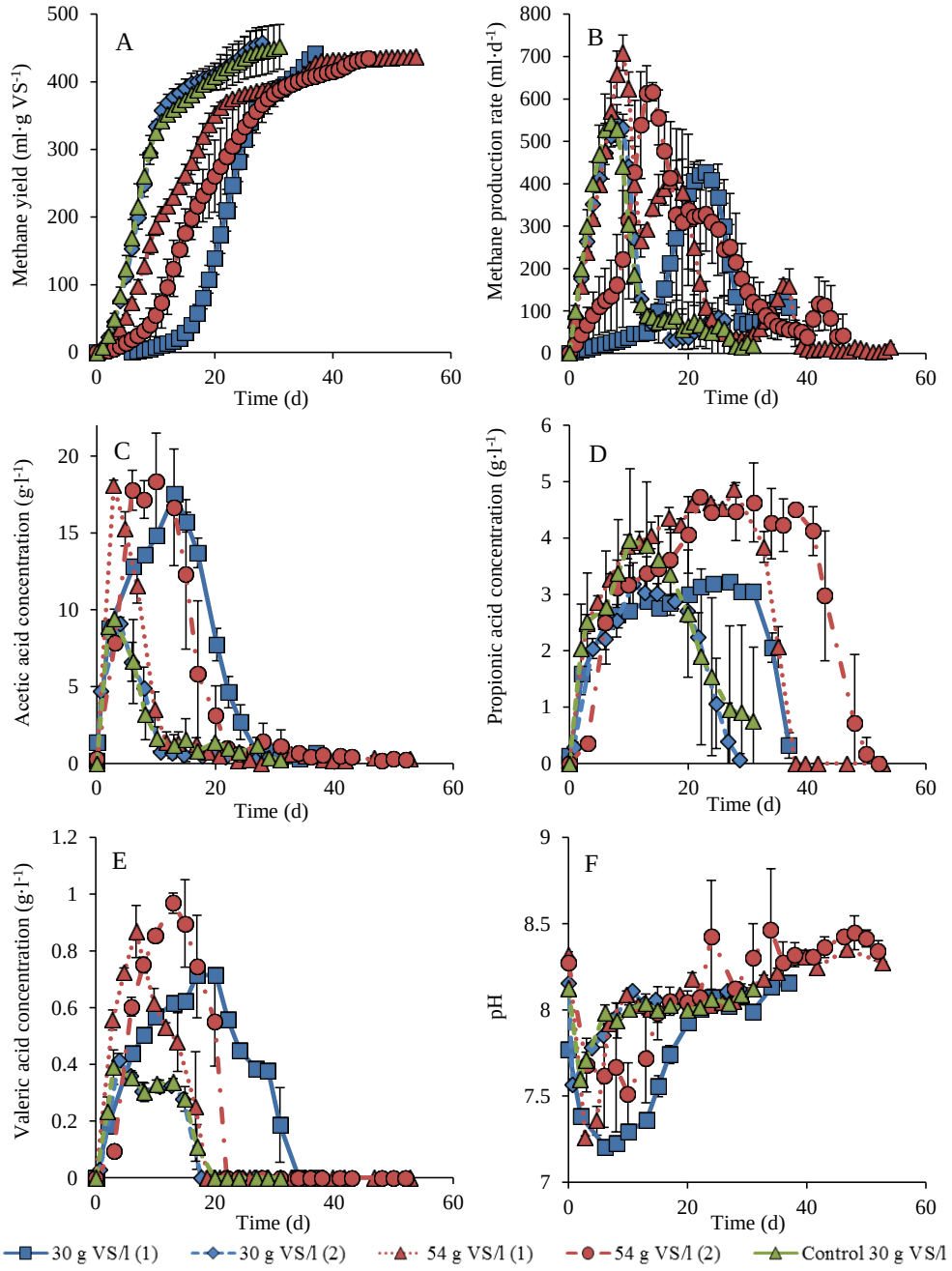

Figure 5.8. Evolution of (A) the methane yields, (B) methane production rates, concentrations of (C) acetic acid, (D) propionic acid and (E) valeric acid and (F) pH in the reactors supplemented with biochar and $FeCl_3$ and the Control reactor from the previous section (second load)

When compared with the Control reactor of the previous section, addition of biochar and $FeCl_3$ improved the AD kinetics. While 29 days were needed for a complete HPr degradation in the first load in the biochar + $FeCl_3$ reactor, more than 31 days were needed in the Control (see Table 5.3). As previously, increasing the load to 54 g $VS \cdot l^{-1}$ of FW led to performant AD processes, keeping high methane yields (437-440 ml·g VS^{-1}) and enhancing the methane production rates (up to 709 $ml \cdot d^{-1}$). However, even higher transitory concentrations of VFAs

were observed at the beginning of AD, with HAc concentrations up to 18.3 $g \cdot l^{-1}$ and times for HPr consumption up to 51 days in the last feeding. Also the initial accumulation of HVal (up to 0.41 $g \cdot l^{-1}$ at 30 g VS $FW \cdot l^{-1}$ and up to 0.97 $g \cdot l^{-1}$ at 54 g VS $FW \cdot l^{-1}$) was more significant at higher loads, leading again to a second peak in the methane production rate (Figure 5.8B and Figure 5.8E). Interestingly, in this case significant differences were observed between the two consecutive loads at 54 VS $FW \cdot l^{-1}$. A lag phase in the methane production (and a corresponding higher initial peak of VFAs) appeared in the second feeding. This led to a longer batch time, which increased from 38 to 51 days for a total degradation of HPr. This suggests, not only that 54 g VS $FW \cdot l^{-1}$ may be a too high substrate load, but also that the added amounts of biochar and $FeCl_3$ were not sufficient to improve the AD performance at this FW concentration. Further experiments aiming to optimize the dosage of these AD enhancers must be performed to draw clear conclusions. It must be mentioned that, although the AD performance was clearly improved from load 1 to load 2 (30 g $VS \cdot l^{-1}$), as in the first load no biochar and no $FeCl_3$ were added into the reactors, this improvement cannot be attributed only to these AD enhancers. It is clear that the acclimation of the initial inoculum also played a major role.

Table 5.7. Final methane yields, required times for total consumption of propionic acid, volumetric productions and volumetric production rates in the reactors supplemented with biochar and $FeCl_3$

Parameter\Load	**30 g $VS \cdot l^{-1}$ (1)**	**30 g $VS \cdot l^{-1}$ (2)**	**54 g $VS \cdot l^{-1}$ (1)**	**54 g $VS \cdot l^{-1}$ (2)**
Methane yield (ml $\cdot g\ VS^{-1}$)	441 ± 5	458 ± 19	437 ± 3	440 ± 1
Time for consumption of propionic acid (d)	37	29	38	51 ± 1
Volumetric production ($l \cdot l^{-1}$)	13.4 ± 0.15	14.0 ± 0.52	23.7 ± 0.51	22.7 ± 0.16
Volumetric production rate ($l \cdot l^{-1} \cdot d^{-1}$) [1]	0.36 ± 0.01	0.48 ± 0.02	0.62 ± 0.01	0.45 ± 0.01

1. This value corresponds to the volumetric production divided by the batch duration (*i.e.* time required for consumption of propionic acid)

The results presented in Table 5.7 show that increasing the FW load improved the volumetric methane productions. Nevertheless, as the batch duration was much larger (from 29 to up to 51 days), the volumetric production rate was not improved at higher loads. In fact, during the second feeding at 54 g VS $FW \cdot l^{-1}$, the volumetric production rate was not significantly different to the one obtained at 30 g VS $FW \cdot l^{-1}$ (0.45 and 0.48 $l \cdot l^{-1} \cdot d^{-1}$, respectively).

When comparing the AD performances obtained using GAC and TEs or biochar and $FeCl_3$ for AD stabilization, it is clear that the first option showed much better results, with

volumetric production rates up to 0.93 $l \cdot l^{-1} \cdot d^{-1}$ and minimum AD times of 15 days. However, as addition of biochar and $FeCl_3$ also improved the AD process when compared to the control reactor this alternative must still be considered and further research must be carried out. Optimal dosages of biochar and industrial $FeCl_3$ must be determined, aiming at obtaining a stabilization option for FW AD that represents an economically feasible alternative from an industrial point of view.

5.3.3 *Conclusions*

Higher substrate loads improved the volumetric methane production but also increased the batch duration, which led to equivalent volumetric methane production rates (up to 0.94 $l \cdot l^{-1} \cdot d^{-1}$). A compromise allowing high concentrations of FW and low batch lengths must be found. A FW load of 86 g $VS \cdot l^{-1}$ led to reactor acidification and negligible amounts of methane produced. The addition of biochar and $FeCl_3$ improved the AD process, but was less performant than addition of GAC and TEs at similar dosed concentrations. GAC and TEs being too expensive, further experiments must be carried out to optimize the dosage of biochar and $FeCl_3$ to obtain an economically feasible option for FW AD stabilization.

5.4 Biochar and industrial $FeCl_3$ as enhancers of FW AD for methane production

5.4.1 *Outcomes from the previous experiments and current objectives*

While the application of GAC and TEs has allowed elucidating the effect of these materials/reagents on the AD performance, their industrial applicability is not feasible from an economic point of view. On the other hand, biochar and $FeCl_3$ also improved the AD kinetics, but with significantly less promising performances when compared with GAC and TEs at the concentrations applied. Therefore, further experiments were carried out to determine if higher concentrations of these substitutes could further improve the AD kinetics. This was the main objective of this last experimental section of the thesis (5.4.2).

Three different experiments were performed: (i) a batch experimental design aiming at assessing the influence of different concentrations of biochar and industrial $FeCl_3$ on the AD performance (allowing also dosage optimization), (ii) a second batch study focused on optimizing the biogas productivities in the most performant reactor from the previous experiment and (iii) a continuous pilot scale essay comparing the performance of a control CSTR fed with FW with that of a CSTR supplemented with biochar and $FeCl_3$. Although a patent is being written, the corresponding results are presented as a scientific publication.

5.4.2 *Biochar and industrial $FeCl_3$ as additives to favor the consumption of VFAs during anaerobic digestion of food waste for methane production*

Submitted to patent office. To be submitted as scientific article after patent acceptance.

Abstract

Batch reactors were used to study the effect of biochar and industrial $FeCl_3$ addition on the performance of anaerobic digestion of food waste, optimizing at the same time their concentrations. Continuous pilot reactors were run in parallel, aiming at obtaining results that could be extrapolated to industrial scale installations. The supplementation of biochar and industrial $FeCl_3$ favored the digestion kinetics in batch reactors, with optimal results at the highest biochar concentration applied (100 $g \cdot l^{-1}$). Biochar addition improved the maximum methane production rates and the average daily methane production rates, related to acetate and propionate consumption, respectively. The continuous reactors confirmed the batch results, with higher methane production rates (up to 1.75 $l \cdot l \cdot d^{-1}$) and lower concentrations of both acetate and propionate when biochar and $FeCl_3$ were added. Although more research is needed, these materials appear as a feasible option for favoring VFA consumption and stabilizing food waste anaerobic digestion.

Graphical abstract

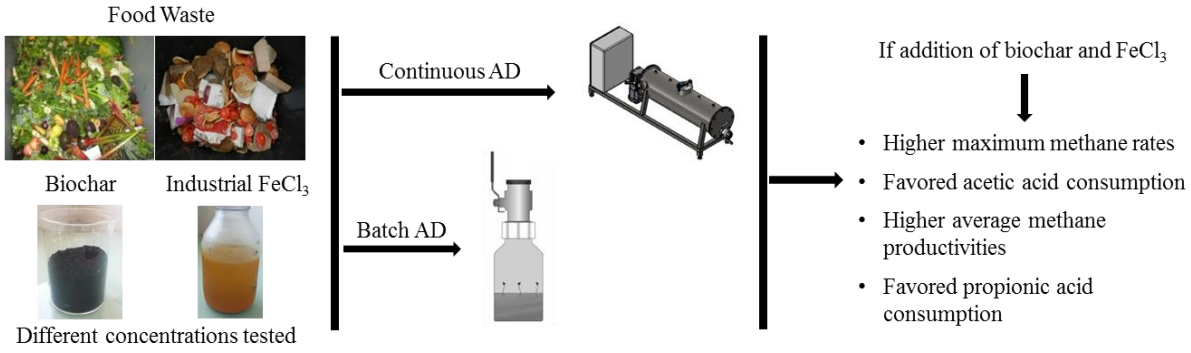

5.4.2.1 Introduction

The increasing production of food waste (FW) and novel international regulations call for the development of novel sustainable technologies for its treatment and valorization (Capson-Tojo et al., 2016). Among the existing options, anaerobic digestion (AD) is an environmental-friendly process that provides an efficient waste treatment, producing biogas and digestate. These products serve as renewable energy source in the case of biogas and for nutrient recovery if the digestate is applied on-land. Because of these advantages, AD has been proved

to be a preferable option when compared to other treatment methods, such as composting, landfilling or incineration (Bernstad and la Cour Jansen, 2012).

Nevertheless, FW AD is a complex biological process that often leads to inefficient results or reactor acidification. The first complication occurring during FW AD is related to the fast biodegradability of this substrate, which is mainly composed of easily degradable carbohydrates. Therefore, the reactors can be easily overloaded, especially in batch systems (Capson-Tojo et al., 2017d. This occurs due to an unbalance between the acidogenesis/acetogenesis and the methanogenesis steps, which results in an initial accumulation of volatile fatty acids (VFAs) and a consequent pH drop (Capson-tojo et al., 2017b; Capson-Tojo et al., 2016). The second issue to be dealt with is related to the high protein content of this substrate and its low water content (20 % total solids; TS). During AD, organic nitrogen (usually in the form of proteins) is reduced into ammonia nitrogen (total ammonia nitrogen; TAN), which, in its free form (free ammonia nitrogen; FAN) is toxic to microorganisms, especially to methanogenic archaea. Thus, different FW AD studies have reported inefficient performances due to high concentrations of FAN (Banks et al., 2008; Capson-Tojo et al., 2017b; Rajagopal et al., 2013b).

These characteristics also affect the microbial communities in the reactors and thus the predominant metabolic pathways taking place. Recent studies have proven that hydrogenotrophic and mixotrophic archaea are predominant in FW AD (De Vrieze et al., 2012; Jiang et al., 2017; P. Wang et al., 2017). This occurs because acetoclastic methanogens (predominant under unstressed conditions) are more sensitive to high TAN/FAN concentrations (TAN over 2.8-3.0 $g \cdot l^{-1}$) and VFA peaks than hydrogenotrophic archaea (De Vrieze et al., 2012). As a consequence, it has been stated that hydrogenotrophic methanogenesis (HM) is the predominant methane-producing pathway during FW AD (Banks et al., 2012; Capson-Tojo et al., 2017d Westerholm et al., 2012; Yirong et al., 2015). Figure 5.9 represents the main pathways that have been hypothesized to occur during FW AD (adapted from Capson-Tojo et al. (2017a)).

During HM, syntrophic interactions between the bacteria producing hydrogen via VFA oxidation and the archaea consuming this hydrogen to produce methane are particularly important. This is so because if hydrogen builds-up in the reactors, the oxidation of VFAs becomes thermodynamically unfavorable and acids start to get accumulated, eventually causing AD acidification. The degradation of propionic acid (HPr) becomes rapidly unfavorable when the concentrations of acetic acid (HAc) and molecular hydrogen (or formic acid) start to increase in the reactors. Therefore, HPr has been found to be a particularly

problematic compound during FW AD, leading to inefficient AD performances and even process failure (Banks et al., 2011, 2008, Capson-Tojo et al., 2017a, 2017b; Wanqin Zhang et al., 2015).

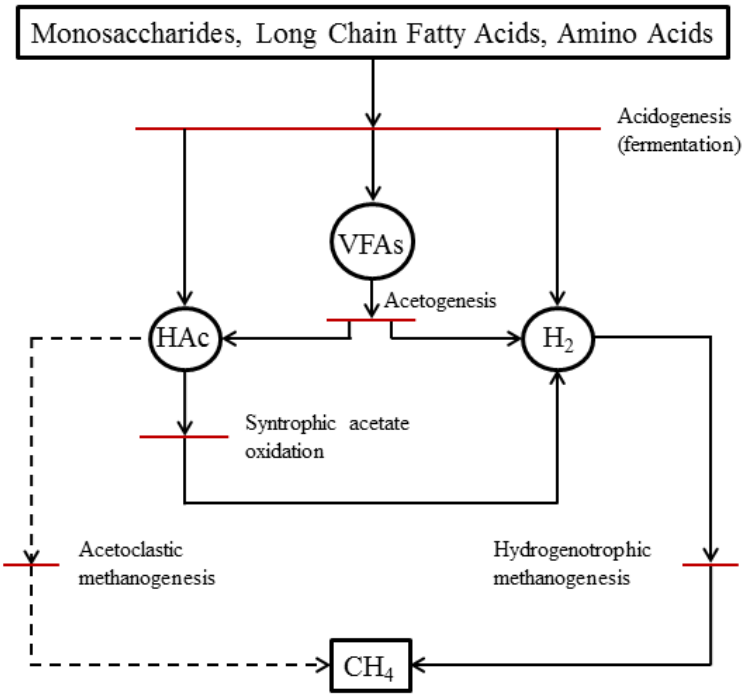

Figure 5.9. Different pathways involved in methane production during AD. The dashed lines represent the pathway inhibited at the high TAN/FAN concentrations associated with FW AD. VFAs stands for volatile fatty acids and HAc for acetic acid (adapted from Capson-Tojo et al. (2017a))

The main alternative that has been applied to favor consumption of VFAs in FW AD is the supplementation of trace elements (TEs) (Banks et al., 2012; Voelklein et al., 2017; Zhang and Jahng, 2012; Wanli Zhang et al., 2015b). Different TEs have been found to favor HPr consumption (and avoid its accumulation) in both mesophilic and thermophilic AD of FW. The reason behind this improvement lays on the addition of the elements required for the synthesis of critical enzymes for syntrophic HM. Banks et al. (2012) stated that the synthesis of formate dehydrogenase was particularly important for reducing formate concentrations and favor VFA oxidation. TEs addition has been successfully applied to avoid accumulation of VFAs at high organic loading rates (OLRs) (Zhang et al., 2011; Wanli Zhang et al., 2015b; Wanqin Zhang et al., 2015) and to recover acidified reactors (Qiang et al., 2013, 2012). Among them, iron, selenium, cobalt, molybdenum, nickel and tungsten have been found to be essential (Banks et al., 2012; Facchin et al., 2013; Qiang et al., 2013, 2012; Zhang and Jahng, 2012; Wanqin Zhang et al., 2015).

Another strategy to favor VFA consumption during AD that has gained attention in the last few years is the addition of conductive materials (Dang et al., 2016; Lovley, 2017). This approach is based on the capability of these materials for improving microbial interactions. They do so by allowing the formation of biofilm onto theirs surfaces and by facilitating the occurrence of direct interspecies electron transfer (DIET), a mechanism in which the transfer of electrons between species occurs through shared physical connections. DIET is an alternative to mediated interspecies electron transfer (MIET), in which hydrogen (or formate) acts as electron shuttle between bacteria and methanogenic archaea. In this context, DIET offers two main advantages when compared to MIET: (i) it is a faster and more efficient route for electron transfer than MIET (Lovley, 2017) and (ii) hydrogen is no longer formed (MIET does not take place) and thus VFA oxidation is thermodynamically independent of its concentration (Dang et al., 2016; Lee et al., 2016). Moreover, recent studies have suggested that HAc, butyric acid (HBu) and HPr can be metabolized through DIET (Cruz Viggi et al., 2014; Dang et al., 2016; Zhao et al., 2016a, 2016b). Materials such as granular activated carbon (GAC), carbon cloth or magnetite have been found to favor VFA consumption and methane production during AD (Cruz Viggi et al., 2014; Dang et al., 2017). Among them, GAC appears as a particularly performant alternative which has a high active surface and that can serve as both electron acceptor and electron donor (F. Liu et al., 2012). GAC has been found to promote the consumption of HAc and HBu during AD of dog food waste (Dang et al., 2017, 2016) and to promote the consumption of HPr during FW AD when co-supplemented with TEs (Section 5.2).

However, both TEs and GAC are expensive and their application at an industrial scale is far from being feasible. Thus, cheaper alternatives must be found. A simple substitute for the TEs solution may be industrial $FeCl_3$, often produced from metal scraps. It consists on an acid solution, highly concentrated in different metals (mainly Fe), that is commonly applied in wastewater treatment plants and anaerobic digesters for pH control worldwide. Concerning GAC, an affordable substitute may be biochar. Although its conductivity depends on the raw material used for its production and the process used (*i.e.* slow or fast pyrolysis), biochar is also a carbon-conductive material with the capacity of accepting and donating electrons (Prévoteau et al., 2016). In addition, biochar may also improve the AD process by providing buffering capacity and by sorption of inhibitors (Fagbohungbe et al., 2017). It favors nutrient retention in the digestates, facilitating nutrient uptake if the digestate is spread on land for plant cultivation (Fagbohungbe et al., 2017; D. Wang et al., 2017). Moreover, as biochar can

be produced from digestate (Monlau et al., 2015) or directly from FW (Rago et al., 2017), its addition for AD improvement clearly fits within the approach of environmental biorefinery.

Few studies have been carried out using biochar as amendment for AD. Biochar has been used for biogas purification (removal of H_2S or CO_2) (Linville et al., 2017; Shen et al., 2015; Y. Shen et al., 2016), as reactor packing for biofilm support (Cooney et al., 2016), as AD substrate (Mumme et al., 2014), for nutrient supplementation (Shen et al., 2017), as matrix for sorption of inhibitors (Fagbohungbe et al., 2016; Torri and Fabbri, 2014) or as means to increase the buffer capacity of the system (D. Wang et al., 2017). However, when dealing with low-dosage of biochar for favoring the degradation of VFAs, only three studies have been carried out so far. Luo et al. (2015) studied the addition of biochar for improving the kinetics of methane production and VFA degradation (HAc and HBu) with glucose as substrate, concluding that a positive effect existed. Zhao et al. (2016a) investigated the effect of biochar and ethanol supplementation in up-flow anaerobic sludge blanket (UASB) reactors degrading HPr and HBu. They observed that the degradation of both VFAs was improved by adding biochar, observing also that bacteria known to participate in DIET (*i.e. Geobacter* species) were attached onto the biochar surface. Finally, Sunyoto et al. (2016) assessed the influence of biochar addition in a two-phase AD reactor treating aqueous carbohydrates FW. They observed that biochar supplementation increased the hydrogen and methane production rates, enhancing VFA production in the first stage and their consumption in the second one. They attributed this improvement to a promotion of the biofilm formation.

To the knowledge of the authors, no study has been carried out so far to assess if addition of biochar can stabilize AD of complex substrates such as FW, reducing the extent of VFAs accumulation and favoring their consumption. Moreover, the stabilizing effect of jointly adding industrial $FeCl_3$ and biochar on the performance of FW AD has never been investigated. Therefore, the goal of this study was to: (i) optimize the concentrations of both biochar and industrial $FeCl_3$ using a batch experimental design to improve the kinetics of FW AD and (ii) evaluate the effect of industrial $FeCl_3$ and biochar supplementation on the AD performance of semi-continuous pilot reactors treating commercial FW.

5.4.2.2 Material and methods

5.4.2.2.1 Inoculum, substrate and AD additives

The reactors were inoculated with digestate from an industrial plant treating different organic streams at high TAN/FAN concentrations (5.04 g TAN·l^{-1}; 615 mg FAN·l^{-1}). Thus, it was assumed that the microorganisms would be adapted to high the high TAN/FAN levels

associated with FW AD. The TS content of the inoculum was 5.81 ± 0.02 %, with a proportion of volatile solids (VS) of 59.13 ± 0.08 %. The commercial FW was collected from five mayor producers from the region of the Grand Narbonne, in the south of France. A proportional mixture (wet weight) was used as substrate. The main characteristics if the FWs, as well as those of the mixture used as substrate and the inoculum are presented in Table 5.8.

Table 5.8. Characteristics of the food waste mixture and the inoculum (Capson-Tojo et al., 2017b)

Parameter	Food waste mixture	Inoculum
TS (%)	21.0	5.81
VS/TS (%)	90.3	59.1
Carbohydrates (g·kg TS^{-1})	618	n.m.[1]
Proteins (g·kg TS^{-1})	187	n.m.[1]
Lipids (g·kg TS^{-1})	121	n.m.[1]
BMPs (ml CH_4·g VS^{-1})	420	n.m.[1]
pH	5.02	8.10
TAN (g·kg TS^{-1})	0.90	5.04
TKN (g·kg TS^{-1})	30.0	93.0
C/N	16.1	3.04

1. n.m. stands for “not measured”

The characteristics of the FW mixture were in agreement with typical values presented in the literature (Capson-Tojo et al., 2016), which indicated that it can be considered as a representative sample of a general FW. It had a TS contents of 21 % (90.3 % VS), it was mainly composed of carbohydrates (618 g·kg TS^{-1}) and it had relatively low C/N ratios (16.1). A more extensive characterization and a deeper discussion of the results can be found in Capson-Tojo et al. (2017b).

The industrial $FeCl_3$ was provided by an industrial AD plant, where it is used for pH controlling purposes. The characteristics and composition of this industrial solution are shown in Table 5.9.

The biochar was natural slow-pyrolyzed wood charcoal. Before utilization, the biochar was grinded and sieved at 600 µm. Its particle size distribution is shown in Figure C.4 (supplementary material).

Table 5.9. Characteristics and composition of the industrial $FeCl_3$ solution

Parameter	Unit	Value
Density at 20 °C	($g \cdot cm^{-3}$)	1.45
$FeCl_3$	(%)	41.1
Cl total	($g \cdot l^{-1}$)	397
Fe total	($g \cdot l^{-1}$)	206
HCl	($g \cdot l^{-1}$)	2.2
Mn	($mg \cdot l^{-1}$)	780
Zn	($mg \cdot l^{-1}$)	390
Pb	($mg \cdot l^{-1}$)	220
Ni	($mg \cdot l^{-1}$)	67
Co	($mg \cdot l^{-1}$)	28
Cu	($mg \cdot l^{-1}$)	65
Cr	($mg \cdot l^{-1}$)	45
Ca	($mg \cdot l^{-1}$)	540
Na	($mg \cdot l^{-1}$)	110
Al	($mg \cdot l^{-1}$)	100
Mg	($mg \cdot l^{-1}$)	15

5.4.2.2.2 Laboratory scale experiments

5.4.2.2.2.1 Batch experimental design for dosage optimization

A multilevel factorial design was used to optimize the dosage of biochar and industrial $FeCl_3$ and to evaluate their individual effect on the methane production and the VFA production-consumption kinetics. For this purpose, digestate from continuous reactors digesting FW was used (after consumption of the remaining VFAs). This sludge had a TS content of 5.17 %, with 60.2 % corresponding to VS and had a TAN content of 7.27 $g \cdot l^{-1}$. Sixty g of FW were added as substrate in all the reactors. A substrate to inoculum (S/X) ratio of 1 g VS·g VS^{-1} was applied, leading to initial FW concentrations of approximately 27 g VS $FW \cdot l^{-1}$. The reactors were incubated at 37 °C. The working volumes ranged from 487 ml to 529 ml. Two different concentrations of the $FeCl_3$ solution (0.1 and 0.2 g $Fe \cdot l^{-1}$) and three of biochar (10, 55 and 100 $g \cdot l^{-1}$) were tested. As results, an experimental design with 12 conditions was defined (Table 5.10).

Table 5.10. Experimental design of the batch experiment. All the reactors were fed with 60 g of FW at an S/X ratio of 1 g VS·g VS^{-1} and incubated at 37 °C

Reactor	Normalized level		Real concentrations ($g \cdot l^{-1}$)	
	Biochar	$FeCl_3$	Biochar	$FeCl_3$
1	0	-1	55	0.1
2	-1	1	10	0.2
3	1	1	100	0.2
4	-1	-1	10	0.1
5	1	-1	100	0.1
6	0	1	55	0.2
7	0	-1	55	0.1
8	-1	-1	10	0.1
9	0	1	55	0.2
10	1	1	100	0.2
11	-1	1	10	0.2
12	1	-1	100	0.1

This experimental design was chosen because it allows analyzing the effects of the selected factors (biochar and $FeCl_3$ concentrations) on a chosen output through the entire experimental region covered. It allows so by predicting the responses using a quadratic model (Eq. 5.6):

$$y = a_0 + \sum_{i-1}^{k} a_i \cdot x_i + \sum_{i-1}^{k} a_{ii} \cdot x_i^2 + \sum_{i<j}^{k} a_{ij} \cdot x_i \cdot x_j \qquad \text{Equation 5.6}$$

Where y is the response to be predicted, x_i are the studied factors and a_i, a_{ii} and a_{ij} are the parameters corresponding to each factor. These parameters represent the linear effects, the quadratic effects and the interactional effects, respectively. The first coefficient a_0 is required for fitting the mathematical model. The p-values from F-tests (95 % confidence) and the coefficient of determination R^2 were used to evaluate the fitness of the model. The experiment was designed and evaluated using the software STATGRAPHICS Centurion XVI Version 16.1.03 (©StatPoint Technologies Inc.).

The reactors were incubated in an Automated Methane Potential Testing System (AMPTSII) (Bioprocess Control, Sweden). Twelve reactors from the AMPTSII system, with a total volume of 600 ml, were used. According to the manufacturer instructions, they were connected to CO_2 traps (NaOH solutions) and to gas flow meters to determine continuously the methane flow rates. The reactors were agitated during one minute every 10 minutes at 40 rpm.

The first batch feeding served for inoculum adaptation (results not presented), and the results of the second feeding were used for modelling purposes. The criterion followed to

decide when the batch had finished was the total consumption of the HPr in the reactors (26 days).

5.4.2.2.2.2 Optimization of the biogas productivities: effect of increasing substrate loads

After optimizing the concentrations of biochar and $FeCl_3$, another batch experiment was carried out. This second batch essay aimed at assessing the effect of increasing the substrate load on the AD performance of the most efficient reactors from the previous section (with fixed biochar and $FeCl_3$ concentrations). From an industrial point of view, determining the maximum feasible load and the biogas productivities is critical. In addition, this allowed comparing the performance of these AD reactors with the results presented in Section 5.3, where GAC and TEs and low concentrations of biochar and $FeCl_3$ were applied.

Two consecutive batches were performed. The first feeding corresponded to the second batch from the previous section (S/X ratio of 1 g VS·g VS^{-1}; ~ 30 g VS·l^{-1}). In the second feeding, the load was doubled (S/X ratio of 2 g VS·g VS^{-1}; ~ 60 g VS·l^{-1}). These conditions were equivalent to the ones used in Section 5.3.

5.4.2.2.3 Continuous pilot scale reactors

In parallel to the batch reactors, two different pilot scale reactors were run: a control system simply digesting FW and a doped reactor supplemented with biochar and the $FeCl_3$ solution. Both reactors were incubated at 37 °C and had a working volume of 12 l. The reactors were fed once per day, initially with an OLR of 1.4 g VS·l^{-1}·d^{-1}, corresponding to a hydraulic retention time (HRT) of 110 days. This value was increased to 2.8 g VS·l^{-1}·d^{-1} (HRT of 55 days) after 77 days of operation. An equivalent amount of digestate was withdrawn to keep the volume of the reactors constant. The $FeCl_3$ solution was diluted with water (x20 vol:vol) and dosed into the supplemented reactor to keep a constant concentration of 100 mg Fe·l^{-1} (value calculated from optimal results reported in the literature from Banks et al. (2012), Zhang and Jahng (2012) and Wanli Zhang et al. (2015b). The initial concentration of biochar in the supplemented reactor was 10 g·l^{-1}. As it will be further explained, this concentration was increased up to 50 g·l^{-1} to favor the consumption of the accumulated VFAs, according to the results obtained from the batch experimental design.

The pilot reactors consisted of jacketed cylindrical vessels made of stainless steel that had inner stirring blades to provide continuous agitation. A more detailed description of the reactors can be found elsewhere (Ganesh et al., 2013). The experiments lasted for 196 days.

5.4.2.2.4 Analytical methods

5.4.2.2.4.1 Physicochemical characterization of the FW

The TS and VS contents were measured as described in the standard methods of the American Public Health Association (APHA, 2005). The concentrations of carbohydrates and lipids were determined using the Dubois method (Dubois et al., 1956) and by a gravimetric method based on accelerated solvent extraction (APHA, 2005), respectively. The protein content was calculated using the total Kjeldahl nitrogen (TKN) contents (6.25 g protein·g N^{-1} (Jimenez et al., 2013)). The TKN and NH_4^+ concentrations were determined using an AutoKjehdahl Unit K-370, BUCHI. The contents of organic (TOC) and inorganic carbon (IC) were measured with a Shimadzu (Kyoto, Japan) TOC-V_{CSN} Total Organic Carbon Analyzer coupled to a Shimadzu ASI-V tube rack. The C/N ratio was calculated as TOC/TKN. A WTW (London, United Kingdom) pHmeter series inoLab pH720 was used for pH measurement. Finally, the biochemical methane potentials (BMPs) of the substrates were measured according to Motte et al. (2014a).

5.4.2.2.4.2 Gas quantification and analysis

The amount of methane produced was automatically measured in the AMPTSII system and the volume of biogas produced in the pilot reactors was continuously measured using Ritter MilliGascounters MGC-1 V3.0. The composition of the biogas was determined by gas chromatography as described in Cazier et al. (2015).

5.4.2.2.4.3 Analysis of metabolites and final products of the digestion

A sample of digestate from the pilot reactors was taken once per week for measurement of the concentrations of VFAs and ionic species in the reactors. Concerning the batch study, a plastic tube submerged in the reaction media served for digestate sampling when required. Before sampling, a clip was used for blocking the gas output and the equivalent volume of digestate to be removed was injected as nitrogen gas, avoiding an overestimation of the produced gas. The concentrations of VFAs and ionic species in the digestates were measured as described in Motte et al. (2013), by gas and ion chromatography, respectively. The methane yields (expressed by VS of substrate added) were corrected to take into account the digestate removed when sampling.

5.4.2.2.4.4 Data analysis

The concentration of FAN was calculated according to Chen et al. (2014) as a function of temperature, pH, and TAN concentration.

5.4.2.3 Results and discussion

5.4.2.3.1 Laboratory scale experiments

5.4.2.3.1.1 Optimization of biochar and $FeCl_3$ dosing in batch reactors

As aforementioned, the objective of this study was to evaluate the effect of different concentrations of both biochar and $FeCl_3$, aiming at optimizing their dosage. The results of the experimental design are shown in Table 5.11.

Table 5.11. Results of the experimental design

Reactor	Methane yield (ml·g VS^{-1})	Maximum methane rate (ml·g VS^{-1}·d^{-1})	Time for HPr consumption (d)	Average daily methane production rate (ml·d^{-1})[1]	Final pH
1	483	1327	18.9	363	8.15
2	505	948.1	23.0	302	8.22
3	484	1498	18.9	376	8.19
4	509	886.4	24.4	280	8.21
5	489	1436	18.9	374	8.18
6	459	1249	18.9	356	8.29
7	461	1281	20.1	329	8.29
8	501	907.0	21.5	316	8.17
9	456	1142	20.1	323	8.29
10	466	1489	18.9	361	8.27
11	496	912.8	21.5	326	8.42
12	496	1457	20.1	360	8.19

1. Calculated as final methane yield divided by the time required for HPr consumption (batch duration)

All the reactors produced methane efficiently, with yields ranging from 456 to 505 ml CH_4·g VS^{-1} and final pH values between 8.15 and 8.42. These high pH values were caused by the high TAN concentrations, up to 9.75 g·l^{-1}. As it can be observed, the main differences were related to the AD kinetics. The maximum methane production rates (consequence of the initial consumption of HAc) varied widely, from 907 to 1498 ml·g VS^{-1}·d^{-1}. The total time for consumption of HPr (most recalcitrant VFA to be degraded) ranged from 18.9 to 24.4 days, making also vary the average daily methane production rates (from 302 to 376 ml CH_4·d^{-1}), which was calculated by dividing the total volume produced of methane by the batch duration (*i.e.* time to completely degrade HPr). The values of the methane yields, the maximum methane rates and the average daily methane production rates were used as inputs for the quadratic model (Equation 5.6), obtaining the results presented in Table 5.12. The raw kinetic curves of the methane yields and production rates, the pH values and the concentrations of the different VFAs are presented in Figure C.5 and Figure C.6 (supplementary material).

Starting with the methane yields, the modeled results indicated that both linear coefficients from the biochar and the $FeCl_3$ (*i.e.* $a_{biochar}$ and a_{FeCl3}) had a significant effect on this variable (p-values linear coefficients < 0.05). However, the quadratic parameter $a_{biochar\text{-}biochar}$ was statistically different than zero with a 99 % of certainty (p-value < 0.01) and the high value of this parameter indicated that the experimental design was not properly centered for predicting the methane yield. The relatively low R^2 value (86.7 %) also suggests the lack of fit of the model. In addition, the Durbin-Wilson test (with a p-value < 0.05) could not exclude that correlations existed due to the order in which the data were used as input. All these results suggest that the model was not able to predict any direct effect of the biochar or the $FeCl_3$ on the final methane yields obtained. Considering that the biodegradable matter content of these two additives should be negligible, this is a logical outcome. In addition, the fact that the batch reactors with low concentrations of biochar lasted for a longer time than the others (see Table 5.11) might have affected the results, allowing the degradation of the most recalcitrant organic matter.

Table 5.12. Coefficients of the quadratic model for the main responses of the experimental design

Parameter/coefficient	Methane yield ($ml \cdot g\ VS^{-1}$)	Maximum methane rate ($ml \cdot g\ VS^{-1} \cdot d^{-1}$)	Average daily methane production rates ($ml \cdot d^{-1}$)[1]
a_0	465	1250	343
$a_{biochar}$	-9.54*	278.2**	37.3***
a_{FeCl3}	-9.04*	-4.71	4.02***
$a_{biochar\text{-}biochar}$	28.3**	-57.9	-12.2***
$a_{biochar\text{-}FeCl3}$	-8.03	3.25	-6.94***
R^2	86.7 %	94.2 %	100 %
p-value Durbin-Wilson	0.025	0.20	-

1. Calculated as final methane yield divided by the time required for HPr consumption (batch duration)
* p-value < 0.05
** p-value < 0.001
*** p-value < 0.0001

Nevertheless, the model was able to reproduce precisely the maximum methane production rates (R^2 of 94.2 % and p-value Durbin-Wilson 0.20) and the average daily methane production rates (R^2 of 100 %). The model responses for these two variables are presented in Figure 5.10.

The maximum methane production rate was mainly affected by the biochar concentration, with a negligible influence of the $FeCl_3$ concentration. This can be verified by the p-values of the parameters in Table 5.12, where it can be observed that the only parameter with a p-value < 0.5 was $a_{biochar}$. This indicates that addition of biochar clearly improved the degradation of the HAc that accumulated at the beginning of the AD process, when the maximum methane

production rates were registered (Figure C.5 and Figure C.6). Regarding the average daily methane production rates (estimated by dividing the total volume of methane produced by the time to completely degrade the HPr) the value of this variable also increased greatly at higher biochar concentrations. However, in this case the effect of the $FeCl_3$ was significant, with both $a_{biochar}$ and a_{FeCl3} showing p-values lower than 0.5. This variable was mainly affected by the batch duration, which was determined by the time required for HPr consumption. Thus, it can be concluded that both biochar and $FeCl_3$ addition favored the degradation of the HPr accumulated during the first days of the batch process. This can be related to favored syntrophic interactions and to the occurrence of DIET in the case of biochar and to the synthesis of enzymes for the $FeCl_3$

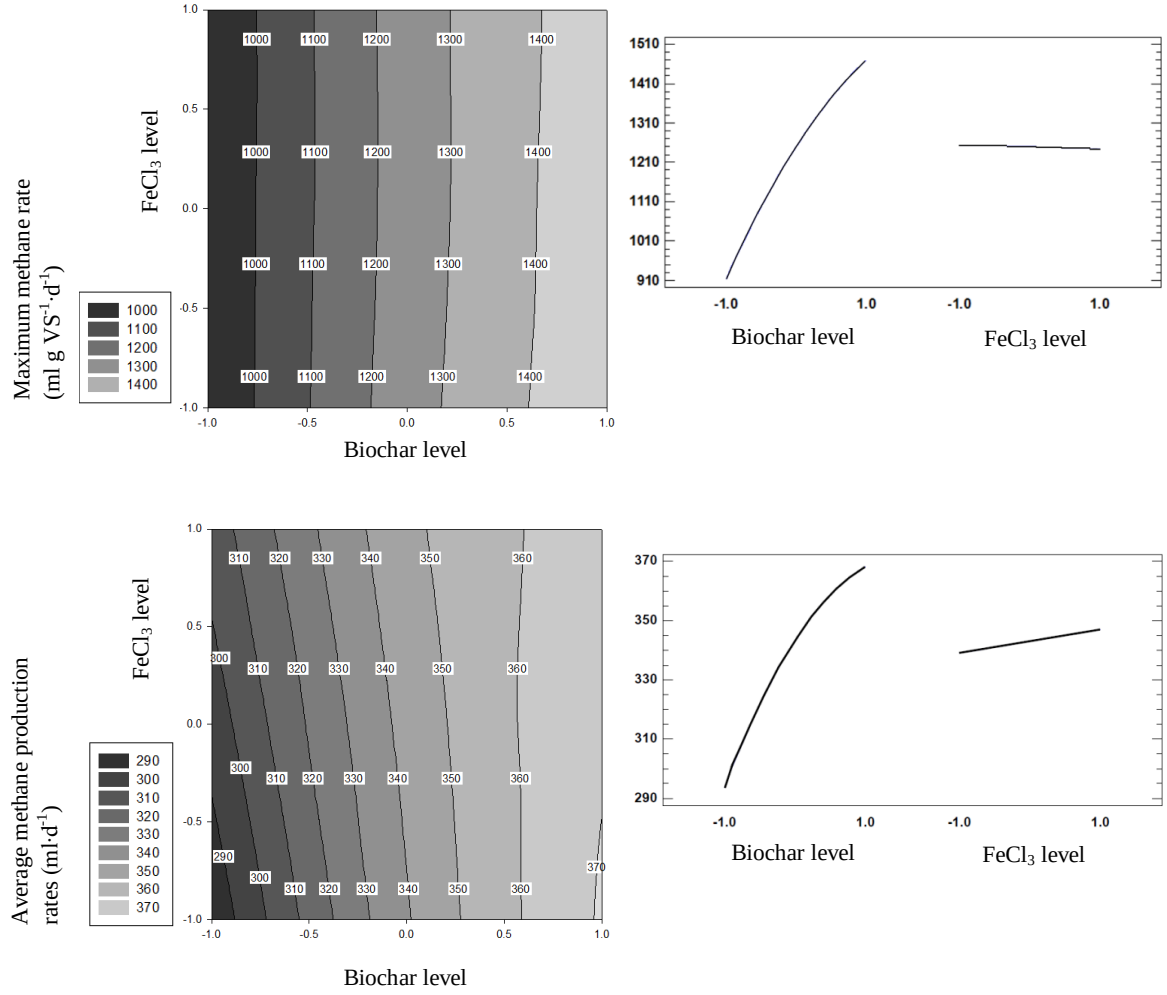

Figure 5.10. Surface responses (left) and average individual effects (right) of (A) the maximum methane rates and (B) the average daily methane production rates

Although optimal values could be extrapolated (162 $g \cdot l^{-1}$ of biochar at 0.1 g $Fe \cdot l^{-1}$ for maximizing the methane production rate and 111 $g \cdot l^{-1}$ of biochar at 0.2 g $Fe \cdot l^{-1}$ for maximizing the average methane production rates), it is clear that the experimental design

was no properly centered and therefore further experiments must be performed to precisely optimize the dosing of these reagents.

5.4.2.3.1.2 Effect of increasing substrate loads and comparison with GAC and TEs addition

As the best performances were obtained at 55 and 100 $g \cdot l^{-1}$ of biochar, these reactors were used for evaluating the influence of the substrate load (S/X ratio of 1 and 2 g VS·g VS^{-1}) on the AD kinetics. The corresponding results are shown in Table 5.13.

Table 5.13. Final methane yields, required times for total consumption of propionic acid, volumetric productions and volumetric production rates in the reactors

Parameter	S/X ratio (g VS·g VS^{-1})	B(55 $g \cdot l^{-1}$) [1] Fe(0.1 $g \cdot l^{-1}$)	B(55 $g \cdot l^{-1}$) [1] Fe(0.2 $g \cdot l^{-1}$)	B(100 $g \cdot l^{-1}$) [1] Fe(0.1 $g \cdot l^{-1}$)	B(100 $g \cdot l^{-1}$) [1] Fe(0.2 $g \cdot l^{-1}$)
Methane yield (ml·g VS^{-1})	1	472 ± 16	458 ± 2	493 ± 5	475 ± 13
	2	468 ± 18	456 ± 4	487 ± 15	496 ± 24
Time for consumption of propionic acid (d)	1	19.5 ± 0.8	19.5 ± 0.8	19.5 ± 0.8	18.9 ± 0.0
	2	24.0 ± 0.0	23.0 ± 2.8	17.7 ± 1.1	21.0 ± 0.0
Volumetric methane production ($l \cdot l^{-1}$)	1	12.9 ± 0.5	12.6 ± 0.3	13.2 ± 0.1	12.8 ± 0.3
	2	22.3 ± 0.3	21.7 ± 0.1	23.1 ± 0.0	23.0 ± 1.2
Volumetric production rate ($l \cdot l^{-1} \cdot d^{-1}$) [2]	1	0.66 ± 0.05	0.64 ± 0.04	0.68 ± 0.02	0.68 ± 0.01
	2	0.93 ± 0.01	0.95 ± 0.11	1.30 ± 0.08	1.09 ± 0.06

1. B stands for biochar and Fe for $FeCl_3$. The concentration of industrial $FeCl_3$ is expressed in g $Fe \cdot l^{-1}$
2. This value corresponds to the volumetric productivity divided by the batch duration (*i.e.* time required for consumption of propionic acid)

The final methane yields did not vary significantly when increasing the substrate load and, as expected, the time required for the total consumption of HPr was generally higher. However, this was compensated by the high volumetric production rates and, as a consequence, the volumetric production rates increased significantly after doubling the substrate loads. The best results (1.30 and 1.09 $l \cdot l^{-1} \cdot d^{-1}$) were achieved at the highest biochar concentrations (100 $g \cdot l^{-1}$), further indicating the positive effect of its addition.

Comparing these results to those obtained using GAC and TEs (Table 5.6; maximum volumetric production rate of 0.94 $l \cdot l^{-1} \cdot d^{-1}$ at an S/X ratio of 1 g VS·g VS^{-1}), it can be concluded that biochar (and $FeCl_3$) successfully acted as substitute of GAC (and TEs) once its concentration was increased, obtaining even better performances at higher substrate loads. However, it must be considered that the concentration of GAC was not optimized and different levels should be tested to avoid unbiased comparisons.

5.4.2.3.2 Performance of the continuous pilot reactors

Two continuous pilot reactors were run in parallel to the batch reactors during 196 days: a control reactor fed only with FW and a reactor supplemented with biochar and $FeCl_3$. The main operational parameters and the obtained results are presented in Figure 5.11.

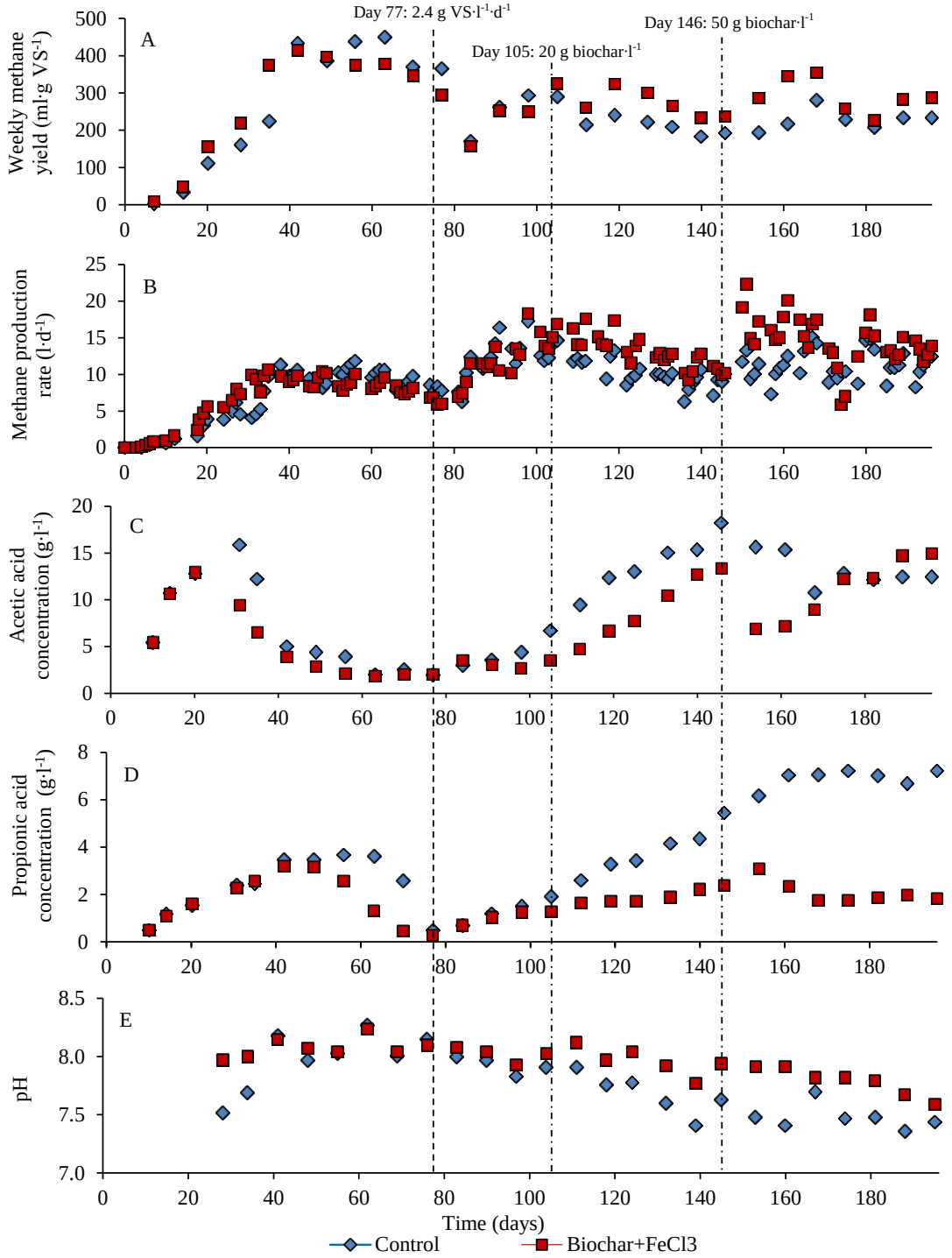

Figure 5.11. Evolution of the (A) average weekly methane yield, (B) methane production rate, (C) acetic acid concentration, (D) propionic acid concentration and (E) pH in the pilot reactors. The days in which an operational parameter (*i.e.* OLR or biochar concentration) was modified are also indicated (vertical lines)

After starting the reactors at an OLR of 1.4 g $VS \cdot l^{-1} \cdot d^{-1}$, it was required to wait around 30-40 days to achieve a stable methane production of 10 $l \cdot d^{-1}$ in both systems. Interestingly, in this start-up period differences between both reactors could already be appreciated. After 15 days, the reactor supplemented with biochar and $FeCl_3$ showed higher methane production rates than the control (Figure 5.11B), which were associated with higher initial methane yields, lower concentrations of HAc and HPr (*i.e.* peaks of HAc of 13 and 16 $g \cdot l^{-1}$, respectively) and higher pH values. This suggests that the added AD enhancers favored the consumption of the VFAs accumulated during the start-up period, even at low biochar concentrations (10 $g \cdot l^{-1}$).

Moving forwards, after 60 days both reactors achieved efficient methane productions at the first OLR applied, with yields around 400 ml $CH_4 \cdot g\ VS^{-1}$ (95 % of the BMP) and with relatively low concentrations of VFAs in the reactors (2 $g \cdot l^{-1}$ of HAc and 0.3 $g \cdot l^{-1}$ for HPr) and high pH values (around 8.1). It must be mentioned that high TAN concentrations were already present in the reactors at this point, with values around 8 $g \cdot l^{-1}$ in both reactors at day 68.

However, due to the low OLR applied, relatively low methane production rates (around 10 l $CH_4 \cdot d^{-1}$) were obtained. Therefore, the OLR was doubled in day 77 to reach 2.8 g $VS \cdot l^{-1} \cdot d^{-1}$. This caused a sudden drop in the methane yields to 160 ml $CH_4 \cdot g\ VS^{-1}$, which was associated with an increase in the HAc and HPr concentrations in the reactors. In agreement with the previous results, the levels of both VFAs were always lower in the supplemented reactor.

In an attempt to reduce the intensity of VFA accumulation in the reactor containing biochar and $FeCl_3$, the biochar concentrations were increased to 20 $g \cdot l^{-1}$ on day 105 and to 50 $g \cdot l^{-1}$ on day 146 (based on the results from the batch optimization experiment described above). While the first increase did not have significant effects, the second one (to 50 $g \cdot l^{-1}$) caused a drop in the HAc concentration from 13 to 7 $g \cdot l^{-1}$, raising the methane yields up to 350 ml $CH_4 \cdot g\ VS^{-1}$. A consequent decrease in the HPr concentration was observed (from 3.1 to 1.8 $g \cdot l^{-1}$). Sadly, on day 167 a problem occurred with the heating of the biochar-supplemented reactor. This caused a temperature drop, which led to a sudden decrease of the methane yields obtained and, again, an accumulation of HAc at the end of the operational period (days 167 to 196). Besides the aforementioned complication, Figure 5.11 clearly shows that addition of biochar and $FeCl_3$ decreased the HPr concentrations in reactors, with considerable differences between the supplemented reactor and the control. This discrepancy was particularly important after increasing the biochar concentrations, with HPr levels of 7.2 $g \cdot l^{-1}$ in the control reactor and of 1.8 $g \cdot l^{-1}$ in the reactor containing biochar and $FeCl_3$ at the end of the operational period.

Although the obtained results further suggest that addition of biochar and $FeCl_3$ can improve the AD kinetics and favor VFA consumption during FW AD, it is also clear that further continuous experiments must be carried out, allowing longer operational periods. These experiments should aim to reach an operational steady-state, with results that can be extrapolated to a potential industrial scale facility.

5.4.2.3.3 Biochar as feasible option for enhancing FW AD

The results obtained both in batch and continuous reactors are in agreement with different studies carried out to study the effect of biochar on AD. The kinetics of consumption of HAc and HBu were reported to be faster when adding biochar using glucose as substrate (Luo et al., 2015). Also the direct degradation of HPr and HBu has been improved by supplementing biochar and ethanol (Zhao et al., 2016a). Sunyoto et al. (2016) observed that biochar supplementation increased the methane production rates and enhanced the consumption of HAc and HBu in the second stage of a 2-phase AD reactor treating aqueous FW.

Using GAC as carbon-based AD enhancer, different studies have suggested that HAc, HBu and HPr can be directly metabolized through DIET, improving the kinetics of consumption of these VFAs (Cruz Viggi et al., 2014; Dang et al., 2016; Zhao et al., 2016a, 2016b). In addition, biochar has also been found to promote the growth of bacteria known to participate in DIET (*i.e. Geobacter* species) onto its surface (Zhao et al., 2016a). Therefore, it can be hypothesized that the improved VFA degradation kinetics were related to an enhancement of the syntrophic interactions between microorganisms via biofilm formation and to the occurrence of DIET. The degradation of HAc through DIET has already been proposed in the literature and, although being more limited thermodynamically (Capson-Tojo et al., 2017b), DIET may have also played an important role in the oxidation of HPr. Besides, even in direct DIET of HPr might not have occurred extensively, its degradation would be favored anyway due to lower HAc and hydrogen/formate concentrations. Further studies analyzing the microbial communities attached on the biochar should be performed to verify this hypothesis. Concerning the $FeCl_3$ addition, this additive favored the HPr degradation due to the supplementation of TEs, critical for enzyme synthesis (Banks et al., 2012).

These experiments proved that a regular biochar (natural slow-pyrolyzed wood charcoal) could also improve greatly the AD performance. It must also be considered that, other than the concentration applied, many parameters and variables which have not been considered in this study have a huge potential for optimization when considering biochar as AD enhancer. It

is clear that the textural characteristics of the biochar (*e.g.* specific surface, pore volume, pore size or pore distribution) as well as its surface chemistry (*e.g.* hydrophobicity) or its particle size play a major role on biofilm formation. In addition, also its resistivity (conductivity) might have a huge impact on its capability for favoring DIET. All these characteristics are dependent on different variables that clearly deserve further study, such as the raw material used for biochar production (Shen et al., 2017), the temperature and pressure applied during pyrolysis (*i.e.* slow or fast pyrolysis) or the pretreatment applied to the biochar before its addition into the AD reactor (*i.e.* mechanical grinding) (Fagbohungbe et al., 2017).

Although deep techno-economic analyses must be carried out before considering its application at industrial scale, the obtained results suggest that biochar and industrial $FeCl_3$ can be a feasible alternative for stabilizing AD of FW, favoring the consumption of VFAs and improving the methane productivities.

5.4.2.4 Conclusions

The addition of biochar and industrial $FeCl_3$ favored the FW AD kinetics in batch reactors, with optimal results at the highest biochar concentration applied (100 $g \cdot l^{-1}$). Biochar supplementation improved the maximum methane rates (related to HAc consumption) and both biochar and $FeCl_3$ significantly enhanced the average daily methane production rates (related to HPr consumption). Continuous reactors confirmed the batch results, with higher methane production rates (up to 1.75 $l \cdot l \cdot d^{-1}$) and lower concentrations of both HAc and HPr when biochar and $FeCl_3$ were dosed in the reactors.

5.5 General conclusions and perspectives

The results from Section 5.2, using GAC and TEs as AD enhancers prove that their combined supplementation enhanced VFA degradation in FW AD. The preliminary analyses of the microbial communities presented in this section suggested that GAC improved the VFA degradation kinetics and favored the growth of microorganisms, which lead to higher concentrations of both bacteria and archaea in the media. These materials favored interactions between syntrophic bacteria and hydrogenotrophic archaea, thus enhancing VFA degradation. Although the occurrence of DIET as mechanism of electron transport could not be confirmed, further experiments must be carried out to elucidate this hypothesis and to identify potential unknown electro-active microorganisms. Section 5.3 allowed applying the enhanced VFA consumption for increasing the FW load, which improved the volumetric methane productivities. However, it also increased the batch duration, thus obtaining similar average

methane production rates at the effective loads tested (30 and 54 g $VS \cdot l^{-1}$). Finally, the results from Section 5.4.2 suggest that biochar and industrial $FeCl_3$ can be used as substitutes for GAC and TEs, respectively, thus providing an economically-feasible option for favoring the consumption of VFAs in FW AD. By increasing the concentrations of these AD enhancers, high volumetric methane productivities and average methane production rates were achieved in the reactors, reaching acceptable values for industrial scale processes. Globally, this final experimental chapter provided a main novel outcome: carbon-based conductive materials (together with trace elements) enhance VFA consumption during FW AD.

To conclude, it can be stated that this chapter provides a potential option for achieving a stable FW AD process at large scale: biochar and industrial $FeCl_3$ dosage. However, different aspects must be addressed before this strategy can become a reality, such as the evaluation of different biochars, the identification of the desired characteristics that this material should have and the optimization of the dosage of these reactants, including a techno-economic analysis.

A general overview of the conclusions drawn from each section of this chapter is shown in Table 5.14. The perspectives to follow are also included.

Table 5.14. Summary of the conclusions of Chapter 5 and the research perspectives

Section	5.2	5.3	5.4.2
Objective	Improve digestion kinetics by adding GAC and TEs	Asses maximum methane production rate in reactors doped with GAC and TEs	Optimize dosage of biochar and $FeCl_3$ and gas productivities in batch reactors; evaluate continuous pilot scale application
Main conclusion	GAC and TEs supplementation improved VFA degradation (mainly HAc and HPr)	Higher substrate loads: improved methane productivity but longer batches; acidification at 86 g VS $FW \cdot l^{-1}$	Biochar and $FeCl_3$ addition improved FW AD kinetics and VFA degradation
Novelty	GAC and TEs addition favored consumption of accumulated VFAs and biomass growth (GAC)	Similar methane production rates at higher loads (up to 0.94 $l \cdot l^{-1} \cdot d^{-1}$)	Biochar and $FeCl_3$ favored consumption HAc and HPr in FW AD, even at high substrate loads
Agreement with literature	VFA degradation GAC (Dang et al., 2016); HPr degradation TEs (Banks et al., 2012)	More intense VFA accumulation at higher loads (Capson-Tojo et al., 2017b)	Biochar boosts AD kinetics and VFA consumption (Sunyoto et al., 2016; Zhao et al., 2016a)
Hypotheses and perspectives	• Conductive carbon-based materials favor syntrophic interactions and allow DIET • HPr degradation is favored thermodynamically due to a faster consumption of HAc and the absence of molecular hydrogen (if DIET occurs) • The microbial communities and the mechanisms involved in the process deserve further study; particularly the identification of extremophile electro-active bacteria • Different biochars must be tested, aiming to determine its optimal characteristics		

GAC stands for granular activated carbon, TEs for trace elements, VFA for volatile fatty acid, HAc for acetic acid, HPr for propionic acid, VS for volatile solid, FW for food waste, AD for anaerobic digestion and DIET for direct interspecies electron transfer

Chapter 6. Conclusions and perspectives

6.1 Outcomes of the thesis: understanding and overcoming the issues associated with food waste valorization via anaerobic processes

This thesis is the result of merging both scientific and industrial interests. Thus, its general objectives pointed in both directions. On one side, this work aimed at assessing the main parameters affecting FW AD and at identifying the mechanisms governing the process. On the other hand, it also comprised the development of an industrial scale AD process for efficient FW valorization.

With these objectives in mind, a common research strategy was applied: (i) literature review to gather existing knowledge and identify gaps in scientific knowledge (Chapter 1), (ii) batch experiments to screen main factors affecting FW dry anaerobic valorization (Chapter 3), (iii) consecutive batch experiments to evaluate potential options for stabilizing FW AD (Chapter 4) and (iv) both continuous and consecutive batch experiments to evaluate the application of carbon-based conductive materials for favoring VFA consumption and to eventually develop and industrially feasible process (Chapter 5). The results from this procedure have allowed drawing different conclusions, which are presented in Figure 6.1, together with global perspectives for future research.

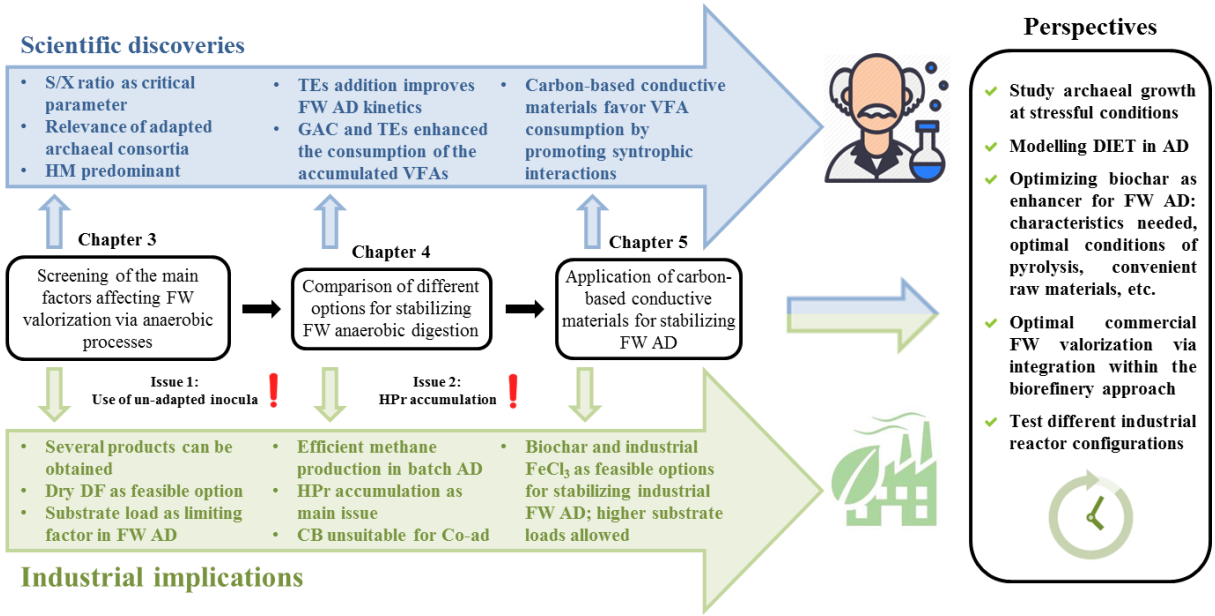

Figure 6.1. Schematic representation of the conclusions and the perspectives. S/X stands for substrate to inoculum, TEs for trace elements, FW for food waste, AD for anaerobic digestion, VFA for volatile fatty acid, DF for dark fermentation, HPr for propionic acid, CB for cardboard and DIET for direct interspecies electron transfer.

The first experiments performed (see Chapter 3) allowed elucidating the critical importance of the S/X ratio in batch conditions, which determined the main metabolic pathways occurring in the reactors due to metabolite accumulation and pH regulation. In addition, it served for identifying the first main issue found during the project: the need of using an adapted inoculum. This microbial consortium should be rich in hydrogenotrophic and mixotrophic methanogens, which are more resistant to high VFA and TAN/FAN concentrations than acetotrophic archaea. From an industrial point of view, different value-added products (other than methane) can be obtained, suggesting that, other than AD, other processes (such as DF) have a great potential for improving the economics of FW valorization. In addition, it was found that low substrate loads were needed to avoid reactor acidification. This might eventually reduce the volumetric production rates of an industrial facility, thus jeopardizing its feasibility.

Moving forwards to the experiments presented in Chapter 4, they allowed identifying the second main issue faced (using already an adapted microbial inoculum): accumulation of HPr. Although efficient methane production was achieved using consecutive batch reactors, VFAs accumulated during the process (mainly HPr), jeopardizing the AD kinetics and eventually causing reactor acidification. TEs supplementation improved the kinetics, but could not avoid VFA accumulation at the applied loads. Moreover, as co-digestion with CB showed the worst performance, this option was discarded for large scale operation.

With the issue of HPr accumulation in mind, the experiments from Chapter 5 were designed. The first conclusion drawn was that GAC and TEs clearly improved the batch kinetics, favoring VFA consumption and increasing the methane productivities. Pursuing an efficient industrial scale option, biochar and industrial $FeCl_3$ were tested as substitutes of GAC and TEs, respectively. The results proved that these reagents are a feasible option for stabilizing FW AD, also improving VFA consumption and allowing higher FW loads.

Summarizing the information aforementioned, the obtained results have proven that FW can be efficiently transformed into different value-added products, such as methane, VFAs, hydrogen and/or digestate through anaerobic processes (*i.e.* AD and DF). However, due to the low water content of FW, high concentrations of organic matter and ionic species were achieved in the reactors. Consequently, AD of FW as treatment option suffers from two main issues: (i) an adapted microbial inoculum (rich in hydrogenotrophic archaea) must be used and (ii) VFAs (mainly HPr) accumulate easily. Supplementation of TEs and carbon-based conductive materials (*i.e.* GAC and biochar) appear as solutions to stabilize FW AD, favoring VFA consumption and improving the kinetics of methane production. From an industrial

point of view, addition of biochar and industrial $FeCl_3$ appears as a feasible option for stabilizing AD of FW both in continuous or batch systems.

This thesis provides novel insights, both on the main mechanisms governing FW AD and on the implications that they present. In addition, novel solutions for the complications found are given, aiming at developing a feasible industrial AD process.

6.2 Future of food waste valorization: remaining questions and industrial perspectives

From a scientific point of view, the results presented in this thesis have opened several research possibilities, leaving many questions unanswered. Starting with the need of using an adapted microbial inoculum to achieve an efficient FW AD, this observation recalls a question that has rarely been addressed in the literature: what is the effect of harsh environmental conditions on the microbial communities in AD reactors? And, more precisely: how do these environmental conditions affect the methane-producing pathways through archaeal selection? Although few recent studies have been carried out to answer these questions (Jiang et al., 2017), further research must be carried out, analyzing the AD performances with simple substrates at different concentrations of inhibitory species (*i.e.* TAN/FAN or total ionic species), pH values and buffering capacities. Radiolabelling substrate marking and –omics studies (*i.e.* genomics, proteomics or transcriptomics) are techniques that can significantly improve the current understanding on the predominant AD pathways in stressed environments. In addition, modelling of archaeal/microbial shifts (coupled to thermodynamic modelling) is another powerful tool that should be applied in the future if a comprehensive understanding of the mechanisms governing AD of complex substrates, such as FW, is to be achieved.

The previous questions highlight a basic procedure that needs to be unified: TAN measurement and FAN estimation. It is widely known that within this equilibrium, FAN is the toxic species for microorganisms (it can pass through the cell membrane, increasing the pH and disrupting homeostasis). However, its proportions in highly concentrated media differ widely from those in ideal solutions. Other than the pH and the temperature, the FAN concentrations depend greatly on the ionic strength on the media (Rajagopal et al., 2013b). Besides the critical relevance of a precise estimation of the concentrations of FAN in FW AD reactors, this value is not always given and, when calculated, different authors use different methods, thus obtaining biased results and precluding potential comparisons (Hafner and Bisogni, 2009). Because of these complications, TAN (not FAN) inhibitory levels have been

given in the literature (De Vrieze et al., 2012). Although this information might be useful, the main species responsible for archaeal inhibition is FAN and thus, a standard method must be developed to obtain representative and comparable data that can be used to produce unbiased results.

Moving forwards, while the mechanisms of AD enhancement associated with TEs addition have been widely studied, it is still unclear why carbon-based conductive materials aid this process. As explained by Lovley (2017), DIET in AD is a novel research field that is still on its infancy. Research focusing on the basic microbial interactions occurring must be performed. As example, radiolabelling substrate marking and –omics studies could be applied to verify if HAc, HBu and HPr are actually metabolized through DIET. This could also serve to identify new electroactive bacteria. Similarly, the application of conductive materials that allow a recovery of the biofilm attached onto its surface (*i.e.* large biochar particles or carbon cloth) is a promising approach that can also provide critical insight on the interactions taking place. Finally, although new research has been carried out focusing on DIET modelling (Storck et al., 2016), this is a novel research field that clearly deserves further exploration. Coupling this approach with thermodynamic modelling and metagenomic analyses can provide essential information to understand the mechanisms taking place and their potential for improving AD performances.

In addition, another interesting aspect that remains to be studied regarding AD of highly-degradable solid substrates is the evolution of the TS contents in the reactor, which modifies the working volume, the rheology and the heterogeneity inside the reactors. Modelling approaches should also be tested, aiming at understanding and predicting the effects of the variable TS concentrations.

Finally, another research approach that should be addressed is the potential recovery of the accumulated propionic acid from the digestates (*i.e.* via electrodialysis), producing this way a high value-added chemical that can improve greatly the economical performance of an environmental biorefinery treating FW. This option changes the current paradigm regarding HPr, looking at it as a potential product instaed of a problematic compound to get rid of.

Concerning the industrial perspectives, the most promising approach drawn from this thesis is the application of biochar for AD stabilization. Other than being a feasible option to improve the biogas productivities, it might also increase the agronomic value of the digestate and favor the reduction of pathogens (Fagbohungbe et al., 2017). Furthermore, the obtained results are clearly of a preliminary nature, implying that the performances are still to be optimized. Studies must be carried out to determine the optimal characteristics of the biochar

to be used (*e.g.* specific surface, pore volume, pore size, pore distribution, hydrophobicity or conductivity). Once these optimal features are known, the variables affecting them, such as the raw material used for biochar production, the temperature and pressure applied during the pyrolysis processes (*i.e.* slow or fast pyrolysis) or the pretreatment applied to the biochar (*i.e.* mechanical grinding), must be assessed. Eventually, the biochar concentrations and the FW loads in the reactor should also be optimized, both in batch and continuous experiments. Local biochar availability must always be assessed when considering its application in industrial AD plants.

Other promising options that deserve further study are: (i) application of fixed carbon cloths/coating in the AD reactors (with a concomitant study focusing on the reactor geometry to optimize the ratio contact surface-total volume), (ii) NH_3 stripping and ammonia recovery coupled to digestate recirculation (Pedizzi et al., 2017) and (iii) co-digestion proportions allowing a sufficient substrate dilution (*i.e.* wastewater) (Pretel et al., 2016).

The FW test collection performed during the project (Appendix B) has also pointed out different practical aspects that must be addressed if FW industrial AD is to be performed efficiently. First of all, if substrate dilution and pretreatment (practices commonly applied nowadays) are to be avoided, a robust AD process must be developed, able to deal with the presence of inerts and the substrate heterogeneity due to the variable characteristics of FW according to its source. In addition, the FW storage has also appeared as an important variable to consider if the methane yields are to be maintained and environmental nuisances are to be avoided. The variability of the FW according to the production source (Appendix B) and seasonal differences is also another factor that must be considered, as it may affect greatly the characteristics of the substarte entering the reactors.

Finally, an environmental biorefinery such as the presented in Figure 1.5 is the future of biomass valorization, and FW is not an exception. Combined carbon and energy recovery through the joint production of value-added VFAs, biofertilizers, hydrogen and methane is a promising approach that has been proved to be feasible but still remains to be optimized and applied industrially. Alternatives for stabilizing FW AD such as biochar addition could be easily incorporated into this scheme. The treatment of another centrally collected waste (*i.e.* green waste) through pyrolysis can be contemplated as biochar source, which afterwards could be dosed into the AD reactors. Recycling of the solid fraction of the digestate could be also applied as method for reducing its dosage. This approach would tackle waste stream integration, a clearly beneficial practice. Both scientific and industrial efforts should be directed towards the development of sustainable valorization facilities such as the presented

above. This would imply a significant step forwards in the pursuit of developing green sustainable societies, based on a circular economy.

Appendix A. Green waste as carbohydrate-rich co-substrate for stabilizing FW AD for methane production

Complementary to the co-digestion strategy presented in Chapter 4 (PW), another co-substrate that was evaluated as a potential option for stabilizing FW AD in consecutive batch reactors was municipal green waste (GW). As for PW, this approach was based upon the idea of using the GW to increase the TS contents, dilute the nitrogen present in the FW and reduce the impact of the initial VFA accumulation occurring during batch AD. As GW is a lignocellulosic material rich in carbon and with high TS contents, this material gathered all the characteristics needed. In addition, as in the Grand Narbonne region GW is already separately collected (and treated by composting), this waste was readily available and could be potentially applied at industrial scale.

The procedure was similar to the one followed in Chapter 4: the substrate load was increased consecutively, repeating each load twice. However, another approach was used to determine if the digestion had finished and thus the reactor needed to be re-alimented. In this case, instead of using the methane yield as indicator, the reactors were reloaded when no HPr was detected. As these experiments were carried out after those presented in Chapter 4, the issue of HPr accumulation had already been identified. The idea was to avoid the progressive accumulation of this VFA by simply waiting until it had been consumed (as in Chapter 5).

The co-digestion ratio was fixed at 75 g FW:25 g PW (w/w) and two different reactors were run: (i) a control fed with the FW and GW mixture and (ii) a reactor fed with same substrate but supplemented also with biochar and the industrial $FeCl_3$ solution (complementary to the reactors shown in Chapter 5). This allowed evaluating the influence of these two AD enhancers on the co-digestion performance. The concentrations of both reactants were fixed at 10 $g \cdot l^{-1}$ for biochar and 0.1 g $Fe \cdot l^{-1}$ for the industrial $FeCl_3$ solution. The characteristics of these two reagents are presented in Chapter 5. The reactors had a working volume if 7.3-8.6 kg. They are described in Section 2.4.4.

The biogas production and the concentrations of ionic species and VFAs were measured as in Chapter 4. Similarly, the TAN concentrations were also calculated as described previously and the modified Gompertz equation was used to model the obtained results (to evaluate precisely the kinetics of the AD process).

Appendix A. Green waste as carbohydrate-rich co-substrate for stabilizing FW AD for methane production

Using the same inoculum as in Chapter 4, the reactors were started at an S/X ratio of 1 g VS·g VS^{-1} (0.218 g substrate·g $inoculum^{-1}$). After two feedings, the load was doubled (0.435 g substrate·g $inoculum^{-1}$) and a single load of 0.871 g substrate·g $inoculum^{-1}$ was applied in the control reactor. Table A.1 shows a summary of the loading regime applied in the reactors.

Table A.1. Loading regime applied to the pilot reactors (kg substrate·kg $inoculum^{-1}$)

Reactor\Cycle #	1	2	3	4	5
Control	0.218	0.218	0.435	0.435	0.871
Biochar + $FeCl_3$	0.218	0.218	0.435	0.435	na[1]

1. Not applicable

Before presenting the AD results, it must be mentioned that, surprisingly, the characterization of the GW showed that, in addition to a high carbon content, it also contained significant proportions of organic nitrogen, which lowered the C/N ratio to 19.8, much lower than for CB (183) and close to that of the FW used as substrate (16.1). Therefore, it can be expected that the concentrations of TAN/FAN in the reactors will not be significantly lower due to the addition of GW to the substrate. However, the low degradability of GW (with a BMP of 55.8 ml CH_4·g VS^{-1}) suggests that it can efficiently serve for lowering the intensity of the initial VFA occurring during batch FW AD.

The obtained kinetics for the methane production (Figure A.1) showed that efficient methane production was achieved initially in both conditions, with methane yields ranging between 183 to 239 ml CH_4·g VS^{-1} (Table A.2). As expected, these yields were lower than those for obtained for FW mono-digestion (with a BMP of 420 ml CH_4·g VS^{-1}). As for the CB, this was related to the lower biodegradability of GW, which decreased the yields (expressed per g VS of substrate fed).

Before discussing the kinetic results, it must be mentioned that the first load applied to the reactor supplemented with biochar and $FeCl_3$ caused a lag phase of over 20 days in the methane production. This was not observed in the control reactor and, as both systems were inoculated with the same microbial consortia, fed with the same substrates and the reactors were physically similar, no explanation was found for this initial lag phase.

The results of the second load at 0.218 kg substrate·kg $inoculum^{-1}$ were similar in both reactors, with improved kinetics when compared to the first feeding, lag phases of 5.6-5.7 days and maximum methane production rates of 18-19 ml CH_4·g VS^{-1}·d^{-1} (Table A.2). This suggests that addition of biochar did not aid the AD process when treating FW and GW at the applied load.

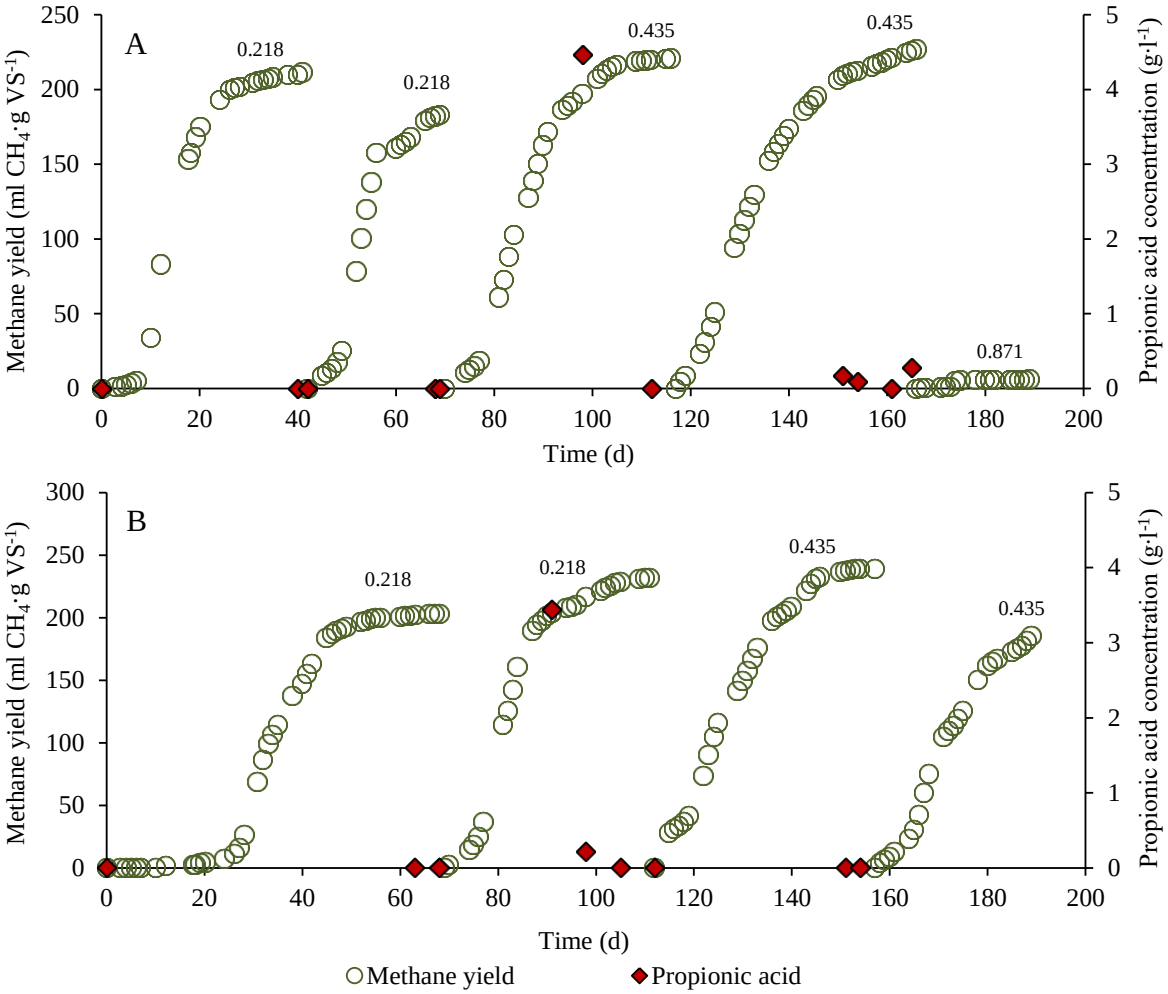

Figure A.1. Kinetics of methane production in the pilot reactors fed with FW and GW: control reactor (A) and reactor supplemented with biochar and $FeCl_3$ (B). The concentrations of propionic acid after each feeding cycle are also presented. The numbers on the top of the methane curves stand for the loads applied in each batch (kg substrate·kg inoculum^{-1})

When doubling the load to 0.435 kg substrate·kg inoculum^{-1}, efficient yields were also achieved in both reactors. However, the maximum methane production rates decreased to values down to 9.9 ml CH_4·g VS^{-1}·d^{-1} and the lag phases increased up to 6 days, suggesting worse kinetic performances. In addition, much longer batch durations were needed in order to consume the accumulated HPr. While a minimum duration of 28 days was obtained in the first load, this value corresponded to 46 days when the load was doubled, meaning that practically the average volumetric methane productivity would not be increased at increasing substrate loads. Again, no significant improvements were observed when adding biochar and $FeCl_3$ into the reactors.

The single load of 0.871 kg substrate·kg inoculum^{-1} applied to the control reactor resulted in acidification of the AD process and negligible methane yields due to overload of the system.

Appendix A. Green waste as carbohydrate-rich co-substrate for stabilizing FW AD for methane production

Table A.2. Experimental methane yields and best-fitting parameters corresponding to the representation of the methane yields from both reactors by the Gompertz equation

Condition	Substrate load (kg substrate·kg inoculum^{-1})	Experimental methane yield (ml CH_4·g VS^{-1})	M_{max}[1] (ml CH_4·g VS^{-1})	R_m[1] (ml CH_4·g VS^{-1}·d^{-1})	L[1] (d)	R^2	p-value F-test
Control reactor	0.218	212	209	17	7.7	0.999	< 0.0001
	0.218	183	179	19	5.6	0.993	< 0.0001
	0.435	221	223	12	5.8	0.999	< 0.0001
	0.435	227	224	9.9	2.9	0.999	< 0.0001
	0.871	neg[1]	na[1]	na[1]	na[1]	na[1]	na[1]
Reactor supplemented with biochar and $FeCl_3$	0.218	203	203	12	25	0.998	< 0.0001
	0.218	232	226	18	5.7	0.997	< 0.0001
	0.435	239	247	11	2.7	0.996	< 0.0001
	0.435	186[2]	191	10	6.0	0.989	< 0.0001

1. M_{max} stands for the final methane yield, R_m for the maximum methane production rate, L for the lag phase, neg for negligible and na for not available
2. The reactor needed to be stopped before the final methane yield was achieved

Concerning the TAN concentrations, values of 8.6 ± 0.6 g·l^{-1} (pH 8.18 ± 0.1) in the control reactor and 9.1 ± 0.3 g·l^{-1} (pH 8.15 ± 0.2) in the reactor supplemented with biochar and $FeCl_3$ were obtained, meaning that, as expected after knowing the values of the C/N ratios of the substrates, GW addition did not dilute the TAN concentrations in the reactors (see for instance Figure 4.1, corresponding to consecutive batch FW mono-digestion and its co-digestion with PW). The average pH values after each batch (8.18 ± 0.1 in the control reactor and 8.15 ± 0.2 in the reactor supplemented with biochar and $FeCl_3$) were also similar to those reported in FW mono-digestion (see for instance Section 4.2.3.1.2), suggesting that GW addition did not increase the buffering capacities.

Altogether, this experiment suggests that FW co-digestion with GW is not a suitable solution for stabilizing FW AD in industrial scale. The batch durations are longer that in FW mono-digestion (see for instance Table 5.6), the methane yields are lower and no significant dilution of the TAN concentrations was achieved. Moreover, addition of biochar and industrial $FeCl_3$ was not found to improve the AD performance.

Finally, it is worth to mention that undegraded GW remained always in the reactors after each batch, floating on the surface of the reaction media, jeopardizing the mixing in the reactors and risking to block the gas outlet (with the consequent pressure build-up inside the vessel). This may have huge implications when designing an industrial scale AD reactor.

Appendix B. Results of the commercial food waste quantification and characterization

As explained in Section 2.2.2, within the project of the thesis a FW collection test was carried out. This collection test consisted on identifying potential FW producers from the region of the Grand Narbonne (France) and informing them about the project and about the possibility of collecting their source-separated FW. Instructions were given to the producers that agreed to participate in the project (Figure C.7 and Figure C.8, in French) and the municipality and SUEZ provided the materials required for the collection (*i.e.* containers, truck and disposal location). With everything set-up, the FW flux was measured weekly at the INRA-LBE and different sampling campaigns were performed throughout the three years. This allowed assessing the FW characteristics from each producer and its seasonal variations.

Seven mayor FW producers from the region participated efficiently in the collection test and were then used as representative FW suppliers. They corresponded to a meat-serving restaurant, a hospital canteen, a high school canteen, a fruit and vegetable supermarket, a fruit and vegetable distribution company, a fast food restaurant and a supermarket. Figure B.1 and Figure B.2 show the results of the weekly-based quantitative measurements. Figure B.1 presents the evolution of the daily FW production throughout the sampling period (99 weeks, equivalent to around 2 years). Figure B.2 shows the average contribution of each producer to the daily waste collected. It must be considered that the collection of the FW produced by the high-school and the hospital canteens started after the others (in week 34 and 70, respectively) and thus their contribution in Figure B.2 is underestimated.

As it can be observed, the daily FW production fluctuated throughout the sampling period, with an average value of 101.6 ± 30.6 $kg \cdot d^{-1}$. This fluctuation was mainly caused by logistic complications and no significant trends or differences were identified according to seasonal variations. From a practical point of view, the main difficulty found was the fast degradation of FW when stored prior its collection, which caused odors that affected both the FW producers and their clients. The simplest solution would be to increase the collection frequency (of one week in this study). However, this would complicate the collection logistics and increase the associated costs. The supermarkets accounted for most of the waste produced (31 and 17 %), followed by the distribution company (17 %) and the fast food restaurant (17 %). To be able to extrapolate these results to the whole region (allowing to accurately estimate the total FW production), a study should be carried out considering the number of

potential FW suppliers present in the region, as well as their particular activity and the number of clients they serve.

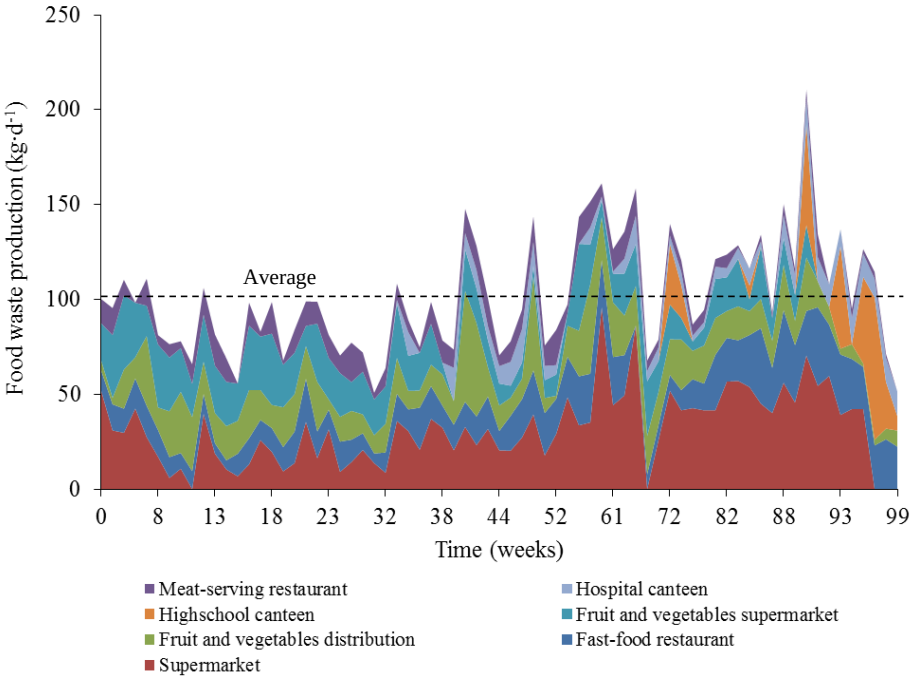

Figure B.1. Evolution of the daily food waste production from each producer throughout the collection period

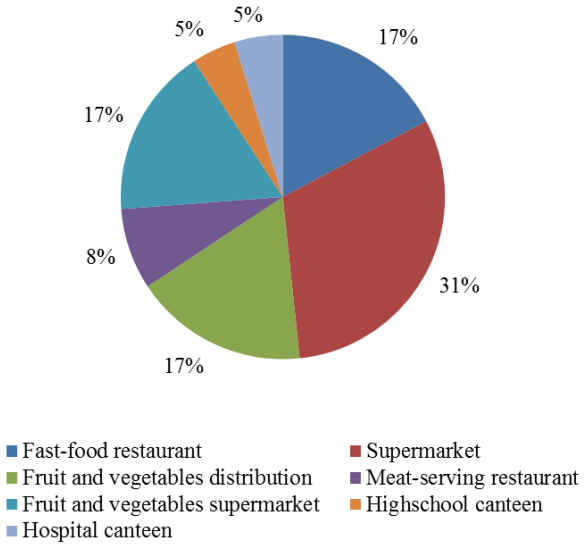

Figure B.2. Average contribution of each food waste supplier to the total daily production

Concerning the characterization results, the raw data are shown in Table B.1. The criteria used to decide if a waste was collected were the FW requirements for the experiments and the variability of the waste. Thus, a different number of sampling campaigns were carried out for each FW supplier. In addition, this was obviously affected by when the waste collection started.

Appendix B. Results of the commercial food waste quantification and characterization

To allow the identification of relationship between the studied variables, a PCA analysis of the data was carried out. In addition, this analysis allowed also evaluating if significant differences between the different samples of each waste existed. Finally, it also enabled to compare the characteristics of the FW from the different FW suppliers, identifying similar groups. The PCA was performed as described in Section 2.7.2.3. The results presented in Table B.1 were used as input data for the PCA analysis. The concentrations of VFAs and FAN and the pH were considered to be mainly dependent on the waste storage time and where therefore excluded from the analysis. As the parameters for the VS/TS and the concentrations of P_2O_5, CaO, Co, Cd, Hg and Pb had p-values over 0.05 (the null hypothesis could not be refused and their values might be zero), these variables were also removed from the PCA analysis. This allowed simplifying the obtained results and improving the variability explained by each PC. The graphical output of the PCA is shown in Figure B.3. The ellipses in the figure represent the results of a clustering analysis performed with the input data.

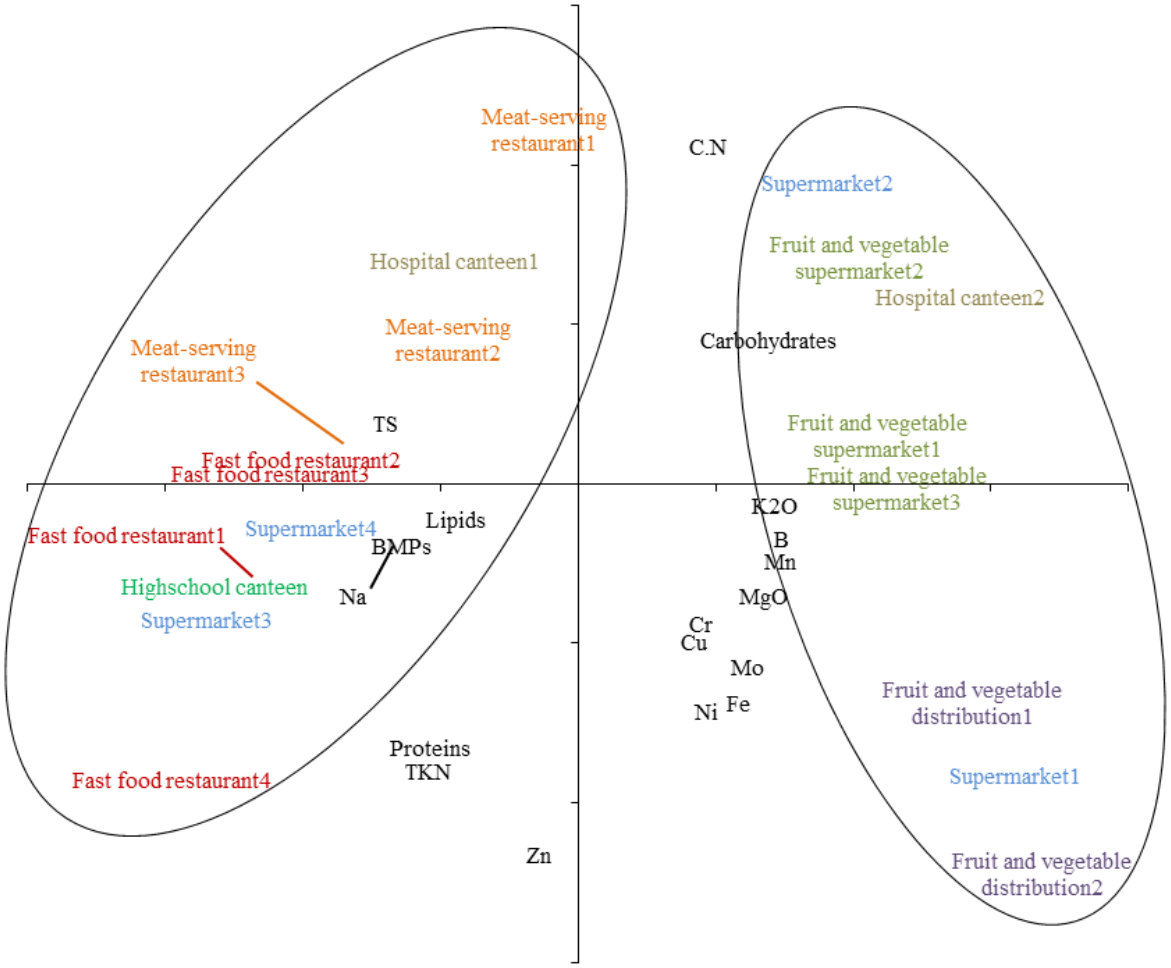

Figure B.3. Results of the PCA analysis using the FW characteristics as input data. The two first principal components, which account for 55.4 and 17.1 % of the variance respectively, were considered. The ellipses represent the two main clusters obtained by HCA

Appendix B. Results of the commercial food waste quantification and characterization

Table B.1. Characteristics of the food waste samples

Provider	Fast food restaurant				Meat-serving restaurant			Supermarket				Fruit and vegetable supermarket			Fruit and vegetable distribution		Hospital canteen		Highschool canteen
Sampling campaign	1	2	3	4	1	2	3	1	2	3*	4*	1	2	3	1	2	1	2	1
TS (%)	34.3	34.3	38.1	38.5	43.1	40.1	44.8	9.70	10.2	33.8	33.0	10.0	12.5	9.41	10.6	10.6	31.3	9.5	27.0
VS/TS (%)	96.2	93.1	86.2	94.2	88.8	88.5	83.3	88.7	94.4	85.0	87.8	89.8	89.8	86.2	85.8	85.8	89.6	88.4	93.0
Carbohydrates ($g \cdot kg\ TS^{-1}$)	387	396	299	297	674	524	391	770	762	331	504	776	776	627	712	634	597	830	81.6
Proteins ($g \cdot kg\ TS^{-1}$)	320	230	282	487	124	190	234	170	129	562	311	170	125	164	225	262	208	108	364
Lipids ($g \cdot kg\ TS^{-1}$)	257	293	215	167	140	127	201	35.2	62.6	15.4	15.0	25.9	24.0	86.3	39.8	99.0	60.7	102	416
BMPs ($ml\ CH_4 \cdot g\ VS^{-1}$)	475	515	465	478	440	449	440	388	377	543	530	388	388	431	371	371	405	334	412
pH	5.2	5.2	5.40	4.1	5.3	5.4	4.8	4.8	4.7	6.1	5.8	5.4	4.7	5.4	5.7	5.1	4.8	3.9	3.9
TOC ($g \cdot kg\ TS^{-1}$)	449	454	432	475	453	431	415	398	457	421	437	437	452	417	434	439	447	449	468
TAN ($g \cdot kg\ TS^{-1}$)	1.63	0.69	0.60	0.70	1.10	1.08	0.90	2.00	0.53	0.90	1.62	0.78	0.40	2.47	4.10	1.80	0.58	2.30	0.70
TKN ($g \cdot kg\ TS^{-1}$)	51.3	36.7	46.0	79.2	19.8	30.4	38.0	27.2	20.7	55.0	53.7	27.1	19.9	26.0	36.0	42.0	31.0	23.8	59.5
C/N	8.8	12.4	9.40	6.0	22.9	14.1	11.0	14.5	21.7	7.61	8.13	15.7	21.8	16.0	11.8	10.3	14.0	18.9	7.90
P_2O_5 ($g \cdot kg\ TS^{-1}$)	7.31	7.59	7.59	7.3	8.3	27	35.6	7.17	5.76	13.1	15.3	7.96	6.97	8.67	7.3	14.2	6.7	9.7	14.5
CaO ($g \cdot kg\ TS^{-1}$)	7.4	14	6.4	9.4	23.6	42.4	54.0	5.43	6.7	30.5	18.7	6.4	12.9	34.1	11.1	10	7.7	11.8	13.5
MgO ($g \cdot kg\ TS^{-1}$)	0.91	1.21	0.97	1.1	1.30	1.86	1.81	2.78	2.56	1.22	1.16	2.57	2.49	3.38	3.46	5.16	1.00	4.10	2.10
K_2O ($g \cdot kg\ TS^{-1}$)	7.32	9.33	8.32	7.5	11.1	13.7	9.8	30.3	31.4	7.90	8.27	29.5	32.8	42.2	34.8	43.9	7.0	54.4	14.5
Na ($g \cdot kg\ TS^{-1}$)	9.77	9.89	9.42	11.2	6.46	7.69	9.99	1.02	0.95	13.3	13.1	1.56	0.74	1.74	3.64	1.97	9.81	5.20	22.2
B ($mg \cdot kg\ TS^{-1}$)	2.64	2.7	2.17	< 2.8	5.60	3.43	4.52	26.0	17.9	2.66	1.86	23.1	15.8	25.2	28.5	24.9	3.2	33.1	7.4
Co ($mg \cdot kg\ TS^{-1}$)	< 9.08	< 9.75	< 8.66	< 0.47	<8.76	<9.75	< 8.64	<9.70	<9.75	< 8.81	< 8.99	<9.8	<9.75	< 9.32	<9.56	< 9.75	< 8.68	< 0.45	< 0.50
Cu ($mg \cdot kg\ TS^{-1}$)	4.85	4.92	5.20	7.10	11.9	9.43	6.59	83.2	12.1	4.72	4.03	11.9	11.6	17.2	16.9	18.0	4.9	9.50	4.10
Fe ($mg \cdot kg\ TS^{-1}$)	271	268	184	380	397	294	334	1878	731	281	279	972	1227	1661	1375	3049	204	68	130
Mn ($mg \cdot kg\ TS^{-1}$)	8.5	12.5	9.2	12.1	15.6	10.3	9.0	35.7	30.7	7.60	7.95	28.2	30.2	41.5	30.8	54.3	11.8	41.2	8.6
Mo ($mg \cdot kg\ TS^{-1}$)	< 0.36	< 0.35	< 0.34	< 0.45	0.64	0.47	< 0.34	1.37	0.48	0.36	0.39	1.41	0.85	1.64	3.25	4.49	0.58	1.5	< 0.47
Zn ($mg \cdot kg\ TS^{-1}$)	58.7	52.6	42.5	64.0	21.8	36.3	45.1	59.6	20.3	40.1	38.0	31.4	27.6	36.3	40.3	55.3	23.9	31.9	31.6
Cd ($mg \cdot kg\ TS^{-1}$)	< 0.19	< 0.19	< 0.18	< 0.14	<0.18	< 0.19	< 0.18	0.27	<0.19	< 0.18	< 0.18	<0.20	<0.19	< 0.19	<0.19	<0.19	< 0.18	0.2	0.20
Cr ($mg \cdot kg\ TS^{-1}$)	1.89	< 1.81	< 1.77	1.30	3.05	3.46	1.90	8.31	3.05	< 1.80	13.0	23.4	6.37	7.50	39.2	13.3	< 1.78	4.8	2.0
Ni ($mg \cdot kg\ TS^{-1}$)	< 1.86	< 1.99	< 1.77	0.90	<1.79	< 1.99	< 1.78	15.8	<1.99	< 1.80	< 1.84	4.68	2.06	2.46	7.23	3.87	< 1.78	< 0.66	1.0
Pb ($mg \cdot kg\ TS^{-1}$)	< 4.59	< 4.93	< 4.38	< 3.70	<4.43	< 4.93	< 4.37	<4.91	<4.93	< 4.46	< 4.55	<4.96	< 4.93	< 4.72	<4.84	<4.93	< 4.39	< 3.50	< 3.90
Hg ($mg \cdot kg\ TS^{-1}$)	< 0.01	0.07	< 0.01	< 0.14	<0.01	< 0.01	< 0.01	<0.01	0.02	0.02	0.01	<0.01	<0.01	0.02	<0.01	0.01	< 0.01	< 0.13	< 0.14
Acetate ($g \cdot kg^{-1}$)	5.78	6.14	6.31	7.46	7.28	5.59	5.32	3.61	1.39	3.23	1.11	1.89	4.21	0.83	6.03	4.18	5.07	0.50	5.07
Propionate ($g \cdot kg^{-1}$)	0.34	0.01	0.08	0.16	0.24	$<5 \cdot 10^{-4}$	0.05	0.04	$<5 \cdot 10^{-4}$	0.46	0.42	$<5 \cdot 10^{-4}$	$<5 \cdot 10^{-4}$	0.08	0.10	$<5 \cdot 10^{-4}$	0.18	0.18	0.18
Isobutyrate ($g \cdot kg^{-1}$)	0.08	0.24	$< 5 \cdot 10^{-4}$	0.01	0.01	0.41	$<5 \cdot 10^{-4}$	0.37	0.07	0.01	0.01	$<5 \cdot 10^{-4}$	0.15	$<5 \cdot 10^{-4}$	$<5 \cdot 10^{-4}$	0.15	$<5 \cdot 10^{-4}$	0.02	$<5 \cdot 10^{-4}$
Butyrate ($g \cdot kg^{-1}$)	2.63	0.32	0.07	0.28	0.25	$<5 \cdot 10^{-4}$	0.04	$<5 \cdot 10^{-4}$	$<5 \cdot 10^{-4}$	0.08	0.16	0.03	$<5 \cdot 10^{-4}$	0.32	0.21	$<5 \cdot 10^{-4}$	0.07	0.11	0.07
Isovalerate ($g \cdot kg^{-1}$)	0.15	$< 5 \cdot 10^{-4}$	$< 5 \cdot 10^{-4}$	0.01	$<5 \cdot 10^{-4}$	$<5 \cdot 10^{-4}$	$<5 \cdot 10^{-4}$	0.13	$<5 \cdot 10^{-4}$	0.01	0.01	$<5 \cdot 10^{-4}$	$<5 \cdot 10^{-4}$	$<5 \cdot 10^{-4}$	$<5 \cdot 10^{-4}$	$<5 \cdot 10^{-4}$	$<5 \cdot 10^{-4}$	0.02	$<5 \cdot 10^{-4}$
Valerate ($g \cdot kg^{-1}$)	0.02	$< 5 \cdot 10^{-4}$	$< 5 \cdot 10^{-4}$	0.01	$<5 \cdot 10^{-4}$	$<5 \cdot 10^{-4}$	$<5 \cdot 10^{-4}$	$<5 \cdot 10^{-4}$	$<5 \cdot 10^{-4}$	$<5 \cdot 10^{-4}$	0.00	$<5 \cdot 10^{-4}$	$<5 \cdot 10^{-4}$	$<5 \cdot 10^{-4}$	$<5 \cdot 10^{-4}$	$<5 \cdot 10^{-4}$	$<5 \cdot 10^{-4}$	$<5 \cdot 10^{-4}$	$<5 \cdot 10^{-4}$
Total VFAs ($g\ COD \cdot kg^{-1}$)	8.00	7.58	6.99	8.77	7.65	6.72	5.82	3.97	1.61	4.33	2.15	1.91	4.76	1.61	6.25	4.73	5.82	1.07	5.82

* Including all the unsold products from the supermarket (also packed products)

Starting with the correlations between variables, it can be observed that the BMP values where directly related to the lipids and protein contents and negatively correlated with the carbohydrates proportions. Considering that the theoretical methane yields of lipids are higher than those of proteins, which are higher than those of carbohydrates, this is a logical result. In addition, the protein content was directly related to the TKN concentrations and inversely related to the C/N ratio, indicating that the proteins were responsible for the high TKN proportions and the low C/N ratios. Interestingly, most of the macronutrients and the TEs (all but Zn) were linked to the carbohydrate concentrations.

Continuing with the sample distribution, the first point to consider is that both the PCA and the HCA analysis showed that two groups of samples existed: one formed by the samples with high contents of lipids, proteins and solids and with high BMP values (left side of Figure B.3; meat-rich samples) and a second one formed by the samples with high contents of carbohydrates and TEs (right side of Figure B.3; vegetable-rich samples). This allowed associating the FW characteristics directly to their source and to their potential impact on the AD process. The samples belonging to the cluster on the left, which were rich in lipids and proteins and poor in carbohydrates, came mainly from the restaurants and canteens, suggesting that samples from these sources may lead to high methane yields but also to high TAN concentrations in the reactors due to their high TKN contents. On the other hand, samples coming from supermarkets and fruit and vegetable distribution (cluster on the right) were rich in carbohydrates and TEs, which may lead to lower methane yields but also to more stable AD performances, with lower TAN concentrations and higher TEs contents. The differences observed between the samples 1-2 and the samples 3-4 from the supermarket were caused by a modification of the FW collection procedure. While in samples 1-2 the FW collected corresponded to the non-packed unsold products, samples 3-4 included also the unsold packed products, mainly consisting of meat, fish and dairy products (*i.e.* cheese, milk and yogurts), all with high contents of fats and proteins, therefore modifying the global FW composition and moving their position towards the protein-rich group. This indicated that including the collection of the packed FW from supermarkets can greatly modify the general FW characteristics, increasing the methane yields but also the TAN concentrations in the AD reactor, which may destabilize the process. These results suggest than the source of the FW collected clearly affects its characteristics and that, if possible, the selective collection of FW from different producers or different FW fractions may also be a solution for stabilizing methane production from this waste.

Interestingly, the different samplings from the fast-food restaurant (1-4), the meat-serving restaurant (1-3), the fruit and vegetable supermarket (1-3) and the fruit and vegetable distribution company (1-2) were close to each other, indicating that the variability on their composition was not significant when compared to the overall variability of the sampling set. However, this was not the case for the samples from the hospital canteen (1-2) and the supermarket (1-4). In both cases, half of the samples characterized belonged to different clusters and sides of the PCA plot. The variability of the samples from the hospital canteen can be directly attributed to the menu served on the collection date (*i.e.* meat-rich meal *vs.* vegetable-rich meal), and that of the samples from the supermarket to the collection of the packed products in samples 3 and 4.

Appendix C. Supplementary material

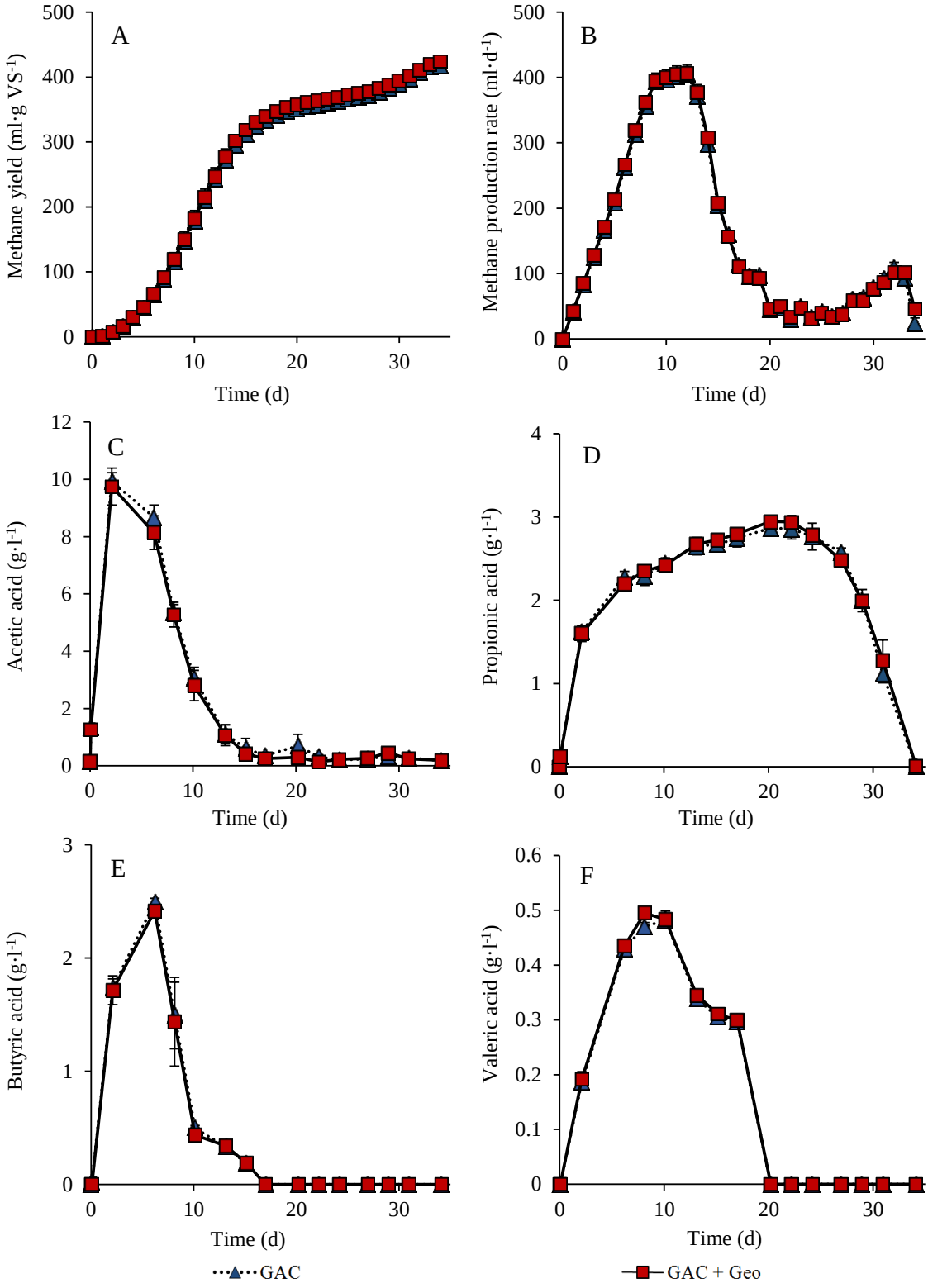

Figure C.1. Evolution of (A) the methane yields, (B) methane production rates and concentrations of (C) acetic, (D) propionic, (E) butyric and (F) valeric acid during the first feed in the reactor supplemented with GAC (GAC) and the reactor supplemented with GAC and inoculated with *Geobacter sulfurreducens* (GAC + Geo)

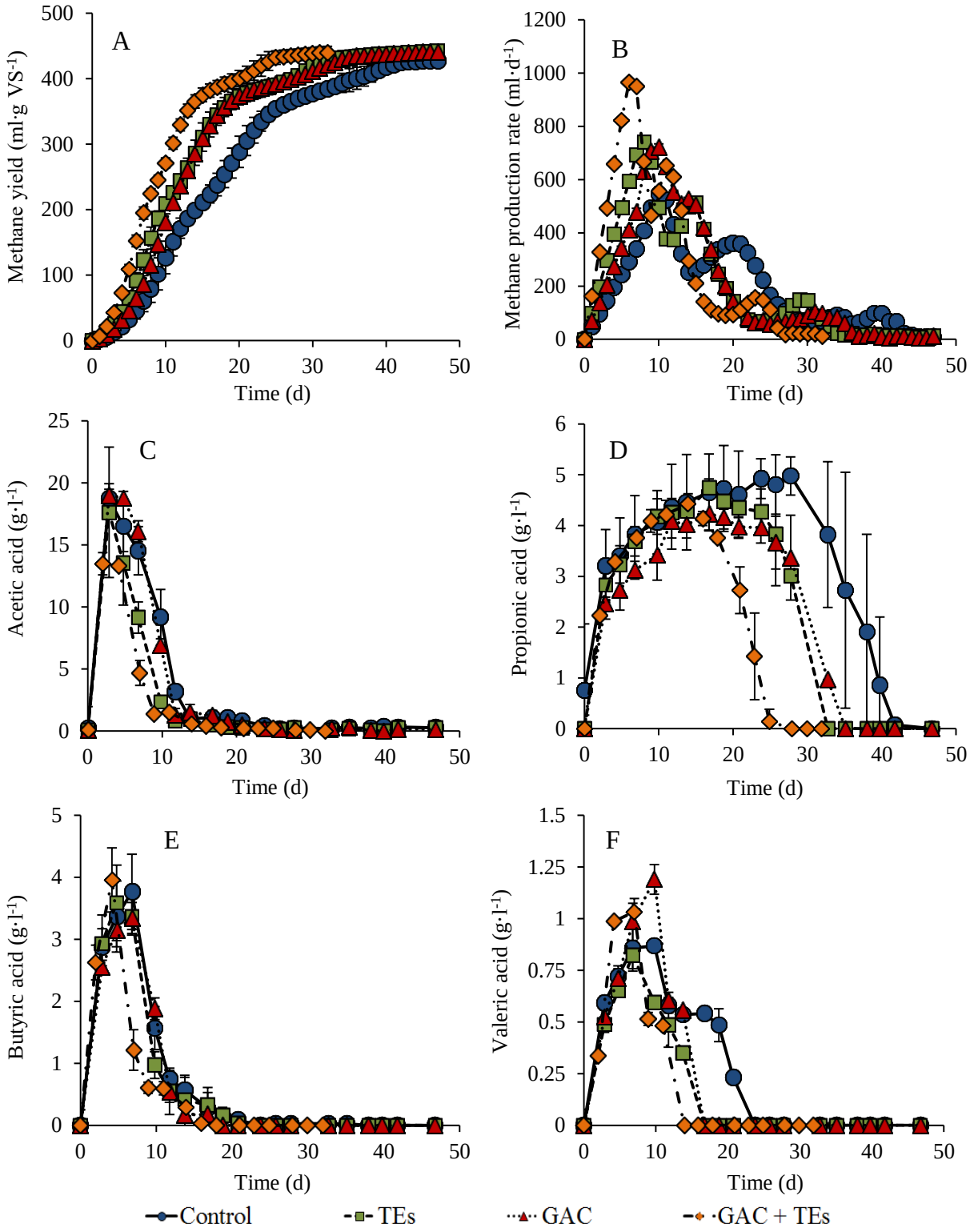

Figure C.2. Evolution of (A) the methane yields, (B) methane production rates and concentrations of (C) acetic, (D) propionic, (E) butyric and (F) valeric acids during the third feeding (~ 55 g VS FW·l^{-1})

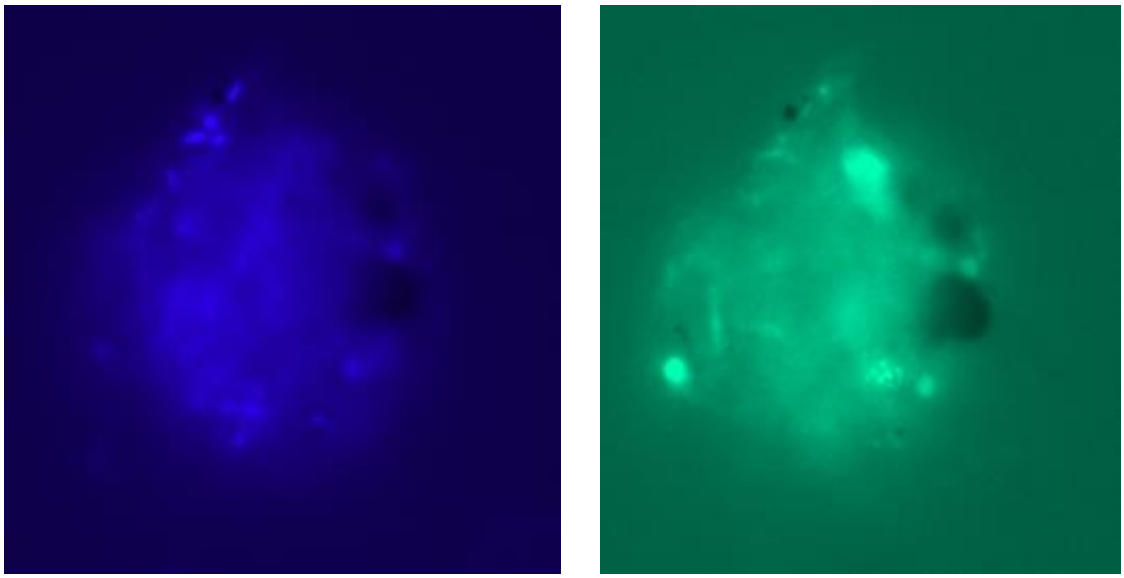

Figure C.3. Microscopy pictures of a GAC particle taken after DAPI coloration (left) and at 420 nm (right). Each picture represents a total length of 50 µm. The presence of bacterial and archaeal cells attached onto the GAC particles was qualitatively assessed using coloration and fluorescence microscopy. DNA was colored using DAPI (4',6-diamino-2-fenilindol). A diluted digestate sample was mixed with the DAPI solution (25 $\mu g \cdot ml^{-1}$) at a volumetric ratio of 19:1 and the mixture was incubated at ambient temperature for 20 min. The natural fluorescence of methanogenic archaea at 420 nm (due to the coenzyme F_{420}) was used for their observation. To avoid crushing the GAC particles (and thus the biofilm), the samples were fixed in agar (1.5 % in Tris pH 7.5 0.1M) while it was still liquid and covered with a layer of Milli-Q water (around 1 mm deep). A submergible lens (Olympus UM Plan FLN 60x/1.00) coupled to a microscope Olympus BX53, a motorized reflected fluorescence system (Olympus BX3-RFAA) and a control box (Olympus U-CBM) was used

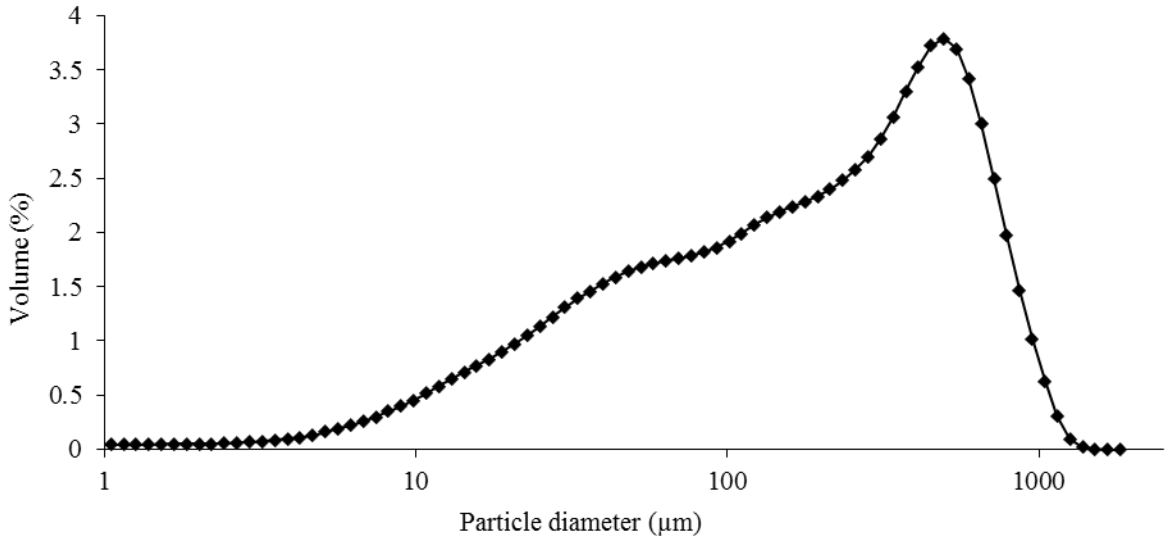

Figure C.4. Particle size distribution of the biochar used in the study

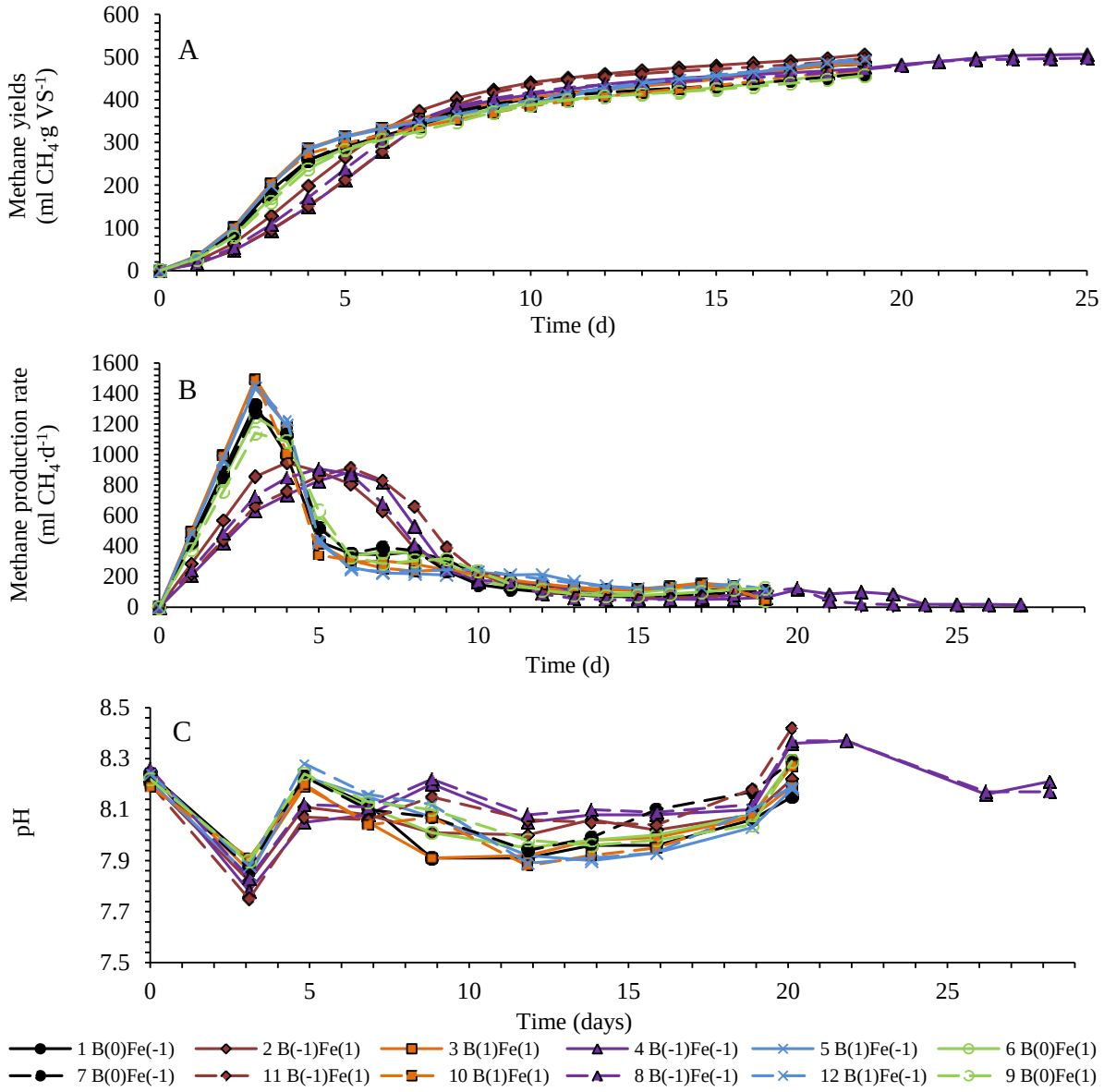

Figure C.5. Evolution of (A) the methane yields, (B) the methane production rates and (C) the pH in the reactors. The legend indicates the reactor number and the normalized levels of each factor (B stands for biochar and Fe for $FeCl_3$ solution)

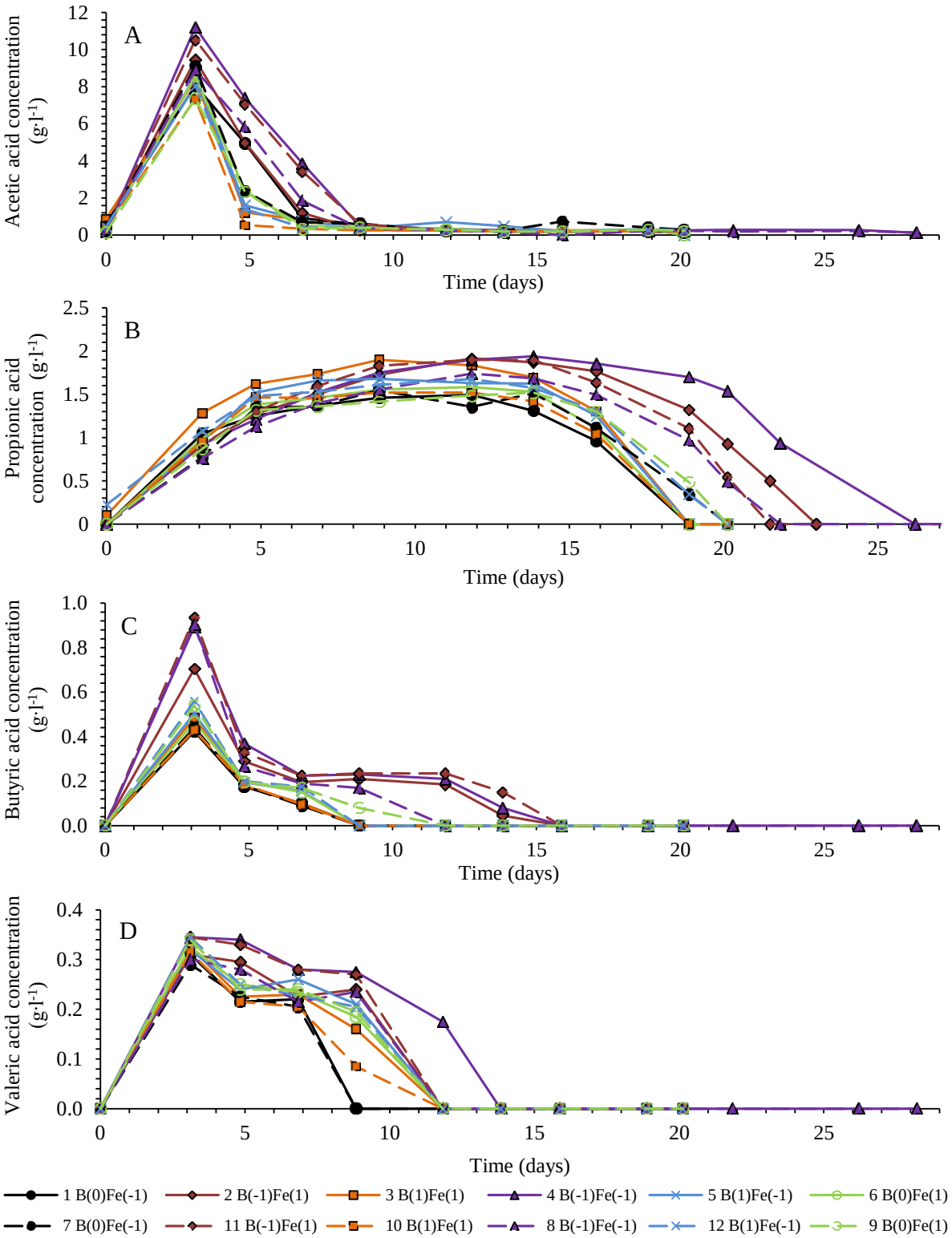

Figure C.6. Evolution of the concentrations of (A) acetic acid, (B) propionic acid, (C) butyric acid and (D) valeric acid in the reactors. The legend indicates the reactor number and the normalized levels of each factor (B stands for biochar and Fe for $FeCl_3$ solution)

Figure C.7. Instructions given to the FW producers working on food distribution (in French)

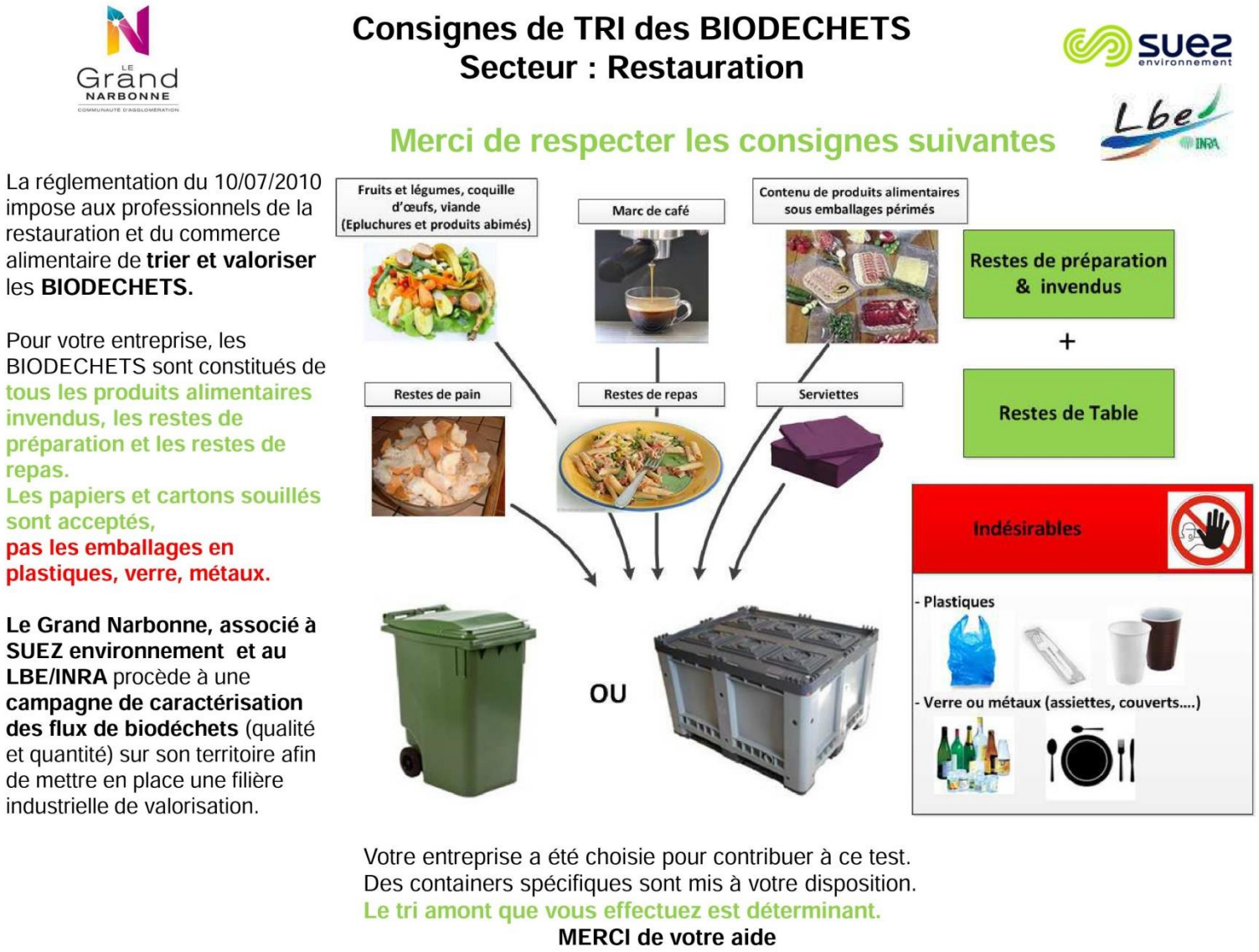

Figure C.8. Instructions given to the FW producers working on the restauration sector (in French

Bibliography

Abbassi-Guendouz, A., Brockmann, D., Trably, E., Dumas, C., Delgenès, J.-P., Steyer, J.-P., Escudié, R., 2012. Total solids content drives high solid anaerobic digestion via mass transfer limitation. Bioresource Technology 111, 55–61.

Abbassi-Guendouz, A., Trably, E., Hamelin, J., Dumas, C., Steyer, J.P., Delgenès, J.-P., Escudié, R., 2013. Microbial community signature of high-solid content methanogenic ecosystems. Bioresource Technology 133, 256–262.

Agyeman, F.O., Tao, W., 2014. Anaerobic co-digestion of food waste and dairy manure: Effects of food waste particle size and organic loading rate. Journal of Environmental Management 133, 268–274.

Ahamed, A., Chen, C.-L., Rajagopal, R., Wu, D., Mao, Y., Ho, I.J.R., Lim, J.W., Wang, J.-Y., 2015. Multi-phased anaerobic baffled reactor treating food waste. Bioresource technology 182, 239–44.

Ako, O.Y., Kitamura, Y., Intabon, K., Satake, T., 2008. Steady state characteristics of acclimated hydrogenotrophic methanogens on inorganic substrate in continuous chemostat reactors. Bioresource Technology 99, 6305–6310.

Anderson, G.K., Donnelly, T., McKeown, K.J., 1982. Identification and control of inhibition in the anaerobic treatment of industrial wastewaters.

Angelidaki, I., Ahring, B.K., 1992. Effects of free long-chain fatty acids on thermophilic anaerobic digestion. Applied Microbiology and Biotechnology 37, 808–812.

Angelidaki, I., Alves, M.M., Bolzonella, D., Borzacconi, L., Campos, J.L., Guwy, A.J., Kalyuzhnyi, S., Jenicek, P., Van Lier, J.B., 2009. Defining the biomethane potential (BMP) of solid organic wastes and energy crops: a proposed protocol for batch assays.Water Science and Technology 59, 927-934.

Angenent, L.T., Richter, H., Buckel, W., Spirito, C.M., Steinbusch, K.J.J., Plugge, C.M., Strik, D.P.B.T.B., Grootscholten, T.I.M., Buisman, C.J.N., Hamelers, H.V.M., 2016. Chain Elongation with Reactor Microbiomes: Open-Culture Biotechnology to Produce Biochemicals. Environmental Science and Technology 50, 2796–2810.

Angeriz-Campoy, R., Álvarez-Gallego, C.J., Romero-García, L.I., 2015. Thermophilic anaerobic co-digestion of organic fraction of municipal solid waste (OFMSW) with food waste (FW): Enhancement of bio-hydrogen production. Bioresource technology 194, 291–296.

APHA, 2005. Standard Methods for the Examination of Water and Wastewater. American Public Health Association, Washington, DC.

Appels, L., Baeyens, J., Degrève, J., Dewil, R., 2008. Principles and potential of the anaerobic digestion of waste-activated sludge. Progress in Energy and Combustion Science 34, 755–781.

Ariunbaatar, J., Panico, A., Frunzo, L., Esposito, G., Lens, P.N.L., Pirozzi, F., 2014. Enhanced anaerobic digestion of food waste by thermal and ozonation pretreatment methods. Journal of environmental management 146, 142–9.

Ariunbaatar, J., Panico, A., Yeh, D.H., Pirozzi, F., Lens, P.N.L., Esposito, G., 2015a. Enhanced mesophilic anaerobic digestion of food waste by thermal pretreatment: Substrate versus digestate heating. Waste Management 46, 176–181.

Bibliography

Ariunbaatar, J., Scotto Di Perta, E., Panico, A., Frunzo, L., Esposito, G., Lens, P.N.L., Pirozzi, F., 2015b. Effect of ammoniacal nitrogen on one-stage and two-stage anaerobic digestion of food waste. Waste management (New York, N.Y.) 38, 388–98.

Arthurson, V., 2009. Closing the global energy and nutrient cycles through application of biogas residue to agricultural land - potential benefits and drawbacks. Energies 2, 226–242.

Asato, C.M., Gonzalez-Estrella, J., Jerke, A.C., Bang, S.S., Stone, J.J., Gilcrease, P.C., 2016. Batch anaerobic digestion of synthetic military base food waste and cardboard mixtures. Bioresource Technology 216, 894–903.

Bajón Fernández, Y., Green, K., Schuler, K., Soares, A., Vale, P., Alibardi, L., Cartmell, E., 2015. Biological carbon dioxide utilisation in food waste anaerobic digesters. Water research 87, 467–75.

Banks, C.J., Chesshire, M., Stringfellow, A., 2008. A pilot-scale trial comparing mesophilic and thermophilic digestion for the stabilisation of source segregated kitchen waste. Water Science & Technology 58, 1475–1481.

Banks, C.J., Chesshire, M., Heaven, S., Arnold, R., 2011a. Anaerobic digestion of source-segregated domestic food waste: Performance assessment by mass and energy balance. Bioresource Technology 102, 612–620.

Banks, C.J., Salter, A.M., Heaven, S., Riley, K., 2011b. Energetic and environmental benefits of co-digestion of food waste and cattle slurry: A preliminary assessment. Resources, Conservation and Recycling 56, 71–79.

Banks, C.J., Zhang, Y., Jiang, Y., Heaven, S., 2012. Trace element requirements for stable food waste digestion at elevated ammonia concentrations. Bioresource Technology 104, 127–135.

Barua, S., Dhar, B.R., 2017. Advances Towards Understanding and Engineering Direct Interspecies Electron Transfer in Anaerobic Digestion. Bioresource Technology *In Press*.

Batstone, D.J., Keller, J., Newell, R.B., Newland, M., 2000. Modelling anaerobic degradation of complex wastewater. I: model development. Bioresource Technology 75, 67–74.

Batstone, D.J., Keller, J., Angelidaki, I., Kalyuzhny, S. V, Pavlostathis, S.G., Rozzi, A., Sanders, W.T.M., Siegrist, H., Vavilin, V.A., 2002a. Anaerobic digestion model no. 1 (ADM1). IWA Publishing.

Batstone, D.J., Keller, J., Angelidaki, I., Kalyuzhnyi, S. V, Pavlostathis, S.G., Rozzi, A., Sanders, W.T.M., Siegrist, H., Vavilin, V.A., 2002b. The IWA Anaerobic Digestion Model No 1 (ADM 1). Water Science & Technology 45, 65–73.

Bernstad, A., la Cour Jansen, J., 2011. A life cycle approach to the management of household food waste–a Swedish full-scale case study. Waste management 31, 1879–1896.

Bernstad, A., la Cour Jansen, J., 2012. Review of comparative LCAs of food waste management systems--current status and potential improvements. Waste management (New York, N.Y.) 32, 2439–55.

Bernstad, A., Andersson, T., 2014. Food waste minimization from a life-cycle perspective. Journal of environmental management 147, 219–226.

Bernstad, A., Wenzel, H., la Cour Jansen, J., 2016. Identification of decisive factors for greenhouse gas emissions in comparative lifecycle assessments of food waste

management – An analytical review. Journal of Cleaner Production 119, 13–24.

Blasco, L., Kahala, M., Tampio, E., Ervasti, S., Paavola, T., Rintala, J., Joutsjoki, V., 2014. Dynamics of microbial communities in untreated and autoclaved food waste anaerobic digesters. Anaerobe 29, 3–9.

Boni, M.R., Sbaffoni, S., Tuccinardi, L., 2013. The influence of slaughterhouse waste on fermentative H2 production from food waste: preliminary results. Waste management (New York, N.Y.) 33, 1362–71.

Bouallagui, H., 2003. Mesophilic biogas production from fruit and vegetable waste in a tubular digester. Bioresource Technology 86, 85–89.

Braun, F., Hamelin, J., Gèvaudan, G., Patureau, D., 2011. Development and application of an enzymatic and cell flotation treatment for the recovery of viable microbial cells from environmental matrices such as anaerobic sludge. Applied and Environmental Microbiology 77, 8487–8493.

Brown, D., Li, Y., 2013. Solid state anaerobic co-digestion of yard waste and food waste for biogas production. Bioresource Technology 127, 275–280.

Browne, J.D., Murphy, J.D., 2013. Assessment of the resource associated with biomethane from food waste. Applied Energy 104, 170–177.

Cao, X., Zhao, Y., 2009. The influence of sodium on biohydrogen production from food waste by anaerobic fermentation. Journal of material cycles and waste management 11, 244–250.

Capson-Tojo, G., Rouez, M., Crest, M., Steyer, J.-P., Delgenès, J.-P., Escudié, R., 2016. Food waste valorization via anaerobic processes: a review. Reviews in Environmental Science and Bio/Technology 15, 499–547.

Capson-Tojo, G., Ruiz, D., Rouez, M., Crest, M., Steyer, J.-P., Bernet, N., Delgenès, J.-P., Escudié, R., 2017a. Accumulation of propionic acid during consecutive batch anaerobic digestion of commercial food waste. Bioresource Technology Volume 245, 724–733.

Capson-Tojo, G., Trably, E., Rouez, M., Crest, M., Steyer, J.-P., Delgenès, J.-P., Escudié, R., 2017b. Dry anaerobic digestion of food waste and cardboard at different substrate loads, solid contents and co-digestion proportions. Bioresource Technology 233, 166–175.

Capson-Tojo, G., Rouez, M., Crest, M., Trably, E., Steyer, J., Bernet, N., Delgenes, J., Escudié, R., 2017c. Kinetic study of dry anaerobic co-digestion of food waste and cardboard for methane production. Waste Management 69, 470-479.

Capson-Tojo, G., Ruiz, D., Rouez, M., Crest, M., Steyer, J.-P., Bernet, N., Delgenès, J.-P., Escudié, R., 2017d. Cardboard proportions and total solids contents as driving factors in dry co-fermentation of food waste. Bioresource Technology 245, 724-733.

Carucci, G., Carrasco, F., Trifoni, K., Majone, M., Beccari, M., 2005. Anaerobic digestion of food industry wastes: effect of codigestion on methane yield. Journal of Environmental Engineering 131, 1037–1045.

Cavinato, C., Giuliano, A., Bolzonella, D., Pavan, P., Cecchi, F., 2012. Bio-hythane production from food waste by dark fermentation coupled with anaerobic digestion process: A long-term pilot scale experience. International Journal of Hydrogen Energy 37, 11549–11555.

Cazier, E.A., Trably, E., Steyer, J.P., Escudie, R., 2015. Biomass hydrolysis inhibition at high hydrogen partial pressure in solid-state anaerobic digestion. Bioresource Technology

190, 106–113.

Chang, H.N., Kim, N.J., Kang, J., Jeong, C.M., 2010. Biomass-derived volatile fatty acid platform for fuels and chemicals. Biotechnology and Bioprocess Engineering 15, 1–10.

Chatellard, L., Trably, E., Carrère, H., 2016. The type of carbohydrates specifically selects microbial community structures and fermentation patterns. Bioresource Technology 221, 541–549.

Chen, G., Liu, G., Yan, B., Shan, R., Wang, J., Li, T., Xu, W., 2016. Experimental study of co-digestion of food waste and tall fescue for bio-gas production. Renewable Energy 88, 273–279.

Chen, H., Jiang, W., Yang, Y., Yang, Y., Man, X., 2016. State of the art on food waste research: a bibliometrics study from 1997 to 2014. Journal of Cleaner Production 140, Part 2, 840-846.

Chen, H., Meng, H., Nie, Z., Zhang, M., 2013. Polyhydroxyalkanoate production from fermented volatile fatty acids: effect of pH and feeding regimes. Bioresource technology 128, 533–8.

Chen, J.L., Ortiz, R., Steele, T.W.J., Stuckey, D.C., 2014. Toxicants inhibiting anaerobic digestion: a review. Biotechnology advances 32, 1523–34.

Chen, J.L., Steele, T.W.J., Stuckey, D.C., 2016. Stimulation and inhibition of anaerobic digestion by nickel and cobalt: a rapid assessment using the resazurin reduction assay. Environmental Science & Technology 50, 11154-11163.

Chen, W.-H., Chen, S.-Y., Khanal, S.K., Sung, S., 2006. Kinetic study of biological hydrogen production by anaerobic fermentation. International Journal of Hydrogen Energy 31, 2170–2178.

Chen, X., Yan, W., Sheng, K., Sanati, M., 2014. Comparison of high-solids to liquid anaerobic co-digestion of food waste and green waste. Bioresource Technology 154, 215–221.

Chen, X., Yuan, H., Zou, D., Liu, Y., Zhu, B., Chufo, A., Jaffar, M., Li, X., 2015. Improving biomethane yield by controlling fermentation type of acidogenic phase in two-phase anaerobic co-digestion of food waste and rice straw. Chemical Engineering Journal 273, 254–260.

Chen, Y., Cheng, J.J., Creamer, K.S., 2008. Inhibition of anaerobic digestion process: A review. Bioresource Technology 99, 4044–4064.

Chen, Y., Luo, J., Yan, Y., Feng, L., 2013. Enhanced production of short-chain fatty acid by co-fermentation of waste activated sludge and kitchen waste under alkaline conditions and its application to microbial fuel cells. Applied Energy 102, 1197–1204.

Chinellato, G., Cavinato, C., Bolzonella, D., Heaven, S., Banks, C.J., 2013. Biohydrogen production from food waste in batch and semi-continuous conditions: Evaluation of a two-phase approach with digestate recirculation for pH control. International Journal of Hydrogen Energy 38, 4351–4360.

Cho, J.K., Park, S.C., Chang, H.N., 1995. Biochemical methane potential and solid state anaerobic digestion of Korean food wastes. Bioresource Technology 52, 245–253.

Cho, S.-K., Im, W.-T., Kim, D.-H., Kim, M.-H., Shin, H.-S., Oh, S.-E., 2013. Dry anaerobic digestion of food waste under mesophilic conditions: Performance and methanogenic community analysis. Bioresource Technology 131, 210–217.

Chu, C.-F., Ebie, Y., Xu, K.-Q., Li, Y.-Y., Inamori, Y., 2010. Characterization of microbial community in the two-stage process for hydrogen and methane production from food waste. International journal of hydrogen energy 35, 8253–8261.

Chu, C.-F., Xu, K.-Q., Li, Y.-Y., Inamori, Y., 2012. Hydrogen and methane potential based on the nature of food waste materials in a two-stage thermophilic fermentation process. International Journal of Hydrogen Energy 37, 10611–10618.

Chynoweth, D.P., Owens, J.M., Legrand, R., 2001. Renewable methane from anaerobic digestion of biomass. Renewable Energy 22, 1–8.

Climenhaga, M.A., Banks, C.J., 2008. Anaerobic digestion of catering wastes: effect of micronutrients and solids retention time. Water Science & Technology 57, 687–692.

Cogan, M., Antizar-Ladislao, B., 2016. The ability of macroalgae to stabilise and optimise the anaerobic digestion of household food waste. Biomass and Bioenergy 86, 146–155.

Cooney, M.J., Lewis, K., Harris, K., Zhang, Q., Yan, T., 2016. Start up performance of biochar packed bed anaerobic digesters. Journal of Water Process Engineering 9, e7–e13.

Cruz Viggi, C., Rossetti, S., Fazi, S., Paiano, P., Majone, M., Aulenta, F., 2014. Magnetite particles triggering a faster and more robust syntrophic pathway of methanogenic propionate degradation. Environmental Science and Technology 48, 7536–7543.

Cuetos, M.J., Martinez, E.J., Moreno, R., Gonzalez, R., Otero, M., Gomez, X., 2016. Enhancing anaerobic digestion of poultry blood using activated carbon. Journal of Advanced Research 297–307.

Curry, N., Pillay, P., 2012. Biogas prediction and design of a food waste to energy system for the urban environment. Renewable Energy 41, 200–209.

Dahiya, S., Sarkar, O., Swamy, Y. V, Mohan, S.V., 2015. Acidogenic fermentation of food waste for volatile fatty acid production with co-generation of biohydrogen. Bioresource technology 182, 103–13.

Dai, X., Duan, N., Dong, B., Dai, L., 2013. High-solids anaerobic co-digestion of sewage sludge and food waste in comparison with mono digestions: Stability and performance. Waste Management 33, 308–316.

Dai, X., Li, X., Zhang, D., Chen, Y., Dai, L., 2016. Simultaneous enhancement of methane production and methane content in biogas from waste activated sludge and perennial ryegrass anaerobic co-digestion: The effects of pH and C/N ratio. Bioresource Technology 216, 323–330.

Dang, Y., Holmes, D.E., Zhao, Z., Woodard, T.L., Zhang, Y., Sun, D., Wang, L.-Y., Nevin, K.P., Lovley, D.R., 2016. Enhancing anaerobic digestion of complex organic waste with carbon-based conductive materials. Bioresource Technology 220, 516–522.

Dang, Y., Sun, D., Woodard, T.L., Wang, L.-Y., Nevin, K.P., Holmes, D.E., 2017. Stimulation of the anaerobic digestion of the dry organic fraction of municipal solid waste (OFMSW) with carbon-based conductive materials. Bioresource Technology 238, 30–38.

Danko, A.S., Pinheiro, F., Abreu, Â.A., Alves, M.M., 2008. Effect of methanogenic inhibitors, inocula type, and temperature on biohydrogen production from food components. Environmental Engineering and Management Journal 7, 531–536.

de Bok, F.A.M., Plugge, C.M., Stams, A.J.M., 2004. Interspecies electron transfer in methanogenic propionate degrading consortia. Water Research 38, 1368–1375.

Bibliography

De Clercq, D., Wen, Z., Fan, F., Caicedo, L., 2016. Biomethane production potential from restaurant food waste in megacities and project level-bottlenecks: A case study in Beijing. Renewable and Sustainable Energy Reviews 59, 1676–1685.

De Vrieze, J., Hennebel, T., Boon, N., Verstraete, W., 2012. Methanosarcina: The rediscovered methanogen for heavy duty biomethanation. Bioresource Technology 112, 1–9.

De Vrieze, J., De Lathouwer, L., Verstraete, W., Boon, N., 2013. High-rate iron-rich activated sludge as stabilizing agent for the anaerobic digestion of kitchen waste. Water Research 47, 3732–3741.

Defays, D., 1977. An efficient algorithm for a complete link method. The Computer Journal 20, 364–366.

Dobbs, R., Oppenheim, J., Thompson, F., Brinkman, M., Zornes, M., 2011. Resource Revolution: Meeting the world's energy, materials, food, and water needs. McKinsey Global Institute.

Drennan, M.F., DiStefano, T.D., 2014. High solids co-digestion of food and landscape waste and the potential for ammonia toxicity. Waste Management 34, 1289–1298.

Dubois, M., Gilles, K.A., Hamilton, J.K., Rebers, P.A., Smith, F., 1956. Colorimetric Method for Determination of Sugars and Related Substances. Analytical Chemistry 28, 350–356.

Dung Thi, N.B., Lin, C.-Y., Kumar, G., 2016. Waste-to-wealth for valorization of food waste to hydrogen and methane towards creating a sustainable ideal source of bioenergy. Journal of Cleaner Production 122, 29-41.

Ebner, J.H., Labatut, R.A., Lodge, J.S., Williamson, A.A., Trabold, T.A., 2016. Anaerobic co-digestion of commercial food waste and dairy manure: Characterizing biochemical parameters and synergistic effects. Waste Management 52, 286–294.

El-Mashad, H.M., McGarvey, J.A., Zhang, R., 2008. Performance and microbial analysis of anaerobic digesters treating food waste and dairy manure. Biological Engineering Transactions 1, 23-242.

El-Mashad, H.M., Zhang, R., 2010. Biogas production from co-digestion of dairy manure and food waste. Bioresource Technology 101, 4021–4028.

Elbeshbishy, E., Hafez, H., Dhar, B.R., Nakhla, G., 2011a. Single and combined effect of various pretreatment methods for biohydrogen production from food waste. International Journal of Hydrogen Energy 36, 11379–11387.

Elbeshbishy, E., Hafez, H., Nakhla, G., 2011b. Ultrasonication for biohydrogen production from food waste. International Journal of Hydrogen Energy 36, 2896–2903.

Elsamadony, M., Tawfik, A., Suzuki, M., 2015. Surfactant-enhanced biohydrogen production from organic fraction of municipal solid waste (OFMSW) via dry anaerobic digestion. Applied Energy 149, 272–282.

Eriksson, O., Bisaillon, M., Haraldsson, M., Sundberg, J., 2016. Enhancement of biogas production from food waste and sewage sludge – Environmental and economic life cycle performance. Journal of Environmental Management 175, 33–39.

European Community, 2011. RÈGLEMENT (UE) No 142/2011 DE LA COMMISSION du 25 février 2011.

European Community, 2009. RÈGLEMENT (CE) No 1069/2009 DU PARLEMENT

EUROPÉEN ET DU CONSEIL du 21 octobre 2009.

European Community, 1999. Directive 1999/31/EC on the landfill of waste, OJ L 182.

European Community, 1975. Directive 775/442/EEC on waste, OJ L194.

Facchin, V., Cavinato, C., Fatone, F., Pavan, P., Cecchi, F., Bolzonella, D., 2013. Effect of trace element supplementation on the mesophilic anaerobic digestion of food waste in batch trials: The influence of inoculum origin. Biochemical Engineering Journal 70, 71–77.

Fagbohungbe, M.O., Herbert, B.M.J., Hurst, L., Li, H., Usmani, S.Q., Semple, K.T., 2016. Impact of biochar on the anaerobic digestion of citrus peel waste. Bioresource Technology 216, 142–149.

Fagbohungbe, M.O., Herbert, B.M.J., Hurst, L., Ibeto, C.N., Li, H., Usmani, S.Q., Semple, K.T., 2017. The challenges of anaerobic digestion and the role of biochar in optimizing anaerobic digestion. Waste Management 61, 236–249.

FAO, 2012. Towards the future we want: end hunger and make the transition to sustainable agricultural and food systems. Rome.

Feng, X.M., Karlsson, A., Svensson, B.H., Bertilsson, S., 2010. Impact of trace element addition on biogas production from food industrial waste–linking process to microbial communities. FEMS microbiology ecology 74, 226–240.

Fernández, B., Porrier, P., Chamy, R., 2001. Effect of inoculum-substrate ratio on the start-up of solid waste anaerobic digesters. Water Science and Technology 44, 103–108.

Ferreira, L.C., Nilsen, P.J., Fdz-Polanco, F., Pérez-Elvira, S.I., 2014. Biomethane potential of wheat straw: Influence of particle size, water impregnation and thermal hydrolysis. Chemical Engineering Journal 242, 254–259.

Fisgativa, H., Tremier, A., Dabert, P., 2016. Characterizing the variability of food waste quality: A need for efficient valorisation through anaerobic digestion. Waste management (New York, N.Y.) 50, 264-274.

Fisgativa, H., Tremier, A., Le Roux, S., Bureau, C., Dabert, P., 2017. Understanding the anaerobic biodegradability of food waste: Relationship between the typological, biochemical and microbial characteristics. Journal of Environmental Management 188, 95–107.

Fitamo, T., Boldrin, A., Boe, K., Angelidaki, I., Scheutz, C., 2016. Co-digestion of food and garden waste with mixed sludge from wastewater treatment in continuously stirred tank reactors. Bioresource Technology 206, 245–254.

Fontanille, P., Kumar, V., Christophe, G., Nouaille, R., Larroche, C., 2012. Bioconversion of volatile fatty acids into lipids by the oleaginous yeast Yarrowia lipolytica. Bioresource technology 114, 443–9.

Forster-Carneiro, T., Pérez, M., Romero, L.I., 2008. Influence of total solid and inoculum contents on performance of anaerobic reactors treating food waste. Bioresource Technology 99, 6994–7002.

Fotidis, I.A., Wang, H., Fiedel, N.R., Luo, G., Karakashev, D.B., Angelidaki, I., 2014. Bioaugmentation as a solution to increase methane production from an ammonia-rich substrate. Environmental Science and Technology 48, 7669–7676.

Frølund, B., Palmgren, R., Keiding, K., Nielsen, P.H., 1996. Extraction of extracellular

polymers from activated sludge using a cation exchange resin. Water research 30, 1749–1758.

Ganesh, R., Torrijos, M., Sousbie, P., Steyer, J.P., Lugardon, A., Delgenes, J.P., 2013. Anaerobic co-digestion of solid waste: Effect of increasing organic loading rates and characterization of the solubilised organic matter. Bioresource technology 130, 559–69.

Ghanem, I.I.., Guowei, G., Jinfu, Z., 2001. Leachate production and disposal of kitchen food solid waste by dry fermentation for biogas generation. Renewable Energy 23, 673–684.

Ghimire, A., Frunzo, L., Pirozzi, F., Trably, E., Escudie, R., Lens, P.N.L., Esposito, G., 2015a. A review on dark fermentative biohydrogen production from organic biomass: Process parameters and use of by-products. Applied Energy 144, 73–95.

Ghimire, A., Valentino, S., Frunzo, L., Trably, E., Escudié, R., Pirozzi, F., Lens, P.N.L., Esposito, G., 2015b. Biohydrogen production from food waste by coupling semi-continuous dark-photofermentation and residue post-treatment to anaerobic digestion: A synergy for energy recovery. International Journal of Hydrogen Energy 40, 16045–16055.

Girotto, F., Alibardi, L., Cossu, R., 2015. Food waste generation and industrial uses: A review. Waste management (New York, N.Y.) 45, 32–41.

Gou, C., Yang, Z., Huang, J., Wang, H., Xu, H., Wang, L., 2014. Effects of temperature and organic loading rate on the performance and microbial community of anaerobic co-digestion of waste activated sludge and food waste. Chemosphere 105, 146–151.

Grim, J., Malmros, P., Schnürer, A., Nordberg, Å., 2015. Comparison of pasteurization and integrated thermophilic sanitation at a full-scale biogas plant – Heat demand and biogas production. Energy 79, 419–427.

Grimberg, S.J., Hilderbrandt, D., Kinnunen, M., Rogers, S., 2015. Anaerobic digestion of food waste through the operation of a mesophilic two-phase pilot scale digester – Assessment of variable loadings on system performance. Bioresource Technology 178, 226–229.

Grootscholten, T.I.M., Kinsky dal Borgo, F., Hamelers, H.V.M., Buisman, C.J.N., 2013. Promoting chain elongation in mixed culture acidification reactors by addition of ethanol. Biomass and Bioenergy 48, 10–16.

Gunders, D., 2012. Wasted: How America is losing up to 40 percent of its food from farm to fork to landfill, National Resource Defense Council Issue Paper.

Guo, X.M., Trably, E., Latrille, E., Carrere, H., Steyer, J.-P., 2014. Predictive and explicative models of fermentative hydrogen production from solid organic waste: Role of butyrate and lactate pathways. International Journal of Hydrogen Energy 39, 7476–7485.

Gustavsson, J., Cederberg, C., Sonesson, U., 2011. Global food losses and food waste: Extent, causes and prevention, FAO-Food and Agriculture Organization of the United Nations.

Hafner, S.D., Bisogni, J.J., 2009. Modeling of ammonia speciation in anaerobic digesters. Water Research 43, 4105–4114.

Haider, M.R., Zeshan, Yousaf, S., Malik, R.N., Visvanathan, C., 2015. Effect of mixing ratio of food waste and rice husk co-digestion and substrate to inoculum ratio on biogas production. Bioresource technology 190, 451–457.

Han, S.-K., Shin, H.-S., 2004. Biohydrogen production by anaerobic fermentation of food waste. International Journal of Hydrogen Energy 29, 569–577.

Han, W., Liu, D.N., Shi, Y.W., Tang, J.H., Li, Y.F., Ren, N.Q., 2015a. Biohydrogen production from food waste hydrolysate using continuous mixed immobilized sludge reactors. Bioresource technology 180, 54–8.

Han, W., Ye, M., Zhu, A.J., Zhao, H.T., Li, Y.F., 2015b. Batch dark fermentation from enzymatic hydrolyzed food waste for hydrogen production. Bioresource technology 191, 24–9.

Han, W., Fang, J., Liu, Z., Tang, J., 2016. Techno-economic evaluation of a combined bioprocess for fermentative hydrogen production from food waste. Bioresource Technology 202, 107–112.

Hao, L., Lü, F., Mazéas, L., Desmond-Le Quéméner, E., Madigou, C., Guenne, A., Shao, L., Bouchez, T., He, P., 2015. Stable isotope probing of acetate fed anaerobic batch incubations shows a partial resistance of acetoclastic methanogenesis catalyzed by Methanosarcina to sudden increase of ammonia level. Water Resource 59, 90-99.

He, M., Sun, Y., Zou, D., Yuan, H., Zhu, B., Li, X., Pang, Y., 2012. Influence of Temperature on Hydrolysis Acidification of Food Waste. Procedia Environmental Sciences 16, 85–94.

Heo, N.H., Park, S.C., Lee, J.S., Kang, H., Park, D.H., 2003. Single-stage anaerobic codigestion for mixture wastes of simulated Korean food waste and waste activated sludge. Applied biochemistry and biotechnology 105–108, 567–579.

Hogg, D., Favoino, E., Nielsen, N., Thompson, J., Wood, K., Penschke, A., Papageorgiou, D., Economides, S., 2002. Economic analysis of options for managing biodegradable municipal waste, Final Report to the European Commission. Bristol, UNITED KINGDOM.

Holmes, D.E., Shrestha, P.M., Walker, D.J.F., Dang, Y., Nevin, K.P., Woodard, T.L., Lovley, D.R., 2017. Metatranscriptomic evidence for direct interspecies electron transfer between Geobacter and Methanothrix species in methanogenic rice paddy soils. Applied and Environmental Microbiology 83.

Hong, C., Haiyun, W., 2010. Optimization of volatile fatty acid production with co-substrate of food wastes and dewatered excess sludge using response surface methodology. Bioresource technology 101, 5487–93.

Iacovidou, E., Ohandja, D.-G., Voulvoulis, N., 2012. Food waste co-digestion with sewage sludge – Realising its potential in the UK. Journal of Environmental Management 112, 267–274.

Ismail, F., Abd-Aziz, S., MeiLing, C., Hassan, M.A., 2009. Statistical optimization of biohydrogen production using food waste under thermophilic conditions. Open Renewable Energy Journal 2, 124-131.

Izumi, K., Okishio, Y., Nagao, N., Niwa, C., Yamamoto, S., Toda, T., 2010. Effects of particle size on anaerobic digestion of food waste. International Biodeterioration & Biodegradation 64, 601–608.

Jabeen, M., Yousaf, S., Haider, M.R., Malik, R.N., 2015. High-solids anaerobic co-digestion of food waste and rice husk at different organic loading rates. International Biodeterioration & Biodegradation 102, 149–153.

Jang, S., Kim, D.-H., Yun, Y.-M., Lee, M.-K., Moon, C., Kang, W.-S., Kwak, S.-S., Kim, M.-S., 2015. Hydrogen fermentation of food waste by alkali-shock pretreatment: microbial community analysis and limitation of continuous operation. Bioresource technology 186, 215–22.

Jiang, J., Zhang, Y., Li, K., Wang, Q., Gong, C., Li, M., 2013. Volatile fatty acids production from food waste: effects of pH, temperature, and organic loading rate. Bioresource technology 143, 525–30.

Jiang, Y., Banks, C., Zhang, Y., Heaven, S., Longhurst, P., 2017. Quantifying the percentage of methane formation via acetoclastic and syntrophic acetate oxidation pathways in anaerobic digesters. Waste Management, *In Press*.

Jimenez, J., Vedrenne, F., Denis, C., Mottet, A., Déléris, S., Steyer, J.-P., Rivero, J.A.C., 2013. A statistical comparison of protein and carbohydrate characterisation methodology applied on sewage sludge samples. Water Research 47, 1751–1762.

Jimenez, J., Aemig, Q., Doussiet, N., Steyer, J.-P., Houot, S., Patureau, D., 2015. A new organic matter fractionation methodology for organic wastes: bioaccessibility and complexity characterization for treatment optimization. Bioresource Technology 194, 344–353.

Jin, Y., Chen, T., Chen, X., Yu, Z., 2015. Life-cycle assessment of energy consumption and environmental impact of an integrated food waste-based biogas plant. Applied Energy 151, 227–236.

Kangle, K.M., Kore, S. V., Kore, V.S., Kulkarni, G.S., 2010. Recent Trends in Anaerobic Codigestion: A Review. Universal Journal of Environmental Research and Technology 2, 210–219.

Karthikeyan, O.P., Visvanathan, C., 2013. Bio-energy recovery from high-solid organic substrates by dry anaerobic bio-conversion processes: a review. Reviews in Environmental Science and Bio/Technology 12, 257–284.

Karthikeyan, O.P., Selvam, A., Wong, J.W.C., 2016. Hydrolysis-acidogenesis of food waste in solid-liquid-separating continuous stirred tank reactor (SLS-CSTR) for volatile organic acid production. Bioresource technology 200, 366–73.

Kawai, M., Nagao, N., Tajima, N., Niwa, C., Matsuyama, T., Toda, T., 2014. The effect of the labile organic fraction in food waste and the substrate/inoculum ratio on anaerobic digestion for a reliable methane yield. Bioresource Technology 157, 174–180.

Kenealy, W.R., Cao, Y., Weimer, P.J., 1995. Production of caproic acid by cocultures of ruminal cellulolytic bacteria and Clostridium kluyveri grown on cellulose and ethanol. Applied Microbiology and Biotechnology 44, 507–513.

Khanal, S.K., Chen, W.-H., Li, L., Sung, S., 2004. Biological hydrogen production: effects of pH and intermediate products. International Journal of Hydrogen Energy 29, 1123–1131.

Khoo, H.H., Lim, T.Z., Tan, R.B.H., 2010. Food waste conversion options in Singapore: environmental impacts based on an LCA perspective. The Science of the total environment 408, 1367–73.

Kim, D.-H., Kim, S.-H., Shin, H.-S., 2009. Hydrogen fermentation of food waste without inoculum addition. Enzyme and Microbial Technology 45, 181–187.

Kim, D.-H., Kim, S.-H., Kim, K.-Y., Shin, H.-S., 2010. Experience of a pilot-scale hydrogen-producing anaerobic sequencing batch reactor (ASBR) treating food waste. International Journal of Hydrogen Energy 35, 1590–1594.

Kim, D.-H., Oh, S.-E., 2011. Continuous high-solids anaerobic co-digestion of organic solid wastes under mesophilic conditions. Waste Management 31, 1943–1948.

Kim, D.-H., Kim, S.-H., Jung, K.-W., Kim, M.-S., Shin, H.-S., 2011a. Effect of initial pH

independent of operational pH on hydrogen fermentation of food waste. Bioresource technology 102, 8646–52.

Kim, D.-H., Kim, S.-H., Kim, H.-W., Kim, M.-S., Shin, H.-S., 2011b. Sewage sludge addition to food waste synergistically enhances hydrogen fermentation performance. Bioresource technology 102, 8501–6.

Kim, D.-H., Wu, J., Jeong, K.-W., Kim, M.-S., Shin, H.-S., 2011c. Natural inducement of hydrogen from food waste by temperature control. International Journal of Hydrogen Energy 36, 10666–10673.

Kim, D.-H., Kim, M.-S., 2013. Development of a novel three-stage fermentation system converting food waste to hydrogen and methane. Bioresource technology 127, 267–74.

Kim, D.-H., Lee, M.-K., Jung, K.-W., Kim, M.-S., 2013. Alkali-treated sewage sludge as a seeding source for hydrogen fermentation of food waste leachate. International Journal of Hydrogen Energy 38, 15751–15756.

Kim, D.-H., Jang, S., Yun, Y.-M., Lee, M.-K., Moon, C., Kang, W.-S., Kwak, S.-S., Kim, M.-S., 2014. Effect of acid-pretreatment on hydrogen fermentation of food waste: Microbial community analysis by next generation sequencing. International Journal of Hydrogen Energy 39, 16302–16309.

Kim, H.-W., Nam, J.-Y., Shin, H.-S., 2011. A comparison study on the high-rate co-digestion of sewage sludge and food waste using a temperature-phased anaerobic sequencing batch reactor system. Bioresource Technology 102, 7272–7279.

Kim, H.J., Kim, S.H., Choi, Y.G., Kim, G.D., Chung, T.H., 2006. Effect of enzymatic pretreatment on acid fermentation of food waste. Journal of Chemical Technology and Biotechnology 81, 974–980.

Kim, M.-S., Na, J.-G., Lee, M.-K., Ryu, H., Chang, Y.-K., Triolo, J.M., Yun, Y.-M., Kim, D.-H., 2016. More value from food waste: lactic acid and biogas recovery. Water Research 96, 208-216.

Kim, M., Chowdhury, M.M.I., Nakhla, G., Keleman, M., 2017. Synergism of co-digestion of food wastes with municipal wastewater treatment biosolids. Waste Management 61, 473–483.

Kim, S.-H., Shin, H.-S., 2008. Effects of base-pretreatment on continuous enriched culture for hydrogen production from food waste. International Journal of Hydrogen Energy 33, 5266–5274.

Kim, S.-H., Han, S.-K., Shin, H.-S., 2008. Optimization of continuous hydrogen fermentation of food waste as a function of solids retention time independent of hydraulic retention time. Process Biochemistry 43, 213–218.

Kim, S.-H., Cheon, H.-C., Lee, C.-Y., 2012. Enhancement of hydrogen production by recycling of methanogenic effluent in two-phase fermentation of food waste. International Journal of Hydrogen Energy 37, 13777–13782.

Kiran, E.U., Trzcinski, A.P., Liu, Y., 2015. Enhancing the hydrolysis and methane production potential of mixed food waste by an effective enzymatic pretreatment. Bioresource technology 183, 47–52.

Kjerstadius, H., la Cour Jansen, J., De Vrieze, J., Haghighatafshar, S., Davidsson, Å., 2013. Hygienization of sludge through anaerobic digestion at 35, 55 and 60° C. Water Science & Technology 68, 2234–2239.

Klappenbach, J., Saxman, P., Cole, J., Schmidt, T., 2001. rrndb: the Ribosomal RNA Operon Copy Number Database. Nucleic Acids Research 29, 181–184.

Kobayashi, T., Xu, K.-Q., Li, Y.-Y., Inamori, Y., 2012. Effect of sludge recirculation on characteristics of hydrogen production in a two-stage hydrogen–methane fermentation process treating food wastes. International Journal of Hydrogen Energy 37, 5602–5611.

Koch, K., Plabst, M., Schmidt, A., Helmreich, B., Drewes, J.E., 2016. Co-digestion of food waste in a municipal wastewater treatment plant: Comparison of batch tests and full-scale experiences. Waste management (New York, N.Y.) 47, 28–33.

Koike, Y., An, M.-Z., Tang, Y.-Q., Syo, T., Osaka, N., Morimura, S., Kida, K., 2009. Production of fuel ethanol and methane from garbage by high-efficiency two-stage fermentation process. Journal of bioscience and bioengineering 108, 508–12.

Komemoto, K., Lim, Y.G., Nagao, N., Onoue, Y., Niwa, C., Toda, T., 2009. Effect of temperature on VFA's and biogas production in anaerobic solubilization of food waste. Waste Management 29, 2950–2955.

Kondusamy, D., Kalamdhad, A.S., 2014. Pre-treatment and anaerobic digestion of food waste for high rate methane production – A review. Journal of Environmental Chemical Engineering 2, 1821–1830.

Kong, X., Wei, Y., Xu, S., Liu, J., Li, H., Liu, Y., Yu, S., 2016a. Inhibiting excessive acidification using zero-valent iron in anaerobic digestion of food waste at high organic load rates. Bioresource Technology 211, 65–71.

Kong, X., Xu, S., Liu, J., Li, H., Zhao, K., He, L., 2016b. Enhancing anaerobic digestion of high-pressure extruded food waste by inoculum optimization. Journal of environmental management 166, 31–7.

Kosseva, M.R., 2009. Processing of food wastes. Advances in food and nutrition research 58, 57–136.

Kumar, M., Ou, Y.-L., Lin, J.-G., 2010. Co-composting of green waste and food waste at low C/N ratio. Waste management (New York, N.Y.) 30, 602–9.

Labatut, R.A., Angenent, L.T., Scott, N.R., 2011. Biochemical methane potential and biodegradability of complex organic substrates. Bioresource technology 102, 2255–64.

Laothanachareon, T., Kanchanasuta, S., Mhuanthong, W., Phalakornkule, C., Pisutpaisal, N., Champreda, V., 2014. Analysis of microbial community adaptation in mesophilic hydrogen fermentation from food waste by tagged 16S rRNA gene pyrosequencing. Journal of environmental management 144, 143–51.

Latif, M.A., Ahmad, A., Ghufran, R., Wahid, Z.A., 2012. Effect of temperature and organic loading rate on upflow anaerobic sludge blanket reactor and CH4 production by treating liquidized food waste. Environmental Progress & Sustainable Energy 31, 114–121.

Le, C., Stuckey, D.C., 2017. The Influence of Feeding Composition on The Production of Soluble Microbial Products (SMPs) in Anaerobic Digestion, in: 1st International ABWET Conference : Waste-to-Bioenergy : Applications in Urban Areas. Paris, 116–117.

Lee, D.-Y., Ebie, Y., Xu, K.-Q., Li, Y.-Y., Inamori, Y., 2010. Continuous H2 and CH4 production from high-solid food waste in the two-stage thermophilic fermentation process with the recirculation of digester sludge. Bioresource technology 101 Suppl, S42-7.

Lee, D.-Y., Xu, K.-Q., Kobayashi, T., Li, Y.-Y., Inamori, Y., 2014. Effect of organic loading rate on continuous hydrogen production from food waste in submerged anaerobic membrane bioreactor. International Journal of Hydrogen Energy 39, 16863–16871.

Lee, D.H., Behera, S.K., Kim, J.W., Park, H.-S., 2009. Methane production potential of leachate generated from Korean food waste recycling facilities: A lab-scale study. Waste Management 29, 876–882.

Lee, J.Y., Lee, S.H., Park, H.D., 2016. Enrichment of specific electro-active microorganisms and enhancement of methane production by adding granular activated carbon in anaerobic reactors. Bioresource Technology 205, 205–212.

Lee, Y.-W., Chung, J., 2010. Bioproduction of hydrogen from food waste by pilot-scale combined hydrogen/methane fermentation. International Journal of Hydrogen Energy 35, 11746–11755.

Levin, D.B., Pitt, L., Love, M., 2004. Biohydrogen production: prospects and limitations to practical application. International Journal of Hydrogen Energy 29, 173–185.

Li, M., Zhao, Y., Guo, Q., Qian, X., Niu, D., 2008. Bio-hydrogen production from food waste and sewage sludge in the presence of aged refuse excavated from refuse landfill. Renewable Energy 33, 2573–2579.

Li, R., Chen, S., Li, X., Saifullah Lar, J., He, Y., Zhu, B., 2009. Anaerobic codigestion of kitchen waste with cattle manure for biogas production. Energy & Fuels 23, 2225–2228.

Li, R., Chen, S., Li, X., 2010. Biogas production from anaerobic co-digestion of food waste with dairy manure in a two-phase digestion system. Applied biochemistry and biotechnology 160, 643–654.

Li, S.-L., Lin, J.-S., Wang, Y.-H., Lee, Z.-K., Kuo, S.-C., Tseng, I.-C., Cheng, S.-S., 2011. Strategy of controlling the volumetric loading rate to promote hydrogen-production performance in a mesophilic-kitchen-waste fermentor and the microbial ecology analyses. Bioresource technology 102, 8682–7.

Liao, X., Zhu, S., Zhong, D., Zhu, J., Liao, L., 2014. Anaerobic co-digestion of food waste and landfill leachate in single-phase batch reactors. Waste Management 34, 2278–2284.

Lim, J.W., Wang, J.-Y., 2013. Enhanced hydrolysis and methane yield by applying microaeration pretreatment to the anaerobic co-digestion of brown water and food waste. Waste management (New York, N.Y.) 33, 813–9.

Lim, J.W., Chen, C.-L., Ho, I.J.R., Wang, J.-Y., 2013. Study of microbial community and biodegradation efficiency for single- and two-phase anaerobic co-digestion of brown water and food waste. Bioresource technology 147, 193–201.

Lim, J.W., Chiam, J.A., Wang, J.-Y., 2014. Microbial community structure reveals how microaeration improves fermentation during anaerobic co-digestion of brown water and food waste. Bioresource technology 171, 132–8.

Lim, S.-J., Choi, D.W., Lee, W.G., Kwon, S., Chang, H.N., 2000. Volatile fatty acids production from food wastes and its application to biological nutrient removal. Bioprocess Engineering 22, 543–545.

Lim, S.-J., Kim, B.J., Jeong, C.-M., Choi, J., Ahn, Y.H., Chang, H.N., 2008. Anaerobic organic acid production of food waste in once-a-day feeding and drawing-off bioreactor. Bioresource technology 99, 7866–74.

Lin, C.S.K., Pfaltzgraff, L.A., Herrero-Davila, L., Mubofu, E.B., Solhy, A., Clark, P.J.,

Koutinas, A., Kopsahelis, N., Stamatelatou, K., Dickson, F., Thankappan, S., Zahouily, M., Brocklesby, R., Luque, R., 2013. Food waste as a valuable resource for the production of chemicals, materials and fuels. Current situation and global perspective. Energy & Environmental Science 426–464.

Lin, J., Zuo, J., Gan, L., Li, P., Liu, F., Wang, K., Chen, L., Gan, H., 2011. Effects of mixture ratio on anaerobic co-digestion with fruit and vegetable waste and food waste of China. Journal of Environmental Sciences 23, 1403–1408.

Linville, J.L., Shen, Y., Ignacio-de Leon, P.A., Schoene, R.P., Urgun-Demirtas, M., 2017. In-situ biogas upgrading during anaerobic digestion of food waste amended with walnut shell biochar at bench scale. Waste Management & Research 35, 669-679.

Liu, F., Rotaru, A.-E., Shrestha, P.M., Malvankar, N.S., Nevin, K.P., Lovley, D.R., 2012. Promoting direct interspecies electron transfer with activated carbon. Energy & Environmental Science 5, 8982-8989.

Liu, G., Zhang, R., El-Mashad, H.M., Dong, R., 2009. Effect of feed to inoculum ratios on biogas yields of food and green wastes. Bioresource Technology 100, 5103–5108.

Liu, X., Li, R., Ji, M., Han, L., 2013. Hydrogen and methane production by co-digestion of waste activated sludge and food waste in the two-stage fermentation process: substrate conversion and energy yield. Bioresource technology 146, 317–23.

Liu, X., Wang, W., Gao, X., Zhou, Y., Shen, R., 2012. Effect of thermal pretreatment on the physical and chemical properties of municipal biomass waste. Waste Management 32, 249–255.

Lorenz, H., Fischer, P., Schumacher, B., Adler, P., 2013. Current EU-27 technical potential of organic waste streams for biogas and energy production. Waste Management 33, 2434–2448.

Lovley, D.R., 2017. Syntrophy Goes Electric: Direct Interspecies Electron Transfer. Annual Review of Microbiology 71, 643-664.

Lowry, O.H., 1951. Protein Measurement by Folin Reagent. Journal of Biological Chemistry 193, 265–276.

Lü, F., Hao, L., Zhu, M., Shao, L., He, P., 2012. Initiating methanogenesis of vegetable waste at low inoculum-to-substrate ratio: importance of spatial separation. Bioresource technology 105, 169–73.

Lü, F., Zhou, Q., Wu, D., Wang, T., Shao, L., He, P., 2015. Dewaterability of anaerobic digestate from food waste: Relationship with extracellular polymeric substances. Chemical Engineering Journal 262, 932–938.

Lü, F., Xu, X., Shao, L., He, P., 2016. Importance of storage time in mesophilic anaerobic digestion of food waste. Journal of Environmental Sciences 45, 76-83.

Lu, J., Li, D., Chen, L., Kitamura, Y., Jiang, W., Li, B., 2013. Simultaneous pretreatment and acidogenesis of solid food wastes by a rotational drum fermentation system with methanogenic leachate recirculation and andesite porphyry addition. Bioresource technology 138, 101–8.

Luo, C., Lü, F., Shao, L., He, P., 2015. Application of eco-compatible biochar in anaerobic digestion to relieve acid stress and promote the selective colonization of functional microbes. Water Research 68, 710–718.

Luo, G., Angelidaki, I., 2013. Co-digestion of manure and whey for in situ biogas upgrading

by the addition of H2: process performance and microbial insights. Applied microbiology and biotechnology 97, 1373–1381.

Ma, H., Xing, Y., Yu, M., Wang, Q., 2014. Feasibility of converting lactic acid to ethanol in food waste fermentation by immobilized lactate oxidase. Applied Energy 129, 89–93.

Ma, J., Duong, T.H., Smits, M., Verstraete, W., Carballa, M., 2011. Enhanced biomethanation of kitchen waste by different pre-treatments. Bioresource technology 102, 592–9.

Mantzouridou, F.T., Paraskevopoulou, A., Lalou, S., 2015. Yeast flavour production by solid state fermentation of orange peel waste. Biochemical Engineering Journal 101, 1–8.

Mao, C., Feng, Y., Wang, X., Ren, G., 2015. Review on research achievements of biogas from anaerobic digestion. Renewable and Sustainable Energy Reviews 45, 540–555.

Marañón, E., Castrillón, L., Quiroga, G., Fernández-Nava, Y., Gómez, L., García, M.M., 2012. Co-digestion of cattle manure with food waste and sludge to increase biogas production. Waste Management 32, 1821–1825.

Marin, J., Kennedy, K.J., Eskicioglu, C., 2010. Effect of microwave irradiation on anaerobic degradability of model kitchen waste. Waste management (New York, N.Y.) 30, 1772–9.

Mata-Alvarez, J., Cecchi, F., Llabrés, P., Pavan, P., 1992. Anaerobic digestion of the Barcelona central food market organic wastes. Plant design and feasibility study. Bioresource Technology 42, 33–42.

Mata-Alvarez, J., Dosta, J., Macé, S., Astals, S., 2011. Codigestion of solid wastes: a review of its uses and perspectives including modeling. Critical reviews in biotechnology 31, 99–111.

Mata-Alvarez, J., Dosta, J., Romero-Güiza, M.S., Fonoll, X., Peces, M., Astals, S., 2014. A critical review on anaerobic co-digestion achievements between 2010 and 2013. Renewable and Sustainable Energy Reviews 36, 412–427.

Maus, I., Wibberg, D., Stantscheff, R., Eikmeyer, F.G., Seffner, A., Boelter, J., Szczepanowski, R., Blom, J., Jaenicke, S., König, H., Pühler, A., Schlüter, A., 2012. Complete genome sequence of the hydrogenotrophic, methanogenic archaeon Methanoculleus bourgensis strain MS2T, isolated from a sewage sludge digester. Journal of Bacteriology 194, 5487–5488.

Mekjinda, N., Ritchie, R.J., 2015. Breakdown of food waste by anaerobic fermentation and non-oxygen producing photosynthesis using a photosynthetic bacterium. Waste management (New York, N.Y.) 35, 199–206.

Melikoglu, M., Lin, C.S.K., Webb, C., 2013. Analysing global food waste problem: pinpointing the facts and estimating the energy content. Central European Journal of Engineering 3, 157–164.

Meng, Y., Li, S., Yuan, H., Zou, D., Liu, Y., Zhu, B., Chufo, A., Jaffar, M., Li, X., 2015. Evaluating biomethane production from anaerobic mono- and co-digestion of food waste and floatable oil (FO) skimmed from food waste. Bioresource technology 185, 7–13.

Micolucci, F., Gottardo, M., Bolzonella, D., Pavan, P., 2014. Automatic process control for stable bio-hythane production in two-phase thermophilic anaerobic digestion of food waste. International Journal of Hydrogen Energy 39, 17563–17572.

Monier, V., Mudgal, S., Escalon, V., O'Connor, C., Anderson, G., Montoux, H., Reisinger, H., Dolley, P., Oglivie, S., Morton, G., 2010. Preparatory study on food waste across EU 27.

Monlau, F., Sambusiti, C., Antoniou, N., Barakat, A., Zabaniotou, A., 2015. A new concept for enhancing energy recovery from agricultural residues by coupling anaerobic digestion and pyrolysis process. Applied Energy 148, 32–38.

Moscoviz, R., Trably, E., Bernet, N., 2016. Consistent 1,3-propanediol production from glycerol in mixed culture fermentation over a wide range of pH. Biotechnology for biofuels 9, 32.

Moscoviz, R., de Fouchécour, F., Santa-Catalina, G., Bernet, N., Trably, E., 2017. Cooperative growth of Geobacter sulfurreducens and Clostridium pasteurianum with subsequent metabolic shift in glycerol fermentation. Scientific Reports 7, 44334.

Motte, J.-C., Trably, E., Escudié, R., Hamelin, J., Steyer, J.-P., Bernet, N., Delgenes, J.-P., Dumas, C., 2013. Total solids content: a key parameter of metabolic pathways in dry anaerobic digestion. Biotechnology for biofuels 6, 164.

Motte, J.-C., Escudié, R., Beaufils, N., Steyer, J.-P., Bernet, N., Delgenès, J.-P., Dumas, C., 2014a. Morphological structures of wheat straw strongly impacts its anaerobic digestion. Industrial Crops and Products 52, 695–701.

Motte, J.-C., Trably, E., Hamelin, J., Escudié, R., Bonnafous, A., Steyer, J.-P., Bernet, N., Delgenes, J.-P., Dumas, C., 2014b. Total solid content drives hydrogen production through microbial selection during thermophilic fermentation. Bioresource Technology 166, 610–615.

Motte, J.-C., Watteau, F., Escudié, R., Steyer, J.-P., Bernet, N., Delgenes, J.-P., Dumas, C., 2015. Dynamic observation of the biodegradation of lignocellulosic tissue under solid-state anaerobic conditions. Bioresource Technology 191, 322–326.

Mumme, J., Srocke, F., Heeg, K., Werner, M., 2014. Use of biochars in anaerobic digestion. Bioresource Technology 164, 189–197.

Nagao, N., Tajima, N., Kawai, M., Niwa, C., Kurosawa, N., Matsuyama, T., Yusoff, F.M., Toda, T., 2012. Maximum organic loading rate for the single-stage wet anaerobic digestion of food waste. Bioresource Technology 118, 210–218.

Nakamura, K., Takahashi, A., Mori, C., Tamaki, H., Mochimaru, H., Nakamura, K., Takamizawa, K., Kamagata, Y., 2013. Methanothermobacter tenebrarum sp. nov., a hydrogenotrophic, thermophilic methanogen isolated from gas-associated formation water of a natural gas field. International Journal of Systematic and Evolutionary Microbiology 63, 715–722.

Nand, K., Sumithra Devi, S., Viswanath, P., Deepak, S., Sarada, R., 1991. Anaerobic digestion of canteen wastes for Biogas production: process optimisation. Process Biochemistry 26, 1–5.

Nathao, C., Sirisukpoka, U., Pisutpaisal, N., 2013. Production of hydrogen and methane by one and two stage fermentation of food waste. International Journal of Hydrogen Energy 38, 15764–15769.

Nazlina, H.M.Y., Aini, A.R.N., Ismail, F., Yusof, M.Z.M., Hassan, M.A., 2009. Effect of different temperature, initial pH and substrate composition on biohydrogen production from food waste in batch fermentation. Asian Journal of Biotechnology 1, 42–50.

Neves, L., Oliveira, R., Alves, M.M., 2004. Influence of inoculum activity on the bio-methanization of a kitchen waste under different waste/inoculum ratios. Process Biochemistry 39, 2019–2024.

Neves, L., Gonçalo, E., Oliveira, R., Alves, M.M., 2008. Influence of composition on the biomethanation potential of restaurant waste at mesophilic temperatures. Waste Management 28, 965–972.

Neves, L., Oliveira, R., Alves, M.M., 2009. Fate of LCFA in the co-digestion of cow manure, food waste and discontinuous addition of oil. Water Research 43, 5142–5150.

Owamah, H.I., Dahunsi, S.O., Oranusi, U.S., Alfa, M.I., 2014. Fertilizer and sanitary quality of digestate biofertilizer from the co-digestion of food waste and human excreta. Waste Management 34, 747–752.

Owamah, H.I., Izinyon, O.C., 2015. The effect of organic loading rates (OLRs) on the performances of food wastes and maize husks anaerobic co-digestion in continuous mode. Sustainable Energy Technologies and Assessments 11, 71–76.

Pagliaccia, P., Gallipoli, A., Gianico, A., Montecchio, D., Braguglia, C.M., 2016. Single stage anaerobic bioconversion of food waste in mono and co-digestion with olive husks: Impact of thermal pretreatment on hydrogen and methane production. International Journal of Hydrogen Energy 41, 905–915.

Pan, J., Zhang, R., El-Mashad, H.M., Sun, H., Ying, Y., 2008. Effect of food to microorganism ratio on biohydrogen production from food waste via anaerobic fermentation. International Journal of Hydrogen Energy 33, 6968–6975.

Pan, J., Chen, X., Sheng, K., Yu, Y., Zhang, C., Ying, Y., 2013. Effect of ammonia on biohydrogen production from food waste via anaerobic fermentation. International Journal of Hydrogen Energy 38, 12747–12754.

Papanikolaou, S., Dimou, A., Fakas, S., Diamantopoulou, P., Philippoussis, A., Galiotou-Panayotou, M., Aggelis, G., 2011. Biotechnological conversion of waste cooking olive oil into lipid-rich biomass using Aspergillus and Penicillium strains. Journal of applied microbiology 110, 1138–1150.

Pedizzi, C., Lema, J.M., Carballa, M., 2017. Enhancing thermophilic co-digestion of nitrogen-rich substrates by air side-stream stripping. Bioresource Technology 241, 397–405.

Pham, T.P.T., Kaushik, R., Parshetti, G.K., Mahmood, R., Balasubramanian, R., 2014. Food-waste-to-energy conversion technologies: Current status and future directions. Waste Management 38, 399–408.

Pisutpaisal, N., Nathao, C., Sirisukpoka, U., 2014. Biological Hydrogen and Methane Production in from Food Waste in Two-stage CSTR. Energy Procedia 50, 719–722.

Pleissner, D., Lau, K.Y., Schneider, R., Venus, J., Lin, C.S.K., 2015. Fatty acid feedstock preparation and lactic acid production as integrated processes in mixed restaurant food and bakery wastes treatment. Food Research International 73, 52–61.

Poirier, S., Desmond-Le Quéméner, E., Madigou, C., Bouchez, T., Chapleur, O., 2016. Anaerobic digestion of biowaste under extreme ammonia concentration: Identification of key microbial phylotypes. Bioresource Technology 207, 92–101.

Pretel, R., Moñino, P., Robles, A., Ruano, M.V., Seco, A., Ferrer, J., 2016. Economic and environmental sustainability of an AnMBR treating urban wastewater and organic fraction of municipal solid waste. Journal of Environmental Management 179, 83–92.

Prévoteau, A., Ronsse, F., Cid, I., Boeckx, P., Rabaey, K., 2016. The electron donating capacity of biochar is dramatically underestimated. Scientific Reports 6, 32870.

Qiang, H., Lang, D.-L., Li, Y.-Y., 2012. High-solid mesophilic methane fermentation of food

waste with an emphasis on Iron, Cobalt, and Nickel requirements. Bioresource technology 103, 21–7.

Qiang, H., Niu, Q., Chi, Y., Li, Y., 2013. Trace metals requirements for continuous thermophilic methane fermentation of high-solid food waste. Chemical Engineering Journal 222, 330–336.

Qu, X., Vavilin, V.A., Mazéas, L., Lemunier, M., Duquennoi, C., He, P.J., Bouchez, T., 2009. Anaerobic biodegradation of cellulosic material: Batch experiments and modelling based on isotopic data and focusing on aceticlastic and non-aceticlastic methanogenesis. Waste Management 29, 1828–1837.

Rago, Y.P., Surroop, D., Mohee, R., 2017. Assessing the potential of biofuel (biochar) production from food wastes through thermal treatment. Bioresource Technology, *In Press*.

Rajagopal, R., Lim, J.W., Mao, Y., Chen, C.-L., Wang, J.-Y., 2013a. Anaerobic co-digestion of source segregated brown water (feces-without-urine) and food waste: for Singapore context. The Science of the total environment 443, 877–86.

Rajagopal, R., Massé, D.I., Singh, G., 2013b. A critical review on inhibition of anaerobic digestion process by excess ammonia. Bioresource Technology 143, 632–641.

Rama Mohan, S., 2016. Strategy and design of Innovation Policy Roadmapping for a waste biorefinery. Bioresource Technology 215, 76-83.

Ranade, D.R., Yeole, T.Y., Godbole, S.H., 1987. Production of biogas from market waste. Biomass 13, 147–153.

Rapport, J., Zhang, R., Jenkins, B.M., Williams, R.B., 2008. Current Anaerobic Digestion Technologies Used for Treatment of Municipal Organic Solid Waste. California Environmental Protection Agency

Ratanatamskul, C., Onnum, G., Yamamoto, K., 2014. A prototype single-stage anaerobic digester for co-digestion of food waste and sewage sludge from high-rise building for on-site biogas production. International Biodeterioration & Biodegradation 95, Part A, 176–180.

Ratanatamskul, C., Wattanayommanaporn, O., Yamamoto, K., 2015. An on-site prototype two-stage anaerobic digester for co-digestion of food waste and sewage sludge for biogas production from high-rise building. International Biodeterioration & Biodegradation 102, 143–148.

Redondas, V., Gómez, X., García, S., Pevida, C., Rubiera, F., Morán, A., Pis, J.J., 2012. Hydrogen production from food wastes and gas post-treatment by CO2 adsorption. Waste Management 32, 60–66.

Redwood, M.D., Orozco, R.L., Majewski, A.J., Macaskie, L.E., 2012. An integrated biohydrogen refinery: synergy of photofermentation, extractive fermentation and hydrothermal hydrolysis of food wastes. Bioresource technology 119, 384–92.

Reungsang, A., Sreela-or, C., Plangklang, P., 2013. Non-sterile bio-hydrogen fermentation from food waste in a continuous stirred tank reactor (CSTR): Performance and population analysis. International Journal of Hydrogen Energy 38, 15630–15637.

Rotaru, A.E., Shrestha, P.M., Liu, F., Markovaite, B., Chen, S., Nevin, K.P., Lovley, D.R., 2014a. Direct interspecies electron transfer between Geobacter metallireducens and Methanosarcina barkeri. Applied and Environmental Microbiology 80, 4599–4605.

Rotaru, A.-E., Shrestha, P.M., Liu, F., Shrestha, M., Shrestha, D., Embree, M., Zengler, K., Wardman, C., Nevin, K.P., Lovley, D.R., 2014b. A new model for electron flow during anaerobic digestion: direct interspecies electron transfer to Methanosaeta for the reduction of carbon dioxide to methane. Energy Environ. Sci. 7, 408–415.

Roy, F., Samain, E., Dubourguier, H.C., Albagnac, G., 1986. Synthrophomonas sapovorans sp. nov., a new obligately proton reducing anaerobe oxidizing saturated and unsaturated long chain fatty acids. Arch Microbiol 145, 142–147.

Salminen, E., Rintala, J., 2002. Anaerobic digestion of organic solid poultry slaughterhouse waste–a review. Bioresource Technology 83, 13–26.

San Martin, D., Ramos, S., Zufía, J., 2016. Valorisation of food waste to produce new raw materials for animal feed. Food Chemistry 198, 68–74.

Savant, D. V., Shouche, Y.S., Prakash, S., Ranade, D.R., 2002. Methanobrevibacter acididurans sp. nov., a novel methanogen from a sour anaerobic digester. International Journal of Systematic and Evolutionary Microbiology 52, 1081–1087.

Sawatdeenarunat, C., Nguyen, D., Surendra, K.C., Shrestha, S., Rajendran, K., Oechsner, H., Xie, L., Khanal, S.K., 2016. Anaerobic biorefinery: current status, challenges, and opportunities. Bioresource Technology 215, 304-131.

Schievano, A., Tenca, A., Lonati, S., Manzini, E., Adani, F., 2014. Can two-stage instead of one-stage anaerobic digestion really increase energy recovery from biomass? Applied Energy 124, 335–342.

Serna-Maza, A., Heaven, S., Banks, C.J., 2014. Ammonia removal in food waste anaerobic digestion using a side-stream stripping process. Bioresource Technology 152, 307–315.

Serna-Maza, A., Heaven, S., Banks, C.J., 2015. Biogas stripping of ammonia from fresh digestate from a food waste digester. Bioresource Technology 190, 66–75.

Shahriari, H., Warith, M., Hamoda, M., Kennedy, K., 2013. Evaluation of single vs. staged mesophilic anaerobic digestion of kitchen waste with and without microwave pretreatment. Journal of environmental management 125, 74–84.

Shen, D., Wang, K., Yin, J., Chen, T., Yu, X., 2016. Effect of phosphoric acid as a catalyst on the hydrothermal pretreatment and acidogenic fermentation of food waste. Waste management (New York, N.Y.) 51, 65–71.

Shen, F., Yuan, H., Pang, Y., Chen, S., Zhu, B., Zou, D., Liu, Y., Ma, J., Yu, L., Li, X., 2013. Performances of anaerobic co-digestion of fruit & vegetable waste (FVW) and food waste (FW): single-phase vs. two-phase. Bioresource technology 144, 80–5.

Shen, Y., Linville, J.L., Urgun-Demirtas, M., Schoene, R.P., Snyder, S.W., 2015. Producing pipeline-quality biomethane via anaerobic digestion of sludge amended with corn stover biochar with in-situ CO2 removal. Applied Energy 158, 300–309.

Shen, Y., Linville, J.L., Ignacio-de Leon, P.A.A., Schoene, R.P., Urgun-Demirtas, M., 2016. Towards a sustainable paradigm of waste-to-energy process: Enhanced anaerobic digestion of sludge with woody biochar. Journal of Cleaner Production 135, 1054–1064.

Shen, Y., Forrester, S., Koval, J., Urgun-Demirtas, M., 2017. Yearlong semi-continuous operation of thermophilic two-stage anaerobic digesters amended with biochar for enhanced biomethane production. Journal of Cleaner Production.

Sheng, K., Chen, X., Pan, J., Kloss, R., Wei, Y., Ying, Y., 2013. Effect of ammonia and nitrate on biogas production from food waste via anaerobic digestion. Biosystems

Engineering 116, 205–212.

Spanish Ministry of Agriculture Food and the Environment, 2013. Spanish Strategy: "More food, less waste" Program to reduce food loss and waste and maximise the value of discarded food.

Spirito, C.M., Richter, H., Rabaey, K., Stams, A.J.M., Angenent, L.T., 2014. Chain elongation in anaerobic reactor microbiomes to recover resources from waste. Current Opinion in Biotechnology 27, 115–122.

Sreela-or, C., Imai, T., Plangklang, P., Reungsang, A., 2011a. Optimization of key factors affecting hydrogen production from food waste by anaerobic mixed cultures. International Journal of Hydrogen Energy 36, 14120–14133.

Sreela-or, C., Plangklang, P., Imai, T., Reungsang, A., 2011b. Co-digestion of food waste and sludge for hydrogen production by anaerobic mixed cultures: Statistical key factors optimization. International Journal of Hydrogen Energy 36, 14227–14237.

Steinbusch, K.J.J., Hamelers, H.V.M., Plugge, C.M., Buisman, C.J.N., 2011. Biological formation of caproate and caprylate from acetate: fuel and chemical production from low grade biomass. Energy & Environmental Science 4, 216-224.

Stoknes, K., Scholwin, F., Krzesiński, W., Wojciechowska, E., Jasińska, A., 2016. Efficiency of a novel "Food to waste to food" system including anaerobic digestion of food waste and cultivation of vegetables on digestate in a bubble-insulated greenhouse. Waste Management 56, 466–476.

Storck, T., Virdis, B., Batstone, D.J., 2016. Modelling extracellular limitations for mediated versus direct interspecies electron transfer. The ISME Journal 10, 621–631.

Sunyoto, N.M.S., Zhu, M., Zhang, Z., Zhang, D., 2016. Effect of biochar addition on hydrogen and methane production in two-phase anaerobic digestion of aqueous carbohydrates food waste. Bioresource Technology 219, 29–36.

Tampio, E., Ervasti, S., Paavola, T., Heaven, S., Banks, C., Rintala, J., 2014. Anaerobic digestion of autoclaved and untreated food waste. Waste Management 34, 370–377.

Thauvin, P., Vernier, A., 2013. Réduire, trier et valoriser les biodéchets des gros producteurs. ADEME, Agence del'Environnement et de la Maîtrise de l'Energie.

Thi, N.B.D., Lin, C.-Y., Kumar, G., 2016. Electricity generation comparison of food waste-based bioenergy with wind and solar powers: A mini review. Sustainable Environment Research 26, 197–202.

Torri, C., Fabbri, D., 2014. Biochar enables anaerobic digestion of aqueous phase from intermediate pyrolysis of biomass. Bioresource Technology 172, 335–341.

Tuck, C.O., Pérez, E., Horváth, I.T., Sheldon, R.A., Poliakoff, M., 2012. Valorization of biomass: deriving more value from waste. Science 337, 695–699.

Uçkun Kiran, E., Trzcinski, A.P., Ng, W.J., Liu, Y., 2014. Bioconversion of food waste to energy: A review. Fuel 134, 389–399.

Uçkun Kiran, E., Liu, Y., 2015. Bioethanol production from mixed food waste by an effective enzymatic pretreatment. Fuel 159, 463–469.

United Nations, 2011. World Population Prospects: The 2010 Revision, Volume I: Comprehensive Tables., ST/ESA/SER.A/313.

Valdez-Vazquez, I., Poggi-Varaldo, H.M., 2009. Alkalinity and high total solids affecting H2

production from organic solid waste by anaerobic consortia. International Journal of Hydrogen Energy 34, 3639–3646. 9

VALORGAS, 2010. D2.1: Compositional analysis of food waste from study sites in geographically distinct regions of Europe, Valorisation of food waste to biogas.

Van Soest, P.J., 1963. Use of detergents in the analysis of fibrous feeds. II. A rapid method for the determination of fiber and lignin. J. Assoc. Off. Anal. Chem. 46, 829–835.

Van Velsen, A.F.M., 1979. Adaptation of methanogenic sludge to high ammonia-nitrogen concentrations. Water Research 13, 995–999.

Venkata, S.M., Nikhil, G.N., Chiranjeevi, P., Nagendranatha Reddy, C., Rohit, M.V., Naresh Kumar, A., Sarkar, O., 2016. Waste Biorefinery Models Towards Sustainable Bioeconomy: Critical Review and Future Perspectives. Bioresource Technology 215, 2-12.

Venkiteshwaran, K., Milferstedt, K., Hamelin, J., Zitomer, D.H., 2016. Anaerobic digester bioaugmentation influences quasi steady state performance and microbial community. Water Research 104, 128–136.

Ventura, J.-R.S., Lee, J., Jahng, D., 2014. A comparative study on the alternating mesophilic and thermophilic two-stage anaerobic digestion of food waste. Journal of Environmental Sciences 26, 1274–1283.

Voelklein, M.A., O'Shea, R., Jacob, A., Murphy, J.D., 2017. Role of trace elements in single and two-stage digestion of food waste at high organic loading rates. Energy, *In Press*.

Walter, A., Probst, M., Hinterberger, S., Müller, H., Insam, H., 2016. Biotic and abiotic dynamics of a high solid-state anaerobic digestion box-type container system. Waste Management 49, 26–35.

Wan, S., Sun, L., Douieb, Y., Sun, J., Luo, W., 2013. Anaerobic digestion of municipal solid waste composed of food waste, wastepaper, and plastic in a single-stage system: Performance and microbial community structure characterization. Bioresource Technology 146, 619–627.

Wang, D., Ai, J., Shen, F., Yang, G., Zhang, Y., Deng, S., Zhang, J., Zeng, Y., Song, C., 2017. Improving anaerobic digestion of easy-acidification substrates by promoting buffering capacity using biochar derived from vermicompost. Bioresource Technology 227, 286–296.

Wang, K., Yin, J., Shen, D., Li, N., 2014. Anaerobic digestion of food waste for volatile fatty acids (VFAs) production with different types of inoculum: effect of pH. Bioresource technology 161, 395–401.

Wang, L.-H., Wang, Q., Cai, W., Sun, X., 2012. Influence of mixing proportion on the solid-state anaerobic co-digestion of distiller's grains and food waste. Biosystems Engineering 112, 130–137.

Wang, L.Y., Nevin, K.P., Woodard, T.L., Mu, B.Z., Lovley, D.R., 2016. Expanding the diet for DIET: Electron donors supporting direct interspecies electron transfer (DIET) in defined co-cultures. Frontiers in Microbiology 7, 1–7.

Wang, M., Sun, X., Li, P., Yin, L., Liu, D., Zhang, Y., Li, W., Zheng, G., 2014. A novel alternate feeding mode for semi-continuous anaerobic co-digestion of food waste with chicken manure. Bioresource Technology 164, 309–314.

Wang, P., Wang, H., Qiu, Y., Ren, L., Jiang, B., 2017. Microbial characteristics in anaerobic

digestion process of food waste for methane production-A review. Bioresource Technology, *In Press*.

Wang, Q., Kuninobu, M., Ogawa, H.I., Kato, Y., 1999. Degradation of volatile fatty acids in highly efficient anaerobic digestion. Biomass and Bioenergy 16, 407–416.

Wang, Q., Jiang, J., Zhang, Y., Li, K., 2015. Effect of initial total solids concentration on volatile fatty acid production from food waste during anaerobic acidification. Environmental Technology 36, 1884–1891.

Wang, X., Zhao, Y., 2009. A bench scale study of fermentative hydrogen and methane production from food waste in integrated two-stage process. International Journal of Hydrogen Energy 34, 245–254.

Wang, Y., Qian, P., 2009. Conservative fragments in bacterial 16S rRNA genes and primer design for 16S ribosomal DNA amplicons in metagenomic studies. PloS one 4.

Wei, Q., Zhang, W., Guo, J., Wu, S., Tan, T., Wang, F., Dong, R., 2014. Performance and kinetic evaluation of a semi-continuously fed anaerobic digester treating food waste: effect of trace elements on the digester recovery and stability. Chemosphere 117, 477–85.

Weimer, P.J., Nerdahl, M., Brandl, D.J., 2015. Production of medium-chain volatile fatty acids by mixed ruminal microorganisms is enhanced by ethanol in co-culture with Clostridium kluyveri. Bioresource Technology 175, 97–101.

Wen, Z., Wang, Y., De Clercq, D., 2016. What is the true value of food waste? A case study of technology integration in urban food waste treatment in Suzhou City, China. Journal of Cleaner Production 118, 88–96.

Westerholm, M., Levén, L., Schnürer, A., 2012. Bioaugmentation of syntrophic acetate-oxidizing culture in biogas reactors exposed to increasing levels of ammonia. Applied and environmental microbiology 78, 7619–25.

Woon, K.S., Lo, I.M.C., 2015. A proposed framework of food waste collection and recycling for renewable biogas fuel production in Hong Kong. Waste Management 47, 3–10.

Wu, L.-J., Kobayashi, T., Li, Y.-Y., Xu, K.-Q., 2015. Comparison of single-stage and temperature-phased two-stage anaerobic digestion of oily food waste. Energy Conversion and Management 106, 1174–1182.

Wu, X.Y., Shi, K.L., Xu, E.W., Wu, M., Oren, A., Zhu, X.F., 2010. Alkaliphilus halophilus sp. nov., a strictly anaerobic and halophilic bacterium isolated from a saline lake, and emended description of the genus Alkaliphilus. International Journal of Systematic and Evolutionary Microbiology 60, 2898–2902.

Wu, Y., Ma, H., Zheng, M., Wang, K., 2015. Lactic acid production from acidogenic fermentation of fruit and vegetable wastes. Bioresource technology 191, 53–58.

Xu, C., Shi, W., Hong, J., Zhang, F., Chen, W., 2015. Life cycle assessment of food waste-based biogas generation. Renewable and Sustainable Energy Reviews 49, 169–177.

Xu, S.Y., Lam, H.P., Karthikeyan, O.P., Wong, J.W.C., 2011. Optimization of food waste hydrolysis in leach bed coupled with methanogenic reactor: effect of pH and bulking agent. Bioresource technology 102, 3702–8.

Xu, S.Y., Karthikeyan, O.P., Selvam, A., Wong, J.W.C., 2012. Effect of inoculum to substrate ratio on the hydrolysis and acidification of food waste in leach bed reactor. Bioresource technology 126, 425–30.

Yabu, H., Sakai, C., Fujiwara, T., Nishio, N., Nakashimada, Y., 2011. Thermophilic two-stage dry anaerobic digestion of model garbage with ammonia stripping. Journal of Bioscience and Bioengineering 111, 312–319.

Yamada, C., Kato, S., Ueno, Y., Ishii, M., Igarashi, Y., 2015. Conductive iron oxides accelerate thermophilic methanogenesis from acetate and propionate. Journal of Bioscience and Bioengineering 119, 678–682.

Yan, B.H., Selvam, A., Wong, J.W.C., 2016. Innovative method for increased methane recovery from two-phase anaerobic digestion of food waste through reutilization of acidogenic off-gas in methanogenic reactor. Bioresource Technology 217, 3-9.

Yang, L., Huang, Y., Zhao, M., Huang, Z., Miao, H., Xu, Z., Ruan, W., 2015. Enhancing biogas generation performance from food wastes by high-solids thermophilic anaerobic digestion: Effect of pH adjustment. International Biodeterioration & Biodegradation 105, 153–159.

Yang, Y., Zhang, Y., Li, Z., Zhao, Z., Quan, X., Zhao, Z., 2017. Adding granular activated carbon into anaerobic sludge digestion to promote methane production and sludge decomposition. Journal of Cleaner Production 149, 1101–1108.

Yasin, N.H.M., Mumtaz, T., Hassan, M.A., Abd Rahman, N., 2013. Food waste and food processing waste for biohydrogen production: a review. Journal of environmental management 130, 375–85.

Ye, J., Li, D., Sun, Y., Wang, G., Yuan, Z., Zhen, F., Wang, Y., 2013. Improved biogas production from rice straw by co-digestion with kitchen waste and pig manure. Waste management (New York, N.Y.) 33, 2653–8.

Yin, J., Wang, K., Yang, Y., Shen, D., Wang, M., Mo, H., 2014. Improving production of volatile fatty acids from food waste fermentation by hydrothermal pretreatment. Bioresource technology 171, 323–9.

Yirong, C., Banks, C.J., Heaven, S., 2013. Comparison of mesophilic and thermophilic anaerobic digestion of food waste, in: IWA (Ed.), AD13 Recovering (Bio) Resources for the World. Santiago de Compostela.

Yirong, C., Heaven, S., Banks, C.J., 2015. Effect of a Trace Element Addition Strategy on Volatile Fatty Acid Accumulation in Thermophilic Anaerobic Digestion of Food Waste. Waste and Biomass Valorization 6, 1–12.

Yong, Z., Dong, Y., Zhang, X., Tan, T., 2015. Anaerobic co-digestion of food waste and straw for biogas production. Renewable Energy 78, 527–530.

Zamanzadeh, M., Hagen, L.H., Svensson, K., Linjordet, R., Horn, S.J., 2016a. Anaerobic digestion of food waste - effect of recirculation and temperature on performance and microbiology. Water Research 96, 246-254.

Zeeman, G., 2005. Anaerobic Wastewater Treatment, 2005th ed. Wageningen University, Wageningen.

Zeng, Y., De Guardia, A., Dabert, P., 2015. Improving composting as a post-treatment of anaerobic digestate. Bioresource Technology 201, 293–303.

Zhan-jiang, P., Jie, L., Feng-mei, S., Su, W., Ya-bing, G., Da-lei, Z., 2014. High-solid Anaerobic Co-digestion of Food Waste and Rice Straw for Biogas Production. Journal of Northeast Agricultural University (English Edition) 21, 61–66.

Zhang, B., Cai, W., He, P., 2007. Influence of lactic acid on the two-phase anaerobic

digestion of kitchen wastes. Journal of Environmental Sciences 19, 244–249.

Zhang, C., Su, H., Tan, T., 2013a. Batch and semi-continuous anaerobic digestion of food waste in a dual solid–liquid system. Bioresource Technology 145, 10–16.

Zhang, C., Xiao, G., Peng, L., Su, H., Tan, T., 2013b. The anaerobic co-digestion of food waste and cattle manure. Bioresource Technology 129, 170–176.

Zhang, C., Su, H., Baeyens, J., Tan, T., 2014. Reviewing the anaerobic digestion of food waste for biogas production. Renewable and Sustainable Energy Reviews 38, 383–392.

Zhang, J., Wang, Q., 2013. Buffering and nutrient effects of white mud from ammonia–soda process on thermophilic hydrogen fermentation from food waste. International Journal of Hydrogen Energy 38, 13564–13571.

Zhang, J., Wang, Q., Jiang, J., 2013. Lime mud from paper-making process addition to food waste synergistically enhances hydrogen fermentation performance. International Journal of Hydrogen Energy 38, 2738–2745.

Zhang, J., Wang, Q., Zheng, P., Wang, Y., 2014. Anaerobic digestion of food waste stabilized by lime mud from papermaking process. Bioresource technology 170, 270–7.

Zhang, J., Lv, C., Tong, J., Liu, J., Liu, J., Yu, D., Wang, Y., Chen, M., Wei, Y., 2015. Optimization and microbial community analysis of anaerobic co-digestion of food waste and sewage sludge based on microwave pretreatment. Bioresource technology 200, 253–261.

Zhang, J., Lv, C., Tong, J., Liu, J., Liu, J., Yu, D., Wang, Y., Chen, M., Wei, Y., 2016. Optimization and microbial community analysis of anaerobic co-digestion of food waste and sewage sludge based on microwave pretreatment. Bioresource Technology 200, 253–261.

Zhang, L., Lee, Y.-W., Jahng, D., 2011. Anaerobic co-digestion of food waste and piggery wastewater: Focusing on the role of trace elements. Bioresource Technology 102, 5048–5059.

Zhang, L., Jahng, D., 2012. Long-term anaerobic digestion of food waste stabilized by trace elements. Waste Management 32, 1509–1515.

Zhang, L., Ouyang, W., Lia, A., 2012. Essential Role of Trace Elements in Continuous Anaerobic Digestion of Food Waste. Procedia Environmental Sciences 16, 102–111.

Zhang, R., El-Mashad, H.M., Hartman, K., Wang, F., Liu, G., Choate, C., Gamble, P., 2007. Characterization of food waste as feedstock for anaerobic digestion. Bioresource Technology 98, 929–935.

Zhang, W., Wu, S., Guo, J., Zhou, J., Dong, R., 2015. Performance and kinetic evaluation of semi-continuously fed anaerobic digesters treating food waste: role of trace elements. Bioresource technology 178, 297–305.

Zhang, W., Zhang, L., Li, A., 2015a. Anaerobic co-digestion of food waste with MSW incineration plant fresh leachate: process performance and synergistic effects. Chemical Engineering Journal 259, 795–805.

Zhang, W., Zhang, L., Li, A., 2015b. Enhanced anaerobic digestion of food waste by trace metal elements supplementation and reduced metals dosage by green chelating agent [S, S]-EDDS via improving metals bioavailability. Water research 84, 266–77.

Zhang, Y., Banks, C.J., Heaven, S., 2012a. Co-digestion of source segregated domestic food

waste to improve process stability. Bioresource Technology 114, 168–178.

Zhang, Y., Banks, C.J., Heaven, S., 2012b. Anaerobic digestion of two biodegradable municipal waste streams. Journal of environmental management 104, 166–74.

Zhao, Z., Zhang, Y., Holmes, D.E., Dang, Y., Woodard, T.L., Nevin, K.P., Lovley, D.R., 2016a. Potential enhancement of direct interspecies electron transfer for syntrophic metabolism of propionate and butyrate with biochar in up-flow anaerobic sludge blanket reactors. Bioresource Technology 209, 148–156.

Zhao, Z., Zhang, Y., Yu, Q., Dang, Y., Li, Y., Quan, X., 2016b. Communities stimulated with ethanol to perform direct interspecies electron transfer for syntrophic metabolism of propionate and butyrate. Water Research 102, 475–484.

Zheng, J., Gao, M., Wang, Q., Wang, J., Sun, X., Chang, Q., Tashiro, Y., 2017. Enhancement of l-lactic acid production via synergism in open co-fermentation of Sophora flavescens residues and food waste. Bioresource Technology 225, 159–164.

Zhou, P., Elbeshbishy, E., Nakhla, G., 2013. Optimization of biological hydrogen production for anaerobic co-digestion of food waste and wastewater biosolids. Bioresource technology 130, 710–8.

Zhou, Q., Shen, F., Yuan, H., Zou, D., Liu, Y., Zhu, B., Jaffu, M., Chufo, A., Li, X., 2014. Minimizing asynchronism to improve the performances of anaerobic co-digestion of food waste and corn stover. Bioresource Technology 166, 31–36.

Zhou, Y., Zhang, Z., Nakamoto, T., Li, Y., Yang, Y., Utsumi, M., Sugiura, N., 2011. Influence of substrate-to-inoculum ratio on the batch anaerobic digestion of bean curd refuse-okara under mesophilic conditions. Biomass and Bioenergy 35, 3251–3256.

Zhu, H., Parker, W., Basnar, R., Proracki, A., Falletta, P., Béland, M., Seto, P., 2009. Buffer requirements for enhanced hydrogen production in acidogenic digestion of food wastes. Bioresource technology 100, 5097–102.

Zhu, H., Parker, W., Conidi, D., Basnar, R., Seto, P., 2011. Eliminating methanogenic activity in hydrogen reactor to improve biogas production in a two-stage anaerobic digestion process co-digesting municipal food waste and sewage sludge. Bioresource technology 102, 7086–92.

Zong, W., Yu, R., Zhang, P., Fan, M., Zhou, Z., 2009. Efficient hydrogen gas production from cassava and food waste by a two-step process of dark fermentation and photo-fermentation. Biomass and Bioenergy 33, 1458–1463.

Zwietering, M.H., Jongenburger, I., Rombouts, F.M., Van't Riet, K., 1990. Modeling of the bacterial growth curve. Applied and environmental microbiology 56, 1875–1881.

VALORIZATION OF COMMERCIAL FOOD WASTE VIA ANAEROBIC PROCESSES

The increasing production of food waste worldwide and new international regulations call for the development of novel processes for the treatment of this waste. Among all the existing possibilities, anaerobic processes represent a sustainable-modern approach that allows waste treatment and valorization. This PhD thesis aims at understanding the biochemical processes governing anaerobic digestion of food waste, eventually providing a stable process applicable at industrial scale.

As a first step, a screening was performed to elucidate the main parameter affecting anaerobic digestion of food waste, evaluating different substrate loads, solid contents, co-digestion proportions and microbial inocula from different origins. After concluding the critical importance of the inoculum used and the substrate load, different strategies for process stabilization for methane production were tested using consecutive batch reactors. This served for confirming the positive effect of supplementation of trace elements and to identify the main issue that was found: accumulation of propionic acid. Aiming at finding a solution, the final experiments were focused on assessing the capability of carbon-based conductive materials to solve this problem. The dosing of these materials favored the digestion kinetics, improving greatly the methane volumetric productivities.

This thesis provides novel insights, both on the main mechanisms governing food waste anaerobic digestion and on the implications that they present for the valorization of this waste. In addition, potential solutions for the complications found are given, aiding to the development of a feasible industrial digestion process.

DEFENDED ON 12TH DECEMBER 2017 AT :

WITH THE FINANCIAL SUPPORT OF :

INRA
SCIENCE & IMPACT

INSTITUT NATIONAL DE LA RECHERCHE AGRONOMIQUE
Unité de recherche (UR0050) - Laboratoire de Biotechnologie de l'Environnement

102, avenue des Etangs
F-11100 Narbonne
France

Tél. : + 33 4 68 42 51 51
Courriel: lbe-contact@supagro.inra.fr
www.montpellier.inra.fr/narbonne